REGULATION OF ANTIBIOTIC PRODUCTION IN ACTINOMYCETES

EDITED BY: Yvonne Mast, Evi Stegmann and Yinhua Lu
PUBLISHED IN: Frontiers in Microbiology

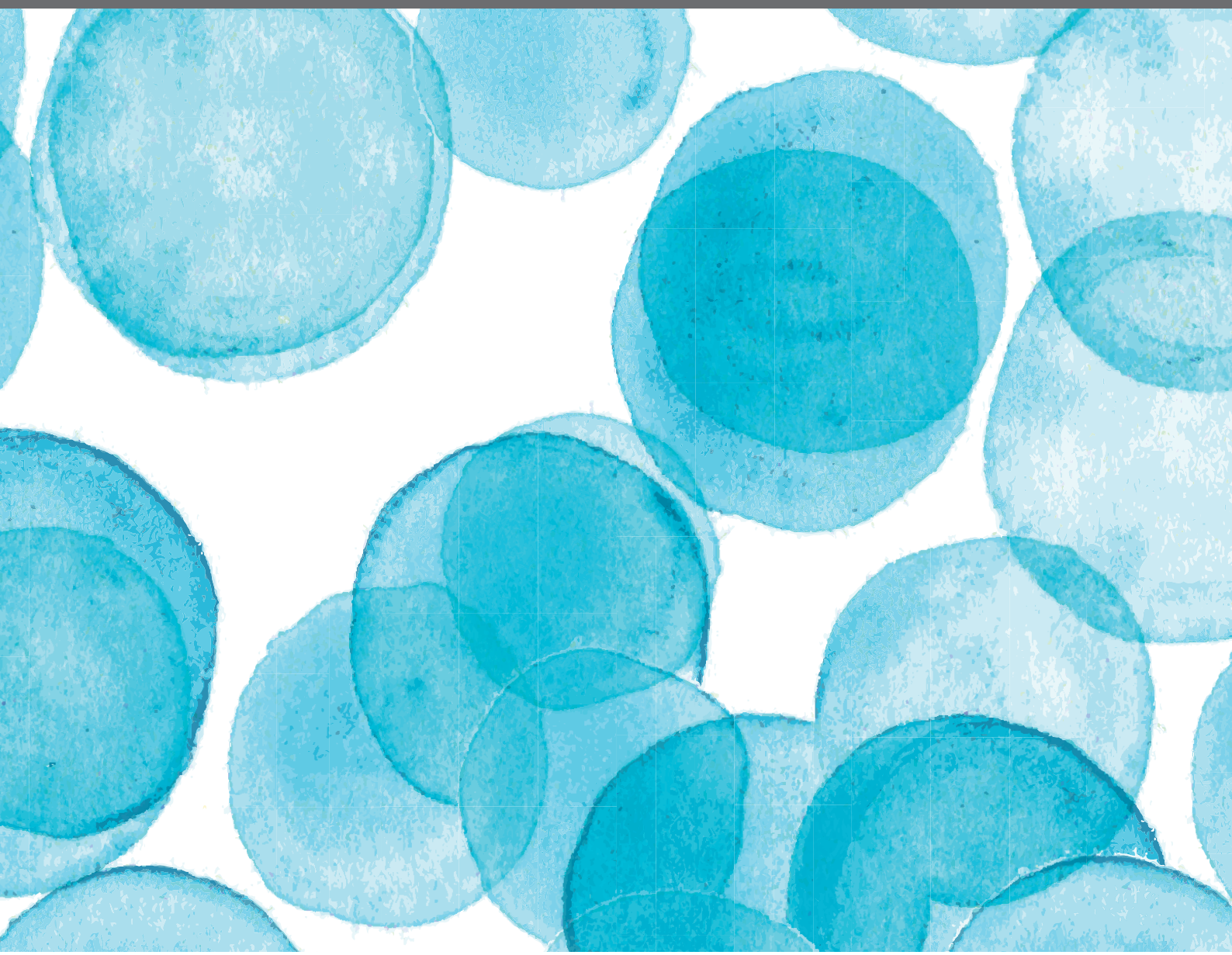

frontiers Research Topics

ISSN 1664-8714
ISBN 978-2-88963-995-3
DOI 10.3389/978-2-88963-995-3

About Frontiers

Frontiers is more than just an open-access publisher of scholarly articles: it is a pioneering approach to the world of academia, radically improving the way scholarly research is managed. The grand vision of Frontiers is a world where all people have an equal opportunity to seek, share and generate knowledge. Frontiers provides immediate and permanent online open access to all its publications, but this alone is not enough to realize our grand goals.

Frontiers Journal Series

The Frontiers Journal Series is a multi-tier and interdisciplinary set of open-access, online journals, promising a paradigm shift from the current review, selection and dissemination processes in academic publishing. All Frontiers journals are driven by researchers for researchers; therefore, they constitute a service to the scholarly community. At the same time, the Frontiers Journal Series operates on a revolutionary invention, the tiered publishing system, initially addressing specific communities of scholars, and gradually climbing up to broader public understanding, thus serving the interests of the lay society, too.

Dedication to Quality

Each Frontiers article is a landmark of the highest quality, thanks to genuinely collaborative interactions between authors and review editors, who include some of the world's best academicians. Research must be certified by peers before entering a stream of knowledge that may eventually reach the public - and shape society; therefore, Frontiers only applies the most rigorous and unbiased reviews.
Frontiers revolutionizes research publishing by freely delivering the most outstanding research, evaluated with no bias from both the academic and social point of view. By applying the most advanced information technologies, Frontiers is catapulting scholarly publishing into a new generation.

What are Frontiers Research Topics?

Frontiers Research Topics are very popular trademarks of the Frontiers Journals Series: they are collections of at least ten articles, all centered on a particular subject. With their unique mix of varied contributions from Original Research to Review Articles, Frontiers Research Topics unify the most influential researchers, the latest key findings and historical advances in a hot research area! Find out more on how to host your own Frontiers Research Topic or contribute to one as an author by contacting the Frontiers Editorial Office: researchtopics@frontiersin.org

REGULATION OF ANTIBIOTIC PRODUCTION IN ACTINOMYCETES

Topic Editors:
Yvonne Mast, German Collection of Microorganisms and Cell Cultures GmbH (DSMZ), Germany
Evi Stegmann, University of Tübingen, Germany
Yinhua Lu, Shanghai Normal University, China

Citation: Mast, Y., Stegmann, E., Lu, Y., eds. (2020). Regulation of Antibiotic Production in Actinomycetes. Lausanne: Frontiers Media SA. doi: 10.3389/978-2-88963-995-3

Table of Contents

frontiers in Microbiology

EDITORIAL
published: 22 July 2020
doi: 10.3389/fmicb.2020.01566

Editorial: Regulation of Antibiotic Production in Actinomycetes

Yvonne Mast[1,2,3]*, *Evi Stegmann*[4] *and Yinhua Lu*[5]

[1] Department Bioresources for Bioeconomy and Health Research, Leibniz Institute DSMZ -German Collection of Microorganisms and Cell Cultures, Brunswick, Germany, [2] Department of Microbiology, Technical University Braunschweig, Brunswick, Germany, [3] German Center for Infection Research (DZIF), Partner Site Tübingen, Tübingen, Germany, [4] Department of Microbial Bioactive Compounds, Interfaculty Institute of Microbiology and Infection Medicine, Faculty of Science, University of Tübingen, Tübingen, Germany, [5] College of Life Sciences, Shanghai Normal University, Shanghai, China

Keywords: actinomycetes, antibiotic, secondary metabolism, regulation, signaling

Editorial on the Research Topic

Regulation of Antibiotic Production in Actinomycetes

Actinomycetes are a well-known resource for the discovery of novel bioactive compounds. Up to two-thirds of all antibiotics in use today are natural products from actinomycetes or semi-synthetic derivatives thereof (Barka et al., 2016). *Streptomyces* species have thus far proven to be a particularly useful resource. It is now 80 years ago (1940) when Selman Waksman isolated the first antibiotic from an actinomycete's species, which was actinomycin A from *Actinomyces* (*Streptomyces*) *antibioticus* (Kresge et al., 2004). Shortly after, he coined the term "antibiotic," which is just one reason why he is considered widely to be the true "Father of Antibiotics" (Kresge et al., 2004). In the following years Waksman's group successfully applied his screening technique for the identification of natural substances and isolated more than 20 additional new bioactive compounds, thereby initiating the so-called "golden era of antibiotic discovery." One of the most important Waksman compounds was streptomycin, which Albert Schatz and he identified in 1943 as a product from *Streptomyces griseus*. As discoverer of the "first antibiotic effective against tuberculosis" he was rewarded with the Nobel Prize in 1952 (Kresge et al., 2004). Since that time, actinomycetes, especially streptomycetes, have been studied intensively, not only because of their gifted metabolic potential but also due to their interesting biological features: e.g., streptomycetes have extraordinarily large genomes with up to ∼13 Mbp, which are of linear style and with a high GC content (>70%). They are characterized by an unique life-cycle, involving the formation of mats of fungus-like mycelium from which aerial branches are formed that carry chains of spores. The spores are then readily released for dissemination (Chater, 2016). Nowadays, actinomycetes are still, or maybe more than ever, a valuable resource for novel drugs. New antibiotics are urgently needed due to the constant rise of infections caused by drug-resistant pathogens (O'Neill, 2016). In recent years, a wealth of expertise has been gained regarding especially knowledge on antibiotic biosynthesis in these organisms. Particularly since the advent of next-generation sequencing technologies, the field of antibiotic research has experienced a remarkable revival, which is due to the upcoming of a large amount of genome sequence information that gave rise to novel approaches in order to exploit actinomycetes for drug discovery. Comparable few studies focus on a better understanding of regulatory mechanism of antibiotic biosynthesis. Understanding regulatory principles in antibiotic producing organisms is, however, fundamental for targeted optimization of antibiotic production yields, activation of silent gene clusters to find novel antibiotics, or facilitating genetic engineering approaches, e.g., to allow heterologous expression of engineered gene clusters. Besides that, regulation is the interface connecting aspects of chemical differentiation with complex

Edited by:
Rustam Aminov, University of Aberdeen, United Kingdom

Reviewed by:
Polpass Arul Jose, The Hebrew University of Jerusalem, Israel
Ryan Seipke, University of Leeds, United Kingdom

***Correspondence:**
Yvonne Mast
yvonne.mast@dsmz.de

Specialty section:
This article was submitted to Antimicrobials, Resistance and Chemotherapy, a section of the journal Frontiers in Microbiology

Received: *02 June 2020*
Accepted: *16 June 2020*
Published: *22 July 2020*

Citation:
Mast Y, Stegmann E and Lu Y (2020) Editorial: Regulation of Antibiotic Production in Actinomycetes. Front. Microbiol. 11:1566. doi: 10.3389/fmicb.2020.01566

morphological differentiation events in actinomycetes. Thus, understanding regulation means also learning about actinomycetal biology.

Regulation of secondary metabolism in actinomycetes is a complex process depending on various factors, such as nutrient limitation, oxygen supply or pH conditions (Liu et al., 2013; Wohlleben et al., 2017). Regulation can occur at the level of transcription and/or translation. Concerning the former, regulatory signaling cascades can include global, as well as pathway-specific (cluster-situated) transcriptional regulators. Thereby, various chemical substances may serve as effectors for transcriptional regulators, such as quorum-sensing-like γ-butyrolactone (GBL) molecules, antibiotics, or intermediates thereof. Groundbreaking scientific achievement in this field has been made already in the 1980s by Sueharu Horinouchi using the above mentioned famous *S. griseus* strain (Ohnishi, 2010). Horinouchi et al., showed that streptomycin production and morphological differentiation of *S. griseus* is under control of a complex regulatory signaling cascade triggered by the microbial hormone-like substance A-factor (Horinouchi et al., 1983; Horinouchi, 2002). The A-factor is a GBL molecule and was initially discovered in the 1960s by Khokhlov et al., as a substance controlling streptomycin production in the originally named strain *Actinomyces streptomycini* (*S. griseus*) (Khokhlov et al., 1967). Horinouchi thereafter worked out in detail that the A-factor is produced in a growth-dependent manner at nanomolar concentrations. When A-factor concentrations reach a certain threshold the cognate repressor-type receptor ArpA dissociates from its target gene *adpA*. *adpA* itself encodes the transcriptional regulator AdpA, which acts as a pleiotropic regulator controlling several hundred genes in *S. griseus*, including a number of genes involved in morphological differentiation and secondary metabolite biosynthesis (Horinouchi, 2002). The A-factor signaling cascade became a model system for understanding regulatory principles in antibiotic-producing actinomycetes. Indeed, GBLs are produced by many, if not all streptomycetes (Bibb, 2005), whereby the signaling cascades that are governed by GBLs and which control transcriptional activation of antibiotic gene clusters can have different compositions in various antibiotic producers (Bibb, 2005; Wohlleben et al., 2017). Furthermore, not only GBLs may function as signaling molecules but also antibiotics or their intermediates, which altogether result in complex regulatory networks including elaborate feedback and feedforward loops (Xu and Yang, 2019). Besides that, such networks themselves are embedded in larger regulatory circuits involving transcriptional as well as translational regulation, which may respond to diverse environmental signals as mentioned above (Bibb, 2005; Liu et al., 2013). Most of these various regulatory interactions have not been explored yet. Thus, there is still a lot to investigate for actinomycetes.

With this Frontiers Research Topic we aimed to create space for current advances and knowledge on regulation of antibiotic biosynthesis in actinomycetes and highlight the importance of this topic for antibiotic research. We collected 13 articles, including nine original articles and four reviews covering a variety of different regulatory aspects of antibiotic production. The articles address the topics of regulatory networks, signaling molecules for antibiotic production, studies on regulator-driven activation of silent gene clusters, optimization of antibiotic production, as well as regulatory effects from small open reading frames (ORFs) and small non-coding RNAs in actinomycetes.

The overarching review article from Juan Martin and Paloma Liras reports on the interplay between various environmental stress signals (e.g., variations in carbon and nitrogen sources, phosphate, oxygen, iron, and other nutrients) and major transcriptional factors in actinomycetes. It is described how these different signals are integrated at the molecular level (Martín and Liras). The authors propose a cross-talk of the transcriptional regulators, which bind to specific DNA regions, so-called "integrator sites," that allow to compensate for unbalances produced by metabolic stresses—a phenomenon designated as the "balance metabolism safety net" (Martín and Liras). The review article from Kong et al., concentrates on autoregulator-driven regulation of secondary metabolite biosynthesis. Here, the authors highlight the recent findings on regulation of antibiotic biosynthesis by small molecules including GBLs, antibiotics and their intermediates. This review is accompanied by four original research articles, which address specific signaling cascades in streptomycetes: Vicente et al., report on the regulatory role of the GBL-receptor-type regulator AlpZ in the kinamycin producer *Streptomyces ambofaciens*. Here, the authors present a molecular dynamics approach, which was applied to investigate the DNA-binding properties of AlpZ to its target DNA sequence and the impact of the potential signaling molecule on receptor-DNA interaction. Misaki et al., explore the repressive function of the pseudo-GBL receptor SrrB on lankacidin and lankamycin production in *Streptomyces rochei* and its hierarchical positioning within the regulatory signaling cascade. The study of Kang et al.., shows the involvement of the pleiotropic AdpA-like regulator $AdpA_{lin}$ from *Streptomyces lincolnensis* in lincomycin production and morphological differentiation; whereas Vior et al., report on a so far less studied cluster-situated gene *btmL*, which encodes a protein that acts as a modulator of the biosynthesis of the ribosomally synthesized and post-translationally modified peptide (RiPP) antibiotic bottromycin from *Streptomyces scabies*. Bottromycin shows an activity against clinical relevant pathogens and exhibits a unique chemical structure and mode of action, which makes it a promising drug lead compound. However, production yields in the known producers are very low, which hampered further drug development so far (Vior et al.). Indeed, this is a well-known issue for several drug development approaches, where further advancement is hindered by low production yields. Understanding regulatory principles is a key aspect, which allows the targeted improvement of antibiotic production yields. This aspect is largely covered by two reviews from Xia et al. and Li et al.: The article from Xia et al., summarizes the latest knowledge on regulatory cascades in streptomycetes and their importance for yield improvement applications and metabolite mining purposes, whereas the article from Li et al. concentrates on recent advances of synthetic biology approaches involving also regulatory components for yield improvement strategies. The importance of regulation for antibiotic yield improvement is also highlighted by two original

research articles (Park et al.; Yushchuk et al.): Park et al. report on the overexpression of a set of pathway-specific regulatory genes (*nppRI–nppRVI*) in *Pseudonocardia autotrophica*, which significantly improved production of the polyene-like substance NPP B2, whereas the study of Yushchuk et al. extended the genetic toolkit for members of the *Nonomurea* genus, involving the usage of suitable promoters and cluster-situated regulators to improve production yields of the glycopeptide antibiotic A40926 in *Nonomurea gerenzanensis*. As outlined in the review of Xia et al. understanding regulatory signaling can also help to activate silent gene clusters for novel natural compounds discovery. This is underpinned by an original research article from Krause et al. who report on the activating function of the SARP-type regulator PapR2 from *Streptomyces pristinaespiralis* and describe how these type of regulators can be used as general devices to activate antibiotic gene clusters in actinomycetes. Besides several studies that deal with transcriptional regulators, also post-transcriptional regulation is the topic in two research articles: The study of Engel et al. disclosed the post-transcriptional regulatory effect of a small RNA *scr5239* on the primary metabolic enzyme phosphoenolpyruvate carboxykinase PEPK and report on the interconnection between central carbon metabolism and secondary metabolism via this small RNA. Furthermore, the study of Vassallo et al. shows that the conserved small ORF *trpM,* of which the product modulates L-tryptophan biosynthesis, has a regulatory effect on morphological development and antibiotic production in *Streptomyces coelicolor*. TrpM is suggested to interact with the putative cytosol aminopeptidase PepA (SCO2179) via a post-transcriptional and/or post-translational regulatory mechanism, whereby PepA plays a key role in antibiotic production and sporulation. Overall, this collection of articles gives a profound overview on the importance of knowledge on regulation of antibiotic biosynthesis for antibiotic research. We are delighted to present this Research Topic in *Frontiers in Microbiology* and hope that it will promote further research in this area.

AUTHOR CONTRIBUTIONS

YM, YL, and ES edited the Frontiers Research Topic on *Regulation of Antibiotic Production in Actinomycetes* and wrote the manuscript. All authors contributed to the article and approved the submitted version.

FUNDING

This work was supported by funding received from the Baden-Württemberg Stiftung (BWST_WSF-035) and the German Center for Infection research (DZIF) (TTU 09.819) given to YM and ES, and the National Natural Science Foundation of China (31770088) given to YL.

ACKNOWLEDGMENTS

The Editors would like to thank all the authors who contributed their valuable work to this Research Topic. We also acknowledge the important comments and suggestions of all the designated peer reviewers, who ensured robustness of research data and helped to improve the articles for the Research Topic. Finally, the authors thank the Chef Editor and the Frontiers Team for their support during handling of the Research Topic.

REFERENCES

Barka, E. A., Vatsa, P., Sanchez, L., Gaveau-Vaillant, N., Jacquard, C., Meier-Kolthoff, J. P., et al. (2016). Taxonomy, physiology, and natural products of actinobacteria. *Microbiol. Mol. Biol. Rev.* 80, 1–44. doi: 10.1128/MMBR.00019-15

Bibb, M. (2005). Regulation of secondary metabolism in streptomycetes. *Curr. Opin. Microbiol.* 8, 208–215. doi: 10.1016/j.mib.2005.02.016

Chater, K. F. (2016). Recent advances in understanding *Streptomyces*. *F1000Res* 5, 1–16. doi: 10.12688/f1000research.9534.1

Horinouchi, S. (2002). A microbial hormone, A-factor, as a master switch for morphological differentiation and secondary metabolism in *Streptomyces coelicolor*. *Front. Biosci.* 7, 2045–2057. doi: 10.2741/horinouc/list.htm

Horinouchi, S., Hara, O., and Beppu, T. (1983). Cloning of a pleiotropic gene that positively controls biosynthesis of A-factor, actinorhodin, and prodigiosin in *Streptomyces coelicolor* A3(2) and *Streptomyces lividans*. *J. Bacteriol.* 155, 1238–1248.

Khokhlov, A. S., Tovarova, I. I., Borisova, L. N., Pliner, S. A., Shevchenko, L. N., Kornitskaia, E. I., et al. (1967). The A-factor, responsible for streptomycin biosynthesis by mutant strains of *Actinomyces streptomycini*. *Dokl. Akad. Nauk SSSR* 177, 232–235.

Kresge, N., Simoni, R. D., and Hill, R. L. (2004). Selman Waksman: the father of antibiotics. *J. Biol. Chem.* 279, 101–103. Available online at: https://www.jbc.org/content/279/48/e7.short

Liu, G., Chater, K. F., Chandra, G., Niu, G., and Tan, H. (2013). Molecular regulation of antibiotic biosynthesis in *Streptomyces*. *Microbiol. Mol. Biol. Rev.* 77, 112–143. doi: 10.1128/MMBR.00054-12

Ohnishi, Y. (2010). Sueharu Horinouchi. *J. Antibiot.* 63, 97–98. doi: 10.1038/ja.2009.120

O'Neill, J. (2016). *Tackling Drug-Resistant Infections Globally: Final Report and Recommendations - The Review on Antimicrobial Resistance*. Available online at: https://amr-review.org/sites/default/files/160518_Finalpaper_with_cover.pdf (accessed July 09, 2020).

Wohlleben, W., Bera, A., Mast, Y., and Stegmann, E. (2017). "Regulation of secondary metabolites of actinobacteria," in *Biology and Biotechnology of Actinobacteria,* eds J. Wink, F. Mohammadipanah, and J. Hamedi (Cham: Springer), 181–232. doi: 10.1007/978-3-319-60339-1_8

Xu, G., and Yang, S. (2019). Regulatory and evolutionary roles of pseudo γ-butyrolactone receptors in antibiotic biosynthesis and resistance. *Appl. Microbiol. Biotechnol.* 103, 9373–9378. doi: 10.1007/s00253-019-10219-0

Conflict of Interest: The authors declare that the research was conducted in the absence of any commercial or financial relationships that could be construed as a potential conflict of interest.

frontiers in Microbiology

ORIGINAL RESEARCH
published: 23 October 2019
doi: 10.3389/fmicb.2019.02428

$AdpA_{lin}$, a Pleiotropic Transcriptional Regulator, Is Involved in the Cascade Regulation of Lincomycin Biosynthesis in *Streptomyces lincolnensis*

Yajing Kang[1], Yingying Wang[1], Bingbing Hou[1,2], Ruida Wang[1], Jiang Ye[2], Xiaoyu Zhu[1], Haizhen Wu[1,2] and Huizhan Zhang[1,2]**

[1] State Key Laboratory of Bioreactor Engineering, East China University of Science and Technology, Shanghai, China,
[2] Department of Applied Biology, East China University of Science and Technology, Shanghai, China

OPEN ACCESS

Edited by:
Yinhua Lu,
Shanghai Normal University, China

Reviewed by:
Xu-Ming Mao,
Zhejiang University, China
Ying Wen,
China Agricultural University (CAU), China

***Correspondence:**
Jiang Ye
yej@ecust.edu.cn
Huizhan Zhang
huizhzh@ecust.edu.cn

Specialty section:
This article was submitted to Antimicrobials, Resistance and Chemotherapy, a section of the journal Frontiers in Microbiology

Received: 14 August 2019
Accepted: 08 October 2019
Published: 23 October 2019

Citation:
Kang Y, Wang Y, Hou B, Wang R, Ye J, Zhu X, Wu H and Zhang H (2019) $AdpA_{lin}$, a Pleiotropic Transcriptional Regulator, Is Involved in the Cascade Regulation of Lincomycin Biosynthesis in Streptomyces lincolnensis. Front. Microbiol. 10:2428. doi: 10.3389/fmicb.2019.02428

Lincomycin is one of the most important antibiotics in clinical practice. To further understand the regulatory mechanism on lincomycin biosynthesis, we investigated a pleiotropic transcriptional regulator $AdpA_{lin}$ in the lincomycin producer *Streptomyces lincolnensis* NRRL 2936. Deletion of $adpA_{lin}$ (which generated $\Delta adpA_{lin}$) interrupted lincomycin biosynthesis and impaired the morphological differentiation. We also found that putative AdpA binding sites were unusually scattered in the promoters of all the 8 putative operons in the lincomycin biosynthetic gene cluster (BGC). In $\Delta adpA_{lin}$, transcript levels of structural genes in 8 putative operons were decreased with varying degrees, and electrophoretic mobility shift assays (EMSAs) confirmed that $AdpA_{lin}$ activated the overall putative operons via directly binding to their promoter regions. Thus, we speculated that the entire lincomycin biosynthesis is under the control of $AdpA_{lin}$. Besides, $AdpA_{lin}$ participated in lincomycin biosynthesis by binding to the promoter of *lmbU* which encoded a cluster sited regulator (CSR) LmbU of lincomycin biosynthesis. Results of qRT-PCR and catechol dioxygenase activity assay showed that $AdpA_{lin}$ activated the transcription of *lmbU*. In addition, $AdpA_{lin}$ activated the transcription of the *bldA* by binding to its promoter, suggesting that $AdpA_{lin}$ indirectly participated in lincomycin biosynthesis and morphological differentiation. Uncommon but understandable, $AdpA_{lin}$ auto-activated its own transcription via binding to its own promoter region. In conclusion, we provided a molecular mechanism around the effect of $AdpA_{lin}$ on lincomycin biosynthesis in *S. lincolnensis*, and revealed a cascade regulation of lincomycin biosynthesis by $AdpA_{lin}$, LmbU, and BldA.

Keywords: AdpA, lincomycin, *Streptomyces lincolnensis*, transcriptional regulator, cascade regulation

INTRODUCTION

Lincomycin is a naturally occurring antibiotic isolated from soil sample, and it was first introduced into clinical practice in 1963 (Macleod et al., 1964). Lincomycin and its derivatives belong to lincosamide antibiotics and exhibit biological activities against anaerobic and some protozoal infections by inhibiting protein synthesis in sensitive targets (Spizek and Rezanka, 2017).

Clindamycin is a semi-synthetic chlorinated derivative of lincomycin and it is marked by being one of the 20 most important antibiotics (Spizek and Rezanka, 2004a). Given the extensive clinical application of lincomycin, multiple attempts have been taken into industrial practice to increase the production yields of lincomycin or to optimize the products (Spizek and Rezanka, 2004b; Li et al., 2007). Genetic manipulations are also adopted as complement to enhance the production of lincomycin (Pang et al., 2015; Xu et al., 2018). Though the pathway of lincomycin biosynthesis was assembled mainly within the recent 10 years (Neusser et al., 1998; Novotna et al., 2004; Sasaki et al., 2012; Lin et al., 2014; Pang et al., 2015; Zhao et al., 2015; Jiraskova et al., 2016), studies on the regulation mechanism of lincomycin biosynthesis are prompted quite slowly. Thus, various methods have limited effect on yield improvement of lincomycin.

Biosynthesis of antibiotics is controlled by elaborate regulatory mechanisms. Hormone-like signaling molecules, for example γ-butyrolactone (Takano et al., 2000; Hsiao et al., 2009; Du et al., 2011), serve as stimuli that interact with their receptor proteins to prelude the secondary metabolism (Niu et al., 2016). Global regulators and/or pleiotropic regulators then deliver these signals to CSRs which directly control the onset of antibiotic biosynthesis. In addition, researches on the secondary metabolism in *Streptomyces* is expanded to the post-transcriptional regulation. For example, BldA, a rare tRNA in *Streptomyces*, has significant importance on morphological differentiation and antibiotic biosynthesis (Hackl and Bechthold, 2015). As for lincomycin biosynthesis, only limited researches contribute to decipher the regulatory network. Lu et al. (2008) found that LmbU contributes to lincomycin biosynthesis. Hou et al. (2018a, 2019) demonstrated that LmbU, as a CSR, positively regulates lincomycin biosynthesis by controlling the transcription of *lmbA*, *lmbC*, *lmbJ*, *lmbK*, *lmbW*, and *lmbU* itself, and subsequently solved the subtle mechanism of LmbU regulon. Besides, Hou et al. (2018b) also found that BldA functions as a global regulator on both morphological differentiation and lincomycin biosynthesis at the level of translation, and genes *lmbB2*, *lmbY*, and *lmbU*, which all contain TTA rare codon, get involved in the regulon. Meng et al. (2017) revealed the regulatory network between nitrate metabolism and lincomycin biosynthesis where GlnR activates the transcription of *lmrA*, the lincomycin exporter gene. Lately, a TetR-type regulator SLCG_2919 has been identified as a repressor of lincomycin biosynthesis that controls the transcription of *lmbA*, *lmbC*, *lmbE*, *lmbG*, *lmbK*, *lmbR*, *lmbV,* and *lmbW* (Xu et al., 2019). However, to complete the regulatory network of lincomycin biosynthesis, there are lots of gaps remained.

AdpA was previously found to be an A-factor dependent regulator and repressed by ArpA (Kato et al., 2007). AdpA amplifies the A-factor signal and thus participates in morphological differentiation and secondary metabolism. By means of chromatin affinity precipitation (ChAP) and chromatin immunoprecipitation (ChIP), Higo et al. (2012) found that AdpA controls more than 500 genes in *Streptomyces griseus*. Afterward AdpA is considered to be a regulator of great importance in *Streptomyces*. In *S. chattanoogensis*, AdpA$_{ch}$ controls the expression of *wblA$_{ch}$*, and thus participates in the regulation of natamycin biosynthesis (Yu et al., 2014). In *S. roseosporus*, AdpA controls the expression of *atrA* and indirectly control daptomycin biosynthesis (Mao et al., 2015). In a recent research, AdpA interacts with the two-component system PhoRP and both of them contribute to the transcription of *atrA* (Zheng et al., 2019). Effects of AdpA on antibiotic biosynthesis is always a popular topic. AdpA always serves as an activator of antibiotic biosynthesis, a classic case is that AdpA activates the transcription of *strR*, which encodes the CSR of streptomycin biosynthesis. Therefore, AdpA regulates streptomycin biosynthesis positively and indirectly (Tomono et al., 2005). Similarly, for the biosynthesis of grixazone (Higashi et al., 2007), nikkomycin (Pan et al., 2009), and natamycin (Yu et al., 2018), AdpA activates the transcription of CSRs in their BGCs and indirectly regulates antibiotic biosynthesis. On the other hand, AdpA has a negative impact on oviedomycin biosynthesis in *S. ansochromogenes* by repressing the transcription of CSR (Xu et al., 2017). Very recently, it was reported that AdpA from *S. xiamenensis* 318 negatively regulates morphological differentiation as well as polycyclic tetramate macrolactams (PTMs) production, while positively regulates xiamenmycin production by activating the transcription of two of the structural genes *ximA* and *ximB* (Bu et al., 2019). As we can speculate from previous studies, AdpA typically controls the CSR and/or some structural genes in an antibiotic BGC. So, we scanned the lincomycin BGC and found that putative AdpA binding sites were extraordinarily scattered upstream all of the 8 putative operons with different amounts and locations. Thus, we focused on the pleiotropic regulator AdpA (GenBank accession no. ANS65440.1) and attempted to investigate its regulatory mechanism of lincomycin biosynthesis in *Streptomyces lincolnensis* in this study.

MATERIALS AND METHODS

Bacterial Strains, Plasmids, and Culture Conditions

Bacterial strains and plasmids used in this study are listed in **Table 1**. *S. lincolnensis* NRRL 2936 which served as wild type (WT) and its mutants were incubated at 28°C on mannitol soya flour (MS) medium (Kieser et al., 2000) for 3–5 days for routine cultivation, phenotype observation, and strain preservation, and then cultivated at 28°C in YEME liquid medium [10 g/L yeast extract (OXOID, United States), 5 g/L polypeptone (Nihon Pharmaceutical, Japan), 10 g/L glucose (Lingfeng, China), 3 g/L maltose (Generay, China), 5 mM $MgCl_2{\cdot}2H_2O$ (Lingfeng, China), 340 g/L sucrose (Titan, China), dissolved in dH_2O] with shaking (210 rpm) for 3–5 days for routine cultivation, total DNA extraction, and sporeless strain preservation. Fermentation medium FM1 [20 g/L lactose (SCRC, China), 20 g/L glucose, 10 g/L polypeptone, 10 g/L corn steep liquor (Aladdin, China), dissolved in dH_2O] is used for primary cultivation, and FM2 [20 g/L lactose, 20 g/L glucose, 10 g/L polypeptone, 10 g/L corn steep liquor, 4 g/L

TABLE 1 | Strains and plasmids used in this study.

Strain or plasmid	Genotype and/or description	Source or references
Strains		
S. lincolnensis		
NRRL 2936	Wild type (WT), lincomycin producer	NRRL, United States
Δ*adpA*	Deletion of *AdpA$_{lin}$*, with an insertion of the neomycin resistance gene cassette	This study
Δ*adpA*:*adpA*	Δ*adpA* attBΦC31:pADO	This study
WT:pADPX	NRRL 2936 attBΦC31:pADPX	This study
Δ*adpA*:pADPX	Δ*adpA* attBΦC31:pADPX	This study
WT:pBLPX	NRRL 2936 attBΦC31:pBLPX	This study
Δ*adpA*:pBLPX	Δ*adpA* attBΦC31:pBLPX	This study
WT:pUPX	NRRL 2936 attBΦC31:pUPX	This study
Δ*adpA*:pUPX	Δ*adpA* attBΦC31:pUPX	This study
WT:pAPX	NRRL 2936 attBΦC31:pAPX	This study
Δ*adpA*:pAPX	Δ*adpA* attBΦC31:pAPX	This study
WT:pCPX	NRRL 2936 attBΦC31:pCPX	This study
Δ*adpA*:pCPX	Δ*adpA* attBΦC31:pCPX	This study
WT:pDPX	NRRL 2936 attBΦC31:pDPX	This study
Δ*adpA*:pDPX	Δ*adpA* attBΦC31:pDPX	This study
WT:pJPX	NRRL 2936 attBΦC31:pJPX	This study
Δ*adpA*:pJPX	Δ*adpA* attBΦC31:pJPX	This study
WT:pKPX	NRRL 2936 attBΦC31:pKPX	This study
Δ*adpA*:pKPX	Δ*adpA* attBΦC31:pKPX	This study
WT:pVPX	NRRL 2936 attBΦC31:pVPX	This study
Δ*adpA*:pVPX	Δ*adpA* attBΦC31:pVPX	This study
WT:pWPX	NRRL 2936 attBΦC31:pWPX	This study
Δ*adpA*:pWPX	Δ*adpA* attBΦC31:pWPX	This study
E. coli		
JM83	F' *ara*Δ(*lac-pro* AB) *rpsL* (Str^r)[a] Φ80 *lacZ*ΔM15	Our lab
BL21 (DE3)	F$^-$ *ompT hsdS gal dcm*	Novagen
ET12567:pUZ8002	*dam-13*::Tn*9 dcm-6 hsdM*; contains the non-transmissible RP4 derivative plasmid pUZ8002	Our lab
M. luteus 28001	Indicator strain used for the bioassay method of lincomycin production	CGMCC
Plasmids		
pOJ260-NEO	A suicide vector in Streptomyces	Our lab (Liu et al., 2015)
pMJ1	A suicide vector in Streptomyces, derived from pOJ260-NEO	Our lab
[0.2pt] pADNU	pMJ1 with *AdpA$_{lin}$* replaced by neomycin resistance cassette	This study
pSET152	Integrative vector based on ΦC31 integrase	Our lab (Bierman et al., 1992)
pADC	pIB152 with *AdpA$_{lin}$* inserted downstream of *ermE*p*	This study
pET-28a (+)	*E. coli* expression vector	Novagen
pADH	AdpA$_{lin}$ cloned in *Nde*I/*Eco*RI sites of pET-28a (+)	This study
pADPX	pSET152 with the *xylTE* reporter gene controlled by *adpAp*	This study
pBLPX	pSET152 with the *xylTE* reporter gene controlled by *bldAp*	This study
pUPX	pSET152 with the *xylTE* reporter gene controlled by *lmbUp*	This study
pAPX	pSET152 with the *xylTE* reporter gene controlled by *lmbAp*	This study
pCPX	pSET152 with the *xylTE* reporter gene controlled by *lmbCp*	This study
pDPX	pSET152 with the *xylTE* reporter gene controlled by *lmbDp*	This study
pJPX	pSET152 with the *xylTE* reporter gene controlled by *lmbJp*	This study
pKPX	pSET152 with the *xylTE* reporter gene controlled by *lmbKp*	This study
pVPX	pSET152 with the *xylTE* reporter gene controlled by *lmbVp*	This study
pWPX	pSET152 with the *xylTE* reporter gene controlled by *lmbWp*	This study

(Continued)

TABLE 1 | Continued

$CaCO_3$ (Lingfeng, China), dissolved in dH_2O] is used for dry cell weight determination and lincomycin production assays. ISP4 medium [10 g/L soluble starch (Lingfeng, China), 1 g/L K_2HPO_4 (Lingfeng, China), 5 g/L $MgSO_4{\cdot}7H_2O$ (Lingfeng, China), 1 g/L NaCl (Titan, China), 2 g/L $(NH_4)_2SO_4$ (Lingfeng, China), 2 g/L $CaCO_3$, 15 g/L Agar (Shize, China), 0.001 g/L $FeSO_4{\cdot}_7H_2O$, 0.001 g/L $MnCl_2{\cdot}4H_2O$ (Lingfeng, China), 0.001 g/L $ZnSO_4{\cdot}7H_2O$ (Lingfeng, China), 0.02 mol/L $MgCl_2$, dissolved in dH_2O] was used for conjugation of *Escherichia coli* and *S. lincolnensis*. Antibiotics were supplemented on demand with the following final concentration: 20 μg/mL apramycin (Sangon Biotech, China), 20 μg/mL kanamycin (Kinglyuan, China), 12 μg/mL chloramphenicol (Sigma-Aldrich, United States), and/or 20 μg/mL nalidixic acid (Aladdin, China).

Escherichia coli strains were cultivated at 37°C in Luria-Bertani (LB) liquid medium with shaking (180 rpm) or on LB solid media. Antibiotics were supplemented on demand with the following final concentration: 50 μg/mL apramycin, 50 μg/mL kanamycin, and/or 30 μg/mL chloramphenicol.

Micrococcus luteus 28001 were cultivated at 37°C in medium III (5 g/L polypeptone, 1.5 g/L beef extract (SCRC, China), 3 g/L yeast extract, 3.5 g/L NaCl, 3.68 g/L K_2HPO_4, 1.32 g/L KH_2PO_4 (Lingfeng, China), 1 g/L glucose, 18 g/L agar) for 16 to 18 h.

Deletion and Complementation of *AdpA$_{lin}$*

To construct *AdpA$_{lin}$* disruption strain Δ*adpA* in *S. lincolnensis*, DNA fragments of upstream and downstream region of *AdpA$_{lin}$* were amplified separately using primers *ad*-F1/R1 and *ad*-F2/R2. Then digested, respectively, with restriction enzyme *Hin*d III/*Xba* I and *Bam*HI/*Eco*R I (Thermo Fisher Scientific, United States) and ligated into the *E. coli-Streptomyces* shuttle plasmid pMJ1 to generate plasmid pADNU. Then *E. coli* ET12567/pUZ8002 was used to introduce pADNU into *S. lincolnensis* NRRL 2936 by conjugal transfer (Hou et al., 2018b). As a result of homologous recombination Δ*adpA* was constructed. DNA sequencing with

primers ID*ad*-F1/IDneo-R1 and IDneo-F2/ID*ad*-R2 was adopted for further identification.

To construct *adpA* complementation strain Δ*adpA*:*adpA*, a DNA fragment covering *AdpA$_{lin}$* was amplified by PCR with primers *ad*-C-F/R and then digested with *Nde* I/*Eco*R I (Thermo Fisher Scientific, United States). Then ligated into the corresponding sites of the integrative vector pSET152. The resulting plasmid pADC was introduced into Δ*adpA* by conjugal transfer and integrated into the chromosome to generate Δ*adpA*:*adpA* where the complemented *AdpA$_{lin}$* was under the control of the promoter *ermE*p*. DNA sequencing with primers 152-F/R was adopted for further identification.

All primers used in this study are listed in **Supplementary Table S1**, and synthesized by Genewiz (China).

Scanning Electron Microscope (SEM)

Scanning electron microscope assay referred to a previously established method (Hou et al., 2018b) with some optimizations. *S. lincolnensis* NRRL 2936, Δ*adpA*, and Δ*adpA*:*adpA* were cultured on SMA medium at 28°C for about 5 days. Equivalent areas of the lawn were harvested and placed in 2.5% glutaraldehyde solution overnight. Dehydrated by vacuum freezing drying and sprayed with platinum by Gatan ALTO 1000E (Gatan, United States). Then observed with Hitachi S-3400N scanning electron microscopy (Hitachi, Japan).

Dry Cell Weight Determination and Lincomycin Bioassay Analysis

Streptomyces lincolnensis NRRL 2936, Δ*adpA*, and Δ*adpA*:*adpA* were inoculated from SMA medium into FM1 at 28°C with shaking (210 rpm) for 3 days and then inoculated into FM2 and cultured for 6 days at 28°C with shaking (210 rpm). Precipitate of each sample was harvested every 24 h and dried at 55°C for 24 h. Then the weights of the dried precipitates represent the dry cell weights. Meanwhile, to analyze the bioassay of lincomycin, supernatant of each sample was harvested at the same time, and previously mentioned method (Pharmacopoeia of the People's Republic of China [PPRC], 1990; Hou et al., 2018a) with some modifications was adopted. *M. luteus* 28001, used as indicator, was cultured on medium III at 37°C for 16–18 h and the lawn was washed off with 0.9% NaCl and suspended readily to use. Lincomycin standard solutions (4, 6, 8, 10, 12, 14, and 16 μg/mL) were used for the standard curve and internal control. Diameters of inhibition zone were linearized with the logarithmic values of the concentrations of the lincomycin standard solutions. Concentration of each sample was calculated on the basis of the standard curves. All assays in this section were performed in duplication and standard errors of the mean were calculated. The software GraphPad Prism 7.00 was used to draw the line graph of dry cell weight and histogram of lincomycin bioassay.

RNA Extraction and Quantitative Real-Time PCR (qRT-PCR)

Streptomyces lincolnensis NRRL 2936, and Δ*adpA* cultured on the second day in FM2 medium were used to extract total RNA. Precipitate of samples were ground in liquid nitrogen (Liu et al., 2013) and followed by the method using TRIzol (Thermo Fisher Scientific, United States) (Setinova et al., 2017). After reacting with Recombinant DNase I (Takara, Japan) to remove the trace amount of DNA, 800 ng of RNA samples (analyzed by NanoDrop 2000, Thermo Fisher Scientific, United States) were reverse transcribed to cDNA using Reverse Transcriptase M-MLV (Takara, Japan). SYBR green PCR master mix (ToYoBo, Japan) was used and qRT-PCR was performed in triplication for each transcript. qRT-PCR conditions were mentioned previously (Hou et al., 2018a). To detect the transcript level of AdpA$_{lin}$ targets, primers q*bl*-F/R, q*U*-F/R, q*A*-F/R, q*C*-F/R, q*D*-F/R, q*J*-F/R, q*K*-F/R, q*V*-F/R, and q*W*-F/R in **Supplementary Table S1** were used. And primers q*hrdB*-F/R were used to detect the transcript level of *hrdB* which served as an internal control. qRT-PCR was performed with samples in triplication and data were treated with the threshold cycle ($2^{-\Delta\Delta C_T}$) method (Livak and Schmittgen, 2001) and standard errors of the mean were calculated. GraphPad Prism 7.00 was used to draw the histogram of relative expression level of each AdpA$_{lin}$ target.

Catechol Dioxygenase Activity Analysis

DNA fragment covering reporter gene *xylTE* was amplified by PCR with primers *xyl*-F/R. Promoters of different AdpA$_{lin}$ targets were amplified separately by PCR with primers *adp-xyl*-F/R (for *adpAp,* from −610 to +4), *blp-xyl*-F/R (for *bldAp*, from −799 to +52), *Up-xyl*-F/R (for *lmbUp*, from −730 to +17), *Ap-xyl*-F/R (for *lmbAp*, from −533 to +3), *Cp-xyl*-F/R (for *lmbCp*, from −513 to −1), *Dp-xyl*-F/R (for *lmbDp*, from −581 to +3), *Jp-xyl*-F/R (for *lmbJp*, from −391 to +3), *Kp-xyl*-F/R (for *lmbKp*, from −896 to +3), *Vp-xyl*-F/R (for *lmbVp*, from −364 to −1), and *Wp-xyl*-F/R (for *lmbWp*, from −456 to +4). In respect to *bldAp*, +1 represents the start point of mature *bldA*. As for other promoters, +1 represents the translation starting point of the genes controlled by them. Promoter fragment and *xylTE* fragment were inserted into Pvu II site of the integrative vector pSET152 using Super Efficiency Fast Seamless Cloning kits (DoGene, China) (Hou et al., 2018b) to construct reporter plasmids pADPX, pBLPX, pUPX, pAPX, pCPX, pDPX, pJPX, pKPX, pVPX, pWPX, and pADPX2. Then introduced into *S. lincolnensis* NRRL 2936 or Δ*adpA* respectively, to investigate the effects of AdpA$_{lin}$ on these targets. Referred to the method optimized by Hou et al. (2018b), Catechol dioxygenase activity analysis was carried out in triplication. Standard errors of the mean were calculated and the software GraphPad Prism 7.00 was used to draw the histogram of catechol dioxygenase activity.

Electrophoretic Mobility Shift Assays (EMSAs)

The *AdpA$_{lin}$* gene was amplified by PCR with primers *ad*-C-F/R and digested with *Nde* I/*Eco*R I. DNA fragment was cloned into corresponding sites of pET-28a (+) vector (Novagen, United States), and the resulting plasmid pADH was transformed into *E. coli* BL21 (DE3). Overexpression and purification of recombinant protein refer to the procedures described previously (Hou et al., 2018a). According to our experience, DNA probes with length around 200 bp are appropriate for EMSAs with

AdpA$_{lin}$. For the first round of amplification, primers *adp*-A-F/R, *adp*-B-F/R, *adp*-B-1-F/R, *adp*-B-F/*adp*-B-2-R, *adp*-B-F/m*adp*-B-2-R, *blp*-A-F/R, *blp*-B-F/R, *blp*-N-F/R, m*blp*-B-F/*blp*-B-R, *Up*-A-F/R, *Up*-B-F/R, *Up*-C-F/R, m*Up*-B-F/R, *Ap*-A-F/R, m*Ap*-F/R, *Cp*-A-F/R, *Cp*-B-F/R, *Cp*-C-F/R, *Dp*-A-F/R, *Jp*-A-F/R, m*Jp*-A-F/R, *Jp*-B-F/R, *Kp*-B-F/R, m*Kp*-B-F/R, and *Vp*-A-F/R in **Supplementary Table S1** were used to amplify DNA probes with putative AdpA binding sites, and primers n*ad*-F/R were used to amplify DNA probe with no AdpA binding site as a negative control. Genes *lmbV* and *lmbW* share the same DNA probe. For the second round, amplified DNA fragments are used as templates with primer Biotin-linker* to harvest DNA probes with biotin labeled at 5′ terminal. EMSAs were performed as previously described (Liao et al., 2015) using chemiluminescent EMSA kits (Beyotime Biotechnology, China). AdpA$_{lin}$ of different concentrations (0, 1.6, 3.2, and/or 6.4 μM, respectively) interacted with 2.5 nM biotin labeled DNA probe in binding buffer TGB [20 mM Tris–HCl (Shize, China), 5% glycerol (Titan, China), and 0.1% BSA (Sangon, China), pH 7.5], and 200-folds excess of unlabeled probes were added as competitive assays.

RESULTS

AdpA$_{lin}$ Positively Regulates Both Lincomycin Biosynthesis and Morphological Differentiation in *S. lincolnensis*

It has been shown that AraC/XylS family regulators control various metabolic pathways including antibiotic biosynthesis (Ibarra et al., 2008). There are about 30 AraC/XylS family regulators in *S. lincolnensis*, among which, AdpA is the most famous one. Based on this, we investigated the effects of AdpA$_{lin}$ on lincomycin biosynthesis and attempted to propose some innovative idea on this classic regulator. Alignment of AdpA from 26 *Streptomyces* species (**Supplementary Figures S1A,B**) showed that AdpA retained the conserved N-terminal ThiJ/PfpI/DJ-1-like (also referenced as GATase-1) dimerization domain and C-terminal AraC/XylS-type DNA-binding domain (DBD) (Ohnishi et al., 2005). The first 340 amino acids possessed an ortholog with over 90% identities, and the main diversity occurred at the tail end of C-terminus with a length of no more than 90 amino acids, after the conserved DNA binding domain (**Supplementary Figure S1A**). To infer the evolutionary history of AdpA, phylogenetic analysis was performed using a maximum likelihood method. The results showed that AdpA$_{lin}$ possessed an ortholog with 89% amino acid identity to AdpA$_{sg}$, and thus we classified AdpA$_{lin}$ to be one member of the AraC/XylS family.

To investigate the effects of AdpA$_{lin}$ on lincomycin biosynthesis, *AdpA$_{lin}$* null mutant was constructed and named as Δ*adpA*. Lincomycin biosynthesis was significantly influenced by the non-functional *AdpA$_{lin}$*. In medium FM2, lincomycin started to be produced on the second day in WT, reached a maximum bioassay of 30.10 μg/mL between the second and the fourth day, and maintained thereafter. However, bioassay of lincomycin in Δ*adpA* remained undetectable throughout the entire 6 days (**Figure 1A**). Furthermore, the lawns of Δ*adpA* on SMA medium exhibited a bald phenotype distinct from WT (**Figure 1B**). Deletion of *AdpA$_{lin}$* blocked the sporulation and caused long, extended aerial hyphae when detected by SEM (**Figure 1C**). Complementation of *AdpA$_{lin}$* in Δ*adpA* strain (Δ*adpA*:*adpA*) restored both lincomycin biosynthesis and sporulation as expected (**Figure 1**) though lincomycin production in complemented strain did not restore to WT level, probably due to using the promoter *ermE*p*. Moreover, the biomasses of WT, Δ*adpA*, and Δ*adpA*:*adpA* were measured at all the four detected days. The data showed that biomasses of the three strains have no significant differences at days 1 and 6, while at day 2, Δ*adpA* had decreased biomass compared to WT and Δ*adpA*:*adpA*, and at day 4, Δ*adpA*:*adpA* had increased biomass compared to WT and Δ*adpA*. These data suggested that AdpA$_{lin}$ is an important regulator of lincomycin biosynthesis in *S. lincolnensis*.

AdpA$_{lin}$ Directly Activates Transcription of the Structural Genes in the *lmb* Cluster

AdpA regulates more than 500 genes in *S. griseus* (Higo et al., 2012), and AdpA binding motifs have been well studied in other *Streptomyces* species such as *S. griseus* (Yamazaki et al., 2004), *S. coelicolor* (Kim et al., 2005), and *S. lividans* (Guyet et al., 2013). Additionally, Ming et al. have solved the complex structure of AdpA-DBD and target DNA in *S. griseus* (Yao et al., 2013). AdpA binding site is recognized as 5′-TGGCSNGWWY-3′ (where S is G or C, W is A or T, Y is T or C, and N is any nucleotide), and G at position 2 and C at position 4 are more highly conserved than the other nucleotides in this motif (Yao et al., 2013). Lincomycin BGC was named as the *lmb* cluster, and the gene organization was shown in **Supplementary Figure S2A**. The *lmb* cluster contains 8 putative operons and the first genes of them are *lmbA*, *lmbC*, *lmbD*, *lmbJ*, *lmbK*, *lmbV*, *lmbW*, and *lmbU*, respectively. We looked into the nucleic acid sequence of the *lmb* cluster and searched with the conserved AdpA binding sequence, and no more than 3 mismatches in the last 3 bp were allowed. We found that putative AdpA binding sites were scattered in the upstream region of all the 8 putative operons (**Supplementary Figures S2B–F**). The numbers of putative AdpA binding sites in the upstream of *lmbA*, *lmbC*, *lmbD*, *lmbJ*, *lmbK*, *lmbV*, *lmbW*, and *lmbU* are 1, 6, 1, 3, 3, 2, 2, and 10, respectively. Therefore, we speculated that the entire biosynthesis process of lincomycin might be under the control of AdpA$_{lin}$.

qRT-PCR analysis showed that the transcript level of *lmbA*, *lmbC*, *lmbD*, *lmbJ*, *lmbV*, and *lmbW* dramatically decreased in Δ*adpA* with fold changes 129.41, 43.64, 60.30, 215.29, 11.95, and 301.20, respectively (**Figure 2A**). It was suggested that in Δ*adpA*, lincomycin biosynthesis was blocked because of the decreased expression of structural genes *lmbA*, *lmbC*, *lmbD*, *lmbJ*, *lmbV*, and *lmbW*. Due to the low transcript level of *lmbK* (data not shown), we failed to calculate the relative expression in both WT and Δ*adpA*. To investigate the regulation between AdpA$_{lin}$

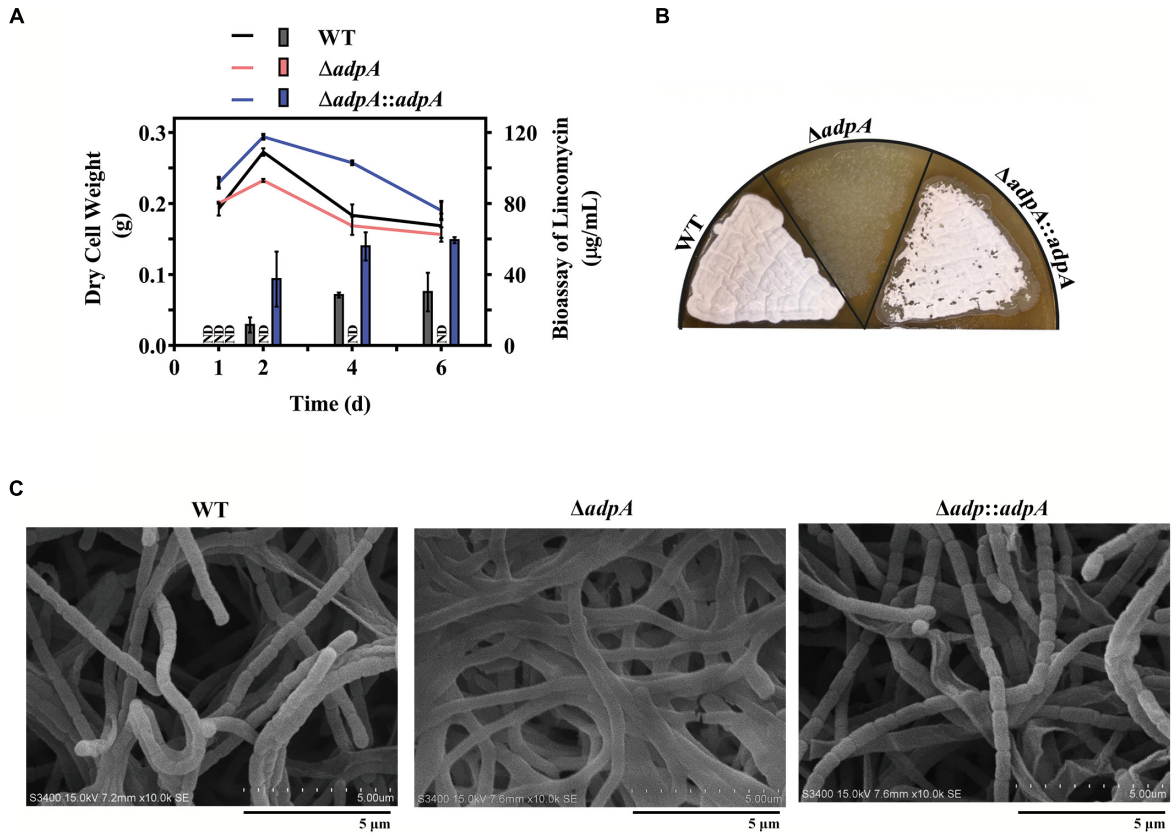

FIGURE 1 | Effects of *AdpA$_{lin}$* on lincomycin biosynthesis and morphological differentiation. **(A)** Changing of dry cell weight (line graph), which represented growth curve. And bioassay of lincomycin (histogram) of WT, Δ*adpA* and Δ*adpA*:*adpA*, which showed the production of lincomycin. ND represents not detected. **(B,C)** Growth of WT and *AdpA$_{lin}$* mutants cultivated on SMA medium. **(B)** Lawns of WT and *AdpA$_{lin}$* mutants grown on SMA medium. **(C)** Scanning electron micrograph with a scale bar of 5 μm.

and *lmbK*, we cloned the 895 bp of DNA sequences upstream from *lmbK* translation starting site (TSS) and constructed reporting plasmid for catechol dioxygenase activity assay. The results demonstrated that AdpA$_{lin}$ got involved in regulating the transcription of *lmbK* (**Figure 2B**). Besides, transcriptions of *lmbA*, *lmbC*, *lmbD*, *lmbJ*, *lmbV*, and *lmbW* were activated by AdpA$_{lin}$ in catechol dioxygenase activity assay as well (**Figure 2B**). These data suggested that AdpA$_{lin}$ has primary effects on the structural genes in the *lmb* cluster.

Then we carried out EMSAs to investigate the interplay between AdpA$_{lin}$ and promotors of above *lmb* structural genes. DNA fragments containing putative AdpA binding sites were labeled with biotin and incubated with purified AdpA$_{lin}$. Results of EMSAs showed that AdpA$_{lin}$ interacted with all of the 8 promoter regions containing putative AdpA binding sites (**Figure 2C**). DNA probe *lmbJp-A* served as part of the promoter regions of both *lmbJ* and *lmbK*, and similarly, DNA probe *lmbVp-A* served as the promoter regions of both *lmbV* and *lmbW*. For promoters containing more than one AdpA binding sites, such as genes *lmbC*, *lmbJ*, *lmbK*, *lmbV*, and *lmbW*, AdpA$_{lin}$ interacted with different putative AdpA binding sites and generated different forms of complexes (**Figure 2C**). DNA fragment without AdpA binding site, i.e., probe-neg, could not interact with AdpA$_{lin}$ (**Supplementary Figure S3**). To confirm the exact binding sites of AdpA$_{lin}$ with promoters, we deleted the putative AdpA binding sites in *lmbAp*-A, *lmbJp*-A and *lmbKp*-B, and EMSAs showed AdpA$_{lin}$ no longer interacted with these DNA probes (**Supplementary Figure S4**). Thus, we speculated that AdpA$_{lin}$ activates all of the 8 promoters in the *lmb* cluster by directly binding to putative AdpA binding sites.

AdpA$_{lin}$ Directly Activates Transcription of the CSR Gene *lmbU*

LmbU was recently reported by Hou et al. (2018a, 2019) to be a novel transcriptional regulator cited in the *lmb* cluster and positively regulate lincomycin biosynthesis. Here, we investigated the regulatory relationship between AdpA$_{lin}$ and *lmbU*. We analyzed the 770 bp of promoter region upstream from *lmbU* TSS, and found 10 putative AdpA binding sites where two of them are overlapped (**Supplementary Figure S2F**). Relative expression of *lmbU* significantly decreased by 26.26 folds in Δ*adpA* compared with WT (**Figure 3A**). We cloned the 770 bp of DNA sequences upstream from *lmbU*

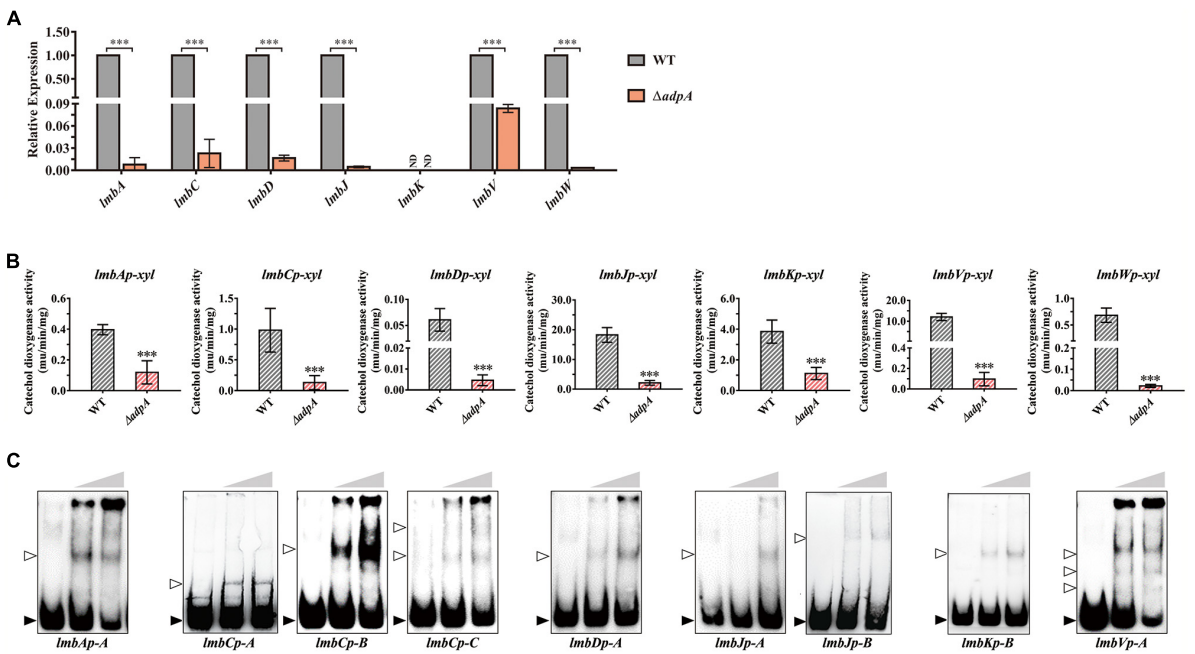

FIGURE 2 | AdpA$_{lin}$ activates the transcription of structural genes in *lmb* cluster. **(A)** Relative expression of *lmbA*, *lmbC*, *lmbD*, *lmbJ*, *lmbK*, *lmbV*, and *lmbW* in WT and Δ*adpA*. ND means not detected. **(B)** Catechol dioxygenase activity assays of WT and Δ*adpA* transformed with corresponding reporter plasmids. **(C)** EMSAs of AdpA$_{lin}$ with 5′-biotin labeled probes in **Supplementary Figure S2**. Solid triangles point to the bands of probes and hollow triangles point to the complexes of AdpA$_{lin}$ and probes. Concentrations of AdpA$_{lin}$ are 0, 1.6, and 3.2 μM, respectively. ***$P < 0.001$.

TSS to construct reporter plasmid for catechol dioxygenase assay. In accordance with qRT-PCR results, catechol dioxygenase assay demonstrated that AdpA$_{lin}$ remarkably activated *lmbU* promoter (**Figure 3B**). As displayed in **Supplementary Figure S2F**, *lmbUp-A*, *lmbUp-B*, and *lmbUp-C* are three DNA probes containing putative AdpA binding sites in the promoter region of *lmbU*. EMSAs indicated that AdpA$_{lin}$ directly bound to *lmbUp-A*, *lmbUp-B*, and *lmbUp-C*, separately (**Figure 3C**). Then, the putative AdpA binding site in *lmbUp*-B was deleted, and EMSA showed that AdpA$_{lin}$ could not bind to this DNA probe (**Supplementary Figure S4**), suggesting that AdpA$_{lin}$ activates the transcription of *lmbU* by directly binding to the *lmbU* promoter and thus gets involved in the activation of lincomycin biosynthesis.

AdpA$_{lin}$ Directly Activates the Expression of the Global Regulator Gene *bldA*

As mentioned above, deletion of *AdpA$_{lin}$* in *S. lincolnensis* not only blocked lincomycin biosynthesis, but also significantly impaired the generation of spores (**Figures 1B,C**), which suggested that AdpA$_{lin}$ had complicated connections with genes outside the *lmb* cluster. Hou et al. (2018b) previously identified that BldA regulates morphological differentiation and lincomycin biosynthesis in *S. lincolnensis*. We analyzed the 799 bp of promoter region upstream from the mature *bldA*, three putative AdpA binding sites were found (**Figure 4A**). Relative expression of *bldA* exhibited a 7.29-fold decreased in Δ*adpA* compared with WT (**Figure 4B**). The 799 bp of DNA sequences upstream from the mature *bldA* was cloned to construct reporter plasmid for catechol dioxygenase activity assay. And the results indicated that AdpA$_{lin}$ significantly activates the transcription of *bldA in vivo* (**Figure 4C**). *BldAp-A* and *bldAp-B* are two DNA probes containing putative AdpA binding sites marked in **Figure 4A**. We performed EMSAs of AdpA$_{lin}$ with *bldAp-A* and *bldAp-B* separately, and as displayed in **Figure 4D**, AdpA$_{lin}$ directly bound to DNA fragments containing putative AdpA binding sites *in vitro*. Thus, we speculated that AdpA$_{lin}$ participates in the lincomycin biosynthesis in *S. lincolnensis* through activating the transcription of *bldA*, and indirectly mediates the morphological differentiation.

Since AdpA has been identified to regulate the transcription of *bldA* in *S. griseus* (Higo et al., 2011), we further analyzed the *bldA* promoter from *S. lincolnensis* and *S. griseus*. The data showed that putative AdpA binding site and its flanking sequence in *bldAp*-A was highly conserved (**Supplementary Figure S5A**), and EMSA of AdpA$_{lin}$ with *bldAp*-A confirmed the binding (**Figure 4D**). However, the sequences upstream *bldAp*-A are various between the two species, which contains the AdpA binding sites in *S. griseus*, but not in *S. lincolnensis* (**Supplementary Figure S5A**). Further EMSA demonstrated that AdpA$_{lin}$ cannot bind to this fragment *bldAp*-N (**Supplementary Figure S5B**), confirming that it is not a functional AdpA binding site in *S. lincolnensis*. Moreover, putative AdpA binding site in *bldAp*-B, which has not

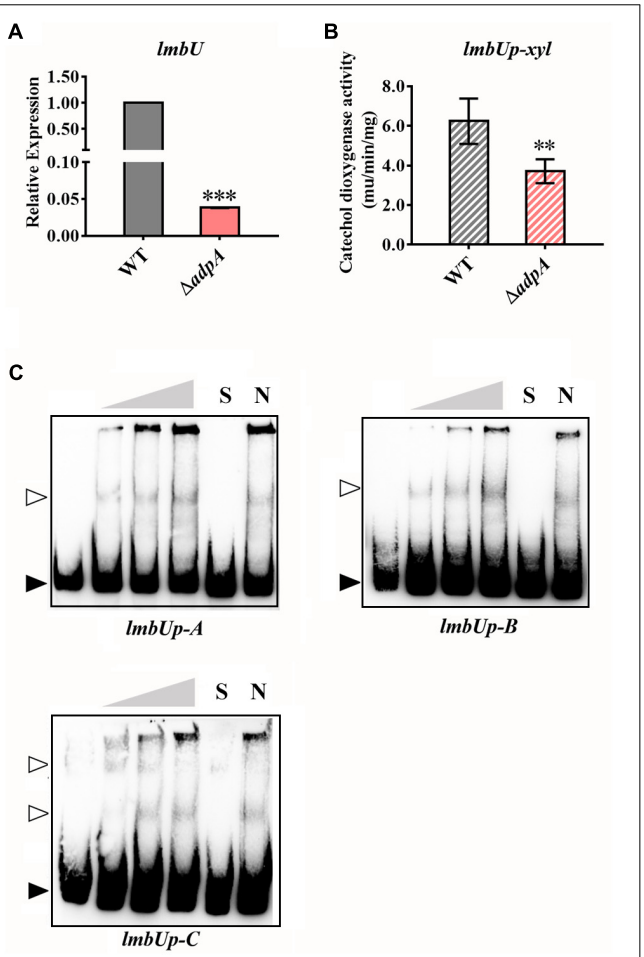

FIGURE 3 | AdpA$_{lin}$ activates the transcription of the CSR gene *lmbU*. **(A)** Relative expression of *lmbU* in WT and Δ*adpA*. **(B)** Catechol dioxygenase activity analysis of WT and Δ*adpA* transformed with pUPX. **(C)** EMSAs of AdpA$_{lin}$ with 5′-biotin labeled DNA probes *lmbUp-A*, *lmbUp-B*, and *lmbUp-C*. Solid triangles point to the bands of probes and hollow triangles point to the complexes of AdpA$_{lin}$ and probes. Concentrations of AdpA$_{lin}$ are 0, 1.6, 3.2, 6.4, 6.4, and 6.4 μM, respectively. Competitive assays were carried out with a 200-fold excess of unlabeled specific probe *lmbUp*-A, *lmbUp*-B, or *lmbUp*-B (lane S) or with a 200-fold excess of unlabeled non-specific probe probe-neg (lane N). ***$P < 0.001$ and **$P < 0.01$, respectively.

been studied before, was confirmed to be a AdpA binding site in *S. lincolnensis* (**Supplementary Figure S5C**).

AdpA$_{lin}$ Positively Autoregulates Its Own Transcription via Directly Binding to Its Own Promoter

We carried out a detailed analysis of 610 bp of upstream DNA sequences from *AdpA$_{lin}$* TSS and found 6 putative AdpA$_{lin}$ binding sites where 4 of them are overlapped in pairs (**Figure 5A**). To investigate the transcriptional regulation between AdpA$_{lin}$ and its own transcription, we cloned the 610 bp of DNA sequence upstream from *AdpA$_{lin}$* TSS to construct a reporter plasmid for catechol dioxygenase activity assay. The results revealed that AdpA$_{lin}$ slightly activated its own transcription *in vivo* (**Figure 5B**). As displayed in **Figure 5A**, *adpAp-A* and *adpAp-B* are two DNA probes containing putative AdpA$_{lin}$ binding sites, and the results of EMSAs verified that AdpA$_{lin}$ directly interacted with the promoter region of *AdpA$_{lin}$ in vitro* (**Figure 5C**).

AdpA also has been identified to autoregulate its own transcription in *S. griseus* (Kato et al., 2005), then we compared *AdpA$_{lin}$* promoter from *S. lincolnensis* with *adpA* promoter from *S. griseus*. In *S. lincolnensis*, the putative AdpA binding site and its flanking sequence in *adpAp*-A was high conserved (**Supplementary Figure S6A**) and the result of EMSA verified the binding (**Figure 5C**). However, the nucleic acid sequences upstream *adpAp*-A were highly diverse (**Supplementary Figure S6A**). Then we designed two probes, *adpAp*-B-1 and *adpAp*-B-2, which contain the unconserved AdpA binding motifs from *S. griseus* (Kato et al., 2005) and putative AdpA binding sites from *S. lincolnensis*, respectively. The results of EMSAs showed that AdpA$_{lin}$ can bind to *adpAp*-B-2, but not to *adpAp*-B-1 (**Supplementary Figures S6B,C**), indicating that two new AdpA binding sites are found in *S. lincolnensis*, and the differences between the two probes may allow them to respond to different regulatory mechanisms.

DISCUSSION

In this study, we elucidated the effect of AdpA$_{lin}$ on lincomycin biosynthesis and morphological differentiation. There are 8 putative operons in the *lmb* cluster. Before this study, none of a regulator has been identified to directly bind to all the eight promoters in the *lmb* cluster and have an overall impact on the entire lincomycin biosynthesis progress. By deciphering the regulations on the 8 putative operons, we attempted to envision the transcriptional regulatory network on lincomycin biosynthesis. Lincomycin biosynthesis contains three main parts: formation of α-methylthiolincosaminide (MTL), formation of propylproline (PPL), and condensation and final methylation (**Supplementary Figure S2A**). AdpA$_{lin}$ activates *lmbKp* and *lmbVp*, therefore we speculate that AdpA$_{lin}$ directly activates the transcription of *lmbK*, *lmbR*, *lmbO*, and *lmbN*, so that AdpA$_{lin}$ positively regulates the biosynthesis of MTL structure (Sasaki et al., 2012; Lin et al., 2014). AdpA$_{lin}$ activates the transcription of *lmbAp*, *lmbWp*, and *lmbUp*, which means *lmbB1*, *lmbB2*, *lmbX* and *lmbY* are also activated by AdpA$_{lin}$, thus we speculated that AdpA$_{lin}$ directly regulates the biosynthesis of PPL structure (Novotna et al., 2004, 2013; Pang et al., 2015; Jiraskova et al., 2016). In addition, AdpA$_{lin}$ activates the transcription *lmbCp*, *lmbDp*, *lmbJp*, and *lmbVp*, which means transcriptions of *lmbT*, *lmbE*, *lmbF*, and *lmbG* are activated by AdpA$_{lin}$ (Hola et al., 2003; Zhao et al., 2015; Kadlcik et al., 2017; Zhong et al., 2017; Zhang et al., 2018). Therefore, we inferred that AdpA$_{lin}$ functions as a primary activator of lincomycin biosynthesis and regulates the entire biosynthetic process. And this is the first case that AdpA directly activates the transcription of the overall structural genes in such a complicated antibiotic biosynthetic gene cluster (BGC). In addition, EMSAs of AdpA$_{lin}$ with targets showed that AdpA$_{lin}$ binds to different binding

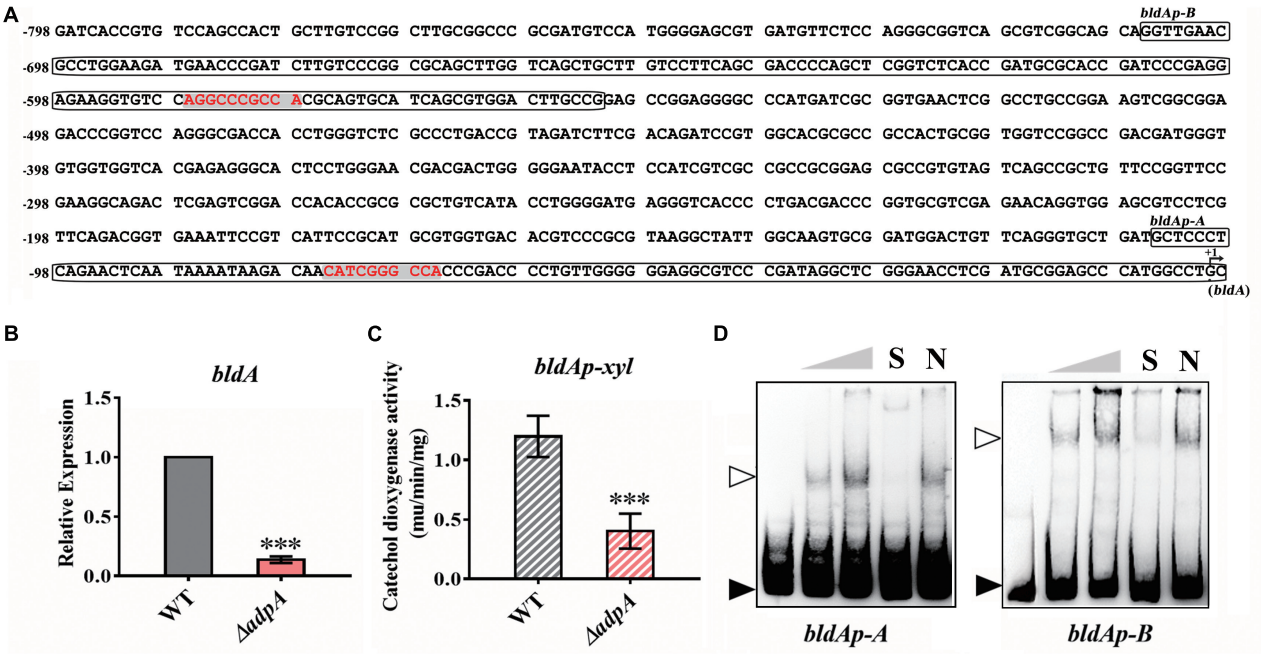

FIGURE 4 | AdpA$_{lin}$ activates the transcription of *bldA*. **(A)** Nucleic acid sequence of *bldA* promoter region where +1 represents the start of mature *bldA*. Putative AdpA binding sites are marked in red color with gray background. Probes for EMSA, *bldAp-A*, and *bldAp-B*, are framed. **(B)** Relative expression of *bldA* in WT and Δ*adpA*. **(C)** Catechol dioxygenase activity analysis of WT and Δ*adpA* transformed with pBLPX. **(D)** EMSAs of AdpA$_{lin}$ with 5′-biotin labeled DNA probes *bldAp-A* and *bldAp-B*. Solid triangles point to the bands of probes and hollow triangles point to the complexes of AdpA$_{lin}$ and DNA probes. Concentrations of AdpA$_{lin}$ are 0, 1.6, 3.2, 3.2, and 3.2 μM, respectively. Competitive assays were carried out with a 200-fold excess of unlabeled specific probe *bldAp*-A or *bldAp*-B (lane S) or with a 200-fold excess of unlabeled non-specific probe probe-neg (lane N). ***$P < 0.001$.

sites with different affinities (**Figure 2C**). Based on these results, some strategies of genetic manipulations may be proposed for hyper-production of lincomycin, such as mutation, deletion or addition of AdpA binding sites in the promoter regions of target genes.

Besides directly participating in lincomycin biosynthesis, as a pleiotropic regulator, AdpA$_{lin}$ controls lincomycin biosynthesis by regulating other transcriptional regulators as well. LmbU has been identified to activate the transcription of *lmbA*, *lmbC*, and *lmbJ*, and repress the transcription of *lmbK* and *lmbU* itself (Hou et al., 2018a). In this study, we confirmed that the transcription of *lmbU* was activated by AdpA$_{lin}$ (**Figure 3**). As described by Hou et al. (2018b) there is a UUA codon in *lmbU*, and translation of *lmbU* is controlled by BldA. Existence of rare codon means very small changes of the tRNA could induce the significant change of protein amount (Chater, 2006). Besides, UUA codons also exist in *lmbB2* and *lmbY* in the *lmb* cluster, indicating that LmbB2 and LmbY might be important regulatory targets during lincomycin biosynthesis. Furthermore, it has been showed that the *adpA* gene contains a UUA codon as well, on the other hand, transcription of *bldA* is regulated by AdpA$_{lin}$ (**Figure 4**), which may function as a feedback regulatory mechanism to keep the organism in balance. In this study, we speculated that AdpA$_{lin}$, LmbU, and BldA formed a regulatory cascade that mediate lincomycin biosynthesis in *S. lincolnensis* (**Figure 6**). In addition, considering AdpA responds to the GBL-involved cascade regulation (Healy et al., 2009; Tan et al., 2015), bioinformatics analysis was performed and two GBL-signaling systems were found in *S. lincolnensis* (**Figure 6**). One system consists of the GBL receptor SLINC_6539 (GenBank accession number ANS68763.1) and biosynthetic enzyme SLINC_6540 (GenBank accession number ANS68764.1) which were highly homology with many receptors and enzymes in *Streptomyces*, whereas SLINC_6539 and SLINC_6540 had identities with ArpA (47%) and AsfA (70%) in *S. griseus*, respectively. The other system consists of SLINC_5093 (GenBank accession number WP_067437987.1) and SLINC_5094 (GenBank accession number WP_067437989.1) which were low similarities with other receptors and enzymes, while SLINC_5093 and SLINC_5094 had identities with ArpA (44%) and AsfA (33%) in *S. griseus*, respectively. But how these two GBL-signaling systems works to affect lincomycin biosynthesis will be needed further research.

In *S. griseus*, AdpA auto-depresses its own transcription (Ohnishi et al., 2005), whereas in *S. lincolnensis*, AdpA$_{lin}$ has a positive impact on its own transcription (**Figure 5B**). Differences of AdpA binding sites in *S. lincolnensis* and *S. griseus* indicated that AdpA homologs from different resource have specialized regulatory mechanism on their own transcription. Catechol dioxygenase activity showed that AdpA$_{lin}$ had a negatively effect on the AdpA binding site near the *AdpA$_{lin}$* TSS (Data not shown). Thus, we speculated that AdpA$_{lin}$ bound to this putative site and prevented the *AdpA$_{lin}$* promotor from being activated.

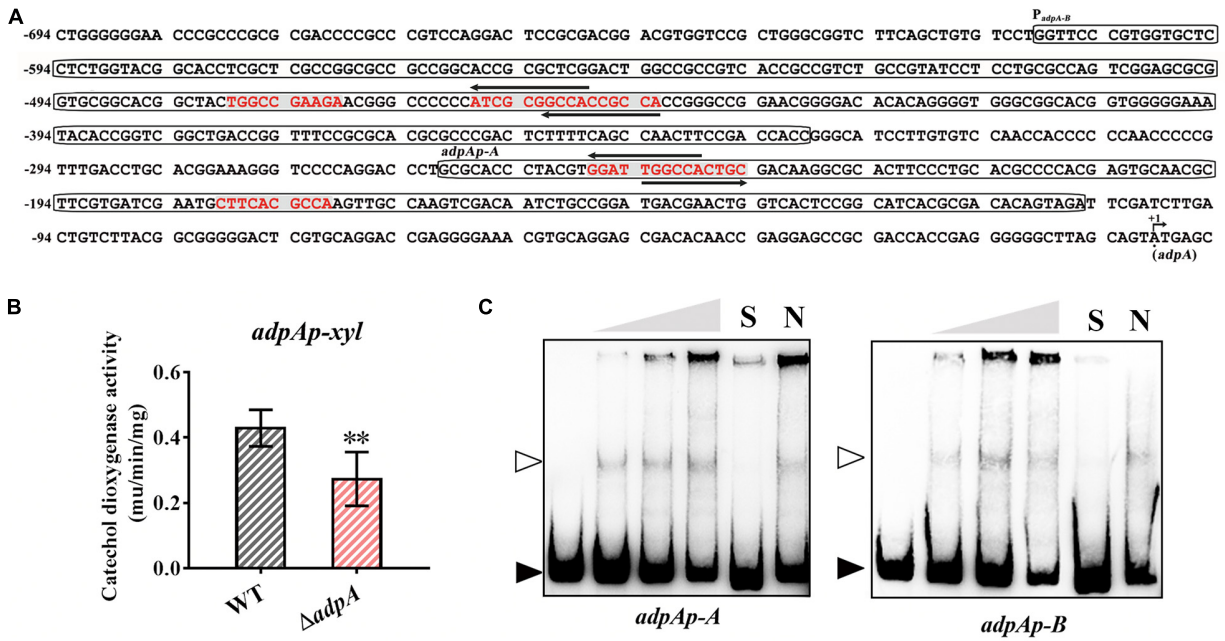

FIGURE 5 | AdpA$_{lin}$ positively regulates its own transcription. **(A)** Nucleic acid sequence of *AdpA$_{lin}$* promoter region where +1 represents the translation starting site (TSS) of *adpA*. Putative AdpA binding sites are marked in red color with gray background. Probes for EMSA, *adpAp-A* and *adpAp-B*, are framed. **(B)** Catechol dioxygenase activity analysis of WT and Δ*adpA* transformed with pADPX. $^{**}P < 0.01$. **(C)** EMSAs of AdpA$_{lin}$ with 5′-biotin labeled DNA probes *adpAp-A* and *adpAp-B*. Solid triangles point to the bands of probes and hollow triangles point to the complexes of AdpA$_{lin}$ and DNA fragments. Concentrations of AdpA$_{lin}$ are 0, 1.6, 3.2, 6.4, 6.4, and 6.4 μM, respectively. Competitive assays were carried out with a 200-fold excess of unlabeled specific probe *adpAp*-A or *adpAp*-B (lane S) or with a 200-fold excess of unlabeled non-specific probe probe-neg (lane N).

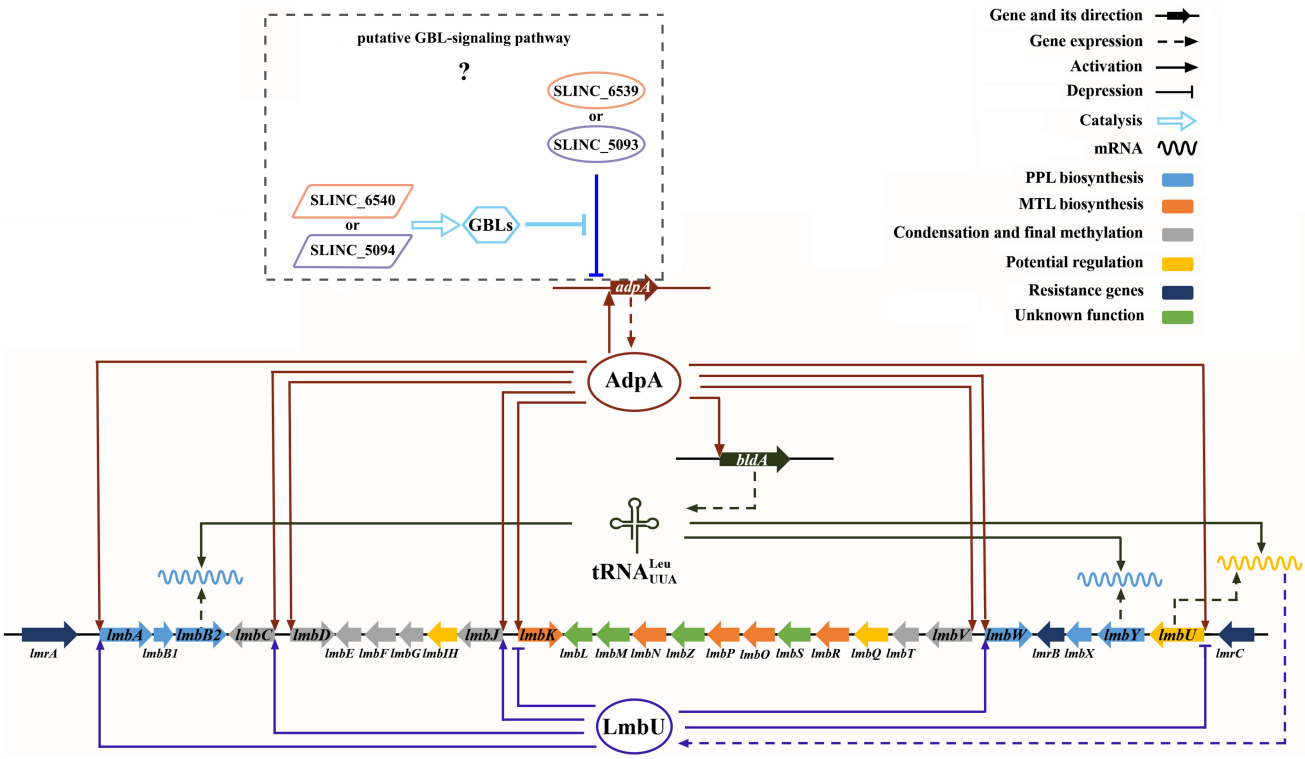

FIGURE 6 | Cascade regulation of AdpA$_{lin}$, LmbU, and BldA on lincomycin biosynthesis in *S. lincolnensis*.

As for another putative AdpA binding sites, we presumed it might recruit RNA polymerase after interacting with AdpA$_{lin}$ and thus the overall effect of AdpA$_{lin}$ on its own promoter appeared to be positive. In the natamycin producer *S. chattanoogensis*, AdpA$_{ch}$ was an activator of natamycin biosynthesis, and 6 AdpA binding sites were identified in the *scnRI-scnRII* intergenic region (Du et al., 2011; Yu et al., 2018). It is notable that although the general effect of AdpA$_{ch}$ on the transcription of *scnRI* is positive, AdpA binding site A and B serve as repression sites. Thus, we speculated that the varying amounts and locations of AdpA binding sites in the promoter region of AdpA$_{lin}$ targets exhibited different effects and constituted a complicated and subtle regulatory network of AdpA regulons.

In summary, we reported a lesser-known case that AdpA$_{lin}$ interacted with all of the 8 putative operons and activated the transcription of structural genes in the *lmb* cluster. Furthermore, we deduced AdpA$_{lin}$, LmbU, and BldA in cascade regulation that controlled lincomycin biosynthesis. Based on these knowledge, more efforts should be devoted to complete the regulatory mechanism of lincomycin biosynthesis and to enhance to production of lincomycin.

DATA AVAILABILITY STATEMENT

All datasets generated for this study are included in the manuscript/**Supplementary Files**.

AUTHOR CONTRIBUTIONS

YK, BH, and HW designed the experiments. YK, YW, and RW carried out the experiments. YK, BH, XZ, JY, and HW analyzed the data. YK, JY, and HW wrote the manuscript. JY and HZ guided the work. All authors assisted with critical reading of the manuscript.

FUNDING

This study was supported by the National Natural Science Foundation of China (NSFC) (31900059), the China Postdoctoral Science Foundation (2019M650079), and the Research Program of State Key Laboratory of Bioreactor Engineering.

ACKNOWLEDGMENTS

We thank Dr. Weihong Jiang for providing the plasmid for catechol dioxygenase activity assay and all the members of our laboratory.

SUPPLEMENTARY MATERIAL

The Supplementary Material for this article can be found online at: https://www.frontiersin.org/articles/10.3389/fmicb.2019.02428/full#supplementary-material

REFERENCES

Bierman, M., Logan, R., O'Brien, K., Seno, E. T., Rao, R. N., and Schoner, B. E. (1992). Plasmid cloning vectors for the conjugal transfer of DNA from *Escherichia coli* to *Streptomyces* spp. *Gene* 116, 43–49. doi: 10.1016/0378-1119(92)90627-2

Bu, X. L., Weng, J. Y., He, B. B., Xu, M. J., and Xu, J. (2019). A novel AdpA homologue negatively regulates morphological differentiation in *Streptomyces xiamenensis* 318. *Appl. Environ. Microbiol.* 85:e3107-18. doi: 10.1128/AEM.03107-18

Chater, K. F. (2006). *Streptomyces* inside-out: a new perspective on the bacteria that provide us with antibiotics. *Philos. Trans. R. Soc. Lond. B Biol. Sci.* 361, 761–768. doi: 10.1098/rstb.2005.1758

Du, Y. L., Li, S. Z., Zhou, Z., Chen, S. F., Fan, W. M., and Li, Y. Q. (2011). The pleitropic regulator AdpAch is required for natamycin biosynthesis and morphological differentiation in *Streptomyces chattanoogensis*. *Microbiology* 157, 1300–1311. doi: 10.1099/mic.0.046607-0

Guyet, A., Gominet, M., Benaroudj, N., and Mazodier, P. (2013). Regulation of the clpP1clpP2 operon by the pleiotropic regulator AdpA in *Streptomyces lividans*. *Arch. Microbiol.* 195, 831–841. doi: 10.1007/s00203-013-0918-2

Hackl, S., and Bechthold, A. (2015). The gene bldA, a regulator of morphological differentiation and antibiotic production in *Streptomyces*. *Arch. Pharm.* 348, 455–462. doi: 10.1002/ardp.201500073

Healy, F. G., Eaton, K. P., Limsirichai, P., Aldrich, J. F., Plowman, A. K., and King, R. R. (2009). Characterization of gamma-butyrolactone autoregulatory signaling gene homologs in the angucyclinone polyketide WS5995B producer *Streptomyces acidiscabies*. *J. Bacteriol.* 191, 4786–4797. doi: 10.1128/JB.00437-439

Higashi, T., Iwasaki, Y., Ohnishi, Y., and Horinouchi, S. (2007). A-factor and phosphate depletion signals are transmitted to the grixazone biosynthesis genes via the pathway-specific transcriptional activator GriR. *J. Bacteriol.* 189, 3515–3524. doi: 10.1128/JB.00055-07

Higo, A., Hara, H., Horinouchi, S., and Ohnishi, Y. (2012). Genome-wide distribution of AdpA, a global regulator for secondary metabolism and morphological differentiation in *Streptomyces*, revealed the extent and complexity of the AdpA regulatory network. *DNA Res.* 19, 259–273. doi: 10.1093/dnares/dss010

Higo, A., Horinouchi, S., and Ohnishi, Y. (2011). Strict regulation of morphological differentiation and secondary metabolism by a positive feedback loop between two global regulators AdpA and BldA in *Streptomyces griseus*. *Mol. Microbiol.* 81, 1607–1622. doi: 10.1111/j.1365-2958.2011.07795.x

Hola, K., Janata, J., Kopecky, J., and Spizek, J. (2003). LmbJ and LmbIH protein levels correlate with lincomycin production in *Streptomyces lincolnensis*. *Lett. Appl. Microbiol.* 37, 470–474. doi: 10.1046/j.1472-765X.2003.01432.x

Hou, B., Lin, Y., Wu, H., Guo, M., Petkovic, H., Tao, L., et al. (2018a). The novel transcriptional regulator LmbU promotes lincomycin biosynthesis through regulating expression of its target genes in S*treptomyces lincolnensis*. *J. Bacteriol.* 200:e00447-e17. doi: 10.1128/JB.00447-17

Hou, B., Tao, L., Zhu, X., Wu, W., Guo, M., Ye, J., et al. (2018b). Global regulator BldA regulates morphological differentiation and lincomycin production in *Streptomyces lincolnensis*. *Appl. Microbiol. Biotechnol.* 102, 4101–4115. doi: 10.1007/s00253-018-8900-1

Hou, B., Zhu, X., Kang, Y., Wang, R., Wu, H., Ye, J., et al. (2019). LmbU, a cluster-situated regulator for lincomycin, consists of a DNA-binding domain, an auto-inhibitory domain, and forms homodimer. *Front. Microbiol.* 10:989. doi: 10.3389/fmicb.2019.00989

Hsiao, N. H., Nakayama, S., Merlo, M. E., de Vries, M., Bunet, R., Kitani, S., et al. (2009). Analysis of two additional signaling molecules in *Streptomyces coelicolor* and the development of a butyrolactone-specific reporter system. *Chem. Biol.* 16, 951–960. doi: 10.1016/j.chembiol.2009.08.010

Ibarra, J. A., Perez-Rueda, E., Segovia, L., and Puente, J. L. (2008). The DNA-binding domain as a functional indicator: the case of the AraC/XylS family of transcription factors. *Genetica* 133, 65–76. doi: 10.1007/s10709-007-9185-y

Jiraskova, P., Gazak, R., Kamenik, Z., Steiningerova, L., Najmanova, L., Kadlcik, S., et al. (2016). New concept of the biosynthesis of 4-Alkyl-l-proline precursors of lincomycin, hormaomycin, and pyrrolobenzodiazepines: could a γ-glutamyltransferase cleave the C-C bond? *Front. Microbiol.* 7:276. doi: 10.3389/fmicb.2016.00276

Kadlcik, S., Kamenik, Z., Vasek, D., Nedved, M., and Janata, J. (2017). Elucidation of salicylate attachment in celesticetin biosynthesis opens the door to create a library of more efficient hybrid lincosamide antibiotics. *Chem. Sci.* 8, 3349–3355. doi: 10.1039/c6sc04235j

Kato, J. Y., Funa, N., Watanabe, H., Ohnishi, Y., and Horinouchi, S. (2007). Biosynthesis of gamma-butyrolactone autoregulators that switch on secondary metabolism and morphological development in *Streptomyces*. *Proc. Natl. Acad. Sci. U.S.A.* 104, 2378–2383. doi: 10.1073/pnas.0607472104

Kato, J. Y., Ohnishi, Y., and Horinouchi, S. (2005). Autorepression of AdpA of the AraC/XylS family, a key transcriptional activator in the A-factor regulatory cascade in *Streptomyces griseus*. *J. Mol. Biol.* 350, 12–26. doi: 10.1016/j.jmb.2005.04.058

Kieser, T., Bibb, M. J., Buttner, M. J., Chater, K. F., and Hopwood, D. A. (2000). *Practical Streptomyces Genetics*. Norwich: John Innes Foundation.

Kim, D. W., Chater, K., Lee, K. J., and Hesketh, A. (2005). Changes in the extracellular proteome caused by the absence of the bldA gene product, a developmentally significant tRNA, reveal a new target for the pleiotropic regulator AdpA in *Streptomyces coelicolor*. *J. Bacteriol.* 187, 2957–2966. doi: 10.1128/JB.187.9.2957-2966.2005

Li, X. B., Zhao, G. R., Zheng, H., and Yuan, Y. J. (2007). Improved industrial fermentation of lincomycin by phosphorus feeding. *Process Biochem.* 42, 662–668. doi: 10.1016/j.procbio.2006.12.007

Liao, C. H., Yao, L., Xu, Y., Liu, W. B., Zhou, Y., and Ye, B. C. (2015). Nitrogen regulator GlnR controls uptake and utilization of non-phosphotransferase-system carbon sources in actinomycetes. *Proc. Natl. Acad. Sci. U.S.A.* 112, 15630–15635. doi: 10.1073/pnas.1508465112

Lin, C. I., Sasaki, E., Zhong, A., and Liu, H. W. (2014). In vitro characterization of LmbK and LmbO: identification of GDP-D-erythro-alpha-D-gluco-octose as a key intermediate in lincomycin a biosynthesis. *J. Am. Chem. Soc.* 136, 906–909. doi: 10.1021/ja412194w

Liu, F., Xu, D., Zhang, Y., Zhu, Y., Ye, J., and Zhang, H. (2015). Identification of BagI as a positive transcriptional regulator of bagremycin biosynthesis in engineered *Streptomyces* sp. Tu 4128. *Microbiol. Res.* 173, 18–24. doi: 10.1016/j.micres.2015.01.011

Liu, Y., Yan, T., Jiang, L., Wen, Y., Song, Y., Chen, Z., et al. (2013). Characterization of SAV7471, a TetR-family transcriptional regulator involved in the regulation of coenzyme a metabolism in *Streptomyces avermitilis*. *J. Bacteriol.* 195, 4365–4372. doi: 10.1128/JB.00716-13

Livak, K. J., and Schmittgen, T. D. (2001). Analysis of relative gene expression data using real-time quantitative PCR and the 2(-ΔΔCT) method. *Methods* 25, 402–408. doi: 10.1006/meth.2001.1262

Lu, C., Yang, J., and Ye, J. (2008). Knockout and retro-complementation of a lincomycin biosynthetic gene lmbU. *J. East China Univ. Sci. Techno.* 34:60. doi: 10.3724/SP.J.1141.2008.00373

Macleod, A. J., Ross, H. B., Ozere, R. L., Digout, G., and Van, R. (1964). Lincomycin: a new antibiotic active against staphylococci and other gram-positive cocci: clinical and laboratory studies. *Can. Med. Assoc. J.* 91, 1056–1060.

Mao, X. M., Luo, S., Zhou, R. C., Wang, F., Yu, P., Sun, N., et al. (2015). Transcriptional regulation of the daptomycin gene cluster in *Streptomyces roseosporus* by an autoregulator. AtrA. *J. Biol. Chem.* 290, 7992–8001. doi: 10.1074/jbc.M114.608273

Meng, S., Wu, H., Wang, L., Zhang, B., and Bai, L. (2017). Enhancement of antibiotic productions by engineered nitrate utilization in actinomycetes. *Appl. Microbiol. Biotechnol.* 101, 5341–5352. doi: 10.1007/s00253-017-8292-7

Neusser, D., Schmidt, H., Spizek, J., Novotna, J., Peschke, U., Kaschabeck, S., et al. (1998). The genes lmbB1 and lmbB2 of *Streptomyces lincolnensis* encode enzymes involved in the conversion of L-tyrosine to propylproline during the biosynthesis of the antibiotic lincomycin A. *Arch. Microbiol.* 169, 322–332. doi: 10.1007/s002030050578

Niu, G., Chater, K. F., Tian, Y., Zhang, J., and Tan, H. (2016). Specialised metabolites regulating antibiotic biosynthesis in *Streptomyces* spp. *FEMS Microbiol. Rev.* 40, 554–573. doi: 10.1093/femsre/fuw012

Novotna, J., Honzatko, A., Bednar, P., Kopecky, J., Janata, J., and Spizek, J. (2004). l-3,4-Dihydroxyphenyl alanine-extradiol cleavage is followed by intramolecular cyclization in lincomycin biosynthesis. *Eur. J. Biochem.* 271, 3678–3683. doi: 10.1111/j.1432-1033.2004.04308.x

Novotna, J., Olsovska, J., Novak, P., Mojzes, P., Chaloupkova, R., Kamenik, Z., et al. (2013). Lincomycin biosynthesis involves a tyrosine hydroxylating heme protein of an unusual enzyme family. *PLoS One* 8:e79974. doi: 10.1371/journal.pone.0079974

Ohnishi, Y., Yamazaki, H., Kato, J. Y., Tomono, A., and Horinouchi, S. (2005). AdpA, a central transcriptional regulator in the A-factor regulatory cascade that leads to morphological development and secondary metabolism in *Streptomyces griseus*. *Biosci. Biotechnol. Biochem.* 69, 431–439. doi: 10.1271/bbb.69.431

Pan, Y., Liu, G., Yang, H., Tian, Y., and Tan, H. (2009). The pleiotropic regulator AdpA-L directly controls the pathway-specific activator of nikkomycin biosynthesis in *Streptomyces ansochromogenes*. *Mol. Microbiol.* 72, 710–723. doi: 10.1111/j.1365-2958.2009.06681.x

Pang, A. P., Du, L., Lin, C. Y., Qiao, J., and Zhao, G. R. (2015). Co-overexpression of lmbW and metK led to increased lincomycin a production and decreased byproduct lincomycin B content in an industrial strain of *Streptomyces lincolnensis*. *J. Appl. Microbiol.* 119, 1064–1074. doi: 10.1111/jam.12919

Pharmacopoeia of the People's Republic of China [PPRC], (1990). *Pharmacopoeia of the People's Republic of China*. Beijing: China Medico-Pharmaceutical Science & Technology Publishing House.

Sasaki, E., Lin, C. I., Lin, K. Y., and Liu, H. W. (2012). Construction of the octose 8-phosphate intermediate in lincomycin a biosynthesis: characterization of the reactions catalyzed by LmbR and LmbN. *J. Am. Chem. Soc.* 134, 17432–17435. doi: 10.1021/ja308221z

Setinova, D., Smidova, K., Pohl, P., Music, I., and Bobek, J. (2017). RNase III-binding-mRNAs revealed novel complementary transcripts in *Streptomyces*. *Front. Microbiol.* 8:2693. doi: 10.3389/fmicb.2017.02693

Spizek, J., and Rezanka, T. (2004a). Lincomycin, clindamycin and their applications. *Appl. Microbiol. Biotechnol.* 64, 455–464. doi: 10.1007/s00253-003-1545-7

Spizek, J., and Rezanka, T. (2004b). Lincomycin, cultivation of producing strains and biosynthesis. *Appl. Microbiol. Biotechnol.* 63, 510–519. doi: 10.1007/s00253-003-1431-3

Spizek, J., and Rezanka, T. (2017). Lincosamides: chemical structure, biosynthesis, mechanism of action, resistance, and applications. *Biochem. Pharmacol.* 133, 20–28. doi: 10.1016/j.bcp.2016.12.001

Takano, E., Nihira, T., Hara, Y., Jones, J. J., Gershater, C. J., Yamada, Y., et al. (2000). Purification and structural determination of SCB1, a gamma-butyrolactone that elicits antibiotic production in *Streptomyces coelicolor* A3(2). *J. Biol. Chem.* 275, 11010–11016. doi: 10.1074/jbc.275.15.11010

Tan, G. Y., Peng, Y., Lu, C., Bai, L., and Zhong, J. J. (2015). Engineering validamycin production by tandem deletion of gamma-butyrolactone receptor genes in *Streptomyces hygroscopicus* 5008. *Metab. Eng.* 28, 74–81. doi: 10.1016/j.ymben.2014.12.003

Tomono, A., Tsai, Y., Yamazaki, H., Ohnishi, Y., and Horinouchi, S. (2005). Transcriptional control by a-factor of strR, the pathway-specific transcriptional activator for streptomycin biosynthesis in *Streptomyces griseus*. *J. Bacteriol.* 187, 5595–5604. doi: 10.1128/JB.187.16.5595-5604.2005

Xu, J., Zhang, J., Zhuo, J., Li, Y., Tian, Y., and Tan, H. (2017). Activation and mechanism of a cryptic oviedomycin gene cluster via the disruption of a global regulatory gene, adpA, in *Streptomyces ansochromogenes*. *J. Biol. Chem.* 292, 19708–19720. doi: 10.1074/jbc.M117.809145

Xu, Y., Ke, M., Li, J., Tang, Y., Wang, N., Tan, G., et al. (2019). TetR-type regulator SLCG_2919 is a negative regulator of lincomycin biosynthesis in *Streptomyces lincolnensis*. *Appl. Environ. Microbiol.* 85:e02091-18. doi: 10.1128/AEM.02091-18

Xu, Y., Tan, G., Ke, M., Li, J., Tang, Y., Meng, S., et al. (2018). Enhanced lincomycin production by co-overexpression of metK1 and metK2 in *Streptomyces lincolnensis*. *J. Ind. Microbiol. Biotechnol.* 45, 345–355. doi: 10.1007/s10295-018-2029-1

Yamazaki, H., Tomono, A., Ohnishi, Y., and Horinouchi, S. (2004). DNA-binding specificity of AdpA, a transcriptional activator in the a-factor regulatory cascade in *Streptomyces griseus*. *Mol. Microbiol.* 53, 555–572. doi: 10.1111/j.1365-2958.2004.04153.x

Yao, M. D., Ohtsuka, J., Nagata, K., Miyazono, K., Zhi, Y., Ohnishi, Y., et al. (2013). Complex structure of the DNA-binding domain of AdpA, the global transcription factor in *Streptomyces griseus*, and a target duplex DNA reveals the structural basis of its tolerant DNA sequence specificity. *J. Biol. Chem.* 288, 31019–31029. doi: 10.1074/jbc.M113.473611

Yu, P., Bu, Q. T., Tang, Y. L., Mao, X. M., and Li, Y. Q. (2018). Bidirectional regulation of AdpAch in controlling the expression of scnRI and scnRII in the natamycin biosynthesis of *Streptomyces chattanoogensis* L10. *Front. Microbiol.* 9:361. doi: 10.3389/fmicb.2018.00316

Yu, P., Liu, S.-P., Bu, Q.-T., Zhou, Z.-X., Zhu, Z.-H., Huang, F.-L., et al. (2014). WblAch, a pivotal activator of natamycin biosynthesis and morphological differentiation in *Streptomyces chattanoogensis* L10, is positively regulated by AdpAch. *Appl. Environ. Microbiol.* 80, 6879–6887. doi: 10.1128/aem.01849-1814

Zhang, D., Tang, Z., and Liu, W. (2018). Biosynthesis of lincosamide antibiotics: reactions associated with degradation and detoxification pathways play a constructive role. *Acc. Chem. Res.* 51, 1496–1506. doi: 10.1021/acs.accounts.8b00135

Zhao, Q., Wang, M., Xu, D., Zhang, Q., and Liu, W. (2015). Metabolic coupling of two small-molecule thiols programs the biosynthesis of lincomycin A. *Nature* 518, 115–119. doi: 10.1038/nature14137

Zheng, Y., Sun, C. F., Fu, Y., Chen, X. A., Li, Y. Q., and Mao, X. M. (2019). Dual regulation between the two-component system PhoRP and AdpA regulates antibiotic production in streptomyces. *J. Ind. Microbiol. Biotechnol.* 46, 725–737. doi: 10.1007/s10295-018-02127-2125

Zhong, G., Zhao, Q., Zhang, Q., and Liu, W. (2017). 4-alkyl-L-(Dehydro)proline biosynthesis in actinobacteria involves N-terminal nucleophile-hydrolase activity of γ-glutamyltranspeptidase homolog for C-C bond cleavage. *Nat. Commun.* 8:16109. doi: 10.1038/ncomms16109

Conflict of Interest: The authors declare that the research was conducted in the absence of any commercial or financial relationships that could be construed as a potential conflict of interest.

frontiers in Microbiology

REVIEW
published: 05 November 2019
doi: 10.3389/fmicb.2019.02467

Recent Advances in Synthetic Biology Approaches to Optimize Production of Bioactive Natural Products in Actinobacteria

Lei Li[1†], Xiaocao Liu[1,2†], Weihong Jiang[1,3] and Yinhua Lu[4]**

[1] Key Laboratory of Synthetic Biology, CAS Center for Excellence in Molecular Plant Sciences, Institute of Plant Physiology and Ecology, Chinese Academy of Sciences, Shanghai, China, [2] School of Life Sciences, Henan University, Kaifeng, China, [3] Jiangsu National Synergetic Innovation Center for Advanced Materials, SICAM, Nanjing, China, [4] College of Life Sciences, Shanghai Normal University, Shanghai, China

OPEN ACCESS

Edited by:
Rustam Aminov,
University of Aberdeen,
United Kingdom

Reviewed by:
Linquan Bai,
Shanghai Jiao Tong University, China
Bertolt Gust,
University of Tübingen, Germany

***Correspondence:**
Weihong Jiang
whjiang@sibs.ac.cn
Yinhua Lu
yhlu@shnu.edu.cn;
yhlu@shnu.edu

† These authors have contributed equally to this work

Specialty section:
This article was submitted to Antimicrobials, Resistance and Chemotherapy, a section of the journal Frontiers in Microbiology

Received: 01 September 2019
Accepted: 15 October 2019
Published: 05 November 2019

Citation:
Li L, Liu X, Jiang W and Lu Y (2019) Recent Advances in Synthetic Biology Approaches to Optimize Production of Bioactive Natural Products in Actinobacteria. Front. Microbiol. 10:2467. doi: 10.3389/fmicb.2019.02467

Actinobacteria represent one of the most fertile sources for the discovery and development of natural products (NPs) with medicinal and industrial importance. However, production titers of actinobacterial NPs are usually low and require optimization for compound characterization and/or industrial production. In recent years, a wide variety of novel enabling technologies for engineering actinobacteria have been developed, which have greatly facilitated the optimization of NPs biosynthesis. In this review, we summarize the recent advances of synthetic biology approaches for overproducing desired drugs, as well as for the discovery of novel NPs in actinobacteria, including dynamic metabolic regulation based on metabolite-responsive promoters or biosensors, multi-copy chromosomal integration of target biosynthetic gene clusters (BGCs), promoter engineering-mediated rational BGC refactoring, and construction of genome-minimized *Streptomyces* hosts. Integrated with metabolic engineering strategies developed previously, these novel enabling technologies promise to facilitate industrial strain improvement process and genome mining studies for years to come.

Keywords: actinobacteria, natural product, synthetic biology, dynamic regulation, BGC amplification, pathway refactoring, genome-minimized host

INTRODUCTION

As a kind of Gram-positive bacteria with high GC content, actinobacteria undergo complex morphological differentiation and secondary metabolism processes (Barka et al., 2016). Actinobacteria, particularly the *Streptomyces* genus, have been recognized as the main sources for microbial bioactive natural products (NPs), such as antibiotics, chemotherapeutics, immunosuppressants and anthelmintics, which make important contributions to health care and crop protection (Jensen et al., 2015; Genilloud, 2017; Nepal and Wang, 2019). With the rapid advances in genome sequencing and genome mining methods (Ziemert et al., 2016; Blin et al., 2019), a wealth of hidden NP biosynthetic gene clusters (BGCs) have been revealed by specialized software (i.e., antiSMASH) and are regarded as an untapped treasure trove for the discovery of novel bioactive compounds (Rutledge and Challis, 2015; Niu, 2018). For instance, a single *Streptomyces* genome usually harbors around 30 NP BGCs, approximately 10-fold more than

previously identified by bioactivity screening (Rutledge and Challis, 2015). However, the majority of NP BGCs in actinobacteria are silent or cryptic under laboratory culture conditions, and must be activated for the isolation and characterization of unknown compounds (Rutledge and Challis, 2015; Zarins-Tutt et al., 2016). Furthermore, production titers of many available actinomycete-derived drugs are still low for the economically viable industrial bioprocess. Construction of highly efficient microbial cell factories becomes increasingly critical for commercial application of desired NPs (Kim et al., 2016; Zhang et al., 2016).

With the advents of metabolic engineering and synthetic biology, genetic engineering of actinobacteria could address several major challenges associated with NP discovery, development and large-scale manufacturing. In the last three decades, a variety of genetic engineering strategies have been developed for strain development, including precursor engineering, BGC amplification, deletion of competing pathways, engineering of translational/transcriptional machineries as well as manipulation of pleiotropic/pathway-specific regulators (Baltz, 2016; Kim et al., 2016; Palazzotto et al., 2019). Interested readers are referred to the detailed reviews of systems biotechnology of actinobacteria (Weber et al., 2015; Baltz, 2016; Kim et al., 2016; Zhang et al., 2016; Palazzotto et al., 2019). It is worth noting that with breakthroughs in CRISPR-based genome editing methods, a series of novel enabling technologies have been developed, greatly facilitating the engineering of actinomycetal genomes (i.e., deletion, insertion, replacement and point mutation) as well as NP BGCs (i.e., cloning, editing, deletion and amplification) (Li et al., 2017a; Tong et al., 2018; Alberti and Corre, 2019). In this review, we briefly summarize the most recent synthetic biology approaches and discuss how these technologies enable the generation of microbial cell factories and the discovery of novel therapeutic drug leads. These include dynamic regulation based on metabolite-responsive elements, multiplex site-specific recombination (SSR) system-mediated BGC amplification (MSGE), systematical and rational BGC refactoring, as well as construction of genome-minimized *Streptomyces* hosts for NP overproduction and discovery. Together with traditional metabolic engineering strategies (Weber et al., 2015; Baltz, 2016), we believe that these newly developed tools will be widely applicable for actinobacteria, providing general strategies for (meta)genome mining-based novel NP discovery as well as for the overproduction of commercially important NPs.

DYNAMIC PATHWAY REGULATION BASED ON METABOLITE-RESPONSIVE PROMOTERS OR REGULATORS

Dynamic metabolic regulation has proved to be an effective strategy to improve production titers of target compounds by balancing bacterial growth and biosynthesis of specific metabolites (Zhang et al., 2012; Dahl et al., 2013; Gupta et al., 2017). Generally, three different approaches – quorum sensing systems, metabolite-responsive promoters and protein/RNA-based biosensors – are used for autonomous control of metabolic pathway flux (Zhang et al., 2015; Polkade et al., 2016; Tan and Prather, 2017). These new concepts were initially developed in *Escherichia coli* or *Saccharomyces cerevisiae*, and the latter two have been extended to actinobacteria for the optimization of antibiotic biosynthetic pathways.

Metabolite-Responsive Promoters

In the last three decades, a large variety of metabolic engineering strategies have been developed to optimize production of secondary metabolites in microbes. However, few approaches could enable the coordination between bacterial growth and biosynthesis of target compounds. Recently, Li et al. (2018) employed time-course transcriptome analysis to identify a series of antibiotic-responsible promoters with a transcription profile similar to the inducible promoters, when under the optimal conditions (**Figure 1A**). These dynamic responsive promoters could be used to efficiently optimize the expression of native actinorhodin and heterogeneous oxytetracycline (OTC) BGCs in *Streptomyces coelicolor*, subsequently improving the production titers of ACT and OTC by 1.3- and 9.1-fold, respectively, compared with constitutive promoters (Li et al., 2018). Xu et al. (2012) reported a metabolite-responsive promoter, which controlled the transcription of *actAB* encoding an antibiotic exporter in *S. coelicolor*. They found that the antibiotic ACT and its biosynthetic intermediates [e.g., (S)-DNPA] could relieve the repression of *actAB* by binding the transcriptional regulator ActR. That means that the *actAB* promoter could indirectly respond to intermediates or end-products, thus synergistically regulating ACT biosynthesis and export. The metabolite-responsible promoter based strategy will achieve an autonomous induction of pathway regulation and provide a universal route for titer improvements of desired NPs in actinobacteria.

Natural Product-Specific Biosensors

Genetically encoded biosensors are a kind of important synthetic biology tool for real-time detection of intracellular metabolites for specific readouts (Zhang et al., 2015). A typical biosensor is composed of three modules: (i) a signal input module, such as transcription factors (TFs) or riboswitches; (ii) a regulatory module, such as TF-dependent promoters; (iii) a signal output module, such as reporter genes (Mahr and Frunzke, 2016; Lim et al., 2018). Until now, three major categories of biosensors - fluorescence resonance energy transfer (FRET)-based sensors, TF-based sensors and riboswitches – have been widely used in metabolic engineering of microbial hosts (Zhang et al., 2015; Lim et al., 2018). As a kind of natural sensory protein, a classical TF has evolved to contain a ligand-binding domain for responding to environmental changes and a DNA-binding domain for regulating gene expression. Interestingly, many NP BGCs encode cluster-situated regulators (CSRs) in actinobacteria, such as TetR-like regulators and *Streptomyces* antibiotic regulatory proteins (SARPs; Liu et al., 2013; Romero-Rodriguez et al., 2015). These CSRs can be used to dynamically detect developmental state, population density or other environmental changes, and

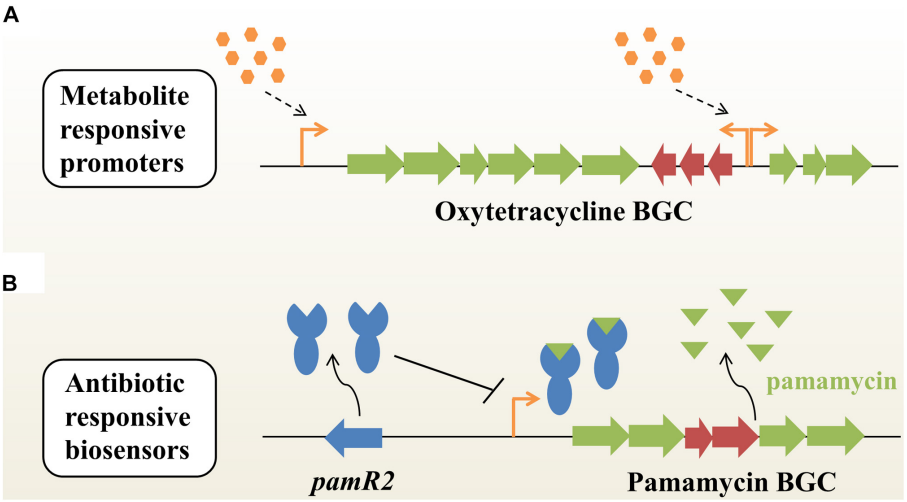

FIGURE 1 | Dynamic pathway regulation balances flux between bacterial growth and antibiotic biosynthesis in actinobacteria. **(A)** Autoregulated fine-tuning of the expression of an antibiotic (e.g., oxytetracycline) BGC based on metabolite-responsive native promoters without specific transcription factors or additional inducers. BGC, biosynthetic gene cluster. **(B)** Antibiotic-responsive biosensors. This strategy is engineered from cluster-situated regulators (e.g., PamR2) that bind to their associated promoters upon interaction with the corresponding secondary metabolites (e.g., pamamycins). Placing antibiotic biosynthetic genes under such promoters enables antibiotic dependent gene expression.

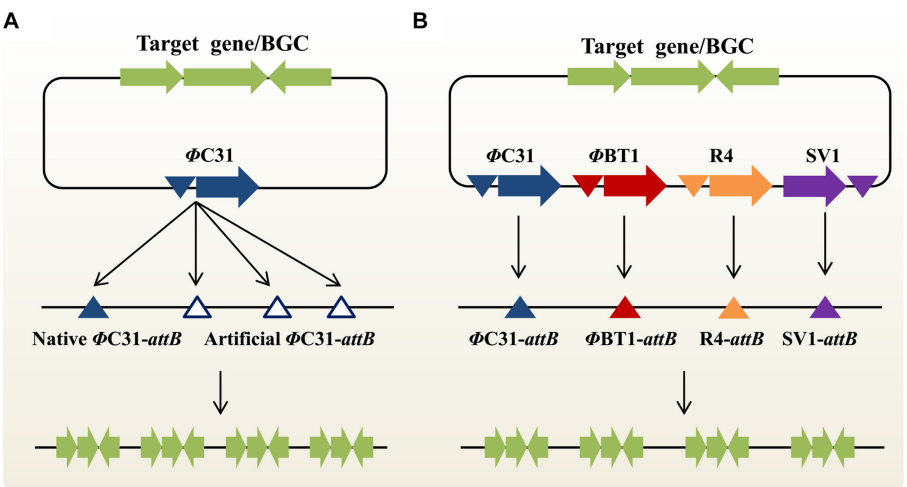

FIGURE 2 | Two emerging synthetic biology approaches for multi-copy integration of target genes or natural products BGCs in actinobacteria. **(A)** Multiplex site-specific genome engineering (MSGE) for discrete amplification of target genes or BGCs. This method is based on the "one integrase-multiple *attB* sites" concept. The blue and blank triangles represent the native and artificial ΦC31 *attB* sites, respectively. **(B)** Advanced multiplex site-specific genome engineering (aMSGE) for multi-locus chromosomal integration of target genes or BGCs. This method is based on the "multiple integrases-multiple *attB* sites" concept. Particularly, these discrete *attB* sites are naturally occurring in the actinomycetal genomes. BGC, biosynthetic gene cluster.

thus determine the onset and production levels of secondary metabolites in actinobacteria. Recently, Rebets et al. (2018) developed a new antibiotic-specific whole-cell biosensor based on a TetR-like repressor for the development of antibiotic-overproducing strains (**Figure 1B**). Briefly, the highly active macrodiolide antibiotic pamamycins BGC encodes a transporter PamW and a corresponding transcriptional repressor PamR2, which can be deactivated by binding to pamamycins (Rebets et al., 2015). Generally, PamW expression is controlled by PamR2 at low level of pamamycins. However, at very high levels of pamamycins, the native PamR2-based biosensors will reach the detection limit and cannot effectively regulate PamW expression (Rebets et al., 2018). The *pamW* promoter was directly used to control expression of the kanamycin resistance gene, thus generating the resistance-based G0 whole-cell biosensor system. After UV-induced mutagenesis, strains resistant to a high-concentration of kanamycin showed a significant increase in pamamycins production (up to 15–16 mg/L). Of note is the fact that the native pamamycins-responsive biosensor showed limited operating and dynamic ranges for further applications.

To overcome this obstacle, the G1 pamamycins biosensor was further developed by combining different promoters, varying the number and position of operators, as well as using diverse reporter genes. Using the new biosensor with higher sensitivity, three mutated strains were obtained, which could produce up to 30 mg/L of pamamycins. Furthermore, to overcome the low detection limit of the G1 biosensor, the binding affinity of PamR2-pamamycins was also efficiently decreased by designing a panel of PamR2 mutations. As expected, the G2 biosensor showed a better operating dynamic range than that of the G1 biosensor (Rebets et al., 2018). In fact, at least 17% of NP BGCs encode TetR-like regulators and putative transporters simultaneously, which provides possibilities for the development of diverse antibiotic-responsive biosensors (Rebets et al., 2018). With the aid of a metabolite-responsive biosensor system, it will become very convenient to assess the functional expression of NP BGCs after random mutagenesis, genetic manipulation or exposure to various cultivation conditions. In the future, TF-based biosensors will hold great promise for accelerating cell factory development for pharmaceutical production and the activation of silent BGCs for the discovery of novel compounds in actinobacteria (Kim et al., 2016; Zarins-Tutt et al., 2016; Sun et al., 2017).

MULTIPLEX SITE-SPECIFIC GENOME ENGINEERING FOR NPs OVERPRODUCTION

In the last three decades, due to their broad host specificities, SSR systems have been widely applied to strain improvements, combinatorial biosynthesis, and heterologous expression of the entire BGCs in *Streptomyces*, *Actinoplanes* and other industrial actinobacteria (Baltz, 2012; Stark, 2017; Merrick et al., 2018). To date, at least ten SSR systems have been identified in actinobacteria, which are derived from bacteriophage CBG73463, R4, SV1, TG1, VWB, ΦBT1, ΦC31, ΦJoe, ΦK38-1 or Φ1/6 (Baltz, 2012; Fogg et al., 2017; Li et al., 2017a; Kormanec et al., 2019). In particular, ΦBT1, ΦC31 and TG1 systems have been widely used for cell factory development via multi-copy amplification of target genes or BGCs (Baltz, 2012). For instance, production titers of the antibiotic goadsporin were increased by 2.3-fold by a step-by-step introduction of two extra copies of the goadsporin BGC based on ΦC31 and TG1 integration systems (Haginaka et al., 2014). However, this strategy requires repeated rounds of conjugal transfer and is limited by the number of selection markers. In 2011, Murakami and coworkers demonstrated that the ZouA-RsA/B-mediated recombination system could be used to achieve tandem amplification of the ACT gene cluster with 4–12 copies, resulting in a 20-fold increase in ACT production (Murakami et al., 2011). However, the engineered strains may be genetically unstable in the absence of antibiotic selection due to the presence of tandem amplification. In addition, the method requires the introduction of the ZouA-RsA/B system into both flanks of target BGCs in advance via two-round conjugal transfer before BGC amplification, which is time-consuming and labor-intensive. To address these limitations, our group has recently developed two novel enabling technologies for multi-locus chromosomal integration of target genes or BGCs, including MSGE and aMSGE (Li et al., 2017b, 2019b).

MSGE: Multiplex Site-Specific Genome Engineering Based on the "One Integrase-Multiple *attB* Sites" Concept

In the actinomycetal genome, there is typically no, or only one, native *attB* site for each SSR system (Baltz, 2012). In theory, one-step, multi-copy integration of target genes or BGCs could be achieved by introducing multiple artificial *attB* sites into the host chromosome in advance. Based on this "one integrase-multiple *attB* sites" concept, an innovative approach MSGE was developed for discrete BGC amplification (**Figure 2A**; Li et al., 2017b). Using the high-efficiency CRISPR/Cas9 genome editing method (Huang et al., 2015), we sequentially introduced three ΦC31 and two ΦBT1 *attB* sites into the genomic loci of deleted, non-target secondary metabolite BGCs in the industrial strain *Streptomyces pristinaespiralis*. Then, five extra copies of the pristinamycin II BGC were integrated into the modified chromosome in two steps using the ΦC31 and ΦBT1 compatible integration systems, which led to significantly improved PII titers (Li et al., 2015, 2017b). Importantly, the novel strategy was also extended to develop a series of powerful *Streptomyces coelicolor* heterologous expression hosts. Up to four copies of the chloramphenicol or YM-216391 BGCs were simultaneously integrated into these new chassis strains, thus resulting in increased production titers (Li et al., 2017b). Using the highly effective heterologous expression system, YM-216391 BGC was engineered to generate aurantizolicin and a hybrid compound 3, which exhibits significantly increased antitumor activity (Pei et al., 2018). Similarly, Myronovskyi et al. (2018) also constructed a panel of cluster-free, powerful *Streptomyces albus* chassis strains based on the "one integrase-multiple *attB* sites" concept. The production titers of a variety of bioactive compounds, including aloesaponarin II, cinnamycin, didesmethylmensacarcin and griseorhodin A, were significantly enhanced in these heterologous expression superhosts (Myronovskyi et al., 2018). It is worth noting that compared with the ZouA-RsA/B recombination system, MSGE-based engineered strains would be genetically stable in the absence of antibiotic selection due to discrete, site-specific integration of target BGCs (Li et al., 2017b). However, when the MSGE method is used to amplify target BGCs with multiple copies in a single step, there is an upper limit to the number of integrated BGCs. For example, we found that the chloramphenicol or YM-216391 BGCs could be simultaneously inserted into *S. coelicolor* with up to 4 copies. The possible reason is that the high-order amplification of BGCs or the accumulation of target products places an excess burden on bacterial growth (Li et al., 2017b). In the near future, we believe that these versatile *Streptomyces* hosts will greatly accelerate (meta)genomic mining and combinatorial biosynthesis studies for novel bioactive NP discovery (Li et al., 2017a; Liu et al., 2018; Zhang et al., 2019).

aMSGE: Advanced Multiplex Site-Specific Genome Engineering With Orthogonal Modular Recombinases

Although the MSGE method could be widely used to construct a variety of suitable chassis organisms for NP discovery and overproduction, two major limitations remains to be addressed. On the one hand, it will be difficult or even impossible to initially insert foreign *attB* sites into the chromosomes of genetically intractable industrial actinobacteria due to the lack of available replicative plasmids and also their low homologous recombination capability, such as spinosad-producing *Saccharopolyspora spinosa* and epoxomicin-producing *Goodfellowiella coeruleoviolacea*. On the other hand, repeated introduction of multiple artificial *attB* sites is still time-consuming and labor-intensive, especially for the slow-growing actinobacteria. To overcome these bottlenecks, our group recently developed an advanced MSGE method (aMSGE) based on the "multiple integrases-multiple *attB* sites" concept (**Figure 2B**; Li et al., 2019b). In this improved method, native *attB* sites of different orthogonal SSR systems in the actinomycetal genome are simultaneously applied to multi-copy integration of target genes or BGCs, rather than introducing foreign *attB* sites into the host chromosome. Accordingly, a plug-and-play amplification toolkit was designed and constructed, which contains 27 modular recombination plasmids with single or multiple SSR systems. Using this innovative technique, we achieved a high-efficiency introduction of the 5-oxomilbemycin A3/A4 BGC into the parental strain *Streptomyces hygroscopicus* with up to four extra copies, thus resulting in a significant increase in the production titers of 5-oxomilbemycin A3/A4 (Li et al., 2019b). Compared with previously developed metabolic engineering tools, the aMSGE method doesn't require the introduction of any genetic modifications before target gene or BGC amplification, which will considerably simplify and accelerate efforts to facilitate NP discovery and overproduction. The whole process for BGC amplification takes only ∼18 days for the construction of high-yield engineered strains (e.g., growth period is ∼6 days). More importantly, the aMSGE method could be applicable to genetically intractable actinobacteria for strain improvements. Given that SSR systems are widely distributed in a variety of microorganisms (Fogg et al., 2014; Stark, 2017), our newly developed methodology should be widely extended to establish more efficient industrial platforms for overproducing valuable chemicals and drugs. However, the aMSGE method could not be used for BGC amplification in actinobacteria without native *attB* sites.

RATIONAL PATHWAY REFACTORING OF NP BIOSYNTHESIS

Generally, NP biosynthesis is under the control of highly complicated transcriptional, translational and metabolic regulation, which hampers the ability of systematic BGC engineering to maximize biosynthetic efficiency (Liu et al., 2013). Pathway refactoring provides an effective synthetic biological approach to decouple gene expression from complex native regulation and to achieve precise control of metabolite production by redesigning target BGCs in versatile surrogate hosts (Tan and Liu, 2017; Niu and Li, 2019). The key steps of BGC refactoring are to develop a set of well-characterized genetic control elements and high-efficiency DNA assembly methods (**Figure 3**).

In the last ten years, a series of synthetic regulatory elements have been identified to precisely regulate gene expression with wide dynamic ranges in actinobacteria, including constitutive or inducible promoters, ribosomal binding sites (RBSs), terminators and protein degradation tags (Myronovskyi and Luzhetskyy, 2016; Horball et al., 2018; Ji et al., 2019). For instance, the expression levels of 200 native or synthetic promoters and 200 artificial RBSs were systematically quantitated, which provides a universal toolbox of synthetic modular regulatory elements for the scalable and cost-effective optimization of NP biosynthetic pathway in different *Streptomyces* (Bai et al., 2015).

Next, a variety of *in vitro* or *in vivo* DNA assembly methods have been established to reconstruct target BGCs for diverse applications (Li et al., 2017a; Zhang et al., 2019). On the one hand, a panel of *in vivo* DNA assembly methods for single-marker or marker-free multiplexed promoter engineering of large BGCs have been developed on the basis of powerful homologous recombination capacity in *S. cerevisiae*, including DNA assembler (Shao et al., 2011), mCRISTAR (multiplexed Cas9-transformation-associated recombination) (Kang et al., 2016) and miCRISTAR (multiplexed *in vitro* Cas9-transformation-associated recombination) (Kim et al., 2019). For example, using the miCRISTAR strategy, the activation of a silent BGC led to the characterization of two bacterial cyclic sesterterpenes atolypene A and B (Kim et al., 2019). In another study, yeast-mediated construction of a riboswitch-controlled pathway achieved a 120-fold increase in bottromycin productivity (Eyles et al., 2018). Intriguingly, multiple new bottromycin-related metabolites were also generated by using high-efficiency, flexible BGC modifications. On the other hand, a range of *in vitro* DNA assembly methods suitable for pathway refactoring have been developed, including modified Gibson assembly (Li et al., 2015), MASTER (methylation-assisted tailorable ends rational) ligation (Chen et al., 2013) and SLIC (Sequence- and Ligation-Independent Cloning) (D'Agostino and Gulder, 2018). Recently, an innovative DNA assembly method, ExoCET (Exonuclease Combined with RecET recombination), was also developed for large-size, multi-operon BGC refactoring (Song et al., 2018; Wang et al., 2018). The artificial 79-kb spinosad BGC with 7 artificial operons under the control of strong constitutive promoters achieved a 328-fold enhanced spinosad production compared to the native BGC (Song et al., 2018). As a simple and robust genetic platform, BGC refactoring will have potentially broad applications in combinatorial biosynthesis and antibiotic overproduction, as well as high-throughput activation of silent BGCs from either metagenomes or uncultured actinobacteria.

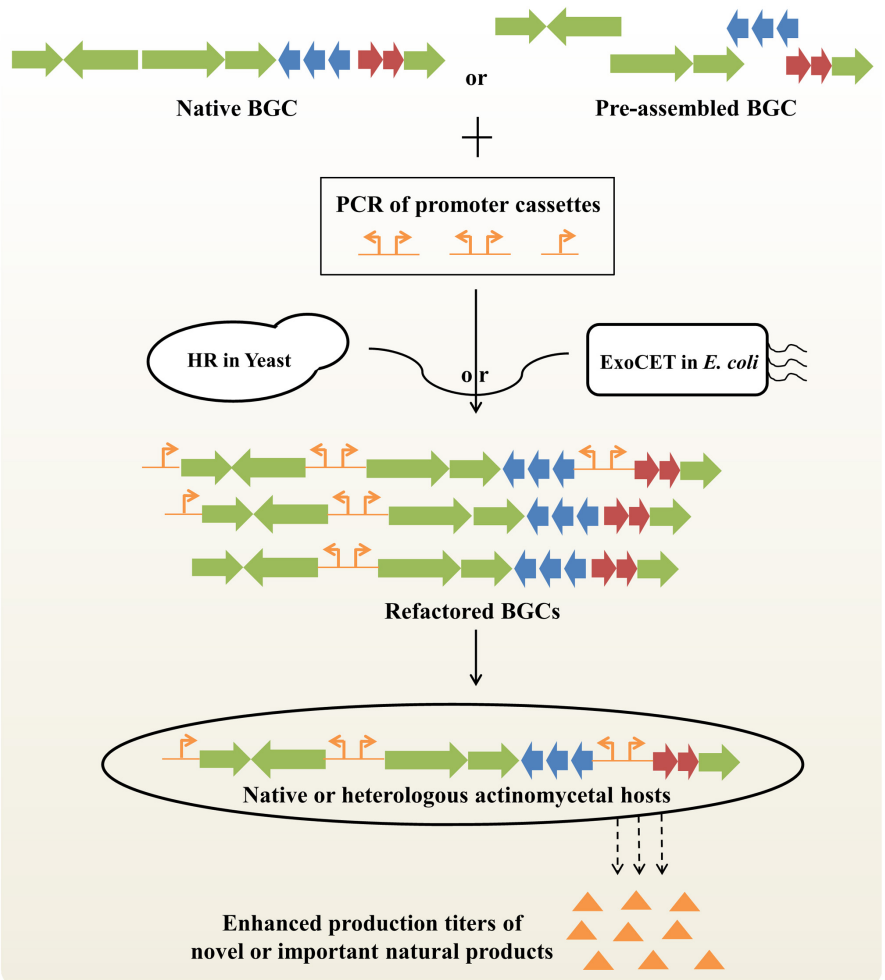

FIGURE 3 | Improved production titers of novel or important natural products by BGC refactoring strategy. Native BGCs can be obtained by *in vivo* or *in vitro* BGC cloning/assembly strategies. Preassembled BGC can be obtained by PCR amplification or CRISPR-mediated *in vitro* digestion of native BGCs. Refactored BGCs can be obtained by partial or complete replacement of native promoters with artificial promoters based on homologous recombination (HR) in *S. cerevisiae* or exonucleases combined with RecET recombination (ExoCET) in *E. coli*. Finally, different refactored BGCs will be integrated into native or heterologous actinomycetal hosts for activating silent BGCs or enhancing production titers of clinically important drugs. BGC, biosynthetic gene cluster.

CONSTRUCTION OF GENOME-REDUCED *Streptomyces* HOSTS FOR NPs DISCOVERY AND OVERPRODUCTION

Streptomyces species are capable of producing a wide range of secondary metabolites, such as polyketides, non-ribosomal peptides and terpenes, and possess the unique metabolic background needed for heterologous expression of NP BGCs from actinobacteria or other bacteria with high-GC content (Liu et al., 2018; Nepal and Wang, 2019). Within the streptomycetes, *S. coelicolor*, *S. albus* J1074 and *Streptomyces lividans* have been widely used as surrogate hosts for NPs discovery and overproduction (Beites and Mendes, 2015; Liu et al., 2018). With the continuous advances of novel bioinformatics tools and genetic manipulation techniques (Zhang et al., 2016, 2019; Ziemert et al., 2016), a series of versatile *Streptomyces* chassis have been developed by deleting non-essential genomic regions, such as redundant BGCs, genome islands and insertion sequences (Liu et al., 2018; Huo et al., 2019; **Table 1**). Particularly, deletion of redundant BGCs are predicted to increase the supply of primary metabolite precursors, remove competing carbon and nitrogen sinks, and also facilitate the biosynthesis of heterologous BGCs. In addition, engineered strains without redundant BGCs will possess simple extracellular metabolite profiles for convenient structural characterization of novel bioactive compounds.

Along with the emergence of genome mining as a robust approach to discover novel drug leads, the development of reliable *Streptomyces* chassis for heterologous expression of cloned BGCs is becoming increasingly important (Huo et al., 2019; Nepal and Wang, 2019). As a model strain, *S. coelicolor* has been widely used to study the molecular regulation of antibiotic biosynthesis and morphological differentiation (Liu et al., 2013;

TABLE 1 | Characteristics of synthetic model *Streptomyces* chassis.

Model strains	***Streptomyces coelicolor* M145**			***Streptomyces albus* J1074**		***Streptomyces lividans* TK24**
Engineered hosts	M1146/M1152	M1246-M1446/M1252-M1452	M1317	Del14	B2P1/B4	SBT5
Characteristics	Deletion of BGCs for ACT, CDA, CPK and RED	Derived from M1146 or M1152 with 1-3 artificial ΦC31 *attB* sites	Derived from M1152 by deleting all three of type III polyketide genes	Deletion of 15 endogenous BGCs	Derived from Del14 with 1-2 artificial ΦC31 *attB* sites	Deletion of BGCs for ACT, RED and CDA and insertion of $afsRS_{cla}$
Deletion sizes	173 kb (2%)	173 kb (2%)	176 kb (2%)	500 kb (7.3%)	500 kb (7.3%)	120 kb (1.4%)
Deletion methods	Resistance gene-assisted recombination	CRISPR-based recombination	RedET-mediated recombination	RedET-mediated recombination	RedET-mediated recombination	Resistance gene-assisted recombination
Compounds	Chaxamycin, Taromycin B, Thiostreptamide et al.	Chloramphenicol and YM-216391	Flaviolin and Germicidin	Cinnamycin, Griseorhodine A, Tunicamycin B2 et al.	Cinnamycin, Griseorhodine A, Tunicamycin B2 et al.	8D1-1 and 8D1-2
Reference	Gomez-Escribano and Bibb, 2011	Li et al., 2017b	Thanapipatsiri et al., 2015	Myronovskyi et al., 2018	Myronovskyi et al., 2018	Bai et al., 2014

ACT, actinorhodin; CDA, calcium-dependent antibiotic; CPK, cryptic type I polyketide; RED, prodiginine; BGC, biosynthetic gene cluster.

Barka et al., 2016). In the last 10 years, a series of advanced genome editing tools and diverse synthetic regulatory elements have been developed for the optimization of heterologous pathways in *S. coeliclor* (Myronovskyi and Luzhetskyy, 2016; Alberti and Corre, 2019). In 2011, on the basis of the wild-type strain *S. coelicolor* M145, two versatile engineered hosts M1146 and M1152 were developed, which contained deletions in four BGCs, responsible for the biosynthesis of ACT, calcium-dependent antibiotic (CDA), cryptic type I polyketides (CPK) and prodiginine (RED), or in combination with a point mutation in *rpoB* (Gomez-Escribano and Bibb, 2011). The productivity of the chloramphenicol or congocidine BGCs was significantly increased compared with the parental strain (Gomez-Escribano and Bibb, 2011). Nowadays, M1146 and M1152 have been widely used to heterologously express different types of compounds from fastidious original producers or metagenomic DNA (Huo et al., 2019; Nepal and Wang, 2019). Similarly, a genome-reduced host *S. lividans* SBT5 was also developed by deleting BGCs responsible for ACT, CDA and RED as well as inserting the regulatory gene $afsRS_{cla}$ (Bai et al., 2014). Furthermore, to specifically facilitate the study of Type III polyketides, an effective surrogate *S. coelicolor* host M1317 was constructed by removing all three endogenous Type III polyketide synthase (PKS) genes (*gcs*, *srsA*, *rppA*) on the basis of M1152, which could potentially increase precursor supply and prevent undesirable interference with expression of heterologous Type III PKS genes (Thanapipatsiri et al., 2015). As another important *Streptomyces* chassis, *S. albus* J1074 provides high success rates of heterologous BGC expression with rapid growth and high productivity (Nepal and Wang, 2019). Recently, on the basis of *S. ablus* J1074, 15 endogenous secondary metabolite BGCs were deleted to generate a powerful engineered host Del14 (Myronovskyi et al., 2018). The production yields of heterologously expressed metabolites in *S. albus* Del14 were higher than those in commonly used *S. albus* J1074 and *S. coelicolor* M1152. Furthermore, the authors also introduced 1-2 artificial ΦC31 *attB* sites into the genomes of *S. albus* Del14, thus resulting in two another versatile engineered hosts, B2P1 and B4. The two powerful chassis could be easily used for BGC amplification of up to four copies, thus efficiently improving fermentation levels of the encoded compounds (Myronovskyi et al., 2018).

In addition to the construction of a model heterologous expression chassis, the genome-reduced strategy has been frequently used to develop non-model *Streptomyces* strains for the discovery and overproduction of important NPs (**Table 2**). *Streptomyces* sp. FR-008 is a fast-growing, potentially industrial production chassis, which produces the macrolide candicidin and other bioactive compounds. By deleting three endogenous polyketide genes, a mutant strain LQ3 was constructed with a stable and streamlined genome structure, which possibly allows for simple separation and purification of heterologously expressed compounds (Liu et al., 2016). As a producer of the anti-infective avermectin, *Streptomyces avermitilis* is already optimized to efficiently supply primary precursors. To construct a versatile industrial chassis for heterologous expression of secondary metabolite BGCs, a series of genome-reduced *S. avermitilis* mutants were obtained by deleting the left subtelomeric region (∼2 Mb) that corresponds to the more variable genome regions (Komatsua et al., 2010). Herein, the SUKA5 and SUKA17 strains were highlighted, which had genome reductions of 17.9 and 18.5%, respectively. *S. avermitilis* SUKA5 strain has the deletions of both oligomycin BGC and the left subtelomeric region, and the SUKA17 strain is a derivative of SUKA5 with the additional deletions of three terpene BGCs (Komatsua et al., 2010). The feasibility and superiority of these two engineered hosts has been widely confirmed by the efficient production of more than 20 exogenous secondary metabolite BGCs (Komatsu et al., 2013; Ikeda et al., 2014). Similarly, 1.3-Mb and 0.7-Mb possible non-essential genomic regions were deleted in the natamycin-producing industrial strian

TABLE 2 | Characteristics of synthetic non-model *Streptomyces* chassis.

Non-model strain	*Streptomyces* sp. FR-008	*Streptomyces avermitilis* wide-type		*Streptomyces albus* BK3-25	*Streptomyces chattanoogensis* L10	
Engineered host	LQ3	SUKA5	SUKA17	ZXJ-6	L320	L321
Characteristic	Deletion of BGCs for three endogenous polyketide genes	Deletion of left subtelomeric region and oligomycin BGC	Derived from SUKA5 and deletion of BGCs for three terpene compounds	Introduction of the ethylmalonyl-CoA biosynthetic pathway and deletion of the salinomycin BGC	Deletion of possible non-essential 0.5–1.8 Mb genomic region	Deletion of possible non-essential 8–8.7 Mb genomic region
Deletion size	150 kb (2.1%)	1.62 Mb (17.9%)	1.67 Mb (18.5%)	77 kb (0.9%)	1.3 Mb (14.4%)	0.7 Mb (7.8%)
Deletion method	Resistance gene-assisted recombination	Cre-loxP recombination	Cre-loxP recombination	Resistance gene-assisted recombination	Cre-loxP recombination	Cre-loxP recombination
Compound	NA	Cephamycin C, Pladienolide, Streptomycin et al.	Kasugamycin, Oxytetracycline, Rebeccamycin et al.	ACT	Natamycin	Natamycin
Reference	Liu et al., 2016	Komatsua et al., 2010	Komatsua et al., 2010	Zhang et al., 2017	Bu et al., 2019	Bu et al., 2019

ACT, actinorhodin; BGC, biosynthetic gene cluster; PKS, polyketide synthase gene; NRPS, non-ribosomal peptide synthase gene; NA, not available.

Streptomyces chattanoogensis L10 by Cre-loxP recombination system, respectively, thus generating two efficient chassis L320 and L321 for the production of valuable polyketides (Bu et al., 2019). In another study, a newly engineered host ZXJ-6 was developed based on a salinomycin-producing industrial strain, *Streptomyces albus* BK3-25, by deleting the salinomycin BGC and chromosomal integration of a three-gene cassette for the biosynthesis of ethylmalonyl-CoA. It was successfully used for the heterologous expression of polyketide BGCs, such as the ACT BGC from *S. coelicolor* (Zhang et al., 2017). In the future, the genome-reduced strategy could be widely implemented in a variety of industrial actinobacteria for the improved production of various bioactive compounds.

CONCLUDING REMARKS

Actinobacteria, especially bacteria from the genus *Streptomyces*, have long been employed as an important source of a wide range of novel bioactive small molecules (Barka et al., 2016; Newman and Cragg, 2016; Genilloud, 2017). To harness the production potential of actinobacteria, a variety of innovative metabolic engineering and synthetic biology strategies have been developed in the last 10 years, including dynamic metabolic regulation, BGC amplification, pathway refactoring and genome-minimized *Streptomyces* chassis (Beites and Mendes, 2015; Tan and Liu, 2017; Tan and Prather, 2017; Li et al., 2019a). We envision that NP discovery and development will be rapidly accelerated by the refactoring and amplification of whole biosynthetic pathways in combination with powerful heterologous expression platforms. Considering that a large number of BGCs are generally silent or expressed at very low levels, it is still important to develop diverse heterologous hosts and universal refactoring approaches to activate silent BGCs or boost production of secondary metabolites. Next, quorum sensing systems are widely distributed in actinobacteria (Polkade et al., 2016), which provide opportunities for bacterial growth-mediated dynamic regulation of metabolic pathways for enhanced production of target compounds. Furthermore, due to the complex regulation between primary and secondary metabolism, iterative application of the design-build-test-learn cycle will be necessary to overproduce different secondary metabolites (Liu et al., 2013; Kim et al., 2016; van der Heul et al., 2018). Finally, the advancements in the fields of genome sequencing, multi-omics and genome editing techniques are paving the way for systems metabolic engineering of industrial actinobacteria, including pathway engineering, regulatory circuit rewiring, host modification and enzyme engineering (Kim et al., 2016; Zhang et al., 2019). Given the requirement for high titers in commercial production, an integrated approach involving traditional mutagenesis screening and rational host/pathway engineering is required to systematically optimize the biosynthesis of target compounds. It is expected that these synthetic biology tools and metabolic engineering strategies presented in this review and future developments will play increasingly important roles in the discovery of novel drug leads, as well as yield improvement for large-scale manufacturing in actinobacteria.

AUTHOR CONTRIBUTIONS

LL and XL wrote the manuscript. LL, WJ, and YL reviewed, edited, and approved its final version.

FUNDING

We gratefully acknowledge the financial support from the National Mega-project for Innovative Drugs (2018ZX09711001-006-012), the National Natural Science Foundation of China (31970083, 31770088, and 31630003), and the Science and Technology Commission of Shanghai Municipality (18ZR1446700).

REFERENCES

Alberti, F., and Corre, C. (2019). Editing streptomycete genomes in the CRISPR/Cas9 age. *Nat. Prod. Rep.* 36, 1237–1248. doi: 10.1039/c8np00081f

Bai, C., Zhang, Y., Zhao, X., Hu, Y., Xiang, S., Miao, J., et al. (2015). Exploiting a precise design of universal synthetic modular regulatory elements to unlock the microbial natural products in *Streptomyces*. *Proc. Natl. Acad. Sci. U.S.A.* 112, 12181–12186. doi: 10.1073/pnas.1511027112

Bai, T.-l., Yu, Y.-f., Xu, Z., and Tao, M.-f. (2014). Construction of *Streptomyces lividans* SBT5 as an efficient heterologous expression host. *J. Huazhong Agric. Univ.* 33, 1–6.

Baltz, R. H. (2012). *Streptomyces* temperate bacteriophage integration systems for stable genetic engineering of actinomycetes (and other organisms). *J. Ind. Microbiol. Biotechnol.* 39, 661–672. doi: 10.1007/s10295-011-1069-6

Baltz, R. H. (2016). Genetic manipulation of secondary metabolite biosynthesis for improved production in *Streptomyces* and other actinomycetes. *J. Ind. Microbiol. Biotechnol.* 43, 343–370. doi: 10.1007/s10295-015-1682-x

Barka, E. A., Vatsa, P., Sanchez, L., Gaveau-Vaillant, N., Jacquard, C., Klenk, H. P., et al. (2016). Taxonomy, physiology, and natural products of actinobacteria. *Microbiol. Mol. Biol. Rev.* 80, 1–43. doi: 10.1128/MMBR.00019-15

Beites, T., and Mendes, M. V. (2015). Chassis optimization as a cornerstone for the application of synthetic biology based strategies in microbial secondary metabolism. *Front. Microbiol.* 6:906. doi: 10.3389/fmicb.2015.00906

Blin, K., Shaw, S., Steinke, K., Villebro, R., Ziemert, N., Lee, S. Y., et al. (2019). antiSMASH 5.0: updates to the secondary metabolite genome mining pipeline. *Nucleic Acids Res.* 47, W81–W87. doi: 10.1093/nar/gkz310

Bu, Q. T., Yu, P., Wang, J., Li, Z. Y., Chen, X. A., Mao, X. M., et al. (2019). Rational construction of genome-reduced and high-efficient industrial *Streptomyces* chassis based on multiple comparative genomic approaches. *Microb. Cell Fact.* 18:16. doi: 10.1186/s12934-019-1055-7

Chen, W. H., Qin, Z. J., Wang, J., and Zhao, G. P. (2013). The Master (methylation-assisted tailorable ends rational) ligation method for seamless DNA assembly. *Nucleic Acids Res.* 41:e93. doi: 10.1093/nar/gkt122

D'Agostino, P. M., and Gulder, T. M. (2018). Direct pathway cloning combined with sequence- and ligation-independent cloning for fast biosynthetic gene cluster refactoring and heterologous expression. *ACS Synth. Biol.* 7, 1702–1708. doi: 10.1021/acssynbio.8b00151

Dahl, R. H., Zhang, F., Alonso-Gutierrez, J., Baidoo, E., Batth, T. S., Redding-Johanson, A. M., et al. (2013). Engineering dynamic pathway regulation using stress-response promoters. *Nat. Biotechnol.* 31, 1039–1046. doi: 10.1038/nbt.2689

Eyles, T. H., Vior, N. M., and Truman, A. W. (2018). Rapid and robust yeast-mediated pathway refactoring generates multiple new bottromycin-related metabolites. *ACS Synth. Biol.* 7, 1211–1218. doi: 10.1021/acssynbio.8b00038

Fogg, P. C. M., Colloms, S., Rosser, S., Stark, M., and Smith, M. C. M. (2014). New applications for phage integrases. *J. Mol. Biol.* 426, 2703–2716. doi: 10.1016/j.jmb.2014.05.014

Fogg, P. C. M., Haley, J. A., Stark, W. M., and Smith, M. C. M. (2017). Genome integration and excision by a new *Streptomyces bacteriophage*, ϕJoe. *Appl. Environ. Microbiol.* 83:e2767-e16. doi: 10.1128/AEM.02767-16

Genilloud, O. (2017). Actinomycetes: still a source of novel antibiotics. *Nat. Prod. Rep.* 34, 1203–1232. doi: 10.1039/c7np00026j

Gomez-Escribano, J. P., and Bibb, M. J. (2011). Engineering *Streptomyces coelicolor* for heterologous expression of secondary metabolite gene clusters. *Microb. Biotechnol.* 4, 207–215. doi: 10.1111/j.1751-7915.2010.00219.x

Gupta, A., Reizman, I. M. B., Reisch, C. R., and Prather, K. L. J. (2017). Dynamic regulation of metabolic flux in engineered bacteria using a pathway-independent quorum-sensing circuit. *Nat. Biotechnol.* 35, 273–279. doi: 10.1038/nbt.3796

Haginaka, K., Asamizu, S., Ozaki, T., Igarashi, Y., Furumai, T., and Onaka, H. (2014). Genetic approaches to generate hyper-producing strains of goadsporin: the relationships between productivity and gene duplication in secondary metabolite biosynthesis. *Biosci. Biotechnol. Biochem.* 78, 394–399. doi: 10.1080/09168451.2014.885824

Horball, L., Siegl, T., and Luzhetskyy, A. (2018). A set of synthetic versatile genetic control elements for the efficient expression of genes in actinobacteria. *Sci. Rep.* 8:491. doi: 10.1038/s41598-017-18846-1

Huang, H., Zheng, G. S., Jiang, W. H., Hu, H. F., and Lu, Y. H. (2015). One-step high-efficiency CRISPR/Cas9-mediated genome editing in *Streptomyces*. *Acta. Biochim. Biophys. Sin* 47, 231–243. doi: 10.1093/abbs/gmv007

Huo, L., Hug, J. J., Fu, C., Bian, X., Zhang, Y., and Muller, R. (2019). Heterologous expression of bacterial natural product biosynthetic pathways. *Nat. Prod. Rep.* doi: 10.1039/C8NP00091C [Epub ahead of print].

Ikeda, H., Shin-Ya, K., and Omura, S. (2014). Genome mining of the Streptomyces avermitilis genome and development of genome-minimized hosts for heterologous expression of biosynthetic gene clusters. *J. Ind. Microbiol. Biotechnol.* 41, 233–250. doi: 10.1007/s10295-013-1327-x

Jensen, P. R., Moore, B. S., and Fenical, W. (2015). The marine actinomycete genus *Salinispora*: a model organism for secondary metabolite discovery. *Nat. Prod. Rep.* 32, 738–751. doi: 10.1039/c4np00167b

Ji, C. H., Kim, H., and Kang, H. S. (2019). Synthetic inducible regulatory systemsoptimized for the modulation of secondary metabolite production in *Streptomyces*. *ACS Synth. Biol.* 8, 577–586. doi: 10.1021/acssynbio.9b00001

Kang, H. S., Charlop-Powers, Z., and Brady, S. F. (2016). Multiplexed CRISPR/Cas9-and TAR-mediated promoter engineering of natural product biosynthetic gene clusters in yeast. *ACS Synth. Biol.* 5, 1002–1010. doi: 10.1021/acssynbio.6b00080

Kim, H. U., Charusanti, P., Lee, S. Y., and Weber, T. (2016). Metabolic engineering with systems biology tools to optimize production of prokaryotic secondary metabolites. *Nat. Prod. Rep.* 33, 933–941. doi: 10.1039/c6np00019c

Kim, S. H., Lu, W. L., Ahmadi, M. K., Montiel, D., Ternei, M. A., and Brady, S. F. (2019). Atolypenes, tricyclic bacterial sesterterpenes discovered using a multiplexed *in vitro* Cas9-TAR gene cluster refactoring approach. *ACS Synth. Biol.* 8, 109–118. doi: 10.1021/acssynbio.8b00361

Komatsu, M., Komatsu, K., Koiwai, H., Yamada, Y., Kozone, I., Izumikawa, M., et al. (2013). Engineered *Streptomyces avermitilis* host for heterologous expression of biosynthetic gene cluster for secondary metabolites. *ACS Synth. Biol.* 2, 384–396. doi: 10.1021/sb3001003

Komatsua, M., Uchiyama, T., Omura, S., Cane, D. E., and Ikeda, H. (2010). Genome-minimized *Streptomyces* host for the heterologous expression of secondary metabolism. *Proc. Natl. Acad. Sci. U.S.A.* 107, 2646–2651. doi: 10.1073/pnas.0914833107

Kormanec, J., Rezuchova, B., Homerova, D., Csolleiova, D., Sevcikova, B., Novakova, R., et al. (2019). Recent achievements in the generation of stable genome alterations/mutations in species of the genus *Streptomyces*. *Appl. Microbiol. Biotechnol.* 103, 5463–5482. doi: 10.1007/s00253-019-09901-0

Li, L., Jiang, W., and Lu, Y. (2017a). New strategies and approaches for engineering biosynthetic gene clusters of microbial natural products. *Biotechnol. Adv.* 35, 936–949. doi: 10.1016/j.biotechadv.2017.03.007

Li, L., Zheng, G., Chen, J., Ge, M., Jiang, W., and Lu, Y. (2017b). Multiplexed site-specific genome engineering for overproducing bioactive secondary metabolites in actinomycetes. *Metab. Eng.* 40, 80–92. doi: 10.1016/j.ymben.2017.01.004

Li, L., Liu, X., Wei, K., Lu, Y., and Jiang, W. (2019a). Synthetic biology approaches for chromosomal integration of genes and pathways in industrial microbial systems. *Biotechnol. Adv.* 37, 730–745. doi: 10.1016/j.biotechadv.2019.04.002

Li, L., Wei, K., Liu, X., Wu, Y., Zheng, G., Chen, S., et al. (2019b). aMSGE: advanced multiplex site-specific genome engineering with orthogonal modular recombinases in actinomycetes. *Metab. Eng.* 52, 153–167. doi: 10.1016/j.ymben.2018.12.001

Li, L., Zhao, Y., Ruan, L., Yang, S., Ge, M., Jiang, W., et al. (2015). A stepwise increase in pristinamycin II biosynthesis by *Streptomyces pristinaespiralis* through combinatorial metabolic engineering. *Metab. Eng.* 29, 12–25. doi: 10.1016/j.ymben.2015.02.001

Li, S., Wang, J., Xiang, W., Yang, K., Li, Z., and Wang, W. (2018). An autoregulated fine-tuning strategy for titer improvement of secondary metabolites using native promoters in *Streptomyces*. *ACS Synth. Biol.* 7, 522–530. doi: 10.1021/acssynbio.7b00318

Lim, H. G., Jang, S., Seo, S. W., and Jung, G. Y. (2018). Design and optimization of genetically encoded biosensors for high-throughput screening of chemicals. *Curr. Opin. Biotechnol.* 54, 18–25. doi: 10.1016/j.copbio.2018.01.011

Liu, G., Chater, K. F., Chandra, G., Niu, G., and Tan, H. (2013). Molecular regulation of antibiotic biosynthesis in streptomyces. *Microbiol. Mol. Biol. Rev.* 77, 112–143. doi: 10.1128/MMBR.00054-12

Liu, Q., Xiao, L., Zhou, Y., Deng, K., Tan, G., Han, Y., et al. (2016). Development of *Streptomyces* sp. *FR*-008 as an emerging chassis. *Synth. Syst. Biotechnol.* 1, 207–214. doi: 10.1016/j.synbio.2016.07.002

Liu, R., Deng, Z. X., and Liu, T. G. (2018). *Streptomyces* species: ideal chassis for natural product discovery and overproduction. *Metab. Eng.* 50, 74–84. doi: 10.1016/j.ymben.2018.05.015

Mahr, R., and Frunzke, J. (2016). Transcription factor-based biosensors in biotechnology: current state and future prospects. *Appl. Microbiol. Biotechnol.* 100, 79–90. doi: 10.1007/s00253-015-7090-3

Merrick, C. A., Zhao, J., and Rosser, S. J. (2018). Serine integrases: advancing synthetic biology. *ACS Synth. Biol.* 7, 299–310. doi: 10.1021/acssynbio.7b00308

Murakami, T., Burian, J., Yanai, K., Bibb, M. J., and Thompson, C. J. (2011). A system for the targeted amplification of bacterial gene clusters multiplies antibiotic yield in *Streptomyces coelicolor*. *Proc. Natl. Acad. Sci. U.S.A.* 108, 16020–16025. doi: 10.1073/pnas.1108124108

Myronovskyi, M., and Luzhetskyy, A. (2016). Native and engineered promoters in natural product discovery. *Nat. Prod. Rep.* 33, 1006–1019. doi: 10.1039/c6np00002a

Myronovskyi, M., Rosenkranzer, B., Nadmid, S., Pujic, P., Normand, P., and Luzhetskyy, A. (2018). Generation of a cluster-free *Streptomyces albus* chassis strains for improved heterologous expression of secondary metabolite clusters. *Metab. Eng.* 49, 316–324. doi: 10.1016/j.ymben.2018.09.004

Nepal, K. K., and Wang, G. (2019). *Streptomycetes*: surrogate hosts for the genetic manipulation of biosynthetic gene clusters and production of natural products. *Biotechnol. Adv.* 37, 1–20. doi: 10.1016/j.biotechadv.2018.10.003

Newman, D. J., and Cragg, G. M. (2016). Natural products as sources of new drugs from 1981 to 2014. *J. Nat. Prod.* 79, 629–661. doi: 10.1021/acs.jnatprod.5b01055

Niu, G. (2018). Genomics-driven natural product discovery in actinomycetes. *Trends Biotechnol.* 36, 238–241. doi: 10.1016/j.tibtech.2017.10.009

Niu, G., and Li, W. (2019). Next-generation drug discovery to combat antimicrobial resistance. *Trends Biochem. Sci.* doi: 10.1016/j.tibs.2019.05.005 [Epub ahead of print].

Palazzotto, E., Tong, Y., Lee, S. Y., and Weber, T. (2019). Synthetic biology and metabolic engineering of actinomycetes for natural product discovery. *Biotechnol. Adv.* 37:107366. doi: 10.1016/j.biotechadv.2019.03.005

Pei, Z. F., Yang, M. J., Li, L., Jian, X. H., Yin, Y., Li, D. H., et al. (2018). Directed production of aurantizolicin and new members based on a YM-216391 biosynthetic system. *Org. Biomol. Chem.* 16, 9373–9376. doi: 10.1039/c8ob02665c

Polkade, A. V., Mantri, S. S., Patwekar, U. J., and Jangid, K. (2016). Quorum sensing: an under-explored phenomenon in the phylum actinobacteria. *Front. Microbiol.* 7:131. doi: 10.3389/fmicb.2016.00131

Rebets, Y., Brotz, E., Manderscheid, N., Tokovenko, B., Myronovskyi, M., Metz, P., et al. (2015). Insights into the pamamycin biosynthesis. *Angew. Chem. Int. Ed. Engl.* 54, 2280–2284. doi: 10.1002/anie.201408901

Rebets, Y., Schmelz, S., Gromyko, O., Tistechok, S., Petzke, L., Scrima, A., et al. (2018). Design, development and application of whole-cell based antibiotic-specific biosensor. *Metab. Eng.* 47, 263–270. doi: 10.1016/j.ymben.2018.03.019

Romero-Rodriguez, A., Robledo-Casados, I., and Sanchez, S. (2015). An overview on transcriptional regulators in *Streptomyces*. *Biochim. Biophys. Acta.* 1849, 1017–1039. doi: 10.1016/j.bbagrm.2015.06.007

Rutledge, P. J., and Challis, G. L. (2015). Discovery of microbial natural products by activation of silent biosynthetic gene clusters. *Nat. Rev. Microbiol.* 13, 509–523. doi: 10.1038/nrmicro3496

Shao, Z. Y., Luo, Y. Z., and Zhao, H. M. (2011). Rapid characterization and engineering of natural product biosynthetic pathways via DNA assembler. *Mol. Biosyst.* 7, 1056–1059. doi: 10.1039/c0mb00338g

Song, C., Luan, J., Cui, Q., Duan, Q., Li, Z., Gao, Y., et al. (2018). Enhanced heterologous spinosad production from a 79-kb synthetic multi-operon assembly. *ACS Synth. Biol.* 8, 137–147. doi: 10.1021/acssynbio.8b00402

Stark, W. M. (2017). Making serine integrases work for us. *Curr. Opin. Microbiol.* 38, 130–136. doi: 10.1016/j.mib.2017.04.006

Sun, Y. Q., Busche, T., Ruckert, C., Paulus, C., Rebets, Y., Novakova, R., et al. (2017). Development of a biosensor concept to detect the production of cluster-specific secondary metabolites. *ACS Synth. Biol.* 6, 1026–1033. doi: 10.1021/acssynbio.6b00353

Tan, G. Y., and Liu, T. (2017). Rational synthetic pathway refactoring of natural products biosynthesis in actinobacteria. *Metab. Eng.* 39, 228–236. doi: 10.1016/j.ymben.2016.12.006

Tan, S. Z., and Prather, K. L. J. (2017). Dynamic pathway regulation: recent advances and methods of construction. *Curr. Opin. Chem. Biol.* 41, 28–35. doi: 10.1016/j.cbpa.2017.10.004

Thanapipatsiri, A., Claesen, J., Gomez-Escribano, J. P., Bibb, M., and Thamchaipenet, A. (2015). A *Streptomyces coelicolor* host for the heterologous expression of Type III polyketide synthase genes. *Microb. Cell Fact.* 14:145. doi: 10.1186/s12934-015-0335-0

Tong, Y., Weber, T., and Lee, S. Y. (2018). CRISPR/Cas-based genome engineering in natural product discovery. *Nat. Prod. Rep.* 36, 1262–1280. doi: 10.1039/c8np00089a

van der Heul, H. U., Bilyk, B. L., Mcdowall, K. J., Seipke, R. F., and Van Wezel, G. P. (2018). Regulation of antibiotic production in actinobacteria: new perspectives from the post-genomic era. *Nat. Prod. Rep.* 35, 575–604. doi: 10.1039/c8np00012c

Wang, H., Li, Z., Jia, R., Yin, J., Li, A., Xia, L., et al. (2018). ExoCET: exonuclease in vitro assembly combined with RecET recombination for highly efficient direct DNA cloning from complex genomes. *Nucleic Acids Res.* 46:e28. doi: 10.1093/nar/gkx1249

Weber, T., Charusanti, P., Musiol-Kroll, E. M., Jiang, X. L., Tong, Y. J., Kim, H. U., et al. (2015). Metabolic engineering of antibiotic factories: new tools for antibiotic production in actinomycetes. *Trends Biotechnol.* 33, 15–26. doi: 10.1016/j.tibtech.2014.10.009

Xu, Y., Willems, A., Au-Yeung, C., Tahlan, K., and Nodwell, J. R. (2012). A two-step mechanism for the activation of actinorhodin export and resistance in *Streptomyces coelicolor*. *mBio* 3, e191–e112. doi: 10.1128/mBio.00191-12

Zarins-Tutt, J. S., Barberi, T. T., Gao, H., Mearns-Spragg, A., Zhang, L., Newman, D. J., et al. (2016). Prospecting for new bacterial metabolites: a glossary of approaches for inducing, activating and upregulating the biosynthesis of bacterial cryptic or silent natural products. *Nat. Prod. Rep.* 33, 54–72. doi: 10.1039/c5np00111k

Zhang, F. Z., Carothers, J. M., and Keasling, J. D. (2012). Design of a dynamic sensor-regulator system for production of chemicals and fuels derived from fatty acids. *Nat. Biotechnol.* 30, 354–359. doi: 10.1038/nbt.2149

Zhang, J., Jensen, M. K., and Keasling, J. D. (2015). Development of biosensors and their application in metabolic engineering. *Curr. Opin. Chem. Biol.* 28, 1–8. doi: 10.1016/j.cbpa.2015.05.013

Zhang, J. J., Tang, X., and Moore, B. S. (2019). Genetic platforms for heterologous expression of microbial natural products. *Nat. Prod. Rep.* 36, 1313–1332. doi: 10.1039/c9np00025a

Zhang, M. M., Wang, Y. J., Ang, E. L., and Zhao, H. M. (2016). Engineering microbial hosts for production of bacterial natural products. *Nat. Prod. Rep.* 33, 963–987. doi: 10.1039/c6np00017g

Zhang, X. J., Lu, C. Y., and Bai, L. Q. (2017). Conversion of the high-yield salinomycin producer *Streptomyces albus* BK3-25 into a surrogate host for polyketide production. *Sci. China Life Sci.* 60, 1000–1009. doi: 10.1007/s11427-017-9122-8

Ziemert, N., Alanjary, M., and Weber, T. (2016). The evolution of genome mining in microbes-a review. *Nat. Prod. Rep.* 33, 988–1005. doi: 10.1039/c6np00025h

Conflict of Interest: The authors declare that the research was conducted in the absence of any commercial or financial relationships that could be construed as a potential conflict of interest.

frontiers in Microbiology

REVIEW
published: 19 December 2019
doi: 10.3389/fmicb.2019.02927

Regulation of Antibiotic Production by Signaling Molecules in *Streptomyces*

Dekun Kong[1,2], *Xia Wang*[1,2], *Ju Nie*[1,3] *and Guoqing Niu*[1,2]*

[1] *Biotechnology Research Center, Southwest University, Chongqing, China,* [2] *State Cultivation Base of Crop Stress Biology for Southern Mountainous Land, Academy of Agricultural Sciences, Southwest University, Chongqing, China,* [3] *College of Horticulture and Landscape Architecture, Southwest University, Chongqing, China*

The genus *Streptomyces* is a unique subgroup of actinomycetes bacteria that are well-known as prolific producers of antibiotics and many other bioactive secondary metabolites. Various environmental and physiological signals affect the onset and level of production of each antibiotic. Here we highlight recent findings on the regulation of antibiotic biosynthesis in *Streptomyces* by signaling molecules, with special focus on autoregulators such as hormone-like signaling molecules and antibiotics themselves. Hormone-like signaling molecules are a group of small diffusible signaling molecules that interact with specific receptor proteins to initiate complex regulatory cascades of antibiotic biosynthesis. Antibiotics and their biosynthetic intermediates can also serve as autoregulators to fine-tune their own biosynthesis or cross-regulators of disparate biosynthetic pathways. Advances in understanding of signaling molecules-mediated regulation of antibiotic production in *Streptomyces* may aid the discovery of new signaling molecules and their use in eliciting silent antibiotic biosynthetic pathways in a wide range of actinomycetes.

Keywords: antibiotic biosynthesis, regulation, *Streptomyces*, hormone-like signaling molecule, antibiotic biosynthetic intermediate, elicitor

OPEN ACCESS

Edited by:
Yinhua Lu,
Shanghai Normal University, China

Reviewed by:
Matthew Ian Hutchings,
University of East Anglia, United Kingdom
Weishan Wang,
Institute of Microbiology (CAS), China

***Correspondence:**
Guoqing Niu
niu062376@swu.edu.cn

Specialty section:
This article was submitted to Antimicrobials, Resistance and Chemotherapy, a section of the journal Frontiers in Microbiology

Received: *29 October 2019*
Accepted: *05 December 2019*
Published: *19 December 2019*

Citation:
Kong D, Wang X, Nie J and Niu G (2019) Regulation of Antibiotic Production by Signaling Molecules in Streptomyces. Front. Microbiol. 10:2927. doi: 10.3389/fmicb.2019.02927

INTRODUCTION

The genus *Streptomyces*, a unique subgroup of actinomycetes bacteria, is best-known for their ability to produce an enormous variety of bioactive secondary metabolites including antibiotics. The onset and production level of each antibiotic is subject to complex control by various environmental and physiological signals (Liu et al., 2013; Niu et al., 2016). Several excellent and comprehensive reviews have focused on the roles of signaling molecules in the regulation of antibiotic production of *Streptomyces* species (Takano, 2006; Sidda and Corre, 2012; Niu et al., 2016; Okada and Seyedsayamdost, 2017). Hormone-like signaling molecules are a group of small diffusible signaling molecules that can elicit antibiotic production and/or induce morphological differentiation at nanomolar concentrations. Typically, a hormone-like signaling molecule binds to its specific receptor, and exerts regulatory function through regulators at different hierarchical levels, including global regulators, pleiotropic regulators, and cluster-situated regulators (CSRs) (Liu et al., 2013; Niu and Tan, 2015; Wei et al., 2018). The most-studied regulatory system is the A-factor cascade that involves the signaling molecule A-factor and its receptor ArpA necessary for streptomycin and grixazone production in *Streptomyces griseus*

(Horinouchi, 2007; Horinouchi and Beppu, 2007). Aside from the hormone-like signaling molecules, accumulating evidence suggests that antibiotics and their biosynthetic intermediates can also serve as autoregulators to modulate their own biosynthesis and as cross-regulators of disparate biosynthetic pathways (Niu et al., 2016). This review is not intended to be comprehensive, but to highlight recent findings on the regulation of antibiotic biosynthesis in *Streptomyces* by small molecules including hormone-like signaling molecules and antibiotics/their biosynthetic intermediates. A better understanding of the regulatory cascade of antibiotic production by signaling molecules in *Streptomyces* may aid the discovery of new signaling molecules and speed up their application in eliciting silent antibiotic biosynthetic pathways in actinomycetes.

REPRESENTATIVE HORMONE-LIKE SIGNALING MOLECULES CONTROLLING ANTIBIOTIC BIOSYNTHESIS

Hormone-like signaling molecules are diffusible small molecules that can elicit antibiotic production and/or induce morphological differentiation at nanomolar concentrations. They exert their regulatory effect via specific receptor proteins that usually belong to the TetR family of transcriptional regulators (Takano, 2006; Niu et al., 2016). The TetR family regulators are characterized by a N-terminal helix-turn-helix (HTH) DNA-binding motif and a C-terminal ligand regulatory domain. They are widely distributed among bacteria and regulate diverse cellular processes in bacteria, especially antibiotic biosynthesis in *Streptomyces* (Cuthbertson and Nodwell, 2013). In *Streptomyces* species, A-factor, the first signaling molecule to be discovered, induces streptomycin production and morphological differentiation through a regulatory cascade involving the receptor ArpA, the pleiotropic regulator AdpA, and the CSR activator StrR in *S. griseus* (Horinouchi, 2007; Horinouchi and Beppu, 2007). Inspired by studies on the A-factor regulatory cascade, many more hormone-like signaling molecules have been identified, and great efforts has been directed to understanding signaling molecules-mediated regulatory cascades of antibiotic biosynthesis in *Streptomyces*.

Five Major Classes of Hormone-Like Signaling Molecules

Similar to the well-documented *N*-acyl-homoserine lactones (AHLs) in Gram-negative bacteria, hormone-like signaling molecules in the Gram-positive *Streptomyces* bacteria are diffusible low molecular weight chemical substances that can elicit antibiotic production and/or induce morphological differentiation at nanomolar concentrations (Swift et al., 1994; Takano, 2006). To date, hormone-like signaling molecules identified from *Streptomyces* are classified into five major classes, including γ-butyrolactones (GBLs), furans, γ-butenolides as well as PI factor and *N*-methylphenylalanyl-dehydrobutyrine diketopiperazine (MDD) (Niu et al., 2016). GBLs, furans and γ-butenolides are based on five-membered heterocyclic rings containing four carbons and one oxygen, while PI factor and MDD have quite different structures (Recio et al., 2004; Matselyukh et al., 2015). As most recent investigations are largely on GBLs and γ-butenolides, we herein only summarize recent findings on these two important classes. GBLs, the largest group of these signaling molecules, share a characteristic 2,3-disubstituted GBL core skeleton but differ in the length, branching and stereochemistry of the acyl side chain (Takano, 2006). So far, a total of 19 GBLs have been identified in streptomycetes, including the A-factor from *S. griseus*, eight butanolides (SCB1-8) from *Streptomyces coelicolor*, five virginiae butanolides (VBs A–E) from *Streptomyces virginiae*, IM-2 from *Streptomyces lavendulae*, factor 1 from *Streptomyces viridochromogenes*, and three Gräfe's factors from *Streptomyces bikinensis* and *Streptomyces cyaneofuscatus* (**Figure 1**; Niu et al., 2016; Sidda et al., 2016). To gain insight to the distribution of GBLs, an A-factor-deficient mutant of *S. griseus* was used as an indicator strain to screen against 203 actinomycete strains. Thirty of the strains tested showed distinct A-factor activity, indicating that A-factor was widely distributed among actinomycetes (Hara and Beppu, 1982). Earlier studies identified the butenolide synthase AfsA as a key enzyme for A-factor biosynthesis in *S. griseus*, and the AfsA homolog ScbA was required for the biosynthesis of the three SCBs in *S. coelicolor* (Takano et al., 2001; Hsiao et al., 2007). Among the eight butanolides identified in the model organism *S. coelicolor*, SCB1-3 were identified in the 2000s (Takano et al., 2000; Hsiao et al., 2009). Recently, the engineered strain *S. coelicolor* M1152 was found to overproduce GBLs SCB1–3 as well as five novel GBLs designated as SCB4–8 (Sidda et al., 2016). The *S. coelicolor* M1152 is a derivative of *S. coelicolor* M145 lacking four biosynthetic gene clusters (BGCs) for the biosynthesis of actinorhodin (ACT), undecylprodigiosin (RED), calcium-dependent antibiotic (CDA) and coelimycin. It should be noted that the deletion of the coelimycin gene cluster included *scbR2*, which encodes a repressor of SCBs biosynthetic gene *scbA*, and thereby contributed to the overproduction of SCBs in *S. coelicolor* M1152 (Gomez-Escribano and Bibb, 2012; Sidda et al., 2016). In a BLAST survey, we found one to three *afsA*-like genes in each of nine *Streptomyces* genomes (Niu et al., 2016). In another study, BLAST search for homologs of AfsA from *S. griseus* within the actinobacteria genomes available from public databases showed that AfsA-like proteins are present in most actinomycetes (Ahmed et al., 2017). The widespread distribution of GBLs was further confirmed by using VB- and IM-2-deficient strains as indicators to examine VB and IM-2 distribution. A total of 10 strains of the 40 *Streptomyces* and 11 endophytic actinomycetes tested produce IM-2, and the same number of strains produced VB active compounds (Thao et al., 2017). These studies reinforce the notion that GBLs are the most common hormone-like signaling molecules among actinomycetes. More efforts should be directed to identifying chemical structures of these signaling molecules.

Representative γ-butenolides include two butenolides (SRB1 and SRB2) from *Streptomyces rochei* (Arakawa et al., 2012; Arakawa, 2014), the avenolide from *Streptomyces avermitilis* (Kitani et al., 2011), four butenolides from *Streptomyces albus*

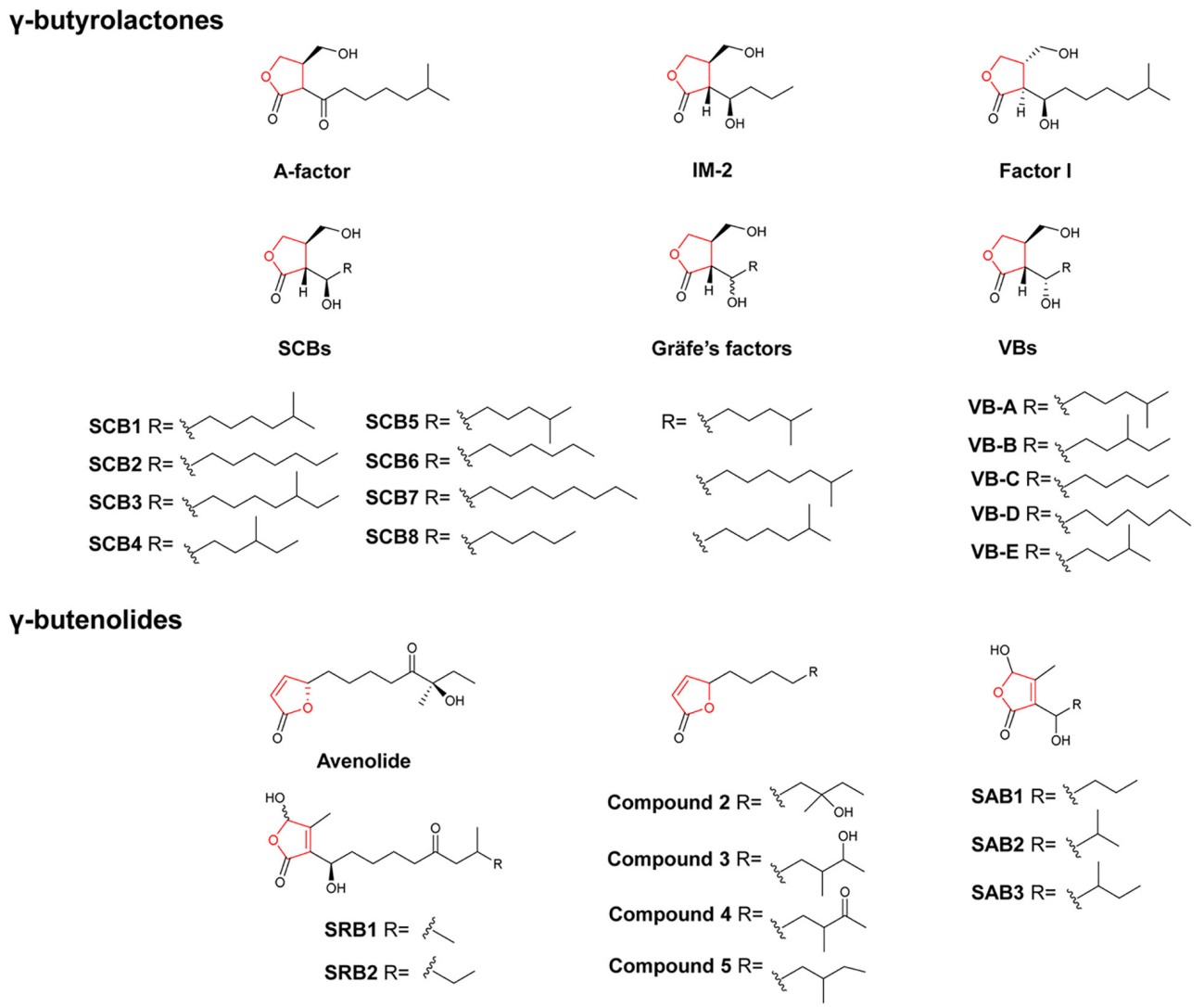

FIGURE 1 | Chemical structures of representative γ-butyrolactones and γ-butenolides. Compounds 2–5: the four γ-butenolides from *Streptomyces albus* J1074.

J1074 (Nguyen et al., 2018), and three butenolides (SAB1-3) from *Streptomyces ansochromogenes* (Wang et al., 2018; **Figure 1**). Of special note is the avenolide that is necessary for triggering avermectin production in *S. avermitilis* (Kitani et al., 2011). The gene cluster responsible for avenolide biosynthesis consists of three genes (*avaR1-3*) that encode GBL receptor homologs, and two genes (*aco* and *cyp17*) that encode an acyl-CoA oxidase and a cytochrome P450 hydroxylase, respectively. Studies suggested that both the acyl-CoA oxidase Aco and the cytochrome P450 hydroxylase Cyp17 were required for the enzymatic production of avenolide. Furthermore, Aco/Cyp17 homologs were also found in the genomes of *Streptomyces fradiae*, *Streptomyces ghanaensis*, *Streptomyces griseoauranticus*, and *S. albus* J1074, suggesting that they have the capacity to produce avenolide or avenolide-like autoregulators (Kitani et al., 2011; Ahmed et al., 2017). Recently, Luzhetskyy and colleagues identified an avenolide-like compound 4 in a genetically modified strain of *S. albus* 1074 (Ahmed et al., 2017). In another study, Nihira and colleagues investigated the distribution of avenolide by using a *S. avermitilis aco* disruptant as a biosensor in a collection of 40 *Streptomyces* and 11 endophytic actinomycetes. They showed that 12 of the 51 actinomycetes strains exhibited avenolide activity with *S. albus* J1074 showing the highest activity (Thao et al., 2017). Metabolite profiling of a disruptant of the *S. albus aco* gene led to the identification of the compound 4 along with three other butenolides (compounds 2, 3, and 5). The four avenolide-like compounds showed different levels of avenolide activity in stimulating avermectin production in *S. avermitilis* (Nguyen et al., 2018). It is interesting to note that the four compounds have been isolated previously from marine-derived *Streptomyces* strains, though there are no reports on their connection with antibiotic biosynthesis in the native producers (Cho et al., 2001; Strand et al., 2014; Viegelmann et al., 2014; Igarashi et al., 2015). In a recent study, Tan and colleagues identified a putative BGC for

autoregulator biosynthesis in *S. ansochromogenes* (nikkomycin producer). Within the gene cluster, *sabA* encodes an AfsA-like enzyme, whereas *sabP* and *sabD* encode phosphatase and dehydrogenase enzymes, respectively. Heterologous expression of *sabAPD* in *E. coli* and *Streptomyces* led to the identification of three novel butenolides (SAB1, 2, and 3) (Wang et al., 2018). Since there are only limited numbers of natural GBLs and γ-butenolides identified in *Streptomyces*, these studies provide effective strategies for the discovery of new signaling molecules, which are normally produced in very small quantities. It is noteworthy that several butenolides have also been identified in *Streptomyces* species (Wang T. et al., 2014; de Oliveira et al., 2019), especially from marine-derived *Streptomyces* (Cho et al., 2001; Strand et al., 2014; Viegelmann et al., 2014; Igarashi et al., 2015). The roles of these butenolides in their native producers await further investigation.

Receptors of Hormone-Like Signaling Molecules

The transmission of chemical signals starts with the binding of an autoregulator to its specific receptor protein, that usually belongs to the TetR family of transcriptional regulators. It is not uncommon that many *Streptomyces* genomes contain multiple genes for ArpA-like GBL receptors. Examples include ScbR, ScbR2, CprA and CprB in *S. coelicolor*, JadR2 and JadR3 in *Streptomyces venezuelae*, and AvaR1, AvaR2, and AvaR3 in *S. avermitilis*, SabR1 and SabR2 in *S. ansochromogenes*. It is noteworthy that most genes encoding these GBL receptors are closely linked both to each other and to the *afsA*-like genes, except that *cprA* and *cprB* are not linked to an *afsA*-like gene and therefore referred to as "orphan GBL receptor" genes (Onaka et al., 1998). To date, only a few identified receptors have been shown to interact with endogenous GBL molecules. In the model organism *S. coelicolor*, ScbR was characterized as a genuine receptor of SCBs (Takano et al., 2005; Gomez-Escribano et al., 2012). ScbR binds the *scbR-scbA* intergenic region to repress its own expression, while interacting with ScbA to activate *scbA* expression in response to SCBs (Takano et al., 2001). Another known target of ScbR is *kasO*, the CSR activator of the coelimycin biosynthetic pathway (Takano et al., 2005). In *S. venezuelae*, JadR3 was identified as a genuine receptor of SVB1, a GBL identical in structure to SCB3 of *S. coelicolor*. The SVB1 receptor JadR3 has dual activation and repression effects on jadomycin biosynthesis (Zou et al., 2014; Niu et al., 2016). In *S. ansochromogenes*, SabR1, the cognate receptor of SABs, was shown to repress the expression of *sabA*, *sabR1*, *sabR2* and *cprC* by binding directly to their promoter regions. Interestingly, CprC, a homolog of CprA and CprB in *S. coelicolor*, was identified as an activator of the pleiotropic regulatory gene *adpA*, which in turn stimulated nikkomycin biosynthesis via activating the transcriptional initiation of the

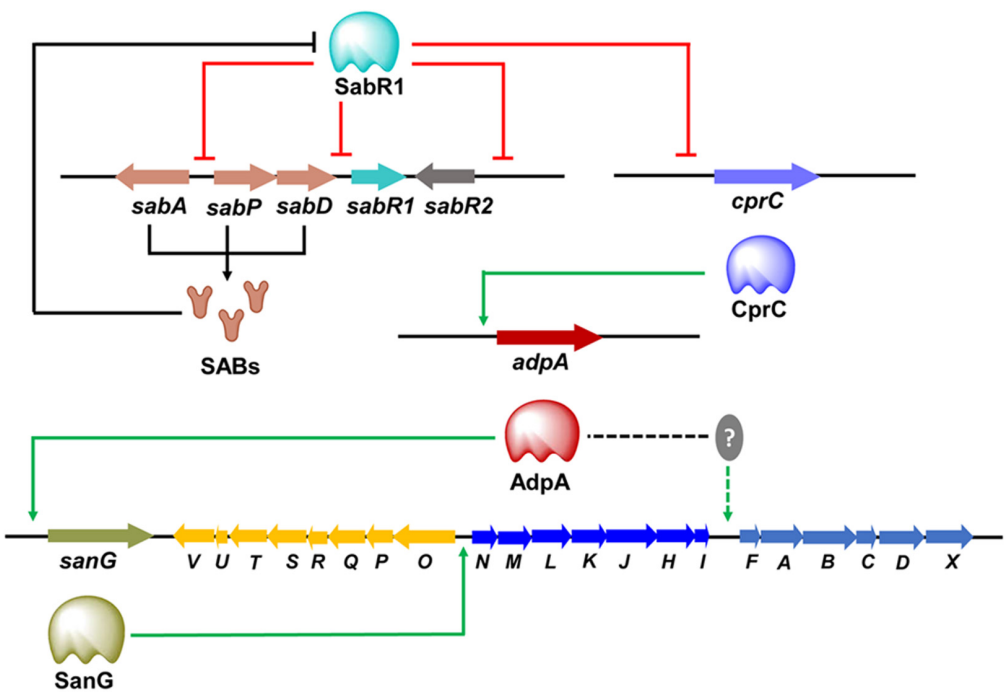

FIGURE 2 | Cascade regulation of nikkomycin biosynthesis. The SABs synthesized by SabA, SabP, and SabD exert regulatory functions via the receptor SabR1. SabR1 represses the transcription of *cprC* and other target genes (*sabA*, *sabR1*, *sabR2*) by binding directly to their promoter regions. Binding of SABs to SabR1 causes the dissociation of SabR1 from *cprC* promoter, and thereby releases its repression on the transcription of *cprC*, which in turn activates *adpA* transcription to stimulate nikkomycin production. AdpA activates nikkomycin biosynthesis via activating the transcriptional initiation of *sanG*. SanG promotes nikkomycin biosynthesis through directly binding to the bidirectional *sanN–sanO* promoter region and activating the transcription of the biosynthetic genes. AdpA can also activate the transcription of *sanF-X* through an unknown mediator.

CSR activator gene *sanG* and biosynthetic genes of the *sanF-X* operon (**Figure 2**; Pan et al., 2009; Wang et al., 2018). Of the three GBL receptors in *S. avermitilis*, AvaR1 acts as an avenolide receptor to control avenolide and avermectin production by directly repressing the transcription of *aco*, *aveR*, its own gene and the other two GBL receptor homologous genes (*avaR2* and *avaR3*) (**Figure 3**; Zhu et al., 2017). ScbR2, JadR2, AvaR2 and SabR2 were identified as pseudo GBL receptors (Xu et al., 2010; Zhu et al., 2016; Wang et al., 2018), and the roles of these pseudo GBL receptors in the regulation of antibiotic biosynthesis will be discussed in a subsequent section. AvaR3 contains an extra 75-amino acid stretch that is not present in typical GBL receptors, and promotes avermectin production through a yet-unknown regulatory mechanism (Miyamoto et al., 2011). It is interesting to note that AvaR3 may represent a new subgroup of GBL receptors, and therefore further studies are needed to reveal its role in avermectin production.

ANTIBIOTICS AS REGULATORY LIGANDS REGULATING ANTIBIOTIC BIOSYNTHESIS

Other than the hormone-like signaling molecules described above, antibiotics and their biosynthetic intermediates can also serve as regulatory ligands to regulate their own biosynthesis or cross-regulators of disparate biosynthetic pathways. In jadomycin biosynthesis, jadomycin and its biosynthetic intermediates actively participate in both feedback and feedforward cascade control of their own production in *S. venezuelae*. Such interplay makes jadomycin biosynthesis an illuminating model for regulatory studies of antibiotic production mediated by antibiotics and their biosynthetic intermediates (Niu et al., 2016). Aside from roles in regulating their own biosynthesis, antibiotics can also serve as autoregulators to control disparate antibiotic biosynthetic pathways. Typically, antibiotics exert their regulatory effect through CSRs that are associated with BGCs or pleiotropic regulators situated elsewhere in the genome (**Table 1**).

Antibiotics and Their Biosynthetic Intermediates as Autoregulators of Their Own Biosynthesis

The first line of antibiotics as autoregulators came from studies on the roles of two atypical response regulators (ARRs) in antibiotic biosynthesis. The CSR activator JadR1, an OmpR-type ARR of *S. venezuelae*, activates the expression of jadomycin B (JdB) biosynthetic genes in the presence of a low concentration of JdB and its homologs, but high JdB concentrations cause the dissociation of JadR1 from its target promoters. Thus, JdB interacts with JadR1 directly in a dose-dependent manner to control JdB production in a feedback regulatory mechanism (Wang et al., 2009). Similarly, a NarL-type ARR RedZ was shown to promote RED biosynthesis in *S. coelicolor* by activating the CSR activator gene *redD*, and the DNA-binding activity of RedZ to its target gene was released by adding RED (Wang et al., 2009). Other than the end-product, studies also suggest that biosynthetic intermediates of antibiotics can also serve as autoregulatory molecules to modulate their own biosynthesis. For example, the TetR family regulator JadR* can respond to early jadomycin intermediates [2,3-dehydro-UWM6 (DHU) and dehydrorabelomycin (DHR)] and release its repression on *jadY*

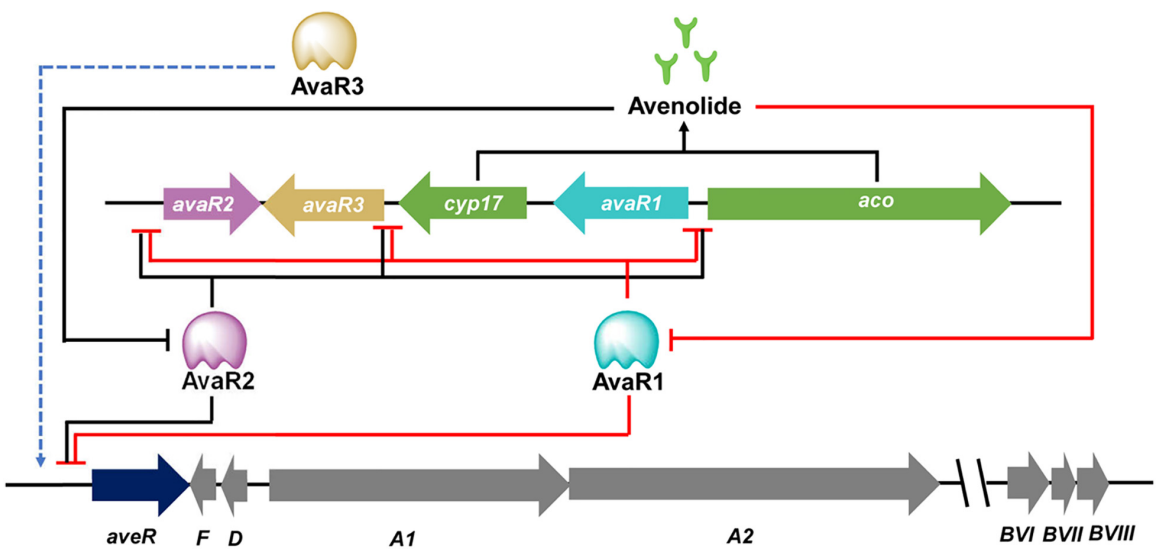

FIGURE 3 | Cascade regulation of avermectin biosynthesis. The complex regulation of avermectin production involves three GBL receptors. The avenolide receptor AvaR1 inhibits avenolide and avermectin production by directly repressing the transcription of *aco*, *aveR*, *avaR1*, *avaR2*, and *avaR3*. The pseudo GBL receptor AveR2 also acts as a repressor of avenolide and avermectin biosynthesis by binding to the same targets as AveR1. Another GBL receptor AvaR3 promotes avermectin production through an unknown regulatory mechanism. The DNA binding activities of AvaR1 and AvaR2 are modulated by avenolide, which are the enzymatic product of Aco and Cyp17.

TABLE 1 | Representative regulators of antibiotic biosynthesis with antibiotics and/or their biosynthetic intermediates as regulatory ligands.

Regulators	Ligands	Description	References
JadR1	JdB, JdA, DHU, DHR	TetR family, activator of jadomycin biosynthesis; repressor of chloramphenicol biosynthesis	Wang et al., 2009
RedZ	RED	TetR family, activator of RED biosynthesis	Wang et al., 2009
JadR*	DHU, DHR, JdA, JdB	TetR family, repressor of jadomycin biosynthesis	Zhang et al., 2013
ChlF1	CHL, DM-CHL, deschloro-CHL	TetR family, repressor of chlorothricin biosynthesis	Li et al., 2016
CalR3	calcimycin, cezomycin	TetR family, repressor of calcimycin biosynthesis	Gou et al., 2017
NosP	NOS, NOS-AC	SARP family, activator of nosiheptide production	Li et al., 2018
RifQ	rifamycin B	TetR family, repressor of rifamycin biosynthesis	Lei et al., 2018
PhlH	2,4-DAPG, MAPG	TetR family, repressor of 2,4-diacetylphloroglucinol biosynthesis	Yan et al., 2017
ScbR2	ACT, RED	TetR family, repressor of coelimycin biosynthesis	Xu et al., 2010
JadR2	JdB, Cm	TetR family, repressor of jadomycin biosynthesis; activator of chloramphenicol	Xu et al., 2010

JdB, jadomycin B; JdA, jadomycin A; DHU, 2,3-dehydro-UWM6; DHR, dehydrorabelomycin; RED, undecylprodigiosin; CHL, chlorothricin; DM-CHL, demethylsalicycloyl chlorothricin; deschloro-CHL, deschloro-chlorothricin; NOS, nosiheptide; NOS-AC, the intermediate of NOS; 2,4-DAPG, 2,4-diacetylphloroglucinol; MAPG, monoacetylphloroglucinol; ACT, actinorhodin; Cm, chloramphenicol.

transcription to ensure the timely supply of cofactors for JadG to convert DHR to the late intermediate jadomycin A (JdA) in jadomycin biosynthesis (Zhang et al., 2013).

Inspired by studies on the regulation of jadomycin biosynthesis in *S. venezuelae*, more antibiotics and their biosynthetic intermediates have been found to serve as autoregulatory molecules to modulate their own biosynthesis in many other streptomycetes. For illustration purposes, we herein only highlight several recent findings. For example, ChlF1, a TetR family regulator involved in chlorothricin biosynthesis of *Streptomyces antibioticus*, was found to repress the transcription of *chlF1*, *chlG* (encoding a major facilitator superfamily transporter), and *chlK* (encoding a type II thioesterase) but activates *chlJ* (encoding acyl-CoA carboxyl transferase) by binding to their promoter regions. However, ChlF1 was disassociated from its target promoters in the presence of chlorothricin and its biosynthetic intermediates (demethyl salicyloyl chlorothricin and deschloro-chlorothricin), which directly interacted with the regulator in a concentration-dependent manner (Li et al., 2016). In another study, CalR3, a TetR family regulator involved in calcimycin biosynthesis of *Streptomyces chartreusis* NRRL 3882, was found to repress the transcription of *calR3* and its adjacent *calT* (encoding a putative transmembrane efflux pump protein of the MMPL family) by binding to their promoter regions. Similarly, both calcimycin and its biosynthetic intermediate (cezomycin) can act as ligands to dissociate CalR3 from its target promoters in a concentration-dependent manner (Gou et al., 2017; Wu et al., 2018). Other than TetR family regulators, *Streptomyces* antibiotic regulatory proteins (SARPs) family regulator was also found to regulate antibiotic biosynthesis in response to antibiotics and their biosynthetic intermediates. For example, NosP was found to regulate nosiheptide production in response to both the end-product nosiheptide (NOS) and biosynthetic intermediate (NOS-AC) (Li et al., 2018). It should be noted that such findings are not limited to the genus *Streptomyces*. One example comes from the actinomycete *Amycolatopsis mediterranei*, in which rifamycin B (the end-product of rifamycin biosynthesis) serves as an extracellular signaling molecule to regulate rifamycin export in a feedback mechanism (Lei et al., 2018). Another study showed that 2,4-diacetylphloroglucinol and its biosynthetic intermediate could serve as autoregulatory ligands to regulate its own biosynthesis in *Pseudomonas fluorescens* (Yan et al., 2017). These studies suggested that antibiotics and their biosynthetic intermediates could function as autoregulators to regulate their own biosynthesis, mainly through the modulation of the binding activity of CSRs to their target genes within their cognate gene clusters.

Antibiotics as Cross-Regulators of the Biosynthesis of Other Antibiotics

Earlier studies suggest that CSRs of one biosynthetic pathway can also control the biosynthesis of disparate antibiotic biosynthetic pathways. For example, RedZ, CSR of the *red* gene cluster, modulates the production of RED as well as that of ACT and CDA (Huang et al., 2005). In another study, the candicidin CSR FscRI was found to control the biosynthesis of candicidin as well as antimycin, the product of a disparate BGC in *Streptomyces albidoflavus* S4 (previously known as *Streptomyces albus* S4) (McLean et al., 2016; Li et al., 2019). Similar observations were also made with coordinated production of geldanamycin and elaiophylin by GdmRIII in *Streptomyces autolyticus* CGMCC0516 (Jiang et al., 2017), production of cephamycin C and clavulanic acid by CcaR in *Streptomyces clavuligerus* (Santamarta et al., 2002), and production of jadomycin and chloramphenicol by JadR1 in *S. venezuelae* (Wang et al., 2009). Recent years see growing evidence that antibiotics can also act as autoregulators regulating other biosynthetic pathways. The first examples to be described involve pseudo GBL receptors. In *S. coelicolor*, ScbR2, represses the same target, *kasO*, as the SCBs-interactive ScbR. Although *scbR2* is linked to the gene cluster for coelimycin biosynthesis, ScbR2 also responds to the endogenous antibiotics ACT and RED, and thereby regulates the production of these antibiotics (Xu et al., 2010). In *S. venezuelae*, JadR2, a close homolog of ScbR2, modulates JdB biosynthesis via direct repression of *jadR1*. This repression is sensitive to the jadomycin end products. Likewise, although *jadR2* is linked to the *jad* gene cluster for jadomycin biosynthesis, JadR2 could also

bind to the endogenous antibiotic chloramphenicol, the product of the distant *cml* biosynthetic gene cluster (Xu et al., 2010). These studies suggest that CSRs of one biosynthetic pathway can also control disparate antibiotic biosynthetic pathways in response to different antibiotics. The pseudo GBL receptor AvaR2 of *S. avermitilis* was as an important repressor of avermectin and avenolide biosynthesis. It directly repressed transcription of *aveR*, *aco*, its own gene and the other two GBL receptor homologous genes (*avaR1* and *avaR3*) (**Figure 3**; Zhu et al., 2016). Interestingly, DNA-binding activity of AvaR2 can be modulated by endogenous avenolide in a concentration-dependent manner, indicating that avenolide serves as ligands for both the genuine GBL receptor AvaR1 and the pseudo GBL receptor AvaR2. Furthermore, DNA-binding activity of AvaR2 can also be modulated by exogenous antibiotics JdB and aminoglycoside antibiotics such as apramycin, hygromycin B, kanamycin and streptomycin (Zhu et al., 2016). It would be interesting to examine if JdB from *S. venezuelae* can serve as signals to modulate avermectin production in *S. avermitilis* under physiological conditions.

SIGNALING MOLECULES IN THE IMPROVEMENT OF ANTIBIOTIC TITERS AND THE CONSTRUCTION OF GENETIC CIRCUITS

As mentioned above, signaling molecules serve as elicitors for antibiotic production in *Streptomyces*. It is reasonable that signaling molecules can be used to improve antibiotic production through exogenous addition. However, due to the fact that natural GBLs are produced in very small quantities, it is impractical to collect sufficient amount of GBLs for the improvement of antibiotic production. Synthetic GBLs and their analogs are then used for this purpose. Early studies showed that addition of chemically synthesized VB-C enhanced virginiamycin production in *Streptomyces virginiae* (Yang et al., 1995, 1996). Similarly, addition of chemically synthesized SCB1 promoted ACT production in *S. coelicolor*. Synthetic GBL analogs are also an alternative (Yang et al., 2009). In two recent studies, the addition of synthetic 1,4-butyrolactone enhanced validamycin A production in *Streptomyces hygroscopicus* 5008 and bitespiramycin production in *Streptomyces spiramyceticus* WS1-195, respectively (Tan et al., 2013; Gao et al., 2019). These studies showed that exogenous addition of signaling molecules can be used as an effective strategy to increase metabolic titers of antibiotics. However, this method has limited application due to the fact that there are only a few natural and synthetic analogs available. Therefore, it is necessary to expand the reservoir of both natural and synthetic signaling molecules. Furthermore, there is a growing interest in the construction of GBL-based genetic circuits in heterologous systems, which has been summarized by Takano and colleagues in 2015 (Biarnes-Carrera et al., 2015). Recently, orthogonal regulatory circuits based on the *S. coelicolor* GBL system have been constructed in *E. coli* (Biarnes-Carrera et al., 2018), reinforcing the promising applications of GBL systems from *Streptomyces* as a regulatory tool for synthetic biology in heterologous systems.

SIGNALING MOLECULES IN THE DISCOVERY OF NOVEL NATURAL PRODUCTS

High-throughput DNA sequencing technologies have resulted in an explosion of microbial genome sequences. Genome sequencing of multiple well-known actinomycetes has revealed that they harbor a great number of BGCs that are predicted to direct the biosynthesis of diverse natural products (Nett et al., 2009). It has become clear that these enormous reservoir of uncharacterized BGCs can serve as an important source of novel bioactive compounds. However, most of these BGCs are not expressed efficiently or not at all under routine laboratory culturing conditions (Mao et al., 2018). Though the reason for the silence of these gene clusters is complicated and remains obscure, a lack of specific signaling molecules may be one of the contributing factors (Liu et al., 2013). Interestingly, antibiotics can be used as chemical elicitors to trigger the expression of these cryptic BGCs and expand the chemical diversity of natural products.

Antibiotics as Chemical Elicitors for the Discovery of Novel Natural Products

In recent years, growing evidence suggests that antibiotics, at sub-inhibitory concentrations, can potentiate antibiotic production in multiple *Streptomyces* species. For example, lincomycin at a sub-inhibitory concentration resulted in an elevated expression of the CSR activator gene *actII-ORF4*, and therefore increased ACT overproduction in *S. coelicolor* (Imai et al., 2015). A recent study suggests that lincomycin produced profound changes in gene expression profiles of *S. coelicolor* (Ishizuka et al., 2018). In another example, a sub-inhibitory concentration of JdB (the angucycline from *S. venezuelae*) induced early RED production and premature differentiation (formation of sporulating aerial mycelium) in *S. coelicolor*. Other angucyclines were also found to elicit similar phenotypes (Wang W. et al., 2014). Examples also include perturbation of antibiotics production by ribosome-targeting antibiotics (thiostrepton, spectinomycin, and chloramphenicol) in multiple *Streptomyces* species (Tanaka et al., 2017; Wang et al., 2017). Furthermore, antibiotics can also be used as chemical elicitors for the discovery of novel natural products. For example, *S. lividans* 1326 grown in the presence of lincomycin at a sub-inhibitory concentration produced abundant antibacterial compounds that were absent in cells grown in lincomycin-free medium. Some of these antibacterial compounds were revealed as novel congeners of CDA (Imai et al., 2015). In another case, polyether antibiotics, including promomycin and closely related salinomycin, monensin, and nigercin, at sub−inhibitory concentrations elicited antibiotic production in multiple *Streptomyces* strains (Amano et al., 2010, 2011). These studies suggest that antibiotics have the potential to

serve as chemical elicitors for the discovery of novel bioactive natural products.

High-Throughput Elicitor Screening for the Discovery of Novel Natural Products

It is well-known that the cryptic gene clusters represent a treasure trove of new natural products, and various strategies and methods has been devised for the activation of these gene clusters (Liu et al., 2013; Niu et al., 2016; Niu, 2018; Niu and Li, 2019). Of special note is a chemogenetic method referred to as high-throughput elicitor screening approach (HiTES) (**Figure 4**). In this approach, a reporter gene is inserted into the BGC of interest to allow a rapid read-out for its expression. The resulting reporter strain is then screened against small molecule libraries to identify candidate elicitors (Seyedsayamdost, 2014). This approach was initially applied to activate two cryptic gene clusters in the Gram-negative bacterium *Burkholderia thailandensis*, leading to the identification of a new malleilactone analog. Interestingly, almost all elicitors identified from a library of 800 compounds were antibiotics (Seyedsayamdost, 2014). Furthermore, Seyedsayamdost and colleagues have employed this approach to identify 14 novel specialized products in *S. albus* J1074 (Xu et al., 2017). HiTES with *S. albus* J1074 using a library of ∼500 natural products identified two classical antibiotics (ivermectin and etoposide) as the best elicitors of a cryptic non-ribosomal peptide synthetase (NRPS) gene cluster (Xu et al., 2017). A major limitation of this method is that genetic manipulations and/or molecular biology approaches are required for the insertion of the reporter gene. To circumvent this problem, HiTES is then combined with bioactivity assays or imaging mass spectrometry (IMS) to identify novel antibiotics. In these approaches, a wild-type microorganism is subjected to HiTES. The resulting induced cultures are then screened directly for biological activity or subject to IMS (**Figure 4**). Application of these modified methods have uncovered two

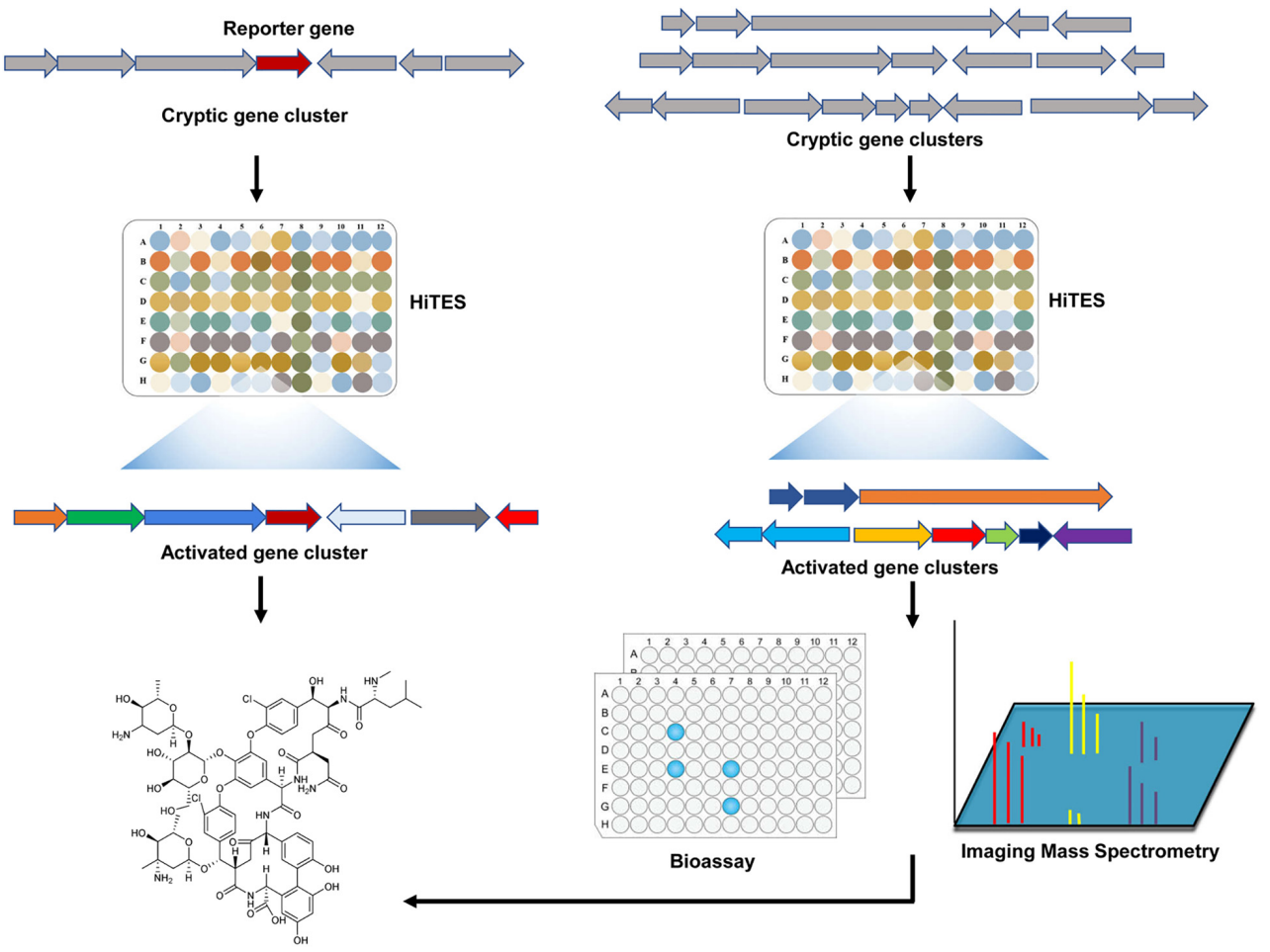

FIGURE 4 | A general workflow of HiTES for the discovery of novel antibiotics. Initially, HiTES uses a reporter gene to allow a rapid read-out for the expression of the target cyptic gene cluster. The resulting reporter strain is then subjected to HiTES screening for the identification of novel antibiotics. Alternatively, microbial genomes encoding numerous cryptic gene clusters are directly subjected to HiTES screening. Cryptic gene clusters activated by small molecule elicitors are then subjected to high throughput bioassays for novel bioactive compounds. They can also be subjected to Imaging Mass Spectrometry to detect the natural products in a rapid and untargeted fashion. HiTES: high-throughput elicitor screening.

novel specialized products in *Streptomyces hiroshimensis* (Moon et al., 2019b), and many other novel specialized metabolites in diverse microorganisms (Moon et al., 2019a; Xu et al., 2019). These studies suggest that HiTES represents a promising new avenue for the discovery of novel bioactive natural products in a high-throughput manner.

CONCLUSION AND PERSPECTIVES

Over the past several decades, significant advances have been made in understanding the regulation of antibiotic biosynthesis in *Streptomyces*. The emerging picture shows a complex interplay of various signals and regulatory proteins. It is interesting to note that both hormone-like signaling molecules and antibiotics/their biosynthetic intermediates actively participate in the regulation of antibiotic production. These small molecule regulators exert their function through the modulation of the binding activity of different regulators to their target genes. Further studies are needed to reveal the complex interplay of autoregulators and multiple GBL receptor homologs in antibiotic biosynthesis of different *Streptomyces*. However, the number of hormone-like signaling molecules identified from *Streptomyces* is still limited, most likely due to the fact that they are produced in very small quantities. BLAST searches for homologs of AfsA from *S. griseus* within the actinobacteria genomes available from public databases indicated that AfsA-like proteins are present in most actinomycetes (Niu et al., 2016; Ahmed et al., 2017). Similar observations have been made with a BLAST search for homologs of Aco and Cyp17 proteins from *S. avermitilis* (Ahmed et al., 2017). It is strongly believed that GBLs and γ-butenolide autoregulators are widely distributed among actinomycetes. It is therefore necessary to identify more hormone-like signaling molecules. Currently, several approaches have been used to discover new signaling molecules in *Streptomyces*, including deletion of gene encoding repressor of signaling molecule biosynthetic gene (Sidda et al., 2016), bioassay using disruptants of known signaling molecule biosynthetic genes as indicator strains (Thao et al., 2017; Nguyen et al., 2018), and heterologous expression of putative signaling molecule biosynthetic genes in model microorganisms (Wang et al., 2018). These approaches will speed up the process of identifying new signaling molecules, and their signal transduction pathways. For autoregulators of antibiotics and their biosynthetic intermediates, more efforts should be geared toward understanding their effect on the fine-tuning regulation of antibiotic biosynthesis under physiological conditions. A better understanding of the complex regulatory pathways of signaling molecules in *Streptomyces* may be used to increase the metabolic titer of industrially and medically important antibiotics as well as activate silent antibiotic BGCs for the discovery of novel bioactive natural products in a wide range of actinomycetes.

AUTHOR CONTRIBUTIONS

All authors listed have made a substantial, direct and intellectual contribution to the work, and approved it for publication.

FUNDING

This work was supported in part by the National Natural Science Foundation of China (31870061), grants from the Chongqing Science and Technology Commission (cstccxljrc201904, cstc2018jcyjAX0066, and cstc2017jcyjAX0467), a start-up grant from the Southwest University (SWU117015), and the Fundamental Research Funds for the Central Universities (SWU119034).

ACKNOWLEDGMENTS

We would like to thank all members of our lab for their helpful comments and discussion during the preparation of this manuscript. We also thank the two reviewers for their helpful comments. We sincerely apologize to those authors whose work we could not cite due to space limitations.

REFERENCES

Ahmed, Y., Rebets, Y., Tokovenko, B., Brotz, E., and Luzhetskyy, A. (2017). Identification of butenolide regulatory system controlling secondary metabolism in *Streptomyces albus* J1074. *Sci. Rep.* 7:9784. doi: 10.1038/s41598-017-10316-y

Amano, S., Morota, T., Kano, Y. K., Narita, H., Hashidzume, T., Yamamoto, S., et al. (2010). Promomycin, a polyether promoting antibiotic production in *Streptomyces* spp. *J. Antibiot.* 63, 486–491. doi: 10.1038/ja.2010.68

Amano, S. I., Sakurai, T., Endo, K., Takano, H., Beppu, T., Furihata, K., et al. (2011). A cryptic antibiotic triggered by monensin. *J. Antibiot.* 64:703. doi: 10.1038/ja.2011.69

Arakawa, K. (2014). Genetic and biochemical analysis of the antibiotic biosynthetic gene clusters on the *Streptomyces* linear plasmid. *Biosci. Biotechnol. Biochem.* 78, 183–189. doi: 10.1080/09168451.2014.882761

Arakawa, K., Tsuda, N., Taniguchi, A., and Kinashi, H. (2012). The butenolide signaling molecules SRB1 and SRB2 induce lankacidin and lankamycin production in *Streptomyces rochei*. *Chembiochem* 13, 1447–1457. doi: 10.1002/cbic.201200149

Biarnes-Carrera, M., Breitling, R., and Takano, E. (2015). Butyrolactone signalling circuits for synthetic biology. *Curr. Opin. Chem. Biol.* 28, 91–98. doi: 10.1016/j.cbpa.2015.06.024

Biarnes-Carrera, M., Lee, C. K., Nihira, T., Breitling, R., and Takano, E. (2018). Orthogonal regulatory circuits for *Escherichia coli* based on the (-butyrolactone system of *Streptomyces coelicolor*. *ACS Synth. Biol.* 7, 1043–1055. doi: 10.1021/acssynbio.7b00425

Cho, K. W., Lee, H. S., Rho, J. R., Kim, T. S., Mo, S. J., and Shin, J. (2001). New lactone-containing metabolites from a marine-derived bacterium of the genus *Streptomyces*. *J. Nat. Prod.* 64, 664–667. doi: 10.1021/np000599g

Cuthbertson, L., and Nodwell, J. R. (2013). The TetR family of regulators. *Microbiol. Mol. Biol. Rev.* 77, 440–475. doi: 10.1128/MMBR.00018-13

de Oliveira, J. A. M., Williams, D. E., Andersen, R. J., Sarragiotto, M. H., and Baldoqui, D. C. (2019). Mycenolide A, new butenolide from a marine sediment-derived bacterium *Streptomyces* sp. 4054. *Nat. Prod. Res.* doi: 10.1080/14786419.2019.1597351 [Epub ahead of print].

Gao, X., Wang, Y., and Chu, J. (2019). A preliminary study on the impact of exogenous A-Factor analogue 1,4-butyrolactone on stimulating bitespiramycin

biosynthesis. *Bioprocess Biosyst. Eng.* 42, 1903–1913. doi: 10.1007/s00449-019-02184-9

Gomez-Escribano, J. P., and Bibb, M. J. (2012). *Streptomyces coelicolor* as an expression host for heterologous gene clusters. *Methods Enzymol.* 517, 279–300. doi: 10.1016/B978-0-12-404634-4.00014-0

Gomez-Escribano, J. P., Song, L., Fox, D. J., Yeo, V., Bibb, M. J., and Challis, G. L. (2012). Structure and biosynthesis of the unusual polyketide alkaloid coelimycin P1, a metabolic product of the *cpk* gene cluster of *Streptomyces coelicolor* M145. *Chem. Sci.* 3, 2716–2720. doi: 10.1039/C2SC20410J

Gou, L., Han, T., Wang, X., Ge, J., Liu, W., Hu, F., et al. (2017). A novel TetR family transcriptional regulator, CalR3, negatively controls calcimycin biosynthesis in *Streptomyces chartreusis* NRRL 3882. *Front. Microbiol.* 8:2371. doi: 10.3389/fmicb.2017.02371

Hara, O., and Beppu, T. (1982). Mutants blocked in streptomycin production in *Streptomyces griseus* - the role of A-factor. *J. Antibiot.* 35, 349–358. doi: 10.7164/antibiotics.35.349

Horinouchi, S. (2007). Mining and polishing of the treasure trove in the bacterial genus *Streptomyces*. *Biosci. Biotechnol. Biochem.* 71, 283–299. doi: 10.1271/bbb.60627

Horinouchi, S., and Beppu, T. (2007). Hormonal control by A-factor of morphological development and secondary metabolism in *Streptomyces*. *Proc. Jpn. Acad. Ser. B Phys. Biol. Sci.* 83, 277–295. doi: 10.2183/pjab/83.277

Hsiao, N. H., Nakayama, S., Merlo, M. E., de Vries, M., Bunet, R., Kitani, S., et al. (2009). Analysis of two additional signaling molecules in *Streptomyces coelicolor* and the development of a butyrolactone-specific reporter system. *Chem. Biol.* 16, 951–960. doi: 10.1016/j.chembiol.2009.08.010

Hsiao, N. H., Soding, J., Linke, D., Lange, C., Hertweck, C., Wohlleben, W., et al. (2007). ScbA from *Streptomyces coelicolor* A3(2) has homology to fatty acid synthases and is able to synthesize (-butyrolactones. *Microbiology* 153, 1394–1404. doi: 10.1099/mic.0.2006/004432-0

Huang, J., Shi, J., Molle, V., Sohlberg, B., Weaver, D., Bibb, M. J., et al. (2005). Cross-regulation among disparate antibiotic biosynthetic pathways of *Streptomyces coelicolor*. *Mol. Microbiol.* 58, 1276–1287. doi: 10.1111/j.1365-2958.2005.04879.x

Igarashi, Y., Ikeda, M., Miyanaga, S., Kasai, H., Shizuri, Y., and Matsuura, N. (2015). Two butenolides with PPAR(agonistic activity from a marine-derived *Streptomyces*. *J. Antibiot.* 68, 345–347. doi: 10.1038/ja.2014.151

Imai, Y., Sato, S., Tanaka, Y., Ochi, K., and Hosaka, T. (2015). Lincomycin at subinhibitory concentrations potentiates secondary metabolite production by *Streptomyces* spp. *Appl. Environ. Microbiol.* 81, 3869–3879. doi: 10.1128/aem.04214-14

Ishizuka, M., Imai, Y., Mukai, K., Shimono, K., Hamauzu, R., Ochi, K., et al. (2018). A possible mechanism for lincomycin induction of secondary metabolism in *Streptomyces coelicolor* A3(2). *Antonie Van Leeuwenhoek* 111, 705–716. doi: 10.1007/s10482-018-1021-0

Jiang, M., Yin, M., Wu, S., Han, X., Ji, K., Wen, M., et al. (2017). GdmRIII, a TetR family transcriptional regulator, controls geldanamycin and elaiophylin biosynthesis in *Streptomyces autolyticus* CGMCC0516. *Sci. Rep.* 7:4803. doi: 10.1038/s41598-017-05073-x

Kitani, S., Miyamoto, K. T., Takamatsu, S., Herawati, E., Iguchi, H., Nishitomi, K., et al. (2011). Avenolide, a *Streptomyces* hormone controlling antibiotic production in *Streptomyces avermitilis*. *Proc. Natl. Acad. Sci. U.S.A.* 108, 16410–16415. doi: 10.1073/pnas.1113908108

Lei, C., Wang, J., Liu, Y., Liu, X., Zhao, G., and Wang, J. (2018). A feedback regulatory model for RifQ-mediated repression of rifamycin export in *Amycolatopsis mediterranei*. *Microb. Cell Fact.* 17:14. doi: 10.1186/s12934-018-0863-5

Li, J., Li, Y., Niu, G., Guo, H., Qiu, Y., Lin, Z., et al. (2018). NosP-regulated nosiheptide production responds to both peptidyl and small-molecule ligands derived from the precursor peptide. *Cell Chem. Biol.* 25, e144. doi: 10.1016/j.chembiol.2017.10.012

Li, Y., Li, J., Tian, Z., Xu, Y., Zhang, J., Liu, W., et al. (2016). Coordinative modulation of chlorothricin biosynthesis by binding of the glycosylated intermediates and end product to a responsive regulator ChlF1. *J. Biol. Chem.* 291, 5406–5417. doi: 10.1074/jbc.M115.695874

Li, Y., Pinto-Tomas, A. A., Rong, X., Cheng, K., Liu, M., and Huang, Y. (2019). Population genomics insights into adaptive evolution and ecological differentiation in *Streptomycetes*. *Appl. Environ. Microbiol.* 85:e2555-18. doi: 10.1128/AEM.02555-18

Liu, G., Chater, K. F., Chandra, G., Niu, G., and Tan, H. (2013). Molecular regulation of antibiotic biosynthesis in *Streptomyces*. *Microbiol. Mol. Biol. Rev.* 77, 112–143. doi: 10.1128/MMBR.00054-12

Mao, D., Okada, B. K., Wu, Y., Xu, F., and Seyedsayamdost, M. R. (2018). Recent advances in activating silent biosynthetic gene clusters in bacteria. *Curr. Opin. Microbiol.* 45, 156–163. doi: 10.1016/j.mib.2018.05.001

Matselyukh, B., Mohammadipanah, F., Laatsch, H., Rohr, J., Efremenkova, O., and Khilya, V. (2015). N-methylphenylalanyl-dehydrobutyrine diketopiperazine, an A-factor mimic that restores antibiotic biosynthesis and morphogenesis in *Streptomyces globisporus* 1912-B2 and *Streptomyces griseus* 1439. *J. Antibiot.* 68, 9–14. doi: 10.1038/ja.2014.86

McLean, T. C., Hoskisson, P. A., and Seipke, R. F. (2016). Coordinate regulation of antimycin and candicidin biosynthesis. *mSphere* 1, 1–35. doi: 10.1128/mSphere.00305-16

Miyamoto, K. T., Kitani, S., Komatsu, M., Ikeda, H., and Nihira, T. (2011). The autoregulator receptor homologue AvaR3 plays a regulatory role in antibiotic production, mycelial aggregation and colony development of *Streptomyces avermitilis*. *Microbiology* 157, 2266–2275. doi: 10.1099/mic.0.048371-0

Moon, K., Xu, F., and Seyedsayamdost, M. R. (2019a). Cebulantin, a cryptic lanthipeptide antibiotic uncovered using bioactivity-coupled HiTES. *Angew. Chem. Int. Ed Engl.* 58, 5973–5977. doi: 10.1002/anie.201901342

Moon, K., Xu, F., Zhang, C., and Seyedsayamdost, M. R. (2019b). Bioactivity-HiTES unveils cryptic antibiotics encoded in actinomycete bacteria. *ACS Chem. Biol.* 14, 767–774. doi: 10.1021/acschembio.9b00049

Nett, M., Ikeda, H., and Moore, B. S. (2009). Genomic basis for natural product biosynthetic diversity in the actinomycetes. *Nat. Prod. Rep.* 26, 1362–1384. doi: 10.1039/b817069j

Nguyen, T. B., Kitani, S., Shimma, S., and Nihira, T. (2018). Butenolides from *Streptomyces albus* J1074 act as external signals to stimulate avermectin production in *Streptomyces avermitilis*. *Appl. Environ. Microbiol.* 84:e2791-17. doi: 10.1128/aem.02791-17

Niu, G. (2018). Genomics-driven natural product discovery in actinomycetes. *Trends Biotechnol.* 36, 238–241. doi: 10.1016/j.tibtech.2017.10.009

Niu, G., Chater, K. F., Tian, Y., Zhang, J., and Tan, H. (2016). Specialised metabolites regulating antibiotic biosynthesis in *Streptomyces* spp. *FEMS Microbiol. Rev.* 40, 554–573. doi: 10.1093/femsre/fuw012

Niu, G., and Li, W. (2019). Next-generation drug discovery to combat antimicrobial resistance. *Trends Biochem. Sci.* 44, 961–972. doi: 10.1016/j.tibs.2019.05.005

Niu, G., and Tan, H. (2015). Nucleoside antibiotics: biosynthesis, regulation, and biotechnology. *Trends Microbiol.* 23, 110–119. doi: 10.1016/j.tim.2014.10.007

Okada, B. K., and Seyedsayamdost, M. R. (2017). Antibiotic dialogues: induction of silent biosynthetic gene clusters by exogenous small molecules. *FEMS Microbiol. Rev.* 41, 19–33. doi: 10.1093/femsre/fuw035

Onaka, H., Nakagawa, T., and Horinouchi, S. (1998). Involvement of two A-factor receptor homologues in *Streptomyces coelicolor* A3(2) in the regulation of secondary metabolism and morphogenesis. *Mol. Microbiol.* 28, 743–753. doi: 10.1046/j.1365-2958.1998.00832.x

Pan, Y., Liu, G., Yang, H., Tian, Y., and Tan, H. (2009). The pleiotropic regulator AdpA-L directly controls the pathway-specific activator of nikkomycin biosynthesis in *Streptomyces ansochromogenes*. *Mol. Microbiol.* 72, 710–723. doi: 10.1111/j.1365-2958.2009.06681.x

Recio, E., Colinas, A., Rumbero, A., Aparicio, J. F., and Martin, J. F. (2004). PI factor, a novel type quorum-sensing inducer elicits pimaricin production in *Streptomyces natalensis*. *J. Biol. Chem.* 279, 41586–41593. doi: 10.1074/jbc.M402340200

Santamarta, I., Rodriguez-Garcia, A., Perez-Redondo, R., Martin, J. F., and Liras, P. (2002). CcaR is an autoregulatory protein that binds to the *ccaR* and *cefD-cmcI* promoters of the cephamycin C-clavulanic acid cluster in *Streptomyces clavuligerus*. *J. Bacteriol.* 184, 3106–3113. doi: 10.1128/jb.184.11.3106-3113.2002

Seyedsayamdost, M. R. (2014). High-throughput platform for the discovery of elicitors of silent bacterial gene clusters. *Proc. Natl. Acad. Sci. U.S.A.* 111, 7266–7271. doi: 10.1073/pnas.1400019111

Sidda, J. D., and Corre, C. (2012). (-butyrolactone and furan signaling systems in *Streptomyces*. *Methods Enzymol.* 517, 71–87. doi: 10.1016/B978-0-12-404634-4.00004-8

Sidda, J. D., Poon, V., Song, L., Wang, W., Yang, K., and Corre, C. (2016). Overproduction and identification of butyrolactones SCB1-8 in the antibiotic

production superhost *Streptomyces* M1152. *Org. Biomol. Chem.* 14, 6390–6393. doi: 10.1039/c6ob00840b

Strand, M., Carlsson, M., Uvell, H., Islam, K., Edlund, K., Cullman, I., et al. (2014). Isolation and characterization of anti-adenoviral secondary metabolites from marine actinobacteria. *Mar. Drugs* 12, 799–821. doi: 10.3390/md12020799

Swift, S., Bainton, N. J., and Winson, M. K. (1994). Gram-negative bacterial communication by N-acyl homoserine lactones: a universal language? *Trends Microbiol.* 2, 193–198. doi: 10.1016/0966-842x(94)90110-q

Takano, E. (2006). Gamma-butyrolactones: *Streptomyces* signalling molecules regulating antibiotic production and differentiation. *Curr. Opin. Microbiol.* 9, 287–294. doi: 10.1016/j.mib.2006.04.003

Takano, E., Chakraburtty, R., Nihira, T., Yamada, Y., and Bibb, M. J. (2001). A complex role for the gamma-butyrolactone SCB1 in regulating antibiotic production in *Streptomyces coelicolor* A3(2). *Mol. Microbiol.* 41, 1015–1028. doi: 10.1046/j.1365-2958.2001.02562.x

Takano, E., Kinoshita, H., Mersinias, V., Bucca, G., Hotchkiss, G., Nihira, T., et al. (2005). A bacterial hormone (the SCB1) directly controls the expression of a pathway-specific regulatory gene in the cryptic type I polyketide biosynthetic gene cluster of *Streptomyces coelicolor*. *Mol. Microbiol.* 56, 465–479. doi: 10.1111/j.1365-2958.2005.04543.x

Takano, E., Nihira, T., Hara, Y., Jones, J. J., Gershater, C. J., Yamada, Y., et al. (2000). Purification and structural determination of SCB1, a (-butyrolactone that elicits antibiotic production in *Streptomyces coelicolor* A3(2). *J. Biol. Chem.* 275, 11010–11016. doi: 10.1074/jbc.275.15.11010

Tan, G. Y., Bai, L., and Zhong, J. J. (2013). Exogenous 1,4-butyrolactone stimulates A-factor-like cascade and validamycin biosynthesis in *Streptomyces hygroscopicus* 5008. *Biotechnol. Bioeng.* 110, 2984–2993. doi: 10.1002/bit.24965

Tanaka, Y., Izawa, M., Hiraga, Y., Misaki, Y., Watanabe, T., and Ochi, K. (2017). Metabolic perturbation to enhance polyketide and nonribosomal peptide antibiotic production using triclosan and ribosome-targeting drugs. *Appl. Microbiol. Biotechnol.* 101, 4417–4431. doi: 10.1007/s00253-017-8216-6

Thao, N. B., Kitani, S., Nitta, H., Tomioka, T., and Nihira, T. (2017). Discovering potential *Streptomyces* hormone producers by using disruptants of essential biosynthetic genes as indicator strains. *J. Antibiot.* 70, 1004–1008. doi: 10.1038/ja.2017.85

Viegelmann, C., Margassery, L. M., Kennedy, J., Zhang, T., O'Brien, C., O'Gara, F., et al. (2014). Metabolomic profiling and genomic study of a marine sponge-associated *Streptomyces* sp. *Mar. Drugs* 12, 3323–3351. doi: 10.3390/md12063323

Wang, H., Zhao, G., and Ding, X. (2017). Morphology engineering of *Streptomyces coelicolor* M145 by sub-inhibitory concentrations of antibiotics. *Sci. Rep.* 7:13226. doi: 10.1038/s41598-017-13493-y

Wang, L., Tian, X., Wang, J., Yang, H., Fan, K., Xu, G., et al. (2009). Autoregulation of antibiotic biosynthesis by binding of the end product to an atypical response regulator. *Proc. Natl. Acad. Sci. U.S.A.* 106, 8617–8622. doi: 10.1073/pnas.0900592106

Wang, T., Jiang, Y., Ma, K. X., Li, Y. Q., Huang, R., Xie, X. S., et al. (2014). Two new butenolides produced by an actinomycete *Streptomyces* sp. *Chem. Biodivers.* 11, 929–933. doi: 10.1002/cbdv.201300321

Wang, W., Ji, J., Li, X., Wang, J., Li, S., Pan, G., et al. (2014). Angucyclines as signals modulate the behaviors of *Streptomyces coelicolor*. *Proc. Natl. Acad. Sci. U.S.A.* 111, 5688–5693. doi: 10.1073/pnas.1324253111

Wang, W., Zhang, J., Liu, X., Li, D., Li, Y., Tian, Y., et al. (2018). Identification of a butenolide signaling system that regulates nikkomycin biosynthesis in *Streptomyces*. *J. Biol. Chem.* 293, 20029–20040. doi: 10.1074/jbc.RA118.005667

Wei, J., He, L., and Niu, G. (2018). Regulation of antibiotic biosynthesis in actinomycetes: perspectives and challenges. *Synth. Syst. Biotechnol.* 3, 229–235. doi: 10.1016/j.synbio.2018.10.005

Wu, H., Liang, J., Wang, J., Liang, W. J., Gou, L., Wu, Q., et al. (2018). Cezomycin is activated by CalC to its ester form for further biosynthesis steps in the production of calcimycin in *Streptomyces chartreusis* NRRL 3882. *Appl. Environ. Microbiol.* 84:e586-18. doi: 10.1128/aem.00586-18

Xu, F., Nazari, B., Moon, K., Bushin, L. B., and Seyedsayamdost, M. R. (2017). Discovery of a cryptic antifungal compound from *Streptomyces albus* J1074 using high-throughput elicitor screens. *J. Am. Chem. Soc.* 139, 9203–9212. doi: 10.1021/jacs.7b02716

Xu, F., Wu, Y., Zhang, C., Davis, K. M., Moon, K., Bushin, L. B., et al. (2019). A genetics-free method for high-throughput discovery of cryptic microbial metabolites. *Nat. Chem. Biol.* 15, 161–168. doi: 10.1038/s41589-018-0193-2

Xu, G., Wang, J., Wang, L., Tian, X., Yang, H., Fan, K., et al. (2010). "Pseudo" (-butyrolactone receptors respond to antibiotic signals to coordinate antibiotic biosynthesis. *J. Biol. Chem.* 285, 27440–27448. doi: 10.1074/jbc.M110.143081

Yan, X., Yang, R., Zhao, R. X., Han, J. T., Jia, W. J., Li, D. Y., et al. (2017). Transcriptional regulator PhlH modulates 2,4-diacetylphloroglucinol biosynthesis in response to the biosynthetic intermediate and end product. *Appl. Environ. Microbiol.* 83:e1419-17. doi: 10.1128/AEM.01419-17

Yang, Y. H., Kim, T. W., Park, S. H., Lee, K., Park, H. Y., Song, E., et al. (2009). Cell-free *Escherichia coli*-based system to screen for quorum-sensing molecules interacting with quorum receptor proteins of *Streptomyces coelicolor*. *Appl. Environ. Microbiol.* 75, 6367–6372. doi: 10.1128/AEM.00019-09

Yang, Y. K., Morikawa, M., Shimizu, H., Shioya, S., Suga, K., Nihira, T., et al. (1996). Maximum virginiamycin production by optimization of cultivation conditions in batch culture with autoregulator addition. *Biotechnol. Bioeng.* 49, 437–444. doi: 10.1002/(sici)1097-0290(19960220)49:4<437::aid-bit11>3.3.co;2-t

Yang, Y. K., Shimizu, H., Shioya, S., Suga, K., Nihira, T., and Yamada, Y. (1995). Optimum autoregulator addition strategy for maximum virginiamycin production in batch culture of *Streptomyces virginiae*. *Biotechnol. Bioeng.* 46, 437–442. doi: 10.1002/bit.260460507

Zhang, Y., Pan, G., Zou, Z., Fan, K., Yang, K., and Tan, H. (2013). JadR*-mediated feed-forward regulation of cofactor supply in jadomycin biosynthesis. *Mol. Microbiol.* 90, 884–897. doi: 10.1111/mmi.12406

Zhu, J., Chen, Z., Li, J., and Wen, Y. (2017). AvaR1, a butenolide-type autoregulator receptor in *Streptomyces avermitilis*, directly represses avenolide and avermectin biosynthesis and multiple physiological responses. *Front. Microbiol.* 8:2577. doi: 10.3389/fmicb.2017.02577

Zhu, J., Sun, D., Liu, W., Chen, Z., Li, J., and Wen, Y. (2016). AvaR2, a pseudo (-butyrolactone receptor homologue from *Streptomyces avermitilis*, is a pleiotropic repressor of avermectin and avenolide biosynthesis and cell growth. *Mol. Microbiol.* 102, 562–578. doi: 10.1111/mmi.13479

Zou, Z., Du, D., Zhang, Y., Zhang, J., Niu, G., and Tan, H. (2014). A (-butyrolactone-sensing activator/repressor, JadR3, controls a regulatory mini-network for jadomycin biosynthesis. *Mol. Microbiol.* 94, 490–505. doi: 10.1111/mmi.12752

Conflict of Interest: The authors declare that the research was conducted in the absence of any commercial or financial relationships that could be construed as a potential conflict of interest.

frontiers in Microbiology

ORIGINAL RESEARCH
published: 21 January 2020
doi: 10.3389/fmicb.2020.00008

New Molecular Tools for Regulation and Improvement of A40926 Glycopeptide Antibiotic Production in *Nonomuraea gerenzanensis* ATCC 39727

Oleksandr Yushchuk[1], Andres Andreo-Vidal[1], Giorgia Letizia Marcone[1], Mervyn Bibb[2], Flavia Marinelli[1] and Elisa Binda[1]*

[1]Department of Biotechnology and Life Sciences, University of Insubria, Varese, Italy, [2]Department of Molecular Microbiology, John Innes Centre, Norwich Research Park, Norwich, United Kingdom

Genome sequencing has revealed that *Nonomuraea* spp. represent a still largely unexplored source of specialized metabolites. *Nonomuraea gerenzanensis* ATCC 39727 is the most studied representative species since it produces the glycopeptide antibiotic (GPA) A40926 – the precursor of the clinically relevant antibiotic dalbavancin, approved by the FDA in 2014 for the treatment of acute skin infections caused by multi-drug resistant Gram-positive pathogens. The clinical relevance of dalbavancin has prompted increased attention on A40926 biosynthesis and its regulation. In this paper, we investigated how to enhance the genetic toolkit for members of the *Nonomuraea* genus, which have proved quite recalcitrant to genetic manipulation. By constructing promoter-probe vectors, we tested the activity of 11 promoters (heterologous and native) using the GusA reporter system in *N. gerenzanensis* and in *Nonomuraea coxensis*; this latter species is phylogenetically distant from *N. gerenzanesis* and also possesses the genetic potential to produce A40926 or a very similar GPA. Finally, the strongest constitutive promoter analyzed in this study, *aac(3) IVp*, was used to overexpress the cluster-situated regulatory genes controlling A40926 biosynthesis (*dbv3* and *dbv4* from *N. gerenzanensis* and *nocRI* from *N. coxensis*) in *N. gerenzanensis*, and the growth and productivity of the best performing strains were assessed at bioreactor scale using an industrial production medium. Overexpression of positive pathway-specific regulatory genes resulted in a significant increase in the level of A40926 production in *N. gerenzanensis*, providing a new knowledge-based approach to strain improvement for this valuable glycopeptide antibiotic.

Keywords: A40926, *Nonomuraea*, glycopeptide antibiotics, pathway-specific regulators, strain improvement

OPEN ACCESS

Edited by:
Yvonne Mast, German Collection of Microorganisms and Cell Cultures GmbH (DSMZ), Germany

Reviewed by:
Max Julian Cryle, Monash University, Australia
Marta Vaz Mendes, University of Porto, Portugal

****Correspondence:***
Flavia Marinelli
flavia.marinelli@uninsubria.it

Specialty section:
This article was submitted to Antimicrobials, Resistance and Chemotherapy, a section of the journal Frontiers in Microbiology

Received: *11 November 2019*
Accepted: *06 January 2020*
Published: *21 January 2020*

Citation:
Yushchuk O, Andreo-Vidal A, Marcone GL, Bibb M, Marinelli F and Binda E (2020) New Molecular Tools for Regulation and Improvement of A40926 Glycopeptide Antibiotic Production in Nonomuraea gerenzanensis ATCC 39727. Front. Microbiol. 11:8. doi: 10.3389/fmicb.2020.00008

INTRODUCTION

Research on glycopeptide antibiotics (GPAs) – drugs of "last resort" for treating severe infections caused by multi-drug resistant Gram-positive pathogens – has experienced a "renaissance" over the last decade (Marcone et al., 2018). Clinically important GPAs include two natural products (vancomycin and teicoplanin) and three second generation antibiotics (telavancin,

dalbavancin, and oritavancin), which are semisynthetic derivatives of natural products endowed with an increased antimicrobial potency and superior pharmacokinetic properties. The urgent need for new potent antibiotics has driven much recent interest in GPAs. For example, chemical synthesis recently resulted in the generation of a plethora of vancomycin derivatives with novel modifications that show superior antimicrobial activities (Okano et al., 2017; Wu and Boger, 2019), while teicoplanin has been conjugated with nanoparticles resulting in increased activity against biofilm-forming pathogens (Armenia et al., 2018).

In contrast, genetic manipulation of GPA producers to yield novel potent derivatives is in its infancy. Recent work (Haslinger et al., 2015; Peschke et al., 2017; Schoppet et al., 2019) has revealed new details of the specificity and timing of non-ribosomal peptide synthesis, including chlorination and cross-linking steps, suggesting that the use of combinatorial biosynthesis to generate GPAs with completely novel oligopeptide scaffolds should be possible. In parallel, heterologous expression of enzymes involved in later stages of GPA biosynthesis (glycosylation, sulfation, acylation etc.) in known producers or *in vitro* has already generated novel GPA derivatives that could not be prepared easily by chemical synthesis (Banik and Brady, 2008; Banik et al., 2010; Yim et al., 2014).

In the meantime, genome sequencing has revealed the organization of GPA biosynthetic gene clusters (BGCs) in industrially valuable actinobacteria (D'Argenio et al., 2016), including long known GPA-producers (Vongsangnak et al., 2012; Truman et al., 2014; Kusserow and Gulder, 2017; Nazari et al., 2017; Adamek et al., 2018) as well as in novel producing strains (Thaker et al., 2013; Stegmann et al., 2014). Although the global regulation of GPA biosynthesis is still largely unexplored, the pathway-specific regulation controlling the expression of BGCs is being elucidated in model systems (Bibb, 2013). The roles of cluster-situated regulatory genes have been investigated in *Amycolatopsis balhimycina* (Shawky et al., 2007), *Nonomuraea gerenzanensis* (Lo Grasso et al., 2015; Alduina et al., 2018), and *Actinoplanes teichomyceticus* (Horbal et al., 2014b; Yushchuk et al., 2019), producing balhimycin, A40926 (the natural precursor of dalbavancin), and teicoplanin, respectively. Overexpression of the teicoplanin cluster-situated regulatory genes (*tei15**, coding for a StrR-like transcriptional regulator, and *tei16**, coding for a LuxR-type regulator) in *A. teichomyceticus* markedly increased teicoplanin production in the wild type strain, representing one of the most successful examples of using molecular tools for improving antibiotic production (Horbal et al., 2012, 2014b). In this work, we investigated the potential of molecular tools to improve the production of A40926, the dalbavancin precursor.

The BGC for A40926, named *dbv*, contains two genes encoding transcriptional regulators: *dbv3* and *dbv4* (Lo Grasso et al., 2015). *dbv3* encodes a LuxR-type regulator, which, however, is non-orthologous to the *tei* cluster encoded LuxR-regulator – Tei16* (Yushchuk et al., 2019). *dbv4* codes for a StrR-like transcriptional regulator with close homologues in every GPA BGC (Yushchuk et al., 2019). The A40926-producing strain, recently re-classified as *N. gerenzanensis* (Dalmastri et al., 2016), belongs to a still poorly investigated genus of actinobacteria that was only recently identified as an untapped source of novel antibiotics and other bioactive metabolites (Sungthong and Nakaew, 2015). More recently, fully sequenced genomes of *N. gerenzanensis* (D'Argenio et al., 2016) and of the kistamicin producer *Nonomuraea* sp. ATCC 55076, previously classified as *Actinomadura parvosata* subsp. *kistnae* S382–8 (Kusserow and Gulder, 2017; Nazari et al., 2017), have confirmed the hidden potential of these uncommon actinomycetes as prolific producers of specialized metabolites. In this paper, we report that another member of this genus, *Nonomuraea coxensis* DSM 45129, which was isolated in Bangladesh in 2007 (Ara et al., 2007), has the genetic potential to produce A40926 or a very similar GPA; its BGC contains two regulatory genes, *nocRI* and *nocRII*, which are close homologs of *dbv3* and *dbv4*, respectively. Thus, we first developed the molecular tools to manipulate both *N. gerenzanensis* and *N. coxensis*, we then selected the strongest heterologous promoter to drive gene expression in *Nonomuraea* spp., and finally we overexpressed both native and heterologous cluster-specific regulatory genes in *N. gerenzanensis*, assessing the best performers at flask and bioreactor scale in industrial media. The overexpression of the positive pathway-specific regulators significantly increased the level of A40926 production in *N. gerenzanensis*, paving the way for knowledge-based strain improvement for the production of this valuable GPA.

MATERIALS AND METHODS

Plasmids, Bacterial Strains, Antibiotics, and Culture Conditions

Plasmids and bacterial strains used in this work are summarized in **Table 1**. Compositions of media are given in ESM. Unless otherwise stated, all media components and antibiotics were supplied by Sigma-Aldrich, St. Louis, MO, United States. For routine maintenance, actinobacterial strains were cultivated on ISP3 or VM0.1 agar media supplemented with 50 μg/ml apramycin-sulfate when appropriate. For genomic DNA isolation, *N. gerenzanensis* ATCC 39727 and *N. coxensis* DSM 45129 were grown in 250 ml Erlenmeyer flasks containing 10 glass beads (ø5 mm) with 50 ml of liquid VSP medium on an orbital shaker at 220 rpm and at 30°C. Working cell banks (WCB) of *Nonomuraea* spp. were prepared as described previously (Marcone et al., 2014). *Escherichia coli* DH5α was used as a routine cloning host and *E. coli* ET12567 pUZ8002 as a donor for intergeneric conjugations. *E. coli* strains were grown at 37°C in LB liquid or agar media supplemented with 100 μg/ml of apramycin-sulfate, 50 μg/ml of kanamycin-sulfate and 25 μg/ml of chloramphenicol when appropriate.

Generation of Recombinant Plasmids

Construction of Promoter-Probe Vectors

To test the activity of different native *N. gerenzanensis* promoters, pSAGA (Koshla et al., 2019), where *gusA* (Myronovskyi et al., 2011) is expressed from *aac(3)IVp*, was chosen as a chassis. Genomic DNA, extracted from *N. gerenzanensis* according to the Kirby procedure (Kieser et al., 2000), was used as a template

to amplify the putative promoter regions of: *BN4615_P641* (coding for the DNA gyrase B subunit – $GyrB_{ng}$) 342 bp; *BN4615_P8899* (coding for the RNA polymerase sigma factor RpoD – $HrdB_{ng}$), 524 bp; *BN4615_P604* (coding for the single-stranded DNA-binding protein – Ssb_{ng}), 207 bp; *BN4615_P1543* (coding for the SSU ribosomal protein S12p – $RpsL_{ng}$), 339 bp; *BN4615_P7269* (coding for the rifamycin-resistant RNA polymerase subunit β – $RpoB_{Rng}$), 558 bp; and *BN4615_P1539* (coding for the rifamycin-sensitive RNA polymerase subunit β – $RpoB_{ng}$), 493 bp. Amplicons were generated using Q5 High-Fidelity DNA Polymerase (New England Biolabs, Ipswich, MA, United States) according to the supplier's protocol and the oligonucleotide primers listed in **Table 2**. All of the amplicons were digested with *Bam*HI and *Eco*RV and cloned in pSAGA cleaved with the same endonucleases, thus replacing *aac(3)IVp* in front of *gusA* with each of the amplified promoter regions. The resulting recombinant plasmids were named pGBP (carrying $gyrB_{ng}p$), pHBP ($hrdB_{ng}p$), pSBP ($ssb_{ng}p$), pRLP ($rpsL_{ng}p$), pRBP1 ($rpoB_{ng}p$), and pRBP2 ($rpoB_{Rng}p$).

Construction of the *dbv3*, *dbv4*, and *nocRI* Overexpression Plasmids

The coding sequences of *dbv3* (2,635 bp) and *dbv4* (1,006 bp) were amplified from the A40Y cosmid (**Table 1**; Marcone et al., 2010a) using Q5 High-Fidelity DNA Polymerase and the dbv3_F/R or dbv4_F/R primer pairs (**Table 2**). The obtained amplicons were digested with *Eco*RI and *Eco*RV and cloned into pSET152A cleaved with the same enzymes. The resulting plasmids were named pSAD3 and pSAD4. To generate a vector for the overexpression of both *dbv3* and *dbv4*, the regions containing the coding sequences of both genes were amplified using the dbv4_F/dbv3_R primer pair and cloned into pSET152A in a similar fashion, generating pSAD3–4.

To construct the vector for overexpression of *nocRI* (the *dbv3* ortholog from *N. coxensis*), the coding sequence of *A3G7_RS0138355* was amplified from the genomic DNA of *N. coxensis* isolated using the Kirby procedure (Kieser et al., 2000) using Q5 High-Fidelity DNA Polymerase and the orfR1_F/R primer pair (**Table 2**). The obtained amplicon (2,661 bp) was digested with *Eco*RI and *Eco*RV and cloned into pSET152A cut with the same enzymes to generate pSAR1. All of the generated recombinant plasmids were verified by restriction endonuclease mapping and sequencing at BMR Genomics (University of Padua, Italy).

Conjugative Transfer of Plasmids Into *Nonomuraea* spp. and Verification of the Recombinant Strains

Conjugative transfer of plasmids into *N. gerenzanensis* was performed essentially as described previously (Marcone et al., 2010c). All recombinant plasmids were transferred individually into the non-methylating *E. coli* ET12567 pUZ8002 and the resulting derivatives used as donor strains for intergeneric conjugation. To prepare fresh vegetative mycelium of *N. gerenzanensis* prior to conjugal transfer, one vial of WCB was inoculated into 50 ml of VSP medium (250 ml Erlenmeyer

TABLE 1 | Bacterial strains and plasmids used in this work.

Name	Description	Source of reference
N. gerenzanensis	Wild type, A40926 producer	ATCC 39727
N. coxensis	Wild type	DSM 45129
N. gerenzanensis pSET152A$^+$	Wild type derivative carrying pSET152A	This work
N. gerenzanensis pSAD3$^+$	Wild type derivative carrying pSAD3	This work
N. gerenzanensis pSAD4$^+$	Wild type derivative carrying pSAD4	This work
N. gerenzanensis pSAD3–4$^+$	Wild type derivative carrying pSAD3–4	This work
N. gerenzanensis pSAR1$^+$	Wild type derivative carrying pSAR1	This work
N. gerenzanensis pSAGA$^+$	Wild type derivative carrying pSAGA	This work
N. gerenzanensis pTEGA$^+$	Wild type derivative carrying pTEGA	This work
N. gerenzanensis pGUSmoeE5script$^+$	Wild type derivative carrying pGUSmoeE5script	This work
N. gerenzanensis pGCymRP21$^+$	Wild type derivative carrying pGCymRP21	This work
N. gerenzanensis pGT2p$^+$	Wild type derivative carrying pGT2p	This work
N. gerenzanensis pGBP$^+$	Wild type derivative carrying pGBP	This work
N. gerenzanensis pHBP$^+$	Wild type derivative carrying pHBP	This work
N. gerenzanensis pSBP$^+$	Wild type derivative carrying pSBP	This work
N. gerenzanensis pRLP$^+$	Wild type derivative carrying pRLP	This work
N. gerenzanensis pRBP1$^+$	Wild type derivative carrying pRBP1	This work
N. gerenzanensis pRBP2$^+$	Wild type derivative carrying pRBP2	This work
N. coxensis pSAGA$^+$	Wild type derivative carrying pSAGA	This work
N. coxensis pTEGA$^+$	Wild type derivative carrying pTEGA	This work
N. coxensis pGUSmoeE5script$^+$	Wild type derivative carrying pGUSmoeE5script	This work
N. coxensis pGCymRP21$^+$	Wild type derivative carrying pGCymRP21	This work
N. coxensis pGT2p$^+$	Wild type derivative carrying pGT2p	This work
N. coxensis pGBP$^+$	Wild type derivative carrying pGBP	This work
N. coxensis pHBP$^+$	Wild type derivative carrying pHBP	This work
N. coxensis pSBP$^+$	Wild type derivative carrying pSBP	This work
N. coxensis pRLP$^+$	Wild type derivative carrying pRLP	This work
N. coxensis pRBP1$^+$	Wild type derivative carrying pRBP1	This work
N. coxensis pRBP2$^+$	Wild type derivative carrying pRBP2	This work
E. coli DH5α	General cloning host	MBI Fermentas, USA
E. coli ET12567 pUZ8002	(*dam-13*::Tn9 *dcm-6*), pUZ8002$^+$ (Δ*oriT*), used for conjugative transfer of DNA	Kieser et al. (2000)

(Continued)

TABLE 1 | Continued

Name	Description	Source of reference
A40Y	SuperCos1 derivative, including 22 kb of *dbv* cluster (*dbv1-dbv17*)	Marcone et al. (2010a)
pGUS	pSET152 derivative, containing promoterless *gusA*	Myronovskyi et al. (2011)
pSET152A	pSET152 derivative, containing *aac(3)IVp* from pIJ773	Horbal et al. (2013)
pSAD3	pSET152A derivative, containing *dbv3* under the control of *aac(3)IVp*	This work
pSAD4	pSET152A derivative, containing *dbv4* under the control of *aac(3)IVp*	This work
pSAD3–4	pSET152A derivative, containing *dbv4* together with *dbv3*	This work
pSAR1	pSET152A derivative, containing *nocRI* under the control of *aac(3)IVp*	This work
pSAGA	pSET152A derivative, containing *gusA* under the control of *aac(3)IVp*	Koshla et al. (2019)
pTEGA	pTES derivative, containing *gusA* under the control of *ermEp*	Yushchuk et al. (2020a)
pGUSmoeE5script	pGUS derivative, containing *gusA* under the control of *moeE5p*	Makitrynskyy et al. (2013)
pGCymRP21	pGUS derivative, containing CymR operator, *P21* promoter and *cymR* gene	Horbal et al. (2014a)
pGT2p	pGUS derivative, containing *gusA* under the control of *tei2p*	Yushchuk et al. (2020b)
pGBP	pSAGA derivative, containing *gusA* under the control of $gyrB_{ng}p$	This work
pHBP	pSAGA derivative, containing *gusA* under the control of $hrdB_{ng}p$	This work
pSBP	pSAGA derivative, containing *gusA* under the control of $ssb_{ng}p$	This work
pRLP	pSAGA derivative, containing *gusA* under the control of $rpsL_{ng}p$	This work
pRBP1	pSAGA derivative, containing *gusA* under the control of $rpoB_{ng}p$	This work
pRBP2	pSAGA derivative, containing *gusA* under the control of $rpoB_{Rng}p$	This work

flask with 10 ø5 mm glass beads) and incubated for 48 h on the orbital shaker at 220 rpm and at 30°C. The mycelium was collected by centrifugation (10 min, 3,220 × *g*), washed twice with sterile 20% v/v glycerol, resuspended in the same solution to a final volume of 20 ml, and stored at −80°C. 1 ml of mycelial suspension was mixed with approximately 10^9 of donor *E. coli* cells and the mixtures were plated on well dried VM0.1 agar plates supplemented with 20 mM of $MgCl_2$. After 12–16 h of incubation at 30°C, each plate was overlaid with 1 ml of sterile deionized water containing 1.25 mg of apramycin-sulfate and 750 μg of nalidixic acid sodium salt. Transconjugants were selected as resistant to 50 μg/ml of apramycin-sulfate.

Spore suspensions of *N. coxensis* were prepared from lawns grown on ISP3 agar for 7 days. Spores from one plate were collected in deionized water and filtered through one layer of Miracloth (Merck KGaA, Darmstadt, Germany) to remove vegetative mycelial fragments. Then, spores were pelleted from a 50 ml suspension by centrifugation (15 min, 3,220 × *g*), resuspended in 1 ml of 15% v/v glycerol, and stored at −80°C. For conjugation, approx. 10^6 spores were mixed with 10^7 *E. coli* donor cells and plated on VM0.1 agar plates supplemented with 20 mM of $MgCl_2$. The overlay for the selection of transconjugants was performed as described previously for *N. gerenzanensis*.

To verify the integration of promoter-probe vectors, an ~1 kbp internal fragment of *gusA* was amplified from the genomic DNA of recombinant *N. gerenzanensis* or *N. coxensis* strains using the gusA_ver_F/R primer pair (**Table 2**). To verify the integration of pSET152A, *aac(3)IV* was amplified using the aac(3)IV_F/R primer pair (**Table 2**). To verify the integration of pSAD4, an ~1 kbp fragment of pSAD4 was amplified with the PAM_seq_F/dbv4_R primer pair (**Table 2**), in which PAM_seq_F anneals within the *aac(3)IVp* sequence. Verification of pSAD3 and pSAD3–4 integration was made by amplification of an ~2 kbp fragment (for pSAD3) or an ~3 kbp fragment (for pSAD3–4), using the PAM_seq_F/dbv3_seq_R primer pair (**Table 2**), in which dbv3_seq_R anneals in the middle of *dbv3*. Finally, to verify the integration of pSAR1 an ~2 kbp fragment was amplified using the PAM_seq_F/orfR1mid_EcoRV_R (**Table 2**) primer pair, in which orfR1mid_EcoRV_R anneals in the middle of *nocRI*.

β-Glucuronidase Activity Assay

β-Glucuronidase (GusA) activity in *Nonomuraea* strains growing on VM0.1 agar medium was assessed by adding, after 6 days of cultivation at 30°C, 10 μl drops of 5-bromo-4-chloro-3-indolyl-β-D-glucuronide (X-Gluc, Thermo Fisher Scientific, Waltham, MA, United States) 50 mg/ml in DMSO to the surfaces of the lawns. Chromogenic conversion of X-Gluc into the blue-colored 5,5′-dibromo-4,4′-dichloro-indigo was monitored after 1 h of incubation. For the quantitative measurements of GusA activity, *Nonomuraea* strains were grown in liquid media. One WCB vial of each of the strains was inoculated into a baffled 500 ml Erlenmeyer flask containing 100 ml of E26 (*N. gerenzanensis* strains) or of VSP (*N. coxensis* strains). After 72 h of cultivation, 10% v/v of this preculture was transferred into a baffled 500 ml Erlenmeyer flask containing 100 ml of FM2 (*N. gerenzanensis* strains) or ISP2 (*N. coxensis* strains). To induce *P21-cmt*-driven *gusA*-expression, cumate was added at the final concentration of 50 μM to cultures carrying pGCymRP21 24 h after inoculation. After 120 h of cultivation, mycelial lysates were prepared as previously reported by Horbal et al., 2013. Glucuronidase activity was measured as previously described (Myronovskyi et al., 2011; Horbal et al., 2013) using

TABLE 2 | Oligonucleotide primers used in this work.

Primer	Nucleotide sequence (5′-3′)*	Purpose
Dbv3_F	TTTGATATCGGAGGGCAAGAGTGCTGTTCGGGC	Cloning of *dbv3* into pSET152A
Dbv3_R	TTTGAATTCCTCTACAGCCGCACTGCCT	
dbv4_F	TTTGATATCGGAGGGGCTAGGTGGACCCGACGG	Cloning of *dbv4* into pSET152A
dbv4_R	TTTGAATTCTCCACTCGTGCTCATCCAG	
PAM_seq_F	GATGTCATCAGCGGTGGAG	Verification of recombinant strains
dbv3_seq_R	CCAGCGCTGGACCGCCTGC	
orfR1nid_EcoRV_rev	TTTGATATCGCAAGGGGCCTCCCCGCCG	
orfR1_F	TTTGATATCGGAGGACTGCGTTGACGAACCGCT	Cloning of *nocRI* into pSET152A
orfR1_R	TTTGAATTCGCGTCATGGGACCACCGCC	
hrdBp_F	TTTGGATCCACCGAAGCGCCGCCTGAGG	Cloning of $hrdB_{ng}p$
hrdBp_R	TTTGATATCGAAGGCCTGACGGACATCC	
rpoB1p_F	TTTGGATCCTCTCGCTGGCTGGTGGCCG	Cloning of $rpoB_{ng}p$
rpoB1p_R	TTTGATATCTCGCGGCGGACTGACTACA	
rpoB2p_F	TTTGGATCCTGTCGTACTGCTC	Cloning of $rpoB_{Rng}p$
rpoB2p_R	TTTGATATCATACGAAGGCGAGGGAGGG	
rpsLp_F	TTTGGATCCATGGACGGCGGAGCTGTAG	Cloning of $rpsL_{ng}p$
rpsLp_R	TTTGATATCTTGGCCGGTGTTACGTCA	
ssbp_F	TTTGGATCCAAGTCCGAAGGCATCTACG	Cloning of $ssb_{ng}p$
ssbp_R	TTTGATATCTGCACGCCTTCGCTTGGGT	
gyrBAp_F	TTTGGATCCAGGCTTCGCACAGTAACGG	Cloning of $gyrB_{ng}p$
gyrBAp_R	TTTGATATCGCGGACACGCGGCGGGGGA	
aac(3)IV_F	ATCGACTGATGTCATCAGCG	Amplification of *aac(3)IV*
aac(3)IV_R	CGAGCTGAAGAAAGACAAT	
gusA_ver_F	GGCGGCTACACGCCCTTCGA	Amplification of *gusA* internal fragment
gusA_ver_R	TGATGGGCCGGGTGGGGTC	

**Restriction sites are underlined in primer sequence.*

a spectrophotometric assay following the conversion of the colorless *p*-nitrophenyl-β-D-glucuronide (Thermo Fisher Scientific, Waltham, MA, United States) into the colored *p*-nitrophenol at 415 nm using an Infinite 200 PRO microplate reader (Tecan, Switzerland). Glucuronidase activity was normalized to dry biomass weight as previously reported (Marcone et al., 2014). One unit of activity is defined as the amount of enzyme that is able to convert 1 μM of substrate in 1 min.

A40926 Production

One WCB vial was inoculated into 300 ml baffled flasks containing 50 ml of vegetative medium E26 with 10 glass beads (ø5 mm). Flask cultures were incubated for 72 h on a rotary shaker at 220 rpm and 30°C and then used to inoculate (10% v/v) 500 ml baffled Erlenmeyer flasks containing 100 ml of FM2 medium or a 3-l P-100 Applikon glass reactor (height 250 mm, ø130 mm) equipped with a AD1030 Biocontroller and AD1032 motor, and containing 2 l of the same production medium. Cultivations in FM2 in shake-flasks were conducted at 30°C and 220 rpm. Bioreactor fermentations were conducted at 30°C, with stirring at 450 rpm (corresponding to 1.17 m/s of tip speed) and 2 l/min aeration rate. Dissolved oxygen (measured as % pO2) was monitored using an Ingold polarographic oxygen electrode. The pH values of culture broths were monitored using a pH meter. Foam production was controlled by adding Hodag antifoam (Hodag Chemical Corporation, Chicago, IL, United States) through an antifoam sensor. Samples were collected at regular cultivation time intervals and analyzed to estimate biomass (dry weight), glucose consumption (Diastix sticks, Bayer AG, Leverkusen, Germany), and A40926 production.

HPLC Analysis of Culture Extracts

A40926 was extracted from *Nonomuraea* spp. cultures as previously reported (Marcone et al., 2014). Chromatography was performed with a VWR Hitachi diode array L-2455 HPLC system with detection at 254 nm. The A40926 titers in the batch cultivations were estimated by injecting 50 μl of sample onto a 5 μm-particle-size Ultrasphere ODS (Beckman) HPLC column (4.6 by 250 mm) and eluting at a flow rate of 1 ml/min with a 30 min linear gradient from 15 to 64% of phase B. Phase A was 32 mM $HCOONH_4$ (pH 7) – CH_3CN [90:10 (vol/vol)], and phase B was 32 mM $HCOONH_4$ (pH 7) – CH_3CN [30:70 (vol/vol)]. A volume of 50 μl of a pure sample of 200 μg/ml A40926 (Sigma-Aldrich, St. Louis, MO, United States) was used as an internal standard.

Tools for the Bioinformatics Analysis

Blastp was used to search for homologs (Altschul, 1990); protein sequence alignments were performed with Clustal Omega (EMBL-EBI, Sievers et al., 2011).

RESULTS

Genetic Manipulation of *Nonomuraea coxensis*, a Novel Putative Producer of a A40926-Like Molecule

According to the 16S rRNA gene-based reconstruction of *Nonomuraea* phylogeny (Dalmastri et al., 2016), *N. coxensis* occupies a relatively distant position from *N. gerenzanensis*. Conversely, mining the partially sequenced genome of *N. coxensis*

(ASM37988v1), we found a close homolog of the *N. gerenzanensis* regulatory gene *dbv3* (locus *A3G7_RS0138355* in the *N. coxensis* genome, coding for WP_020547054.1 with 86.6% predicted amino acid sequence identity with Dbv3, ESM **Figure 1**). Dbv3 is a unique LuxR-regulator controlling the expression of the A40926 BGC and it is not closely related to the better-characterized family of Tei16*-like regulators controlling teicoplanin biosynthesis, sharing only 32% of amino acid sequence identity with Tei16* (Yushchuk et al., 2019). This *dbv3*-like gene (we named it *nocRI*) was found on a short *N. coxensis* contig (NZ_KB904006) flanking a gene coding for a putative StrR-like transcriptional regulator apparently orthologous to *dbv4* (locus *A3G7*_RS0138355, coding for WP_026215141.1 with 94.39% of amino acid sequence identity with Dbv4); *dbv4* is the other known cluster-situated regulatory gene in the *dbv* BGC and we named the *N. coxensis* homolog *nocRII* (ESM **Figure 2**). AntiSMASH (Blin et al., 2019) analysis of *N. coxensis* genome revealed the presence of three short contigs (NZ_KB904006, NZ_KB903995, NZ_KB903969, ESM **Figure 3**) covering the majority of a *dbv*-like BGC, suggesting that *N. coxensis* might produce A40926 or a very similar GPA. Thus, we considered *N. coxensis* an interesting candidate for developing *Nonomuraea*-targeted genetic tools.

Initially, we tried to transfer *φC31*-based integrative plasmids (**Table 1**) into *N. coxensis* by using the protocol of intergeneric conjugation optimized for conjugal transfer from a DNA-non-methylating *E. coli* donor strain to *N. gerenzanensis* vegetative mycelium (Marcone et al., 2010c). Transconjugants were obtained at a very low frequency (*ca.* 1×10^{-7}) and only for the relatively small pSAGA-based promoter-probe vectors (approx. 6 kbp). Increasing the amount of donor and recipient cells, changing the time of overlay, and adjusting medium composition (including increasing or decreasing $MgCl_2$ concentration) did not allow the transfer of the larger pGUS-based promoter-probe vectors (such as pGUSmoeE5script or pGCymRP21, both more than 9 kbp). Since, unlike *N. gerenzanensis*, *N. coxensis* sporulates abundantly when grown on ISP3 agar medium (ESM **Figure 4**), we tried to use spores for conjugal transfer. This resulted in transfer rates of approximately 1×10^{-3} when 10^6 spores were mixed with 10^7 *E. coli* donor cells, regardless of plasmid size.

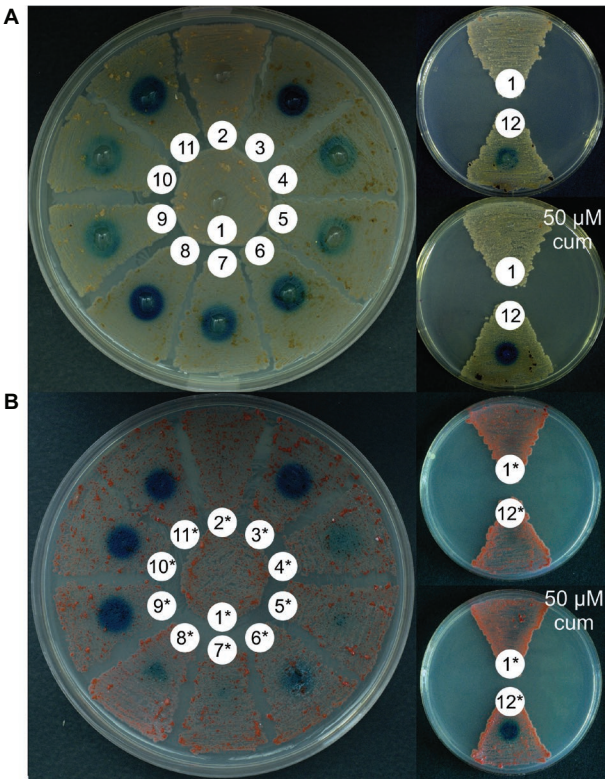

FIGURE 1 | Comparison of GusA activity in recombinant strains of *N. gerenzanensis* **(A)** and *N. coxensis* **(B)**, carrying the following promoter-probe vectors: 2, 2* – pTEGA (*gusA* under the control of *ermEp*); 3, 3* – pSAGA (*gusA* under the control of *aac(3)IVp*); 4, 4* – pHBP (*gusA* under the control of $hrdB_{ng}p$); 5, 5* – pRBP2 (*gusA* under the control of $rpoB_{Rng}p$); 6, 6* – pRBP1 (*gusA* under the control of $rpoB_{ng}p$); 7, 7* – pSBP (*gusA* under the control of $ssb_{ng}p$); 8, 8* – pRLP (*gusA* under the control of $rpsL_{ng}p$); 9, 9* – pGUSmoeE5script (*gusA* under the control of *moeE5p*); 10, 10* – pGT2p (*gusA* under the control of *tei2p*); 11, 11* – pGBP (*gusA* under the control of $gyrB_{ng}p$); 12, 12* – pGCymRP21 (*gusA* under the control of *P21-cmt*). The control parental strains (1, *N. gerenzanensis* and 1*, *N. coxensis*) do not display chromogenic conversion of X-Gluc. Strains were cultivated for 6 days on VM0.1 medium.

Using the GusA-Reporter System to Assess the Activity of Native and Heterologous Promoters in *Nonomuraea* Species

The set of *φC31*-based integrative plasmids transferred to *N. gerenzanensis* and *N. coxensis* were promoter-probe vectors utilizing the GusA reporter system and carrying a selection of native and heterologous promoters, the latter having been used previously to drive gene expression in streptomycetes or actinoplanetes (Horbal et al., 2013, 2014a; Makitrynskyy et al., 2013). Glucuronidase activity of the recombinant *Nonomuraea* strains was assessed qualitatively (on agar plates) and quantitatively (in cell lysates obtained from mycelium grown in liquid medium). Both of the *N. coxensis* and *N. gerenzanensis* wild type strains did not display any glucuronidase activity (**Figure 1**). The heterologous promoters tested were: *aac(3)IVp* (in pSAGA) – the apramycin acetyltransferase gene promoter, derived from pSET152A (Horbal et al., 2013); *ermEp* (in pTEGA, Yushchuk et al., 2020a) – the erythromycin resistance gene promoter from pTES (Herrmann et al., 2012); *moeE5p* (in pGUSmoeE5script) – the *S. ghanaensis* moenomycin biosynthesis gene *moeE5* promoter (Makitrynskyy et al., 2013); *tei2p* (pGT2p, Yushchuk et al., 2020b) – the *A. teichomyceticus* teicoplanin resistance gene *tei2* promoter; and *P21*, a synthetic promoter fused with the cumate inducible *Pseudomonas putida* F1 *cmt* operon operator (in pGCymRP21, Horbal et al., 2014a). In parallel, we tested the activity of six native promoters derived from *N. gerenzanensis* house-keeping genes: $gyrB_{ng}p$ (in pGBP – the promoter of the DNA gyrase B subunit gene); $hrdB_{ng}p$

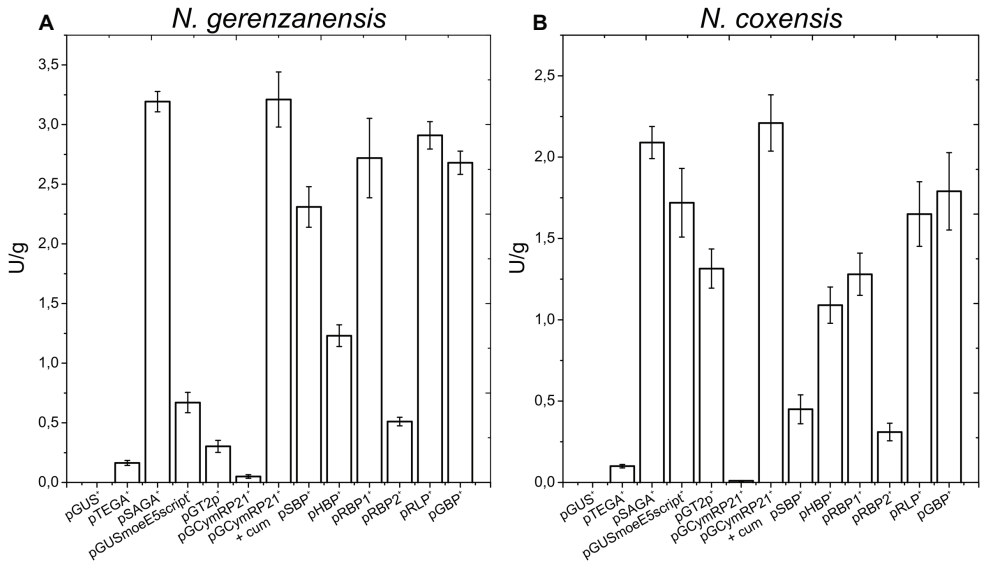

FIGURE 2 | Quantitative measurement of GusA activity (U/gram of dry biomass) in *N. gerenzanensis* **(A)** and *N. coxensis* **(B)** recombinant strains grown in liquid media for 120 h (see growth curves in ESM **Figure 5**), carrying different promoter-probe plasmids. Control strains carried the promoterless pGUS vector and exhibited no GusA activity. Activities are the mean values of three independent experiments. Error bars represent standard deviations.

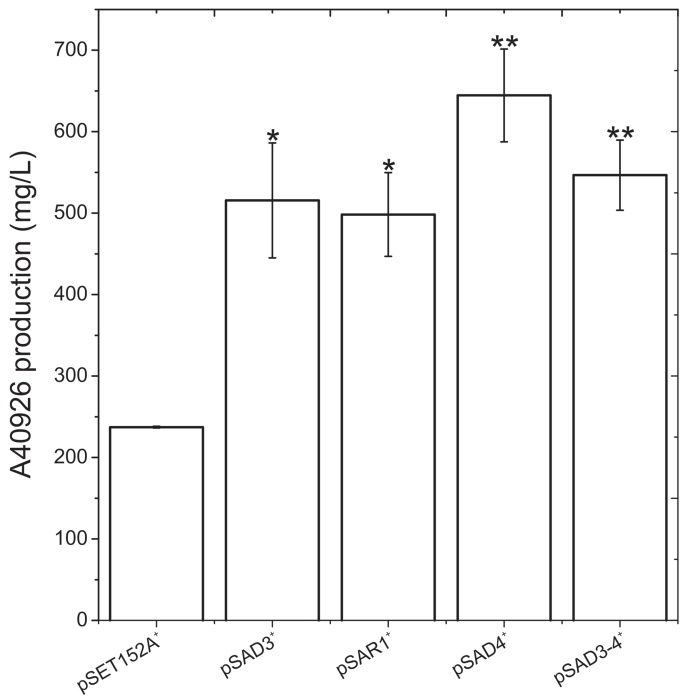

FIGURE 3 | A40926 production in *N. gerenzanensis* carrying the empty vector pSET152A+ and in its recombinant strains overexpressing *dbv3* (pSAD3), *nocRI* (pSAR1), *dbv4* (pSAD4), and co-expressing *dbv3* and *dbv4* genes (pSAD3–4) cultivated in FM2 industrial medium at 500 ml Erlenmeyer flasks-scale. A40926 production was measured after 120 h of cultivation. The results given represent three independent fermentations, error bars represent standard deviations. Statistical significance of the differences in A40926 production between the control and the recombinant strains was estimated using Welch's *t*-test: $*p < 0.05$; $**p < 0.01$.

(in pHBP – the promoter of the RNA polymerase σ-factor RpoD gene); $ssb_{ng}p$ (in pSBP – the promoter of the single-stranded DNA-binding protein); $rpsL_{ng}p$ (in pRLP – the promoter of the SSU ribosomal protein S12p gene); $rpoB_{Rng}p$ (in pRBP2 – the promoter of the rifamycin-resistant RNA polymerase subunit β gene); and $rpoB_{ng}p$ (in pRBP1 – the

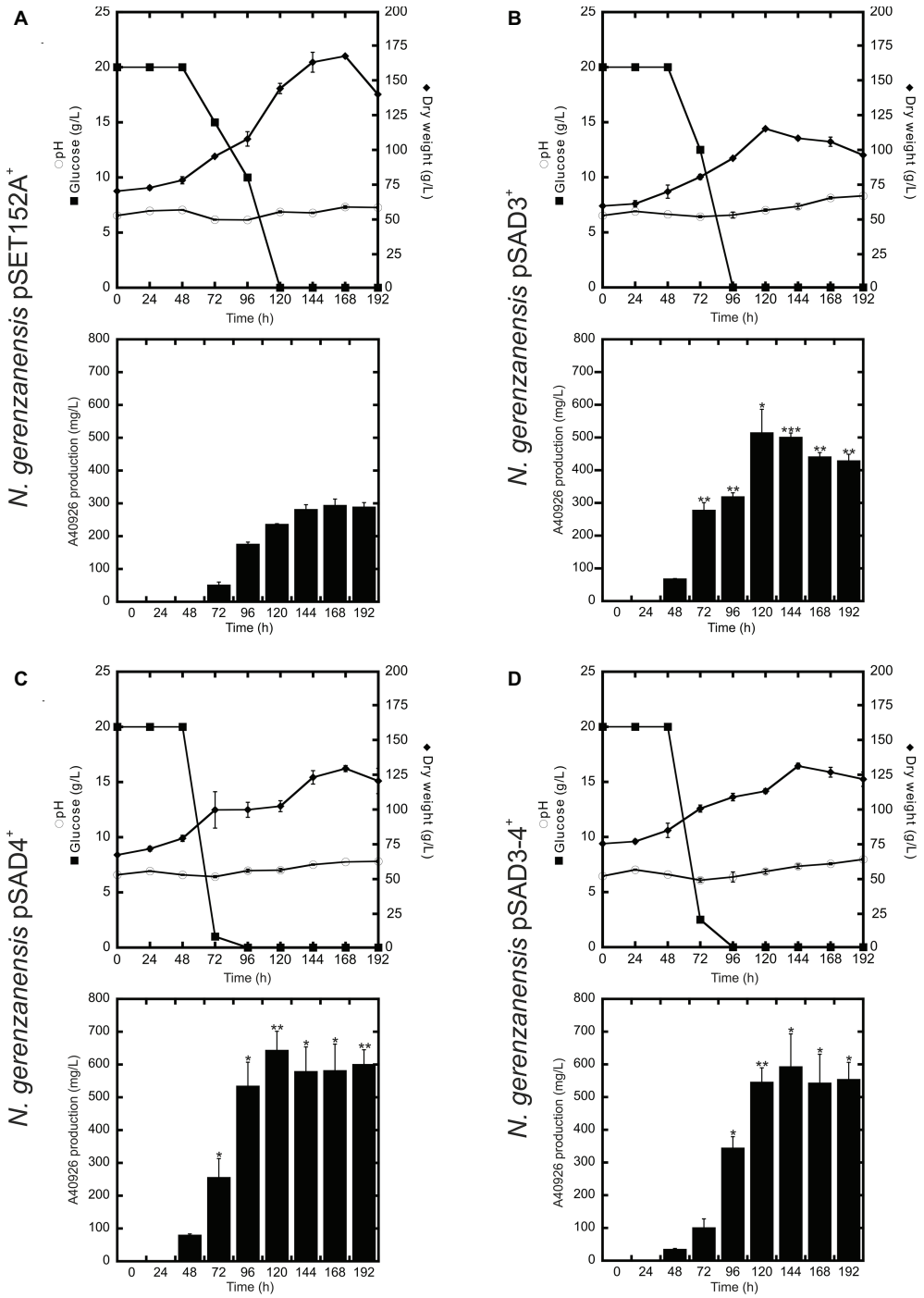

FIGURE 4 | Time courses of *N. gerenzanensis* pSET152A+ **(A)** and recombinant strains overexpressing *dbv3* **(B)**, *dbv4* **(C)** and co-expressing both genes **(D)** cultivated in FM2 industrial medium in 500 ml Erlenmeyer flasks. Glucose consumption (filled rectangles), biomass accumulation (filled rhombi), pH (circles), and A40926 production were monitored every 24 h. Results given are mean values of three independent experiments. Error bars represent standard deviations. Statistical significance of the differences in A40926 production between the control and the recombinant strains was estimated using Welch's *t*-test: $^{*}p < 0.05$; $^{**}p < 0.01$; $^{***}p < 0.001$.

promoter of the rifamycin-sensitive RNA polymerase subunit β gene). In contrast to the wild type strains, all of the recombinant derivatives grown on VM0.1 agar plates converted X-Gluc to its colored derivative 5,5′-dibromo-4,4′-dichloro-indigo, albeit to different extents (**Figure 1**). *N. gerenzanensis* pSAGA+ and *N. coxensis* pSAGA+, carrying *aac(3)IVp*, produced

the most intensive color (**Figures 1A,B**), while the chromogenic conversion of X-Gluc in *N. gerenzanensis* pTEGA$^+$ and *N. coxensis* pTEGA$^+$, carrying the *ermEp*, was only slightly visible. In strains carrying the inducible pGCymRP21, GusA activity was induced by the addition of 50 μM of cumate, proving inducible gene expression (**Figures 1A,B**). However, in *N. gerenzanensis* pGCymRP21$^+$, a basal level of GusA activity was detected even in the absence of cumate (**Figure 1A**). Contrary to this, no basal level of expression from *P21-cmt* was detected in *N. coxensis* pGCymRP21$^+$ (**Figure 1B**).

When the glucuronidase activity present in cell lysates obtained from liquid cultures grown for 120 h (late exponential/early stationary growth phase, see ESM **Figure 5**) was measured using a spectrophotometric assay, overall these quantitative results (normalized for the dry weight of the differently growing strains) correlated with those observed on agar plates: *aac(3)IVp* behaved as a strong promoter in both *N. gerenzanensis* and *N. coxensis*, surpassed only by *cmt-P21p* when induced by the addition of 50 μM cumate (**Figures 2A,B**). Also $rpsL_{ng}p$ and $hrdB_{ng}p$ proved to be strong promoters in both of the *Nonomuraea* spp. whereas the weakest was the *ermEp* (**Figures 2A,B**). Interestingly, the activity of $rpoB_{ng}P$ was higher than that of $rpoB_{Rng}p$ (**Figures 1**, **2**), consistent with previously reported data about differences in transcription levels of the two alleles (Vigliotta et al., 2004).

Knowledge-Based Generation of A40926 Overproducing Strains

Since *aac(3)IVp* was identified as the strongest constitutive promoter for *Nonomuraea* spp., we used it to overexpress *dbv3* and *dbv4* in *N. gerenzanensis*. Both genes were cloned into the integrative pSET152A vector (Horbal et al., 2013) yielding the recombinant vectors pSAD3 and pSAD4, respectively (**Table 1**). Benefiting from the neighboring positions of *dbv3* and *dbv4*, we also cloned them together, generating pSAD3–4, where *dbv4* was directly under the control of *aac(3)IVp*, but *dbv3* remained under the control of its native promoter (**Table 1**). Additionally, the *dbv3*-like *nocRI* from *N. coxensis* was cloned into pSET152A, generating pSAR1, and transferred to *N. gerenzanensis* to determine if it could improve A40926 production, and to assess possible cross-talk between the regulators from the two different *Nonomuraea* spp. All the *N. gerenzanensis* recombinant strains were grown for 120 h in parallel with the control strain carrying the empty vector and A40926 production was measured (**Figure 3**). The production of A40926 in *N. gerenzanensis* carrying pSET152A reached almost 250 mg/l after 120 h of cultivation (**Figure 3**). The four recombinant strains overexpressing the cluster-situated regulatory genes produced more antibiotic than the control strain (**Figure 3**). A40926 production in *N. gerenzanensis* pSAD3$^+$ and pSAR1$^+$ was comparable (*ca*. 500 mg/l), proving that *nocRI* had a similar impact in *N. gerenzanensis* as *dbv3*. The recombinant strain carrying pSAD3–4 vector produced slightly more, around 550 mg/l, whereas the best producer in these conditions was the strain overexpressing *dbv4*, which produced more than 650 mg/l.

Time Courses of A40926 Production in *Nonomuraea gerenzanensis* Recombinant Strains at Flask and at Bioreactor Scale

Although further investigations will be devoted to the expression of the heterologous *nocRI* and *nocRII in N. gerenzanensis*, in our strain improvement work we then focused on *N. gerenzanensis* strains overexpressing native regulators. Consequently, *N. gerenzanensis* strains containing pSET152A, pSAD3, pSAD4, or pSAD3–4 were grown for 192 h in parallel with the control strain carrying the empty vector using the previously optimized industrial medium FM2 (Marcone et al., 2010a, 2014) at flask scale. Samples for the analysis of dry weight, pH, glucose consumption, and A40926 production were collected at regular 24 h intervals. All three recombinant strains expressing the regulatory genes from *aac(3)IVp* accumulated detectable amounts of A40926 earlier than the empty vector control (**Figure 4**). A40926 production reached its peak after 120 h of growth for *N. gerenzanensis* pSAD3$^+$ (*ca.* 500 mg/l) (**Figure 4B**) and pSAD4$^+$ (nearly 650 mg/l) (**Figure 4C**), whereas in pSAD3–4$^+$ the maximum productivity (*ca*. 600 mg/l) was delayed to 144 h (**Figure 4D**). The control strain produced *ca.* 300 mg/l after 144–168 h from inoculation (**Figure 4A**). Although glucose consumption was faster in the recombinant strains containing the cloned regulatory genes in comparison to the control, they accumulated less biomass than *N. gerenzanensis* pSET152A$^+$ (**Figure 4**). Maximum biomass production was around 125 g/l (dry weight) in the overexpression strains versus the 175 g/l produced by the empty vector control strain. These data suggest that part of the consumed glucose was used by the strains carrying the regulatory genes under the control of the strong constitutive promoter *aac(3)IVp* to support antibiotic production at the detriment of biomass formation.

When the cultivation of recombinant strains was scaled up in 3 l vessel-bioreactors containing 2 l working volume of FM2, all of the strains produced significantly more A40926 and grew better than in flask culture with the exception of *N. gerenzanensis* pSAD3$^+$ (**Figure 5**). The control strain with the empty vector grew and produced the antibiotic faster than at the flask level (**Figure 5A**). Maximum biomass (300 g/l dry weight, more than the double of that achieved in flasks) and A40926 production (nearly 400 mg/l) were reached after 120 h from inoculation; glucose was completely consumed within 96 h versus the 120 h needed at flask level. The recombinant strain pSAD4$^+$ grew more (maximum biomass production of 220 g/l after 144 h of growth) than in flask culture, although less than the control strain in the bioreactor. Glucose was consumed faster than in the control strain and glucose concentration tended to zero at 48 h of fermentation (**Figure 5C**), and antibiotic production reached a peak of 700 mg/l after 168 h. The best performance in terms of A40926 productivity in the bioreactor was shown by the pSAD3–4$^+$ strain, which grew better (nearly 250 g/l dry weight biomass) than in flask culture and produced the maximum concentration of the antibiotic (800 mg/l) after 168 h of cultivation (**Figure 5D**). Conversely, the pSAD3$^+$ strain showed a reduced biomass production in comparison to all of the other strains, with consumption of glucose markedly delayed and A40926 production

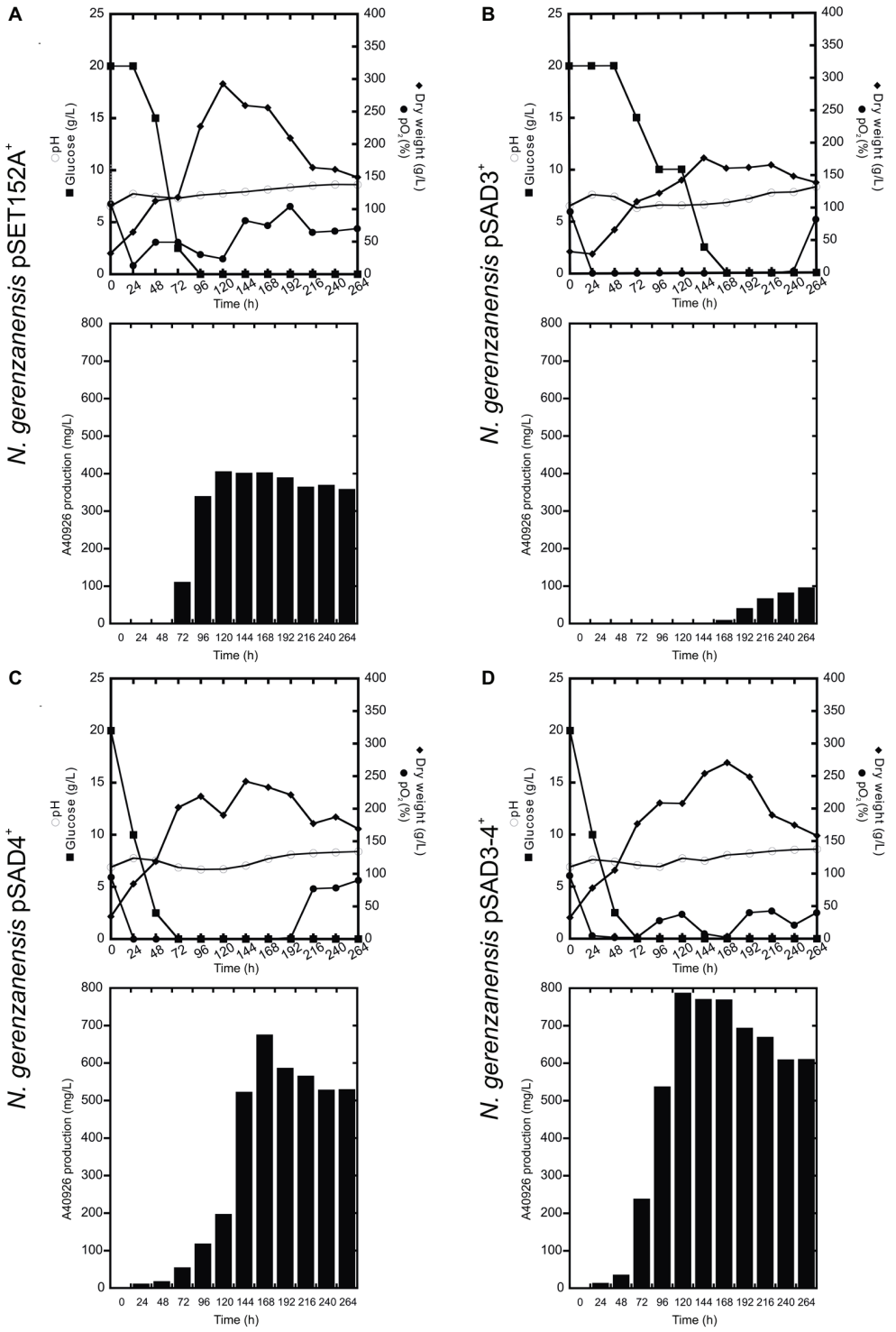

FIGURE 5 | Time courses of *N. gerenzanensis* pSET152A+ **(A)** and recombinant strains, overexpressing *dbv3* **(B)**, *dbv4* **(C)** and co-expressing both genes **(D)** cultivated in 2 l FM2 industrial medium in a 3 l fermenter. Glucose consumption (filled rectangles), biomass accumulation (filled rhombi), pH (circles), O_2 level (filled circles), and A40926 production were monitored every 24 h.

starting very late (after 168 h of cultivation) and never exceeding 100 mg/l (**Figure 5B**). Microscopical observation of pSAD3+ strain showed that the mycelium was highly fragmented (data not shown), suggesting some kind of physiological stress resulting from *dbv3* overexpression. Some fragmentation of the pSAD3+ strain (as well as of the pSAR1 strain carrying the *dbv3*-like

nocRI from *N. coxensis*) was also observed in flask culture, in contrast to the other strains which produced dense mycelial pellets; the fragmentation was less pronounced, indicating that scaling up in the bioreactor dramatically enhanced this effect. Interestingly, in the best performer at the bioreactor scale – the pSAD3–4^{+} strain – *dbv4* was expressed from the strong constitutive *aac(3)IVp* but *dbv3* was left under its endogenous promoter, suggesting that the balance between the expression level of the two cluster-situated regulatory genes is important for optimal improvement of A40926 production.

DISCUSSION

Apart from some reports on cultivating and manipulating the industrially valuable A40926 producer *N. gerenzanensis* (Stinchi et al., 2003, 2006; Marcone et al., 2010a,b,c; Alt et al., 2019) and the kistamicin producer *Nonomuraea* sp. ATCC 55076 (Greule et al., 2019), we are not aware of any other attempt to develop genetic tools for manipulating *Nonomuraea* spp. However, some other glycopeptide producers, like *A. teichomyceticus*, already possess well-developed toolkits for genetic manipulation which has greatly simplified investigations in these strains (Horbal et al., 2013; Yushchuk et al., 2016). Therefore, our first goal in this work was to develop a set of genetic tools for manipulating diverse species of *Nonomuraea*. To do this, we decided to work in parallel with the better-known A40926 producer, recently re-classified as *N. gerenzanensis* (Dalmastri et al., 2016), and with the little investigated *N. coxensis*, which was isolated in Bangladesh in 2007 (Ara et al., 2007). Although the available *N. coxensis* genome sequence is still incomplete, we could identify three contigs covering most of a *dbv*-like gene cluster including the *dbv*-like cluster-situated regulatory genes, which we named *nocRI* (*dbv3* homolog) and *nocRII* (*dbv4* homolog). The next step of our work will be additional sequencing to yield a properly annotated *N. coxensis* genome. Interestingly, during the course of our investigations, Waglechner et al. (2019), systematically screening the available sequences in genomic databases, also reported the presence of a BGC encoding for a A40926-like GPA in the genome of *N. coxensis*. In addition, the same authors reported that a newly isolated *Nonomuraea* sp. WAC01424 possess a BGC which could produce another A40926-related compound (Waglechner et al., 2019). Our preliminary analysis of this BGC suggests that it could be a sulfated A40926-like GPA, lacking the aliphatic side chains.

In the meantime, we tested both in *N. gerenzanensis* and *N. coxensis*, a set of heterologous and native promoters (the latter derived from a set of house-keeping genes in *N. gerenzanensis*) with the final goal of using them for driving gene expression in these strains. Besides the practical outcome of this screening (all of the generated promoter-probe vectors could be easily used as expression vectors simply by exchanging *gusA* for a gene of interest, offering a set of variable tools for gene expression), it is interesting to observe that the studied promoters had similar strengths in the two phylogenetically distant *Nonomuraea* species and that the native promoters from *N. gerenzanensis* worked similarly in *N. coxensis*. Consistently, we detected a comparable difference in the two strains between the strength of promoters driving the expression of rifamycin-sensitive and rifamycin-resistant *rpoB* alleles of *N. gerenzanensis* ($rpoB_{ng}p$ and $rpoB_{Rng}p$). Since we found the two *rpoB* alleles in *N. coxensis* draft genome (on a short genomic scaffolds KB904038 and KB904038), we might suppose that their manipulation could improve antibiotic production in this strain as already reported for *N. gerenzanensis* (Vigliotta et al., 2004). More generally, these vectors should be useful for the genetic manipulation of other members of the genus *Nonomuraea*, which have the potential to produce novel valuable specialized metabolites (Sungthong and Nakaew, 2015; Nazari et al., 2017).

As in the case of *Actinoplanes* spp. (Horbal et al., 2013), the strongest heterologous promoter was *aac(3)IVp*, although some *N. gerenzanensis* native promoters like $hrdB_{ng}p$ and $rpsL_{ng}p$ appeared to have comparable strength and merit further investigations. When we used *aac(3)IVp* to overexpress the cluster-situated regulatory genes *dbv3* and *dbv4* from the *N. gerenzanensis dbv* gene cluster and *nocRI* (*dbv3*-like) from the A40926-like BGC of *N. coxensis*, the recombinant *N. gerenzanensis* strains produced significantly more A40926 than the parental strain. The evidence that the heterologous expression of *nocRI* increased A40926 production in *N. gerenzanensis* confirmed its role in regulating the expression of a A40926-like BGC in *N. coxensis*. Additionally, it represents another case of cross-talk between regulators controlling GPA BGCs in producing actinomycetes (Spohn et al., 2014). Our next goal will be to investigate if and how (in which cultivation conditions) *N. coxensis* produces A40926 or a A40926-like molecule.

Previous work (Lo Grasso et al., 2015) reported that overexpression of *dbv3* (under the control of the thiostrepton-inducible *tipA** promoter in the integrative plasmid pIJ8600) in *N. gerenzanensis* increased A40926 production from 13 to 27 mg/l using the laboratory medium R3 (Lo Grasso et al., 2015). In this paper, we tested the real industrial potential of overexpressing not only *dbv3*, but also *dbv4*, and *dbv3* and *dbv4* together, cloning them under the strong constitutive *aac(3)IVp* promoter, scaling up their cultivation at bioreactor scale and using a previously optimized industrial medium where A40926 is produced in hundreds of milligrams per liter (Marcone et al., 2010a, 2014). At the bioreactor level, where strains could have a different performance from the flask-cultivation due to different mixing and mass transfer rates of nutrients and oxygen, the best performer was the strain carrying both *dbv4* under *aac(3)IVp* and *dbv3* under its own endogenous promoter. This strain produced nearly 800 mg/l of A40926, which is twice that of the parental strain grown under the same conditions. Conversely, the strain carrying only *dbv3* expressed from *aac(3)IVp* showed reduced production capacity and an altered phenotype particularly after scaling up from flask to bioreactor; in contrast, the *dbv4* overexpressing recombinant grew similarly under both conditions. It is widely recognized that any potentially higher producing mutant or derivative needs to be validated in a bioreactor-scale fermentation since unpredictable discrepancies

in strain performance can occur during scaling up from flask culture (Lee and Kim, 2015). In the case of the *dbv3* overexpressing recombinant, we believe that the fragmented mycelial phenotype, which was much more apparent in the bioreactor, could be a specific consequence of the overexpression of the *dbv7* gene encoding a D,D-carboxypeptidase known as VanYn (Binda et al., 2012). The level of VanYn activity in cell extracts from the *dbv3*-carrying recombinant cultivated at bioreactor scale was found to be much higher than in the parental strain (unpublished data). Consistent with this, overexpression of VanYn altered the mycelial morphology in *N. gerenzanensis* as well as in heterologous hosts such as streptomycetes strains (Binda et al., 2013).

In conclusion, only a few GPAs are used in clinical practice and those produced by semi-synthesis from natural products, such as dalbavancin derived from A40926, are still quite expensive. Dalbavancin is the first antibiotic designated as a Qualified Infection Diseases Product by the FDA because of its potency, extended dosing interval, and unique dose regimen, but its cost largely exceeds that of first-generation GPAs and consequently its use in hospitals is still limited (Chiasson and White, 2016; Agarwal et al., 2018). Improving A40926-producing strains might lead to a decrease in the cost of dalbavancin. As demonstrated in this paper, A40926 production could be significantly enhanced by manipulating the expression of *dbv* cluster-situated regulators. An important and often-neglected aspect is testing the genetic stability and productivity of the selected recombinant strains in a fully developed industrial process at bioreactor level, which mimics the conditions of antibiotic large scale production. We were able to demonstrate here that the improvements we made to A40926 production levels in shake flasks were also achieved in the bioreactor, indicating the relevance of this approach to industrial-scale strain improvement.

DATA AVAILABILITY STATEMENT

All datasets generated for this study are included in the article/**Supplementary Material**.

AUTHOR CONTRIBUTIONS

OY, EB, MB, and FM conceived and designed the experiments and wrote the paper. OY, AA-V, GM, and EB performed the experiments. OY, GM, and EB analyzed the data.

FUNDING

This work was supported by public grants "Fondo di Ateneo per la Ricerca" 2018 and 2019 to FM and GM and by Federation of European Microbiological Societies (FEMS) Research Fellowship 2015 to EB.

ACKNOWLEDGMENTS

Consorzio Interuniversitario per le Biotecnologie is acknowledged for its support to traveling and attending congresses for EB and GM.

SUPPLEMENTARY MATERIAL

The Supplementary Material for this article can be found online at: https://www.frontiersin.org/articles/10.3389/fmicb.2020.00008/full#supplementary-material

REFERENCES

Adamek, M., Alanjary, M., Sales-Ortells, H., Goodfellow, M., Bull, A. T., Winkler, A., et al. (2018). Comparative genomics reveals phylogenetic distribution patterns of secondary metabolites in *Amycolatopsis* species. *BMC Genomics* 19, 1–15. doi: 10.1186/s12864-018-4809-4

Agarwal, R., Bartsch, S., Kelly, B., Prewitt, M., Liu, Y., Chen, Y., et al. (2018). Newer glycopeptide antibiotics for treatment of complicated skin and soft tissue infections: systematic review, network meta-analysis and cost analysis. *Clin. Microbiol. Infect.* 24, 361–368. doi: 10.1016/j.cmi.2017.08.028

Alduina, R., Sosio, M., and Donadio, S. (2018). Complex regulatory networks governing production of the glycopeptide A40926. *Antibiotics* 7, pii: E30. doi: 10.3390/antibiotics7020030

Alt, S., Bernasconi, A., Sosio, M., Brunati, C., Donadio, S., and Maffioli, S. I. (2019). Toward single-peak dalbavancin analogs through biology and chemistry. *ACS Chem. Biol.* 14, 356–360. doi: 10.1021/acschembio.9b00050

Altschul, S. (1990). Basic local alignment search tool. *J. Mol. Biol.* 215, 403–410. doi: 10.1016/S0022-2836(05)80360-2

Ara, I., Kudo, T., Matsumoto, A., Takahashi, Y., and Omura, S. (2007). *Nonomuraea bangladeshensis* sp. nov. and *Nonomuraea coxensis* sp. nov. *Int. J. Syst. Evol. Microbiol.* 57, 1504–1509. doi: 10.1099/ijs.0.65054-0

Armenia, I., Marcone, G. L., Berini, F., Orlandi, V. T., Pirrone, C., Martegani, E., et al. (2018). Magnetic nanoconjugated teicoplanin: a novel tool for bacterial infection site targeting. *Front. Microbiol.* 9, 1–17. doi: 10.3389/fmicb.2018.02270

Banik, J. J., and Brady, S. F. (2008). Cloning and characterization of new glycopeptide gene clusters found in an environmental DNA megalibrary. *Proc. Natl. Acad. Sci.* 105, 17273–17277. doi: 10.1073/pnas.0807564105

Banik, J. J., Craig, J. W., Calle, P. Y., and Brady, S. F. (2010). Tailoring enzyme-rich environmental DNA clones: a source of enzymes for generating libraries of unnatural natural products. *J. Am. Chem. Soc.* 132, 15661–15670. doi: 10.1021/ja105825a

Bibb, M. J. (2013). Understanding and manipulating antibiotic production in actinomycetes. *Biochem. Soc. Trans.* 41, 1355–1364. doi: 10.1042/BST20130214

Binda, E., Marcone, G. L., Berini, F., Pollegioni, L., and Marinelli, F. (2013). *Streptomyces* spp. as efficient expression system for a D,D-peptidase/D,D-carboxypeptidase involved in glycopeptide antibiotic resistance. *BMC Biotechnol.* 13, 1–14. doi: 10.1186/1472-6750-13-24

Binda, E., Marcone, G. L., Pollegioni, L., and Marinelli, F. (2012). Characterization of VanYn, a novel D,D-peptidase/D,D-carboxypeptidase involved in glycopeptide antibiotic resistance in *Nonomuraea* sp. ATCC 39727. *FEBS J.* 279, 3203–3213. doi: 10.1111/j.1742-4658.2012.08706.x

Blin, K., Shaw, S., Steinke, K., Villebro, R., Ziemert, N., Lee, S. Y., et al. (2019). AntiSMASH 5.0: updates to the secondary metabolite genome mining pipeline. *Nucleic Acids Res.* 47, W81–W87. doi: 10.1093/nar/gkz310

Chiasson, J., and White, R. (2016). Comparison of dalbavancin, oritavancin and vancomycin pharmacodynamics using clinical targets against ABSSSI pathogens. *Open Forum Infect. Dis.* 3:S515. doi: 10.1093/ofid/ofw172.1506

Dalmastri, C., Gastaldo, L., Marcone, G. L., Binda, E., Congiu, T., and Marinelli, F. (2016). Classification of *Nonomuraea* sp. ATCC 39727, an actinomycete that produces the glycopeptide antibiotic A40926, as *Nonomuraea gerenzanensis* sp. nov. *Int. J. Syst. Evol. Microbiol.* 66, 912–921. doi: 10.1099/ijsem.0.000810

D'Argenio, V., Petrillo, M., Pasanisi, D., Pagliarulo, C., Colicchio, R., Talà, A., et al. (2016). The complete 12 Mb genome and transcriptome of *Nonomuraea gerenzanensis* with new insights into its duplicated "magic" RNA polymerase. *Sci. Rep.* 6, 1–13. doi: 10.1038/s41598-016-0025-0

Greule, A., Izoré, T., Iftime, D., Tailhades, J., Schoppet, M., Zhao, Y., et al. (2019). Kistamicin biosynthesis reveals the biosynthetic requirements for production of highly crosslinked glycopeptide antibiotics. *Nat. Commun.* 10, 1–15. doi: 10.1038/s41467-019-10384-w

Haslinger, K., Peschke, M., Brieke, C., Maximowitsch, E., and Cryle, M. J. (2015). X-domain of peptide synthetases recruits oxygenases crucial for glycopeptide biosynthesis. *Nature* 521, 105–109. doi: 10.1038/nature14141

Herrmann, S., Siegl, T., Luzhetska, M., Petzke, L., Jilg, C., Welle, E., et al. (2012). Site-specific recombination strategies for engineering actinomycete genomes. *Appl. Environ. Microbiol.* 78, 1804–1812. doi: 10.1128/AEM.06054-11

Horbal, L., Fedorenko, V., and Luzhetskyy, A. (2014a). Novel and tightly regulated resorcinol and cumate-inducible expression systems for *Streptomyces* and other actinobacteria. *Appl. Microbiol. Biotechnol.* 98, 8641–8655. doi: 10.1007/s00253-014-5918-x

Horbal, L., Kobylyanskyy, A., Truman, A. W., Zaburranyi, N., Ostash, B., Luzhetskyy, A., et al. (2014b). The pathway-specific regulatory genes, tei15* and tei16*, are the master switches of teicoplanin production in *Actinoplanes teichomyceticus*. *Appl. Microbiol. Biotechnol.* 98, 9295–9309. doi: 10.1007/s00253-014-5969-z

Horbal, L., Kobylyanskyy, A., Yushchuk, O., Zaburannyi, N., Luzhetskyy, A., Ostash, B., et al. (2013). Evaluation of heterologous promoters for genetic analysis of *Actinoplanes teichomyceticus* – producer of teicoplanin, drug of last defense. *J. Biotechnol.* 168, 367–372. doi: 10.1016/j.jbiotec.2013.10.018

Horbal, L., Zaburannyy, N., Ostash, B., Shulga, S., and Fedorenko, V. (2012). Manipulating the regulatory genes for teicoplanin production in *Actinoplanes teichomyceticus*. *World J. Microbiol. Biotechnol.* 28, 2095–2100. doi: 10.1007/s11274-012-1013-6

Kieser, T., Bibb, M. J., Buttner, M. J., Chater, K. F., and Hopwood, D. A. (2000). *Practical streptomyces genetics*. Norwich: John Innes Foundation.

Koshla, O., Yushchuk, O., Ostash, I., Dacyuk, Y., Myronovskyi, M., Jäger, G., et al. (2019). Gene *miaA* for post-transcriptional modification of tRNA XXA is important for morphological and metabolic differentiation in *Streptomyces*. *Mol. Microbiol.* 112, 249–265. doi: 10.1111/mmi.14266

Kusserow, K., and Gulder, T. A. M. (2017). Complete genome sequence of *Actinomadura parvosata* subsp. *kistnae*, a rich source of novel natural product (bio-)chemistry. *J. Genomics* 5, 75–76. doi: 10.7150/jgen.19673

Lee, S. Y., and Kim, H. U. (2015). Systems strategies for developing industrial microbial strains. *Nat. Biotechnol.* 33, 1061–1072. doi: 10.1038/nbt.3365

Lo Grasso, L. L., Maffioli, S., Sosio, M., Bibb, M., Puglia, A. M., and Alduina, R. (2015). Two master switch regulators trigger A40926 biosynthesis in *Nonomuraea* sp. strain ATCC 39727. *J. Bacteriol.* 197, 2536–2544. doi: 10.1128/JB.00262-15

Makitrynskyy, R., Ostash, B., Tsypik, O., Rebets, Y., Doud, E., Meredith, T., et al. (2013). Pleiotropic regulatory genes *bldA*, *adpA* and *absB* are implicated in production of phosphoglycolipid antibiotic moenomycin. *Open Biol.* 3:130121. doi: 10.1098/rsob.130121

Marcone, G. L., Beltrametti, F., Binda, E., Carrano, L., Foulston, L., Hesketh, A., et al. (2010a). Novel mechanism of glycopeptide resistance in the A40926 producer *Nonomuraea* sp. ATCC 39727. *Antimicrob. Agents Chemother.* 54, 2465–2472. doi: 10.1128/AAC.00106-10

Marcone, G. L., Binda, E., Berini, F., and Marinelli, F. (2018). Old and new glycopeptide antibiotics: from product to gene and back in the post-genomic era. *Biotechnol. Adv.* 36, 534–554. doi: 10.1016/j.biotechadv.2018.02.009

Marcone, G. L., Binda, E., Carrano, L., Bibb, M., and Marinelli, F. (2014). Relationship between glycopeptide production and resistance in the actinomycete *Nonomuraea* sp. ATCC 39727. *Antimicrob. Agents Chemother.* 58, 5191–5201. doi: 10.1128/AAC.02626-14

Marcone, G. L., Carrano, L., Marinelli, F., and Beltrametti, F. (2010b). Protoplast formationa and reversion to normal growth in antibiotic-producing uncommon actinomycetes. *J. Antibiot.* 63, 83–88. doi: 10.1038/ja.2009.127

Marcone, G. L., Foulston, L., Binda, E., Marinelli, F., Bibb, M., and Beltrametti, F. (2010c). Methods for the genetic manipulation of *Nonomuraea* sp. ATCC 39727. *J. Ind. Microbiol. Biotechnol.* 37, 1097–1103. doi: 10.1007/s10295-010-0807-5

Myronovskyi, M., Welle, E., Fedorenko, V., and Luzhetskyy, A. (2011). β-Glucuronidase as a sensitive and versatile reporter in actinomycetes. *Appl. Environ. Microbiol.* 77, 5370–5383. doi: 10.1128/AEM.00434-11

Nazari, B., Forneris, C. C., Gibson, M. I., Moon, K., Schramma, K. R., and Seyedsayamdost, M. R. (2017). *Nonomuraea* sp. ATCC 55076 harbours the largest actinomycete chromosome to date and the kistamicin biosynthetic gene cluster. *MedChemComm* 8, 780–788. doi: 10.1039/C6MD00637J

Okano, A., Isley, N. A., and Boger, D. L. (2017). Peripheral modifications of [Ψ[CH_2NH]Tpg4]vancomycin with added synergistic mechanisms of action provide durable and potent antibiotics. *Proc. Natl. Acad. Sci.* 114, E5052–E5061. doi: 10.1073/pnas.1704125114

Peschke, M., Brieke, C., Goode, R. J. A., Schittenhelm, R. B., and Cryle, M. J. (2017). Chlorinated glycopeptide antibiotic peptide precursors improve cytochrome P450-catalyzed cyclization cascade efficiency. *Biochemistry* 56, 1239–1247. doi: 10.1021/acs.biochem.6b01102

Schoppet, M., Peschke, M., Kirchberg, A., Wiebach, V., Süssmuth, R. D., Stegmann, E., et al. (2019). The biosynthetic implications of late-stage condensation domain selectivity during glycopeptide antibiotic biosynthesis. *Chem. Sci.* 10, 118–133. doi: 10.1039/C8SC03530J

Shawky, R. M., Puk, O., Wietzorrek, A., Pelzer, S., Takano, E., Wohlleben, W., et al. (2007). The border sequence of the balhimycin biosynthesis gene cluster from *Amycolatopsis balhimycina* contains *bbr*, encoding a StrR-like pathway-specific regulator. *J. Mol. Microbiol. Biotechnol.* 13, 76–88. doi: 10.1159/000103599

Sievers, F., Wilm, A., Dineen, D., Gibson, T. J., Karplus, K., Li, W., et al. (2011). Fast, scalable generation of high-quality protein multiple sequence alignments using clustal omega. *Mol. Syst. Biol.* 7, 1–6. doi: 10.1038/msb.2011.75

Spohn, M., Kirchner, N., Kulik, A., Jochim, A., Wolf, F., Muenzer, P., et al. (2014). Overproduction of ristomycin a by activation of a silent gene cluster in *Amycolatopsis japonicum* MG417-CF17. *Antimicrob. Agents Chemother.* 58, 6185–6196. doi: 10.1128/AAC.03512-14

Stegmann, E., Albersmeier, A., Spohn, M., Gert, H., Weber, T., Wohlleben, W., et al. (2014). Complete genome sequence of the actinobacterium *Amycolatopsis japonica* MG417-CF17T (=DSM 44213T) producing (S,S)-N,N′-ethylenediaminedisuccinic acid. *J. Biotechnol.* 189, 46–47. doi: 10.1016/j.jbiotec.2014.08.034

Stinchi, S., Azimonti, S., Donadio, S., and Sosio, M. (2003). A gene transfer system for the glycopeptide producer *Nonomuraea* sp. ATCC39727. *FEMS Microbiol. Lett.* 225, 53–57. doi: 10.1016/S0378-1097(03)00490-7

Stinchi, S., Carrano, L., Lazzarini, A., Feroggio, M., Grigoletto, A., Sosio, M., et al. (2006). A derivative of the glycopeptide A40926 produced by inactivation of the β-hydroxylase gene in *Nonomuraea* sp. ATCC39727. *FEMS Microbiol. Lett.* 256, 229–235. doi: 10.1111/j.1574-6968.2006.00120.x

Sungthong, R., and Nakaew, N. (2015). The genus *Nonomuraea*: a review of a rare actinomycete taxon for novel metabolites. *J. Basic Microbiol.* 55, 554–565. doi: 10.1002/jobm.201300691

Thaker, M. N., Wang, W., Spanogiannopoulos, P., Waglechner, N., King, A. M., Medina, R., et al. (2013). Identifying producers of antibacterial compounds by screening for antibiotic resistance. *Nat. Biotechnol.* 31, 922–927. doi: 10.1038/nbt.2685

Truman, A. W., Kwun, M. J., Cheng, J., Yang, S. H., Suh, J.-W., and Hong, H.-J. (2014). Antibiotic resistance mechanisms inform discovery: identification and characterization of a novel *Amycolatopsis* strain producing ristocetin. *Antimicrob. Agents Chemother.* 58, 5687–5695. doi: 10.1128/AAC.03349-14

Vigliotta, G., Tredici, S. M., Damiano, F., Montinaro, M. R., Pulimeno, R., Summa, R. D., et al. (2004). Natural merodiploidy involving duplicated *rpoB* alleles affects secondary metabolism in a producer actinomycete. *Mol. Microbiol.* 55, 396–412. doi: 10.1111/j.1365-2958.2004.04406.x

Vongsangnak, W., Figueiredo, L. F., Förster, J., Weber, T., Thykaer, J., Stegmann, E., et al. (2012). Genome-scale metabolic representation of *Amycolatopsis balhimycina*. *Biotechnol. Bioeng.* 109, 1798–1807. doi: 10.1002/bit.24436

Waglechner, N., Mcarthur, A. G., and Wright, G. D. (2019). Phylogenetic reconciliation reveals the natural history of glycopeptide antibiotic biosynthesis and resistance. *Nat. Microbiol.* 4, 1862–1871. doi: 10.1038/s41564-019-0531-5

Wu, Z.-C., and Boger, D. L. (2019). Exploration of the site-specific nature and generalizability of a trimethylammonium salt modification on vancomycin: A-ring derivatives. *Tetrahedron* 75, 3160–3165. doi: 10.1016/j.tet.2019.02.008

Yim, G., Kalan, L., Koteva, K., Thaker, M. N., Waglechner, N., Tang, I., et al. (2014). Harnessing the synthetic capabilities of glycopeptide antibiotic tailoring enzymes: characterization of the UK-68,597 biosynthetic cluster. *ChemBioChem* 15, 2613–2623. doi: 10.1002/cbic.201402179

Yushchuk, O., Homoniuk, V., Datsiuk, Y., Ostash, B., Marinelli, F., and Fedorenko, V. (2020a). Development of a gene expression system for the uncommon actinomycete *Actinoplanes rectilineatus* NRRL B-16090. *J. Appl. Genet.* doi: 10.1007/s13353-019-00534-7 [Epub ahead of print].

Yushchuk, O., Homoniuk, V., Ostash, B., Marinelli, F., and Fedorenko, V. (2020b). Genetic insights into the mechanism of teicoplanin self-resistance in *Actinoplanes teichomyceticus*. *J. Antibiot.* (in press). doi: 10.1038/s41429-019-0274-9

Yushchuk, O., Horbal, L., Ostash, B., Marinelli, F., Wohlleben, W., Stegmann, E., et al. (2019). Regulation of teicoplanin biosynthesis: refining the roles of *tei* cluster-situated regulatory genes. *Appl. Microbiol. Biotechnol.* 103, 4089–4102. doi: 10.1007/s00253-019-09789-w

Yushchuk, O., Ostash, B., Pham, T. H., Luzhetskyy, A., Fedorenko, V., Truman, A. W., et al. (2016). Characterization of the post-assembly line tailoring processes in teicoplanin biosynthesis. *ACS Chem. Biol.* 11, 2254–2264. doi: 10.1021/acschembio.6b00018

Conflict of Interest: The authors declare that the research was conducted in the absence of any commercial or financial relationships that could be construed as a potential conflict of interest.

frontiers in Microbiology

REVIEW
published: 22 January 2020
doi: 10.3389/fmicb.2019.03120

The Balance Metabolism Safety Net: Integration of Stress Signals by Interacting Transcriptional Factors in *Streptomyces* and Related Actinobacteria

Juan F. Martín and Paloma Liras*

Área de Microbiología, Departamento de Biología Molecular, Universidad de León, León, Spain

Soil dwelling *Streptomyces* species are faced with large variations in carbon or nitrogen sources, phosphate, oxygen, iron, sulfur, and other nutrients. These drastic changes in key nutrients result in an unbalanced metabolism that have undesirable consequences for growth, cell differentiation, reproduction, and secondary metabolites biosynthesis. In the last decades evidence has accumulated indicating that mechanisms to correct metabolic unbalances in *Streptomyces* species take place at the transcriptional level, mediated by different transcriptional factors. For example, the master regulator PhoP and the large SARP-type regulator AfsR bind to overlapping sequences in the *afsS* promoter and, therefore, compete in the integration of signals of phosphate starvation and *S*-adenosylmethionine (SAM) concentrations. The cross-talk between phosphate control of metabolism, mediated by the PhoR–PhoP system, and the pleiotropic orphan nitrogen regulator GlnR, is very interesting; PhoP represses GlnR and other nitrogen metabolism genes. The mechanisms of control by GlnR of several promoters of ATP binding cassettes (ABC) sugar transporters and carbon metabolism are highly elaborated. Another important cross-talk that governs nitrogen metabolism involves the competition between GlnR and the transcriptional factor MtrA. GlnR and MtrA exert opposite effects on expression of nitrogen metabolism genes. MtrA, under nitrogen rich conditions, represses expression of nitrogen assimilation and regulatory genes, including GlnR, and competes with GlnR for the GlnR binding sites. Strikingly, these sites also bind to PhoP. Novel examples of interacting transcriptional factors, discovered recently, are discussed to provide a broad view of this interactions. Altogether, these findings indicate that cross-talks between the major transcriptional factors protect the cell metabolic balance. A detailed analysis of the transcriptional factors binding sequences suggests that the transcriptional factors interact with specific regions, either by overlapping the recognition sequence of other factors or by binding to adjacent sites in those regions. Additional interactions on the regulatory backbone are provided by sigma factors, highly phosphorylated nucleotides, cyclic dinucleotides, and small ligands that interact with cognate receptor proteins and with TetR-type transcriptional regulators. We propose to define the signal integration DNA regions (so called integrator sites) that assemble responses to different stress, nutritional or environmental signals.

OPEN ACCESS

Edited by:
Yvonne Mast, German Collection of Microorganisms and Cell Cultures GmbH (DSMZ), Germany

Reviewed by:
Andrew Hesketh, University of Brighton, United Kingdom
Gang Liu, Institute of Microbiology (CAS), China

***Correspondence:**
Juan F. Martín
jf.martin@unileon.es

Specialty section:
This article was submitted to Microbial Physiology and Metabolism, a section of the journal Frontiers in Microbiology

Received: *04 November 2019*
Accepted: *24 December 2019*
Published: *22 January 2020*

Citation:
Martín JF and Liras P (2020) The Balance Metabolism Safety Net: Integration of Stress Signals by Interacting Transcriptional Factors in Streptomyces and Related Actinobacteria. Front. Microbiol. 10:3120. doi: 10.3389/fmicb.2019.03120

These integrator sites constitute nodes recognized by two, three, or more transcriptional factors to compensate the unbalances produced by metabolic stresses. This interplay mechanism acts as a safety net to prevent major damage to the metabolism under extreme nutritional and environmental conditions.

Keywords: Actinobacteria, stress signals, overlapping binding sequences, transcriptional factors, sigma factors, cyclic nucleotides, safety net, signal integration nodes

COORDINATION OF PRIMARY AND SECONDARY METABOLISM IN *Streptomyces:* INTERACTION OF MULTIPLE TRANSCRIPTIONAL FACTORS AT SIGNAL INTEGRATION SITES

Evidence accumulated in the last decades shows that coordination of primary and secondary metabolism takes place by multiple interactions of pleiotropic and cluster situated transcriptional factors that work in networks and cascades (Martín and Liras, 2010; van Wezel and McDowall, 2011; Martín et al., 2012b; Liu et al., 2013; Romero-Rodríguez et al., 2016a,b). Some pleiotropic transcriptional factors, such as PhoP, GlnR, or MtrA, control, directly or indirectly, hundreds of reactions in the bacterial cells, and we will refer to them in this article as master regulators. Master transcriptional factors interact with upstream regions of cluster situated regulatory genes. This is the case of several transcriptional factors that regulate the *act* and *red* clusters in *Streptomyces coelicolor*. The promoter region of the actinorhodin regulatory gene *actII-orf4* is recognized by at least nine transcriptional factors of different families, including GlnR, AfsS, AfsQ1, AdpA, AtrA, DasR, DraR, AbsA2, and AbsC (Floriano and Bibb, 1996; Ohnishi et al., 2005; Uguru et al., 2005; McKenzie and Nodwell, 2007; Rigali et al., 2008; Yu et al., 2012; He J.M. et al., 2016; Lewis et al., 2019). This phenomenon raises the question of how these transcriptional factors compete for binding to the *actII-orf4* promoter region. In other words, these regions (hereafter named integrators sites) serve to integrate multiple signal cascades that respond to different nutritional and environmental stress signals in *Streptomyces* (**Figure 1**).

An important question is whether these different transcriptional factors interact in some way in the control of expression of a particular gene. Taking into account the large size of some transcriptional regulators (see below), it is likely that each of these transcriptional factors covers at least the major groove or a full turn of DNA (11 nucleotides). Moreover, some of these regulators, e.g., GlnR or PhoP, act as dimers or even oligomers and therefore cover a relatively large stretch of DNA. Mutations affecting these integrator sites alter not only the binding to one transcriptional factor but also to other interacting factors.

The interactions between transcriptional factors and regions upstream of some gene clusters are really elaborated and suggests that there is a fine tuning of the expression of important gene clusters by alternative transcriptional factors. There are many reports of putatively interacting transcriptional factors that affect the biosynthesis of secondary metabolites but the molecular evidence supporting those interactions is scarce. In this article we focus on the most relevant and best-known cases of overlapping interactions between transcriptional factors that allow us to get an insight into how the cells integrate inputs from environmental and nutritional stresses. Those studied for which there are experimental evidence of DNA binding and/or footprinting data are summarized in **Table 1**.

MECHANISM OF CONTROL OF PHOSPHATE METABOLISM: THE PhoP MASTER REGULATOR

Phosphate is an essential nutrients of living beings. Phosphate starvation causes the slow-down of primary metabolism and triggers production of secondary metabolites in different microorganisms (Martín and Demain, 1980). Phosphate control of metabolism is mediated by the two-component system (TCS) PhoR-PhoP (Hutchings et al., 2004; Martín et al., 2012b) that controls not only primary metabolism but also the biosynthesis of secondary metabolites (e.g., actinorhodin and undecylprodigiosin) in *Streptomyces lividans* and *S. coelicolor* (Sola-Landa et al., 2003, 2005; Ghorbel et al., 2006). The PhoP/PhoR TCS has been also studied in *Streptomyces natalensis*, *Streptomyces tsukubaensis*, *Streptomyces avermitilis*, *Streptomyces hygroscopicus* var. *geldanus*, and orthologous sequences have been found in most Actinobacteria genomes. The genes encoding these TCS are well conserved in all *Streptomyces* (Martín et al., 2017, 2019; Ordóñez-Robles et al., 2017b; Martínez-Castro et al., 2018). The *Streptomyces* PhoR-PhoP system belongs to class IIIA of TCSs (Hutchings et al., 2004). PhoR is a protein sensor kinase with signal transducer activity (Cheung and Hendrickson, 2010) of 426 amino acids in *S. lividans* and *S. coelicolor*. It is membrane-anchored through a stretch of hydrophobic amino acids, and contains a cytoplasmic C-terminal region that putatively serves to interact with the phosphate starvation signal, although in some other TCS, the sensor kinase may have an extra-cytoplasmic signal sensor region (McKenzie and Nodwell, 2009). However, in *Streptomyces* species it is unclear if the phosphate limitation signal that interacts with PhoR is extracellular or if it is an internal signal molecule (Xp in **Figure 1**). In *Bacillus subtilis* it has been proposed that the signal molecule is an intracellular intermediate of teichoic acid biosynthesis. This intermediate is an inhibitor of the PhoR autokinase activity and is regulated by the phosphate concentration. Under phosphate limitation conditions the concentration of this intermediate decreases and, therefore, the autophosphorylation of PhoR

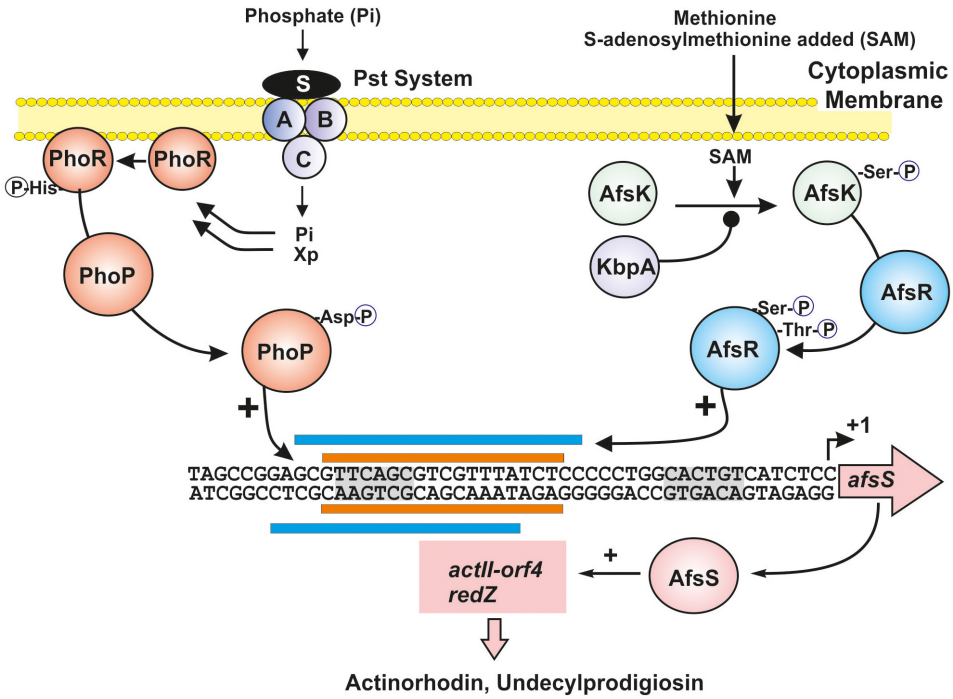

FIGURE 1 | Integration of phosphate limitation and *S*-adenosylmethionine signals through overlapping transcriptional factors. The TCS regulatory proteins PhoR and PhoP are shown in dark orange. Xp indicates the proposed intracellular signal in *B. subtilis*. The methionine signal transduction cascade through AfsK (green sphere) and AfsR (blue sphere) is shown at the right site; KbpA (purple sphere) acts as an inhibitor of AfsK phosphorylation. The sites for PhoP and AfsR binding, in the region upstream of the *afsS* gene, are shown with orange and blue bars, respectively. The -10 and -35 sites (gray shadows) and the transcription start point of the *afsS* gene are indicated. Positive regulation is indicated by arrows and negative regulations by black spheres. See text for additional details.

TABLE 1 | Well-known examples of interacting transcriptional factors in Actinobacteria[1].

Actinobacteria	Integrative DNA region	Interacting transcriptional factors	Input signals
S. coelicolor	*actII-orf4*	AdpA, AtrA, DasR, DraR, AbsA2, AfsQ1, AfsS	GBL, *N*-acetylglucosamine levels, high glutamate levels, Pi limitation, SAM levels
	redZ	DasR, AbsA2, AfsQ1	*N*-acetylglucosamine levels, high glutamate levels
	afsS promoter	PhoP, AfsR	Pi limitation, SAM level
	phoRP promoter	PhoP, AfsR	Pi limitation, SAM level
	glnR promoter	PhoP, AfsR, AfsQ1	Pi limitation, SAM level, high glutamate levels
	pstS promoter	PhoP, AfsR, AfsQ1	Pi limitation, SAM level, high glutamate levels
	cdaR promoter	PhoP, AfsQ1, AbsA2	Pi limitation, high glutamate levels
	scbA promoter	PhoP, ScbR	Pi limitation, GBL
	glnA promoter	PhoP, GlnR, MtrA	Pi limitation, nitrogen limitation, complex nitrogen source
	amtB promoter, a3b3 site	PhoP, GlnR, MtrA, AfsQ1	Pi limitation, nitrogen limitation, complex nitrogen source, high glutamate levels
	glnII	PhoP, GlnR, MtrA	Pi limitation, nitrogen limitation, complex nitrogen source
	ureA	GlnR, PhoP, MtrA	
	glnR promoter	PhoP, MtrA	Pi limitation, complex nitrogen source
	nirB1B2C/D promoter	GlnR, MtrA	Nitrogen limitation, complex nitrogen source
	malEFG promoter	MalR, GlnR	Maltose, nitrogen limitation
S. avermitilis	*aveR* promoter	PhoP, GlnR	Pi limitation, nitrogen limitation
	olmR promoter	GlnR, AveR	Nitrogen limitation
S. roseosporus	*atrA promoter*	PhoP, BldA	Pi limitation, GBL
Sac. erythraea	*pstS* promoter	PhoP, GlnR	Pi limitation, nitrogen limitation
	malEFG promoter	MalR, GlnR, CRP-like[2]	Maltose, nitrogen limitation

[1]Only examples of interaction confirmed by DNA-binding and/or footprinting assays are included. [2]CRP has been proposed to bind to the malEFG promoter but there is no experimental confirmation of this binding. See text for references and details.

and transfer of the phosphate group to PhoP are enhanced (Botella et al., 2014). PhoP is a member of the OmpR family of DNA-binding response regulators (223 amino acids). Under phosphate starvation conditions, the PhoR sensor protein kinase self phosphorylates, and then transfers its phosphate group to a receiver aspartate (D^{49}) in PhoP, that causes a rearrangement of the protein structure resulting in an activation of the DNA-binding domain in the carboxy-terminal region of this transcriptional regulator. The phosphorylated form of PhoP binds specific sequences named PHO boxes and generally activates, but occasionally represses, the expression of genes of the Pho regulon. The *Streptomyces* PHO boxes are formed by direct repeat units (DRus) of 11 nucleotides of which seven nucleotides (GTTCACC) are well conserved (Sola-Landa et al., 2005; Rodríguez-García et al., 2007; Allenby et al., 2012; Santos-Beneit, 2015). Two DRus are required for binding of PhoP to DNA (Sola-Landa et al., 2008) in agreement with the binding of dimer forms of PhoP (Blanco et al., 2002).

The PHO Regulon: PhoP-Regulated Genes

The core Pho regulon is formed by more than 100 genes, of which about 50 are well characterized (Santos-Beneit, 2015; Martín et al., 2017). Using chromatin immunoprecipitation, Allenby et al. (2012) found PhoP binding sites in 150 loci in *S. coelicolor*, not all of them corresponding to promoter regions of characterized genes. Phosphate depletion results in PhoP-mediated induction of genes involved in scavenging, transport, and mobilization of phosphate, and in repression of genes for utilization of nitrogen sources. PhoP reduces expression of genes for aerobic respiration and activates nitrate respiration genes. This master regulator activates expression of genes for teichuronic acid formation and decreases that of genes for phosphate-rich teichoic acid biosynthesis. In *S. coelicolor* PhoP repressed several differentiation genes that affect development and indirectly antibiotic biosynthesis (Rodríguez-García et al., 2007; Allenby et al., 2012; Martín et al., 2017).

Modification of PhoP Binding Affinity to Recognition Sequences by Acylation at Lysine Residues

The chemical structure of some regulatory proteins of the OmpR family, which includes PhoP, is known (Martínez-Hackert and Stock, 1997; Blanco et al., 2002, 2012; He X. et al., 2016). The DNA binding domain (DBD) of PhoP, and other OmpR-family regulators, includes a winged helix turn helix (HTH) structure in the carboxyl terminal region, that recognizes the PhoP binding sequence (PHO boxes) in the promoters of the target genes (Li et al., 2008). This DBD is highly positively charged and, therefore, has a strong affinity for the negative charged DNA backbone. It is known that several regulatory proteins are modified by acylation at the lysine rich region of their DBD (Li et al., 2008; Thao and Escalante-Semerena, 2011; Tiffert et al., 2011; Yao et al., 2014).

Particularly relevant for this review article is the acylation of residues in the lysine rich region of OmpR family regulators (Luo et al., 2004; Matsuzaki et al., 2005; Qin et al., 2016) that may alter the binding affinity to their recognition sequences (Banerjee et al., 2016). Recently, it was reported that the PhoP regulator of *Saccharopolyspora erythraea* is propionylated by an acyl transferase encoded by the *acuA* gene (Xu et al., 2018). Mass spectrometry analysis of the acylated PhoP revealed that the PhoP protein is propionylated at lysines K^{198} or K^{203}. The AcuA enzyme in other organisms utilizes acetyl-CoA as acetyl donor, but in this particular case appears to use propionyl-CoA (You et al., 2014).

Mutation of K^{198} and K^{203} to arginine, glutamate, or glutamine provided evidence that whereas mutation to arginine conserves the polarity of the DNA binding region, the mutation to glutamine (or glutamate) changes the charge of this region thus weakening the binding of the mutated PhoP to the DNA backbone. These observations were supported by electrophoretic mobility-shift assay (EMSA) which showed that the mutation to glutamate removed the binding ability of PhoP and, therefore, altered the control of expression of the Pho regulon genes (Xu et al., 2018). In conclusion, highly propionylated forms of PhoP decrease the binding affinity of PhoP to the PHO boxes in the DNA, and therefore weaken control of the Pho regulon.

Since the 1970s, it is known that erythromycin is formed by condensation of 7-three carbon units provided by one propionyl-CoA as starter unit and six methylmalonyl-CoA elongation units (Cortés et al., 1990). Propionate or propanol addition to *Sac. erythraea* cultures enhances erythromycin production (Guo et al., 2016). Interestingly, propionate addition to erythromycin producing cultures also enhances the propionylated form of PhoP thus reducing the intensity of phosphate control (Xu et al., 2018). This is another interesting aspect of cross-talk between phosphate regulation and carbon source utilization, particularly propionate. It is unclear, however, if acylation of Omp-type response regulators, other than PhoP, in *Streptomyces* may also produce similar alterations of their regulatory effects. Indeed, the GlnR nitrogen regulator is modified both by phosphorylation and acetylation (see below).

Modification of AfsR by Phosphorylation: Involvement in the Transduction of the *S*-Adenosylmethionine Concentration Signal

Expression of actinorhodin and undecylprodigiosin genes in *S. coelicolor* is controlled by the AfsR regulator that belongs to the large size SARP family (Horinouchi, 2003). AfsR (993 amino acids) contains a DBD in its N-terminal region and an internal ATP/GTP binding pocket in the middle of the protein. The AfsR regulatory effect is exerted on expression of the *afsS* gene, encoding a small protein (63 amino acids) that controls expression of the *act* and *red* gene transcriptional regulators (Floriano and Bibb, 1996; Lee et al., 2002) by binding upstream of these cluster specific regulatory genes. AfsR recognizes and binds the promoter of the *afsS* gene, and this binding is essential since no transcription of *afsS* occurs in mutants lacking AfsR. The synthesis of AfsS in turns activates the *act* and *red* transcriptional regulators, and therefore enhances

the biosynthesis of actinorhodin, undecylprodigiosin, and the calcium-dependent antibiotic (CDA).

AfsR is phosphorylated at serine/threonine residues by the AfsK kinase (Hong et al., 1991; Lee et al., 2002). Phosphorylation of AfsR increases significantly the binding affinity of AfsR to the *afsS* promoter and therefore enhances actinorhodin, undecylprodigiosin, and CDA production. In addition, phosphorylation of AfsR modulates the ATPase activity of this regulator, that is required to rearrange the closed RNA polymerase–AfsR complex in the *afsS* promoter to an open transcriptionally active form. Genes orthologous to *afsK* and *afsR* occur in several *Streptomyces* species genomes suggesting that the mechanism of regulation through this phosphorylation cascade is important in these actinobacteria. Noteworthy, the autophosphorylating activity of AfsK is inhibited by KbpA, a protein encoded by a gene located upstream of the *afsK* gene in *S. coelicolor*. The KbpA protein binds to the unphosphorylated AfsK and inhibits its self-phosphorylation at serine/threonine residues. In AfsK–AfsR "*in vitro*" reaction mixtures KbpA inhibits the transmission of phosphate from AfsK to AfsR (Umeyama and Horinouchi, 2001; **Figure 1**). In summary, KbpA acts as a negative regulator in the AfsK–AfsR phosphorylation cascade, an important mechanism for the control of secondary metabolism and differentiation in some *Streptomyces* species, e.g., sporulation in *Streptomyces griseus*. Disruption of *kbpA* increases the phosphorylation cascade flux and results in an increase of actinorhodin production in *S. coelicolor*.

An important advance was the finding that the AfsK/AfsR proteins serve to integrate the signal of *S*-adenosylmethionine (SAM) concentration level. Methionine is one of the major methyl donors in microbial metabolism. This amino acid regulates positively or negatively the biosynthesis of many antibiotics, including actinorhodin (Kim et al., 2003), although the methionine signal transduction cascade has not been elucidated until recently. The methylation reactions are mediated by SAM, an activated form of methionine (Fontecave et al., 2004). The stimulatory effect of SAM is not observed in mutants blocked in the genes *afsR*, *afsS*, or *afsK*, or in the specific regulator gene *actII-orf4* (Jin et al., 2011). NMR studies of the serine/threonine kinase AfsK showed that SAM interacts with the carboxy-terminal moiety of this protein kinase and through this interaction increases the autophosphorylation of the AfsK protein in a dose-dependent mode (Jin et al., 2011). These authors propose that enhanced autophosphorylation of AfsK transmits the SAM signal leading to an increase in phosphorylation of AfsR, that in turns activates *afsS*, and therefore the production of actinorhodin and undecylprodigiosin (**Figure 1**).

Interplay of PhoP With Other Regulatory Factors: Binding to Overlapping DNA Sequences

Although phosphate control of actinorhodin and undecylprodigiosin biosynthesis in *S. coelicolor* is mediated by PhoP, no direct binding of PhoP to the region upstream of the translation start triplet of genes of the *act* and *red* gene clusters was observed (Martín, 2004; Santos-Beneit et al., 2009b; Allenby et al., 2012).

Rather, the phosphate control of these antibiotics biosynthesis is exerted by interference of PhoP and AfsR by binding to the same sequence in the promoter region of the *asfS* gene. Both phosphorylated PhoP and AfsR are competing positive regulators that integrate signals derived from different inputs (Lee et al., 2002; Santos-Beneit et al., 2009b, 2011b; **Figure 1**). Although both PhoP and AfsR overlap completely there is a preference for one particular nucleotide in the sequence, different for PhoP or AfsR. Indeed, nucleotides in the PHO and AfsR boxes at positions 2, 3, 4, and 6 are invariant but the nucleotide at position 5 may be a T or a G. When there is a G at position 5 it promotes binding of PhoP, whereas a T at this position promotes binding of AfsR. AfsR and PhoP compete not only in binding the PHO box upstream of *afsS* but also AfsR binds to PHO boxes in the upstream regions of *pstSCAB*, *glnR*, and *phoRP* (Santos-Beneit et al., 2009b, 2011b).

Additional examples of overlapping recognition sequences, by PhoP and other transcriptional factors, have been reported in the last decades. In one example PhoP controls directly *cdaR* expression, the cluster situated regulator of the CDA in *S. coelicolor*. In addition to PhoP, other master transcriptional factors, including AbsA2 and AfsQ1, bind the upstream sequence of *cdaR* (Allenby et al., 2012). Other interesting example is the regulation of the *scbA* gene, encoding the γ-butyrolactone synthase (D'Alia et al., 2011) by both PhoP and ScbR regulators (Allenby et al., 2012). Both *scbA* and *scbR* are expressed from a divergent promoter and expression of *scbA* is regulated by ScbR, while PhoP binding to the divergent promoter represses *scbA* expression. Therefore, there is a close connection of the regulation by the γ-butyrolactone system and the PhoP-mediated phosphate control in *S. coelicolor* (Allenby et al., 2012).

Cross Regulation of Phosphate and Carbon Sources

Cross-talk regulation between phosphate and carbon sources has been described in *Corynebacterium glutamicum* and also in a few *Streptomyces* species. Initial studies in *S. lividans* on carbon source control of phosphate transport through the high affinity PstSCAB transport system reveal that formation and release of the PstS protein takes place only in cultures with high concentration of fructose, galactose, or mannose but not with other carbon sources (Díaz et al., 2005). The PstS phosphate binding protein is partially released from the PstSCAB complex located in the cells envelopes and this release seems to be due to glycosylation of the PstS protein (Díaz et al., 2005; Wehmeier et al., 2009). The released PstS protein becomes not functional and unable to bind phosphate (Esteban et al., 2008). Using Northern analysis of the *pstSCAB* gene and Western blot assays of the PstS protein in *S. lividans* and *S. coelicolor*, Esteban et al. (2008) observed that the *pstS* gene expression takes place in media containing glucose or fructose as carbon sources but does not occur in complex medium. A stretch of DNA upstream of the *pstS* translation start triplet, including 8 degenerated repeats of a sequence of 12 nucleotides, is involved in negative control

of the transcription from the *pstS* promoter by fructose. This stretch of DNA is adjacent to, but does not overlap with, the well-characterized PHO box recognized by PhoP, though both DNA regions affect expression of the *pstS* gene. However, further detailed analysis of PhoP and the putative role of the repeated 12 nucleotides sequence in regulation by carbon sources needs to be made. Similarly, in *C. glutamicum* the GlxR regulator, which is a cAMP-dependent transcriptional regulator, functionally similar to CRP in Enterobacteria, regulates phosphate transport by binding to a sequence upstream of the phosphate transporter gene *pstS* under phosphate limiting condition and activates its expression (Panhorst et al., 2011).

Another interesting example in *S. coelicolor* is the regulation of *glpQ1* and *glpQ2*, that encode glycerophosphodiester phosphodiesterases, and are regulated by PhoP and also by glycerol and other carbon sources. PHO boxes have been identified in the promoter regions of *glpQ1* and *glpQ2* but the putative regulatory proteins recognizing glycerol or other carbon sources have not been studied yet (Santos-Beneit et al., 2009a). Increasing evidence indicates that coordination of phosphate and carbon source utilization, e.g., through the glycolysis have an important role in the metabolism of *Streptomyces* species. Recently, Ordóñez-Robles et al. (2017a) reported that in the tacrolimus producer *S. tsukubaensis* the use of glucose (but not maltose) as carbon source promotes drastically the expression of *phoR–phoP*, *pstS*, and other key genes of the Pho regulon. The findings that in *S. tsukubaensis* glucose stimulates significantly the genes involved in phosphate transport, and the similar effect of fructose in *S. lividans* indicates that an increase in the concentration of these hexoses in the culture medium favors the uptake of inorganic phosphate to balance the carbon and phosphate metabolism through the glycolysis, pentoses phosphate pathway, and TCA cycle. Reciprocally, inorganic phosphate affects many of the genes of the carbon metabolism and this regulation is mediated by PhoP (Rodríguez-García et al., 2007; Allenby et al., 2012), including enzymes involved in glycogen metabolism and gluconeogenesis (Thomas et al., 2012).

REGULATION OF NITROGEN METABOLISM IN ACTINOBACTERIA: THE GlnR MASTER REGULATOR

One of the most interesting examples of cross-talk between transcriptional regulators is the overlapping binding of PhoP and GlnR in the promoters of several nitrogen metabolism genes. *Streptomyces* and other Actinobacteria use a variety of nitrogen sources for growth. These include ammonium ions, nitrate and nitrite, and complex organic nitrogen sources including urea, amino acids, peptones, and several other nitrogen-containing compounds, including polyamines (Krysenko et al., 2017). In addition, some Actinobacteria, e.g., *Frankia* species are able to utilize atmospheric nitrogen for the production of organic nitrogen compounds in the cells (Nouioui et al., 2019). These different nitrogen sources are converted to glutamate and glutamine that serve as amino donors in transamination reactions to form other nitrogen containing compounds. In *Streptomyces* species there are two glutamine synthetases, encoded by the genes *glnA* and *glnII*, that convert glutamate to glutamine but the major glutamine synthetase activity is that of GlnA (Fink et al., 2002). Other glutamine synthetase-like enzyme, e.g., GlnA3, is known to be involved in polyamine utilization but has no glutamine synthetase activity (Krysenko et al., 2017). The ammonium ions are transported in the cells by the *amtB* transporter, which is clustered with genes *glnK* and *glnD*. On the other hand, nitrate and nitrite ions are reduced to ammonium by the nitrate reductases NasA (Amin et al., 2012), and nitrite reductase NirB1B2C/D (Tiffert et al., 2011). The urea is metabolized by a system encoded by the *ureABC* cluster.

All nitrogen metabolism genes respond to the nitrogen availability in the culture (Tiffert et al., 2008). Two regulatory genes, *glnR* and *glnRII*, control expression of several nitrogen metabolism genes at the transcriptional level (Fink et al., 2002). GlnR (267 amino acids) contains the domains defining a response regulator but is not linked to a cognate sensor kinase (Wray et al., 1991; Fink et al., 2002) and is classified as an orphan response regulator (Hutchings et al., 2004). It has been shown that GlnR in *Streptomyces* species is atypical in its lack of phosphorylation of the D^{49} residue (Hong et al., 2007); in PhoP this amino acid in its phosphorylated form activates the DBD but this activation does not seems to be required in GlnR. The protein region surrounding D^{49} is phosphorylated in serine and threonine residues and is essential for maintaining the biologically active homodimer conformation (Lin et al., 2014). Nucleotide sequences for GlnR binding upstream of many different nitrogen metabolism genes were shown to correspond to 22 nucleotides forming a direct tandem repeat of 11 nucleotides each (Tiffert et al., 2008; Sola-Landa et al., 2013). Under nitrogen limitation conditions GlnR induces expression of *glnA*, *glnII*, and the *amtB–glK–glD* cluster, but represses the cluster of urea utilization genes.

Post-translational Phosphorylation or Acetylation of GlnR Affect Nitrogen Regulation in *S. coelicolor*

Mass spectrometry analysis of GlnR showed that this regulator is post-translationally phosphorylated at serine/threonine residues in six positions and acetylated at four lysine residues. The degree of phosphorylation correlates well with growth on nitrogen rich medium and is reduced, and even absent, in nitrogen limiting minimal medium. DNA binding studies using EMSA showed that the phosphorylated form of GlnR does not bind to its target sequences. Moreover, initial structural studies of GlnR indicated that the serine/threonine phosphorylated residues prevent formation of the active GlnR dimeric form (Amin et al., 2016). Overimposing the amino acid sequences of GlnR with the crystal structure of PhoP it was observed that the serine/threonine residues which are phosphorylated and the lysine residues which are acetylated in GlnR are conserved with respect to the same amino acids in PhoP. Regarding modification by acetylation, four lysine residues are acetylated in GlnR in nitrogen limiting medium but only one lysine is modified in nitrogen rich conditions. Therefore, it was proposed that the

modifications in GlnR are similar to those reported in PhoP except phosphorylation at D^{49}. However, the lysine acetylation does not appear to respond to the nitrogen availability in the medium but rather it responds to carbon sources (Amin et al., 2016), as described above for lysine acylation in PhoP in response to propionate or propanol.

GlnR Regulates Secondary Metabolites Biosynthesis Through Pathway Specific Regulators

Detailed studies on nitrogen regulation mediated by GlnR were performed in the model actinobacteria *S. coelicolor* (Tiffert et al., 2011) and in *Streptomyces venezuelae* (Pullan et al., 2011). Other studies have been performed in *Sac. erythraea* (Yao et al., 2014), in *Amycolatopsis mediterranei* (Yu et al., 2007), and also in *S. hygroscopicus* var. *jinggangensis*, producer of validamycin (Qu et al., 2015). Transcriptional studies of a *S. coelicolor* mutant deleted "in frame" in *glnR*, confirmed that GlnR represses actinorhodin biosynthesis, and induces undecylprodigiosin formation. These observations were supported by DNA binding studies using purified GlnR. Noteworthy, it was found that GlnR binds directly to the promoter regions of genes for the pathway specific regulators ActII-orf4 and RedZ, respectively. He J.M. et al. (2016) identified a GlnR binding nucleotide sequence, 5-GTGAC-3, in the promoter regions of *actII-orf4* and *redZ* genes that has similarity to the nucleotide sequence of the A fragment in GlnR binding site described by Tiffert et al. (2008). Mutation of nucleotides in this putative GlnR binding site supported the conclusion that GlnR binds to the promoters of actinorhodin and undecylprodigiosin gene clusters in a sequence which is slightly different from those identified in primary nitrogen metabolism genes. It is possible that to bind these different sequences GlnR needs cooperation with either a sigma factor or other transcriptional regulators. In the case of genes for nitrate–nitrite assimilation, the recognition by GlnR is promoted by NnaR, which might act as a GlnR co-activator for *nirB1* expression (Amin et al., 2012).

In *S. avermitilis*, which produces the antihelminthic avermectin and the unrelated macrolide oligomycin, a mutant deleted in the *glnR* gene reduces drastically the production of avermectin but increased the biosynthesis of oligomycin (He J.M. et al., 2016). Transcriptional studies of the two regulatory genes involved in the control of avermectin, *aveR*, and oligomycin, *olmR*, indicate that GlnR in *S. avermitilis* binds to the promoter regions of these two regulatory genes. A very interesting aspect of this regulation in *S. avermitilis* is that the regulatory gene *aveR* contains also consensus binding sequences for PhoP (Yang et al., 2015; Martín et al., 2017), suggesting that there are regions upstream of the avermectin regulatory gene that integrate the response to different nutritional signals.

In summary, it may be concluded that GlnR is not only a master transcriptional regulator of nitrogen metabolism but it also coordinates primary metabolism and expression of secondary metabolites biosynthetic gene cluster through binding to the promoters of specific regulators of those gene clusters.

CROSS TALK OF PHOSPHATE AND NITROGEN REGULATION IN *Streptomyces*

One of the most interesting recent development on interaction between master regulators is the cross-talk between GlnR and PhoP in the control of primary metabolism and also secondary metabolites biosynthesis in Actinobacteria.

PhoP and GlnR are related proteins of the OmpR response regulators family (Hutchings et al., 2004; Martín et al., 2012b). The expression of several genes involved in nitrogen metabolism is increased in a *S. coelicolor* Δ*phoP* mutant (Rodríguez-García et al., 2007). The control of PhoP over these genes is exerted in two ways. On the one hand, there is a binding of PhoP to the promoter of the *glnR* gene decreasing its expression when phosphate is limiting (Rodríguez-García et al., 2009; Allenby et al., 2012). In addition, PhoP binds directly to the promoters of at least six other genes related to nitrogen metabolism: *glnA*, *glnII*, the *amtB–glnK–glnD* operon, *ureA*, and some additional uncharacterized genes, interfering with the GlnR activation of these genes (Rodríguez-García et al., 2009; Sola-Landa et al., 2013). The interaction of PhoP with GlnR differs depending on the relative position of the sequences recognized by each of these proteins. In the *glnA* promoter, there is a direct competition between PhoP and GlnR because both regulators recognize overlapping sequences. In the *amtB* promoter, the PhoP and GlnR binding sequences are not fully overlapping, although they are very close and the binding of PhoP may alter the correct recognition of GlnR (Sola-Landa et al., 2013; **Figure 2**).

The Nitrogen Regulator GlnR Controls Phosphate Transport by the PstS System in *A. mediterranei*

The interplay between GlnR and PhoP in *S. coelicolor* is well studied, but it is unknown if these conclusions are valid for other actinobacteria. A relevant example is the interaction of these regulators in *A. mediterranei*, a strain of industrial importance that produces rifamycin. Zhang et al. (2018) cloned the *pstSCAB* cluster of *A. mediterranei* and demonstrated its involvement in phosphate transport under phosphate limiting conditions. A mutant disrupted in the *pstS* gene showed a decreased production of rifamycin and, interestingly, revealed different morphology (swollen, near spherical cells rather than filamentous hyphae).

The *pstSCAB* operon was expressed as a transcriptional unit in *A. mediterranei* (Zhang et al., 2018) as reported also in *S. coelicolor* (Esteban et al., 2008) and confirmed by RNAseq studies (Martín-Martín et al., 2019). Nitrate has a well-known stimulatory effect on rifamycin biosynthesis by *A. mediterranei*. Transcriptional analysis revealed that formation and release of the PstS protein was induced by nitrate and regulated positively by GlnR. Expression of *pst*SCAB in a *glnR*-null mutant of *A. mediterranei* revealed a fourfold decrease of *pst*S transcription even in the presence of added nitrate; in other words, the nitrate stimulation of *pst*S expression is dependent upon GlnR. DNA binding

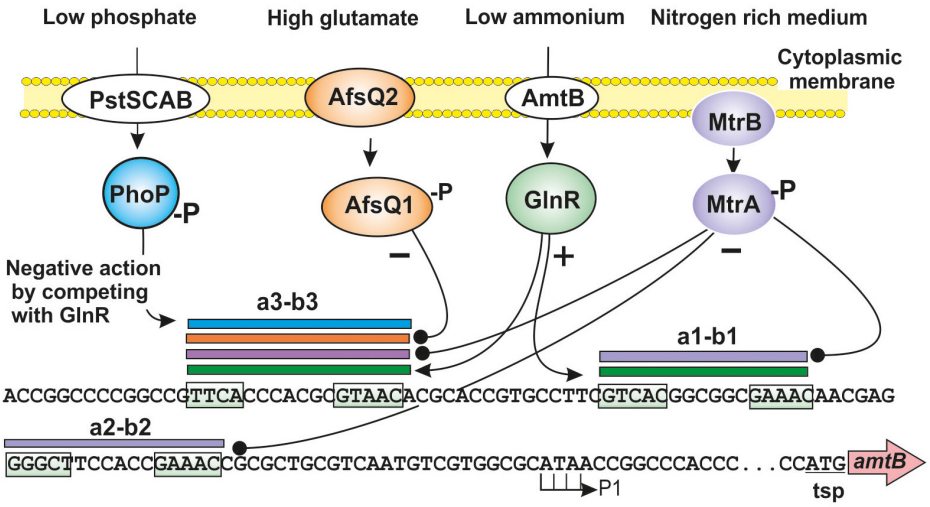

FIGURE 2 | Signal integration sites upstream of *S. coelicolor amtB* gene. Interaction of the regulatory proteins GlnR (green sphere), PhoP (blue sphere), MtrA (purple sphere), and AfsQ1 (orange sphere) on the *amtB* promoter region. The binding sites of GlnR, PhoP, MtrA, and AfsQ1 on the a1-b1, a2-b2, and a3-b3 sites are indicated with green, blue, purple, and orange horizontal bars, respectively. The transcription start point (P1) and the translation start point (tsp) of *amtB* are indicated. Positive regulation is indicated by arrows and negative regulations by black spheres. The consensus GlnR binding sequences are boxed. See text for additional details.

studies with purified GlnR proved that this regulator binds to the upstream region of *pst*S, thus confirming that the high affinity phosphate transport system is under the control of GlnR in this actinobacteria. As indicated above, the *pstSCAB* cluster of many actinobacteria is strongly regulated by PhoP and, indeed, there is a PhoP binding sequence upstream of the *pstSCAB* genes in many bacteria. Therefore, the DNA sequences upstream of *pstSCAB* constitute an integrator site that combines signals of phosphate starvation and nitrogen availability (Zhang et al., 2018).

INTERPLAY OF THE DEVELOPMENTAL REGULATOR MtrA WITH GlnR: COMPETITION FOR THE GlnR BINDING SITE

In 2017, it was observed that the response regulator MtrA (master transcriptional regulator A), member of the MtrAB TCS has an important role in nitrogen regulation (Som et al., 2017a,b; Zhang et al., 2017). The *mtrA* gene was initially discovered in *Mycobacterium tuberculosis*, where it has an important role in cell development and antigen secretion, and was also characterized in *C. glutamicum* (Möker et al., 2004). In *S. coelicolor* the MtrA protein is well conserved compared to the homologous proteins of *M. tuberculosis* and *C. glutamicum.* Initial studies indicated that in *S. coelicolor* MtrA has an important role in cell development since mutation of this regulator results in the lack of mycelium formation (*bald* phenotype) and also alters secondary metabolism (Som et al., 2017a,b). These studies revealed that MtrA binds a 17 nucleotides sequence consisting in two repeats of six nucleotides, separated by a five nucleotides non-conserved stretch, that surprisingly, overlap with the GlnR binding site in several nitrogen metabolism genes.

Role of the Two Components System MtrAB in Nitrogen Metabolism in *S. coelicolor*

Recently, it was experimentally demonstrated that MtrA binds to one of the three putative GlnR binding sequences upstream of the *amtB–glnK–glnD* cluster (Zhu et al., 2019). Previously, three putative GlnR binding sites (named a1-b1, a2-b2, and a3-b3), each consisting in two binding repeats had been identified in the *amtB* promoter region (Wang et al., 2012; Li et al., 2018). More recently, Zhu et al. (2019) showed that the developmental regulator MtrA recognizes the a3-b3 binding sequence which also binds GlnR efficiently. This was confirmed by EMSA DNA binding assays using the a3-b3 sequence as probe (**Figure 2**). MtrA was also able to bind the a1-b1 and a2-b2 sites, although GlnR did not recognizes the a2-b2 site indicating that minor differences in nucleotides in these binding sequences determine the affinity of binding for MtrA versus GlnR. Additionally, binding of MtrA to GlnR boxes upstream of other nitrogen metabolism genes such as *glnA*, *glnII*, *nirB1B2C/D*, and *ureA* was also found. In all cases MtrA was bound to the GlnR recognition sites although the affinity of binding changes depending on the nucleotide sequences of the different GlnR boxes. It is worth to note that the a3-b3 site was also recognized by PhoP (**Figure 2**; Wang et al., 2012; Sola-Landa et al., 2013).

Similarly, competition experiments and EMSA assays on the *nirB1B2C/D* promoter using different amounts of MtrA and GlnR showed that the intensity of the DNA–protein

complexes varies depending on the relative amount of MtrA to GlnR. In other words, both proteins compete for the same nucleotide sequence, demonstrating that there is an overlapping binding of the two regulators to the upstream sequence of the *nirB1B2C/D* cluster.

In vivo binding of MtrA to GlnR recognition sequences in different nitrogen metabolism genes was shown by ChIP-qPCR analysis using anti-Flag antibodies and a *S. coelicolor* Δ*mtrA* mutant transformed with the Mtr-Flag fused gene (Zhu et al., 2019). Comparative transcriptional analysis of gene expression in the parental strain and the *mtrA*-deleted mutant showed that several nitrogen metabolism genes including the *amtB–glnk–glnD* cluster, *glnII*, *nasA*, and *nirB1–nirB2–nirC/D* were highly overexpressed in the *mtrA*-deleted mutant under nitrogen rich medium whereas the urea utilization cluster was not significantly upregulated under these conditions.

These results clearly indicate that under nitrogen rich conditions MtrA represses nitrogen metabolism genes, i.e., this is a regulation opposed to that of GlnR in minimal medium. Interestingly, comparative transcriptional experiments were also performed under nitrogen limiting conditions using the *mtrA*- or the *glnR*-deleted mutant, compared to the parental strain (Zhu et al., 2019); the results clearly indicated that expression of several nitrogen metabolism genes respond to the GlnR concentration in the cells but not to the MtrA levels. In other words under nitrogen limiting conditions the positive regulatory effect of GlnR dominates over the MtrA repression.

Noteworthy, although GlnR does not regulates its own expression, binding of the purified MtrA protein to a sequence upstream of *glnR* was found. Indeed, there was no binding of purified GlnR to the upstream sequence of the *glnR* gene itself, although it is recognized by MtrA. These results are difficult to explain if it is assumed that both GlnR and MtrA recognized the same binding sequences. Probably other proteins interact with MtrA and modify its affinity compared to that of GlnR.

Similarly, NtrA of *S. lividans* regulates expression of several nitrogen metabolism genes under nitrogen rich conditions, as occurs in *S. coelicolor* (Zhu et al., 2019). Furthermore, the *ntrA* gene has been characterized in *M. tuberculosis* and *C. glutamicum*. Initial experiments using NtrA purified protein from these actinobacteria indicate that potentially MtrA is also able to regulate nitrogen metabolism genes both in *Mycobacterium* and in *Corynebacterium*. It is likely that a similar regulatory mechanism occurs in other actinobacteria. In summary, the wide distribution of genes encoding GlnR and MtrA in several actinobacteria suggests that these two master regulators play a very important role in nitrogen metabolism.

Interplay of Nitrogen and Carbon Regulatory Mechanisms Mediated by GlnR

Early studies on GlnR-mediated regulation of metabolism in *Streptomyces* suggested that this regulator is also involved in the control of carbon sources assimilation (Tiffert et al., 2008; Pullan et al., 2011).

An interesting recent development is the finding that GlnR interacts with metabolism of many carbon sources at the transport level (Liao et al., 2015). The actinobacteria use a large variety of carbon sources (Bertram et al., 2004; Titgemeyer et al., 2007). Some of them, e.g., glucose or glycerol, are preferred carbon sources but the utilization of many other hexoses, oligosaccharides, and polysaccharides is non-constitutive and is only induced when required. In *Streptomyces* species, glucose is transported by a well-known permease system (van Wezel et al., 2005). In contrast 87% of the total carbohydrate carbon sources are transported by ATP binding cassettes (ABC) transporter systems (van Wezel et al., 1997; Davidson et al., 2008). Studies on the control by GlnR of several ABC sugar transporters have been done in *Sac. erythraea* and in *S. coelicolor* (Liao et al., 2015). These authors identified a sequence similar to the GlnR-binding site in the upstream region of the *malEFG* operon of *Sac. erythraea*, that encodes an ABC transport system for maltose and maltodextrines (**Figure 3**). Immediately upstream of the *malEFG* operon in the complementary strand and in the opposite orientation are two genes *malR* and *aglA*, encoding the MalR repressor protein and an α-glucosidase involved in the cleavage of maltose and maltodextrins to produce glucose. Both in *Sac. erythraea* and in *S. coelicolor* two MalR binding sites were detected and confirmed in DNA binding assays in the intergenic region *malEFG-malR*, one of which overlap with the GlnR binding sequence (Liao et al., 2015; **Figure 3**). Mutants of *Sac. erythraea* or *S. coelicolor* deleted in the *glnR* gene showed impaired growth in media containing maltose as only carbon source but not in media supplemented with glucose. Transcriptional studies revealed that expression of the *mal* operon was dependent on the GlnR regulator, i.e., there is no expression of this operon in the *glnR*-deleted mutant. Binding of purified GlnR to the upstream region of the *mal* operon was shown by DNA binding assays. Transcription of the *mal* operon increases in response to nitrogen starvation, indicating that the nitrogen availability controls expression of the *mal* transport system (**Figure 3**).

In *S. coelicolor* 12 out of 37 putative ABC sugar transporters were found to contain GlnR binding sites. The same situation was found in *A. mediterranei*, *Mycobacterium smegmatis*, and three additional *Streptomyces: S. griseus*, *S. venezuelae*, and *S. avermitilis* (Liao et al., 2015). Similarly, GlnR binding sites were found in 8 of the 19 putative ABC-type sugar transporters in *Sac. erythraea*. It seems that in all these cases expression of the sugar binding subunits of the respective ABC transporters was dependent on the GlnR regulator.

Altogether these findings indicate that there is a cross-talk between the limitation of nitrogen sources and the transport of several sugars by ABC systems. This interplay between the nitrogen regulation and sugar transport system protects the cell against imbalances in nitrogen and carbon abundance by controlling the utilization of alternative sugar sources. When nitrogen is limiting the GlnR levels increase, and therefore favor the utilization of alternative nitrogen (Tiffert et al., 2011) and carbon sources (Liao et al., 2015).

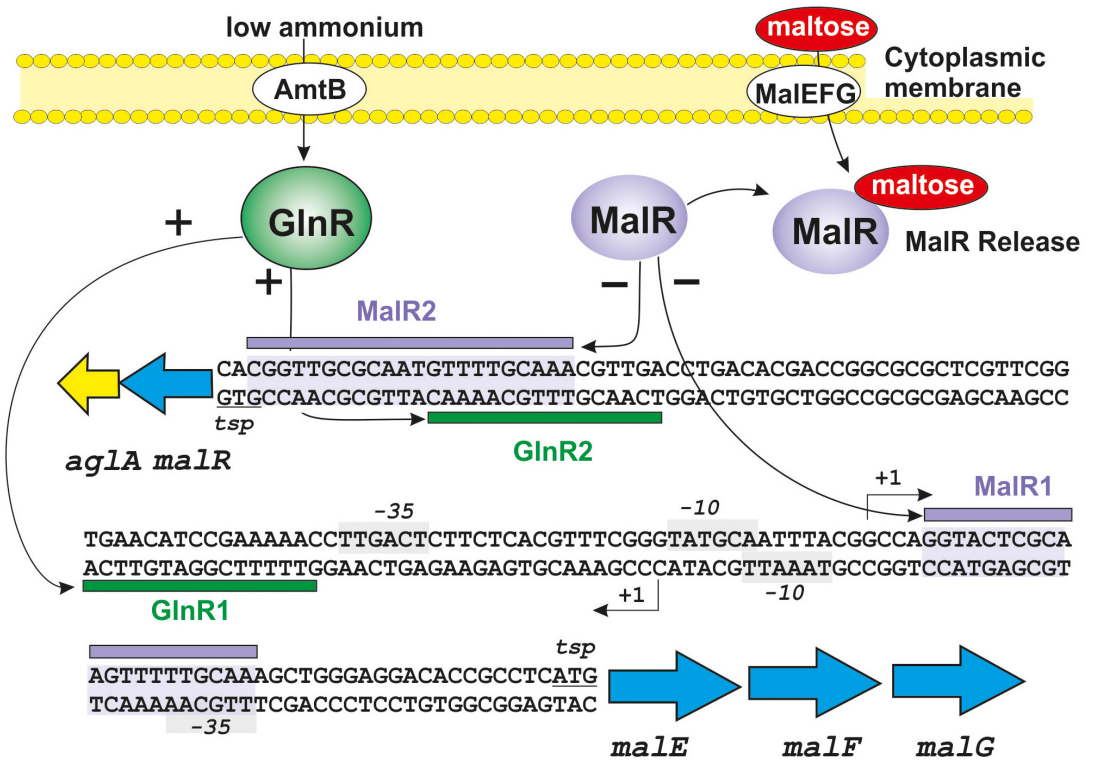

FIGURE 3 | Interaction between the repressor protein MalR and the activator protein GlnR on the *mal* operon of *Sac. erythraea*. The intergenic *aglAmalR-malEFG* region is shown with the MalR binding sites shadowed in purple. The binding sites for MalR and GlnR are indicated with purple and green horizontal bars, respectively. The -10 and -35 sites for both operons are shown in gray boxes. The +1 transcription sites and the translation starting points for both operons are indicated. Positive regulation is indicated by arrows and a (+) sign; negative regulation is indicated by arrows and a (–) sign. Maltose (red ellipse) induces the *malEFG* operon by binding to the MalR repressor and releasing it from the DNA. See text for additional details.

POSSIBLE INTERACTION BETWEEN THE cAMP RECEPTOR PROTEIN AND THE GlnR NITROGEN REGULATOR

Glucose is the preferred carbon source by *Streptomyces* and many other bacteria, and there is a regulation by glucose of alternative non-preferred carbon sources utilization. This regulation in Enterobacteria is mediated by the cAMP receptor protein (CRP) and is dependent on the cAMP levels in the cells. Several studies have reported that in *S. coelicolor*, the carbon catabolite regulation of alternative carbon sources by glucose is not mediated by a CRP-homologous protein. Instead, carbon catabolite regulation is mediated by the glycolytic enzyme glucose kinase (Ikeda et al., 1984; Angell et al., 1994; van Wezel et al., 2007; Romero-Rodríguez et al., 2016a,b). However, in *Sac. erythraea* there is a CRP-like protein that seems to be involved in carbon catabolite control of utilization of alternative carbon sources. This regulation involves binding of the CRP-like protein to promoter regions of several ABC-type sugar transporters. Bioinformatic studies revealed that there are putative CRP binding sequences in the upstream regions of several ABC sugar transporters in *Sac. erythraea* and possibly also in other actinobacteria (Liao et al., 2015). This finding adds a new level of regulation by interaction of CRP with promoters of ABC sugar transporters, such as *malEFG*. Indeed, Liao et al. (2015) proposed that CRP binds to the same region recognized by GlnR in the intergenic region between *malEFG* and *malR-aglA* (**Figure 3**). However, the putative interaction at this level needs further experimental confirmation. In summary, the possible interaction between the CRP protein, the GlnR and the MalR regulator in the *mal* operon for maltose/maltodextrins metabolism, is another provocative example of interaction of several regulatory proteins on the promoter region of key sugar transporters and therefore constitutes an elaborate mechanism of control by interacting transcriptional regulators.

INTERPLAY BETWEEN THE TWO COMPONENTS SYSTEM *AFSQ1/Q2* AND THE NITROGEN REGULATOR GlnR

The two components system AfsQ1–AfsQ2 (of which *afsQ1* encodes the response regulator) was initially found as a result of the observation that it increases the production of actinorhodin and undecylprodigiosin in *S. coelicolor* (Shu et al., 2009). In the opposite orientation of *afsQ1–AfsQ2* is located the *sigQ* gene, encoding a putative sigma factor involved in antibiotic biosynthesis, that is regulated by AfsQ1 (Wang et al., 2013).

The observed regulation takes place only in minimal medium supplemented with 75 mM glutamate. Transcriptional studies using cell grown under these glutamate rich conditions revealed that the expression of *actII-orf4*, *cdaR*, and *redZ* genes was significantly reduced in the *afsQ1-Q2* mutant. EMSA studies with purified AfsQ1 revealed that, indeed, this response regulator was able to bind to the *actII-orf4*, *cdaR*, and *redZ* promoters but not to the *redD* promoter region. The AfsQ1 regulator enhances the expression of *sigQ* but not that of the *afsQ1–afsQ2* operon itself. In other words, there is a bidirectional transcription region that expressed *afsQ1-Q2* in one orientation and *sigQ* in the other and AfsQ1 does not regulates directly its own expression. The AfsQ1 binding sequence was first identified in the promoters of *sigQ* and *redZ* and later also in *actII-orf4* and *cdaR*. In all cases, except in *actII-orf4*, a 16 nucleotides sequence was protected by AfsQ1. This sequence, GTnAC-n6-GTnAC, consists of two repeated GTnAC nucleotides sequences separated by an intervening non-conserved six nucleotides stretch. Surprisingly, the sequence recognized by AfsQ1 in *actII-orf4* does not adjust to the consensus five nucleotides repeated sequence indicating that there are factors, still unknown, that affect the specificity of the binding sequences recognized by AfsQ1 (Wang et al., 2013). These authors using a matrix based on the conserved 16 nucleotides binding sequence were able to recognize 17 sites that correspond to: (1) the upstream regions of nitrogen metabolism genes, such as *glnA* and *nirB1*; (2) the *pstS* gene involved in high affinity phosphate transport; and (3) several bidirectional promoters related to cell differentiation including *whiD* and *bldM* (Wang et al., 2013).

The putative AfsQ1-binding sequence contains the same five nucleotide core repeats that form part of the 16 nucleotides consensus sequence recognized by GlnR. EMSA studies with purified AfsQ1 revealed that this regulator binds to the promoter regions of several nitrogen metabolism genes but not to the promoter of *glnR* or *glnII* indicating that there are differences in the affinity of distinct regulatory proteins for nitrogen metabolism genes. Transcriptional studies using a mutant deleted in *afsQ1–afsQ2* showed that AfsQ1 acts as a transcriptional repressor of several nitrogen assimilation genes under conditions of high glutamate concentration. Competition DNA binding experiments using both purified AfsQ1 and GlnR proteins lead to the conclusion that both regulators compete for the same nucleotide sequence in the upstream region of several nitrogen assimilation genes; in other words, AfsQ1 represses the expression of genes encoding enzymes for assimilation of alternative nitrogen sources in conditions of glutamate excess by competing with GlnR that would activate these promoters under nitrogen limitation conditions.

An important observation is the finding that AfsQ1 regulates expression of the *pstSCAB* cluster that is also strongly regulated by PhoP and AfsR (Santos-Beneit et al., 2009b; Martín et al., 2012a). Indeed, PhoP also regulates expression of several nitrogen assimilation genes as described above in this article. Taken together all this information suggests that these five master regulators PhoP, AfsR, AfsQ1, GlnR, and MtrA, interact in the fine tuning of regulation of key genes in carbon, nitrogen, and phosphate metabolism. This interaction protects the cell against unbalance metabolism due to lack or excess of some key nutrients, such as ammonium or glutamate (**Table 1** and **Figure 2**). Not all five regulators bind to the same integrative node; two, three, or more transcriptional factors may recognize certain sequences whereas combinations of other factors regulate expression of genes at alternative nodes.

OVERLAPPING TRANSCRIPTIONAL FACTORS REGULATE EXPRESSION OF AtrA

Other interesting example of interplay between transcriptional factors is the cross regulation between PhoP and the AdpA regulator, that in turn responds to the γ-butyrolactone signaling mechanism. In the quorum sensing system the γ-butyrolactones are recognized by specific butyrolactone receptor proteins (Brps) (Horinouchi, 2002; Ohnishi et al., 2005) that when combined with its own cognate butyrolatone derepressed the binding of the Brps to the pleiotropic regulator AdpA (Takano, 2006). This occurs in different *Streptomyces* species (Higo et al., 2012; Salehi-Najafabadi et al., 2014) and has been studied with detail in *Streptomyces roseosporus*. The butyrolactone triggered signaling cascade in *S. roseosporus* is known to proceeded through the TetR-type regulator AtrA, that controls expression of the biosynthesis of the lipopeptide antibiotic daptomycin (Mao et al., 2015). Expression of AtrA is controlled by the pleiotropic regulator AdpA. Recently, Zheng et al. (2019) observed that expression of AtrA is regulated in addition by PhoP. Binding of these two regulators overlaps in the upstream region of the *atrA* gene as confirmed by DNA binding studies. Moreover, in turn PhoP indirectly controls expression of the *adpA* gene (Allenby et al., 2012). Therefore, PhoP controls AtrA at two different levels in a cumulative form. In conclusion, this is other excellent example of overlapping regulation exerted by two different master regulators, PhoP and AdpA, on the expression of the *atrA* gene. Since AdpA is regulated by the γ-butyrolactone quorum sensing system the overall mechanism connects the regulation by small ligands (Xu et al., 2010; Martín et al., 2019) with the regulation exerted by the master regulators of phosphate metabolism.

BINDING OF INTERACTING TRANSCRIPTIONAL FACTORS: THE CONCEPT OF SIGNAL INTEGRATIVE DNA REGIONS

Increasing evidence indicates that there are numerous examples of overlapping sequences that integrate nutritional and environmental stress signals in *Streptomyces* species (Romero-Rodríguez et al., 2018). As described above six or even more transcriptional factors may bind to a specific promoter region. Therefore, the concept of a metabolic safety net is of interest to understand how the interaction of these stress signals, through integrator DNA sites, protect the metabolism of the cells against

nutritional and environmental damage by achieving a balance of the key metabolic pathways.

The evidence that different master transcriptional factors interact on overlapping DNA sequences has been supported by studies on ChIP-on-chip analysis. This technique that uses antibodies against one of the binding proteins immunoprecipitates the DNA region bound by the specific factor targeted by the antibody and also results in coprecipitation of other interacting proteins (Allenby et al., 2012). This study indicated that there are many more binding sites for PhoP or other transcriptional factors, e.g., DasR (Świątek-Połatyńska et al., 2015), than those expected from previous transcriptomic studies. The authors propose that interaction of PhoP with other transcriptional factors increase the affinity of PhoP for some poorly conserved PHO boxes. For example, Allenby et al. (2012) observed a massive binding of PhoP to the *cpk* gene cluster corresponding to internal sequences of *cpkB* and *cpkC* genes involved in coelimycin P1 biosynthesis (Gomez-Escribano et al., 2012). It is possible that this intense PhoP binding may be due to some interaction with some other factors that control those genes in the *cpk* gene cluster.

Moreover, these master regulators in turn control several other transcriptional factors at lower levels, that regulates differentiation, osmotic stress responses, oxygen metabolism, and secondary metabolite biosynthesis.

ADDITIONAL INTERTWINING LAYERS OF REGULATION REINFORCE THE SAFETY NET

In this article we have focused on interactions of transcriptional factors that control expression of different gene clusters in *Streptomyces*. These interactions constitute the backbone of the safety net but there are many other regulatory factors at distinct levels that provide different layers of control (**Figure 4**). These include sigma factors and anti-sigma factors (Paget, 2015), guanosine tetraphosphate, guanosine pentaphosphate, and novel cyclic guanine and adenine nucleotides, all of which act the transcriptional level, and ancillary subunits of the RNA polymerase. In this article we are concentrating on the interactions at the transcriptional level. Life of Actinobacteria is subject to frequent changes in nutritional and environmental conditions and this requires adaptation to the stress produced by those changes. To adjust to those changing conditions Actinobacteria have developed a variety of alternative sigma factors that recognize and activate adequate promoters in response to the novel conditions. Housekeeping genes that are strictly required for growth are transcribed by RNA polymerase that contain sigma factors of the Sig70 family, namely the HrdB factor; however, there are several paralogous genes similar to *hrdB* (e.g., *hrdA*, *hrdC*, and *hrdD*), whose function is still partially unclear. Sequencing of *Streptomyces* genomes has revealed that these actinobacteria contain many alternative sigma factors, 69 (66 in the chromosome and 3 in plasmids) in *S. coelicolor* (Bentley et al., 2002) and 62 in *S. lividans* (Rückert et al., 2015; Rebets et al., 2018), whereas *Escherichia coli* contains only 7 sigma factors and *B. subtilis* has 18. Alternative sigma factors play an important role on expression of genes involved in many aspects related to growth, differentiation, stress response, and secondary metabolites biosynthesis (Sun et al., 2017). Therefore, the interactions of these alternative sigma factors with promoter regions that also are regulated by the above described transcriptional factors provide an intertwining mechanism of control of gene expression. Several sigma factors are antagonized by anti-sigma proteins (19 in the *S. lividans* genome). The result is that the interaction of the cognate sigma factor with the RNA polymerase is blocked by binding of the corresponding anti-sigma factor. This adds an additional level of control on the interaction of transcriptional factors and sigma factors in the safety network. An additional protein that interacts with the RNA polymerase core enzyme is the ancillary protein RpoZ that in *S. coelicolor* is controlled by the phosphate regulator PhoP; mutant in *rpoZ* are impaired in cell differentiation and secondary metabolites biosynthesis (Santos-Beneit et al., 2011a).

Another group of molecules that interact with the RNA polymerase are the guanosine hyperphosphorylated molecules, namely guanosine tetra-phosphate (ppGpp) and guanosine pentaphosphate (pppGpp) These compounds initially characterized in *E. coli* have been found in many other bacteria including actinobacteria. These molecules are formed in response to carbon and nitrogen limitation, particularly in amino acid starvation caused be the absence of an essential amino acid (Dalebroux and Swanson, 2012) and constitutes the so called stringent response that limits transcription of several genes involved in vegetative growth (e.g., genes involved in ribosomal protein synthesis) and stimulates expression of stress response genes. The highly phosphorylated guanosine nucleotides are synthesized by a ppGpp synthetase encoded by the *relA* gene. In Enterobacteria the ppGpp is degrade by a ppGpp phosphohydrolase whereas in *Streptomyces* the *relA* gene appears to have both biosynthetic and degradative activities, being named *relA*/*spoT* (Martínez-Costa et al., 1998). Based on the information derived from *S. coelicolor relA* gene it was proposed that accumulation of ppGpp in response to nitrogen limitation increases biosynthesis of secondary metabolites (Bibb, 2005). Indeed, this increase is mediated by the extracytoplasmic factor SigT, thus providing an interesting example of interaction between sigma factors and stringent response (Feng et al., 2011). Mutants deleted in the *relA* gene showed greatly reduced transcription of the *actII-orf4* and *redD* genes, which are required for expression of the *act* and *red* gene clusters (Chakraburtty and Bibb, 1997; Hesketh et al., 2001). Global transcriptomic studies comparing the S. *coelicolor* parental strain and the *relA*-null mutant showed that *relA* controls expression of 598 genes most of them involved in growth and differentiation and some of them affecting secondary metabolite biosynthesis (Hesketh et al., 2007). Among the impacted genes was the major vegetative sigma factor HrdB that is repressed following ppGpp accumulation. The biosynthesis of alternative sigma factors was also affected in the *relA*-deleted mutant (Hesketh et al., 2001). However, more recent information indicates that biosynthesis of ppGpp is not strictly required for triggering biosynthesis of secondary metabolites, even in some *Streptomyces* species such

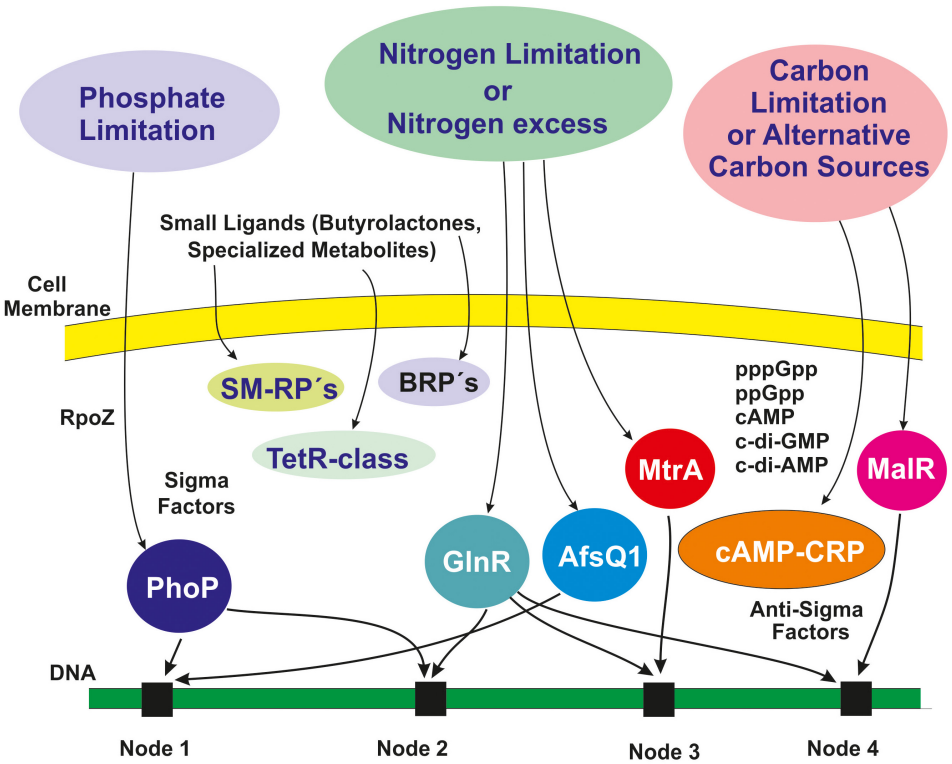

FIGURE 4 | Schematic representation of overlapping layers of regulation that reinforce the safety net. The outer circles represent nutritional stresses that elicit regulatory responses (detailed in **Figures 1–3**). Additional regulatory elements including sigma factors, highly phosphorylated and cyclic nucleotides are shown inside the cell. Receptors proteins (SM-RPs, BRPs) and the TetR-class transcriptional regulators are receptors of signal molecules that are secreted and re-enter the cell. Four integration nodes are highlighted in black boxes in the DNA. The different regulatory sigma and anti-sigma factors and the ligand receptor proteins are connected to distinct nodes (not shown; see text). BRPs, γ-butyrolactone receptor proteins; SM-RPs, specialized metabolites receptor proteins; CRP, cAMP receptor protein.

as *Streptomyces clavuligerus* deletion of the *relA*-gene resulted in a 2–2.5-fold overproduction of cephamycin C and clavulanic acid, indicating that (p)ppGpp may influence positively or negatively antibiotic biosynthesis (Gomez-Escribano et al., 2008). The highly phosphorylated guanine nucleotides form part of a family of second messengers that have been paid more attention recently; these include in addition to ppGpp and pppGpp, cyclic adenosine 3′5′-monophosphate (cAMP), cyclic guanosine 3′5′-monophosphate (cGMP), and purine cyclic dimers as bis (3′,5′)-cyclic di guanosine monophosphate (c-di-GMP) or cyclic dimer adenosine monophosphate (c-di-AMP) (Latoscha et al., 2019). There is still little information on these second messenger nucleotides in *Streptomyces* species. A putative adenylate cyclase encoded by the *cyaA* gene was found in *S. coelicolor* (Danchin et al., 1993). Bioinformatic analysis reveals that the *S. coelicolor* adenylate cyclase encoded by *cyaA* has the same domains as the adenylate cyclase of *M. tuberculosis*. This mycobacterial protein has been crystalized and has been proposed to have a role on acid pH recognition (Tews et al., 2005). The *S. coelicolor cyaA*-null mutant is unable to neutralize the acidic pH produced during growth of the culture and is bald. The aerial mycelium formation was restored when exogenous cAMP was added to the mutant culture (Süsstrunk et al., 1998). Interestingly, a CRP protein has been identified in *S. coelicolor* and found to bind cAMP *in vitro* (Derouaux et al., 2004). However, cAMP does not seem to play a role similar to that of carbon catabolite regulation by glucose of alternative carbon sources. Noteworthy, immunoprecipitation studies have shown that CRP co-precipitates with the upstream region of *actII-orf4* and *redD* (Gao et al., 2012). cAMP has a CRP-dependent inducing effect on expression of these regulatory genes. These finding are consistent with the observation that CRP mutants are impaired in the biosynthesis of actinorhodin and undecylprodigiosin. In conclusion, it seems that the cAMP–CRP complex interacts with the upstream region of *actII-orf4* and *red* and, therefore, regulates expression of the corresponding gene clusters. The possible mechanism, if any, of cAMP–CRP on carbon catabolite regulation in *Streptomyces* needs to be further studied (see the section "Possible Interaction Between the cAMP Receptor Protein and the GlnR Nitrogen Regulator").

Another modified nucleotide, c-di-GMP, has been studied recently in *S. venezuelae* (Al-Bassam et al., 2018). This nucleotide is synthesized by a dimeric guanylate cyclase using two GMP molecules as substrate. The c-di-GMP level is maintained by degradation catalyzed by a phosphodiesterase

to form a linear GMP di-nucleotide. Similar enzymes exist in *S. coelicolor*. Disruption of genes encoding these c-di-GMP biosynthetic and degradative enzymes impaired actinorhodin and undecylprodigiosin formation but the mechanism involved in this effect is unknown. Cell differentiation and spore pigmentation were also affected in the c-di-GMP-null mutant (Tran et al., 2011; Hull et al., 2012). The last of this group of modified nucleotides is bis (3′,5′)-cyclic di adenosine monophosphate (c-di-AMP) that is formed by an adenylate cyclase from two ATP molecules. The genes forming c-di-AMP have been studied in *B. subtilis* and they are also present in actinobacteria including *Streptomyces* species (Witte et al., 2008). The intracellular balance of c-di-AMP is maintained by at least two different mechanisms, one of them involves secretion by a multidrug efflux pump and the second implicates hydrolysis by a phosphodiesterase. Interestingly, the gene encoding this enzyme, that occurs in other bacteria, is not present in *Streptomyces* genomes. The intracellular c-di-AMP levels affect many aspects of cell metabolism, including cell wall preservation and DNA integrity maintenance, but the major aspect regulated by this nucleotide is the ion homeostasis of the cell, particularly osmotic stress balance (Commichau et al., 2018). The interactions between the different second messenger nucleotides and phosphate control is still obscure. It is well known that synthesis of high levels of hyperphosphorylated guanine nucleotides results in a decrease of GTP pool in the cell and vice versa the level of GTP increases in the guanosine tetraphosphate null mutants. The cellular signals that regulate the levels of these modified nucleotides and their relationship with the global phosphate control need to be further investigated.

A further layer of interactions in the protection net is exerted by small ligands that bind to receptor proteins and caused distinct regulatory effects. These ligands are small organic molecules different from normal nutrients that are produced by bacteria and fungi in complex habitats and exert effect in the same species or between different species (Keller and Surette, 2006; Shank and Kolter, 2009; Straight and Kolter, 2009). Several of these ligands are themselves specialized metabolites that are secreted in small amount but exert potent communication effects on competing microorganisms. One group of these ligands are the so-called quorum sensing ligands (Bassler and Losick, 2006). One of the typical classes of quorum sensing molecules are the γ-butyrolactones that are well known in *Streptomyces* and related actinobacteria (Takano, 2006; Nodwell, 2014). The distinct γ-butyrolactones that differ in the modifications of their short fatty acid chains are recognized by γ-butyrolactone receptor proteins. Another important group of receptor proteins, that were initially designated pseudo-γ-butyrolactone receptor proteins (Xu et al., 2010), and have been renamed specialized metabolites receptor proteins (Martín and Liras, 2019), do not recognize γ-butyrolactones but interact with different biosynthetic intermediates and natural products that act as signals in the bacterial intercommunication. In addition to the specialized metabolite receptor proteins other well-known molecules recognize small ligands; this is the case of the TetR-class of transcriptional regulators. The TetR cluster regulators have a ligand binding site in the carboxyterminal region that interact with diverse signal molecules (Cuthbertson and Nodwell, 2013). In conclusion, the number of reported examples of interactions between ligands and transcriptional factors is increasing and the overall picture is that these additional layers of regulation reinforce the safety net with a more intricate connections between the nods. In addition, translational and post-translational regulatory mechanisms also reinforce the safety net.

Related Protection Nets in Other Bacteria

This article focuses on the protection net in *Streptomyces* species and related actinobacteria but equivalent protection nets exist in many other bacteria and in lower eukaryotes. However, the molecular mechanisms that protect the cells in response to nutrient starvation and environmental stresses are rather different from those observed in *Streptomyces*. For example, in *E. coli* there are only seven alternative sigma factors. The mechanism of control of the Pho regulon in *E. coli* is somehow different from that observed in *Streptomyces* species (Hsieh and Wanner, 2010; Antiqueira et al., 2012). In contrast to the strict dependence on the sensor histidine kinase PhoR in *S. coelicolor* (Fernández-Martínez et al., 2012), in *E. coli* the phosphorylation of the response regulator PhoB occurs also by acetyl-phosphate. Moreover, the phosphorylation of the PhoB regulator is also performed by histidine kinases of other two-components systems, as is the case of CreC histidine kinase (Wanner, 1993; Hsieh and Wanner, 2010). Interplay of regulatory systems has been also studied in *B. subtilis* and again there are differences with respect to the *Streptomyces* network; for example, the phosphate starvation response is mediated by a phosphorelay mechanism that involves at least three different steps in a cascade through the PhoR–PhoP TCS, the Spo0 system, and the ResD/ResP system (Hulett, 1996). In conclusion, it is clear that different bacteria have adapted their control mechanisms to the habitat in which they survive and the network of response mechanisms is adapted to those specific niches.

CONCLUSION

All available evidence indicates that there are signal integration sites in the genome of *Streptomyces* that are recognized by interacting transcriptional factors.

These nucleotide sequences upstream of key genes constitute integrative nodes that serve to compensate the unbalance produced by the lack of a key nutrient or for its excess that would impair the cell metabolism. Probably there are several hundreds of these integrator sites; however, it remains to be confirmed that some of these sites serve to integrate signals for the major transcriptional factors such a PhoP, GlnR, MtrA, and so on, whereas other sites probably integrate two or a few signals as appears to be the case of the *atrA* promoter region that is bound by PhoP and AdpA. It will be of utmost interest to establish the hierarchy of the integration sites to get a clear idea of the role of these sites on regulation of overall metabolism,

particularly to advance our knowledge of the system biology of these actinobacteria.

Finally, an interesting conclusion is that mutations that initially may be designed to change a specific regulatory phenomenon that affects a single cluster may, however, alter the expression of many different clusters through the interplay of these major transcriptional factors. An intriguing question is whether the signal integration sites in the DNA correspond to open "unprotected DNA region" at difference of other DNA regions that may be protected by histone-like proteins.

AUTHOR CONTRIBUTIONS

All authors listed have made a substantial, direct and intellectual contribution to the work, and approved it for publication.

REFERENCES

Al-Bassam, M., Julian Haist, J., Neumann, S. A., Lindenberg, S., and Tschowri, N. (2018). Expression patterns, genomic conservation and input into developmental regulation of the GGDEF/EAL/HD-GYP domain proteins in *Streptomyces*. *Front. Microbiol.* 9:2524. doi: 10.3389/fmicb.2018.02524

Allenby, N. E. E., Laing, E., Bucca, G., Kierzek, A. M., and Collin, C. P. (2012). Diverse control of metabolism and other cellular processes in *Streptomyces coelicolor* by the PhoP transcription factor: genome-wide identification of in vivo targets. *Nucleic Acid Res.* 40, 9543–9556. doi: 10.1093/nar/gks766

Amin, R., Franz-Wachtel, M., Tiffert, Y., Heberer, M., Meky, M., Ahmed, Y., et al. (2016). Post-translational serine/threonine phosphorylation and lysine acetylation: a novel regulatory aspect of the global nitrogen response regulator GlnR in *S. coelicolor M*145. *Front. Mol. Biosci.* 3:38. doi: 10.3389/fmolb.2016.00038

Amin, R., Reuther, J., Bera, A., Wohlleben, W., and Mast, Y. (2012). A novel GlnR target gene, *nnaR*, is involved in nitrate/nitrite assimilation in *Streptomyces coelicolor*. *Microbiology* 158, 1172–1182. doi: 10.1099/mic.0.054817-0

Angell, S., Lewis, C. G., Buttner, M. J., and Bibb, M. J. (1994). Glucose repression in *Streptomyces coelicolor* A3(2): a likely regulatory role for glucose kinase. *Mol. Gen. Genet.* 244, 135–143.

Antiqueira, L., Janga, S. C., and Costa, L. F. (2012). Extensive cross-talk and global regulators identified from an analysis of the integrated transcriptional and signaling network in *Escherichia coli*. *Mol. Biosyst.* 8, 3028–3035. doi: 10.1039/c2mb25279a

Banerjee, S. K., Kumar, M., Alokam, R., Sharma, A. K., Chatterjee, A., Kumar, R., et al. (2016). Targeting multiple response regulators of *Mycobacterium tuberculosis* augments the host immune response to infection. *Sci. Rep.* 6:25851. doi: 10.1038/srep25851

Bassler, B. L., and Losick, R. (2006). Bacterially speaking. *Cell* 125, 237–246. doi: 10.1016/j.cell.2006.04.001

Bentley, S. D., Chater, K. F., Cerdeño-Tárraga, A. M., Challis, G. L., Thomson, N. R., James, K. D., et al. (2002). Complete genome sequence of the model actinomycete *Streptomyces coelicolor* A3(2). *Nature* 417, 141–147.

Bertram, R., Schlicht, M., Mahr, K., Nothaft, H., Saier, M. H. Jr., and Titgemeyer, F. (2004). *In silico* and transcriptional analysis of carbohydrate uptake systems of *Streptomyces coelicolor* A3(2). *J. Bacteriol.* 186, 1362–1373. doi: 10.1128/jb.186.5.1362-1373.2004

Bibb, M. J. (2005). Regulation of secondary metabolism in streptomycetes. *Curr. Opin. Microbiol.* 8, 208–215. doi: 10.1016/j.mib.2005.02.016

Blanco, A. G., Canals, A., and Coll, M. (2012). PhoB transcriptional activator binds hierarchically to pho box promoters. *Biol.Chem.* 393, 1165–1171. doi: 10.1515/hsz-2012-0230

Blanco, A. G., Sola, M., Gomis-Rüth, F. X., and Coll, M. (2002). Tandem DNA recognition by PhoB, a two-component signal transduction transcriptional activator. *Structure* 10, 701–713. doi: 10.1016/s0969-2126(02)00761-x

Botella, E., Devine, S. K., Hubner, S., Salzberg, L. I., Gale, R. T., Brown, E. D., et al. (2014). PhoR autokinase activity is controlled by an intermediate in wall teichoic acid metabolism that is sensed by the intracellular PAS domain during the PhoPR-mediated phosphate limitation response of *Bacillus subtilis*. *Mol. Microbiol.* 94, 1242–1259. doi: 10.1111/mmi.12833

Chakrabartty, R., and Bibb, M. (1997). The ppGpp synthetase gene (*relA*) of *Streptomyces coelicolor* A3(2) plays a conditional role in antibiotic production and morphological differentiation. *J. Bacteriol.* 179, 5854–5861. doi: 10.1128/jb.179.18.5854-5861.1997

Cheung, J., and Hendrickson, W. A. (2010). Sensor domains of two-component regulatory systems. *Curr. Opin. Microbiol.* 13, 116–123. doi: 10.1016/j.mib.2010.01.016

Commichau, F. M., Gibhardt, J., Halbedel, S., Gundlach, J., and Stülke, J. (2018). A delicate connection: c-di-AMP affects cell integrity by controlling osmolyte transport. *Trends Microbiol.* 26, 175–185. doi: 10.1016/j.tim.2017.09.003

Cortés, J., Haydock, S. F., Roberts, G. A., Bevitt, D. J., and Leadlay, P. F. (1990). An unusually large multifunctional polypeptide in the erythromycin-producing polyketide synthase of *Saccharopolyspora erythraea*. *Nature* 348, 176–178. doi: 10.1038/348176a0

Cuthbertson, L., and Nodwell, J. R. (2013). The TetR family of regulators. *Microbiol. Mol. Biol. Rev.* 201, 440–475. doi: 10.1128/mmbr.00018-13

Dalebroux, Z. D., and Swanson, M. S. (2012). ppGpp: magic beyond RNA polymerase. *Nat. Rev. Microbiol.* 10, 203–212. doi: 10.1038/nrmicro2720

D'Alia, D., Eggle, D., Nieselt, K., Hu, W. S., Breitling, R., and Takano, E. (2011). Deletion of the signalling molecule synthase ScbA has pleiotropic effects on secondary metabolite biosynthesis, morphological differentiation and primary metabolism in *Streptomyces coelicolor* A3(2). *Microb. Biotechnol.* 4, 239–251. doi: 10.1111/j.1751-7915.2010.00232.x

Danchin, A., Pidoux, J., Krin, E., Thompson, C. J., and Ullmann, A. (1993). The adenylate cyclase catalytic domain of *Streptomyces coelicolor* is carboxy-terminal. *FEMS Microbiol. Lett.* 114, 145–151. doi: 10.1016/0378-1097(93)90511-y

Davidson, A. L., Dassa, E., Orelle, C., and Chen, J. (2008). Structure, function, and evolution of bacterial ATP-binding cassette systems. *Microbiol. Mol. Biol. Rev.* 72, 317–364. doi: 10.1128/MMBR.00031-07

Derouaux, A., Halici, S., Nothaft, H., Neutelings, T., Moutzourelis, G., Dusart, J., et al. (2004). Deletion of a cyclic AMP receptor protein homologue diminishes germination and affects morphological development of *Streptomyces coelicolor*. *J. Bacteriol.* 186, 1893–1897. doi: 10.1128/jb.186.6.1893-1897.2004

Díaz, M., Esteban, A., Fernández-Abalos, J. M., and Santamaría, R. I. (2005). The high-affinity phosphate-binding protein PstS is accumulated under high fructose concentrations and mutation of the corresponding gene affects differentiation in *Streptomyces lividans*. *Microbiology* 151, 2583–2592. doi: 10.1099/mic.0.27983-0

Esteban, A., Díaz, M., Yepes, A., and Santamaría, R. I. (2008). Expression of the *pstS* gene of *Streptomyces lividans* is regulated by the carbon source and is partially independent of the PhoP regulator. *BMC Microbiol.* 8:201. doi: 10.1186/1471-2180-8-201

Feng, W. H., Mao, X. M., Liu, Z. H., and Li, Y. Q. (2011). The ECF sigma factor SigT regulates actinorhodin production in response to nitrogen stress in *Streptomyces coelicolor*. *Appl. Microbiol. Biotechnol.* 92, 1009–1021. doi: 10.1007/s00253-011-3619-2

Fernández-Martínez, L. T., Santos-Beneit, F., and Martín, J. F. (2012). Is PhoR-PhoP partner fidelity strict? PhoR is required for the activation of the pho regulon in *Streptomyces coelicolor*. *Mol. Genet. Genomics* 287, 565–573. doi: 10.1007/s00438-012-0698-4

Fink, D., Weisschuh, N., Reuther, J., Wohlleben, W., and Engels, A. (2002). Two transcriptional regulators GlnR and GlnRII are involved in regulation of nitrogen metabolism in *Streptomyces coelicolor* A3(2). *Mol. Microbiol.* 46, 331–347. doi: 10.1046/j.1365-2958.2002.03150.x

Floriano, B., and Bibb, M. (1996). afsR is a pleiotropic but conditionally required regulatory gene for antibiotic production in Streptomyces coelicolor A3(2). *Mol Microbiol.* 21, 385–396. doi: 10.1046/j.1365-2958.1996.6491364.x

Fontecave, M., Atta, M., and Mulliez, E. (2004). S-adenosylmethionine: nothing goes to waste. *Trends Biochem. Sci.* 29, 243–249. doi: 10.1016/j.tibs.2004.03.007

Gao, C., Hindra, Mulder, D., Yin, C., and Elliot, M. A. (2012). Crp is a global regulator of antibiotic production in Streptomyces. *mBio* 3:e00407-12. doi: 10.1128/mBio.00407-12

Ghorbel, S., Kormanec, J., Artus, A., and Virolle, M. J. (2006). Transcriptional studies and regulatory interactions between the phoR-phoP operon and the phoU, mtpA, and ppk genes of Streptomyces lividans TK24. *J. Bacteriol.* 188, 677–686. doi: 10.1128/jb.188.2.677-686.2006

Gomez-Escribano, J. P., Martín, J. F., Hesketh, A., Bib, M. J., and Liras, P. (2008). *Streptomyces clavuligerus* relA-null mutants overproduce clavulanic acid and cephamycin C: negative regulation of secondary metabolism by (p)ppGpp. *Microbiology* 154, 744–755. doi: 10.1099/mic.0.2007/011890-0

Gomez-Escribano, J. P., Song, L., Fox, D. J., Yeo, V., Bibb, M. J., and Challis, G. L. (2012). Structure and biosynthesis of the unusual polyketide alkaloid coelimycin P1, a metabolic product of the *cpk* gene cluster of *Streptomyces coelicolor* M145. *Chem. Sci.* 3, 2716–2720.

Guo, Q., Chu, J., Zhuang, Y., and Gao, Y. (2016). Controlling the feed rate of propanol to optimize erythromycin fermentation by on-line capacitance and oxygen uptake rate measurement. *Bioprocess Biosyst. Eng.* 39, 255–265. doi: 10.1007/s00449-015-1509-1

He, J. M., Zhu, H., Zheng, G. S., Liu, P. P., Wang, J., Zhao, G. P., et al. (2016). Direct involvement of the master nitrogen metabolism regulator GlnR in antibiotic biosynthesis in *Streptomyces*. *J. Biol. Chem.* 291, 26443–26454. doi: 10.1074/jbc.m116.762476

He, X., Wang, L., and Wang, S. (2016). Structural basis of DNA sequence recognition by the response regulator PhoP in *Mycobacterium tuberculosis*. *Sci. Rep.* 6:24442. doi: 10.1038/srep24442

Hesketh, A., Chen, W. J., Ryding, J., Chang, S., and Bibb, M. (2007). The global role of ppGpp synthesis in morphological differentiation and antibiotic production in *Streptomyces coelicolor A3(2)*. *Genome Biol.* 8:R161.

Hesketh, A., Sun, J., and Bibb, M. (2001). Induction of ppGpp synthesis in *Streptomyces coelicolor* A3(2) grown under conditions of nutritional sufficiency elicits actII-ORF4 transcription and actinorhodin biosynthesis. *Mol. Microbiol.* 39, 136–144. doi: 10.1046/j.1365-2958.2001.02221.x

Higo, A., Hara, H., Horinouchi, S., and Ohnishi, Y. (2012). Genome-wide distribution of AdpA, a global regulator for secondary metabolism and morphological differentiation in *Streptomyces*, revealed the extent and complexity of the AdpA regulatory network. *DNA Res.* 19, 259–273. doi: 10.1093/dnares/dss010

Hong, E., Lee, H. M., Ko, H., Kim, D. U., Jeon, B. Y., Jung, J., et al. (2007). Structure of an atypical orphan response regulator protein supports a new phosphorylation-independent regulatory mechanism. *J. Biol. Chem.* 282, 20667–20675. doi: 10.1074/jbc.m609104200

Hong, S. K., Kito, M., Beppu, T., and Horinouchi, S. (1991). Phosphorylation of the AfsR product, a global regulatory protein for secondary-metabolite formation in *Streptomyces coelicolor* A3(2). *J. Bacteriol.* 173, 2311–2318. doi: 10.1128/jb.173.7.2311-2318.1991

Horinouchi, S. (2002). A microbial hormone, A-factor, as a master switch for morphological differentiation and secondary metabolism in *Streptomyces griseus*. *Front. Biosci.* 7:d2045–d2057.

Horinouchi, S. (2003). AfsR as an integrator of signals that are sensed by multiple serine/threonine kinases in *Streptomyces coelicolor* A3(2). *J. Ind. Microbiol. Biotechnol.* 30, 462–467. doi: 10.1007/s10295-003-0063-z

Hsieh, Y. J., and Wanner, B. L. (2010). Global regulation by the seven-component Pi signaling system. *Curr. Opin. Microbiol.* 13, 198–203. doi: 10.1016/j.mib.2010.01.014

Hulett, F. M. (1996). The signal-transduction network for Pho regulation in *Bacillus subtilis*. *Mol. Microbiol.* 19, 933–939. doi: 10.1046/j.1365-2958.1996.421953.x

Hull, T. D., Ryu, M.-H., Sullivan, M. J., Johnson, R. C., Klena, N. T., Geiger, R. M., et al. (2012). Cyclic Di-GMP phosphodiesterases RmdA and RmdB Are involved in regulating colony morphology and development in *Streptomyces coelicolor*. *J. Bacteriol.* 194, 4642–4651. doi: 10.1128/JB.00157-12

Hutchings, M. I., Hoskisson, P. A., Chandra, G., and Buttner, M. J. (2004). Sensing and responding to diverse extracellular signals? Analysis of the sensor kinases and response regulators of *Streptomyces coelicolor* A3(2). *Microbiology* 150, 2795–2806. doi: 10.1099/mic.0.27181-0

Ikeda, H., Seno, E. T., Bruton, C. J., and Chater, K. F. (1984). Genetic mapping, cloning and physiological aspects of the glucose kinase gene of *Streptomyces coelicolor*. *Mol. Gen. Genet.* 196, 501–507. doi: 10.1007/bf00436199

Jin, Y. Y., Cheng, J., Yang, S. H., Meng, L., Palaniyandi, S. A., Zhao, X. Q., et al. (2011). S-adenosyl-L-methionine activates actinorhodin biosynthesis by increasing autophosphorylation of the Ser/Thr protein kinase AfsK in *Streptomyces coelicolor* A3(2). *Biosci. Biotechnol. Biochem.* 75, 910–913. doi: 10.1271/bbb.100873

Keller, L., and Surette, M. G. (2006). Communication in bacteria: an ecological and evolutionary perspective. *Nat. Rev. Microbiol.* 4, 249–258. doi: 10.1038/nrmicro1383

Kim, D. J., Huh, J. H., Yang, Y. Y., Kang, C. M., Lee, I. H., Hyun, C. G., et al. (2003). Accumulation of S-adenosyl-L-methionine enhances production of actinorhodin but inhibits sporulation in *Streptomyces lividans* TK23. *J. Bacteriol.* 185, 592–600. doi: 10.1128/jb.185.2.592-600.2003

Krysenko, S., Okoniewski, N., Kulik, A., Matthews, A., Grimpo, J., Wohlleben, W., et al. (2017). Gamma-glutamylpolyamine synthetase GlnA3 is involved in the first step of polyamine degradation pathway in *Streptomyces coelicolor* M145. *Front. Microbiol.* 8:726. doi: 10.3389/fmicb.2017.00726

Latoscha, A., Wörmann, M. E., and Tschowri, N. (2019). Nucleotide second messengers in *Streptomyces*. *Microbiology* 165, 1153–1165. doi: 10.1099/mic.0.000846

Lee, P.-C., Umeyama, T., and Horinouchi, S. (2002). *afsS* is a target of AfsR, a transcriptional factor with ATPase activity that globally controls secondary metabolism in *Streptomyces coelicolor* A3(2). *Mol. Microbiol.* 43, 1413–1430. doi: 10.1046/j.1365-2958.2002.02840.x

Lewis, R. A., Wahab, A., Bucca, G., Laing, E. E., Möller-Levet, C. S., Kierzek, A., et al. (2019). Genome-wide analysis of the role of the antibiotic biosynthesis regulator AbsA2 in *Streptomyces coelicolor* A3(2). *PLoS One* 14:e0200673. doi: 10.1371/journal.pone.0200673

Li, Y., Gao, H., Qin, L., Li, B., Han, Y., Guo, Z., et al. (2008). Identification and characterization of PhoP regulon members in Yersinia pestis biovar Microtus. *BMC Genomics* 9:143. doi: 10.1186/1471-2164-9-143

Li, Z., Liu, X., Wang, J., Wang, Y., Zheng, G., Lu, Y., et al. (2018). Insight into the molecular mechanism of the transcriptional regulation of *amtB* operon in *Streptomyces coelicolor*. *Front. Microbiol.* 9:264. doi: 10.3389/fmicb.2018.00264

Liao, C. H., Yao, L., Xu, Y., Liu, W. B., Zhou, Y., and Ye, B. C. (2015). Nitrogen regulator GlnR controls uptake and utilization of non-phosphotransferase-system carbon sources in Actinomycetes. *Proc. Natl. Acad. Sci. U.S.A.* 112, 15630–15635. doi: 10.1073/pnas.1508465112

Lin, W., Wang, Y., Han, X., Zhang, Z., Wang, C., Wang, J., et al. (2014). Atypical OmpR/PhoB subfamily response regulator GlnR of actinomycetes functions as a homodimer, stabilized by the unphosphorylated conserved Asp-focused charge interactions. *J. Biol. Chem.* 289, 15413–15425. doi: 10.1074/jbc.M113.543504

Liu, G., Chater, K. F., Chandra, G., Niu, G., and Tan, H. (2013). Molecular regulation of antibiotic biosynthesis in streptomyces. *Microbiol. Mol. Biol. Rev.* 77, 112–143. doi: 10.1128/MMBR.00054-12

Luo, J., Li, M., Tang, Y., Laszkowska, M., Roeder, R. G., and Gu, W. (2004). Acetylation of p53 augments its site-specific DNA binding both *in vitro* and *in vivo*. *Proc. Natl. Acad. Sci. U.S.A.* 101, 2259–2264. doi: 10.1073/pnas.0308762101

Mao, X. M., Luo, S., Zhou, R. C., Wang, F., Yu, P., Sun, N., et al. (2015). Transcriptional regulation of the daptomycin gene cluster in *Streptomyces roseosporus* by an autoregulator. AtrA. *J. Biol. Chem.* 290, 7992–8001. doi: 10.1074/jbc.M114.608273

Martín, J. F. (2004). Phosphate control of the biosynthesis of antibiotics and other secondary metabolites is mediated by the PhoR-PhoP system: an unfinished story. *J. Bacteriol.* 186, 5197–5201. doi: 10.1128/jb.186.16.5197-5201.2004

Martín, J. F., and Demain, A. L. (1980). Control of antibiotic synthesis. *Microbiol. Rev.* 44, 230–251.

Martín, J. F., and Liras, P. (2010). Engineering of regulatory cascades and networks controlling antibiotic biosynthesis in *Streptomyces*. *Curr. Opin. Microbiol.* 13, 263–273. doi: 10.1016/j.mib.2010.02.008

Martín, J. F., and Liras, P. (2019). Harnessing microbiota interactions to produce bioactive metabolites: communication signals and receptor proteins. *Curr. Opin. Pharmacol.* 48, 8–16. doi: 10.1016/j.coph.2019.02.014

Martín, J. F., Ramos, A., and Liras, P. (2019). Regulation of geldanamycin biosynthesis by cluster-situated transcription factors and the master regulator PhoP. *Antibiotics* 8, 87–103. doi: 10.3390/antibiotics8030087

Martín, J. F., Rodríguez-García, A., and Liras, P. (2017). The master regulator PhoP coordinates phosphate and nitrogen metabolism, respiration, cell differentiation and antibiotic biosynthesis: comparison in *Streptomyces coelicolor* and *Streptomyces avermitilis*. *J. Antibiot.* 70, 534–541. doi: 10.1038/ja.2017.19

Martín, J. F., Santos-Beneit, F., Rodríguez-García, A., Sola-Landa, A., Smith, M. C., Ellingsen, T. E., et al. (2012a). Transcriptomic studies of phosphate control of primary and secondary metabolism in *Streptomyces coelicolor*. *Appl. Microbiol. Biotechnol.* 95, 61–75. doi: 10.1007/s00253-012-4129-6

Martín, J. F., Sola-Landa, A., and Rodríguez-García, A. (2012b). "Two-component systems in *Streptomyces*," in *Two-component Systems in Bacteria*, eds R. Gross, and D. Beier, (Würzburg: Caister Academic), 315–332.

Martínez-Castro, M., Barreiro, C., and Martín, J. F. (2018). Analysis and validation of the *pho* regulon in the tacrolimus-producer strain *Streptomyces tsukubaensis*: differences with the model organism *Streptomyces coelicolor*. *Appl. Microbiol. Biotechnol.* 102, 7029–7045. doi: 10.1007/s00253-018-9140-0

Martínez-Costa, O. H., Fernández-Moreno, M. A., and Malpartida, F. (1998). The *relA/spoT*-homologous gene in *Streptomyces coelicolor* encodes both ribosome-dependent (p)ppGpp-synthesizing and -degrading activities. *J. Bacteriol.* 180, 4123–4132.

Martínez-Hackert, E., and Stock, A. M. (1997). The DNA-binding domain of OmpR: crystal structures of a winged helix transcription factor. *Structure* 5, 109–124. doi: 10.1016/s0969-2126(97)00170-6

Martín-Martín, S., Rodríguez-García, A., Santos-Beneit, F., Franco-Domínguez, E., Sola-Landa, A., and Martín, J. F. (2019). Self-control of the PHO regulon: the PhoP-dependent protein PhoU controls negatively expression of genes of PHO regulon in *Streptomyces coelicolor*. *J. Antibiot.* doi: 10.1038/ja.2017.130 [Epub ahead of print].

Matsuzaki, H., Daitoku, H., Hatta, M., Aoyama, H., Yoshimochi, K., and Fukamizu, A. (2005). Acetylation of Foxo1 alters its DNA-binding ability and sensitivity to phosphorylation. *Proc. Natl. Acad. Sci. U.S.A.* 102, 11278–11283. doi: 10.1073/pnas.0502738102

McKenzie, N. L., and Nodwell, J. R. (2007). Phosphorylated AbsA2 negatively regulates antibiotic production in *Streptomyces coelicolor* through interactions with pathway-specific regulatory gene promoters. *J. Bacteriol.* 189, 5284–5292. doi: 10.1128/JB.00305-07

McKenzie, N. L., and Nodwell, J. R. (2009). Transmembrane topology of the AbsA1 sensor kinase of *Streptomyces coelicolor*. *Microbiology* 155, 1812–1818. doi: 10.1099/mic.0.028431-0

Möker, N., Brocker, M., Schaffer, S., Krämer, R., Morbach, S., and Bott, M. (2004). Deletion of the genes encoding the MtrA-MtrB two-component system of *Corynebacterium glutamicum* has a strong influence on cell morphology, antibiotics susceptibility and expression of genes involved in osmoprotection. *Mol. Microbiol.* 54, 420–438. doi: 10.1111/j.1365-2958.2004.04249.x

Nodwell, J. R. (2014). Are you talking to me? A possible role for γ-butyrolactones in interspecies signalling. *Mol. Microbiol.* 94, 483–485. doi: 10.1111/mmi.12787

Nouioui, I., Cortés-Albayay, C., Carro, L., Castro, J. F., Gtari, M., Ghodhbane-Gtari, F., et al. (2019). Genomic insights into plant-growth-promoting potentialities of the genus *Frankia*. *Front. Microbiol.* 10:1457. doi: 10.3389/fmicb.2019.01457

Ohnishi, Y., Yamazaki, H., Kato, J. Y., Tomono, A., and Horinouchi, S. (2005). AdpA, a central transcriptional regulator in the A-factor regulatory cascade that leads to morphological development and secondary metabolism in *Streptomyces griseus*. *Biosci. Biotechnol. Biochem.* 69, 431–439. doi: 10.1271/bbb.69.431

Ordóñez-Robles, M., Santos-Beneit, F., Albillos, S. M., Liras, P., Martín, J. F., and Rodríguez-García, A. (2017a). *Streptomyces tsukubaensis* as a new model for carbon repression: transcriptomic response to tacrolimus repressing carbon sources. *Appl. Microbiol. Biotechnol.* 101, 8181–8195. doi: 10.1007/s00253-017-8545-5

Ordóñez-Robles, M., Santos-Beneit, F., Rodríguez-García, A., and Martín, J. F. (2017b). Analysis of the Pho regulon in *Streptomyces tsukubaensis*. *Microbiol. Res.* 205, 80–87. doi: 10.1016/j.micres.2017.08.010

Paget, M. S. (2015). Bacterial sigma factors and anti-sigma factors: structure, function and distribution. *Biomolecules* 5, 1245–1265. doi: 10.3390/biom5031245

Panhorst, M., Sorger-Herrmann, U., and Wendisch, V. F. (2011). The *pstSCAB* operon for phosphate uptake is regulated by the global regulator GlxR in *Corynebacterium glutamicum*. *J. Biotechnol.* 154, 149–155. doi: 10.1016/j.jbiotec.2010.07.015

Pullan, S. T., Chandra, G., Bibb, M. J., and Merrick, M. (2011). Genome wide analysis of the role of GlnR in *Streptomyces venezuelae* provides new insights into global nitrogen regulation in actinomycetes. *BMC Genomics* 12:175. doi: 10.1186/1471-2164-12-175

Qin, R., Sang, Y., Ren, J., Zhang, Q. F., Li, S. X., Cui, Z. L., et al. (2016). The bacterial two-hybrid system uncovers the involvement of acetylation in regulating of Lrp activity in *Salmonella typhimurium*. *Front. Microbiol.* 7:1864. doi: 10.3389/fmicb.2016.01864

Qu, S., Kang, Q., Wu, H., Wang, L., and Bai, L. (2015). Positive and negative regulation of GlnR in validamycin A biosynthesis by binding to different loci in promoter region. *Appl. Microbiol. Biotechnol.* 99, 4771–4783. doi: 10.1007/s00253-015-6437-0

Rebets, Y., Tsolis, K. C., Guðmundsdóttir, E. E., Koepff, J., Wawiernia, B., Busche, T., et al. (2018). Characterization of sigma factor genes in *Streptomyces lividans* TK24 using a genomic library-based approach for multiple gene deletions. *Front. Microbiol.* 9:3033. doi: 10.3389/fmicb.2018.03033

Rigali, S., Titgemeyer, F., Barends, S., Mulder, S., Thomae, A. W., Hopwood, D. A., et al. (2008). Feast or famine: the global regulator DasR links nutrient stress to antibiotic production by *Streptomyces*. *EMBO Rep.* 9, 670–675. doi: 10.1038/embor.2008.83

Rodríguez-García, A., Barreiro, C., Santos-Beneit, F., Sola-Landa, A., and Martín, J. F. (2007). Genome-wide transcriptomic and proteomic analysis of the primary response to phosphate limitation in *Streptomyces coelicolor* M145 and in a Δ*phoP* mutant. *Proteomics* 7, 2410–2429. doi: 10.1002/pmic.200600883

Rodríguez-García, A., Sola-Landa, A., Apel, K., Santos-Beneit, F., and Martín, J. F. (2009). Phosphate control over nitrogen metabolism in *Streptomyces coelicolor*: direct and indirect negative control of *glnR*, *glnA*, *glnII* and *amtB* expression by the response regulator PhoP. *Nucleic Acids Res.* 37, 3230–3242. doi: 10.1093/nar/gkp162

Romero-Rodríguez, A., Maldonado-Carmona, N., Ruiz-Villafán, B., Koirala, N., Rocha, D., and Sánchez, S. (2018). Interplay between carbon, nitrogen and phosphate utilization in the control of secondary metabolite production in *Streptomyces*. *Antonie Van Leeuwenhoek* 111, 761–781. doi: 10.1007/s10482-018-1073-1

Romero-Rodríguez, A., Rocha, D., Ruiz-Villafan, B., Tierrafría, V., Rodríguez-Sanoja, R., Segura-González, D., et al. (2016a). Transcriptomic analysis of a classical model of carbon catabolite regulation in *Streptomyces coelicolor*. *BMC Microbiol.* 16:77. doi: 10.1186/s12866-016-0690-y

Romero-Rodríguez, A., Ruiz-Villafán, B., Tierrafría, V. H., Rodríguez-Sanoja, R., and Sánchez, S. (2016b). Carbon catabolite regulation of secondary metabolite formation and morphological differentiation in *Streptomyces coelicolor*. *Appl. Biochem. Biotechnol.* 180, 1152–1166. doi: 10.1007/s12010-016-2158-9

Rückert, C., Albersmeier, A., Busche, T., Jaenicke, S., Winkler, A., Friðjónsson, ÓH., et al. (2015). Complete genome sequence of *Streptomyces lividans* TK24. *J. Biotechnol.* 199, 21–22. doi: 10.1016/j.jbiotec.2015.02.004

Salehi-Najafabadi, Z., Barreiro, C., Rodríguez-García, A., Cruz, A., López, G. E., and Martín, J. F. (2014). The gamma-butyrolactone receptors BulR1 and BulR2 of *Streptomyces tsukubaensis:* tacrolimus (FK506) and butyrolactone synthetases production control. *Appl. Microbiol. Biotechnol.* 98, 4919–4936. doi: 10.1007/s00253-014-5595-9

Santos-Beneit, F. (2015). The Pho regulon: a huge regulatory network in bacteria. *Front. Microbiol.* 6:402. doi: 10.3389/fmicb.2015.00402

Santos-Beneit, F., Barriuso-Iglesias, M., Fernández-Martínez, L. T., Martínez-Castro, M., Sola-Landa, A., Rodríguez-García, A., et al. (2011a). The RNA polymerase omega factor RpoZ is regulated by PhoP and has an important role in antibiotic biosynthesis and morphological differentiation in *Streptomyces coelicolor*. *Appl. Environ. Microbiol.* 77, 7586–7594. doi: 10.1128/AEM.00465-11

Santos-Beneit, F., Rodríguez-García, A., and Martín, J. F. (2011b). Complex transcriptional control of the antibiotic regulator *afsS* in *Streptomyces*: PhoP and AfsR are overlapping, competitive activators. *J. Bacteriol.* 193, 2242–2251. doi: 10.1128/JB.01462-10

Santos-Beneit, F., Rodríguez-García, A., Apel, A. K., and Martín, J. F. (2009a). Phosphate and carbon source regulation of two PhoP-dependent glycerophosphodiester phosphodiesterase genes of *Streptomyces coelicolor*. *Microbiology* 155, 1800–1811. doi: 10.1099/mic.0.026799-0

Santos-Beneit, F., Rodríguez-García, A., Sola-Landa, A., and Martín, J. F. (2009b). Crosstalk between two global regulators in *Streptomyces*: PhoP and AfsR interact in the control of *afsS, pstS* and *phoRP* transcription. *Mol. Microbiol.* 72, 53–68. doi: 10.1111/j.1365-2958.2009.06624.x

Shank, E. A., and Kolter, R. (2009). New developments in microbial interspecies signaling. *Curr. Opin. Microbiol.* 12, 205–214. doi: 10.1016/j.mib.2009.01.003

Shu, D., Chen, L., Wang, W., Yu, Z., Ren, C., Zhang, W., et al. (2009). afsQ1-Q2-sigQ is a pleiotropic but conditionally required signal transduction system for both secondary metabolism and morphological development in *Streptomyces coelicolor*. *Appl. Microbiol. Biotechnol.* 81, 1149–1160. doi: 10.1007/s00253-008-1738-1

Sola-Landa, A., Moura, R. S., and Martín, J. F. (2003). The two component PhoR-PhoP system controls both primary metabolism and secondary metabolite biosynthesis in *Streptomyces lividans*. *Proc. Natl. Acad. Sci. U.SA.* 100, 6133–6138. doi: 10.1073/pnas.0931429100

Sola-Landa, A., Rodríguez-García, A., Amin, R., Wohlleben, W., and Martín, J. F. (2013). Competition between the GlnR and PhoP regulators for the *glnA* and *amtB* promoters in *Streptomyces coelicolo*r. *Nucleic Acids Res.* 41, 1767–1782. doi: 10.1093/nar/gks1203

Sola-Landa, A., Rodríguez-García, A., Apel, A. K., and Martín, J. F. (2008). Target genes and structure of the direct repeats in the DNA-binding sequences of the response regulator PhoP in Streptomyces coelicolor. *Nucleic Acids Res.* 36, 1358–1368. doi: 10.1093/nar/gkm1150

Sola-Landa, A., Rodríguez-García, A., Franco-Domínguez, E., and Martín, J. F. (2005). Binding of PhoP to promoters of phosphate regulated genes in *Streptomyces coelicolor*: identification of PHO boxes. *Mol. Microbiol.* 56, 1373–1385. doi: 10.1111/j.1365-2958.2005.04631.x

Som, N. F., Heine, D., Holmes, N., Knowles, F., Chandra, G., Seipke, R. F., et al. (2017a). The MtrAB two-component system controls antibiotic production in *Streptomyces coelicolor* A3(2). *Microbiology* 163, 1415–1419. doi: 10.1099/mic.0.000524

Som, N. F., Heine, D., Holmes, N. A., Munnoch, J. T., Chandra, G., Seipke, R. F., et al. (2017b). The conserved actinobacterial two-component system MtrAB coordinates chloramphenicol production with sporulation in *Streptomyces venezuelae* NRRL B-65442. *Front. Microbiol.* 8:1145. doi: 10.3389/fmicb.2017.01145

Straight, P. D., and Kolter, R. (2009). Interspecies chemical communication in bacterial development. *Annu. Rev. Microbiol.* 63, 99–118. doi: 10.1146/annurev.micro.091208.073248

Sun, D., Liu, C., Zhu, J. R., and Liu, W. J. (2017). Connecting metabolic pathways: sigma factors in *Streptomyces* spp. *Front. Microbiol.* 8:e02546. doi: 10.3389/fmicb.2017.02546

Süsstrunk, U., Pidoux, J., Taubert, S., Ullmann, A., and Thompson, C. J. (1998). Pleiotropic effects of cAMP on germination, antibiotic biosynthesis and morphological development in *Streptomyces coelicolor*. *Mol. Microbiol.* 30, 33–46. doi: 10.1046/j.1365-2958.1998.01033.x

Świątek-Połatyńska, M. A., Bucca, G., Laing, E., Gubbens, J., Titgemeyer, F., Smith, C. P., et al. (2015). Genome-wide analysis of in vivo binding of the master regulator DasR in *Streptomyces coelicolor* identifies novel non-canonical targets. *PLoS One* 10:e0122479. doi: 10.1371/journal.pone.0122479

Takano, E. (2006). Gamma-butyrolactones: *Streptomyces* signalling molecules regulating antibiotic production and differentiation. *Curr. Opin. Microbiol.* 3, 287–294. doi: 10.1016/j.mib.2006.04.003

Tews, I., Findeisen, F., Sinning, I., Schultz, A., Schultz, J. E., and Linder, J. U. (2005). The structure of a pH-sensing mycobacterial adenylyl cyclase holoenzyme. *Science* 308, 1020–1023. doi: 10.1126/science.1107642

Thao, S., and Escalante-Semerena, J. C. (2011). Control of protein function by reversible N+-lysine acetylation in bacteria. *Curr. Opin. Microbiol.* 14, 200–204. doi: 10.1016/j.mib.2010.12.013

Thomas, L., Hodgson, D. A., Wentzel, A., Nieselt, K., Ellingsen, T. E., Moore, J., et al. (2012). Metabolic switches and adaptations deduced from the proteomes of *Streptomyces coelicolor* wild type and *phoP* mutant grown in batch culture. *Mol. Cell. Proteomics* 11, M111.013797. doi: 10.1074/mcp.M111.013797

Tiffert, Y., Franz-Wachtel, M., Fladerer, C., Nordheim, A., Reuther, J., Wohlleben, W., et al. (2011). Proteomic analysis of the GlnR-mediated response to nitrogen limitation in S*treptomyces coelicolor* M145. *Appl. Microbiol. Biotechnol.* 89, 1149–1159. doi: 10.1007/s00253-011-3086-9

Tiffert, Y., Supra, P., Wurm, R., Wohlleben, W., Wagner, R., and Reuther, J. (2008). The *Streptomyces coelicolor* GlnR regulon: identification of new GlnR targets and evidence for a central role of GlnR in nitrogen metabolism in actinomycetes. *Mol. Microbiol.* 67, 861–880. doi: 10.1111/j.1365-2958.2007.06092.x

Titgemeyer, F., Amon, J., Parche, S., Mahfoud, M., Bail, J., Schlicht, M., et al. (2007). A genomic view of sugar transport in *Mycobacterium smegmatis* and *Mycobacterium tuberculosis*. *J. Bacteriol.* 189, 5903–5915. doi: 10.1128/jb.00257-07

Tran, N. T., Den Hengst, C. D., Gomez-Escribano, J. P., and Buttner, M. J. (2011). Identification and characterization of CdgB, a diguanylate cyclase involved in developmental processes in *Streptomyces coelicolor*. *J. Bacteriol.* 193, 3100–3108. doi: 10.1128/JB.01460-10

Uguru, G. C., Stephens, K. E., Stead, J. A., Towle, J. E., Baumberg, S., and McDowall, K. J. (2005). Transcriptional activation of the pathway-specific regulator of the actinorhodin biosynthetic genes in *Streptomyces coelicolor*. *Mol. Microbiol.* 58, 131–150. doi: 10.1111/j.1365-2958.2005.04817.x

Umeyama, T., and Horinouchi, S. (2001). Autophosphorylation of a bacterial serine/threonine kinase, AfsK, is inhibited by KbpA, an AfsK-binding protein. *J. Bacteriol.* 183, 5506–5512. doi: 10.1128/jb.183.19.5506-5512.2001

van Wezel, G. P., König, M., Mahr, K., Nothaft, H., Thomae, A. W., Bibb, M., et al. (2007). A new piece of an old jigsaw: glucose kinase is activated posttranslationally in a glucose transport-dependent manner in *Streptomyces coelicolor* A3(2*). J. Mol. Microbiol. Biotechnol.* 12, 67–74. doi: 10.1159/000096461

van Wezel, G. P., Mahr, K., König, M., Traag, A., Pimentel-Schmitt, E. F., Willimek, A., et al. (2005). GlcP constitutes the major glucose uptake system of *Streptomyces coelicolor* A3(2). *Mol. Microbiol.* 55, 624–636. doi: 10.1111/j.1365-2958.2004.04413.x

van Wezel, G. P., and McDowall, K. J. (2011). The regulation of the secondary metabolism of *Streptomyces*: new links and experimental advances. *Nat. Prod. Rep.* 28, 1311–1333. doi: 10.1039/c1np00003a

van Wezel, G. P., White, J., Young, P., Postma, P. W., and Bibb, M. J. (1997). Substrate induction and glucose repression of maltose utilization by *Streptomyces coelicolor* A3(2) is controlled by MalR, a member of the lacI-galR family of regulatory genes. *Mol. Microbiol.* 23, 537–549. doi: 10.1046/j.1365-2958.1997.d01-1878.x

Wang, R., Mast, Y., Wang, J., Zhang, W., Zhao, G., Wohlleben, W., et al. (2013). Identification of two-component system AfsQ1/Q2 regulon and its cross-regulation with GlnR in *Streptomyces coelicolor*. *Mol. Microbiol.* 87, 30–48. doi: 10.1111/mmi.12080

Wang, Y., Cen, X., Zhao, G. P., and Wang, J. (2012). Characterization of a new GlnR binding box in the promoter of *amtB* in *Streptomyces coelicolor* inferred a PhoP/GlnR competitive binding mechanis for transcriptional regulation of *amtB*. *J. Bacteriol.* 194, 5237–5244. doi: 10.1128/JB.00989-12

Wanner, B. L. (1993). Gene regulation by phosphate in enteric bacteria. *J. Cell Biochem.* 51, 47–54. doi: 10.1002/jcb.240510110

Wehmeier, S., Varghese, A. S., Gurcha, S. S., Tissot, B., Panico, M., Hitchen, P., et al. (2009). Glycosylation of the phosphate binding protein, PstS, in *Streptomyces coelicolor* by a pathway that resembles protein O-mannosylation in eukaryotes. *Mol. Microbiol.* 71, 421–433. doi: 10.1111/j.1365-2958.2008.06536.x

Witte, G., Hartung, S., Büttner, K., and Hopfner, K. P. (2008). Structural biochemistry of a bacterial checkpoint reveals deadenylate cyclase activity regulated by DNA recombination intermediates. *Mol. Cell* 30, 167–178. doi: 10.1016/j.molcel.2008.02.020

Wray, L. V. Jr., Atkinson, M. R., and Fisher, S. H. (1991). Identification and cloning of the glnR locus, which is required for transcription of the *glnA* gene in *Streptomyces coelicolor* A3(2). *J. Bacteriol.* 173, 7351–7360. doi: 10.1128/jb.173.22.7351-7360.1991

Xu, G., Wang, J., Wang, L., Tian, X., Yang, H., Fan, K., et al. (2010). Pseudo' gamma-butyrolactone receptors respond to antibiotic signals to coordinate antibiotic biosynthesis. *J. Biol. Chem.* 285, 27440–27448. doi: 10.1074/jbc.m110.143081

Xu, Y., Li, Y. X., and Ye, B. C. (2018). Lysine propionylation modulates the transcriptional activity of phosphate regulator PhoP in *Saccharopolyspora erythraea*. *Mol. Microbiol.* 110, 648–661. doi: 10.1111/mmi.14122

Yang, R., Liu, X., Wen, Y., Song, Y., Chen, Z., and Li, J. (2015). The PhoP transcription factor negatively regulates avermectin biosynthesis in *Streptomyces avermitilis*. *Appl. Microbiol. Biotechnol.* 99, 1047–1057. doi: 10.1007/s00253-015-6921-6

Yao, L. L., Liao, C. H., Huang, G., Zhou, Y., Rigali, S., Zhang, B., et al. (2014). GlnR-mediated regulation of nitrogen metabolism in the actinomycete *Saccharopolyspora erythraea*. *Appl. Microbiol. Biotechnol.* 98, 7935–7948. doi: 10.1007/s00253-014-5878-1

You, D., Yao, L. L., Huang, D., Escalante-Semerena, J. C., and Ye, B. C. (2014). Acetyl coenzyme A synthetase is acetylated on multiple lysine residues by a protein acetyltransferase with a single Gcn5-type N-acetyltransferase (GNAT) domain in *Saccharopolyspora erythraea*. *J. Bacteriol.* 196, 3169–3178. doi: 10.1128/JB.01961-14

Yu, H., Yao, Y., Liu, Y., Jiao, R., Jiang, W., and Zhao, G. P. (2007). A complex role of *Amycolatopsis mediterranei* GlnR in nitrogen metabolism and related antibiotics production. *Arch. Microbiol.* 188, 89–96. doi: 10.1007/s00203-007-0228-7

Yu, Z., Zhu, H., Dang, F., Zhang, W., Qin, Z., Yang, S., et al. (2012). Differential regulation of antibiotic biosynthesis by DraR-K, a novel two-component system in *Streptomyces coelicolor*. *Mol. Microbiol.* 85, 535–556. doi: 10.1111/j.1365-2958.2012.08126.x

Zhang, P., Wu, L., Zhu, Y., Liu, M., Wang, Y., Cao, G., et al. (2017). Deletion of MtrA inhibits cellular development of *Streptomyces coelicolor* and alters expression of developmental regulatory genes. *Front. Microbiol.* 8:2013. doi: 10.3389/fmicb.2017.02013

Zhang, Y., Zhang, Y., Li, P., Wang, Y., Wang, J., Shao, Z., et al. (2018). GlnR positive transcriptional regulation of the phosphate-specific transport system *pstSCAB* in *Amycolatopsis mediterranei* U32. *Acta Biochim. Biophys. Sin.* 50, 757–765. doi: 10.1093/abbs/gmy073

Zheng, Y., Sun, C. F., Fu, Y., Chen, X. A., Li, Y. Q., and Mao, X. M. (2019). Dual regulation between the two-component system PhoRP and AdpA regulates antibiotic production in *Streptomyces*. *J. Ind. Microbiol. Biotechnol.* 46, 725–737. doi: 10.1007/s10295-018-02127-5

Zhu, Y., Zhang, P., Zhang, J., Xu, W., Wang, X., Wu, L., et al. (2019). The developmental regulator MtrA binds GlnR boxes and represses nitrogen metabolism genes in *Streptomyces coelicolor*. *Mol. Microbiol.* 112, 29–46. doi: 10.1111/mmi.14252

Conflict of Interest: The authors declare that the research was conducted in the absence of any commercial or financial relationships that could be construed as a potential conflict of interest.

frontiers in Microbiology

ORIGINAL RESEARCH
published: 23 January 2020
doi: 10.3389/fmicb.2019.03121

sRNA scr5239 Involved in Feedback Loop Regulation of *Streptomyces coelicolor* Central Metabolism

Franziska Engel[1], Elena Ossipova[2], Per-Johan Jakobsson[2], Michael-Paul Vockenhuber[1] and Beatrix Suess[1]**

[1] Synthetic Genetic Circuits, Department of Biology, Darmstadt University Technology, Darmstadt, Germany, [2] Division of Rheumatology, Department of Medicine, Karolinska Institutet, Karolinska University Hospital, Solna, Sweden

OPEN ACCESS

Edited by:
Yvonne Mast, German Collection of Microorganisms and Cell Cultures GmbH (DSMZ), Germany

Reviewed by:
Bohdan Ostash, Ivan Franko National University of Lviv, Ukraine
Antonio Rodríguez-García, Instituto de Biotecnología de León, Spain
Paula Yagüe, University of Oviedo, Spain

***Correspondence:**
Michael-Paul Vockenhuber
vockenhuber@bio.tu-darmstadt.de
Beatrix Suess
bsuess@bio.tu-darmstadt.de

Specialty section:
This article was submitted to Microbial Physiology and Metabolism, a section of the journal Frontiers in Microbiology

Received: *04 October 2019*
Accepted: *24 December 2019*
Published: *23 January 2020*

Citation:
Engel F, Ossipova E, Jakobsson P-J, Vockenhuber M-P and Suess B (2020) sRNA scr5239 Involved in Feedback Loop Regulation of Streptomyces coelicolor Central Metabolism. Front. Microbiol. 10:3121. doi: 10.3389/fmicb.2019.03121

In contrast to transcriptional regulation, post-transcriptional regulation and the role of small non-coding RNAs (sRNAs) in streptomycetes are not well studied. Here, we focus on the highly conserved sRNA scr5239 in *Streptomyces coelicolor*. A proteomics approach revealed that the sRNA regulates several metabolic enzymes, among them phosphoenolpyruvate carboxykinase (PEPCK), a key enzyme of the central carbon metabolism. The sRNA scr5239 represses *pepck* at the post-transcriptional level and thus modulates the intracellular level of phosphoenolpyruvate (PEP). The expression of scr5239 in turn is dependent on the global transcriptional regulator DasR, thus creating a feedback loop regulation of the central carbon metabolism. By post-transcriptional regulation of PEPCK and in all likelihood other targets, scr5239 adds an additional layer to the DasR regulatory network and provides a tool to control the metabolism dependent on the available carbon source.

Keywords: sRNA, *Streptomyces*, DasR, carbon metabolism, phosphoenolpyruvate, PEPCK

INTRODUCTION

Streptomycetes are Gram-positive, filamentous, GC-rich, soil-dwelling bacteria. They are best known for their complex life cycle and their ability to produce a wide range of secondary metabolites. These include two thirds of all known antibiotics but also other bioactive compounds such as immunosuppressants, antivirals, and herbicides (Flärdh and Buttner, 2009). This biochemical potential is associated with a large genome size (usually 7–12 Mbp) and requires an equally large repertoire of regulatory proteins to control the network and adapt to changing environmental conditions (Bentley et al., 2002). *Streptomyces coelicolor* serves as a model organism for this large group of bacteria. Its regulatory repertoire includes ∼12% of its protein coding genes but also a large number of regulatory RNAs are known. The function of most of them, however, remains unknown (Pánek et al., 2008; Swiercz et al., 2008; D'Alia et al., 2010; Vockenhuber et al., 2011; Moody et al., 2013; Jeong et al., 2016; Setinova et al., 2017).

Small non-coding RNAs (sRNAs), approximately 50–500 nucleotides (nts) in length, are found in a broad range of bacteria and play an important role in the post-transcriptional regulation. Most small non-coding RNA act by base-pairing with their target mRNAs, which may affect both stability and/or translation of the target mRNA in a positive or negative manner (reviewed in Romby and Wagner, 2012). Depending on their genomic context, sRNAs are divided

into *trans*-encoded regulatory RNAs, which are encoded at different genomic locations from their target genes and often share only limited complementarity with them, and *cis*-encoded (antisense) regulatory RNAs. They are transcribed opposite to annotated genes and share complete complementarity with their targets. Most knowledge about sRNAs, their targets and regulatory networks has so far been derived from Gram-negative bacteria such as *Escherichia coli* and *Salmonella* (Frohlich et al., 2012; Guo et al., 2014; Porcheron et al., 2014; Kim et al., 2019). In contrast, only a few sRNAs in streptomycetes have been experimentally characterized so that their function is known. Examples include scr4677, which is thought to impact the actinorhodin production under specific growth conditions (Hindra et al., 2014) and scr3097, which in combination with a riboswitch influences *rpf*A expression post-transcriptionally (St-Onge and Elliot, 2017). Furthermore, there are the antisense RNA cnc2198.1 that regulates glutamine synthase *glnA* (D'Alia et al., 2010) and scr5239. The latter was identified using a deep sequencing approach (Vockenhuber et al., 2011). scr5239 expression is constitutive under several stress and growth conditions but dependent on the nitrogen supply. It is conserved in two thirds of all currently available *Streptomyces* genomes. The 159 nt long sRNA consists of five stem-loops P1–P5, of which stem P4 is involved in the interaction with both currently known target mRNAs. These targets – the genes for the methionine synthase *metE* and the agarase *dagA* – are crucial for both primary and secondary metabolisms, as they are important for methionine synthesis and the degradation and utilization of agar as a carbon source. Whereas *S. coelicolor* is the only known *Streptomyces* species that carries the agarase gene *dagA*, *metE* is conserved in a wide number of streptomycetes (Vockenhuber et al., 2011; Vockenhuber and Suess, 2012; Vockenhuber et al., 2015). Since non-coding RNAs are known to often control more than one target, and because of its remarkable conservation, we aimed to identify further targets of scr5239. Our previous studies indicated that in contrast to the majority of the characterized sRNAs to date, scr5239 did not induce degradation of the both validated target mRNAs *metE* and *dagA* (Vockenhuber et al., 2011; Vockenhuber et al., 2015). Therefore, we decided to carry out a proteomics study to identify new targets controlled by scr5239.

Here, we present the characterization of a new sRNA target that resulted from the proteomics study, the phosphoenolpyruvate carboxykinase (PEPCK, SCO4979). PEPCK is a key enzyme of the primary metabolism as it connects glycolysis with the tricarboxylic acid (TCA) cycle and is thought to catalyze the first step of gluconeogenesis in all organisms. In the presence of GTP it catalyzes the conversion of oxaloacetate (OAA) to phosphoenolpyruvate (PEP). This reaction is the rate-limiting step in the metabolic pathway that produces glucose from lactate and other precursors derived from the TCA cycle (Delbaere et al., 2004). Here we show that scr5239 controls PEPCK and thus the level of the metabolite PEP. scr5239 itself is controlled by DasR, one of the most important pleiotropic regulators of the primary and secondary metabolism in *S. coelicolor*. It controls more than 50 genes including the biosynthetic pathways for several antibiotics (Świątek-Połatyńska et al., 2015), developmental control (Rigali et al., 2006) or the response to cold shock stress (Nazari et al., 2013). We propose that scr5239 adds an additional layer to the DasR regulatory network by creating a feedback loop regulation for the control of the central metabolism.

MATERIALS AND METHODS

Cultivation of *S. coelicolor*

For growth on solid medium, 10^8 spores per 300 μl were pregerminated (Kieser et al., 2014), plated out on R2YE with cellophane overlays and incubated at 30°C for 3–4 days. For growth in liquid medium, 10^8 spores per 50 ml were pregerminated and incubated at 28°C under continuous shaking for 3–4 days in Jasenka medium (10% sucrose, 3% tryptic soy broth, 0,1% $MgCl_2$ and 0,1% yeast extract).

Plasmids and *S. coelicolor* Strains

A list of all plasmids used may be found in **Table 1**. All integrating plasmids were constructed based on pAR933a (Rodríguez-García et al., 2005). It contains origin of replication for maintenance in *E. coli*, an apramycin resistance gene for selection in *E. coli* and *S. coelicolor*, an integrase gene and attachment site of the phiC31 phage and an origin of transfer. The plasmids used here all enable a stable integration of one single copy per chromosome (Kuhstoss et al., 1991), avoiding possible problems associated with the copy number of multicopy plasmids. The luciferase gene was excised from pAR933a using *Xba*I and *Spe*I and a 3x FLAG-tag (for western blot detection) was inserted, thus converting the *Xba*I site to an *Mfe*I site. Then, an insert containing two *Bsa*I sites for golden gate cloning was cloned into the *Spe*I/*Mfe*I digested vector resulting in pGold_F3. *E. coli* ET12567/pUZ8002 was used to transfer the plasmids into *S. coelicolor* via intergeneric conjugation (Kieser et al., 2014). A list of *S. coelicolor* strains used may be found in **Table 2**.

Mass Spectrometry-Based Quantitative Proteomics

For quantitative liquid chromatography mass spectrometry (LC-MS/MS) analysis, the *S. coelicolor* M145 and the sRNA overexpression and deletion strains (scr5239+ and Δscr5239, respectively) where grown on solid R2YE medium as described above. Cells where harvested at the end of exponential growth when the mycelium just started to turn red. Cell lysis and whole proteome preparation were done as described in section "SDS-PAGE and Western Blot Analysis."

Proteins were precipitated from the lysates using ReadyPrep™ 2-D Cleanup Kit (Bio-Rad). Obtained protein pellets were suspended in dissolving buffer containing 2% SDS, 8 M urea, 25 mM HEPES, 1 mM DTT (pH 7.4) and the protein concentration was measured using Bradford assay (Bio-Rad). For the digestion, aliquots containing 200 μg of total protein amount were added onto Microcon-10 kDa Centrifugal Filter Units (Millipore) and processed using FASP protocol (Wisniewski et al., 2009) with modified digestion buffer containing 0.2% sodium deoxycholate, 0.25 M urea, in 100 mM HEPES, pH 7.6.

TABLE 1 | List of plasmids used in this study.

Plasmid	Characteristics	References
pAR933a	integrating plasmid	Rodríguez-García et al., 2005
pFT241	pFT74-derivative for DasR overexpression	Schlicht, 2003
pGold_F3	integrating plasmid, with FLAG-Tag to detect integrated genes	This work
pPEPC_F3	plasmid for integrating and detecting PEPCK (5416135–5418114)	This work
pSP4_PEPC_F3	plasmid for integrating and detecting PEPCK, natural promoter replaced by the synthetic Promoter SP4	This work
pPEPC_F3 M1	plasmid for integrating and detecting PEPCK, part of the original 5′ UTR replaced by the metH 5′ UTR	This work
pPEPC_F3_scr5239+	plasmid for integrating and detecting PEPC, with scr5239 in control of the SF14 promoter	This work
pPEPC_F3_scr5239+_M1	plasmid for integrating and detecting PEPC, with a mutated scr5239 in control of the SF14 promoter	This work
pGUS_pscr5239	plasmid for integrating scr5239 promoter and detecting its activity using *gusA*	This work
pGUS_pscr5239_M1	plasmid for integrating a shortened scr5239 promoter variant and detecting its activity using *gusA*	This work
pGUS_pscr5239_M2	plasmid for integrating a scr5239 promoter with mutated *dre* site and detecting its activity using *gusA*	This work

After digestion, sodium deoxycholate was removed from the samples by precipitation in the presence of formic acid followed by centrifugation at 12,000 × *g*. Concentration of obtained peptides was measured using Lowry assay. Equal amount of protein digests (100 μg) from each sample were labeled with Tandem Mass Tag (TMT) 6-plex Isobaric Mass Tagging Kit (Thermo Fisher Scientific) according to the manufacturer's instructions. Labeled samples were dissolved in loading buffer (3% ACN, 0.1% FA), resulting in a final concentration of 10 μg/μl prior to LC-MS/MS analysis. Before analysis on the Q Exactive (Thermo Fischer Scientific), peptides were separated using an Agilent 1200 nano-LC system. Samples were trapped on a Zorbax 300SB-C18, and separated on a NTCC-360/100-5-153 (Nikkyo Technos, Ltd.) column using a gradient of A (5% DMSO, 0.1% FA) and B (90% ACN, 5% DMSO, 0.1% FA), ranging from 5 to 37% B in 240 min with a flow of 0.4 μl/min. The Q Exactive was operated in a data-dependent manner, selecting top five precursors for fragmentation by HCD. The survey scan was performed at 70,000 resolution from 300 to 1700 m/z, with a max injection time of 100 ms and target of 1×10^6 ions. For generation of HCD fragmentation spectra, a max ion injection time of 500 ms and AGC of 1×10^5 were used before fragmentation at 30% normalized collision energy, 35,000 resolution. Precursors were isolated with a width of 2 m/z and put on the exclusion list for 70 s. Single and unassigned charge states were rejected from precursor selection.

Acquired MS raw files were searched against the UniProtKB/*S. coelicolor* database and filtered to a 1% FDR cut off. Ion mass tolerance of precursors equals ±10 ppm, whereas the fragments have a more limited mass tolerance of 0.02 Da for HCD-FTMS. The search algorithm assessed tryptic peptides with maximum one missed cleavage; carbamidomethylation (C), TMT 10-plex (K, N-term) as fixed modifications and oxidation (M) as variable modification. Only unique peptides in the data set were used for quantification, while reporter ions were quantified by Proteome Discoverer on HCD-FTMS tandem mass spectra (integration tolerance 20 ppm).

TABLE 2 | List of *S. coelicolor* strains used in this study.

Strain	Features	References
M145	SCP1$^-$, SCP2$^-$	Kieser et al., 2014
Δscr5239	M145scr5329::KanR	Vockenhuber and Suess, 2012
scr5239+	M145scr5239p::SF14p	Vockenhuber and Suess, 2012
M145 [pFT241]	M145 [pFT241]	Schlicht, 2003
BAP29	M145dasR::aacC4	Rigali et al., 2006
FE01	M145::pPEPC_F3	This work
FE02	Δscr5239::pPEPC_F3	This work
FE03	scr5239+::pPEPC_F3	This work
FE04	M145::pSP4_PEPC_F3	This work
FE05	Δscr5239::pSP4_PEPC_F3	This work
FE06	scr5239+::pSP4_PEPC_F3	This work
FE07	M145::pPEPC_F3_M1	This work
FE08	Δscr5239::pPEPC_F3_M1	This work
FE09	scr5239+::pPEPC_F3_M1	This work
FE11	Δscr5239::pPEPC_F3_scr5239+	This work
FE12	Δscr5239::pPEPC_F3_scr5239+_M1	This work
FE13	M145::pGUS_pscr5239	This work
FE14	M145::pGUS_pscr5239_M1	This work
FE15	M145::pGUS_pscr5239_M2	This work

SDS-PAGE and Western Blot Analysis

A total of 1 ml liquid culture or 100 mg mycelium from solid medium were harvested and mixed with 1 ml 1× ZAP (50 mM NaCl, 50 mM Tris–HCl pH 8.0, 10% glycerol, 10 mM PMSF). The subsequent disruption of the cells was done using 200 μl glass beads (0.4 mm diameter) and the FastPrep-24 instrument (MP Biomedicals) for 4 × 1 min at 5.5 m/s. Mycelial debris was removed by centrifugation at 4°C. Protein concentration of the supernatant was determined by Bradford assay (Bradford, 1976). Twenty to fifty μg of crude extract were separated by a 6% or 12% SDS-PAGE. 0,5% 2,2,2-trichloroethanol (TCE) in the polyacrylamide gels allowed fluorescent detection of proteins using the ChemiDoc^{TM} MP Imaging System (Bio-Rad). Gels were blotted using the Trans-Blot® Turbo^{TM} Transfer System (Bio-Rad). Membranes were blocked for 1 h in 2% ECL^{TM} Blocking Agent (GE Healthcare) in TBS-T (20 mM

Tris base, 150 mM NaCl and 0.1% Tween 20), followed by incubation with a Monoclonal ANTI-FLAG® M2 antibody (Sigma-Aldrich #F1804; 1:50000 in 2% ECL™ Blocking Agent in TBS-T) for 1 h at RT and 3 × 10 min wash in TBS-T. Blots were developed using ECL™ Select Western Blotting Detection Reagent (GE Healthcare) and signals detected with the ChemiDoc™ MP Imaging System. Protein bands were quantified using Image Lab Software 6.0.1. Total protein was used as loading control.

RNA Isolation

Total RNA was isolated following Vockenhuber et al. (2015). In brief, 1 ml culture or ∼100 mg mycelium were harvested and resuspended in 300 µl lysis buffer (10 mM sodium acetate, 150 mM sucrose, pH 4.8). Glass beads (200 µl, 0.4 mm diameter) and 300 µl acidic phenol were added. Cells were disrupted using a FastPrep-24 instrument (MP Biomedicals) for 4 × 1 min at 5.5 m/s. After phenol/chloroform extraction and ethanol precipitation, the RNA was resuspended in 500 µl ddH_2O and the concentration was determined (usually 2–4 µg/µl). One hundred µg of total RNA were incubated with 30 U Turbo DNase (Ambion) for 1 h to remove residual DNA, subsequently precipitated and resuspended in 50 µl ddH_2O. The yield was usually a concentration of 1–1.5 µg/µl, of which 1 µg was quality-checked on a 1% agarose gel.

RT-qPCR

A total of 1 µg RNA was reverse-transcribed using the SuperScript IV Reverse Transcriptase (Thermo Fisher Scientific) and random hexamers according to the manufacturer's protocol. After transcription, the 20 µl reaction was filled up to 200 µl with ddH_2O. mRNA levels were analyzed using 5 µl of 1:1 diluted cDNA product, the Fast SYBR Green PCR Master Mix (Applied Biosystems) and specific primers for the *pepck* (PEPCK_fwd and PEPCK_rev). The genes for *hrdB* (Primers: hrdB_fwd and hrdB_rev) and SCO1544 (Primers: 1544_fwd and 1544_rev) served as an endogenous control (Li et al., 2015). RT-qPCR was carried out on a StepOnePlus machine. All oligonucleotides used may be found in **Table 3**.

β-Glucuronidase Measurement

The β-glucuronidase gene (*gusA*) was used to determine promoter activity in *S. coelicolor* (Myronovskyi et al., 2011). Here, 10–40 mg of protein crude extract (cell disruption protocol, see section "SDS-PAGE and Western Blot Analysis") obtained from mycelium harvested from solid medium were used for the enzymatic reaction. The assay was performed as previously described (Rudolph et al., 2015).

TABLE 3 | List of oligonucleotides used in this study.

Primer	Sequence (5′–3′)
PEPCK_fwd	GTCACCGAGTCCTTCGACTG
PEPCK_rev	GATCTTCGGCAGCTTGGACT
hrdB_fwd	AGTTCGAAGCCTCCACTTGT
hrdB_rev	TGCTGACGCCGCTACTCGT
1544_fwd	TCGAGGTCGCCCGGGAACT
1544_rev	GATCACGTAGGTGGGGGTGCC
scr5239_A	CCGGTCGGCCGAAGGATG
5S_A	CGAAATGTAACCGGGCGTTT

Measurement of PEP Concentration

The PEP Colorimetric/Fluorometric Assay Kit from Sigma-Aldrich was used to determine the PEP concentration in *S. coelicolor* according to the manufacturer's protocol. 2–4 mg of mycelium harvested from solid medium were used for the enzymatic reaction. Signals were quantified by fluorescence using a Tecan infinite 200 pro multiwell plate reader.

Northern Blot Analysis

A total of 30 µg total RNA was separated on 6% denaturing polyacrylamide gels and transferred to a positively charged nylon membrane (Hybond-N+, GE Healthcare) in a tank blotting device (Peqlab) at 4°C. As probe for detection, 10 pmol oligonucleotide were radiolabeled at the 5′ end using 5 µl γ-[^{32}P] ATP (∼3.3 pmol/µl, Hartmann-Analytic) and 1 µl T4 polynucleotide kinase (Roche) in the supplied buffer for 1 h at 37°C and subsequently purified using Illustra MicroSpin G-25 columns (GE Healthcare). 25 µl radiolabeled oligonucleotides (approximately 300 kc.p.m./µl) where used as probe for each experiment. Signals were quantified by phosphoimaging using a FLA-5000 phosphoimager (Fujifilm life Science). Expression of scr5239 (probe: scr5239_A) was normalized to the amount of 5S rRNA (probe: 5S_A).

Bioinformatics

RNAhybrid

RNAhybrid (Kruger and Rehmsmeier, 2006) is a tool for the prediction of microRNA/target duplexes. It predicts multiple potential binding sites of microRNAs in large target mRNAs by finding the energetically most favorable hybridization sites of a small RNA in a large RNA. To predict potential binding sites, we used RNAhybrid Version 2.2 with default parameters. Judging from past experience, the predicted mRNA/sRNA interaction sites are more reliable with this program than with other available prediction tools.

Target Explorer and PREDetector

For prediction of *dre* sites, an evaluation matrix ranking the individual nucleotides of the binding site according to their importance was required. For this purpose, the program Target Explorer was used (Sosinsky et al., 2003). To create the position matrix, the sequences of five different known *dre* sites were used. These can be found in **Supplementary Table S1**. The position matrix thus created is shown in **Supplementary Figure S1**. Using this matrix and PREDetector (Hiard et al., 2007), we predicted 15 new *dre* sites in the genome of *S. coelicolor*. The results, ranked according to the degree of matching with the matrix (score), can be found in **Supplementary Table S2**. The *dre* site upstream of scr5239 ranked fourth of all predicted sites.

RESULTS

Quantitative Proteomics Reveals 32 Proteins That Show scr5239-Dependent Changes in Expression

To identify new targets of scr5239, we compared the proteome of *S. coelicolor* wild type (M145) with its respective scr5239 deletion (Δscr5239) and overexpression (scr5239+) strain. We applied quantitative proteomics based on the stable isotope labeling method to all three strains grown on R2YE solid medium and harvested in the transition phase. After protein extraction and fragmentation, the peptides where labeled with a different TMT labels for each strain and analyzed using LC-MS/MS (**Figure 1A**). This method has already been successfully applied in *S. coelicolor* to characterize differentiation and activation of the secondary metabolism (Rioseras et al., 2018).

A total of 1669 proteins were found to be expressed in all three strains (**Supplementary Table S3**). However, only 32 of them showed a significant change in expression level depending on scr5239, i.e., at least a two-fold change in mass spec. signal strength (Δscr5239 vs. M145 or M145 vs. scr5239+) (**Figure 1B**). Functional analysis revealed that potential targets of the sRNA cluster in five main groups. The largest group, comprising about half of the identified annotated proteins (12), are metabolic enzymes. In addition to that, eight proteins cluster in the group of DNA-binding and regulatory proteins. Another three identified proteins are part of the CDA antibiotic biosynthesis cluster and two are involved in proteolysis. The remaining eight proteins are of unknown function. **Figure 1B** shows the detected changes in protein expression upon deletion or overexpression of the sRNA along with a functional analysis.

Since metabolic enzymes were the most abundant, we focused on potential targets within this group. Moreover, the fact that the previously identified targets of this sRNA, *metE* and *dagA* (Vockenhuber et al., 2011, 2015) play a role in central carbon and amino acid metabolism further encouraged us to prioritize metabolic enzymes. The candidate with the most interesting functionality here was SCO4979, which encodes the PEPCK. It connects glycolysis with the TCA cycle and catalyzes the rate-limiting step in the gluconeogenese. In consequence, it is of key importance for the central carbon metabolism. We therefore continued with this candidate.

PEPCK Protein and mRNA Levels Are Dependent on scr5239 Expression

To investigate the role of scr5239 in the regulation of PEPCK, we initially analyzed the mRNA and protein levels of PEPCK depending on the scr5239 level. To validate the quantitative proteomics data, we performed western blot analyses. We used an integrating plasmid and fused a 3x FLAG-tag to the C-terminus of PEPCK resulting in pPEPCK_F3. We attached the tag to the C-terminus as sRNA/mRNA interactions usually take place in the 5′UTR or close to the 5′ end of the coding region of the mRNA. The plasmid was integrated into the genome of wild type (M145), Δscr5239 and scr5239+ into the attachment site of the phiC31 phage, thus resulting in strains FE01, FE02, and FE03, respectively. A list of all strains used and constructed across all experiments may be found in **Table 2**. We used the same growth conditions as in the TMT-based experiment and harvested the cells in the transition phase. The western blot analysis shown in **Figure 2A** effectively confirms the TMT data with a two-fold increase in PEPCK expression in FE02 (Δscr5239) and approximately two-fold decrease in FE03 (scr5239+) compared to the wild type (FE01). To exclude an effect on the transcription of PEPCK, we replaced the wild type *pepck* promoter in pPEPCK_F3 with the synthetic promoter SP4 (Horbal et al., 2018), thus generating the integrating plasmid pSP4_PEPCK_F3. Integration resulted in the respective strains FE04, FE05, and FE06 for M145, Δscr5239, and scr5239+, respectively. Western blot analyses of these strains show similar regulation, which indicates that the observed regulation is not promoter-dependent and therefore taking place on the posttranscriptional level (**Figure 2B**). mRNA levels of *pepck* were measured in M145, Δscr5239 and scr5239+. The RT-qPCR results revealed a four-fold increase of *pepck*-levels in Δscr5239 and a slight decrease (0.6-fold) in scr5239+ compared to the levels in M145 (**Figure 2C**).

Most known sRNAs base pair with the translational initiation region (TIR) and thus initiate mRNA degradation (Saramago et al., 2014). The results of the western blot and RT-qPCR analyses indicate that the PEPCK regulation by scr5239 follows this mechanism.

Deletion of scr5239 Leads to an Increase of the Energy Donor Phosphoenolpyruvate in *S. coelicolor*

Next, we aimed to investigate the metabolic impact of PEPCK regulation through scr5239. We determined the steady state level of PEP, the product converted by PEPCK from OAA. M145, Δscr5239, and scr5239+ were grown and harvested under the same conditions as for the quantitative proteomics analysis. As shown in **Figure 3**, deletion of scr5239 dramatically modulates the cellular PEP level. In Δscr5239 we were able to detect an increase of 70% in PEP level compared to M145. Increasing the scr5239 level (scr5239+) did not significantly alter the PEP level (**Figure 3A**). **Figure 3B** illustrates the influence of the sRNA on PEPCK and consequently on the level of PEP.

Phosphoenolpyruvate is a key intermediate in carbohydrate metabolism and involved in glycolysis and gluconeogenesis. Its metabolization to pyruvic acid by pyruvate kinase generates ATP and is vitally important for the energy balance of the cell, as PEP has the highest-energy phosphate bond found in organisms. The influence the sRNA exerts on the cellular concentration of this key metabolite indicates its crucial role in the regulation of the primary metabolism.

Interaction of PEPCK and scr5239

To mechanistically characterize the regulation of PEPCK by scr5239, we analyzed the interaction between the sRNA and the target mRNA. We used RNAhybrid (Kruger and Rehmsmeier, 2006) to identify potential interaction sites. RNAhybrid predicted an 8 nt region within stem P4 of the sRNA to interact with the TIR

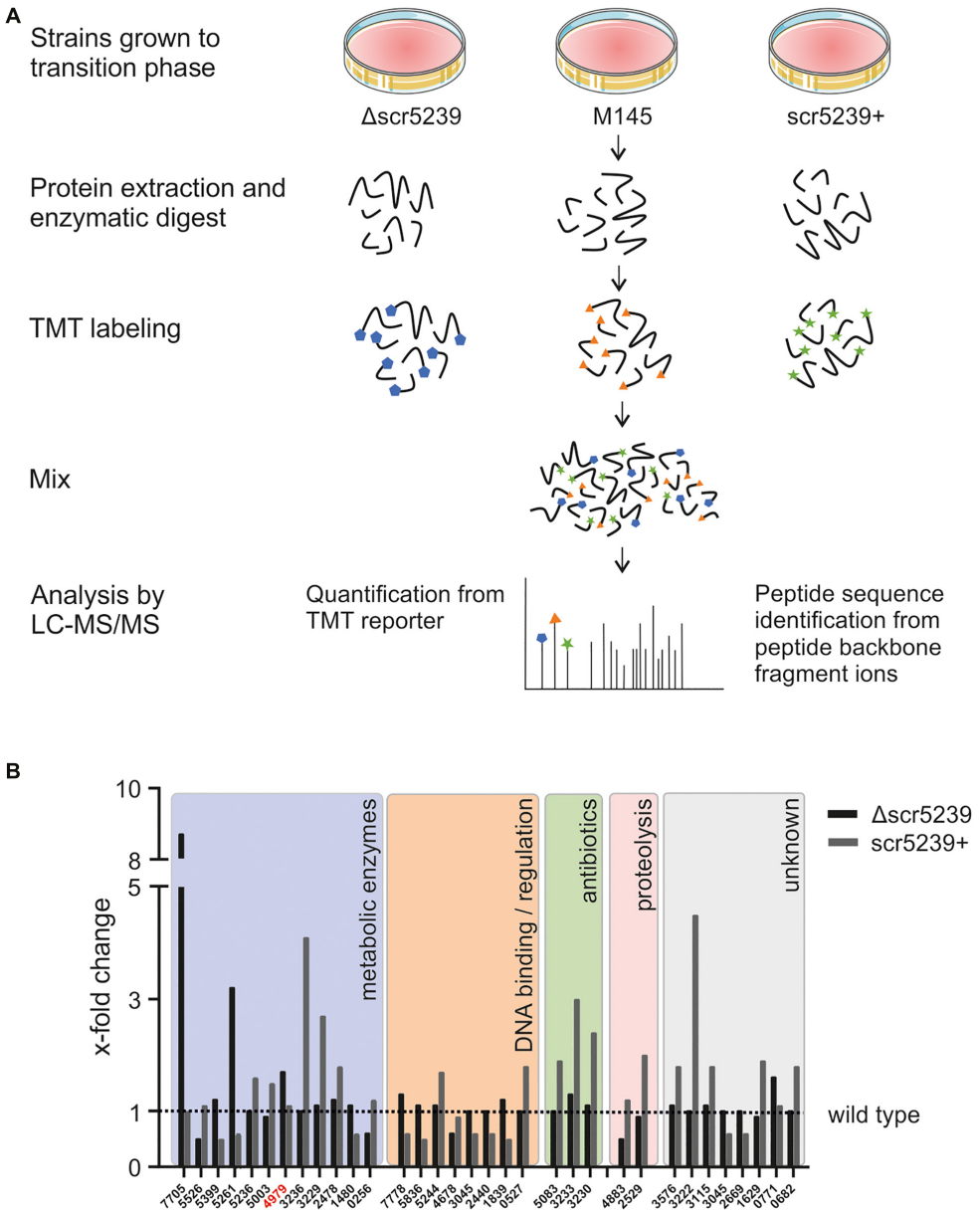

FIGURE 1 | Quantitative proteomics analysis of three different *S. coelicolor* strains. **(A)** LS-MS/MS workflow. *S. coelicolor* Δscr5239, M145, and scr5239+ were grown on rich media and harvested in the transition phase. The samples of the three strains were labeled with different TMT labels. The peptides of the three strains where pooled and the fragments where analyzed in tandem MS. As a result, a fragment of the TMT label is cleaved of each peptide. The mass of the cleaved part of the label differs with each label type. In consequence, we were able to quantify the relative amount of each peptide fragment in the input strains. The signal strength of the cleaved-off part of the labels was then used for input normalization. Thus, this method allows relative quantification of proteins. **(B)** Results of the quantitative proteomics and subsequent functional analysis. Bars indicate the x-fold change in protein expression in the Δscr5239 and scr5239+ strain compared to the wild type. Only hits with a minimum change of 50% in expression are shown (Δ vs. wt or wt vs. +). Colored boxes show categorization of proteins depending on their functional characteristics. Numbers on the *x*-axis refer to the SCO numbers of the expressed genes. The SCO number of PEPCK is highlighted in red.

of the *pepck* mRNA (**Figure 4A**). In consequence, the interaction site with PEPCK predicted for scr5239 was in the same region of the sRNA as the binding sites of the other two targets *dagA* and *metE*.

To verify the predicted interaction site, we introduced mutations within the PEPCK sequence that disrupted potential base pairing. We used plasmid pPEPCK_F3 and exchanged the PEPCK 5′UTR including the ribosomal binding site (RBS) for an 5′UTR of an unrelated gene (methionine synthase MetH), resulting in pPEPCK_F3 M1. The methionine synthase MetH is not regulated by the sRNA (Vockenhuber et al., 2015). **Figure 4B** illustrates the relevant sequence for *pepck* mRNA. The construct pPEPCK_F3 M1 was integrated into the genome of the three strains M145, Δscr5239, and scr5239+,

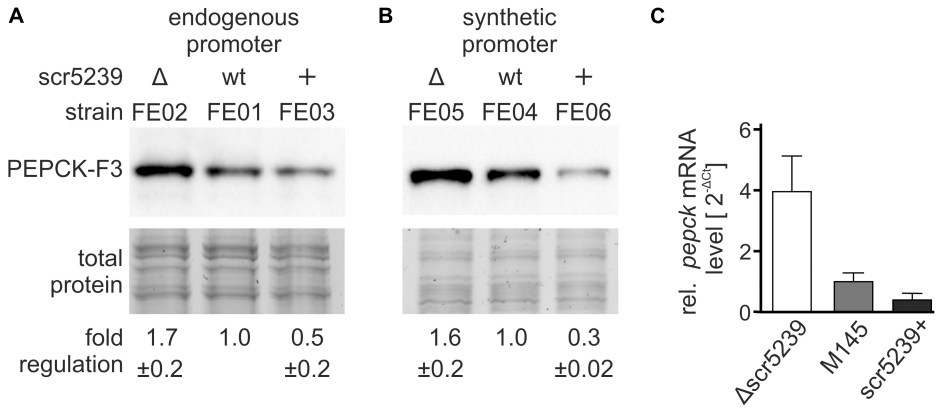

FIGURE 2 | Expression analysis of PEPCK in different strains. The strains were grown on rich media and harvested in the transition phase. **(A)** Western blot analysis using FE01, FE02, and FE03 to detect PEPCK-F3 under control of its endogenous promoter. **(B)** Western blot analysis using FE04, FE05, and FE06 to detect PEPCK-F3 under control of the synthetic promoter SP4. **(C)** RT-qPCR results. mRNA levels of *pepck* were detected in *S. coelicolor* M145, Δscr5239, and scr5239+ and normalized to the levels in M145. Measurements were normalized to the respective strain expressing wild type scr5239; error bars represent the standard deviation calculated from three independent experiments.

resulting in FE07, FE08, and FE09. **Figure 4B** shows that the expression levels of PEPCK are comparable for all three strains. PEPCK expression is not influenced by the scr5239 level as in the corresponding strains FE01, FE02, and FE03 that harbor a functional wild type PEPCK 5′UTR (compare **Figure 2B**). Hence, the mutated PEPCK-F3 does not show dependency on the sRNA.

Furthermore, we mutated scr5239 and analyzed the influence on PEPCK expression. We introduced two mutations (U113A, G114C) into the predicted interaction site of the sRNA. U113 and G114 are central in the predicted binding motif and should prevent both interaction and, consequently, regulation. **Figure 4C** illustrates the relevant sequence of the mutated sRNA. We designed two variants of a plasmid carrying the PEPCK-F3 sequence and the sequence for scr5239. The former, pPEPC_F3_scr5239+, encoded for the wild type scr5239, the latter, pPEPC_F3_scr5239+_M1, encoded for scr5239 with the described mutations. These constructs were integrated in Δscr5239 resulting in FE10 and FE11. The strains express the sRNA exclusively from the integrated plasmid (expression level of the scr5239 was confirmed by Northern blot, data not shown). Western blot analyses show that the PEPCK is more abundant in the strain with the mutated sRNA than in the strain with the wild type sRNA (**Figure 4C**), which indicates that the sRNA represses PEPCK expression more strongly than the mutated sRNA. These results suggest that the mutated sRNA is no longer able to bind *pepck* mRNA.

In sum, the results of the mutational analysis confirmed the predicted interaction site of scr5239 with the PEPCK mRNA.

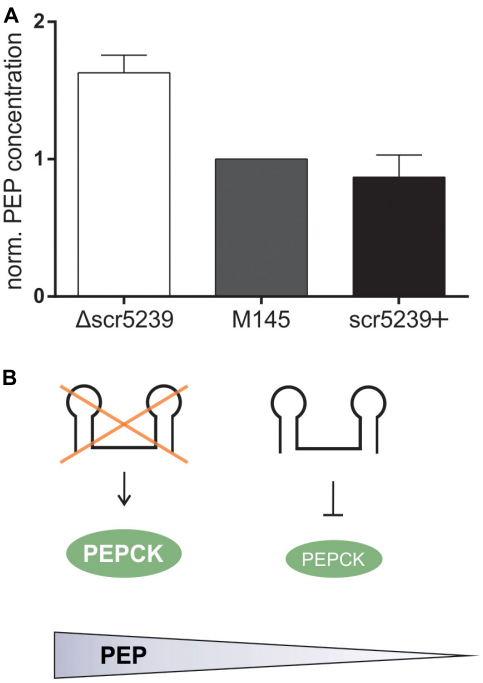

FIGURE 3 | PEP levels in M145, Δscr5239, and scr5239+. **(A)** PEP levels were determined in *S. coelicolor* M145, Δscr5239, and scr5239+ and normalized to the levels in M145; error bars represent the standard deviation calculated from three independent experiments. **(B)** Schematic overview of the connection between scr5239, PEPCK, and PEP levels in *S. coelicolor*.

Regulation of scr5239 by DasR

DasR is a global transcriptional regulator of the metabolism in *S. coelicolor* with more than 50 validated target genes. It is one of the most important pleiotropic regulators of the primary and secondary metabolism in this organism. It controls the *N*-acetylglucosamine metabolism, the monomer unit of the polymer chitin and the primary carbon and nitrogen source for *S. coelicolor* (Rigali et al., 2006; Colson et al., 2007). DasR binds to so called DasR responsive elements (*dre* sites) and prevents the transcription of downstream genes (Rigali et al., 2006; Colson et al., 2007; Rigali et al., 2008; Świątek-Połatyńska et al., 2015). After binding its ligand glucosamine-6-phosphate or

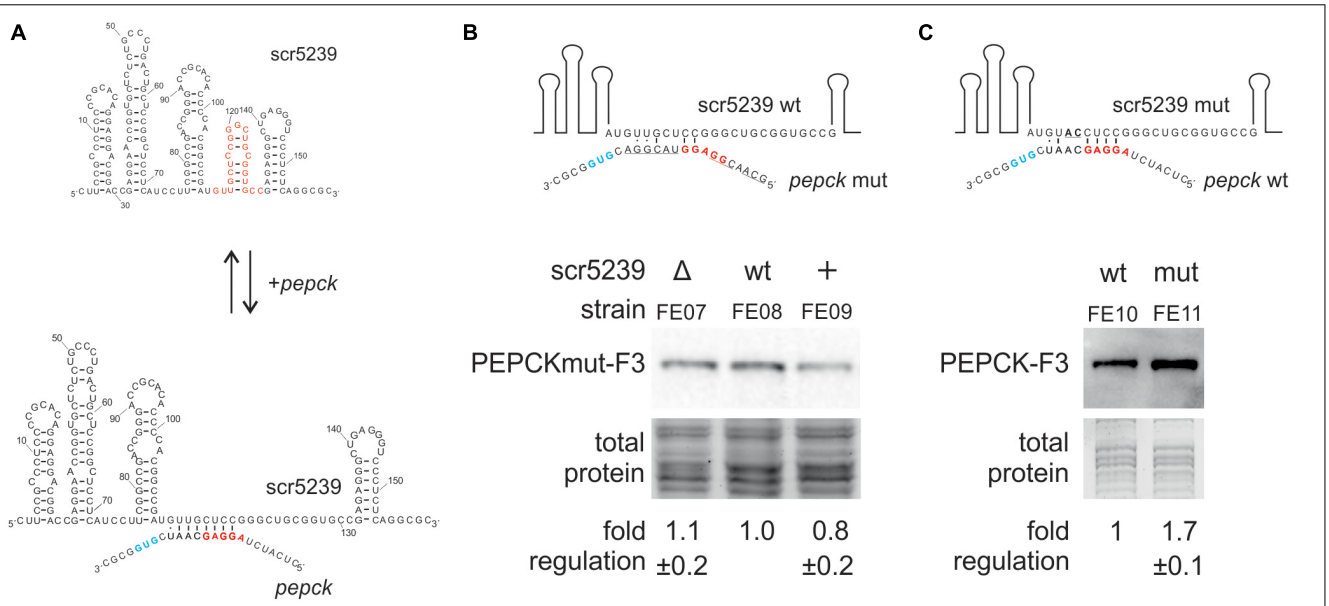

FIGURE 4 | Analysis of the interaction of scr5239 and PEPCK mRNA. **(A)** Predicted interaction site. The sequence of the sRNA is shown completely, that of the *pepck* mRNA only partially. The RBS (red) and the start codon (blue) of *pepck* are highlighted. The interaction site of *dagA* and *metE* is highlighted in red on the sRNA. **(B)** PEPCK was mutated at the predicted interaction site (PEPCmut-F3) and integrated in the genome of the M145, Δscr5239, and scr5239+. Mutated bases in the sequence are underlined. Western blot analysis using FE07, FE08, and FE09 and thus detecting PEPCmut-F3. **(C)** scr5239 was mutated at the predicted interaction site. Mutated bases in the sequence are underlined. The mutated and the wild type scr5239 in combination with PEPC-F3 were integrated into Δscr5239. Western blot analysis using FE10 and FE11 and thus detecting with PEPC-F3. Measurements were normalized to the respective strain expressing wild type scr5239; errors represent the standard deviation calculated from three independent experiments.

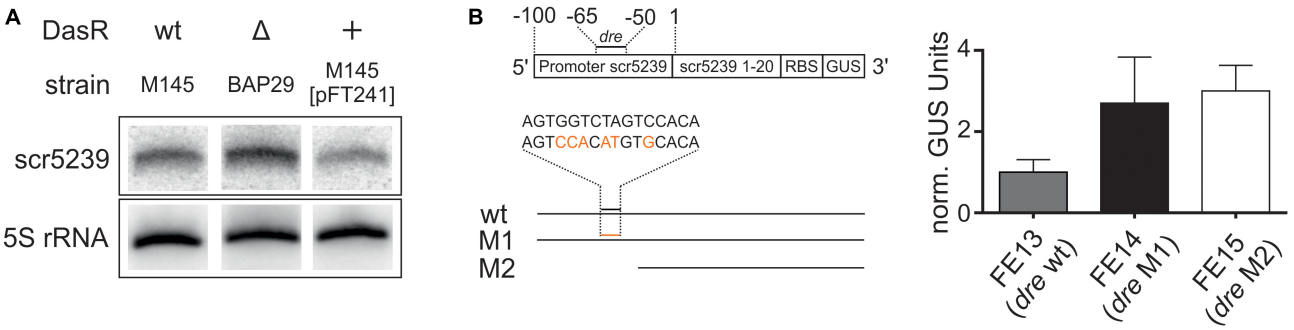

FIGURE 5 | Regulation of scr5239 by DasR. **(A)** Northern blot of scr5239 with RNA harvested from strains with different DasR expression levels. **(B)** Reporter gene measurements of different variants of the scr5239 promoter fused to a *gusA* gene. **(A)** Scheme of the used constructs. The *dre* site of scr5239 is indicated. The sequences of the wild type and the mutated *dre* site are shown. The mutated bases are highlighted in red. **(B)** Results of the reporter gene measurements for FE13, FE14, and FE15. *dre*: DasR responsive element, wt: scr5239 Promoter with wild type *dre* site, M1: scr5239 Promoter with mutated *dre* site, M2: First 50 bp of scr5239 Promoter without *dre* site. Measurements were normalized to FE13; error bars represent the standard deviation calculated from three independent experiments.

N-acetylglucosamine, respectively, DasR releases the DNA and transcription can take place. Using PREDetector software (Hiard et al., 2007), we identified a potential *dre* site upstream of scr5239. As the findings of this study clearly indicate a role of the scr5239 in the central metabolism, we decided to explore whether scr5239 is a direct target of DasR.

First, we analyzed whether scr5239 expression is dependent on DasR. We compared the expression of scr5239 in M145 with a strain lacking the *dasR* gene (BAP29; Rigali et al., 2006 and a strain overexpressing *dasR* (M145 [pFT241]; Schlicht, 2003). Northern blot analysis showed clear DasR-dependent changes in scr5239 expression (**Figure 5A**). Deletion or overexpression of DasR lead to significant increase and decrease of scr5239 expression, respectively. We then validated the significance of the *dre* site of scr5239 by reporter gene measurements. The scr5239 promoter along with the first 20 bases of the sRNA was fused to a *gusA* reporter gene (pGUS_pscr5239). Two mutants were constructed, one with 6 nt of the *dre* site exchanged (pGUS_pscr5239_M1) and a second one that contained only the first 50 bp of the promoter with the *dre* site

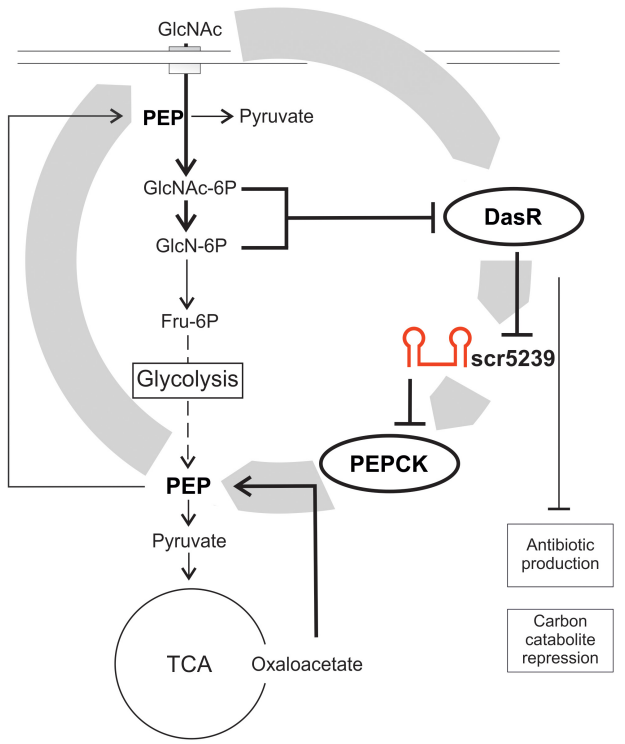

FIGURE 6 | Model of the scr5239 feedback loop. scr5239 is regulated by the global transcriptional regulator DasR that also regulates the antibiotic production and the carbon catabolite repression. scr5239 inhibits the expression of PEPCK and thus influences the PEP levels. Higher PEP levels lead to an enhanced GlcNAc uptake, which as a result inhibits DasR.

deleted (pGUS_pscr5239_M2, **Figure 5B**, left). The constructs (pGUS_pscr5239, _M1, _M2) were integrated into the genome of M145 resulting in the strains FE13, FE14, and FE15. The strains were grown to the transition phase and the GUS activity was measured. Both mutations lead to an approximately three-fold increase in Δ-glucuronidase activity when compared to the wild type promoter (**Figure 5B**, right).

The Northern blot analysis and the reporter gene measurements of the promoter activity confirm that DasR regulates scr5239 transcription by interacting with the upstream *dre* site. However, please note that DasR, even when overexpressed, does not fully repress scr5239. Consequently, there are likely more factors that influence the expression rate of the sRNA *in vivo*.

DISCUSSION

Starting from proteomics data, we confirmed *pepck* as a new target of scr5239 in *S. coelicolor*. Consequently, the sRNA has now three validated targets, which renders it the best characterized sRNA in streptomycetes to our knowledge.

The binding site of scr5239 in the *pepck* gene is located between the RBS and the start codon of the mRNA. In contrast, the binding sites of the other two known scr5239 targets are located within the open reading frame (*dagA* + 33 – + 52, *metE* + 7 – + 30). Furthermore, for *dagA* and *metE*, only the protein levels are changing while their mRNA levels stay constant. However, in the case of PEPCK, mRNA levels change in the same pattern as the protein levels, which is common for mRNA/sRNA interactions. The regulation described here thus follows the conventional mechanism described for the majority of sRNAs, mostly characterized in the well-studied organisms *E. coli* and *Salmonella* (Wagner and Romby, 2015). They regulate the expression of their target genes by blocking access to the RBS and/or start codon, which impedes translation and initiates mRNA degradation.

In the present study, we were able to show that scr5239 is involved in the regulation of the central metabolism of *S. coelicolor*. PEPCK is a key enzyme of the primary metabolism that catalyzes the conversion of OAA to PEP, the first and rate-limiting step of the gluconeogenesis (Delbaere et al., 2004). Since the regulation of glycolysis and gluconeogenesis is mutually exclusive, the control of PEPCK must be exactly adapted to the metabolic demand/situation of the cell. We show that scr5239 is involved in this regulation. It binds to the *pepck* mRNA leading to a reduced level of the enzyme. Consequently, a reduced level of the sRNA significantly increases the intercellular PEP level (see deletion studies). PEP can then be further converted into fructose-1,6-bisphosphate toward glucose but is also involved in carbon uptake and signaling through the phosphotransferase system (PTS) (Bruckner and Titgemeyer, 2002).

Most sRNAs are transcriptionally controlled by σ- or transcription factors. We were able to show that this is also the case for scr5239, which is regulated by the global transcription regulator DasR. We identified a functional *dre* site in the promoter of scr5239. Our findings match the results of previously performed ChIP-on-chip experiments and EMSAs (Świątek-Połatyńska et al., 2015). They showed that the *dre* site of scr5239 was one of the most tightly bound targets of DasR. Moreover, DasR binding to the *dre* site of scr5239 could be observed in the samples taken during vegetative growth and sporulation, which was only the case for a small fraction of the found targets. Furthermore, the genomic locations of DasR and scr5239 provide further insight. DasR is encoded in ORF5231, which puts protein and sRNA in a close evolutionary context. These findings indicate that scr5239 is at least one of the most preferred targets of DasR, thus suggesting a key role of the sRNA in the DasR regulatory network.

Small non-coding RNAs are often involved in forming (negative) feedback loops with the transcription factors they regulate (reviewed in Wagner and Romby, 2015). A feedback loop regulation can also be described for the scr5239 regulation by DasR. DasR is regulated by the PTS in streptomycetes with GlcNAc as preferred carbon source (Nothaft et al., 2003). If the supply of nutrients is sufficient (high level of GlcNAc that is converted via GlcN6-P into Fru-6P as input to glycolysis), DasR in its GlcN6-P-bound conformation cannot act as repressor, hence the sc5239 level is high. As a result, gluconeogenesis is switched off by binding and repressing *pepck* via scr5239,

the first and rate-limiting step of gluconeogenesis. If the nutrient supply deteriorates, DasR in its free form can act as repressor and the level of scr5239 decreases. In consequence, the PEP level increases, which initiates gluconeogenesis. However, PEP is not just important as intermediate for glycolysis and gluconeogenesis, but although for carbon uptake via the PTS. Increased PEP levels allow the cells to take up more GlcNAc through the PTS, which leads to a higher concentration of GlcN-6-P. GlcN-6-P in turn represses DasR, which then again leads to higher levels of scr5239. Through this feedback loop scr5239 can to influence its own repressor. A model of such feedback loop regulation including the DasR and scr5239 is depicted in **Figure 6**. Such regulatory feedback loops have already been described for sRNAs. An example is the transcription factor OmpR that activates the sRNAs OmpA and OmpB whereas these inhibit OmpR (Brosse et al., 2016).

The carbohydrate metabolism is often governed by complex regulatory networks. They allow the survival of bacteria in ever-changing habitats with fluctuating nutrient supplies by rapid adaptation of their metabolic capabilities. Such metabolic networks not only exploit transcription regulation but also include posttranscriptional regulation e.g., the control by sRNAs. Within the last years, sRNAs emerged as an important additional layer to fine-tune regulatory response. sRNAs are proposed to limit the response to substrate availability, set the threshold concentration or module the delay time for activation or shutdown of the system (Durica-Mitic et al., 2018). Prominent examples are the sRNA Spot42 that is involved in the carbon catabolite repression in *E. coli* or the sRNA CsrB and CsrC that control the RNA-binding protein CsrA – a posttranscriptional regulator responsible for the switch between glycolysis and gluconeogenesis. These examples impressively show that bacterial carbohydrate metabolism is controlled at all levels by large and densely interconnected regulatory networks. In *Streptomyces*, DasR is the major hub for the control of the central carbohydrate metabolism. We identified scr5239 as additional player in this regulatory network representing a switch for the cell to decide between gluconeogenese and glycolysis.

DATA AVAILABILITY STATEMENT

The datasets generated for this study can be found in the PRIDE repository project accession: PXD016811.

AUTHOR CONTRIBUTIONS

BS, M-PV, and FE contributed to the conception, design of the study, and wrote the manuscript. FE and M-PV performed most of the experiments. EO and P-JJ were responsible for quantitative proteomics analysis.

FUNDING

This work was funded by the Deutsche Forschungsgemeinschaft CRC902(A2), the Swedish Research Council (grant no. 2017-02577), and Innovative Medicines Initiative (EU/EFPIA, ULTRA-DD, grant no. 115766).

ACKNOWLEDGMENTS

The authors thank Dr. J. E. Weigand for fruitful discussions and for critically reading the manuscript.

SUPPLEMENTARY MATERIAL

The Supplementary Material for this article can be found online at: https://www.frontiersin.org/articles/10.3389/fmicb.2019.03121/full#supplementary-material

FIGURE S1 | *dre* site prediction matrix.

TABLE S1 | *dre* sites that were used to create the position martix.

TABLE S2 | Predicted *dre* sites.

TABLE S3 | Quantitative proteomics results.

REFERENCES

Bentley, S. D., Chater, K. F., Cerdeño-Tárraga, A.-M., Challis, G. L., Thomson, N. R., James, K. D., et al. (2002). Complete genome sequence of the model actinomycete *Streptomyces coelicolor* A3(2). *Nature* 417, 141–147. doi: 10.1038/417141a

Bradford, M. M. (1976). A rapid and sensitive method for the quantitation of microgram quantities of protein utilizing the principle of protein-dye binding. *Anal. Biochem.* 72, 248–254. doi: 10.1006/abio.1976.9999

Brosse, A., Korobeinikova, A., Gottesman, S., and Guillier, M. (2016). Unexpected properties of sRNA promoters allow feedback control via regulation of a two-component system. *Nucleic Acids Res.* 44, 9650–9666. doi: 10.1093/nar/gkw642

Bruckner, R., and Titgemeyer, F. (2002). Carbon catabolite repression in bacteria: choice of the carbon source and autoregulatory limitation of sugar utilization. *FEMS Microbiol. Lett.* 209, 141–148. doi: 10.1111/j.1574-6968.2002.tb11123.x

Colson, S., Stephan, J., Hertrich, T., Saito, A., van Wezel, G. P., Titgemeyer, F., et al. (2007). Conserved cis-acting elements upstream of genes composing the chitinolytic system of streptomycetes are DasR-responsive elements. *J. Mol. Microbiol. Biotechnol.* 12, 60–66. doi: 10.1159/000096460

D'Alia, D., Nieselt, K., Steigele, S., Müller, J., Verburg, I., and Takano, E. (2010). Noncoding RNA of glutamine synthetase I modulates antibiotic production in *Streptomyces coelicolor* A3(2). *J. Bacteriol.* 192, 1160–1164. doi: 10.1128/JB.01374-09

Delbaere, L. T., Sudom, A. M., Prasad, L., Leduc, Y., and Goldie, H. (2004). Structure/function studies of phosphoryl transfer by phosphoenolpyruvate carboxykinase. *Biochim. Biophys. Acta* 1697, 271–278. doi: 10.1016/j.bbapap.2003.11.030

Durica-Mitic, S., Göpel, Y., and Görke, B. (2018). Carbohydrate utilization in bacteria: making the most out of sugars with the help of small regulatory RNAs. *Microbiol. Spectr.* 6, 229–248. doi: 10.1128/microbiolspec.RWR-0013-2017

Flärdh, K., and Buttner, M. J. (2009). *Streptomyces* morphogenetics: dissecting differentiation in a filamentous bacterium. *Nat. Rev.* 7, 36–49. doi: 10.1038/nrmicro1968

Frohlich, K. S., Papenfort, K., Berger, A. A., and Vogel, J. (2012). A conserved RpoS-dependent small RNA controls the synthesis of major porin OmpD. *Nucleic Acids Res.* 40, 3623–3640. doi: 10.1093/nar/gkr1156

Guo, M. S., Updegrove, T. B., Gogol, E. B., Shabalina, S. A., Gross, C. A., and Storz, G. (2014). MicL, a new sigmaE-dependent sRNA, combats envelope stress by

repressing synthesis of Lpp, the major outer membrane lipoprotein. *Genes Dev.* 28, 1620–1634. doi: 10.1101/gad.243485.114

Hiard, S., Marée, R., Colson, S., Hoskisson, P. A., Titgemeyer, F., van Wezel, G. P., et al. (2007). PREDetector: a new tool to identify regulatory elements in bacterial genomes. *Biochem. Biophys. Res. Commun.* 357, 861–864. doi: 10.1016/j.bbrc.2007.03.180

Hindra, Moody, M. J., Jones, S. E., and Elliot, M. A. (2014). Complex intra-operonic dynamics mediated by a small RNA in *Streptomyces coelicolor*. *PLoS One* 9:e85856. doi: 10.1371/journal.pone.0085856

Horbal, L., Siegl, T., and Luzhetskyy, A. (2018). A set of synthetic versatile genetic control elements for the efficient expression of genes in *Actinobacteria*. *Nat. Publish. Group* 8, 491. doi: 10.1038/s41598-017-18846-1

Jeong, Y., Kim, J.-N., Kim, M. W., Bucca, G., Cho, S., Yoon, Y. J., et al. (2016). The dynamic transcriptional and translational landscape of the model antibiotic producer Streptomyces coelicolor A3(2). *Nat. Commun.* 7, 1–11. doi: 10.1038/ncomms11605

Kieser, T., Bibb, M. J., Buttner, M. J., Chater, K., and Hopwood, D. A. (2014). *Practical Streptomyces Genetics: A Laboratory Manual*. Norwich: NHBS.

Kim, K., Palmer, A. D., Vanderpool, C. K., and Slauch, J. M. (2019). The small RNA PinT contributes to PhoP-mediated regulation of the *Salmonella* pathogenicity island 1 type III secretion system in *Salmonella enterica Serovar typhimurium*. *J. Bacteriol.* 201, 312–319. doi: 10.1128/jb.00312-19

Kruger, J., and Rehmsmeier, M. (2006). RNAhybrid: microRNA target prediction easy, fast and flexible. *Nucleic Acids Res.* 34, W451–W454. doi: 10.1093/nar/gkl243

Kuhstoss, S., Richardson, M. A., and Rao, R. N. (1991). Plasmid cloning vectors that integrate site-specifically in *Streptomyces* spp. *Gene* 97, 143–146. doi: 10.1016/0378-1119(91)90022-4

Li, S., Wang, W., Li, X., Fan, K., and Yang, K. (2015). Genome-wide identification and characterization of reference genes with different transcript abundances for *Streptomyces coelicolor*. *Sci. Rep.* 5, 15840–15840. doi: 10.1038/srep15840

Moody, M. J., Young, R. A., Jones, S. E., and Elliot, M. A. (2013). Comparative analysis of non-coding RNAs in the antibiotic-producing *Streptomyces* bacteria. *BMC Genomics* 14:558. doi: 10.1186/1471-2164-14-558

Myronovskyi, M., Welle, E., Fedorenko, V., and Luzhetskyy, A. (2011). Beta-glucuronidase as a sensitive and versatile reporter in actinomycetes. *Appl. Environ. Microbiol.* 77, 5370–5383. doi: 10.1128/AEM.00434-11

Nazari, B., Kobayashi, M., Saito, A., Hassaninasab, A., Miyashita, K., and Fujii, T. (2013). Chitin-induced gene expression in secondary metabolic pathways of *Streptomyces coelicolor* A3(2) grown in soil. *Appl. Environ. Microbiol.* 79, 707–713. doi: 10.1128/AEM.02217-12

Nothaft, H., Dresel, D., Willimek, A., Mahr, K., Niederweis, M., and Titgemeyer, F. (2003). The phosphotransferase system of *Streptomyces coelicolor* is biased for N-acetylglucosamine metabolism. *J. Bacteriol.* 185, 7019–7023. doi: 10.1128/jb.185.23.7019-7023.2003

Pánek, J., Bobek, J., Mikulík, K., Basler, M., and Vohradský, J. (2008). Biocomputational prediction of small non-coding RNAs in *Streptomyces*. *BMC Genomics* 9:217. doi: 10.1186/1471-2164-9-217

Porcheron, G., Habib, R., Houle, S., Caza, M., Lepine, F., Daigle, F., et al. (2014). The small RNA RyhB contributes to siderophore production and virulence of uropathogenic *Escherichia coli*. *Infect. Immun.* 82, 5056–5068. doi: 10.1128/iai.02287-14

Rigali, S., Nothaft, H., Noens, E. E. E., Schlicht, M., Colson, S., Muller, M., et al. (2006). The sugar phosphotransferase system of *Streptomyces coelicolor* is regulated by the GntR-family regulator DasR and links N-acetylglucosamine metabolism to the control of development. *Mol. Microbiol.* 61, 1237–1251. doi: 10.1111/j.1365-2958.2006.05319.x

Rigali, S., Titgemeyer, F., Barends, S., Mulder, S., Thomae, A. W., Hopwood, D. A., et al. (2008). Feast or famine: the global regulator DasR links nutrient stress to antibiotic production by *Streptomyces*. *EMBO Rep.* 9, 670–675. doi: 10.1038/embor.2008.83

Rioseras, B., Shliaha, P. V., Gorshkov, V., Yagüe, P., López-García, M. T., Gonzalez-Quiñonez, N., et al. (2018). Quantitative proteome and phosphoproteome analyses of *Streptomyces coelicolor* reveal proteins and phosphoproteins modulating differentiation and secondary metabolism. *Mol. Cell. Proteomics* 17, 1591–1611. doi: 10.1074/mcp.RA117.000515

Rodríguez-García, A., Combes, P., Pérez-Redondo, R., Smith, M. C. A., and Smith, M. C. M. (2005). Natural and synthetic tetracycline-inducible promoters for use in the antibiotic-producing bacteria *Streptomyces*. *Nucleic Acids Res.* 33, e87–e87. doi: 10.1093/nar/gni086

Romby, P., and Wagner, E. G. H. (2012). Exploring the complex world of RNA regulation. *Biol. Cell* 100, e1–e3. doi: 10.1042/BC20070146

Rudolph, M. M., Vockenhuber, M. P., and Suess, B. (2015). Conditional control of gene expression by synthetic riboswitches in *Streptomyces coelicolor*. *Methods Enzymol.* 550, 283–299. doi: 10.1016/bs.mie.2014.10.036

Saramago, M., Barria, C., Dos Santos, R. F., Silva, I. J., Pobre, V., Domingues, S., et al. (2014). The role of RNases in the regulation of small RNAs. *Curr. Opin. Microbiol.* 18, 105–115. doi: 10.1016/j.mib.2014.02.009

Schlicht, M. (2003). *C-Regulation von Streptomyces coelicolor-Analyse des Proteoms von Mutanten der Regulation des Phosphotransferase Systems*. Bavaria: Friedrich-Alexander-Universität Erlangen-Nürnberg.

Setinova, D., Smidova, K., Pohl, P., Music, I., and Bobek, J. (2017). RNase III-binding-mRNAs revealed novel complementary transcripts in *Streptomyces*. *Front. Microbiol.* 8:2693. doi: 10.3389/fmicb.2017.02693

Sosinsky, A., Bonin, C. P., Mann, R. S., and Honig, B. (2003). Target explorer: an automated tool for the identification of new target genes for a specified set of transcription factors. *Nucleic Acids Res.* 31, 3589–3592. doi: 10.1093/nar/gkg544

St-Onge, R. J., and Elliot, M. A. (2017). Regulation of a muralytic enzyme-encoding gene by two non-coding RNAs. *RNA Biol.* 14, 1592–1605. doi: 10.1080/15476286.2017.1338241

Świątek-Połatyńska, M. A., Bucca, G., Laing, E., Gubbens, J., Titgemeyer, F., Smith, C. P., et al. (2015). Genome-wide analysis of in vivo binding of the master regulator DasR in *Streptomyces coelicolor* identifies novel non-canonical targets. *PLoS One* 10:e122479. doi: 10.1371/journal.pone.0122479

Swiercz, J. P., Hindra, Bobek, J., Haiser, H. J., Di Berardo, C., Tjaden, B., et al. (2008). Small non-coding RNAs in *Streptomyces coelicolor*. *Nucleic Acids Res.* 36, 7240–7251. doi: 10.1093/nar/gkn898

Vockenhuber, M. P., Heueis, N., and Suess, B. (2015). Identification of metE as a second target of the sRNA scr5239 in *Streptomyces coelicolor*. *PLoS One* 10:e0120147. doi: 10.1371/journal.pone.0120147

Vockenhuber, M. P., Sharma, C. M., Statt, M. G., Schmidt, D., Xu, Z., Dietrich, S., et al. (2011). Deep sequencing-based identification of small non-coding RNAs in *Streptomyces coelicolor*. *RNA Biol.* 8, 468–477. doi: 10.4161/rna.8.3.14421

Vockenhuber, M. P., and Suess, B. (2012). Streptomyces coelicolor sRNA scr5239 inhibits agarase expression by direct base pairing to the dagA coding region. *Microbiology* 158(Pt 2), 424–435. doi: 10.1099/mic.0.054205-0

Wagner, E. G. H., and Romby, P. (2015). Small RNAs in bacteria and archaea: who they are, what they do, and how they do it. *Adv. Genet.* 90, 133–208. doi: 10.1016/bs.adgen.2015.05.001

Wisniewski, J. R., Zougman, A., Nagaraj, N., and Mann, M. (2009). Universal sample preparation method for proteome analysis. *Nat. Methods* 6, 359–362. doi: 10.1038/nmeth.1322

Conflict of Interest: The authors declare that the research was conducted in the absence of any commercial or financial relationships that could be construed as a potential conflict of interest.

frontiers in Microbiology

ORIGINAL RESEARCH
published: 24 January 2020
doi: 10.3389/fmicb.2020.00019

Stimulated Biosynthesis of an C10-Deoxy Heptaene NPP B2 *via* Regulatory Genes Overexpression in *Pseudonocardia autotrophica*

*Heung-Soon Park, Hye-Jin Kim, Chi-Young Han, Hee-Ju Nah, Si-Sun Choi and Eung-Soo Kim**

Department of Biological Engineering, Inha University, Incheon, South Korea

Polyene macrolides, such as nystatin A1, amphotericin B, and NPP A1, belong to a large family of valuable antifungal polyketide compounds that are typically produced by soil actinomycetes. Previously, NPP B1, a novel NPP A1 derivative harboring a heptaene core structure, was generated by introducing two amino acid substitutions in the putative NADPH-binding motif of the enoyl reductase domain in module 5 of the NPP A1 polyketide synthase in *Pseudonocardia autotrophica*. This derivative showed superior antifungal activity to NPP A1. In this study, another novel derivative called NPP B2 was developed, which lacks a hydroxyl group at the C10 position by site-specific gene disruption of the P450 hydroxylase NppL. To stimulate the extremely low expression of the NPP B2 biosynthetic pathway genes, the 32-kb NPP-specific regulatory gene cluster was overexpressed *via* site-specific chromosomal integration. The extra copy of the six NPP-specific regulatory genes led to a significant increase in the NPP B2 yield from 0.19 to 7.67 mg/L, which is the highest level of NPP B2 production ever achieved by the *P. autotrophica* strain. Subsequent *in vitro* antifungal activity and toxicity studies indicated that NPP B2 exhibited similar antifungal activity but significantly lower hemolytic toxicity than NPP B1. These results suggest that an NPP biosynthetic pathway refactoring and overexpression of its pathway-specific regulatory genes is an efficient approach to stimulating the production of an extremely low-level metabolite, such as NPP B2 in a pathway-engineered rare actinomycete strain.

Keywords: ***Pseudonocardia autotrophica*, polyene, regulatory genes, hemolytic toxicity, antifungal activity**

OPEN ACCESS

Edited by:
Yinhua Lu,
Shanghai Normal University, China

Reviewed by:
Patrick Caffrey,
University College Dublin, Ireland
Haoxin Wang,
Shandong University, China

***Correspondence:**
Eung-Soo Kim
eungsoo@inha.ac.kr

Specialty section:
This article was submitted to Microbial Physiology and Metabolism, a section of the journal Frontiers in Microbiology

Received: *30 October 2019*
Accepted: *07 January 2020*
Published: *24 January 2020*

Citation:
Park H-S, Kim H-J, Han C-Y, Nah H-J, Choi S-S and Kim E-S (2020) Stimulated Biosynthesis of an C10-Deoxy Heptaene NPP B2 via Regulatory Genes Overexpression in Pseudonocardia autotrophica. Front. Microbiol. 11:19. doi: 10.3389/fmicb.2020.00019

INTRODUCTION

More than 45% of the bioactive compounds discovered from microbial secondary metabolites are derived from actinomycetes (Bu et al., 2019). A significant number of these secondary metabolites produced by actinomycetes were utilized further as the lead compounds in the field of medicine as clinically important anticancer, antibiotic, anti-inflammatory, antiviral, antiparasitic, and antioxidant drugs (Bérdy, 2005; Subramani and Aalbersberg, 2012; Manivasagan et al., 2014; Abdelmohsen et al., 2015). Among them are polyene macrolide antibiotics, such as nystatin,

amphotericin, candicidin, and pimaricin, which are potent antifungal compounds that are comprised typically of a polyketide core macrolactone ring with about 20–40 carbon atoms, including 3–8 conjugated double bonds (**Figure 1**; Caffrey et al., 2016). The major antifungal mechanism of these polyene antibiotics is believed to be the formation of ion channels *via* fungal ergosterol binding that mediates the leakage of cellular K^+ and Mg^{2+}, which leads to the death of fungal cells (Bolard, 1986; Neumann et al., 2016).

Over the last several decades, complete polyene biosynthetic gene clusters from nystatin, amphotericin, pimaricin, and candicidin have been isolated and characterized (Aparicio et al., 1999, 2003; Zotchev et al., 2000; Caffrey et al., 2001). Polyene compounds are biosynthesized typically by a giant enzyme complex called polyketide synthase (PKS), followed by further modification of the core macrolide ring by post-PKS modification enzymes, including P450 hydroxylases and glycosyltransferases (Kim et al., 2015). Subsequent attempts to generate a range of derivatives of these antifungal polyene macrolides were pursued to enhance the antifungal activity and/or reduce their intrinsic toxicities through both semisynthetic and biosynthetic pathway refactoring approaches (Byrne et al., 2003; Nedal et al., 2007; Silveira and Husain, 2007; Caffrey et al., 2016). A heptaene version of nystatin A1 called S44HP displayed considerably higher antifungal activity than the original tetraene nystatin A1, which is comparable to that of amphotericin B (Bruheim et al., 2004). Mannosyl-8-deoxy-amphotericins produced by inactivation of the *amphL* gene and introduction of the pIJ02567-*nypY* construct in *Streptomyces nodosus* exhibited lower hemolytic toxicity (Walmsley et al., 2017). In addition, highly water-soluble amphotericin B analogues were produced by the addition of extra sugar residues to amphotericin B (Caffrey et al., 2016). Recently, the discovery of C35deOAmB revealed that the antifungal activity was critical for binding to ergosterol, not for ion-channel formation (Gray et al., 2012), which generated toxicity-reduced amphotericin B derivatives (Cioffi et al., 2015; Muraglia et al., 2019). Overall, the engineering of polyene PKS to change the number of conjugated double bonds as well as post-PKS modifications for manipulation of the sugar and hydroxyl moieties is considered an important strategy for the generation of pharmacokinetically improved novel polyene derivatives (Bruheim et al., 2004; Gray et al., 2012; Caffrey et al., 2016; Walmsley et al., 2017; Muraglia et al., 2019).

NPP A1 is a disaccharide-containing polyene antifungal compound produced by a rare actinomycete, *Pseudonocardia autotrophica*, with an identical core macrolactone structure to nystatin A1 except for an additional *N*-acetyl-glucosamine (**Figure 1**; Lee et al., 2012). In the NPP A1 biosynthesis process, the macrolide backbone is synthesized by six type I PKSs, and the unique di-sugar moiety, mycosaminyl-(α1-4)-*N*-acetyl-glucosamine, is then attached by two glycosyltransferases-encoding *nppDI* and *nppY* and finally hydroxylated by P450 hydroxylase-encoding *nppL* (Kim et al., 2015). In terms of the biological activities, this polyene has superior water solubility and reduced hemolytic toxicity but shows slightly lower antifungal activity than nystatin A1 (Lee et al., 2012). Elucidation of the post-PKS modification steps of NPP A1 biosynthesis in

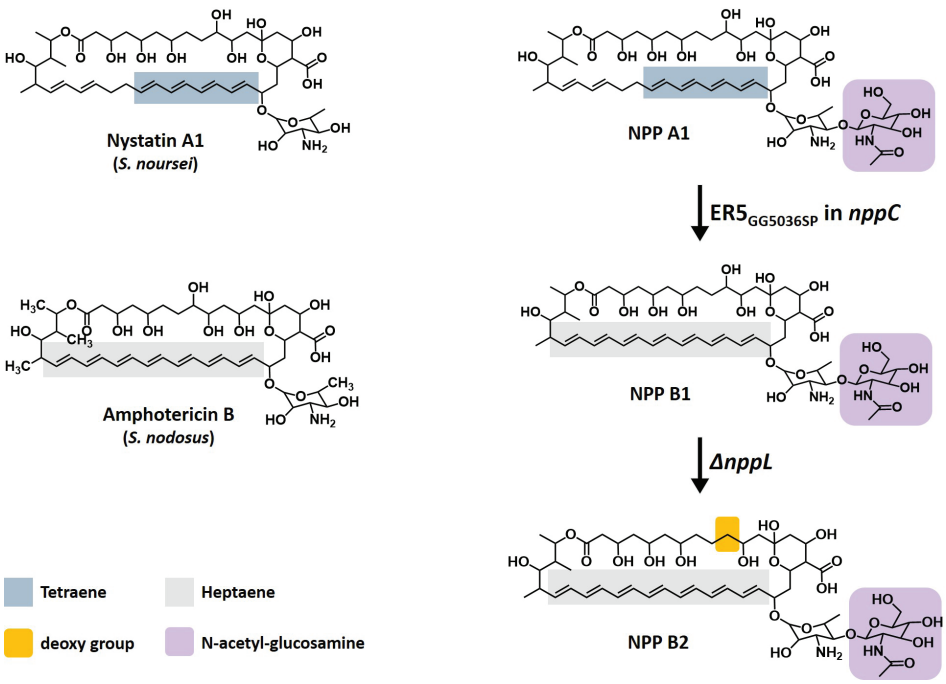

FIGURE 1 | Structure of polyene macrolides. **Nystatin A1**, a typical tetraene polyene macrolide produced by *Streptomyces noursei*. **Amphotericin B**, the most potent polyene macrolide produced by *Streptomyces nodosus*. **Nystatin-like Pseudonocardia polyene (NPP) A1**, a disaccharide-containing tetraene polyene macrolide produced by *Pseudonocardia autotrophica*. **NPP B1**, a disaccharide-containing heptaene polyene macrolide produced by *P. autotrophica* ER5 $_{GG5036SP}$ mutant. **NPP B2**, C10-deoxy NPP B1 produced by inactivation of the *nppL* gene in *P. autotrophica* ER5 $_{GG5036SP}$ mutant.

P. autotrophica highlighted the potential to develop novel NPP A1 derivatives (Kim et al., 2015). Several studies were conducted to develop NPP A1 derivatives to enhance the antifungal activity, resulting in two analogues, NPP A2 and NPP B1. NPP A2 lacks a C10 hydroxyl group that was generated by the inactivation of the P450 hydroxylase-encoding *nppL* gene in *P. autotrophica* (Kim et al., 2016). NPP B1 was generated by changing its core macrolactone structure from tetraene to heptaene through site-specific, two amino acid substitutions in the putative NADPH-binding motif of the enoyl reductase domain in module 5 of the NPP A1 polyketide synthase NppC (**Figure 1**; Kim et al., 2018). Interestingly, both NPP A2 and NPP B1 exhibited higher antifungal activities than those of NPP A1.

In this study, another NPP A1 analogue called NPP B2 was developed, which was generated by the inactivation of the polyketide enoyl reductase (ER) domain in the fifth module as well as the P450 hydroxylase-encoding *nppL* gene in the NPP A1 producing *P. autotrophica* strain (**Figure 1**). To overcome the extremely low level of NPP B2 production because of its pathway refactoring, the 32-kb NPP-specific regulatory gene cluster was overexpressed in the NPP B2 production strain, followed by isolation and characterization of the biological activities of NPP B2.

MATERIALS AND METHODS

Strains and Growth Conditions

P. autotrophica KCTC9441 purchased from the Korean Collection for Type Cultures was used for NPP production. The strain was grown routinely in ISP2 agar (malt extract 10 g, yeast extract 4 g, glucose 4 g, and agar 20 g/L) at 28°C for the sporulation and seed culture. YEME medium (yeast extract 3 g, peptone 5 g, malt extract 3 g, glucose 10 g, sucrose 340 g/L, and 5 mM $MgCl_2$) was used to produce the NPP derivatives (Lee et al., 2012). *Candida albicans* ATCC 14053 was grown on YM medium (dextrose 10 g, peptone 5 g, yeast extract 3 g, Malt extract 3 g, and agar 20 g/L) at 30°C for 24 h. All *Escherichia coli* strains were incubated at 37°C in Luria-Bertani medium supplemented with the appropriate antibiotics where needed.

Inactivation of NppL and Overexpression of NPP-Specific Regulatory Gene Cluster

A *nppL* gene inactivation cassette, including the upstream and downstream regions, was constructed by PCR amplification using the following primer pairs: upstream region, DELL_1F (5′-GAATTCCGTCCTGTACTCGTCGGT-3′) and DELL_1R (5′-CTGCAGTCA TGACGCGTCCTCCGT-3′) and downstream region, DELL_2F (5′-CTGCAGAC GCGGTCACGATGGCGC-3′) and DELL_2R (5′-AAGCTTACCTGGCCGAGCAGATGG-3′) (Kim et al., 2015). The amplified fragments were digested with *Hind*III-*Eco*RI and ligated into pKC1132. The recombinants were selected on LB medium containing apramycin. The *nppL* gene-inactivation plasmid was introduced into the chromosome of the NPP B1 production strain, *P. autotrophica* ER5 mutant.

To overexpress the NPP-specific regulatory genes, the previously constructed pNPPREG, encompassing the 32-kb NPP-specific regulatory gene cluster, was integrated into the chromosome of the B2 production strain (Han et al., 2019). The recombination conjugants were selected on ISP2 medium containing apramycin.

Production and Purification of NPP Derivatives

NPP or its derivative production strains were inoculated in 300 ml of ISP2 medium containing the appropriate antibiotics at 30°C and 220 rpm for 72 h. The pre-cultures were added to 3 L YEME medium in a 5 L bioreactor for batch fermentation. After 48 h of cultivation, 150 g of Amberlite XAD16 resin (Sigma-Aldrich, USA) was added to the culture broth. After 24 h of resin addition, the mycelia and resin from the culture broth were separated and then extracted twice in 600 ml of *n*-butanol. The extract was concentrated using a vacuum evaporator, after which the concentrated extract was dissolved in methanol and loaded onto a column packed with a C18 reversed-phase silica gel (Daiso, Japan) along with methanol-water (30:70, v/v) to remove any residual sugar from the production media. The extracts with sugar removed were purified using a fraction collector (Interchim, France) on a gradient consisted of solvents A (water) and B (methanol): 30% B (v/v) (0–10 min) and 100% B (v/v) (100 min) at a flow rate of 20 ml/min. The fractions containing NPP or its derivatives with >80% purity were detected at 405 nm and analyzed by high performance liquid chromatography (HPLC). The column was equilibrated with 50% solvent A (0.05 M ammonium acetate, pH 6.5) and 50% solvent B (methanol); the flow rate was set to 1.0 ml/min using the following conditions: 0–3 min, 50–75% B; 3–30 min, 75–100% B; 30–33 min, 100–50% B; and 33–40 min, 50% B (Won et al., 2017).

Liquid Chromatography-Mass Spectrometry/Mass Spectrometry Analysis

NPP B2 showing >80% purity was analyzed using A Triple TOF 5600 + (AB Sciex, USA) coupled with Ultimate3000 (Thermo Scientific, USA). Mass spectrometry was operated in both positive and negative ion modes over a mass range from 50 to 2,000 *m*/*z* using an electrospray ionization source. The settings were nitrogen gas for nebulization at 50 psi, heater gas pressure at 50 psi, curtain gas at 25 psi, temperature of 500°C, and an ion spray voltage at 5,500 V in positive ion mode and −4,500 V in negative ion mode. The optimized declustering potential (DP) and collision energy (CE) were set to 60 and 10 eV in positive ion mode, and to −60 and −10 eV in negative ion mode, respectively. A sweeping collision energy setting at 35/−35 ± 15 eV was applied for collision-induced dissociation (CID). Chromatographic conditions: solution A (0.1% formic acid in distilled water) and solution B (0.1% formic acid in acetonitrile) were used for elution and loaded onto Phenomenex Kinetex 1.7 μ C18 (2.1 mm × 150 mm, 1.7 μm). The flow rate was set to 0.4 ml/min using the following conditions: 0–1 min, 90% A; 1–5 min, 90–50%

A; 5–18 min, 50–0% A; 18–25 min, 0% A; 25–27 min, 0–90% A; and 27–30 min, 90% A.

RNA Analysis by Quantitative Real-Time Polymerase Chain Reaction

RNA was prepared using the RNeasy Mini Kit (Qiagen, Germany). cDNA conversion was carried out using a PrimeScript 1ST strand cDNA Synthesis Kit (TaKaRa, Japan) according to the manufacturer's instructions. Real-time PCR was performed using TaKaRa SYBR Premix Ex Taq (Perfect Real Time) with a Thermal Cycler Dice Real Time System Single (code TP850; TaKaRa, Japan). **Supplementary Table S1** lists the primer pairs. The PCR conditions included activation for 10 min at 95°C, followed by 35 cycles of 30 s at 95°C, 30 s at 58°C, and 30 s at 72°C. The data were collected during each 72°C step, and melting curve analysis was performed at default settings ranging from 60 to 95°C. The relative level of amplified mRNA was normalized to the mRNA expression level of the housekeeping gene, *P. autotrophica hrdB*, which was amplified as an internal control using the primer pairs *hrdB*_F (5′-GCGGTGGAGA AGTTCGACTA-3′) and *hrdB*_R (5′-TTGATGACCTCGACCATGTG-3′) (Han et al., 2019).

In vitro Assays for Biological Activities

For *in vitro* antifungal assay, we adapted to the Clinical and Laboratory Standards Institute document M27-A3 (Wayne, 2008). After *C. albicans* was cultured in YM medium at 30°C for 24 h, the cultured solution was diluted with YM medium until the OD value is 0.3 at 530 nm. A working suspension was made by a 1:2,000 dilution with RPMI-1640 broth media (with glutamine and phenol red, without bicarbonate, Sigma-Aldrich, USA), which resulted in 5.0×10^2 to 2.5×10^3 cells per μl. Ten microliters of the DMSO containing polyene antibiotics at various concentrations (3.125–1600 μg/ml) were added to the working suspension of 990 μl, and then, the mixtures were incubated at 30°C without shaking for 48 h. The colorimetric change of the mixture from red to yellow indicated the growth of *C. albicans*. The minimum inhibitory concentration (MIC) values were determined by measuring the minimum concentration that changed color to yellow. The experiment was performed in the duplicate.

For *in vitro* hemolysis assay, we adapted from a previously reported method (Nedal et al., 2007). Briefly, defibrinated horse blood was purchased from Kisan Biotech (South Korea). The polyene compounds were then prepared to the following concentrations with DMSO: 1–200 μg/ml. A 50 μl of each polyene solution was added to 450 μl of 2.5% defibrinated horse blood buffered with RBC buffer (10 mM NaH_2PO_4, 150 mM NaCl, 1 mM $MgCl_2$, and pH 7.4), which resulted in a 1:10 dilution of each concentration of polyene. The samples were then incubated at 37°C for 30 min. After incubation, the samples were centrifuged at 10,000 ×*g* for 2 min. Next, 100 μl of the supernatant from each sample was added to a 96-well plate, after which the absorbance was read at 540 nm using a microplate reader (TECAN, Switzerland). The percentage hemolysis of each sample was defined as $(Abs_{sample} - Abs_{negative}/Abs_{positive} - Abs_{negative}) \times 100$ (%) to calculate the minimum hemolysis concentration (MHC). The positive hemolysis sample was prepared by adding defibrinated horse blood 11.25 μl and DMSO 50 μl to distilled water 438.75 μl, and the negative hemolysis sample was prepared by adding defibrinated horse blood 11.25 μl and DMSO 50 μl to RBC buffer 438.75 μl.

RESULTS

Construction of the NPP B2 Production Strain

An *in vitro* antifungal assay confirmed that the NPP B1, a heptaene version of NPP A1, showed much higher antifungal activity than the tetraene NPP A1 (Kim et al., 2018). Therefore, we tried to generate pharmacokinetically improved heptaene NPP B1 derivative through the engineering of post-PKS modification. Based on the previous results that characterization of the P450 hydroxylases, which were a region-specific hydroxylation such as AmphL (amphotericin), NysL (nystatin), and NppL (NPP) (Byrne et al., 2003; Volokhan et al., 2006; Kim et al., 2016), the NPP B1 production strain was engineered by inactivation of the *nppL* gene, which was involved in NPP C10 region-specific hydroxylation (**Figures 2A,B; Supplementary Figure S1**). Inactivation of the *nppL* gene was performed successfully by homologous recombination using the pKC1132 *Streptomyces* suicide vector system, and the mutation was verified genetically by PCR product sequencing analysis (**Figure 2C; Supplementary Figure S2**). LC-MS analysis of purified NPP B2 contained a signal at *m*/*z* 1111.5807 for $[C_{53}H_{85}N_2O_{22}]^+$ (calculated mass of NPP B2 is 1110.57) confirming that NPP B2 had been produced, as expected in the constructed mutant strain (**Supplementary Figure S3**).

Stimulation of NPP B2 Production Through Overexpression of the NPP Pathway-Specific Regulatory Genes

Although the NPP B2 production strain was developed successfully by inactivation of the ER domain of module 5 followed by the P450 hydroxylase-encoding *nppL* gene from the NPP A1 production strain, the NPP B2 production level was reduced approximately 40-fold to 0.2 mg/L compared to the NPP A1 production level in the *P. autotrophica* wild type. Among the attempts to increase the production of NPP derivatives, a strategy was conducted to increase the production level of NPP B2 through overexpression of the NPP pathway-specific regulatory genes. In previous studies, pNPPREG was constructed by cloning a 32-kb right-hand portion of BGC containing the six NPP-specific regulatory genes (*nppRI–nppRVI*) into a *Streptomyces* artificial chromosomal vector pSBAC (Han et al., 2019). To stimulate NPP B2 production, pNPPREG containing the entire regulatory genes was integrated into the chromosome of the NPP B2 production strain (**Figure 3A**). As a result, the level of NPP B2 production was increased significantly (approximately 39-fold to 7.67 mg/L) (**Figure 3B**).

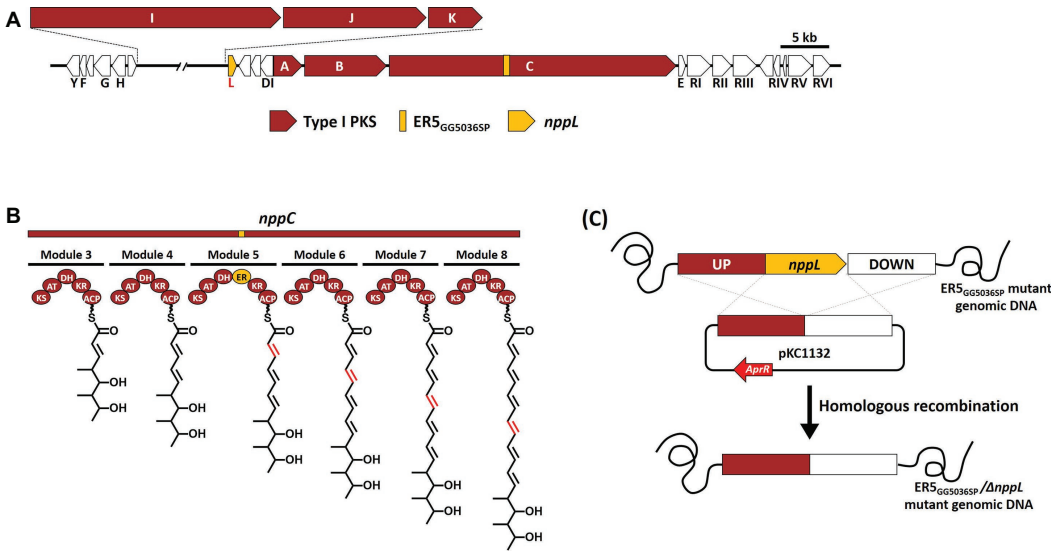

FIGURE 2 | (A) Development of NPP B2 production strains in *P. autotrophica*. **(B)** Organization of modular polyketide synthases involved in mutated NppC by inactivation of enoyl reductase domain in module 5 (ER5). ACP, acyl carrier protein; AT, acyl-transferase; KS, ketosynthase; KR, ketoreductase; DH, dehydratase; ER, enoyl reductase. **(C)** Inactivation scheme of *nppL* gene in NPP B1 production strain (ER5 domain mutant).

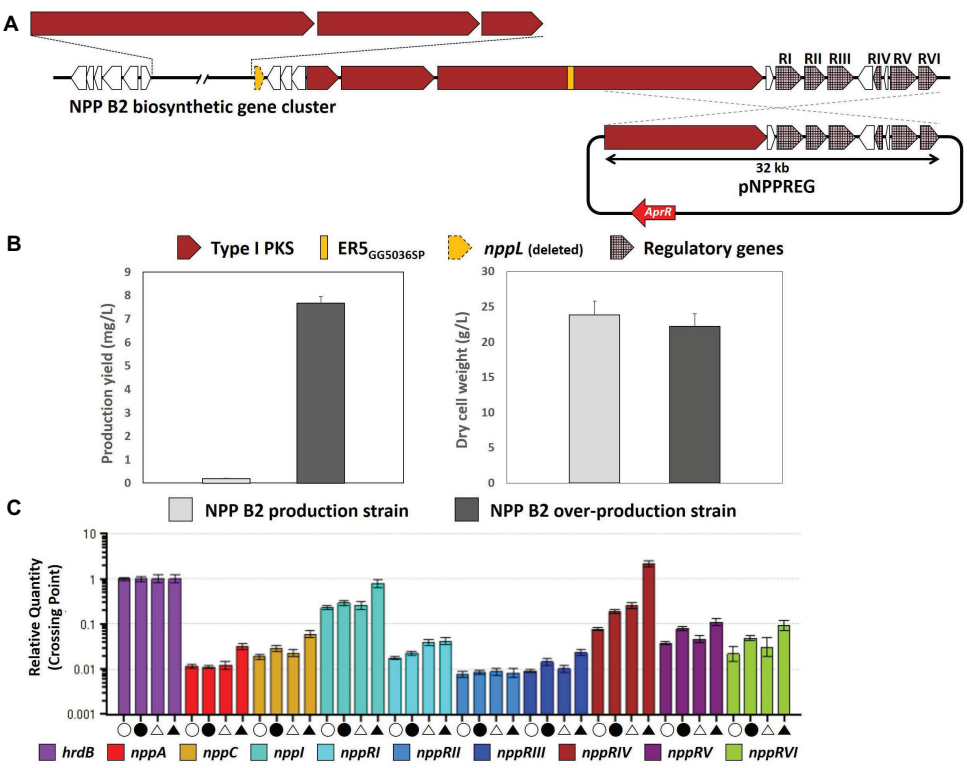

FIGURE 3 | (A) Overexpression scheme of NPP-specific regulatory gene cluster in NPP B2 production strain. **(B)** Comparison of NPP B2 production yields with newly constructed NPP B2 over-production strain after 72 h culture. **(C)** Transcript analysis of NPP B2 production strains by qRT-PCR. Open circle, transcripts from the NPP B2 production strain at 24 h; closed circle, transcripts from the NPP B2 production strain at 48 h; open triangle, transcripts from the NPP B2 over-production mutant at 24 h; closed triangle, transcripts from the NPP B2 over-production mutant at 48 h; house-keeping gene, *hrdB* (light purple); PKS genes, *nppA* (red), *nppC* (yellow), and *nppI* (emerald green); regulatory genes related to NPP B2 biosynthesis, *nppRI* (sky blue), *nppRII* (blue), *nppRIII* (dark blue), *nppRIV* (brown), *nppRV* (dark purple), and *nppRVI* (light green). All transcript measurements were performed in duplicate.

The transcription levels of the NPP B2 biosynthetic genes were analyzed to further understand the molecular basis responsible for enhanced NPP B2 production in the engineered NPP B2 over-production strain. qRT-PCR analysis revealed increased transcription of the PKS genes, such as *nppA* and *nppC*, in the NPP B2 over-production strain compared to the parental strain (**Figure 3C**). As expected, the transcription levels of all five NPP-pathway specific regulatory genes, except *nppRII,* were also stimulated (**Figure 3C**), suggesting that the enhanced transcription level of the refactored NPP B2 biosynthetic pathway genes is critical for the titer improvement.

In vitro Antifungal Activity and Hemolytic Toxicity

Based on successful NPP B2 yield improvement, the purified NPP B2 was evaluated for both *in vitro* antifungal activity and the hemolytic toxicity. Minimum inhibitory concentration (MIC) evaluation assays of *in vitro* antifungal activity using the colorimetric change in the RPMI-1640 media containing *C. albicans* were employed (Wayne, 2008). The MIC value of NPP B2 against *C. albicans* (1.0 μg/ml) was slightly higher than amphotericin B (0.25 μg/ml) and NPP B1 (0.5 μg/ml) (**Table 1; Supplementary Figure S4**). Interestingly, however, *in vitro* hemolytic toxicity evaluation, NPP B2 exhibited much reduced hemolytic toxicity than its parental NPP B1. The minimum hemolytic concentration (MHC) value for NPP B2 was measured as 80.18 μg/ml, whereas the MHC value of amphotericin B was 3.26 μg/ml under the conditions tested, indicating that the *in vitro* toxicity of NPP B2 was approximately 25-fold lower than that of amphotericin B (**Table 1; Supplementary Figure S5**). Moreover, the *in vitro* toxicity was 4.5-fold lower than the MHC value of NPP B1 (17.72 μg/ml). These results suggest that the absence of the hydroxyl moiety at the C10 position of NPP B2 could play an important role in controlling both antifungal acidity and hemolytic toxicity.

DISCUSSION

The genome mining approach of rare actinomycetes followed by the activation of its cryptic biosynthetic gene cluster (BGC) has become an attractive strategy to screen and develop novel bioactive compounds (Choi et al., 2018). The *P. autotrophica* strain described here was classified originally as a polyene non-production strain, which was later proven to be a producer of a novel di-saccharide-containing NPP A1 through culture optimization and whole genome sequencing (Lee et al., 2012). Although an NPP A1 BGC refactoring strategy generated a C10-deoxy NPP A1 (named NPP A2) and a heptaene version of NPP A1 (named NPP B1), their extremely low titers were major hurdles for further characterization of their biological activities.

Previously, several strategies, including overexpression of the pathway-specific regulatory gene, deletion of the global antibiotic downregulator, *in situ* screening of random mutants, co-culture system, and cultivation with xenobiotics, all failed to improve NPP B1 production (Kim et al., 2018). Recently, the entire cluster containing all six NPP pathway-specific genes in a pSBAC system followed by its re-integration into the *P. autotrophica* chromosome led to a significant increase in the NPP B1 titer (Han et al., 2019).

In this study, another novel derivative, called the NPP B2 production strain, was first generated by site-specific inactivation of the *nppL* gene in the NPP B1 production of the *P. autotrophica* mutant strain. C10-deoxy NPP B1 (NPP B2) was also generated based on a previous report that the C8-deoxy amphotericin produced by the inactivation of *amphL* in *S. nodosus* and C10-deoxy nystatin by the inactivation of *nysL* in *Streptomyces noursei* (Byrne et al., 2003; Volokhan et al., 2006). Owing to the extremely low titer of NPP B2, however, its biological characterization could not be pursued without strain improvement. Through the chromosomal integration of all six NPP pathway-specific genes in the NPP B2 production strain, its titer was improved significantly (approximately 39-fold), which was sufficient to proceed for further biological assays, including antifungal and hemolytic toxicity assays.

This paper described for the first time the *in vitro* biological activities of NPP B2, a novel heptaene version of the NPP derivative. Although the *in vitro* antifungal activity of NPP B2 was higher than that of tetraene-type polyenes, such as nystatin A1, NPP A1, and A2, it showed slightly lower antifungal activity than other heptaene-type polyenes, including amphotericin B and NPP B1. Interestingly, the *in vitro* hemolytic activity of NPP B2 was approximately 25 times lower than those of amphotericin B and NPP B1, suggesting that the hydroxyl moiety at the C10 position of NPP could play a critical role in controlling both the antifungal activity and the hemolytic toxicity, probably by affecting its binding affinity to cholesterol and ergosterol. Overall, these results suggest that the combination of rational BGC refactoring and its genetic strain improvement approach is an efficient strategy to stimulate the production of an extremely low-level metabolite, such as NPP B2 in a rare actinomycetes strain.

TABLE 1 | *In vitro* antifungal activity and toxicity of polyene macrolides.

	Amphotericin B	NPP B1	NPP B2
Antifungal activity (MIC, μg/ml)[a]			
Candida albicans ATCC 14053	0.25	0.5	1.0
Hemolytic toxicity (MHC, μg/ml)[b]			
	3.26 ± 0.259	17.71 ± 1.235 (5.4-fold)	80.18 ± 1.168 (25-fold)

[a]*MIC, minimum inhibitory concentration (values resulting in no visible growth of C. albicans).*
[b]*MHC, minimum hemolytic concentration (values causing 90% hemolysis against horse blood cells ± percentage standard deviation).*

DATA AVAILABILITY STATEMENT

The datasets generated for this study can be found in the EU108007.

AUTHOR CONTRIBUTIONS

H-SP, S-SC, and E-SK designed the experiments. H-SP, H-JK, and C-YH performed the experiments. H-SP, H-JN, and E-SK wrote the manuscript.

FUNDING

This study was supported by Agricultural Microbiome R&D Program, Ministry of Agriculture, Food and Rural Affairs, Republic of Korea [as part of the (multi-ministerial) Genome Technology to Business Translation Program] No. 918008-04. This work was also funded by National Research Foundation of Korea (NRF) (Project No. NRF-2017R1A2A2A05069859).

SUPPLEMENTARY MATERIAL

The Supplementary Material for this article can be found online at: https://www.frontiersin.org/articles/10.3389/fmicb.2020.00019/full#supplementary-material

REFERENCES

Abdelmohsen, U. R., Grkovic, T., Balasubramanian, S., Kamel, M. S., Quinn, R. J., and Hentschel, U. (2015). Elicitation of secondary metabolism in actinomycetes. *Biotechnol. Adv.* 33, 798–811. doi: 10.1016/j.biotechadv.2015.06.003

Aparicio, J. F., Caffrey, P., Gil, J. A., and Zotchev, S. B. (2003). Polyene antibiotic biosynthesis gene clusters. *Appl. Microbiol. Biotechnol.* 61, 179–188. doi: 10.1007/s00253-002-1183-5

Aparicio, J. F., Colina, A. J., Ceballos, E., and Martín, J. F. (1999). The biosynthetic gene cluster for the 26-membered ring polyene macrolide pimaricin. *J. Biol. Chem.* 274, 10133–10139. doi: 10.1074/jbc.274.15.10133

Bérdy, J. (2005). Bioactive microbial metabolites: a personal view. *J. Antibiot.* 58, 1–26. doi: 10.1038/ja.2005.1

Bolard, J. (1986). How do the polyene macrolide antibiotics affect the cellular membrane properties? *Biochim. Biophys. Acta Rev. Biomembr.* 864, 257–304. doi: 10.1016/0304-4157(86)90002-X

Bruheim, P., Borgos, S. E., Tsan, P., Sellta, H., Ellingsen, T. E., Lancelin, J. M., et al. (2004). Chemical diversity of polyene macrolides produced by *Streptomyces noursei* ATCC11455 and recombinant strain ERD44 with genetically altered polyketide synthase NysC. *Antimicrob. Agents Chemother.* 48, 4120–4129. doi: 10.1128/AAC.48.11.4120-4129.2004

Bu, Q. T., Yu, P., Wang, J., Li, Z. Y., Chen, X. A., and Mao, X. M. (2019). Rational construction of genome-reduced and high-efficient industrial *Streptomyces chassis* based on multiple comparative genomic approaches. *Microb. Cell Factories* 18:16. doi: 10.1186/s12934-019-1055-7

Byrne, B., Carmody, M., Gibson, E., Rawlings, B., and Caffrey, P. (2003). Biosynthesis of deoxyamphotericins and deoxyamphoteronolides by engineered strains of *Streptomyces nodosus*. *Chem. Biol.* 10, 1215–1224. doi: 10.1016/j.chembiol.2003.12.001

Caffrey, P., De Poire, E., Sheehan, J., and Sweeney, P. (2016). Polyene macrolide biosynthesis in streptomycetes and related bacteria: recent advances from genome sequencing and experimental studies. *Appl. Microbiol. Biotechnol.* 100, 3893–3908. doi: 10.1007/s00253-016-7474-z

Caffrey, P., Lynch, S., Flood, E., Finnan, S., and Oliynyk, M. (2001). Amphotericin biosynthesis in *Streptomyces nodosus* deductions from analysis of polyketide synthase and late genes. *Chem. Biol.* 8, 713–723. doi: 10.1016/S1074-5521(01)00046-1

Choi, S. S., Katsuyama, Y., Bai, L., Deng, Z., Ohnishi, Y., and Kim, E. S. (2018). Genome engineering for microbial natural product discovery. *Curr. Opin. Microbiol.* 45, 53–60. doi: 10.1016/j.mib.2018.02.007

Cioffi, A. G., Hou, J., Grillo, A. S., Diaz, K. A., and Burke, M. D. (2015). Restored physiology in protein-deficient yeast by a small molecule channel. *J. Am. Chem. Soc.* 137, 10096–10099. doi: 10.1021/jacs.5b05765

Gray, K. C., Palacios, D. S., Dailey, I., Endo, M. M., Uno, B. E., Wilcock, B. C., et al. (2012). Amphotericin primarily kills yeast by simply binding ergosterol. *Proc. Natl. Acad. Sci. USA* 109, 2234–2239. doi: 10.1073/pnas.1117280109

Han, C. Y., Jang, J. Y., Kim, H. J., Choi, S. S., and Kim, E. S. (2019). Pseudonocardia strain improvement for stimulation of the di-sugar heptaene Nystatin-like Pseudonocardia polyene B1 biosynthesis. *J. Ind. Microbiol. Biotechnol.* 46, 649–655. doi: 10.1007/s10295-019-02149-7

Kim, H. J., Han, C. Y., Park, J. S., Oh, S. H., Kang, S. H., Choi, S. S., et al. (2018). Nystatin-like Pseudonocardia polyene B1, a novel disaccharide-containing antifungal heptaene antibiotic. *Sci. Rep.* 8:13584. doi: 10.1038/s41598-018-31801-y

Kim, H. J., Kim, M. K., Lee, M. J., Won, H. J., Choi, S. S., and Kim, E. S. (2015). Post-PKS tailoring steps of a disaccharide-containing polyene NPP in *Pseudonocardia autotrophica*. *PLoS One* 7:10. doi: 10.1371/journal.pone.0123270

Kim, M. K., Won, H. J., Kim, H. J., Choi, S. S., Lee, H. S., Kim, P., et al. (2016). Carboxyl-terminal domain characterization of polyene specific P450 hydroxylase in *Pseudonocardia autotrophica*. *J. Ind. Microbiol. Biotechnol.* 43, 1625–1630. doi: 10.1007/s10295-016-1813-z

Lee, M. J., Kong, D., Han, K., Sherman, D. H., Bai, L., Deng, Z., et al. (2012). Structural analysis and biosynthetic engineering of a solubility-improved and less-hemolytic nystatin-like polyene in *Pseudonocardia autotrophica*. *Appl. Microbiol. Biotechnol.* 95, 157–168. doi: 10.1007/s00253-012-3955-x

Manivasagan, P., Venkatesan, J., Sivakumar, K., and Kim, S. K. (2014). Pharmaceutically active secondary metabolites of marine actinobacteria. *Microbiol. Res.* 169, 262–278. doi: 10.1016/j.micres.2013.07.014

Muraglia, K. A., Chorghade, R. S., Kim, B. R., Tang, X. X., Shah, V. S., Grillo, A. S., et al. (2019). Small-molecule ion channels increase host defences in cystic fibrosis airway epithelia. *Nature* 567, 405–408. doi: 10.1038/s41586-019-1018-5

Nedal, A., Sletta, H., Brautaset, T., Borgos, S. E., Sekurova, O. N., Ellingsen, T. E., et al. (2007). Analysis of the mycosamine biosynthesis and attachment genes in the nystatin biosynthetic gene cluster of *Streptomyces noursei* ATCC 11455. *Appl. Microbiol. Biotechnol.* 73, 7400–7407. doi: 10.1128/AEM.01122-07

Neumann, A., Wieczor, M., Zielinska, J., Baginski, M., and Czub, J. (2016). Membrane sterols modulate the binding mode of amphotericin B without affecting its affinity for a lipid bilayer. *Langmuir* 32, 3452–3461. doi: 10.1021/acs.langmuir.5b04433

Silveira, F. P., and Husain, S. (2007). Fungal infections in solid organ transplantation. *Med. Mycol.* 45, 305–320. doi: 10.1080/13693780701200372

Subramani, R., and Aalbersberg, W. (2012). Marine actinomycetes an ongoing source of novel bioactive metabolites. *Microbiol. Res.* 167, 571–580. doi: 10.1016/j.micres.2012.06.005

Volokhan, O., Sletta, H., Ellingsen, T. E., and Zotchev, S. B. (2006). Characterization of the P450 monooxygenase NysL, responsible for C-10 hydroxylation during biosynthesis of the polyene macrolide antibiotic nystatin in *Streptomyces noursei*. *Appl. Environ. Microbiol.* 72, 2514–2519. doi: 10.1128/AEM.72.4.2514-2519.2006

Walmsley, S., De Poire, E., Rawlings, B., and Caffrey, P. (2017). Engineered biosynthesis and characterization of disaccharide-modified 8-deoxyamphoteronlides. *Appl. Microbiol. Biotechnol.* 101, 1899–1905. doi: 10.1007/s00253-016-7986-6

Wayne, P. A. (2008). *Reference for broth dilution antifungal susceptibility testing of yeasts; approved standard. 3rd Edn.* Clinical and Laboratory Standards Institute document, M27–A3.

Won, H. J., Kim, H. J., Jang, J. Y., Kang, S. H., Choi, S. S., and Kim, E. S. (2017). Improved recovery and biological activities of an engineered polyene NPP analogue *in Pseudonocardia autotrophica*. *J. Ind. Microbiol. Biotechnol.* 44, 1293–1299. doi: 10.1007/s10295-017-1954-8

Zotchev, S., Haugan, K., Sekurova, O., Sletta, H., Ellingsen, T. E., and Valla, S. (2000). Identification of a gene cluster for antibacterial polyketide derived

antibiotic biosynthesis in the nystatin producer *Streptomyces noursei* ATCC 11455. *Microbiology* 146, 611–619. doi: 10.1099/00221287-146-3-611

Conflict of Interest: The authors declare that the research was conducted in the absence of any commercial or financial relationships that could be construed as a potential conflict of interest.

frontiers in Microbiology

ORIGINAL RESEARCH
published: 18 February 2020
doi: 10.3389/fmicb.2020.00225

Disclosing the Potential of the SARP-Type Regulator PapR2 for the Activation of Antibiotic Gene Clusters in Streptomycetes

*Janina Krause[1], Ira Handayani[1,2], Kai Blin[3], Andreas Kulik[1] and Yvonne Mast[1,4,5,6]**

[1] Department of Microbiology/Biotechnology, Interfaculty Institute of Microbiology and Infection Medicine, Faculty of Science, University of Tübingen, Tübingen, Germany, [2] Research Center for Biotechnology, Indonesian Institute of Sciences (LIPI), Cibinong, Indonesia, [3] Novo Nordisk Foundation Center for Biosustainability, Technical University of Denmark, Lyngby, Denmark, [4] German Center for Infection Research (DZIF), Partner Site Tübingen, Tübingen, Germany, [5] Department of Bioresources for Bioeconomy and Health Research, Leibniz Institute DSMZ – German Collection of Microorganisms and Cell Cultures, Braunschweig, Germany, [6] Department of Microbiology, Technical University Braunschweig, Braunschweig, Germany

OPEN ACCESS

Edited by:
Rustam Aminov, University of Aberdeen, United Kingdom

Reviewed by:
Marie-Joelle Virolle, Centre National de la Recherche Scientifique (CNRS), France
Jean-Luc Pernodet, Centre National de la Recherche Scientifique (CNRS), France
Javier Santos Aberturas, John Innes Centre (JIC), United Kingdom
Juan F. Martin, Universidad de León, Spain

***Correspondence:**
Yvonne Mast
yvonne.mast@dsmz.de

Specialty section:
This article was submitted to Antimicrobials, Resistance and Chemotherapy, a section of the journal Frontiers in Microbiology

Received: *29 October 2019*
Accepted: *30 January 2020*
Published: *18 February 2020*

Citation:
Krause J, Handayani I, Blin K, Kulik A and Mast Y (2020) Disclosing the Potential of the SARP-Type Regulator PapR2 for the Activation of Antibiotic Gene Clusters in Streptomycetes. Front. Microbiol. 11:225. doi: 10.3389/fmicb.2020.00225

Streptomyces antibiotic regulatory protein (SARP) family regulators are well-known activators of antibiotic biosynthesis in streptomycetes. The respective genes occur in various types of antibiotic gene clusters encoding, e.g., for polyketides, ribosomally and non-ribosomally synthesized peptides, or β-lactam antibiotics. We found that overexpression of the SARP-type regulator gene *papR2* from *Streptomyces pristinaespiralis* in *Streptomyces lividans* leads to the activation of the silent undecylprodigiosin (Red) gene cluster. The activation happens upon the inducing function of PapR2, which takes over the regulatory role of RedD, the latter of which is the intrinsic SARP regulator of Red biosynthesis in *S. lividans*. Due to the broad abundance of SARP genes in different antibiotic gene clusters of various actinomycetes and the uniform activating principle of the encoded regulators, we suggest that this type of regulator is especially well suited to be used as an initiator of antibiotic biosynthesis in actinomycetes. Here, we report on a SARP-guided strategy to activate antibiotic gene clusters. As a proof of principle, we present the PapR2-driven activation of the amicetin/plicacetin gene cluster in the novel Indonesian strain isolate *Streptomyces* sp. SHP22-7.

Keywords: actinomycetes, *Streptomyces*, antibiotic, regulator, SARP, silent gene cluster

INTRODUCTION

In 2018, the WHO warned that the dramatic increase of antibiotic resistances coupled with the scarcity of new antibiotics will lead to a global health crisis in the 21st century (World Health Organization, 2015). Even nowadays, infections that are caused by drug-resistant pathogens are suggested to account for 700,000 deaths worldwide annually (United Nations Foundation and the Wellcome Charitable Trust, 2016). According to the World Bank Group "by 2050, drug-resistant infections could cause global economic damage on par with the 2008 financial crisis" (Worldbank, 2016). Thus, there is a substantial need for new antibiotics in order to combat drug-resistances. Bacteria have long been recognized as a prolific source for antibiotics

(Newman and Cragg, 2016). Especially actinomycetes are potent producers of bioactive molecules, as they provide up to 70% of all medically important antibiotic agents (Tanaka and Omura, 1990). The capability to produce these natural compounds is genetically encoded in the actinomycetes genome, whereby the respective genes usually are organized as biosynthetic gene clusters (BGCs). In recent years, genomic analyses of actinomycetes have revealed the presence of numerous "silent" or "cryptic" BGCs, meaning that these clusters remain silent or are only weakly expressed under standard lab conditions. Indeed it is estimated that actinomycetes encode ∼10-times the number of secondary metabolites than anticipated from prior fermentation studies (Baltz, 2017). Thus, these microorganisms still hold the genetic potential to produce new bioactive compounds. Consequently, there are several attempts to activate silent gene cluster expression in order to find new antibiotics. However, most of these activation efforts are either (a) completely unspecific in terms of the BGC(s) to be activated [e.g., by adding general elicitors to the cell culture, co-cultivation approaches, or strain-cultivations following the "one strain-many compounds" (OSMAC) strategy] or (b) they are absolutely specific for the BGC of interest (e.g., heterologous expression of the BGC, introduction of an artificial promoter in front of the BGC, or manipulation of a cluster-situated regulator) as reviewed in Ochi and Hosaka (2013) and Zhu et al. (2014). Both approaches have their drawbacks, as there are either major analytical efforts to identify the product from the silent gene cluster [in terms of (a)] or tedious genetic engineering efforts to manipulate the producer strain [in terms of (b)]. Thus, it would be highly beneficial to have a more general activation strategy that targets a defined set of BGCs, which would tackle both issues. In a recent study from Martínez-Burgo et al. (2019) it has been shown that conserved pathway-specific activators can be used to activate BGC expression in a foreign *Streptomyces* strain. In this study the heterologous expression of the PAS-LuxR type regulator gene *pimM* from *Streptomyces natalensis* in *Streptomyces clavuligerus* led to the activation of clavulanic acid, cephamycin C, and tunicamycin production.

Here we demonstrate that *Streptomyces* Antibiotic Regulatory Protein (SARP)-type regulators can be used as activators of certain antibiotic gene clusters in actinomycetes and describe a genome-based approach to screen for SARP-activated gene clusters. SARPs have exclusively been found in actinomycetes, especially in streptomycetes, where they act as pathway-specific activators of secondary metabolite biosynthesis (Bibb, 2005). They are known to be associated with various antibiotic gene clusters, encoding type I- (Bate et al., 2002; Takano et al., 2005; Novakova et al., 2011) and type II-PKS derived polyketides (Lombó et al., 1999; Sheldon et al., 2002; Aigle et al., 2005; Novakova et al., 2011), ribosomally (Widdick et al., 2003; Wu et al., 2018) and non-ribosomally synthesized peptides (Ryding et al., 2002), hybrid polyketide-peptide compounds (Pulsawat et al., 2009; Suzuki et al., 2010; Xie et al., 2012; Salehi-Najafabadi et al., 2014; Mast et al., 2015; Ye et al., 2018), β-azachinones (Santamarta et al., 2002; Rodríguez et al., 2008; Kurniawan et al., 2014), and azoxy compounds (Garg et al., 2002). SARP genes usually are located within the BGC they are regulating. The encoded SARP gene products are characterized by a winged helix-turn-helix (HTH) DNA-binding motif at the N-terminus that binds to a conserved recognition sequence within the major groove of the target DNA (Wietzorrek and Bibb, 1997; Liu et al., 2013). The DNA recognition sequence constitutes direct heptameric repeat sequences followed by 4 bp spacers, which are often localized between the −10 and the −35 promoter element of the respective target DNA. Such a localization has already been described for the SARP type regulator AfsR from *Streptomyces coelicolor*, which binds to a recognition sequence 8 bp upstream of the −10 element (Tanaka et al., 2007). Also the SARP regulators Aur1PR4 from *Streptomyces aureofaciens* and FdmR1 from *Streptomyces griseus* bind to heptameric repeat sequences, which are located 8 bp upstream of the −10 region (Chen et al., 2008; Rehakova et al., 2013). ActII-ORF4 from *S. coelicolor* interacts with the −35 element for transcriptional activation (Arias et al., 1999). DnrI from *Streptomyces peucetius* and SanG from *Streptomyces ansochromogenes* bind to interaction sites that occur within the −35 element (Sheldon et al., 2002; He et al., 2010). It is suggested that in general the SARP binding site overlaps with the −35 region of the target promoter, which is a binding region of the majority of repressors but not activators. Thus, SARP-driven transcriptional activation has been proposed to occur via a novel mechanism (Tanaka et al., 2007). The C-terminal bacterial activation domain (BTAD) of the SARP protein activates the transcription of the target genes by recruiting the RNA polymerase (RNAP) to the respective promoter, where a ternary DNA–SARP–RNAP complex is formed allowing for transcriptional initiation (Tanaka et al., 2007). "Small" SARP-type activators only contain the HTH DNA binding and BTAD domain, whereas "large" SARPS carry additional domains at the C-terminal side of the protein. These domains include a domain of unknown function belonging to the P-loop NTPase family, and one or more copies of a tetratricopeptide repeat (TPR) motif (Liu et al., 2013). A typical "small" SARP-type activator is represented by PapR2, which has been identified as the major activator of pristinamycin biosynthesis in *Streptomyces pristinaespiralis* (Mast et al., 2015). A *papR2* deletion mutant is unable to produce any pristinamycin, depicting that PapR2 is essential for pristinamycin biosynthesis (Mast et al., 2015). In contrast, overexpression of *papR2* in *S. pristinaespiralis* leads to an increased pristinamycin production, which shows that PapR2 has an activating function (Mast et al., 2015). With the help of electromobility shift assays (EMSAs) and (quantitative) reverse transcription PCR [RT-(q)PCR] analysis the PapR2 target genes have been identified in the pristinamycin producer and a conserved PapR2 binding site was proposed (Mast et al., 2015).

In this study, we report on the potential of SARP-type regulators as genetic engineering devices for the activation of (silent) BGCs in actinomycetes. SARP-type regulators are present predominantly in actinomycetes with an abundance of 98% in the genus *Streptomyces*. We demonstrate that the SARP-type regulator PapR2 activates the silent undecylprodigiosin (Red) gene cluster in *Streptomyces lividans*. Additionally, we provide evidence for a PapR2-guided activation of a BGC in the poorly studied Indonesian strain isolate *Streptomyces* sp.

SHP22-7 (SHP22-7), which yielded an increased production of the nucleoside antibiotic plicacetin.

MATERIALS AND METHODS

Bacterial Strains, Plasmids, and Cultivation Conditions

The bacterial strains and plasmids used in this study are listed in **Supplementary Table S1**. For routine cloning strategies *Escherichia coli* Novablue (Novagen) was used. *S. lividans* T7 (Fischer, 1996) and SHP22-7 (Handayani et al., 2018) were applied for antibiotic production analysis, generation of overexpression strains, and transcriptional analysis. Cloning procedures and strain cultivation were carried out as described before (Mast et al., 2015). For cultivation and isolation of RNA, *Streptomyces* strains were grown in 100 ml of R5 medium in 500-ml Erlenmeyer flasks (with steel springs) on an orbital shaker (180 rpm) at 28°C (Kieser et al., 2000). For isolation of genomic DNA and protoplast transformation experiments, strains were grown in 100 ml of S-medium (Kieser et al., 2000). Kanamycin (50 μg/ml), apramycin (50 μg/ml), or thiostrepton (20 μg/ml) were used for selection when appropriate. For antibiotic production experiments with *S. lividans*, strains were grown in YEME medium as reported before (Mast et al., 2015). For antibiotic production experiments with SHP22-7, strains (SHP22-7*papR2-OE*; references: SHP22-7*pRM4* and SHP22-7 WT) were grown in 50 ml NL410 medium consisting of glucose (10 g l^{-1}), glycerol (10 g l^{-1}), oat meal (5 g l^{-1}), soy flour (10 g l^{-1}), yeast extract (5 g l^{-1}), Bacto casamino acids (5 g l^{-1}), $CaCO_3$ (1 g l^{-1}), and distilled water (pH was adjusted to 7.0 with NaOH) as a preculture. After 3 days, 10 ml of preculture was transferred to 100 ml of sterile main culture medium NL19, consisting of mannitol (20 g l^{-1}), soy flour (20 g l^{-1}), and distilled water (pH adjusted to pH 7.5 with NaOH). Cells were grown for 168 h at 28°C.

Molecular Cloning

Basic procedures for DNA manipulation were performed as described previously (Sambrook et al., 1989; Kieser et al., 2000). Primers used for PCR were obtained from MWG Biotech AG (MWG, Ebersberg, Germany) and are listed in **Supplementary Table S1**.

Construction of the papR2 Overexpression Strain SHP22-7papR2-OE

For *papR2* overexpression experiments with SHP22-7, the *papR2* gene was isolated as a *Nde*I/*Hin*dIII-fragment from plasmid pGM190/papR2 (Mast et al., 2015) and was cloned into the *Nde*I/*Hin*dIII restriction site of the integrative expression vector pRM4. In the resulting overexpression construct pRM4/papR2, the *papR2* gene is under control of the constitutive promoter of the erythromycin resistance gene *ermEp**. pRM4/papR2 was transferred to SHP22-7 by protoplast transformation. Transformants were selected with apramycin (50 μg/ml), which resulted in the overexpression strain SHP22-7*papR2-OE*. Strain SHP22-7*pRM4*, harboring the empty pRM4 vector, was generated by protoplast transformation accordingly and served as a reference.

PapR2 Protein Expression in *S. lividans*

For *papR2* overexpression experiments *SLpapR2-OE* precultures were grown in 100 ml of YEME liquid medium for 2 days at 28°C. Five milliliters of preculture was used as inoculum for 100 ml YEME liquid medium as main culture with thiostrepton (12.5 μg/ml) as inductor for gene expression (Mast et al., 2015). The main culture was cultivated for 3 days at 28°C. PapR2 protein purification was carried out as reported before (Mast et al., 2015).

Spectrophotometrical Analysis for Red Detection

For Red detection, culture supernatant from *SLpapR2-OE* and *SLpGM190* (reference) was treated as reported in Onaka et al. (2011) and absorption was measured with a Hitachi U-2000 spectrophotometer.

Sample Treatment for SHP22-7 Bioassays and Compound Detection

For SHP22-7 compound detection and bioassay tests, 5 ml culture samples of SHP22-7*papR2-OE* (references: SHP22-7*pRM4* and SHP22-7 WT) was extracted with 5 ml ethyl acetate for 30 min at RT. Ethyl acetate samples were concentrated *in vacuo* completely and then redissolved in 0.75 ml of methanol. Methanolic extracts were used for bioassays and high-performance liquid chromatography/mass spectrometry (HPLC–MS) analysis.

Bioassays

Antibiotic activity was analyzed in disc diffusion assays using *Bacillus subtilis* ATCC6051 as test organism. Thirty microliters of methanolic extract from three independent biological samples of SHP22-7 WT, SHP22-7*pRM4*, and SHP22-7*papR2-OE*, respectively, was pipetted on a filter disc, which was placed on a *B. subtilis* test plate. Five microliters of kanamycin (50 μg/ml) was applied as a positive control and 30 μl of methanol as negative control to test the functionality of the *B. subtilis* bioassay plates. The plates were incubated overnight at 37°C. Antibiotic activity was quantified by measuring the diameter of the inhibition zone around the filter discs. The bioassay was carried out as 10 independent biological replicates.

HPLC and HPLC–MS Analysis for Amicetin/Plicacetin Detection

High-performance liquid chromatography analyses were performed with a HP1090M system with ChemStation 3D software rev. A.08.03 (Agilent Technologies, Waldbronn, Germany) on a Nucleosil C18 column (5 μm, 125 mm × 3 mm) fitted with a precolumn (20 × 3 mm) and with a flow rate of 850 μl min^{-1}. Chromatography was done by linear gradient elution from 95.5 solvent A (water with 0.1% phosphoric acid) to 100% solvent B [acetonitrile (ACN)] over 15 min. The injection volume was 5 μl. Multiple wavelength monitoring was

performed at 210, 230, 260, 280, 310, 435, and 500 nm. UV-Vis spectra were measured from 200 to 600 nm. The evaluation of the chromatograms (210 nm only) was done by means of an in-house HPLC–UV–Vis database.

High-performance liquid chromatography–mass spectrometry analysis of amicetin/plicacetin was performed with an Agilent 1200 series chromatography system (binary pump, high performance autosampler, DAD-detector) coupled with an LC/MSD Ultra Trap System XCT 6330 (Agilent Technologies, Waldbronn, Germany). The sample (5 μl) was injected on a Nucleosil 100 C18 column (3 μm, 100 × 2 mm) fitted with a precolumn (3 μm, 10 × 2 mm) at a flow rate of 400 μl/min and a linear gradient from 100% solvent A (0.1% HCOOH in water) to 100% solvent B (0.06% HCOOH in ACN) over 15 min at 40°C. UV–Vis-detection was done at 220, 260, 280, 360, and 435 nm. Electrospray ionization was performed in positive and negative ultra-scan mode (alternating) with a capillary voltage of 3.5 kV and a drying gas temperature of 350°C. Detection of *m/z* values was conducted with Agilent DataAnalysis for 6300 Series IonTrap LC/MS Version 3.4 (Bruker Daltonik). Upon HPLC–MS analyses amicetin, plicacetin, and plicacetin isomer were identified by comparisons of their UV/visible spectra, retention times, and molecular masses with authentic standards, as *m/z* 617.1 $[M\text{-}H]^-$ and *m/z* 516.1 $[M\text{-}H]^-$, respectively.

AntiSMASH Analysis

With the webtool antiSMASH whole genomes can be scanned for the occurrence of BGCs. Gene cluster similarity is given in % and indicates the number of similar genes to a known cluster. Genes are similar if a BLAST-alignment results in an *e*-value $<10^{-5}$ and the sequence identity is >30%. Additionally, the shortest alignment must enclose >25% of the sequence. If all genes of a known cluster can be found in the query cluster, the similarity of the sequences is 100%. The similarity lowers if less genes of the known cluster can be found in the query cluster (Medema et al., 2011).

PatScan Analysis

PatScan analysis (Blin et al., 2018) was performed with the *S. lividans* T7 genome (GenBank Accession Number ACEY00000000) and the PapR2 consensus sequence 5′-GTCAGSS-3′ using the software at https://patscan.secondarymetabolites.org/.

PapR2 Electromobility Shift Assays

For EMSAs with Red-specific promoter regions, 182 bp DNA fragments of the upstream regions of *redP* and *redQ* were amplified by PCR from genomic DNA of *S. lividans* T7 with primer pairs PredPfw/rv and PredQfw/rv, respectively (**Supplementary Table S1**). For EMSAs with the *pliA* promoter region, a 230 bp DNA fragment of the upstream region of *pliA* was amplified by PCR from genomic DNA of strain SHP22-7 as template and primer pair PpliAfw/rv (**Supplementary Table S1**). Promoter DNA amplificates included a 16 bp Cy5 adapter sequence, each at the 3′- and 5′-end, which was added via the respective primer sequences. The generated amplificates were used as templates in a second PCR approach together with a Cy5 primer (**Supplementary Table S1**) in order to conduct Cy5 labeling of the promoter regions. Promoter labeling and PapR2 EMSAs were carried out with variable concentrations of PapR2 protein sample as reported before (Mast et al., 2015). To verify the specificity of the PapR2-DNA binding, an excess of unlabeled, specific, and non-specific DNA, respectively, was added to the EMSA mixture as described previously (Mast et al., 2015). DNA bands were visualized by fluorescence imaging using a Typhoon Trio^{TM} Variable Mode Imager (GE Healthcare).

Transcriptional Analysis by Reverse Transcription Analysis (RT-PCR)

SLpGM190 and *SLpapR2-OE*, as well as SHP22-7, SHP22-7*pRM4*, and SHP22-7*papR2-OE* were each grown under *papR2*-overexpression conditions as described above. Thirty milliliters of each cell culture was harvested after 48 h. Cell disruption was carried out with glass beads (150–212 μm; Sigma) at 6,500 rpm, 1 × 20-30 s, using a Precellys Homogenizer (Peqlab). Total RNA was isolated as described previously (Sambrook et al., 1989) and served as the basis for RT-PCR experiments. DNA was removed by digestion with DNase (Thermo Fisher Scientific) and absence of DNA was verified via PCR analysis. RNA concentrations and quality were checked using a NanoDrop ND-1000 spectrophotometer (Thermo Fisher Scientific). cDNA from 3 μg RNA was generated with random primers, reverse transcriptase, and cofactors (Fermentas). For RT-PCRs, primers were used that amplify cDNA of 200–250 bp from internal gene sequences. PCR conditions were 98°C for 5 min, followed by 30 cycles of 95°C for 30 s, 60°C for 30 s, and 72°C for 45 s, and a final cycling step at 72°C for 5 min. As a positive control, cDNA was amplified from the 16S rRNA transcript, which is transcribed constitutively. To exclude DNA contamination, negative controls were carried out by using total RNA as a template for each RT-PCR reaction. At least three independent biological replicates have been tested.

Transcriptional Analysis by Real-Time qPCR

Real-time qPCR analysis was applied for quantitative cDNA determination. PCR reactions were run with SYBR® Green Supermix (BioRad) on an iQ5 Multicolor Real-Time-PCR Detection System (BioRad). The SYBR® Green Dye shows increased fluorescence when bound to double-stranded DNA. The fluorescence is measured at 494 and 521 nm and gives the proportional amount of generated dsDNA. cDNA was generated from cultures of *SLpGM190* and *SLpapR2-OE* as described above. The primer pairs redPintfw/rv and redQintfw/rv, respectively (**Supplementary Table S1**), which amplify fragments of about 180 bp from internal gene sequences, were used together with cDNA as template in qPCR reactions. *hrdB* was used as housekeeping gene in each experiment in order to standardize the results by eliminating variation in RNA and cDNA quantity and quality. Each reaction mixture of 10 μL volume contained 5 μL SYBR® Green Supermix (BioRad), 3.85 μL nuclease-free water, 0.2 μL of each primer, and 0.75 μL template. PCR conditions were 98°C for 5 min, followed by 35 cycles of

95°C for 20 s, and 57°C for 30 s. To determine amplification specificity, melting curve analyses were performed after the last cycle, showing in all cases one single peak. Results were analyzed using the ΔΔCT-method (Livak and Schmittgen, 2001). Changes in gene expression are represented in relation to the data from samples of *SLpGM190*. Data are presented as the results from six independent biological replicates.

Database Analysis

FASTA sequences of SARP proteins were extracted from the antiSMASH database version 2 (Blin et al., 2019) by querying for all genes that hit the antiSMASH smCoG (secondary metabolite clusters of orthologous groups) profile SMCOG1041 (transcriptional regulator, SARP family). These hits were checked for the presence of at least one out of four SARP-related profiles from the PFAM database: PF00486.27 (Trans_reg_C, the HTH-style DNA binding domain), PF93704.16 (BTAD, the transcriptional activator), PF00931.22 (NB-ARC, a domain of unknown function found, e.g., in *Saccharopolyspora erythraea* SARPs), and PF13424.6 (TPR_12, a TPR found in many larger SARPs). Sequences that did not hit at least one of these domains were discarded. Sequences were then annotated by which of the four profiles were hit and grouped by taxonomic order and BCG type.

RESULTS

PapR2 Induces Expression of the Silent Red Gene Cluster in *S. lividans*

Streptomyces lividans is a widely used heterologous host strain, which under specific laboratory conditions does not exhibit production of the two pigmented secondary metabolites actinorhodin and undecylprodigiosin (Hu et al., 2002; Martinez et al., 2005; Rodríguez et al., 2013). In frame of analyzing the regulatory role of PapR2 in *S. pristinaespiralis*, the *papR2* gene was heterologously expressed in *S. lividans* T7 for protein purification purposes (Mast et al., 2015). For overexpression experiments the *S. lividans* strain *SLpapR2-OE* was used, which harbors the *papR2* gene under control of the thiostrepton-inducible promoter P_{tipA} on the replicative medium-copy plasmid pGM190 (Mast et al., 2015). *S. lividans* strain *SLpGM190* was used as a reference, containing the pGM190 empty vector. After 2–3 days of growth in YEME liquid medium with thiostrepton as inductor for gene expression, the whole *SLpapR2-OE* culture, as well as the culture supernatant showed an intensive red pigment formation, which was not observed for samples of *SLpGM190* (**Figure 1A**). This phenomenon was also observed on R5 agar with thiostrepton, where *SLpapR2-OE* mycelium was intensively red colored after 3–4 days of cultivation, whereas *SLpGM190* mycelium was not (**Supplementary Figure S1**). *S. lividans* is known to harbor a Red BCG, which remains silent under normal growth conditions (Horinouchi et al., 1986). Red biosynthesis has mainly been studied in *S. coelicolor*; however, since *S. coelicolor* and *S. lividans* are very closely related species, knowledge on Red biosynthesis and regulation can be transferred to *S. lividans* (van Wezel et al., 2000; Lewis et al., 2010).To investigate, whether the red color of the *SLpapR2-OE* cultures originates from the formation of the Red metabolite, we performed spectrophotometrical analysis. A pH shift was carried out with the culture supernatant of *SLpapR2-OE* and the absorption maxima of the sample was determined by using a Hitachi U-2000 spectrophotometer. Spectrophotometrical analysis led to the detection of the Red-specific spectral absorption maxima (Onaka et al., 2002) at 533 and 468 nm under acidic and basic conditions, respectively (**Figure 1B**), which proved that the *SLpapR2-OE* samples contained Red (**Figure 1C**). These data suggested that the overexpression of *papR2* in *S. lividans* induced Red biosynthesis.

PapR2 Mimics the Function of the *S. lividans* SARP-Type Regulator RedD

In *S. lividans* Red biosynthesis is under control of the SARP-type regulator RedD, which directly activates the Red biosynthetic genes (Takano et al., 1992; White and Bibb, 1997). An amino acid sequence comparison using BLASTP revealed that PapR2 and RedD are highly similar to each other (44% identity, 55% similarity) (Mast et al., 2015). This amino acid sequence similarity was even higher for the HTH motif of the protein (66% identity, 75% similarity). Thus, we suspected that PapR2 may substitute for the function of RedD and activates Red biosynthesis in *S. lividans.* In order to identify potential SARP-type binding motifs within the *S. lividans* Red BGC, the genome was analyzed with the bioinformatic tool PatScan, which allows for the identification of specific sequence patterns in a given genome sequence (Blin et al., 2018). PatScan analysis was performed with the previously described PapR2 consensus motif (5'-GTCAGSS-3') (Mast et al., 2015) as sequence pattern on the *S. lividans* genome sequence. Thereby, two highly conserved PapR2-like motifs were identified within the intergenic region of the Red-specific biosynthetic genes *redP* (SCO5888) and *redQ* (SCO5887) with each 100 and 96.5% identity, respectively (**Figure 2A**). *redP* encodes a 3-ketoacyl-acyl carrier protein synthase, whereas *redQ* codes for an acyl carrier protein, both of which have been shown to be involved in Red biosynthesis (Mo et al., 2008). To analyze the functionality of the identified SARP motifs, EMSAs were performed with the PapR2 protein and the upstream regions of *redP* (P*redP*, 182 bp) and *redQ* (P*redQ*, 182 bp), respectively, harboring the PapR2 consensus sequence. EMSAs showed that PapR2 specifically binds to the P*redP* and P*redQ* fragment, respectively (**Figure 2B**), revealing the functionality of the identified SARP-type motifs.

To confirm the regulatory effect of PapR2 on the transcription of the Red BGC, we performed RT-PCR and quantitative qPCR experiments. For these studies *SLpapR2-OE*, as well as the reference strain *SLpGM190* were grown in R5 medium. After 72 h of cultivation samples were harvested for RNA isolation. For each strain six biological replicates were performed. Isolated RNA was used as a template in RT-PCR experiments as a negative control (**Figure 3A**), whereas cDNA was used together with 16S primers as a positive control (**Figure 3B**). For *red* gene-specific transcriptional analysis, isolated RNA was used as template for RT-PCR experiments with the primer pairs redPintfw/rv

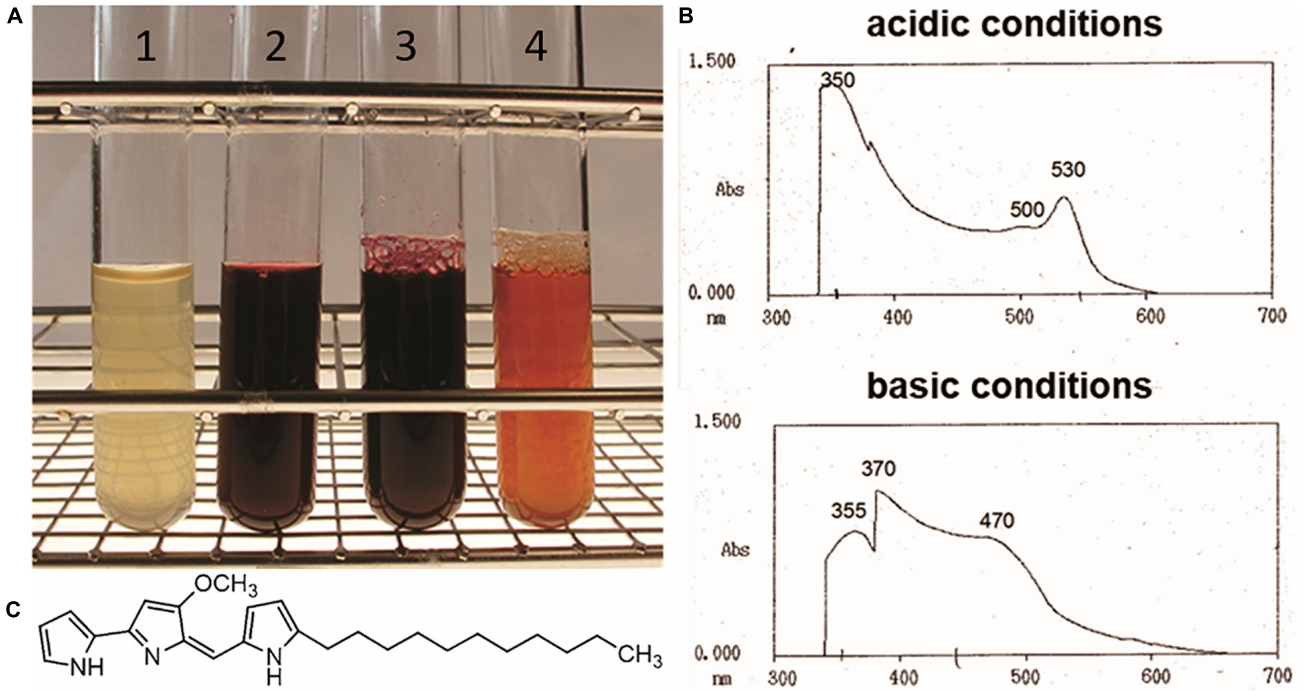

FIGURE 1 | Culture filtrates from *SLpGM190* (1) and *SLpapR2-OE* (2) samples after 3 days of cultivation. Culture filtrate of *SLpapR2-OE* under acidic (3) and basic (4) conditions **(A)**. Absorption profile of the *SLpapR2-OE* culture filtrate under acidic (upper graph) and basic condition (lower graph) **(B)**. Chemical structure of Red **(C)**.

and redQintfw/rv, which annealed to internal parts of *redP* and *redQ*, respectively. The transcriptional analysis revealed that there are stronger signals for the *redP* and *redQ* cDNA amplificates in *SLpapR2-OE* samples compared to *SLpGM190* samples (**Figures 3C,D**, respectively). In order to quantify the amount of *redP* and *redQ* RT-qPCR was performed. Based on the threshold cycle it was calculated that *redP* and *redQ* transcripts were increased to 57- and 492-fold, respectively, in samples of *SLpapR2-OE* compared to samples of *SLpGM190* (**Supplementary Figure S2**). Thus, transcriptional analyses demonstrated that PapR2 activates the transcription of the Red biosynthetic genes *redP* and *redQ*. Due to the intensive Red production of strain *SLpapR2-OE* together with the data obtained from PapR2 EMSA studies and transcriptional analysis, we propose that overexpressed PapR2 in *S. lividans* takes over the regulatory function of RedD and activates the transcription of the Red biosynthetic genes, which leads to the formation of the red colored secondary metabolite Red.

PapR2 Expression Improves Antibiotic Activity of SHP22-7

In order to study the general application of SARP-type regulators for activation of antibiotic biosynthesis, we exemplary tested strain SHP22-7 as a host for *papR2* expression. SHP22-7 is a novel strain isolate from a soil sample of the unique desert island Enggano, Indonesia (Handayani et al., 2018). SHP22-7 shows broad-spectrum antibacterial activity against Gram-positive and Gram-negative bacteria, including *E. coli*, *Staphylococcus carnosus*, *Micrococcus luteus*, and *B. subtilis*. The SHP22-7 genome has been sequenced recently and antiSMASH analysis led to the identification of 25 potential secondary metabolite gene clusters (Handayani et al., 2018; **Table 1**). Four of the gene clusters (clusters 3, 6, 10, and 15) contain SARP genes, which makes SHP22-7 a good candidate strain for a SARP-guided activation. For *papR2* expression studies in SHP22-7, the *papR2* gene was cloned into the integrative plasmid pRM4 under control of the constitutive *ermE** promoter, resulting in construct pRM4/papR2. The pRM4 vector was used as expression plasmid in these analyses to avoid addition of thiostrepton as inductor (see above), which would influence subsequent antibacterial bioassays. The plasmid was transferred to SHP22-7 by protoplast transformation. The resulting expression strain SHP22-7*papR2-OE*, as well as the two reference strains SHP22-7*pRM4*, which harbors the empty pRM4 vector, and the SHP22-7 wild-type (WT) were used for antibacterial bioassay studies. SHP22-7*papR2-OE*, SHP22-7pRM4, and SHP22-7 WT were each cultivated in NL19 medium and samples were taken at 168 h. Methanolic culture extracts were applied for antibacterial bioassays using *B. subtilis* as test organism. Filter discs with kanamycin and methanol served as positive and negative control, respectively. Bioassays were carried out as 10 independent biological replicates. Thereby, significantly larger inhibition zones against *B. subtilis* were observed on average with extracts from SHP22-7*papR2-OE* compared to extracts from SHP22-7*pRM4* or SHP22-7 WT (**Figure 4A**). The extract of SHP22-7*papR2-OE* caused a zone of inhibition of 11.7 ± 2.1 mm, whereas the extracts of SHP22-7*pRM4* and SHP22-7 WT yielded smaller

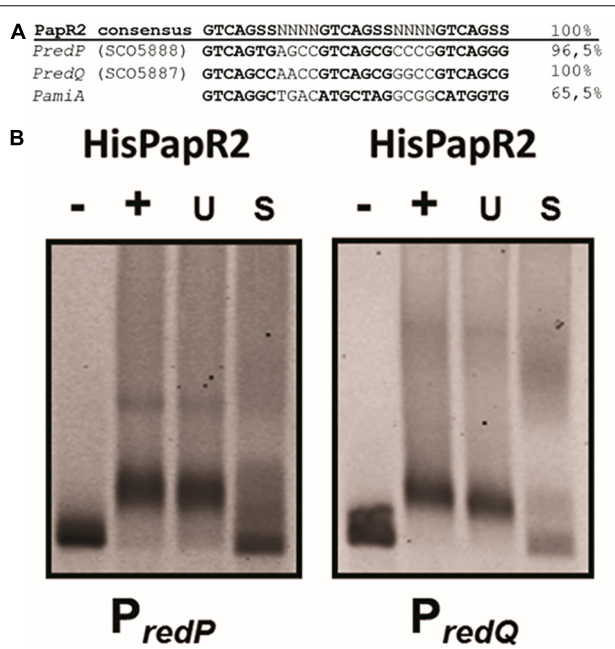

FIGURE 2 | SARP binding sequences within the upstream region of the RED-biosynthetic genes *redP* (SCO5888), *redQ* (SCO5887), and *pliA* **(A)**. EMSAs with undefined HisPapR2 concentrations and Cy5-labeled promoter regions of *redP* and *redQ*. – indicates negative control without protein, + indicates addition of HisPapR2 protein. The specificity of the reaction was checked by the addition of 500-fold specific (S) and unspecific (U) unlabeled DNA **(B)**.

inhibitions zones of 8.3 ± 2.6 and 7.3 ± 2.7 mm, respectively (**Figure 4B**). These data showed that *papR2* expression in SHP22-7 leads to a significantly improved antibiotic activity.

PapR2 Activates Transcription of Cluster 9 in SHP22-7

To identify the substance that is responsible for the antibiotic activity of SHP22-7 but avoid elaborative chemical analytics in the first place, we screened the SHP22-7 genome sequence for the occurrence of PapR2-like consensus sequences by using the PatScan tool. Here, we only considered motifs that were located within intergenic regions of genes from suggested SHP22-7 BGCs. The motif search led to the identification of PapR2-like consensus sequences within 5 of the 25 predicted BGCs from SHP22-7. These included clusters 6 and 10 (NRPS-like gene cluster), cluster 15 (type 2 PKS-butyrolactone-like gene cluster), as well as clusters 3 and 9 ("other" type of gene cluster) (**Table 1**). In order to find out which of the five gene clusters is activated by PapR2, comparative RT-PCR analysis was carried out with SHP22-7*papR2-OE*, SHP22-7pRM4, and SHP22-7 WT in four independent biological replicates. Cells were grown under antibiotic production conditions and samples were harvested at 168 h of cultivation. Two samples were collected for each strain and growth time point, whereby one sample was used for RT-PCR analysis and the second one for HPLC–MS analysis (see the section "SARP-Type Regulatory Genes Are Widespread in BGCs From Diverse Actinobacteria"). RT-PCR was carried out with RNA isolated from cell pellets of SHP22-7*papR2-OE*, SHP22-7*pRM4*, and SHP22-7 WT, respectively. Isolated RNA was used as a template in RT-PCR experiments as a negative control (**Figure 5A**), whereas cDNA was used together with *16S* primers as a positive control (**Figure 5B**). For cluster specific transcriptional analysis, cDNA was generated with primer pairs cl3fw/rv, cl6fw/rv, cl9fw/rv, cl10fw/rv, and cl15fw/rv (**Supplementary Table S1**), each aligning to a predicted biosynthesis gene of clusters 3, 6, 9, 10, and 15, respectively. The transcriptional analysis revealed that there is a stronger signal for the cluster 9 amplificate in the SHP22-7*papR2-OE* samples compared to the samples of SHP22-7*pRM4* and SHP22-7 WT, where there is nearly no signal at all (**Figure 5C**). This difference in signal intensity could not be observed for clusters 3, 6, 10, and 15 (**Figure 5C**). Thus, these data suggested that PapR2 activates the transcription of cluster 9 in SHP22-7*papR2-OE*.

Cluster 9 Resembles an Amicetin Gene Cluster

In order to deduce for what type of metabolite cluster 9 encodes for, we analyzed the cluster sequence region in detail. The antiSMASH output predicted a 75% similarity of cluster 9 to the plicacetin/amicetin gene cluster from *Streptomyces vinaceusdrappus* NRRL 2363 (**Table 1**). The cluster similarity describes the number of genes with a similarity above the ClusterBlast threshold of 30% sequence similarity at over 25% coverage. Manually cluster analysis by sequence alignments yielded a 100% sequence similarity since the sequence region from *amiA–amiD* was not recognized by antiSMASH to be part of the amicetin BGC (**Figures 6A** vs. **B**). Plicacetin (**Figure 6C**) and amicetin (**Figure 6D**) are disaccharide pyrimidine nucleoside antibiotics with a broad-spectrum antibacterial (especially against *Mycobacterium tuberculosis*) and antiviral activity. They act as peptidyl transferase inhibitors and thus inhibit protein synthesis. Amicetin consists of the two deoxysugar moieties, D-amosamine and D-amicetose, as well as cytosine, *p*-aminobenzoic acid (PABA), and a terminal methylserine moiety, whereby the latter moiety is missing in plicacetin (Zhang G.G. et al., 2012; Korzybski et al., 2013). The gene cluster analysis of SHP22-7 revealed that the PapR2-like motif is located directly in front of the *orf pliA* (**Figure 6B**) and shows a rather weak sequence identity of 65.5% to the PapR2 consensus motif (**Figure 2A**). The same motif is present upstream of *amiA* in *S. vinaceusdrappus*. The *pliA* gene presents 99.75% gene nucleotide sequence identity to *amiA* of *S. vinaceusdrappus*, which translates to a 100% amino acid sequence identity among the predicted gene products. In *S. vinaceusdrappus amiA* is the first gene of the amicetin BCG and encodes a putative 4-amino-4-deoxychorismate lyase, which is suggested to catalyze the conversion from 4-amino-4-deoxychorismate to PABA (Zhang G.G. et al., 2012). Remarkably, all genes in the amicetin gene cluster of *S. vinaceusdrappus* and the amicetin-like gene cluster of SHP22-7 are organized in one direction, suggesting a unidirectional transcription. In this context, it would make sense that regulatory activation targets the promoter of the first gene of the unidirectional BGC. In order to

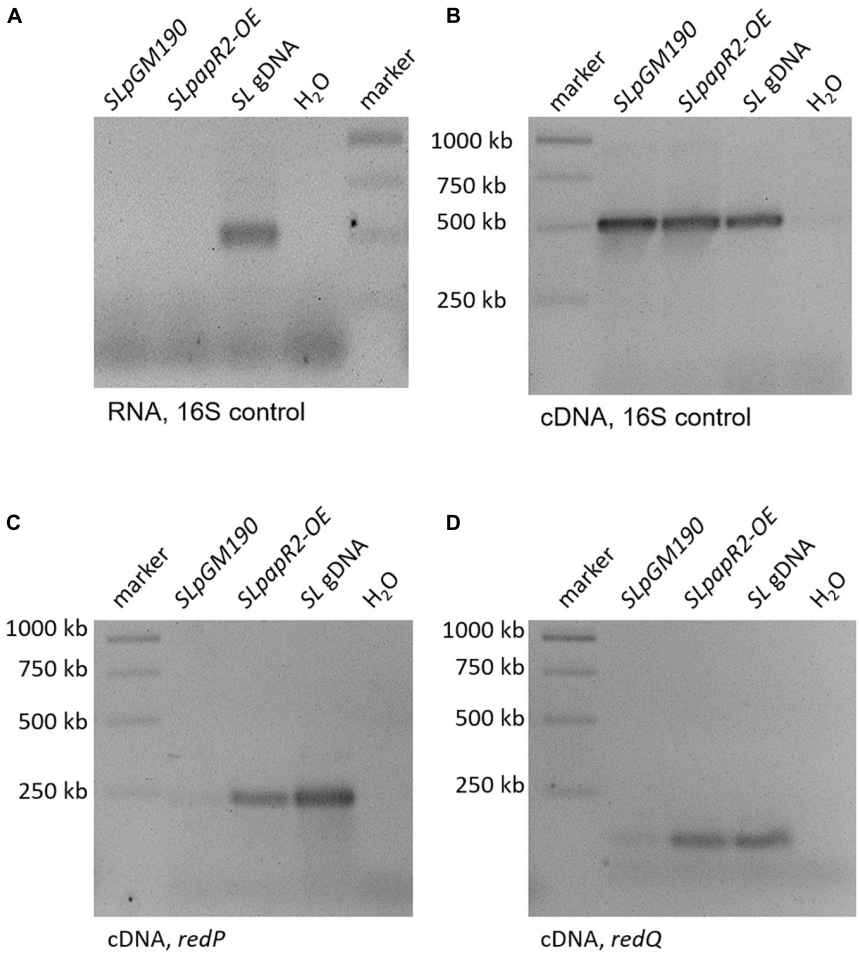

FIGURE 3 | Transcriptional analysis of samples from *SLpGM190* and *SLpapR2-OE* after 168 h. gDNA of *S. lividans* was used as internal positive control (SL gDNA) and water as internal negative control. RT-PCR analysis with RNA samples as template and 16S-specific primers in order to test the absence of DNA **(A)**. RT-PCR analysis with cDNA samples as template and 16S-specific primers in order to test for successful cDNA synthesis **(B)**. RT-PCR analysis of the gene *redP* and in the strains SLpGM190 and SLpapR2-OE **(C)**. RT-PCR analysis of the gene *redQ* and in the strains SLpGM190 and SLpapR2-OE **(D)**.

find out if PapR2 can bind to the *pliA* promoter region, EMSAs were performed with the PapR2 protein and the *pliA* upstream region containing the PapR2 consensus sequence. However, no shifted band was detected in these assays (data not shown). Thus, it might be that the motif is not functional at all and does not constitute a SARP binding motif. It could also be that due to the less conserved PapR2 consensus sequence, the motif is not functional in such an *in vitro* assay. The presence of a SARP consensus sequence would hint for a pathway-specific regulatory gene located within the amicetin(-like) BGC. However, a SARP-type regulatory gene has not been identified in any of the amicetin(-like) clusters from SHP22-7 nor *S. vinaceusdrappus* (**Table 1**; Zhang X. et al., 2012). Overall, six SARP genes have been identified in total within the SHP22-7 genome (**Supplementary Table S2**). All of them are part of BGCs (clusters 3, 6, 10, and 15). Cluster 15 harbors three SARP genes, whereas the other BGCs each contain one SARP gene (**Table 1**). Furthermore, putative SARP binding motifs have been found within the promoter regions of the BGCs (**Table 1** and **Supplementary Table S2**). It might be possible that one of these SARP-type regulators plays a role in *trans*-activating amicetin cluster transcription. So far, regulation of amicetin biosynthesis is not understood. In *S. vinaceusdrappus* three genes [*orf*(*-3*), *orf*(*-2*), *amiP*] have been identified, which encode for putative transcriptional regulators, whereby *orf*(*-3*) and *orf*(*-2*) seem not to be part of the amicetin BGC and *amiP* codes for TetR-like transcriptional regulator, which usually function as repressors of antibiotic biosynthesis (Zhang G.G. et al., 2012). Thus far, it cannot be excluded that also *trans*-acting regulator(s) are involved in the regulation of amicetin biosynthesis.

PapR2 Activates Plicacetin Production in SHP22-7

To investigate if an amicetin(-like) antibiotic is produced by SHP22-7, we analyzed methanolic extracts of cell culture samples from SHP22-7*papR2-OE* by HPLC/MS. To analyze if production is influenced by *papR2* expression, extracts from samples of

TABLE 1 | Secondary metabolite gene clusters of *Streptomyces* sp. SHP22-7 as predicted by antiSMASH 4.0 with an indication of the presence of cluster-situated SARP genes (count), predicted SARP proteins with amino acid sequence homology to PapR2 (I = identity, S = similarity), as well as identified SARP-type motifs.

Cluster	Type of secondary metabolite gene cluster	Similarity to known cluster	Localization	Cluster-situated SARP gene	Sequence homology to PapR2 I/S	SARP consensus motif(s) identified
1	Terpene	Albaflavenone (100%)	Contig 1 49588-70841	–		–
2	T2PKS	Spore pigment (66%)	Contig 1 121312-163740	–		–
3	Other	Granaticin (8%)	Contig 2 304806-348126	+ (1)	41/52%	+
4	Melanin	Melanin (60%)	Contig 3 1-5936	–		–
5	Ectoine	Ectoine (100%)	Contig 4 119873-130271	–		–
6	NRPS	Phosphonoglycans (5%)	Contig 5 129226-170626	+ (1)	31/44%	+
7	Bacteriocin	–	Contig 7 213837-225168	–		–
8	Terpene	–	Contig 7 240589-262769	–		–
9	Other	Amicetin (75%)	Contig 10 129625-170245	–		+
10	NRPS	Calcium dependent antibiotic (47%)	Contig 10 243082-272180	+ (1)	38/56%	+
11	T3PKS	Herboxidiene (8%)	Contig 11 20911-62017	–		–
12	Siderophore	Desferrioxamine B (100%)	Contig 13 127488-139260	–		–
13	Indole	Antimycin (20%)	Contig 17 55086-76126	–		–
14	Terpene	Carotenoid (36%)	Contig 17 133951-147999	–		–
15	T2PKS-Butyrolactone	Fluostatin (26%)	Contig 19 32007-96281	+ (3)	41/59% 67/76% 40/51%	+
16	Terpene	Hopene (84%)	Contig 20 8526-35239	–		–
17	Lanthipeptide	–	Contig 21 82417-98812	–		–
18	T1PKS-NRPS	Candicidin (90%)	Contig 22 1-86799	–		–
19	Arylpolyene-NRPS	Lipopeptide (29%)	Contig 24 1-40688	–		–
20	Siderophore	Grincamycin (8%)	Contig 24 46763-57062	–		–
21	T1PKS	Oligomycin (44%)	Contig 32 4049-49007	–		–
22	OtherKS	Sanglifehrin A (13%)	Contig 42 1-35910	–		–
23	Bacteriocin	Informatipeptin (57%)	Contig 44 22689-32904	–		–
24	NRPS	Coelichelin (27%)	Contig 59 1-16803	–		–
25	Lanthipeptide	–	Contig 96 1-5597	–		–

+, cluster contains gene/motif; –, cluster does not contain gene/motif.

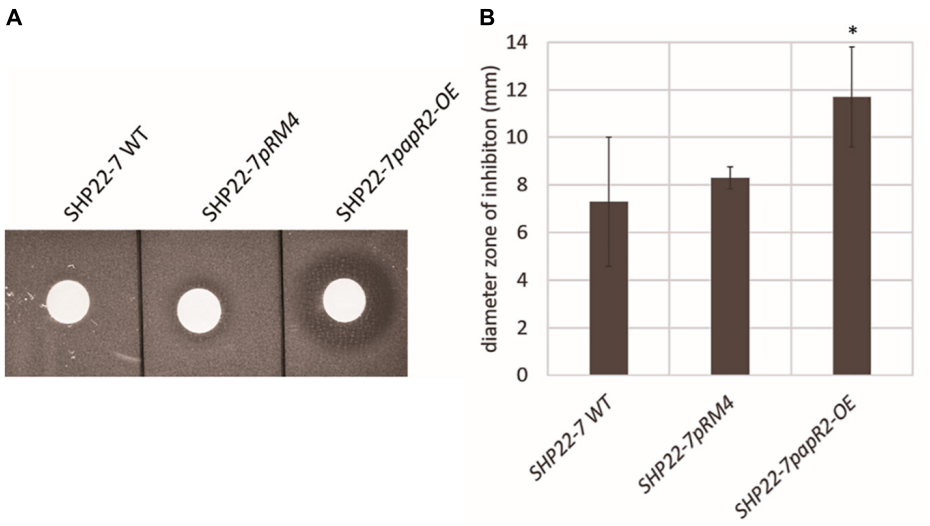

FIGURE 4 | One representative example of culture extracts from SHP22-7 WT, SHP22-7*pRM4*, and SHP22-7*papR2-OE*, respectively, against *B. subtilis*. Filter disk diffusion assay; red arrow indicates inhibition zone **(A)**. Graphical representation of the inhibition zone diameters (mm) from 10 independent biological replicates (n = 10), * indicates significance **(B)**.

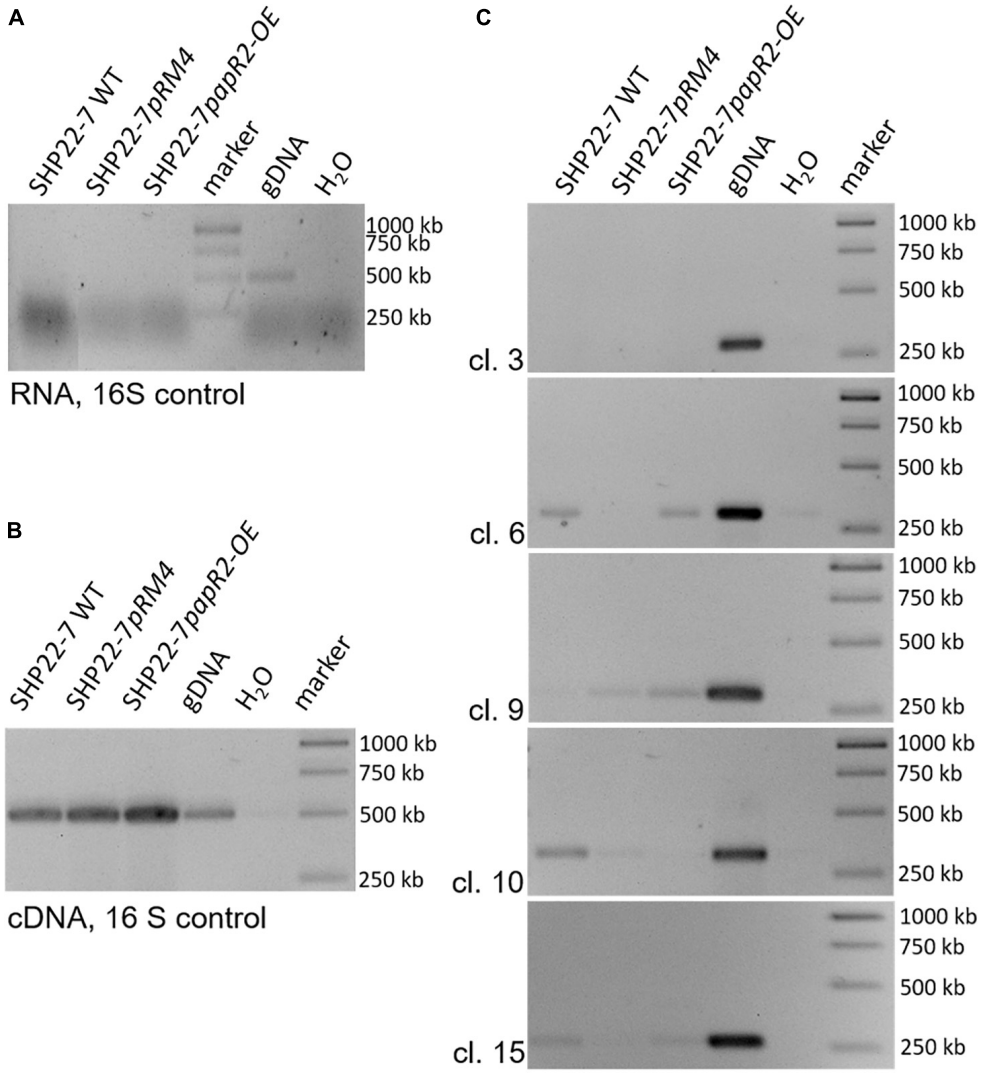

FIGURE 5 | Transcriptional analysis of the SHP22-7 strains SHP22-7 WT, SHP22-7pRM4, and SHP22-7papR2; gDNA of SHP22-7 was used as internal positive (gDNA) and water as internal negative control. The data are representative for four independent experiments. RT-PCR analysis with RNA as template and 16S-specific primers **(A)**. RT-PCR analysis with cDNA and 16S-specific primers **(B)**. Transcriptional analysis of the SARP motif containing gene clusters (cl.) 3, 6, 9, 10, and 15 with samples from SHP22-7 WT, SHP22-7pRM4, and SHP22-7papR2 **(C)**.

SHP22-7*pRM4* and SHP22-7 WT served as references. For these analyses we used the second culture samples obtained from SHP22-7*papR2-OE*, SHP22-7*pRM4*, and SHP22-7 WT, respectively (see above). Based on comparisons with an in-house substance database, HPLC analysis revealed the presence of amicetin [retention time (RT) 4.0 min], plicacetin (RT 4.8 min), and a plicacetin isomer (RT 5.6 min) in all three samples (**Figure 7A**). The identity of the compounds was verified by MS/MS analysis (amicetin *m/z* 617.1 [M-H]; plicacetin *m/z* 516.1 [M-H]; plicacetin isomer *m/z* 516.1 [M-H]) (**Figure 7B**; for HRMS data see **Supplementary Figures S3**, **S4**). Comparisons between the HPLC spectra from samples of SHP22-7*papR2-OE*, SHP22-7*pRM4*, and SHP22-7 WT displayed that peak intensities were especially increased for plicacetin (mAU 605) and the plicacetin isomer (mAU 259) in samples of SHP22-7*papR2-OE* compared to samples of SHP22-7pRM4 [plicacetin (mAU 120), plicacetin isomer (mAU 97)] and SHP22-7 WT [plicacetin (mAU 66), plicacetin isomer (mAU 57)] (**Figure 7C**). Thus, it could be shown that *papR2* expression in SHP22-7 activates explicitly plicacetin biosynthesis, whereas amicetin biosynthesis seems not to be affected. Overall, with this result it could be confirmed that PapR2 induced cluster 9 transcription, which resulted in an increased plicacetin production. Thus, it can be concluded that the increased bioactivity of SHP22-7*papR2-OE* samples against *B. subtilis* arises from the increased production of the nucleoside antibiotic plicacetin. However, since no direct interaction of the PapR2 regulator with the amicetin promoter region could be shown by EMSA analysis, it cannot be deduced if the activation effect is a direct or an indirect one. The SARP consensus motif harbors the central TCA triad, which is also present in the Pho

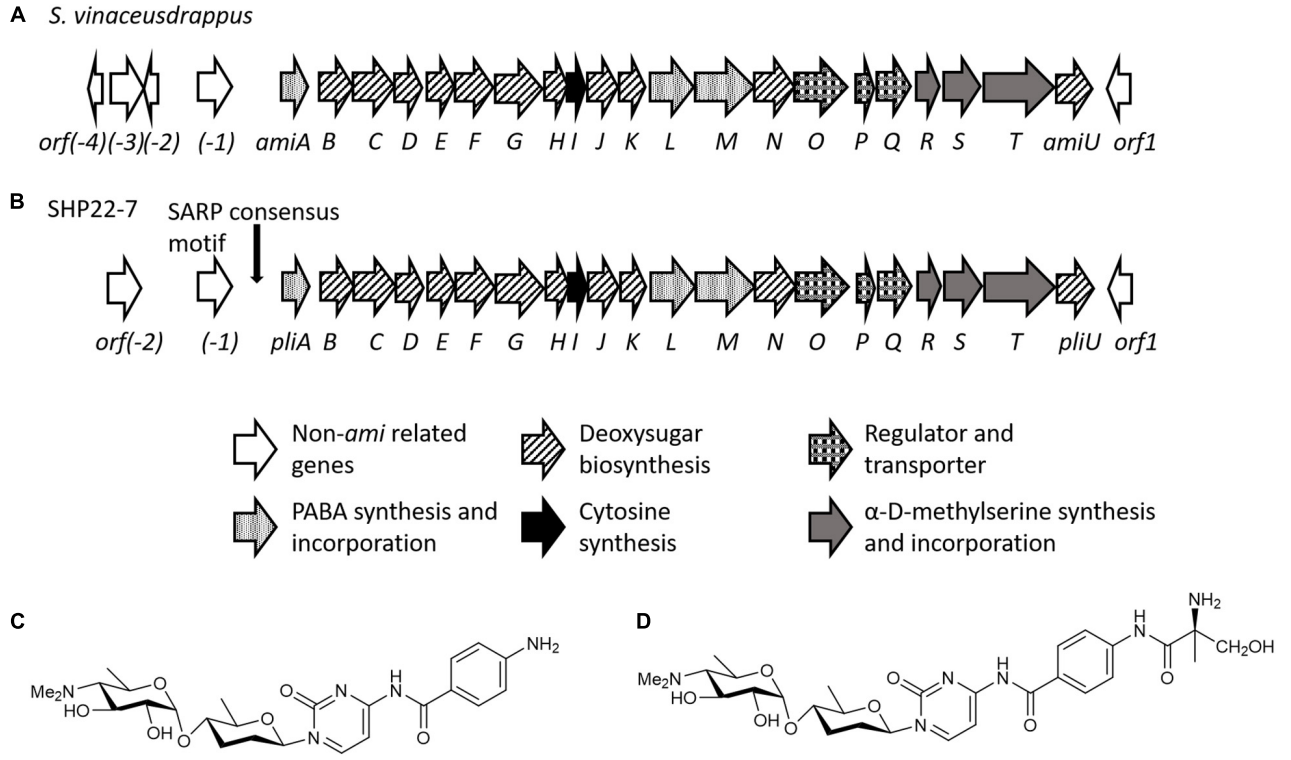

FIGURE 6 | Schematic organization of the amicetin biosynthetic gene cluster of *S. vinaceusdrappus* according to Zhang G.G. et al. (2012) **(A)** and of SHP22-7 **(B)**. Chemical structures of plicacetin **(C)** and amicetin **(D)**.

box (GTTCACC), resembling the target site of the phosphate control two-component system PhoP/PhoR (Martin and Liras, 2020). This sequence region is also known to be bound by the large size SARP regulator AfsR (Martin and Liras, 2020). Additionally, the central TCA triad can be present in binding motifs recognized by the nitrogen regulator GlnR or the DmdR1 (Flores and Martín, 2004; Martin and Liras, 2020). Cross-talk between different transcriptional regulators via the interaction of the same binding sites have been shown before (Martín et al., 2011; Martin and Liras, 2020). Thus, it is also possible that transcriptional activation of the amicetin BGC is an effect from multiple regulatory interactions.

SARP-Type Regulatory Genes Are Widespread in BGCs From Diverse Actinobacteria

Of the top 10 genera containing SARP-type regulators in the antiSMASH database 2 (Blin et al., 2019), 9 belong to the phylum Actinobacteria. Broken up by genus, 98% of *Streptomyces* (611/625), 81% of *Nocardia* (78/96), 100% of *Salinispora* (72/72), 100% of *Micromonospora* (62/62), and 97% of *Amycolatopsis* (38/39) genomes harbor SARP-type regulatory genes, showing their prevalence in filamentous Actinobacteria. On the other hand, only 42% of *Mycobacterium* (115/276) species have SARP-type regulators. Outside of Actinobacteria, mainly Proteobacteria have hits for the SMCOG1041 profile, but mostly lack hits for the HTH motif domain or the BTAD (transcriptional activator domain) [e.g., 6% (79/1236) of *Pseudomonas* hit the smCoG profile, but none of them contain a BTAD match]. Thus, SMCOG1041 profiles from Proteobacteria may not represent typical SARP-type regulators.

Of the total of 6525 proteins containing a hit against any of the four SARP-related PFAM domains, 3289 (50%) are from the order *Streptomycetales* (**Figure 8**). These again break down into 47% "small" SARPs (only containing the HTH and BTAD domains) and 36% "large" SARPs (also containing the NB-ARC and/or TPR domains). The remaining proteins miss the HTH and/or BTAD domains, likely an artifact of bad sequencing data in published draft genomes. The overrepresentation of SARP-type regulators in *Streptomycetales* may also be explained by the higher abundance of available genomes in the database. *Pseudonocardiales* cover 17% of the SARP-type proteins (1080/6525). 31% (330/1080) are "small" SARPs and 39% (421/1080) "large" SARPs. In *Micromonosporales*, accounting for 13% (822/6526) of the dataset, 30% (244/822) are "small" SARPs, and 40% (330/822) are "large" SARPs (**Figure 8**). Interestingly, *Micromonosporales* is the only order to contain a significant amount (22%, 184/882) of SARP-type proteins only containing a hit against BTAD without hitting the HTH domain, suggesting a different subfamily of transcriptional activator. Furthermore, SARP genes were found to be present in various different types of BGCs with a prominent abundance in NRPS

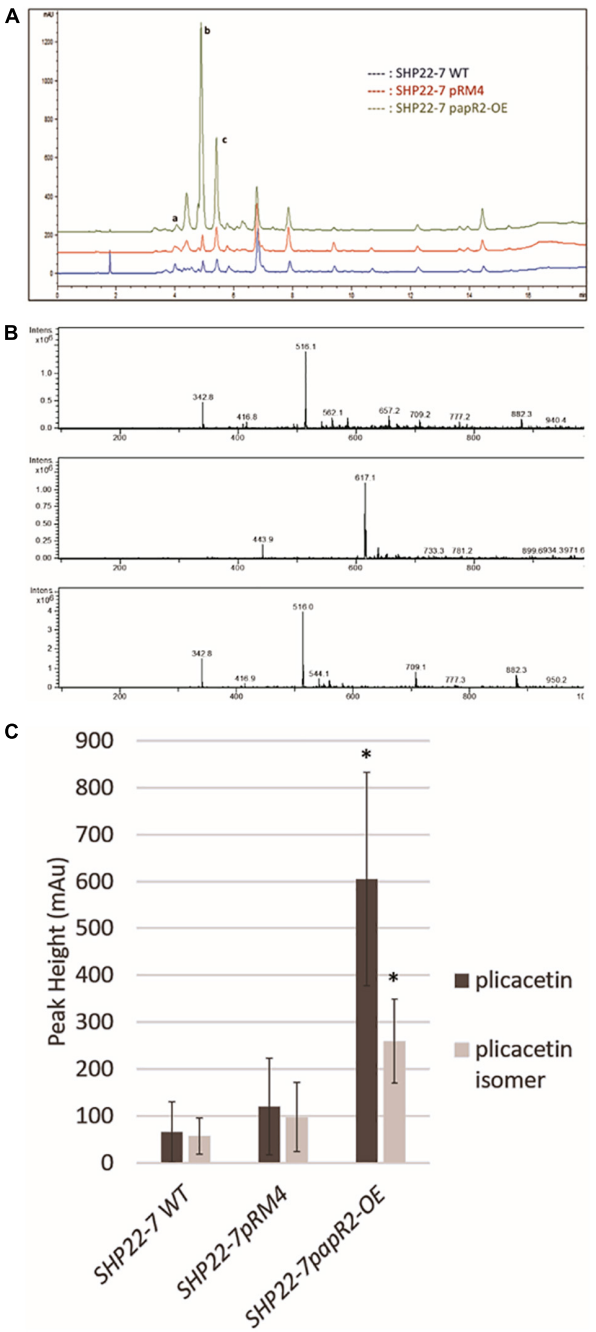

FIGURE 7 | Plicacetin and plicacetin isomer production in the strains SHP22-7 WT, SHP22-7*pRM4*, and SHP22-7*papR2-OE*, respectively. HPLC profile of all three strains. Peaks in the HPLC spectrum representing amicetin are marked with a, plicacetin marked with b, and plicacetin isomer marked with c **(A)**. Mass spectra of plicacetin **(Upper)**, amicetin **(Middle)**, and a plicacetin isomer **(Lower) (B)** isolated from SHP22-7 WT. Graphical representation of production levels of plicacetin and plicacetin isomer in each strain. *n* = 10; * means significance **(C)**.

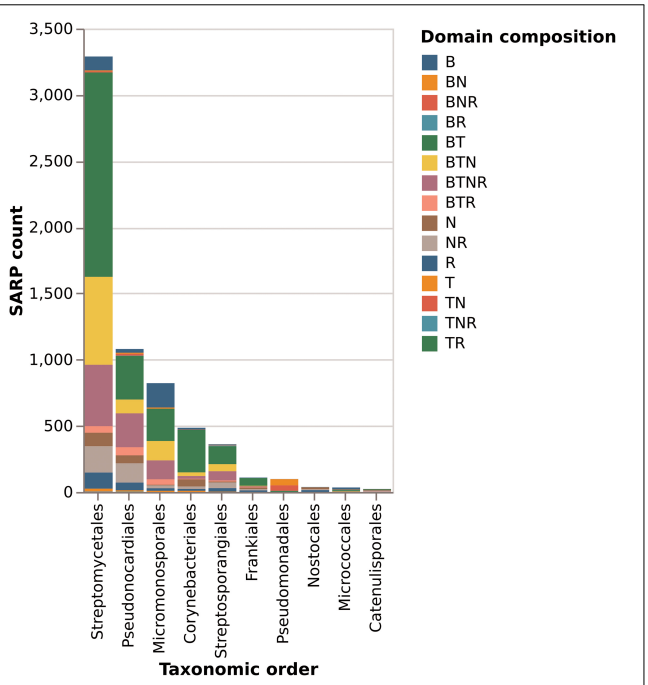

FIGURE 8 | Domain composition of SARP-like proteins in the 10 orders with most protein hits. Letters in the legend denote which domains are present. B is the BTAD domain, T is the HTH-motif DNA binding domain, N is the NB-ARC domain of unknown function, and R is the tetratricopeptide repeat domain.

and PKS gene clusters (**Figure 9**), which however might also be associated with the higher frequency of these cluster types in the database.

DISCUSSION

Regulation is the screw plug to unlock the biosynthetic potential of natural compound producers. Here, we showed that heterologous expression of the SARP-type regulatory gene *papR2* in the foreign host *S. lividans* leads to transcriptional activation of the silent Red BGC. Since SARP regulators show a comparable protein architecture and bind to similar recognition sequences at the DNA, they can substitute for their regulatory functions as exemplified for PapR2 and RedD. This is also underpinned by a previous study, where it has been shown that overexpression of the SARP gene *vlml* from the valanimycin producer *Streptomyces viridifaciens* in a *redD* mutant of *S. coelicolor* M512 restores Red production, demonstrating that *vlmI* can complement a *redD* mutation (Garg and Parry, 2010). Besides having gained indications for such kind of cross-regulation, our data also contribute to a better understanding of the regulation of Red biosynthesis in general. So far, there have been only bioinformatic predictions on potential regulatory binding regions within the Red BGC (Iqbal et al., 2012). Here, we provide first experimental evidence by EMSA studies and (q)RT-PCR experiments for the SARP-binding capability to promoter regions (P*redP*, P*redQ*) of the Red BGC. These data clearly show that *redP* and *redQ* are direct targets of a SARP-driven regulation during Red biosynthesis.

In the literature SARPs often are designated as "pathway-specific" transcriptional activators, which means that they control

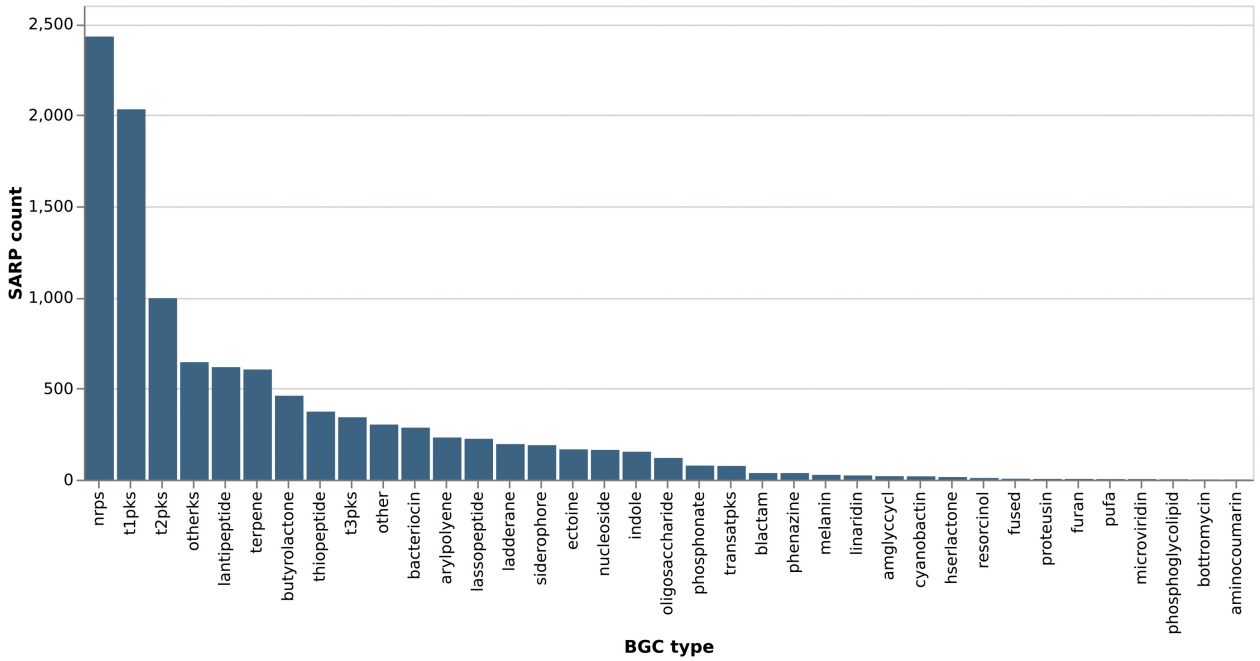

FIGURE 9 | Distribution of SARP-like genes across different biosynthetic gene cluster types. SARP-like genes in hybrid clusters are counted once per type they occur in (e.g., a SARP in a NRPS/PKS type I hybrid cluster would count for both "nrps" and "t1pks").

the expression of an individual BCG. However, SARPs indeed can have activating effects on the biosynthesis of different substances. One example occurring in nature is provided by the SARP-type regulator CcaR from *S. clavuligerus*, which activates the cephamycin gene cluster, where *ccaR* is part of, as well as the adjacent clavulanic acid gene cluster (Pérez-Llarena et al., 1997). Thus, the term "pathway-specific" is not accurate for SARPs and should better be replaced by "cluster-situated" as suggested previously (Huang et al., 2005; Liu et al., 2013). Our results show that SARPs have the potential to control different BGCs, when present in different producer organisms: The SARP regulator PapR2 activates the transcription of the corresponding pristinamycin gene cluster in *S. pristinaespiralis* (Mast et al., 2015) but it also affects different antibiotic BGCs, such as Red and plicacetin, when expressed in foreign strains, such as *S. lividans* or SHP22-7, respectively. Especially, in SHP22-7 *papR2* expression significantly improved plicacetin production and as a result also led to an improved production of a so far not further characterized plicacetin derivative. This derivative is dissimilar from the plicacetin isomer since it shows a different retention time in HPLC analysis (∼6.5 min) (**Figure 9**) and a smaller mass of 481 *m*/*z* (data not shown). If PapR2-driven plicacetin gene cluster activation is a direct or an indirect regulatory effect is unclear at the moment since no direct interaction of the PapR2 regulator with the plicacetin gene cluster could be demonstrated. Furthermore, no SARP gene is present in the plicacetin gene cluster. However, SARP genes have been found in four other SHP22-7 BGCs, which would allow the possibility that one of these regulators may act as the natural activator of amicetin/plicacetin biosynthesis. A similar untargeted effect has been observed when the PAS-LuxR-type regulator PimM from *S. natalensis* was expressed in *S. clavuligerus*, which led to an improved production of cephamycin, clavulanic acid, and tunicamycins (Martínez-Burgo et al., 2019). For tunicamycin production the regulatory effect upon *pimM* expression is unclear. *pimM* expression improved tunicamycin production without affecting tunicamycin gene cluster transcription. Besides, no pathway-specific activator has been identified within the tunicamycin BGC. In this study, the authors speculated that PimM may exert its effect on tunicamycin production, e.g., due to a positive influence on precursor supply (Martínez-Burgo et al., 2019). Furthermore, they found that PimM from *S. natalensis* shows some similarity to a PimM-like regulator, encoded by a gene of the *S. clavuligerus* genome (Martínez-Burgo et al., 2019). Thus, also in these analyses the non-native PimM regulator may have occupied the regulatory role of a homologous natural regulator and along this path provoked antibiotic production. Interspecies cross-regulation has also been shown for the LuxR-family type (LAL) regulator PikD. In *Streptomyces. venezuelae* PikD regulates the expression of pikromycin. The heterologous expression of the *pikD* homologous genes *rapH* and *fkbN* from *Streptomyces hygroscopicus* in *S. venezuelae* increased the production of the antibiotic pikromycin. LAL-family regulators resemble SARP-type regulators in the ATP-binding motif at the N-terminus and in the DNA-binding motif to some extent, which in both regulator types consists of an HTH-motif (Mo and Yoon, 2016).

The fact that SARP genes are widely distributed among actinomycetes, where they occur in many different types of secondary metabolite gene clusters makes them good candidates

to be used as engineering tools for the activation of BCGs. Especially in *Streptomyces* they are predominant occurring with a ∼100% abundance. Interestingly, there might be a phylogenetic grouping of different SARP regulator types from different actinobacterial genera. If so this would raise the question if there is a co-evolution of certain regulator genes with their corresponding gene clusters. Besides that, the statistical analysis revealed that there is a different abundance of different types of SARP regulators, belonging either to the small SARPs (<400 amino acids) with only HTH and BTAD domains (e.g., ActII-ORF4 or RedD) or the large SARPs, which contain an additional NTPase domain and/or a conserved C-terminal TPR domain of unknown function (∼1000 residues) (Liu et al., 2013). Overall small SARP type regulators are more abundant in actinomycetes than the large ones (**Figure 8**). Besides, more experimental data are available on small SARP-guided regulations, and the unclear function of the additional domains included in the large SARPs likely causes further constraints in the function of the regulatory activity. Thus, we propose that especially representatives from the group of small SARP regulators are good candidates to be used for activation approaches. As outlined above, SARP regulators can bind to recognition sequences, which occur at various positions within the promoter of the target genes. The variety of binding sites may also reflect the diversity of SARP-type activators. Thus, it would be interesting to bioinformatically group the SARP regulators by taking into account their DNA-binding domains, which may provide a better picture of the different SARP subsets.

That SARP expression can lead to the activation of silent gene cluster expression has been shown in a recent study. Here, the aim was to activate some of the more than 20 cryptic gene clusters from *Streptomyces* sp. MSC090213JE08 (Du et al., 2016). In this study the authors combined an OSMAC approach with the expression of several native SARP genes from *Streptomyces* sp. MSC090213JE08. Thereby, four of the seven generated recombinant SARP expression strains produced nine metabolites that were hardly detected in the control strains. Expression of one of the SARP genes (SARP-7) in *Streptomyces* sp. MSC090213JE08 led to the production of the novel polyene-like substance ishigamide (Du et al., 2016). This study successfully showed the potency of a SARP-guided silent gene cluster activation. However, the drawback of this approach is that several conditions (number of different culture media) need to be tested and a set of genetic manipulations (cloning of each individual SARP gene) has to be done in order to provoke cluster activation. Further experimental setup is then linked to untargeted laborious compound purifications and analytics. Indeed, this is also the main problem of several other efforts to activate secondary metabolite synthesis in actinomycetes as outlined above. Thus, based on our gained knowledge we propose a targeted SARP-guided strategy for the activation of BGCs in actinomycetes. Our strategy involves (1) prioritization of strains with SARP genes and SARP binding motifs in the BGC. In our experimental setup we focus on SARP genes that encode for predicted proteins with high similarity to PapR2 (>55% amino acid sequence similarity), as well as the occurrence of a PapR2 consensus motif within the promoter region(s) of the SARP-gene containing BGCs, (2) introduction of a SARP-expression construct [in our approach this means heterologous expression of the PapR2 regulator with the help of the pGM190/papR2 and/or pRM4/papR2 expression construct(s)], (3) comparative biological and chemical analyses of SARP-activated expression samples with samples from non-manipulated strains. In our study we focus on PapR2 as the activator brick, however, of course any other type of SARP regulator with a known consensus sequence might be used as the basis for such an activation approach. For sure there might be limitations in such an activation strategy, e.g., transcriptional activation may fail due to SARP-specificity reasons or a lack of a broader set of well-characterized SARP regulators to be tested as candidate elicitors. However, here we disclose a screening idea or a kind of dragnet investigation, which does not aim to cover all possible SARP-regulated clusters but highlights the most probable ones to be activated upon SARP expression. Our strategy has two main advantages: (1) In contrast to completely unspecific cluster activation efforts, such as addition of general elicitors, co-culture approaches or the OSMAC strategy, our approach is more targeted, as it focuses only on a defined set of BGCs, namely those ones that are bioinformatically predicted to be under SARP control. Applying combinatory bioinformatics, such as antiSMASH and PatScan allows to directly identify the associated BGC. In addition, the detection of the activated compound is more straightforward if the outline of the structure can be deduced from the cluster sequence. (2) In contrast to activation strategies that are absolutely specific for the respective BGC, e.g., heterologous expression of the BGC, introduction of artificial promoters in front of the BGC, or the manipulation of cluster-situated regulators, no major effort to manipulate the genome is necessary with our procedure since it only involves cloning of one SARP gene-containing expression construct into the respective strain(s) of interest. These major benefits make the activation of BGCs by SARPs a promising strategy to be applied on putative antibiotic producers.

DATA AVAILABILITY STATEMENT

The complete genome sequence of *S. lividans* T7 has been deposited at DDBJ/ENA/GenBank under the accession number ACEY00000000. The main genome scaffold sequence of SHP22-7 has been deposited at DDBJ/ENA/GenBank under the accession number QXMM00000000. Raw sequencing data are available under SRA accession number PRJNA489221.

AUTHOR CONTRIBUTIONS

YM generated the strains *SLpGM190* and *SLpapR2-OE*, carried out the bioinformatic analyses, and designed, supervised, and coordinated the study. KB performed the statistical analyses. JK created the vector pRM4/papR2 while the vector was inserted in SHP22-7 by IH. IH tested the bioactivity. JK performed all qualitative and quantitative transcriptional analyses. AK and IH performed the HPLC analyses. YM, JK, IH, and KB wrote the manuscript.

FUNDING

We gratefully acknowledge the funding received from the BMBF German–Indonesian Cooperation project NAbaUnAk. The study was supported by a DAAD scholarship given to JK and a scholarship from the Indonesian Ministry for Research and Technology for IH.

ACKNOWLEDGMENTS

We thank Vera Kübler for performing the EMSAs. We also thank Regina Ort-Winklbauer from the University of Tübingen for excellent technical assistance. We acknowledge help from Harald Gross, Nico Ortlieb, and Dorothee Wistuba from the University of Tübingen for High-Resolution Mass Spectrometric analysis. Finally, we thank Puspita Lisdiyanti and Shanti Ratna Komala from the Indonesian Institute of Sciences for providing us with the Indonesian strain isolate SHP 22-7.

SUPPLEMENTARY MATERIAL

The Supplementary Material for this article can be found online at: https://www.frontiersin.org/articles/10.3389/fmicb.2020.00225/full#supplementary-material

REFERENCES

Aigle, B., Pang, X., Decaris, B., and Leblond, P. (2005). Involvement of AlpV, a new member of the *Streptomyces* antibiotic regulatory protein family, in regulation of the duplicated type II polyketide synthase *alp* gene cluster in *Streptomyces ambofaciens*. *J. Bacteriol.* 187, 2491–2500. doi: 10.1128/JB.187.7.2491-2500.2005

Arias, P., Fernández-Moreno, M. A., and Malpartida, F. (1999). Characterization of the pathway-specific positive transcriptional regulator for actinorhodin biosynthesis in *Streptomyces coelicolor* A3(2) as a DNA-binding protein. *J. Bacteriol.* 181, 6958–6968. doi: 10.1128/jb.181.22.6958-6968.1999

Baltz, R. H. (2017). Gifted microbes for genome mining and natural product discovery. *J. Ind. Microbiol. Biotechnol.* 44, 573–588. doi: 10.1007/s10295-016-1815-x

Bate, N., Stratigopoulos, G., and Cundliffe, E. (2002). Differential roles of two SARP-encoding regulatory genes during tylosin biosynthesis. *Mol. Microbiol.* 43, 449–458. doi: 10.1046/j.1365-2958.2002.02756.x

Bibb, M. J. (2005). Regulation of secondary metabolism in streptomycetes. *Curr. Opin. Microbiol.* 8, 208–215. doi: 10.1016/j.mib.2005.02.016

Blin, K., Pascal Andreu, V., de los Santos, E. L. C., Del Carratore, F., Lee, S. Y., Medema, M. H., et al. (2019). The antiSMASH database version 2: a comprehensive resource on secondary metabolite biosynthetic gene clusters. *Nucleic Acids Res.* 47, D625–D630. doi: 10.1093/nar/gky1060

Blin, K., Wohlleben, W., and Weber, T. (2018). Patscanui: an intuitive web interface for searching patterns in DNA and protein data. *Nucleic Acids Res.* 46, W205–W208. doi: 10.1093/nar/gky321

Chen, Y., Wendt-Pienkowski, E., and Shen, B. (2008). Identification and utility of FdmR1 as a *Streptomyces* antibiotic regulatory protein activator for fredericamycin production in Streptomyces griseus ATCC 49344 and heterologous hosts. *J. Bacteriol.* 190, 5587–5596. doi: 10.1128/JB.00592-08

Du, D., Katsuyama, Y., Onaka, H., Fujie, M., Satoh, N., Shin-ya, K., et al. (2016). Production of a novel amide-containing polyene by activating a cryptic biosynthetic gene cluster in Streptomyces sp. MSC090213JE08. *ChemBioChem* 17, 1464–1471. doi: 10.1002/cbic.201600167

Fischer, J. (1996). *Entwicklung Eines Regulierbaren Expressionssystems zur Effizienten Synthese Rekombinanter Proteine in Streptomyces Lividans*. Stuttgart: University of Stuttgart. Ph.D. thesis.

Flores, F. J., and Martín, J. F. (2004). Iron-regulatory proteins DmdR1 and DmdR2 of *Streptomyces coelicolor* form two different DNA-protein complexes with iron boxes. *Biochem. J.* 380, 497–503. doi: 10.1042/BJ20031945

Garg, R. P., Ma, Y., Hoyt, J. C., and Parry, R. J. (2002). Molecular characterization and analysis of the biosynthetic gene cluster for the azoxy antibiotic valanimycin. *Mol. Microbiol.* 46, 505–517. doi: 10.1046/j.1365-2958.2002.03169.x

Garg, R. P., and Parry, R. J. (2010). Regulation of valanimycin biosynthesis in *Streptomyces viridifaciens*: characterization of VlmI as a *Streptomyces* antibiotic regulatory protein (SARP). *Microbiology* 156, 472–483. doi: 10.1099/mic.0.033167-0

Handayani, I., Ratnakomala, S., Lisdiyanti, P., Fahrurrozi Kusharyoto, W., Alanjary, M., et al. (2018). Complete genome sequence of *Streptomyces* sp. *strain SHP*22-7, a new species isolated from mangrove of Enggano island. *Indonesia. Microbiol. Resour. Announc.* 7, 1–3. doi: 10.1128/MRA.01317-18

He, X., Li, R., Pan, Y., Liu, G., and Tan, H. (2010). SanG, a transcriptional activator, controls nikkomycin biosynthesis through binding to the *sanN-sanO* intergenic region in *Streptomyces ansochromogenes*. *Microbiology* 156, 828–837. doi: 10.1099/mic.0.033605-0

Horinouchi, S., Suzuki, H., and Beppu, T. (1986). Nucleotide sequence of *afsB*, a pleiotropic gene involved in secondary metabolism in *Streptomyces coelicolor* A3(2) and *Streptomyces lividans*. *J. Bacteriol.* 168, 257–269. doi: 10.1128/JB.168.1.257-269.1986

Hu, H., Zhang, Q., and Ochi, K. (2002). Activation of antibiotic biosynthesis by specified mutations in the *rpoB* gene (encoding the RNA polymerase β subunit) of *Streptomyces lividans*. *J. Bacteriol.* 184, 3984–3991. doi: 10.1128/JB.184.14.3984-3991.2002

Huang, J., Shi, J., Molle, V., Sohlberg, B., Weaver, D., Bibb, M. J., et al. (2005). Cross-regulation among disparate antibiotic biosynthetic pathways of *Streptomyces coelicolor*. *Mol. Microbiol.* 58, 1276–1287. doi: 10.1111/j.1365-2958.2005.04879.x

Iqbal, M., Mast, Y., Amin, R., Hodgson, D. A., Stream Consortium, Wohlleben, W., et al. (2012). Extracting regulator activity profiles by integration of *de novo* motifs and expression data: characterizing key regulators of nutrient depletion responses in *Streptomyces coelicolor*. *Nucleic Acids Res.* 40, 5227–5239. doi: 10.1093/nar/gks205

Kieser, T., Bibb, M. J., Buttner, M. J., Chater, K. F., and Hopwood, D. A. (2000). Practical *Streptomyces* genetics. *John Innes Found. Norwich, Engl.* 3, 260–261. doi: 10.2436/im.v3i4.9291

Korzybski, T., Kowszyk-Gindifer, Z., Kuryłowicz, W., and Paryski, E. (2013). *Antibiotics. Volume 1: Origin, Nature and Properties*. Oxford: Pergamon Press.

Kurniawan, Y. N., Kitani, S., Maeda, A., and Nihira, T. (2014). Differential contributions of two SARP family regulatory genes to indigoidine biosynthesis in *Streptomyces lavendulae* FRI-5. *Appl. Microbiol. Biotechnol.* 98, 9713–9721. doi: 10.1007/s00253-014-5988-9

Lewis, R. A., Laing, E., Allenby, N., Bucca, G., Brenner, V., Harrison, M., et al. (2010). Metabolic and evolutionary insights into the closely-related species *Streptomyces coelicolor* and *Streptomyces lividans* deduced from high-resolution comparative genomic hybridization. *BMC Genomics* 11:682. doi: 10.1186/1471-2164-11-682

Liu, G., Chater, K. F., Chandra, G., Niu, G., and Tan, H. (2013). Molecular regulation of antibiotic biosynthesis in *Streptomyces*. *Microbiol. Mol. Biol. Rev.* 77, 112–143. doi: 10.1128/MMBR.00054-12

Livak, K. J., and Schmittgen, T. D. (2001). Analysis of relative gene expression data using real-time quantitative PCR and the 2-ΔΔCT method. *Methods* 25, 402–408. doi: 10.1006/METH.2001.1262

Lombó, F., Braña, A. F., Méndez, C., and Salas, J. A. (1999). The mithramycin gene cluster of *Streptomyces argillaceus* contains a positive regulatory gene and two repeated DNA sequences that are located at both ends of the cluster. *J. Bacteriol.* 181, 642–647. doi: 10.1128/jb.181.2.642-647.1999

Martin, J., and Liras, P. (2020). The balance metabolism safety net: integration of stress signals by interacting transcriptional factors in *Streptomyces* and related

Actinobacteria. *Front. Microbiol.* accepted 10:3120. doi: 10.3389/fmicb.2019.03120

Martín, J. F., Sola-Landa, A., Santos-Beneit, F., Fernández-Martínez, L. T., Prieto, C., and Rodríguez-García, A. (2011). Cross-talk of global nutritional regulators in the control of primary and secondary metabolism in *Streptomyces*. *Microb. Biotechnol.* 4, 165–174. doi: 10.1111/j.1751-7915.2010.00235.x

Martinez, A., Kolvek, S. J., Hopke, J., Yip, C. L. T., and Osburne, M. S. (2005). Environmental DNA fragment conferring early and increased sporulation and antibiotic production in *Streptomyces* species. *Appl. Environ. Microbiol.* 71, 1638–1641. doi: 10.1128/AEM.71.3.1638-1641.2005

Martínez-Burgo, Y., Santos-Aberturas, J., Rodríguez-García, A., Barreales, E. G., Tormo, J. R., Truman, A. W., et al. (2019). Activation of secondary metabolite gene clusters in *Streptomyces clavuligerus* by the PimM regulator of *Streptomyces natalensis*. *Front. Microbiol.* 10:580. doi: 10.3389/fmicb.2019.00580

Mast, Y., Guezguez, J., Handel, F., and Schinko, E. (2015). A complex signaling cascade governs pristinamycin biosynthesis in *Streptomyces pristinaespiralis*. *Appl. Environ. Microbiol.* 81, 6621–6636. doi: 10.1128/AEM.00728-15

Medema, M. H., Blin, K., Cimermancic, P., de Jager, V., Zakrzewski, P., Fischbach, M. A., et al. (2011). antiSMASH: rapid identification, annotation and analysis of secondary metabolite biosynthesis gene clusters in bacterial and fungal genome sequences. *Nucleic Acids Res.* 39, W339–W346. doi: 10.1093/nar/gkr466

Mo, S., Sydor, P. K., Corre, C., Alhamadsheh, M. M., Stanley, A. E., Haynes, S. W., et al. (2008). Elucidation of the *Streptomyces coelicolor* pathway to 2-undecylpyrrole, a key intermediate in undecylprodiginine and streptorubin B biosynthesis. *Chem. Biol.* 15, 137–148. doi: 10.1016/j.chembiol.2007.11.015

Mo, S., and Yoon, Y. J. (2016). Interspecies complementation of the LuxR family pathway-specific regulator involved in macrolide biosynthesis. *J. Microbiol. Biotechnol.* 26, 66–71. doi: 10.4014/jmb.1510.10085

Newman, D. J., and Cragg, G. M. (2016). Natural products as sources of new drugs from 1981 to 2014. *J. Nat. Prod.* 79, 629–661. doi: 10.1021/acs.jnatprod.5b01055

Novakova, R., Rehakova, A., Kutas, P., Feckova, L., and Kormanec, J. (2011). The role of two SARP family transcriptional regulators in regulation of the auricin gene cluster in *Streptomyces aureofaciens* CCM 3239. *Microbiology* 157, 1629–1639. doi: 10.1099/mic.0.047795-0

Ochi, K., and Hosaka, T. (2013). New strategies for drug discovery: activation of silent or weakly expressed microbial gene clusters. *Appl. Microbiol. Biotechnol.* 97, 87–98. doi: 10.1007/s00253-012-4551-9

Onaka, H., Mori, Y., Igarashi, Y., and Furumai, T. (2011). Mycolic acid-containing bacteria induce natural-product biosynthesis in *Streptomyces species*. *Appl. Environ. Microbiol.* 77, 400–406. doi: 10.1128/AEM.01337-10

Onaka, H., Nakagawa, T., and Horinouchi, S. (2002). Involvement of two A-factor receptor homologues in *Streptomyces coelicolor* A3(2) in the regulation of secondary metabolism and morphogenesis. *Mol. Microbiol.* 28, 743–753. doi: 10.1046/j.1365-2958.1998.00832.x

Pérez-Llarena, F. J., Liras, P., Rodríguez-García, A., and Martín, J. F. (1997). A regulatory gene (*ccaR*) required for cephamycin and clavulanic acid production in *Streptomyces clavuligerus*: amplification results in overproduction of both beta-lactam compounds. *J. Bacteriol.* 179, 2053–2059. doi: 10.1128/jb.179.6.2053-2059.1997

Pulsawat, N., Kitani, S., Fukushima, E., and Nihira, T. (2009). Hierarchical control of virginiamycin production in *Streptomyces virginiae* by three pathway-specific regulators: VmsS. VmsT and VmsR. *Microbiology* 155, 1250–1259. doi: 10.1099/mic.0.022467-0

Rehakova, A., Novakova, R., Feckova, L., Mingyar, E., and Kormanec, J. (2013). A gene determining a new member of the SARP family contributes to transcription of genes for the synthesis of the angucycline polyketide auricin in *Streptomyces aureofaciens* CCM 3239. *FEMS Microbiol. Lett.* 346, 45–55. doi: 10.1111/1574-6968.12200

Rodríguez, H., Rico, S., Díaz, M., and Santamaría, R. I. (2013). Two-component systems in *Streptomyces*: key regulators of antibiotic complex pathways. *Microb. Cell Fact.* 12:127. doi: 10.1186/1475-2859-12-127

Rodríguez, M., Núñez, L. E., Braña, A. F., Méndez, C., Salas, J. A., and Blanco, G. (2008). Identification of transcriptional activators for thienamycin and cephamycin C biosynthetic genes within the thienamycin gene cluster from *Streptomyces cattleya*. *Mol. Microbiol.* 69, 633–645. doi: 10.1111/j.1365-2958.2008.06312.x

Ryding, N. J., Anderson, T. B., and Champness, W. C. (2002). Regulation of the *Streptomyces coelicolor* calcium-dependent antibiotic by *absA*, encoding a cluster-linked two-component system. *J. Bacteriol.* 184, 794–805. doi: 10.1128/jb.184.3.794-805.2002

Salehi-Najafabadi, Z., Barreiro, C., Rodríguez-García, A., Cruz, A., López, G. E., and Martín, J. F. (2014). The gamma-butyrolactone receptors BulR1 and BulR2 of *Streptomyces tsukubaensis*: tacrolimus (FK506) and butyrolactone synthetases production control. *Appl. Microbiol. Biotechnol.* 98, 4919–4936. doi: 10.1007/s00253-014-5595-9

Sambrook, J., Fritsch, E. F., and Maniatis, T. (1989). *Molecular Cloning: a Laboratory Manual*. Berlin: Cold Spring Harbor Laboratory Press.

Santamarta, I., Rodríguez-García, A., Pérez-Redondo, R., Martín, J. F., and Liras, P. (2002). CcaR is an autoregulatory protein that binds to the *ccaR* and *cefD-cmcI* promoters of the cephamycin C-clavulanic acid cluster in *Streptomyces clavuligerus*. *J. Bacteriol.* 184, 3106–3113. doi: 10.1128/JB.184.11.3106-3113.2002

Sheldon, P. J., Busarow, S. B., and Hutchinson, C. R. (2002). Mapping the DNA-binding domain and target sequences of the *Streptomyces peucetius* daunorubicin biosynthesis regulatory protein. *DnrI*. *Mol. Microbiol.* 44, 449–460. doi: 10.1046/j.1365-2958.2002.02886.x

Suzuki, T., Mochizuki, S., Yamamoto, S., Arakawa, K., and Kinashi, H. (2010). Regulation of lankamycin biosynthesis in *Streptomyces rochei* by two SARP genes, *srrY* and *srrZ*. *Biosci. Biotechnol. Biochem.* 74, 819–827. doi: 10.1271/bbb.90927

Takano, E., Gramajo, H. C., Strauch, E., Andres, N., White, J., and Bibb, M. J. (1992). Transcriptional regulation of the RedD transcriptional activator gene accounts for growth-phase-dependent production of the antibiotic undecylprodigiosin in *Streptomyces coelicolor* A3(2). *Mol. Microbiol.* 6, 2797–2804. doi: 10.1111/j.1365-2958.1992.tb01459.x

Takano, E., Kinoshita, H., Mersinias, V., Bucca, G., Hotchkiss, G., Nihira, T., et al. (2005). A bacterial hormone (the SCB1) directly controls the expression of a pathway-specific regulatory gene in the cryptic type I polyketide biosynthetic gene cluster of *Streptomyces coelicolor*. *Mol. Microbiol.* 56, 465–479. doi: 10.1111/j.1365-2958.2005.04543.x

Tanaka, A., Takano, Y., Ohnishi, Y., and Horinouchi, S. (2007). AfsR recruits RNA polymerase to the *afsS* promoter: a model for transcriptional activation by SARPs. *J. Mol. Biol.* 369, 322–333. doi: 10.1016/J.JMB.2007.02.096

Tanaka, Y., and Omura, S. (1990). Metabolism and products of actinomycetes. *An introduction. Actinomycetologica* 4, 13–14. doi: 10.3209/saj.4_13

United Nations Foundation and the Wellcome Charitable Trust, (2016). *Review on Antimicrobial Resistance*. Available at: https://amr-review.org/ (Accessed September 6, 2018).

van Wezel, G. P., White, J., Hoogvliet, G., and Bibb, M. J. (2000). Application of *redD*, the transcriptional activator gene of the undecylprodigiosin biosynthetic pathway, as a reporter for transcriptional activity in *Streptomyces coelicolor* A3(2) and *Streptomyces lividans*. *J. Mol. Microbiol. Biotechnol.* 2, 551–556.

White, J., and Bibb, M. (1997). *bldA* dependence of undecylprodigiosin production in *Streptomyces coelicolor* A3(2) involves a pathway-specific regulatory cascade. *J. Bacteriol.* 179, 627–633. doi: 10.1128/JB.179.3.627-633.1997

Widdick, D. A., Dodd, H. M., Barraille, P., White, J., Stein, T. H., Chater, K. F., et al. (2003). Cloning and engineering of the cinnamycin biosynthetic gene cluster from *Streptomyces cinnamoneus cinnamoneus* DSM 40005. *Proc. Natl. Acad. Sci. U.S.A.* 100, 4316–4321. doi: 10.1073/pnas.0230516100

Wietzorrek, A., and Bibb, M. (1997). A novel family of proteins that regulates antibiotic production in streptomycetes appears to contain an OmpR-like DNA-binding fold. *Mol. Microbiol.* 25, 1181–1184. doi: 10.1046/j.1365-2958.1997.5421903.x

World Health Organization, (2015). *Global Action plan on Antimicrobial Resistance*. Available at: http://www.who.int/antimicrobial-resistance/publications/global-action-plan/en/ (Accessed September 6, 2018).

Worldbank, (2016). *Drug-Resistant Infections: A Threat to our Economic Future*. Available at: http://www.worldbank.org/en/news/press-release/2016/09/18/by-2050-drug-resistant-infections-could-cause-global-economic-damage-on-par-with-2008-financial-crisis (Accessed September 6, 2018).

Wu, X., Jin, L., Zhang, H., Tong, R., Ma, M., and Chen, Y. (2018). Identification of truncated form of NosP as a transcription factor to regulate the biosynthesis of nosiheptide. *FASEB J.* 32, 453–465. doi: 10.1096/fj.201700556R

Xie, Y., Wang, B., Liu, J., Zhou, J., Ma, J., Huang, H., et al. (2012). Identification of the biosynthetic gene cluster and regulatory cascade for the synergistic antibacterial antibiotics griseoviridin and viridogrisein in *Streptomyces griseoviridis*. *ChemBioChem* 13, 2745–2757. doi: 10.1002/cbic.201200584

Ye, S., Braña, A. F., González-Sabín, J., Morís, F., Olano, C., Salas, J. A., et al. (2018). New insights into the biosynthesis pathway of polyketide alkaloid argimycins P in *Streptomyces argillaceus*. *Front. Microbiol.* 9:252. doi: 10.3389/fmicb.2018.00252

Zhang, G. G., Zhang, H., Li, S., Xiao, J., Zhang, G. G., Zhu, Y., et al. (2012). Characterization of the amicetin biosynthesis gene cluster from *Streptomyces vinaceusdrappus* NRRL 2363 implicates two alternative strategies for amide bond formation. *Appl. Environ. Microbiol.* 78, 2393–2401. doi: 10.1128/AEM.07185-11

Zhang, X., Davenport, K. W., Gu, W., Daligault, H. E., Munk, A. C., Tashima, H., et al. (2012). Improving genome assemblies by sequencing PCR products with PacBio. *Biotechniques* 53, 61–62. doi: 10.2144/0000113891

Zhu, H., Sandiford, S. K., and van Wezel, G. P. (2014). Triggers and cues that activate antibiotic production by actinomycetes. *J. Ind. Microbiol. Biotechnol.* 41, 371–386. doi: 10.1007/s10295-013-1309-z

Conflict of Interest: The authors declare that the research was conducted in the absence of any commercial or financial relationships that could be construed as a potential conflict of interest.

The reviewer JA declared a past co-authorship with one of the authors AK to the handling Editor.

frontiers in Microbiology

ORIGINAL RESEARCH
published: 19 February 2020
doi: 10.3389/fmicb.2020.00224

The *Streptomyces coelicolor* Small ORF *trpM* Stimulates Growth and Morphological Development and Exerts Opposite Effects on Actinorhodin and Calcium-Dependent Antibiotic Production

Alberto Vassallo[1,2], Emilia Palazzotto[3], Giovanni Renzone[4], Luigi Botta[5], Teresa Faddetta[1], Andrea Scaloni[4], Anna Maria Puglia[1] and Giuseppe Gallo[1]*

[1] Laboratory of Molecular Microbiology and Biotechnology, STEBICEF Department, University of Palermo, Palermo, Italy, [2] Laboratory of Microbial and Molecular Evolution, Department of Biology, University of Florence, Sesto Fiorentino, Italy, [3] Novo Nordisk Foundation Center for Biosustainability, Technical University of Denmark, Lyngby, Denmark, [4] Proteomic and Mass Spectrometry Laboratory, ISPAAM, National Research Council, Naples, Italy, [5] Dipartimento di Ingegneria, Università di Palermo, Palermo, Italy

OPEN ACCESS

Edited by:
Yvonne Mast,
German Collection of Microorganisms and Cell Cultures GmbH (DSMZ), Germany

Reviewed by:
Marie-Joelle Virolle,
Centre National de la Recherche Scientifique (CNRS), France
Angel Manteca,
Universidad de Oviedo Mieres, Spain

***Correspondence:**
Alberto Vassallo
alberto.vassallo@unipa.it

Specialty section:
This article was submitted to Antimicrobials, Resistance, and Chemotherapy, a section of the journal Frontiers in Microbiology

Received: 16 October 2019
Accepted: 30 January 2020
Published: 19 February 2020

Citation:
Vassallo A, Palazzotto E, Renzone G, Botta L, Faddetta T, Scaloni A, Puglia AM and Gallo G (2020) The Streptomyces coelicolor Small ORF trpM Stimulates Growth and Morphological Development and Exerts Opposite Effects on Actinorhodin and Calcium-Dependent Antibiotic Production. Front. Microbiol. 11:224. doi: 10.3389/fmicb.2020.00224

In actinomycetes, antibiotic production is often associated with a morpho-physiological differentiation program that is regulated by complex molecular and metabolic networks. Many aspects of these regulatory circuits have been already elucidated and many others still deserve further investigations. In this regard, the possible role of many small open reading frames (smORFs) in actinomycete morpho-physiological differentiation is still elusive. In *Streptomyces coelicolor*, inactivation of the smORF *trpM* (SCO2038) – whose product modulates L-tryptophan biosynthesis – impairs production of antibiotics and morphological differentiation. Indeed, it was demonstrated that TrpM is able to interact with PepA (SCO2179), a putative cytosol aminopeptidase playing a key role in antibiotic production and sporulation. In this work, a *S. coelicolor trpM* knock-in (Sco-*trpM*KI) mutant strain was generated by cloning *trpM* into overexpressing vector to further investigate the role of *trpM* in actinomycete growth and morpho-physiological differentiation. Results highlighted that *trpM*: (i) stimulates growth and actinorhodin (ACT) production; (ii) decreases calcium-dependent antibiotic (CDA) production; (iii) has no effect on undecylprodigiosin production. Metabolic pathways influenced by *trpM* knock-in were investigated by combining two-difference in gel electrophoresis/nanoliquid chromatography coupled to electrospray linear ion trap tandem mass spectrometry (2D-DIGE/nanoLC-ESI-LIT-MS/MS) and by LC-ESI-MS/MS procedures, respectively. These analyses demonstrated that over-expression of *trpM* causes an over-representation of factors involved in protein synthesis and nucleotide metabolism as well as a

down-representation of proteins involved in central carbon and amino acid metabolism. At the metabolic level, this corresponded to a differential accumulation pattern of different amino acids – including aromatic ones but tryptophan – and central carbon intermediates. PepA was also down-represented in Sco-*trpM*KI. The latter was produced as recombinant His-tagged protein and was originally proven having the predicted aminopeptidase activity. Altogether, these results highlight the stimulatory effect of *trpM* in *S. coelicolor* growth and ACT biosynthesis, which are elicited through the modulation of various metabolic pathways and PepA representation, further confirming the complexity of regulatory networks that control antibiotic production in actinomycetes.

Keywords: small open reading frame, *trpM*, actinorhodin production, *Streptomyces coelicolor*, cytosol aminopeptidase, calcium-dependent antibiotic, primary and secondary metabolism

INTRODUCTION

Bacteria belonging to the *phylum Actinomycetales* are widely recognized as a very prolific source of biologically active natural compounds, such as antibiotics, immunosuppressants, and herbicides. As reviewed by Palazzotto et al. (2019), different approaches have been adopted to increase production of these molecules in actinomycetes, ranging from metabolic engineering strategies – driving the nutrient catabolism toward an increased supply of precursors – to the modification of the expression of regulators taking directly part in natural product biosynthesis. Besides being studied as a model for investigation of bacterial differentiation, the filamentous Gram-positive bacterium *Streptomyces coelicolor* is a model organism for the study of polyketide antibiotic production in *Actinomycetales*. *S. coelicolor* produces different biologically active metabolites whose biosynthesis has been widely documented – including the blue-pigmented Type II polyketide actinorhodin (ACT), the red-pigmented alkaloid undecylprodigiosin (RED), and the cyclic lipoundecapeptide calcium-dependent antibiotic (CDA) (Liu et al., 2013). In *S. coelicolor*, many aspects of regulatory circuits controlling antibiotic production have been already elucidated although many others still deserve further investigations. As an example, Xu et al. (2019) demonstrated that ACT biosynthesis is affected by a number of genes spread along the chromosome that have been never previously associated with production of ACT. Also, supplementation of specific nutriments exerts a control on *S. coelicolor* morphological and physiological differentiation: as an example, Palazzotto et al. (2015) demonstrated that the supplementation of L-tryptophan (L-Trp) promotes sporulation and stimulates the production of CDA – that contains proteinogenic and non-proteinogenic amino acids, including L-Trp and D-Trp – and the production of ACT – that does not contain any Trp in its structure. In this regard, it is noteworthy that in *S. coelicolor* the expression of genes involved in L-Trp biosynthesis (i.e., *trp* genes) is not repressed by Trp supplementation (Hu et al., 1999; Palazzotto et al., 2016). In addition, *trp* genes are organized either as gene clusters (i.e., *trpC1MBA* and *trpC2D2GE2*) or single genes (i.e., *trpE3*, *trpE1* and *priA*/*trpF*) spread in the genome with *trpC2D2GE2* localized within the CDA biosynthetic gene cluster. So, this gene organization probably allows *S. coelicolor* to express a subset of *trp* genes independently from the others and in response to specific metabolic needs (Xie et al., 2003).

trpM (SCO2038) is part of the *trpC1MBA locus* (Hu et al., 1999; Palazzotto et al., 2016). Because of its small size (just 64 codons), *trpM* and the corresponding protein can be listed as a small open reading frame (smORF) and a small open reading frame-encoded protein (SEP), respectively. smORFs and SEPs have been extensively ignored so far and discovered mostly serendipitously. Nonetheless, they are known to take part in different important cell processes in bacteria – e.g., spore formation, cell division, membrane transport, regulation of enzymatic activities and signal transduction – and nowadays they are gaining more and more attention (Storz et al., 2014; Chu et al., 2015; Chugunova et al., 2018; Delcourt et al., 2018). It was previously demonstrated that TrpM is involved in L-Trp biosynthesis (Palazzotto et al., 2016). Indeed, a *trpM*-knockout mutant strain showed an impaired growth on minimal medium but a normal growth was restored upon addition of L-Trp or its precursors (i.e., L-serine and indole) to the medium. These results were corroborated through a proteomic investigation that compared the *trpM*-knockout mutant and wild type strains, showing that the list of differentially abundant proteins included some components directly involved in L-Trp biosynthesis (Palazzotto et al., 2016). Moreover, the inactivation of *trpM* significantly affected ACT biosynthesis, since the *trpM*-knockout mutant produced 10-fold less ACT than the WT strain. In addition, a pull-down assay using immobilized His-tagged TrpM allowed to identify the putative cytosol L-leucine-aminopeptidase PepA belonging to M17 metalloprotease family (SCO2179), the ribosomal protein S1 (SCO1998) and the ribosomal protein S2 (SCO5624) as probable interacting proteins of this SEP. TrpM and PepA interaction was also demonstrated by bacterial two-hybrid assay (Palazzotto et al., 2016).

In this work, a *trpM* knock-in mutant strain was obtained to characterize the role of TrpM in both morphological differentiation and antibiotic biosynthesis of *S. coelicolor*; results from different comparative experiments on this mutant and wild type strains allowed us to suggest a possible molecular model explaining its mode of action.

MATERIALS AND METHODS

Bacterial Strains, Plasmids, and Cultivation Conditions

All *Streptomyces coelicolor* strains and plasmids used in this work are listed in **Table 1**. Besides, *Escherichia coli* TOP10 (Invitrogen), *E. coli* S17-1 (Simon et al., 1983), and *E. coli* BL21-AI (Invitrogen) were used as described below.

The *Escherichia coli* strains were cultivated in LB medium (Sambrook and Russell, 2001) supplemented with apramycin (50 μg/mL) and ampicillin (100 μg/mL) in the case of strains carrying pIJ8600/pIJ8600:*trpM* and pRSET-B/pRSET-B:*pepA*, respectively, at 37°C and 200 rpm. For *S. coelicolor* cultures, minimal medium [$NaNO_3$ (1 g/L), $MgSO_47H_2O$ (0.5 g/L), KCl (0.5 g/L), KH_2PO_4 (1 g/L), glucose (10 g/L), trace element solution (1 mL/L), pH 7 as adjusted before sterilization] was used; trace element solution contained $FeSO_47H_2O$ (1 g/100 mL), $ZnCl_2$ (1 g/100 mL), and biotin (0.1 g/100 mL). Glucose and trace element solution were added upon sterilization, and solid media were prepared adding bacto agar (15 g/L) to the recipes reported. If not otherwise indicated, 1.5×10^7 spores of *S. coelicolor* strains were spread on solid minimal medium, and incubated at 30°C, for 7 days. In the case of cultures used for RNA, protein and metabolite extraction, a disc of cellophane (Cellophane Membrane Backing, Bio-Rad, United States) was placed on the surface of medium to facilitate mycelium harvesting.

Construction of Recombinant *Streptomyces coelicolor* Strains

DNA manipulation, purification, ligation, restriction analysis, gel electrophoresis and transformation of *E. coli* were performed according to standard techniques (Sambrook and Russell, 2001). *trpM* and *pepA* were amplified from genomic DNA of *S. coelicolor* M145 using the couple of primers trpM_exp_F/trpM_exp_R and pepA_exp_F/pepA_exp_R, respectively, which are reported in **Table 2**. *Taq* DNA Polymerase Recombinant (Invitrogen) was used in both cases, and standard conditions indicated by the manufacturer were adopted. Purified PCR products containing *trpM* and *pepA* genes were digested with restriction enzymes (*Nde*I and *Bam*HI in case of *trpM*, while *Bam*HI and *Hin*dIII were used for *pepA*), and ligated into previously restricted pIJ8600 and pRSET-B vectors, respectively (**Tables 1**, **2**). Ligation mix was then used for transformation of One Shot Chemically Competent *E. coli* TOP10 cells (Invitrogen). The identity of all DNA fragments amplified by PCR was confirmed by DNA sequencing. The pIJ8600 and pIJ8600:*trpM* plasmids were used to transform chemically competent *E. coli* S17-1 cells, which were used as donor ones to transform *S. coelicolor* M145 through a conjugation-based protocol (Kieser et al., 2000). Integration of either pIJ8600 and pIJ8600:*trpM* plasmids in the *attBΦC31* site of the chromosomal DNA of *S. coelicolor* was verified through Southern blotting. The 1480 bp-long restriction fragment derived from digestion of pIJ8600 with *Sty*I was labeled using the Dig High Prime DNA Labeling and Detection Starter kit I (Roche), and used as probe. Chromosomal DNA of *S. coelicolor* strains was digested with *Bam*HI and blotting was performed according to the manufacturer's instructions and Sambrook and Russell (2001).

TABLE 1 | List of strains and plasmids used in this work.

Strain/plasmid	Genotype	References
S. coelicolor M145	SCP1$^-$ SCP2$^-$	Kieser et al., 2000
S. coelicolor M145 carrying pIJ8600 (Sco-EV)	SCP1$^-$ SCP2$^-$*attBΦC31*:pIJ8600	This work
S. coelicolor M145 carrying pIJ8600:*trpM* (Sco-*trpM*KI)	SCP1$^-$ SCP2$^-$*attBΦC31*:pIJ8600:*trpM*	This work
pIJ8600	AprR, TsrR	Sun et al., 1999
pIJ8600:*trpM*	AprR, TsrR	This work
pRSET-B	AmpR	Thermo Fisher Scientific
pRSET-B:*pepA*	AmpR	This work

TABLE 2 | List of primers used in this work.

Primer	Sequence (5′ > 3′)*	Application
trpM_exp_F	CGGACATATGATGACGCTCC	Construction of pIJ8600:*trpM*
trpM_exp_R	CGGGGATCCTCAATACAGC	
pepA_exp_F	ATAAGGATCCGTGACTGCTC	Construction of pRSET-B:*pepA*
pepA_exp_R	GATCAAGCTTCTAGCCCAG	
hrdB_F	GGTCGAGGTCATCAACAAGC	qRT-PCR (*hrdB*)
hrdB_R	CTCGATGAGGTCACCGAACT	
SCO2038_F	CGCTCCCGCTCGTCCC	qRT-PCR (*trpM*)
SCO2038_R	CCTGATGGGGCGCTTGA	
SCO2179_F	CGCCCAGGCCGTGGACA	qRT-PCR (*pepA*)
SCO2179_R	CCACGACGACGGGAGCCT	

**Underlined sequence corresponds to restriction sites.*

Transcriptional Analysis

RNA was extracted using the Illustra RNAspin Midi RNA Isolation Kit (GE Healthcare, United States) and according to the protocol provided by the manufacturer. A two-step protocol was applied for qRT-PCR and the High-Capacity cDNA Reverse Transcription Kit with RNase Inhibitor (Applied Biosystems) was firstly used to convert RNA in cDNA. Thus, Power SYBR Green PCR Master Mix (Applied Biosystems) was used for relative RNA quantification. To this purpose, primers reported in **Table 2** were used, and *hrdB* was chosen as internal standard. Two biological replicates and three technical replicates were used for each condition.

Scanning Electron Microscope Observations

Agar block samples (1 cm × 1 cm × 0.5 cm) were cut from agar-medium cultures, washed three times with phosphate-buffered saline (PBS) for 3 min, and then fixed using 4% v/v glutaraldehyde for 5 min, under gentle agitation. Upon removing of glutaraldehyde solution, samples were washed

with 15% v/v ethanol for 3 min, and incubated at 65°C until obtaining a thin slice. Samples were sputter-coated with gold to avoid electrostatic charging under the electron beam and examined by Scanning Electronic Microscopy (SEM) (Phenom ProX, PhenomWorld).

Bacterial Growth Kinetics

An amount of $\simeq 10^8$ spores of *S. coelicolor* M145 strains carrying pIJ8600:*trpM* (Sco-*trpM*KI) and pIJ8600 (Sco-EV) were inoculated in 25 mL of J medium (Kieser et al., 2000), respectively, using 250 mL baffled flasks, and incubated for 30 h (30°C, 200 rpm in an orbital shaker). Cultures were centrifuged at 3000 × *g* for 15 min, and pellets were washed twice with sterile water. Finally, pellets were resuspended in 50 mL of sterile water, and 3 mL of the obtained suspensions were inoculated in 200 mL of minimal medium (MM), using 1 L baffled flasks, and incubated for 4 days (30°C, 200 rpm in an orbital shaker). Every 12 h, three aliquots of 1 mL were sampled for dry weight determination. Thus, they were centrifuged, decanted, dried at 65°C for 24 h, and finally weighed.

Spore Counting and Antibiotic Assays

An amount of $\simeq 1.5 \times 10^7$ spores of Sco-*trpM*KI and Sco-EV were spread on six MM agar plates, and incubated at 30°C, for 7 days. Three of them were used for spore harvesting and a subsequent serial dilution counting, while the others were used for determination of ACT and undecylprodigiosin production. Antibiotic assays were performed as described by Kieser et al. (2000). In particular, total ACT and undecylprodigiosin (RED) were sequentially extracted by treating cultivations with a 1 N KOH aqueous solution and a 0.5 N HCl/methanol solution, respectively. Insoluble matter, resulting as pellet after 1 N KOH treatment and centrifugation (13000 x *g*, for 15 min), was washed twice with 1 M Tris–HCl, pH 7.5, before treatment with a solution of 0.5 N HCl/methanol 50:50 v/v (Scaffaro et al., 2017). The amount of ACT and RED, whose identity was confirmed by visible absorption spectra (Horinouchi and Beppu, 1984), was spectrophotometrically evaluated at 640 and 530 nm as the mean value measured for three independent cultivations. Concentrations of ACT and RED were determined using molar extinction coefficients of pure compounds. They are ε_{640} = 25320 M^{-1} x cm^{-1} and ε_{530} = 100500 M^{-1} x cm^{-1} for ACT and RED, respectively. CDA production was evaluated according to Kieser et al. (2000) and Palazzotto et al. (2015).

Proteomic Analysis

Proteins were extracted from the mycelium of Sco-*trpM*KI and Sco-EV according to Puglia et al. (1995), and proteomic investigation was conducted by 2D-DIGE as described by Palazzotto et al. (2016), except that 1.3 was chosen as threshold value for the identification of differentially represented proteins. ANOVA test was used to assess the statistical significance of protein abundance fold change, using a $p \leq 0.05$ to consider differentially represented proteins. Proteins were extracted from three biological replicas for each strain and 2D-DIGE procedure was conducted with two technical replicas with a total of six replicas *per* strain. Identification of protein material present in each differentially represented spot was performed by nanoLC-ESI-LIT-MS/MS analysis, which was performed with an LTQ XL mass spectrometer (Thermo Fisher Scientific, United States) equipped with a Proxeon nanospray source connected to an Easy nanoLC (Thermo Fisher Scientific, United States) (Lirussi et al., 2012). Peptide mixtures were resolved on an Easy C18 column (10 – 0.075 mm, 3 μm) (Thermo Fisher Scientific, United States) as previously reported (Palazzotto et al., 2016).

MASCOT search engine version 2.2.06 (Matrix Science, United Kingdom) was used to identify protein spots from an updated NCBI non-redundant database (downloaded January 2018) also containing protein sequences for *S. coelicolor* A3(2), using mass spectrometric data. Database searching was performed selecting trypsin as proteolytic enzyme, a missed cleavages maximum value of 2, Cys carbamidomethylation as fixed modification, Met oxidation and N-terminal Gln conversion to pyro-Glu as variable modifications, respectively. Candidates with at least 2 assigned peptides with an individual peptide expectation value less than 0.05, which corresponds to a confidence level for peptide attribution greater than 95%, were further evaluated by the comparison with their calculated mass and p*I* values, using the experimental data obtained from electrophoresis. Protein assignment was always associated with manual verification. Finally, in case of multiple protein identifications, unambiguous protein identity was assigned according to an emPAI ratio criterion calculated between the two most abundant protein species (i.e., emPAI 1^{st}/emPAI $2^{nd} > 1.50$) (Shinoda et al., 2010). The mass spectrometry proteomics data have been deposited to the ProteomeXchange Consortium via the PRIDE (Perez-Riverol et al., 2019) partner repository with the dataset identifier PXD015937.

Metabolic Profile Determination

Metabolic profiles of Sco-*trpM*KI and Sco-EV were investigated through LC-ESI-MS/MS analysis in multiple reaction monitoring (MRM) mode coupled with protein precipitation and extraction of metabolites using organic solvents. All procedures reported below were carried out at Centro di Ingegneria Genetica (CEINGE) – Biotecnologie avanzate (Naples, Italy). Samples were lysed in 250 μL of a buffer containing 10 mM NH_4CO_3, 10 mM NaF, 7 M urea, 75 mM NaCl, and the suspension thus obtained was homogenized. Cellular lysates were fivefold diluted with a cold solution of acetonitrile/methanol (50:50 v/v) containing 0.1% v/v acetic acid. Samples were sonicated for 10 min, and centrifuged at 12000 rpm for 10 min, at 4°C. Supernatants were dried and resuspended in 500 μL of a solution of acetonitrile/methanol/water (40:40:20 v/v/v) containing 0.1% v/v acetic acid. Upon centrifugation at 12000 rpm for 10 min, supernatants were filtered using 0.22 μm centrifugal filters and analyzed by LC-ESI-MS/MS. Quantitative analysis was performed by the external calibration method. Standard solutions were prepared dissolving 1 mg of each analyte in 1 mL of 5% v/v acetonitrile (1000 ppm), and serial dilutions of them were used for the generation of calibration curves. 1 μL of supernatants obtained from

samples were analyzed with a 6420 Triple Quadrupole System (SCIEX, United States) coupled to a HPLC 1100 Series Binary Pump (Agilent, United States). Analytes were separated using a Kinetex 5 μm C18 analytical column (100 mm × 2.1 mm) (Phenomenex). The mobile phase was generated by mixing eluent A (0.1% v/v acetic acid containing 3 mM ammonium acetate) and eluent B (50% v/v acetonitrile, 50% v/v 2-propanol and 0.1% v/v acetic acid), at a flow rate of 0.3 mL/min. The elution gradient ranged from 5% to 95% of eluent B in 7 min. Tandem mass spectrometry was performed using a turbo ion spray source operating in negative mode and MRM mode was used for the selected analytes. Metabolites were tuned for ionization polarity, optimal declustering potential, precursor and daughter product ions, and collision energy. Metabolites were extracted from two biological replicates of both strains and three technical replicates of each one were processed. Student's *t*-test was applied to verify the statistical significance of metabolite abundance fold change, using a $p \leq 0.05$ to consider differentially represented metabolites.

Over-Expression of PepA in *Escherichia coli*

One Shot Chemically Competent *E. coli* BL21-AI cells (Invitrogen) were transformed with either pRSET-B:*pepA* or pRSET-B, with the former used to obtain a 6xHis-tagged recombinant PepA and the latter to have a control protein extract. In particular, an amount of 50 mL of LB medium was inoculated with 2.5 mL of an overnight-grown culture of *E. coli* BL21-AI carrying pRSET-B:*pepA*. The culture was incubated (37°C, at 200 rpm in an orbital shaker) until OD_{600} reached a value of 0.8. Then, a sterile solution of the inducer L-arabinose was added to have a final concentration of 0.1% w/v, and induction of *pepA* over-expression was performed at 30°C, for 3 h. *E. coli* BL21-AI carrying pRSET-B was used as negative control, and aliquots from all cultures were collected as further control before adding the inducer. Cultures were centrifuged, and the pellet resuspended in 2 mL of 50 mM Tris–HCl, pH 8. Then, suspensions were sonicated with 3 pulses (10 sec each and 4 as output control) in an ice bath and centrifuged (30 min, 7000 × *g*, at 4°C). Supernatants containing the water-soluble (WS) protein fraction of the cell lysate were directly used for leucine aminopeptidase assay measurements. Bradford reagent was used to determine WS protein concentration (Bradford, 1976).

Leucine Aminopeptidase Assay

An aliquot of 400 μg of WS proteins was added to the reaction mix (0.25 mM L-leucine-*p*-nitroanilide, 1 mM $CoCl_2$ or $MnCl_2$, 50 mM Tris–HCl, pH 8) in a final volume of 500 μL. After incubation at 60°C for 10 min, a volume of 10% v/v acetic acid was added, and the solution was incubated at 100°C, for 5 min. Samples were finally centrifuged at 13000 × *g*, for 5 min, at 4°C, and the absorbance of supernatants was measured at 405 nm (Kuo et al., 2003; Song et al., 2013). This assay was performed with three different technical replicates.

RESULTS

Construction and Characterization of a *trpM* Knock-in Mutant Strain

For the construction of a *S. coelicolor trpM* knock-in mutant strain (thereof named Sco-*trpM*KI), *trpM* was PCR-amplified and cloned within the multiple cloning site of the integrative expression vector pIJ8600 under the control of the thiostrepton-inducible promoter (P*tipA*) (Murakami et al., 1989; Kieser et al., 2000). This plasmid was delivered to *S. coelicolor* through interspecific conjugation, and the correct integration in the *attB* ΦC31 site was verified by PCR, sequencing and Southern blotting. Analogously, a strain having the empty vector pIJ8600 integrated in its genome (indicated as Sco-EV) was constructed and used as control during all the following experiments. Since qRT-PCR showed that the expression of *trpM* in Sco-*trpM*KI was already twofold greater than that in Sco-EV (**Supplementary Figure S1**), thiostrepton was not added to the growth medium as inducer to avoid the introduction of any possible negative effects on antibiotic production and on protein expression pattern as described by Wang et al. (2017) and Chiu et al. (1999), respectively.

During solid-medium growth, Sco-*trpM*KI had a faster growth in comparison to Sco-EV since the former showed an evident substrate mycelium after 24 h, which was not present in the latter (**Supplementary Figures S2A,B**, respectively). After 48 h of growth, both strains showed developed hyphae with few and faint septal constrictions that were more evident in Sco-*trpM*KI (**Supplementary Figures S2C,D**). Spore chains were clearly visible in the 72 h-old Sco-*trpM*KI (**Supplementary Figure S2E**) as well as quite lagging in Sco-EV (**Supplementary Figure S2F**). Nonetheless, after 120 h of growth both Sco-*trp*MKI and Sco-EV had a comparable phenotype with no major morphological differences (**Supplementary Figures S2G,H**). This finding is in good agreement with the faster and higher biomass-yielding growth kinetics in liquid medium cultures, in which Sco-*trpM*KI had a more rapid and abundant production of biomass up to 72 h (**Figure 1**). Accordingly, a higher alkalinization of the growth medium was observed in

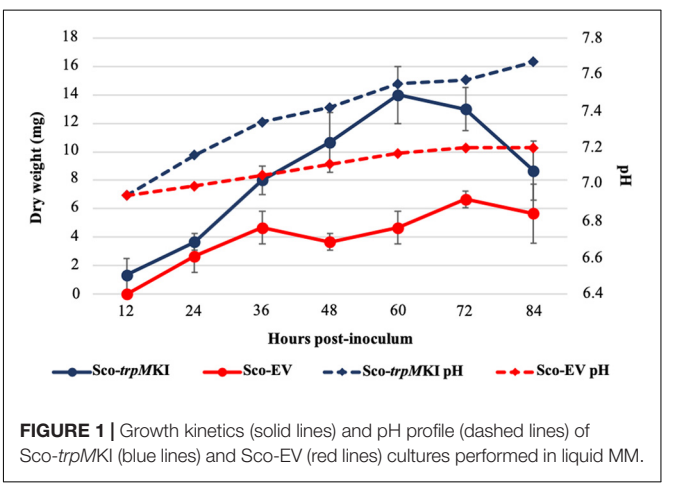

FIGURE 1 | Growth kinetics (solid lines) and pH profile (dashed lines) of Sco-*trpM*KI (blue lines) and Sco-EV (red lines) cultures performed in liquid MM.

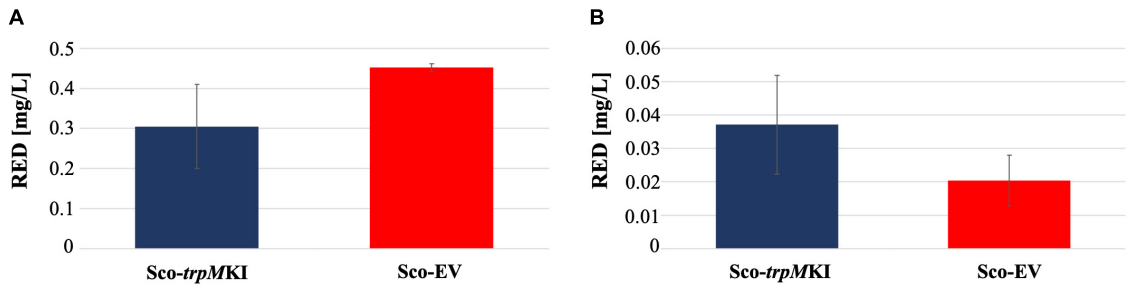

FIGURE 2 | Undecylprodigiosin (RED) production in cultures of Sco-*trpM*KI and Sco-EV strains performed using liquid **(A)** and solid **(B)** MM growth-medium.

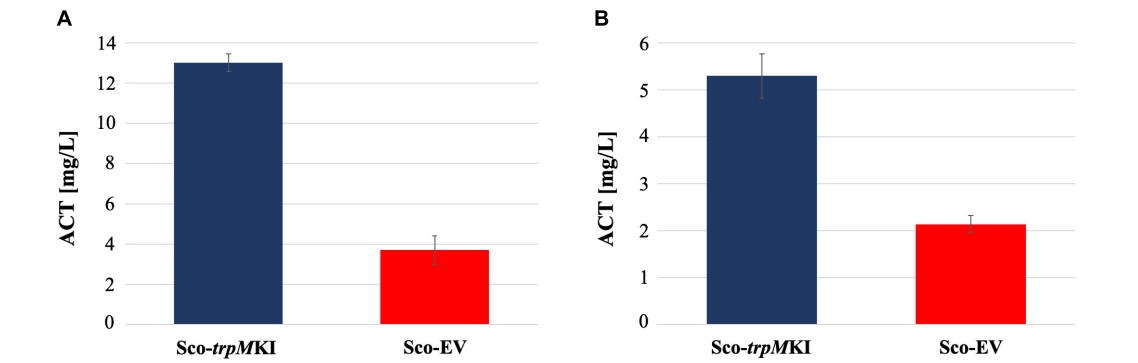

FIGURE 3 | Actinorhodin (ACT) production in cultures of Sco-*trpM*KI and Sco-EV strains performed using liquid **(A)** and solid **(B)** MM growth-medium.

Sco-*trpM*KI that was attributed to conversion of $NaNO_3$ (the sole nitrogen source in the growth medium) into ammonia (Fischer et al., 2012). This suggested that Sco-*trpM*KI had an increased utilization of nitrogen consistently with its higher growth rate, further confirming that the expression of the extra copy of *trpM* influenced the growth rate accelerating morphological development progress. However, *trpM* expression did not affect the final amount of spores and undecylprodigiosin (**Figure 2**), but exerted a positive effect on the production of the polyketide antibiotic ACT, both in liquid and on solid media, with an amount increment ranging from 2.5 to 3 times in comparison to Sco-EV (**Figure 3**). On the other hand, the expression of the extra copy of *trpM* had a negative effect on CDA, with a more than fivefold decrement of CDA production compared to Sco-EV (**Figure 4**).

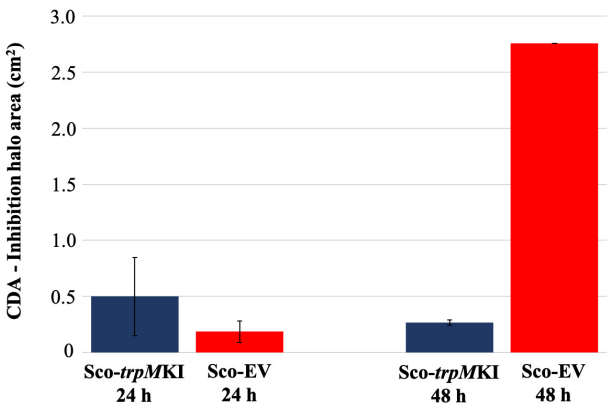

FIGURE 4 | Calcium-dependent antibiotic (CDA) production in Sco-*trpM*KI and Sco-EV cultures determined by bacterial growth inhibition assay.

Proteomic and Metabolic Profiles of the *trpM* Knock-in Mutant Strain

A 2D-DIGE proteomic analysis (**Supplementary Figure S3**) coupled with nanoLC-ESI-LIT-MS/MS was performed to infer metabolic pathways influenced by the expression of *trpM* in Sco-*trpM*KI. This investigation led to the identification of 40 differentially represented proteins, with 23 and 17 over- and down-represented ones in Sco-*trpM*KI compared to Sco-EV, respectively (**Table 3**, **Supplementary Figure S4A** and **Supplementary Tables S1**, **S2**). According to a KEGG orthology-based classification, most of them are involved in translation, carbon metabolism and folding-sorting-degradation of proteins (**Table 3**). Above all, the over-representation of proteins involved in protein synthesis, DNA synthesis and energy metabolism was consistent with the improved growth of Sco-*trpM*KI. On the other hand, the effect of *trpM* expression on growth was associated with a down-representation of several glycolytic enzymes as well as with the simultaneous over- and down-representation of SCO5042 (fumarate hydratase) and SCO4827 (malate dehydrogenase),

TABLE 3 | Differentially represented proteins in Sco-*trpM*KI in comparison to Sco-EV.

SCO ID	Protein description	Differential abundance[1]	*p* (ANOVA)	Functional classification[2]
SCO2179	Probable cytosol aminopeptidase	−1.31	4.42×10^{-3}	Amino acid metabolism; Folding, sorting, and degradation
SCO4837	Serine hydroxymethyltransferase	−1.30	2.04×10^{-4}	Amino acid metabolism
SCO1947	Glyceraldehyde-3-phosphate dehydrogenase	−1.32	1.67×10^{-2}	Carbon metabolism
SCO3649	Fructose-bisphosphate aldolase	−1.52	1.87×10^{-4}	
SCO3649	Fructose-bisphosphate aldolase	−1.61	1.22×10^{-4}	
SCO4209	2,3-bisphosphoglycerate-dependent phosphoglycerate mutase	−1.37	2.01×10^{-3}	
SCO4827	Malate dehydrogenase	−1.54	4.44×10^{-5}	
SCO5042	Fumarate hydratase class II	2.14	1.82×10^{-5}	
SCO2619	ATP-dependent Clp protease proteolytic subunit 1	1.70	1.77×10^{-2}	Cell growth and death; Folding, sorting and degradation
SCO5371	ATP synthase subunit alpha	1.35	2.00×10^{-3}	Energy metabolism
SCO5374	ATP synthase epsilon chain	1.90	1.13×10^{-3}	
SCO1644	Proteasome subunit beta	1.75	1.62×10^{-3}	Folding, sorting and degradation
SCO4296	60 kDa chaperonin 2	1.35	1.18×10^{-2}	
SCO4296	60 kDa chaperonin 2	1.52	1.85×10^{-2}	
SCO4296	60 kDa chaperonin 2	2.33	1.54×10^{-3}	
SCO4296	60 kDa chaperonin 2	1.63	8.03×10^{-4}	
SCO1523	Pyridoxal 5′-phosphate synthase subunit PdxS	−1.83	1.71×10^{-3}	Metabolism of cofactors and vitamins
SCO1523	Pyridoxal 5′-phosphate synthase subunit PdxS	−2.23	9.56×10^{-7}	
SCO1523	Pyridoxal 5′-phosphate synthase subunit PdxS	−1.31	6.82×10^{-3}	
SCO4824	Bifunctional protein FolD	4.61	5.59×10^{-8}	
SCO4041	Uracil phosphoribosyltransferase	2.05	2.12×10^{-4}	Nucleotide metabolism
SCO0409	Spore-associated protein A	1.45	1.19×10^{-2}	Other
SCO0409	Spore-associated protein A	−2.42	4.11×10^{-4}	
SCO4636	UPF0336 protein SCO4636	−1.34	3.56×10^{-2}	
SCO2633	Superoxide dismutase [Fe-Zn] 1	2.08	2.75×10^{-7}	Oxidoreduction; Stress response
SCO2633	Superoxide dismutase [Fe-Zn] 1	−1.47	1.91×10^{-3}	
SCO2633	Superoxide dismutase [Fe-Zn] 1	−1.69	7.44×10^{-4}	
SCO3907	Single-stranded DNA-binding protein 2	1.77	9.16×10^{-4}	Replication and repair; Stress response
SCO0527	Cold shock protein ScoF	−1.50	3.63×10^{-2}	Transcription; Stress response
SCO1505	30S ribosomal protein S4	1.82	8.98×10^{-5}	Translation
SCO1599	50S ribosomal protein L35	−1.59	3.90×10^{-3}	
SCO4702	50S ribosomal protein L3	1.47	1.65×10^{-2}	
SCO4702	50S ribosomal protein L3	−1.30	3.66×10^{-2}	
SCO4702	50S ribosomal protein L3	2.53	3.36×10^{-6}	
SCO4703	50S ribosomal protein L4	1.46	1.42×10^{-3}	
SCO4711	30S ribosomal protein S17	1.53	3.01×10^{-2}	
SCO4713	50S ribosomal protein L24	1.30	6.14×10^{-3}	
SCO4735	30S ribosomal protein S9	1.61	1.18×10^{-6}	
SCO5624	30S ribosomal protein S2	1.32	2.52×10^{-3}	
SCO5624	30S ribosomal protein S2	1.96	3.94×10^{-6}	

[1]*Positive and negative values stand for up- and down-representation in Sco-trpMKI, respectively.* [2]*Functional classification is based on KEGG orthology.*

respectively, which take part into tricarboxylic acid (TCA) cycle. Interestingly, the serine hydroxymethyltransferase (GlyA) involved in interconversion of serine and glycine was down-represented in the Sco-*trpM*KI strain, thus revealing that TrpM can affect the biosynthesis of serine, which is in turn a direct precursor of Trp.

Notwithstanding these proteomic determinations, similar intracellular levels for serine and Trp were ascertained in Sco-*trpM*KI and Sco-EV strains by quantitative metabolite measurements (**Table 4** and **Supplementary Tables S3**, **S4**). Indeed, this analysis showed a down-representation of tyrosine and phenylalanine (**Table 4** and **Supplementary Table S3**) competing with Trp for metabolic intermediates. In general, most differentially abundant compounds were related to: (i) amino acid, (ii) carbon metabolism intermediates; (iii) nucleotide metabolism intermediates (**Supplementary Figure S4B**); most of these compounds were down-represented in Sco-*trpM*KI strain. Exceptions were histidine, inosine, AMP, methylmalonate and succinate, which were over-represented in the Sco-*trpM*KI in the respect of Sco-EV (**Table 4** and **Supplementary Table S3**). This observation, together with the down-representation of compounds belonging to carbon metabolism pathways (i.e., glycolysis and TCA cycle), depicted a metabolic profile that was in good agreement with that deriving from proteomic results (**Supplementary Figure S5**).

Enzymatic Activity of PepA

Different experimental data suggested functional relations between PepA and TrpM. In particular, Palazzotto et al. (2016) identified PepA as a putative TrpM-interacting protein through pull-down experiments, and then confirmed this protein-protein interaction *in vitro* by an adenylate cyclase-based bacterial two-hybrid assay. In this work, PepA was down-represented in Sco-*trpM*KI in comparison with Sco-EV (**Table 3** and **Supplementary Tables S1**, **S2**); on the contrary, a higher expression of this gene was observed by qRT-PCR (**Supplementary Figure S6**). This finding suggested the presence of putative post-transcriptional and/or post-translational regulatory mechanisms controlling the final representation of the active protein, as already globally described elsewhere (Jayapal et al., 2008; Jeong et al., 2016).

As reported in the UniProtKB database, the protein product of *pepA* is a putative cytosol aminopeptidase (entry identifier Q9S2Q7) belonging to the peptidase M17 family. In order to have an experimental confirmation of the PepA function, *pepA* was cloned in the expression vector pRSET-B and over-expressed in *E. coli* as His-tagged protein. Purification of His-tagged PepA

TABLE 4 | Differentially represented metabolites in Sco-*trpM*KI in comparison to Sco-EV.

Compound	Differential abundance[1]	*P* (Student's *t*-test)	Functional classification[2]
Aspartic acid	−3.23	2.76×10^{-2}	Amino acid metabolism
Arginine	−1.37	4.65×10^{-2}	
Phenylalanine	−1.73	3.31×10^{-2}	
Tyrosine	−1.53	2.45×10^{-6}	
Histidine	NA	NA	
Glutamic acid	−1.37	3.86×10^{-2}	
Glutamine	−1.69	1.26×10^{-2}	
Glucosamine 6-phosphate	−2.26	2.81×10^{-2}	Glycolysis; Pentose phosphate pathway
3-phosphoglycerate	−1.91	4.79×10^{-2}	
Fructose 6-phosphate	−1.67	3.43×10^{-2}	
Glucose 6-phosphate	−3.13	4.20×10^{-3}	
6-phosphogluconate	−1.84	4.62×10^{-2}	
2-oxoglutarate	−1.63	2.78×10^{-2}	TCA cycle
Fumarate	NA	NA	
Citrate	−1.36	4.20×10^{-2}	
Methylmalonate	1.70	4.91×10^{-2}	
Succinate	1.72	4.59×10^{-2}	
Malate	−1.90	4.21×10^{-2}	
Oxalate	NA	NA	
AMP	NA	NA	Nucleotide metabolism
CMP	−2.97	2.33×10^{-2}	
UMP	−3.37	4.64×10^{-3}	
Uracil	−2.15	4.91×10^{-2}	
GMP	NA	NA	
Inosine	2.04	4.54×10^{-2}	
Guanosine	−1.34	1.41×10^{-2}	

[1]Positive and negative values stand for up- and down-representation in Sco-trpMKI, respectively. NA, not applicable. [2]Functional classification is based on KEGG orthology.

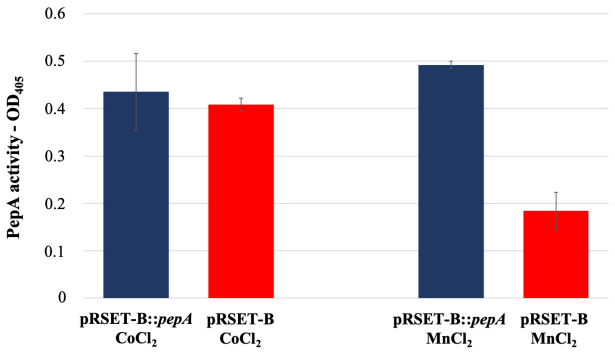

FIGURE 5 | Leucine aminopeptidase activity measured in the WS protein fraction extracted from cultures of *E. coli* BL21-AI pRSET-B:*pepA* and *E. coli* BL21-AI pRSET-B.

under native conditions was not successful, because of the low amount of the soluble protein, due to the undesired formation of inclusion bodies. Thus, WS protein fractions obtained from the *pepA*-overexpressing *E. coli* strain and from the strain carrying the vector pRSET-B were used for comparative enzymatic assay experiments, using the latter as control. In agreement with Song et al. (2013), PepA activity was not revealed in the protein extraction in presence of $CoCl_2$, while the use of $MnCl_2$ notably highlighted for the first time that PepA exerted the predicted aminopeptidase activity (**Figure 5**).

DISCUSSION

The results described in this work revealed that *trpM* boosts the morpho-physiological differentiation of *S. coelicolor*. This positive effect was inferred from the accumulation of biomass in liquid cultures and by the mycelium morphology on solid growth medium observed in Sco-*trpM*KI in comparison to Sco-EV. In agreement, SCO0409 product – known as spore-associated protein A or SapA – is deregulated as shown by differential proteomic analysis. This protein, along with SapB, is expressed in aerial hyphae and is localized on the external surface of spores, contributing to the shaping of spores and to their hydrophobicity (Guijarro et al., 1988; Willey et al., 1991).

The synthesis of the three major secondary metabolites of *S. coelicolor* – i.e., ACT, undecylprodigiosin and CDA – was studied in the *trpM* knock-in strain. It revealed a stimulatory effect only on ACT production. This finding is consistent with the results described by Palazzotto et al. (2016) concerning a *trpM*-knockout mutant strain, whose production of ACT was impaired upon cultivation on minimal medium. These results suggest that *trpM* expression could influence ACT biosynthesis through an indirect regulation of central carbon metabolism. Indeed, the biosynthesis of antibiotics in *S. coelicolor* is greatly affected by precursor supply. In the *trpM* knock-in strain, the relative abundances of two TCA cycle enzymes – i.e., malate dehydrogenase (SCO4827) and fumarate hydratase class II (SCO5042) – suggested a differential abundance of TCA intermediates. Accordingly, the metabolite profile analysis revealed the accumulation of succinate, which can be related also with the accumulation of methylmalonate, a metabolic intermediate of the branched-chain amino acid catabolism providing precursors for the biosynthesis of type II polyketide antibiotics, like ACT (Stirrett et al., 2009). However, the exact metabolic routes possibly leading to an increment of malonyl-CoA, which is an extending unit precursor of the ACT backbone (Revill et al., 1995; Hopwood, 1997; Rawlings, 1999) were not inferred from the proteomic and metabolic profiles of Sco-*trpM*KI strain.

On the other hand, the decrement of CDA production may be related to the altered amounts of amino acids observed in Sco-*trpM*KI strain. Indeed, the biosynthesis of CDA is dependent on amino acid availability. In particular, the peptide moiety of CDA includes residues of serine, threonine, tryptophan, glutamic acid, hydroxyphenylglycine, aspartic acid, glycine, and asparagine (Hojati et al., 2002). Although tyrosine is not part of CDA backbone directly, it is known that CDA biosynthesis intersects tyrosine metabolism since the metabolic intermediary compound 4-hydroxyphenylpyruvate – a product of tyrosine catabolism that is also involved in CDA precursor biosynthesis – exerts a positive effect on the regulatory protein HpdR. This regulator in turn controls genes required for tyrosine catabolism and CDA biosynthesis (Liu et al., 2013). In this work, both glutamic and aspartic acid, which are present in CDA backbone, were down-represented in Sco-*trpM*KI reinforcing the hypothesis that CDA yield was strongly affected by amino acid availability. However, it is noteworthy that Trp levels – along with some of its precursors anthranilate, chorismate and phenylpyruvate – seemed to be not limiting for CDA biosynthesis, since these chemical species were not differentially represented in Sco-*trpM*KI in comparison to Sco-EV.

In the *trpM* knock-in mutant, the decreased intracellular amount of tyrosine and phenylalanine – sharing different biosynthetic steps with Trp – parallels the decrement of arginine, glutamate and glutamine: these three amino acids derive from TCA cycle intermediates oxaloacetate (i.e., arginine) and alpha-ketoglutarate (i.e., glutamate and glutamine) and, moreover, biosynthesis of arginine is directly linked to glutamate/glutamine through ammonium assimilation (Lu, 2006; Lewis et al., 2011). On the other hand, the decreased amount of these amino acids is coupled with increment of histidine whose biosynthesis intersects different metabolic pathways, including those involved in Trp, purine and pyrimidine biosynthesis, as well as in C1 metabolism (Schwentner et al., 2019). In fact, Trp, purine, pyrimidine and histidine biosyntheses share the phosphoribosyl pyrophosphate (PRPP), a metabolite intermediate originating from ribose-5P. Tetrahydrofolate (THF) is a key cofactor in C1 metabolism; a metabolic source for the generation of loaded THF molecules is the reaction of serine hydroxymethyltransferase (GlyA – SCO4837) that interconverts glycine and serine. This last amino acid is a Trp precursor required in the last biosynthetic step of condensation with indole. Interestingly, a differential abundance was observed in Sco-*trpM*KI strain for GlyA and FolD (SCO4824, a bifunctional protein with methylenetetrahydrofolate dehydrogenase and methenyltetrahydrofolate cyclohydrolase activities), with the

latter enzyme being required in biosynthesis of THF derivatives. Additionally, THF is involved in the synthesis of pantothenate that is a key precursor for the biosynthesis of essential cofactor coenzyme A (CoA) and carrier proteins having a phosphopantetheine prosthetic group such as polyketide synthases and non-ribosomal peptide synthetases (Leonardi and Jackowski, 2007). Altogether these results suggest that *trpM* over-expression stimulates metabolic circuits that are interconnected with each other and with Trp biosynthesis but whose regulation and functions still deserve further investigations. The alteration of amino acid biosynthetic pathways due to *trpM* over-expression could be also linked to the observed alkalinization of medium in liquid culture of Sco-*trpM*KI. Indeed, glutamate/glutamine and arginine play a key role in nitrogen assimilation (Lu, 2006; Lewis et al., 2011) and their down-representation could account for an increased amount of free ammonium causing medium alkalinization. In addition, it has been recently reported that different *Streptomyces* species, including *S. coelicolor*, are able to produce ammonia in presence of higher levels of glycine, exerting (i) an antimicrobial activity and (ii) reinforcing the efficiency of other antibiotics through perturbation of membrane permeability in target cells (Avalos et al., 2019). At this regard, it would be interesting to clarify the role of GlyA, which converts serine in glycine, and its putative interplay with TrpM.

The altered metabolism of amino acids could also indirectly contribute to increase ACT biosynthesis in two different manners. Indeed, on one hand, the augmented synthesis of some amino acids (e.g., histidine) could cause the occurrence of oxidative stress in Sco-*trpM*KI and, at this regard, it has been proposed that ACT could be a mean to reduce oxidative metabolism in *S. coelicolor* (Esnault et al., 2017). On the other hand, same authors proposed that metabolite shortage (like that of aspartic acid, arginine, phenylalanine, tyrosine, glutamic acid and glutamine in Sco-*trpM*KI) could act as a trigger as well. In particular, considering that *trpM* expression is positively correlated with ACT biosynthesis, its possible role in limiting oxidative stress through control of ACT concentration deserves further investigation: structural studies of TrpM could clarify, for example, if the two cysteine residues in position 19 and 24 are part of a 2Fe-2S cluster able to sense redox stress and induce conformational changes in TrpM structure. If this is the case, the experimental proof reported by Palazzotto et al. (2016) about the ability of TrpM to form dimers would suggest that a 2Fe-2S cluster could form upon dimerization, providing the four cysteine residues needed.

The differential proteomic analysis revealed that proteins involved in protein synthesis were more abundant in Sco-*trpM*KI strain. These ones included ribosomal proteins and chaperonins. The over-representation of GroEL (SCO4296) was in agreement with its well-documented involvement in metabolism during stationary phase, in morpho-physiological differentiation and in production of secondary metabolites, such as ACT (Kim et al., 2008). Moreover, proteins taking part in nucleotide metabolism and in replication and repair of DNA were more abundant as well, mirroring, at molecular level, the higher accumulation of biomass in Sco-*trpM*KI strain. As it is inferred from metabolite profile analysis, Trp biosynthesis does not seem dramatically altered in Sco-*trpM*KI, in opposition to the findings obtained for the *trpM*-knockout mutant strain (Palazzotto et al., 2016). Indeed, in the latter, some proteins involved in Trp biosynthesis (AroF and TrpE) or its utilization (TrpS) were more abundant, suggesting a compensatory effect probably due to Trp shortage. In Sco-*trpM*KI we did not observe up-regulation of proteins involved in Trp biosynthesis, neither an accumulation of Trp or its precursors (i.e., anthranilate and chorismite), suggesting that the *trpM* knock-in mutation does not exert dramatic effects on Trp metabolism as *trpM*-knockout mutation does. Main differences regarding these two mutant strains are reported in **Table 5**.

In addition, the relationship between stress response proteins and streptomycete development is well known since it has been described by Puglia et al. (1995). In the *trpM* knock-in strain there was also an accumulation of stress response proteins. Analogously, a stimulatory role of Trp on *S. coelicolor* morphological and physiological differentiation was described in Palazzotto et al. (2015) and, among the proteins accumulated in the strain upon Trp supplementation into growth medium, proteins related to stress response were observed, including also oxidative stress proteins. Anyhow, it is still unclear how the up-regulation of *trpM* can exert the pleiotropic effects observed.

As reported by Palazzotto et al. (2016), TrpM interacts with PepA. In addition, qRT-PCR analysis showed that *pepA* was more expressed in Sco-*trpM*KI strain, while proteomics showed that the corresponding protein was less abundant therein. These results suggest the presence of post-transcriptional and/or post-translational regulatory mechanisms that regulate PepA levels. It would be very interesting to find out if this putative regulation is actually due to the TrpM-PepA interaction; this point deserves further investigations.

In this work, *pepA* was cloned and over-expressed in *E. coli* to study the putative enzymatic activity of the corresponding protein. Here, we demonstrated for the first time that PepA has an enzymatic activity that corresponds to the predicted one, shedding new lights on the role of TrpM-PepA interaction. It will be important to know whether or not TrpM affects PepA activity upon binding and, if this is the case, whether

TABLE 5 | Main differences between Sco-*trpM*KI and the *trpM*-knockout mutant strains in comparison to their corresponding control strains (Sco-EV and *S. coelicolor* M145, respectively).

Phenotype	Sco-*trpM*KI[1]	*trpM*-knockout[1]*
Growth rate	+	−
Morphological differentiation	+	−
Spore amount	=	−
ACT	+	−
RED	=	N.D.
CDA	−	N.D.
L-Trp biosynthetic enzymes	=	+
L-Trp precursors	=	N.D.

[1]*+, yield increment/stimulation; −, yield decrement/inhibition; =, no difference observed; N.D., not determined. *Palazzotto et al. (2016).*

the effect is positive or negative. It is well documented that bacterial differentiation can be regulated through the protease-mediated selective degradation of regulators (Gottesman and Maurizi, 1992; Baker and Sauer, 2006). For instance, in *S. coelicolor*, the ATP-dependent serine proteases ClpP have a role in differentiation; in addition, protease inactivation was shown to induce both "bald" phenotype and lack of pigmentated antibiotics (i.e., ACT and undecylprodigiosin) (de Creìcy-Lagard et al., 1999; Bellier and Mazodier, 2004). Although PepA does not belong to the same protease class of ClpP proteins, it is interesting to note that its inactivation caused an enhancement of sporulation and production of ACT, thus suggesting a key role in *S. coelicolor* differentiation (Song et al., 2013; Xu et al., 2019).

Many genes involved in diverse cellular processes different from ACT production – such as metabolism of amino acids, carbohydrate, cell wall and DNA – or having unknown functions were shown to affect ACT production and/or actinomycete development (Gehring et al., 2004; Xu et al., 2019). In this work, TrpM was shown to play a role in regulating *S. coelicolor* growth and differentiation, specifically stimulating ACT production. In particular, our experimental data highlighted the stimulation of a regulatory circuit involving amino acid, cofactor and protein biosynthesis. In this circuit, a possible role could be exerted by the interplay between TrpM and the aminopeptidase PepA. Further studies are necessary to deeply understand the specific molecular mode of action of TrpM, explaining if and how TrpM-PepA interaction has a direct influence on the growth, antibiotic biosynthesis and developmental program of *S. coelicolor*. To such purpose, it will be important to determine the temporal expression profile of both TrpM and PepA and to identify cellular targets of the aminopeptidase activity of PepA, also considering that the augmented expression of *trpM* and the inactivation of *pepA* (Song et al., 2013) both positively influence ACT production in *S. coelicolor*. Furthermore, even the putative interaction between TrpM and the ribosomal protein S2 (SCO5624) will deserve a specific investigation: in fact, it was previously identified as a putative interacting protein of TrpM (Palazzotto et al., 2016) and it was interestingly over-represented in Sco-*trpM*KI as well. Finally, considering that TrpM is conserved among *Streptomyces* species, it should be investigated whether it is able to exert a positive effect even on other secondary metabolite biosynthesis, especially polyketides. Indeed, this chemical class includes several compounds with antibiotic, antitumoral and immunosuppressant activity. So, the development of recombinant strains with altered expression of TrpM and/or PepA could be promising to enhance industrial production of these molecules.

DATA AVAILABILITY STATEMENT

Proteomic data have been submitted to the PRIDE database under the project accession PXD015937.

AUTHOR CONTRIBUTIONS

AV, EP, GR, LB, and TF performed the experiments. AS and GG supervised the experiments and analyzed the results. AV, AP, and GG designed the experiments. AP and GG conceived the project. AV wrote the manuscript with the help of AS and GG. All authors read and approved the manuscript.

FUNDING

This work was partly supported by MIUR FFABR 2017 and University of Palermo FFR 2018 to GG.

SUPPLEMENTARY MATERIAL

The Supplementary Material for this article can be found online at: https://www.frontiersin.org/articles/10.3389/fmicb.2020.00224/full#supplementary-material

FIGURE S1 | qRT-PCR analysis showing the relative quantification (RQ) of *trpM* expression in Sco-*trpM*KI and Sco-EV.

FIGURE S2 | SEM images of Sco-*trpM*KI and Sco-EV after 24, 48, 72, and 120 h of growth on solid MM. **(A)** Sco-*trpM*KI 24 h. **(B)** Sco-EV 24 h. **(C)** Sco-*trpM*KI 48 h. **(D)** Sco-EV 48 h. **(E)** Sco-*trpM*KI 72 h. **(F)** Sco-EV 72 h. **(G)** Sco-*trpM*KI 120 h. **(H)** Sco-EV 120 h.

FIGURE S3 | Representative 2D-proteome map of whole protein extracts obtained from Sco-*trpM*KI. Differentially represented proteins listed in **Supplementary Tables S1**, **S2** are labeled.

FIGURE S4 | Distribution into functional classes of differentially represented proteins **(A)** and metabolites **(B)** when Sco-*trpM*KI and Sco-EV strains were compared. Percentages indicate the relative abundance of each functional class.

FIGURE S5 | Metabolic pathway map showing over-represented proteins (red), down-represented proteins (light green), over-represented metabolites (maroon), and down-represented metabolites (dark green) in Sco-*trpM*KI in comparison to Sco-EV. Only proteins involved in the labeled metabolic pathways are reported. Proteins are indicated with the corresponding genomic locus (i.e., SCOXXXX), while metabolites with their KEGG identifier (i.e., CXXXXX). This map was generated using the web-based tool Interactive Pathways Explorer v3 (iPath3) (Darzi et al., 2018).

FIGURE S6 | qRT-PCR analysis showing relative quantification (RQ) of *pepA* expression in Sco-*trpM*KI and Sco-EV.

TABLE S1 | Description, abundance profile, functional classification and mass spectrometry identification parameters of differentially represented proteins. Functional classification is based on KEGG orthology.

TABLE S2 | Protein identification details of spots observed as differentially represented.

TABLE S3 | Description, abundance profile and functional classification of differentially represented metabolites. Functional classification is based on KEGG orthology.

TABLE S4 | Description, abundance profile and functional classification of not differentially represented metabolites. Functional classification is based on KEGG orthology.

REFERENCES

Avalos, M., Garbeva, P., Raaijmakers, J. M., and van Wezel, G. P. (2019). Production of ammonia as a low-cost and long-distance antibiotic strategy by *Streptomyces* species. *ISME J.* 14, 1–15. doi: 10.1038/s41396-019-0537-2

Baker, T. A., and Sauer, R. T. (2006). ATP-dependent proteases of bacteria: recognition logic and operating principles. *Trends Biochem. Sci.* 31, 647–653. doi: 10.1016/j.tibs.2006.10.006

Bellier, A., and Mazodier, P. (2004). ClgR, a novel regulator of *clp* and *lon* expression in *Streptomyces*. *J. Bacteriol.* 186, 3238–3248. doi: 10.1128/jb.186.10.3238-3248.2004

Bradford, M. M. (1976). A rapid and sensitive method for the quantitation of microgram quantities of protein utilizing the principle of protein-dye binding. *Anal. Biochem.* 72, 248–254. doi: 10.1006/abio.1976.9999

Chiu, M. L., Folcher, M., Katoh, T., Puglia, A. M., Vohradsky, J., Yun, B. S., et al. (1999). Broad spectrum thiopeptide recognition specificity of the *Streptomyces lividans* TipAL protein and its role in regulating gene expression. *J. Biol. Chem.* 274, 20578–20586. doi: 10.1074/jbc.274.29.20578

Chu, Q., Ma, J., and Saghatelian, A. (2015). Identification and characterization of sORF-encoded polypeptides. *Crit. Rev. Biochem. Mol. Biol* 50, 134–141. doi: 10.3109/10409238.2015.1016215

Chugunova, A., Navalayeu, T., Dontsova, O., and Sergiev, P. (2018). Mining for small translated ORFs. *J. Proteome Res.* 17, 1–11. doi: 10.1021/acs.jproteome.7b00707

Darzi, Y., Letunic, I., Bork, P., and Yamada, T. (2018). iPath3.0: interactive pathways explorer v3. *Nucleic Acids Res.* 46, W510–W513. doi: 10.1093/nar/gky299

de Crècy-Lagard, V., Servant-Moisson, P., Viala, J., Grandvalet, C., and Mazodier, P. (1999). Alteration of the synthesis of the Clp ATP-dependent protease affects morphological and physiological differentiation in *Streptomyces*. *Mol. Microbiol.* 32, 505–517. doi: 10.1046/j.1365-2958.1999.01364.x

Delcourt, V., Staskevicius, A., Salzet, M., Fournier, I., and Roucou, X. (2018). Small proteins encoded by unannotated ORFs are rising stars of the proteome, confirming shortcomings in genome annotations and current vision of an mRNA. *Proteomics* 8:e1700058. doi: 10.1002/pmic.201700058

Esnault, C., Dulermo, T., Smirnov, A., Askora, A., David, M., Deniset-Besseau, A., et al. (2017). Strong antibiotic production is correlated with highly active oxidative metabolism in *Streptomyces coelicolor* M145. *Sci. Rep.* 7:200. doi: 10.1038/s41598-017-00259-9

Fischer, M., Schmidt, C., Falke, D., and Sawers, R. G. (2012). Terminal reduction reactions of nitrate and sulfate assimilation in *Streptomyces coelicolor* A3(2): identification of genes encoding nitrite and sulfite reductases. *Res. Microbiol.* 63, 340–348. doi: 10.1016/j.resmic.2012.05.004

Gehring, A. M., Wang, S. T., Kearns, D. B., Storer, N. Y., and Losick, R. (2004). Novel genes that influence development in *Streptomyces coelicolor*. *J. Bacteriol.* 186, 3570–3577. doi: 10.1128/JB.186.11.3570-3577.2004

Gottesman, S., and Maurizi, M. R. (1992). Regulation by proteolysis: energy-dependent proteases and their targets. *Microbiol. Rev.* 56, 592–621.

Guijarro, J., Santamaria, R., Schauer, A., and Losick, R. (1988). Promoter determining the timing and spatial localization of transcription of a cloned *Streptomyces coelicolor* gene encoding a spore-associated polypeptide. *J. Bacteriol.* 170, 1895–1901. doi: 10.1128/jb.170.4.1895-1901.1988

Hojati, Z., Milne, C., Harvey, B., Gordon, L., Borg, M., Flett, F., et al. (2002). Structure, biosynthetic origin, and engineered biosynthesis of calcium-dependent antibiotics from *Streptomyces coelicolor*. *Chem. Biol.* 9, 1175–1187. doi: 10.1016/s1074-5521(02)00252-1

Hopwood, D. A. (1997). Genetic contributions to understanding polyketide synthases. *Chem. Rev.* 97, 2465–2498. doi: 10.1021/cr960034i

Horinouchi, S., and Beppu, T. (1984). Production in large quantities of actinorhodin and undecyl-prodigiosin induced by *afsB* in *Streptomyces lividans*. *Agric. Biol. Chem.* 48, 2131–2133. doi: 10.1080/00021369.1984.10866459

Hu, D. S., Hood, D. W., Heidstra, R., and Hodgson, D. A. (1999). The expression of the *trpD*, *trpC* and *trpBA* genes of *Streptomyces coelicolor* A3(2) is regulated by growth rate and growth phase but not by feedback repression. *Mol. Microbiol.* 32, 869–880. doi: 10.1046/j.1365-2958.1999.01407.x

Jayapal, K. P., Philp, R. J., Kok, Y. J., Yap, M. G., Sherman, D. H., Griffin, T. J., et al. (2008). Uncovering genes with divergent mRNA-protein dynamics in *Streptomyces coelicolor*. *PLoS One* 3:e2097. doi: 10.1371/journal.pone.0002097

Jeong, Y., Kim, J. N., Kim, M. W., Bucca, G., Cho, S., Yoon, Y. J., et al. (2016). The dynamic transcriptional and translational landscape of the model antibiotic producer *Streptomyces coelicolor* A3(2). *Nat. Commun.* 7:11605. doi: 10.1038/ncomms11605

Kieser, T., Bibb, M. J., Buttner, M. J., Chater, K. F., and Hopwood, D. A. (2000). *Practical Streptomyces Genetics*. Norwich: The John Innes Foundation.

Kim, Y. J., Moon, M. H., Song, J. Y., Smith, C. P., Hong, S. K., and Chang, Y. K. (2008). Acidic pH shock induces the expressions of a wide range of stress-response genes. *BMC Genomics* 9:604. doi: 10.1186/1471-2164-9-604

Kuo, L. Y., Hwang, G. Y., Lai, Y. J., Yang, S. L., and Lin, L. L. (2003). Overexpression, purification, and characterization of the recombinant Leucine Aminopeptidase II of *Bacillus stearothermophilus*. *Curr. Microbiol.* 47, 40–45. doi: 10.1007/s00284-002-3950-z

Leonardi, R., and Jackowski, S. (2007). Biosynthesis of pantothenic acid and Coenzyme A. *EcoSal Plus* 2. doi: 10.1128/ecosalplus.3.6.3.4

Lewis, R. A., Shahi, S. K., Laing, E., Bucca, G., Efthimiou, G., Bushell, M., et al. (2011). Genome-wide transcriptomic analysis of the response to nitrogen limitation in *Streptomyces coelicolor* A3(2). *BMC Res. Notes* 4:78. doi: 10.1186/1756-0500-4-78

Lirussi, L., Antoniali, G., Vascotto, C., D'Ambrosio, C., Poletto, M., Romanello, M., et al. (2012). Nucleolar accumulation of APE1 depends on charged lysine residues that undergo acetylation upon genotoxic stress and modulate its BER activity in cells. *Mol. Biol. Cell* 23, 4079–4096. doi: 10.1091/mbc.E12-04-0299

Liu, G., Chater, K. F., Chandra, G., Niu, G., and Tan, H. (2013). Molecular regulation of antibiotic biosynthesis in *Streptomyces*. *Microbiol. Mol. Biol. Rev.* 77, 112–143. doi: 10.1128/MMBR.00054-12

Lu, C. D. (2006). Pathways and regulation of bacterial arginine metabolism and perspectives for obtaining arginine overproducing strains. *Appl. Microbiol. Biotechnol.* 70, 261–272. doi: 10.1007/s00253-005-0308-z

Murakami, T., Holt, T. G., and Thompson, C. J. (1989). Thiostrepton-induced gene expression in *Streptomyces lividans*. *J. Bacteriol.* 171, 1459–1466. doi: 10.1128/jb.171.3.1459-1466.1989

Palazzotto, E., Gallo, G., Renzone, G., Giardina, A., Sutera, A., Silva, J., et al. (2016). TrpM, a small protein modulating tryptophan biosynthesis and morpho-physiological differentiation in *Streptomyces coelicolor* A3(2). *PLoS One* 11:e0163422. doi: 10.1371/journal.pone.0163422

Palazzotto, E., Renzone, G., Fontana, P., Botta, L., Scaloni, A., Puglia, A. M., et al. (2015). Tryptophan promotes morphological and physiological differentiation in *Streptomyces coelicolor*. *Appl. Microbiol. Biotechnol.* 99, 10177–10189. doi: 10.1007/s00253-015-7012-4

Palazzotto, E., Tong, Y., Lee, S. Y., and Weber, T. (2019). Synthetic biology and metabolic engineering of actinomycetes for natural product discovery. *Biotechnol. Adv.* 37:107366. doi: 10.1016/j.biotechadv.2019.03.005

Perez-Riverol, Y., Csordas, A., Bai, J., Bernal-Llinares, M., Hewapathirana, S., Kundu, D. J., et al. (2019). The PRIDE database and related tools and resources in 2019: improving support for quantification data. *Nucleic Acids Res.* 47, D442–D450. doi: 10.1093/nar/gky1106

Puglia, A. M., Vohradsky, J., and Thompson, C. J. (1995). Developmental control of the heat-shock stress regulon in *Streptomyces coelicolor*. *Mol. Microbiol.* 17, 737–746. doi: 10.1111/j.1365-2958.1995.mmi_17040737.x

Rawlings, B. J. (1999). Biosynthesis of polyketides (other than actinomycete macrolides). *Nat. Prod. Rep.* 16, 425–484. doi: 10.1039/A900566H

Revill, W. P., Bibb, M. J., and Hopwood, D. A. (1995). Purification of a malonyltransferase from *Streptomyces coelicolor* A3(2) and analysis of its genetic determinant. *J. Bacteriol.* 177, 3946–3952. doi: 10.1128/jb.177.14.3946-3952.1995

Sambrook, J., and Russell, D. W. (2001). *Molecular Cloning: A Laboratory Manual*. Cold Spring Harbor, NY: Cold Spring Harbor Laboratory Press.

Scaffaro, R., Lopresti, F., Sutera, A., Botta, L., Fontana, R. M., and Gallo, G. (2017). Plasma modified PLA electrospun membranes for actinorhodin production intensification in *Streptomyces coelicolor* immobilized-cell cultivations. *Colloids Surf. B Biointerfaces* 157, 233–241. doi: 10.1016/j.colsurfb.2017.05.060

Schwentner, A., Feith, A., Münch, E., Stiefelmaier, J., Lauer, I., Favilli, L., et al. (2019). Modular systems metabolic engineering enables balancing of relevant pathways for L-histidine production with *Corynebacterium glutamicum*. *Biotechnol. Biofuels* 12:65. doi: 10.1186/s13068-019-1410-2

Shinoda, K., Tomita, M., and Ishihama, Y. (2010). emPAI Calc–for the estimation of protein abundance from large-scale identification data by liquid chromatography-tandem mass spectrometry. *Bioinformatics* 26, 576–577. doi: 10.1093/bioinformatics/btp700

Simon, R., Priefer, U., and Pühler, A. (1983). A broad host range mobilization system for in vivo genetic engineering: transposon mutagenesis in gram negative bacteria. *Biotechnology* 1, 784–791. doi: 10.1038/nbt1183-784

Song, E., Rajesh, T., Lee, B. R., Kim, E. J., Jeon, J. M., Park, S. H., et al. (2013). Deletion of an architectural unit, leucyl aminopeptidase (SCO2179), in *Streptomyces coelicolor* increases actinorhodin production and sporulation. *Appl. Microbiol. Biotechnol.* 97, 6823–6833. doi: 10.1007/s00253-013-4847-4

Stirrett, K., Denoya, C., and Westpheling, J. (2009). Branched-chain amino acid catabolism provides precursors for the Type II polyketide antibiotic, actinorhodin, via pathways that are nutrient dependent. *J. Ind. Microbiol. Biotechnol.* 36, 129–137. doi: 10.1007/s10295-008-0480-0

Storz, G., Wolf, Y. I, and Ramamurthi, K. S. (2014). Small proteins can no longer be ignored. *Ann. Rev. Biochem.* 83, 753–777. doi: 10.1146/annurev-biochem-070611-102400

Sun, J., Kelemen, G. H., Fernandez-Abalos, J. M., and Bibb, M. J. (1999). Green fluorescent protein as a reporter for spatial and temporal gene expression in *Streptomyces coelicolor* A3(2). *Microbiology* 145, 2221–2227. doi: 10.1099/00221287-145-9-2221

Wang, H., Zhao, G., and Ding, X. (2017). Morphology engineering of *Streptomyces coelicolor* M145 by sub-inhibitory concentrations of antibiotics. *Sci. Rep.* 7:13226. doi: 10.1038/s41598-017-13493-y

Willey, J., Santamaria, R., Guijarro, J., Geistlich, M., and Losick, R. (1991). Extracellular complementation of a developmental mutation implicates a small sporulation protein in aerial mycelium formation by *S. coelicolor*. *Cell* 65, 641–650. doi: 10.1016/0092-8674(91)90096-h

Xie, G., Keyhani, N. O., Bonner, C. A., and Jensen, R. A. (2003). Ancient origin of the tryptophan operon and the dynamics of evolutionary change. *Microbiol. Mol. Biol. Rev.* 67, 303–342. doi: 10.1128/mmbr.67.3.303-342.2003

Xu, Z., Li, Y., Wang, Y., Deng, Z., and Tao, M. (2019). Genome-wide mutagenesis links multiple metabolic pathways with actinorhodin production in *Streptomyces coelicolor*. *Appl. Environ. Microbiol.* 85, e03005-18. doi: 10.1128/AEM.03005-18

Conflict of Interest: The authors declare that the research was conducted in the absence of any commercial or financial relationships that could be construed as a potential conflict of interest.

frontiers in Microbiology

REVIEW
published: 24 March 2020
doi: 10.3389/fmicb.2020.00406

The Application of Regulatory Cascades in *Streptomyces*: Yield Enhancement and Metabolite Mining

Haiyang Xia[1], Xiaofang Li[1], Zhangqun Li[1], Xinqiao Zhan[1], Xuming Mao[1,2] and Yongquan Li[1,2]**

[1] *Institute of Biopharmaceuticals, Taizhou University, Taizhou, China,* [2] *Institute of Pharmaceutical Biotechnology, School of Medicine, Zhejiang University, Hangzhou, China*

Streptomyces is taken as an important resource for producing the most abundant antibiotics and other bio-active natural products, which have been widely used in pharmaceutical and agricultural areas. Usually they are biosynthesized through secondary metabolic pathways encoded by cluster situated genes. And these gene clusters are stringently regulated by interweaved transcriptional regulatory cascades. In the past decades, great advances have been made to elucidate the regulatory mechanisms involved in antibiotic production in *Streptomyces*. In this review, we summarized the recent advances on the regulatory cascades of antibiotic production in *Streptomyces* from the following four levels: the signals triggering the biosynthesis, the global regulators, the pathway-specific regulators and the feedback regulation. The production of antibiotic can be largely enhanced by rewiring the regulatory networks, such as overexpression of positive regulators, inactivation of repressors, fine-tuning of the feedback and ribosomal engineering in *Streptomyces*. The enormous amount of genomic sequencing data implies that the *Streptomyces* has potential to produce much more antibiotics for the great diversities and wide distributions of biosynthetic gene clusters in *Streptomyces* genomes. Most of these gene clusters are defined cryptic for unknown or undetectable natural products. In the synthetic biology era, activation of the cryptic gene clusters has been successfully achieved by manipulation of the regulatory genes. Chemical elicitors, rewiring regulatory gene and ribosomal engineering have been employed to crack the potential of cryptic gene clusters. These have been proposed as the most promising strategy to discover new antibiotics. For the complex of regulatory network in *Streptomyces*, we proposed that the discovery of new antibiotics and the optimization of industrial strains would be greatly promoted by further understanding the regulatory mechanism of antibiotic production.

Keywords: antibiotic production, regulatory cascades, rewiring regulatory network, unlocking cryptic metabolites, *Streptomyces*

OPEN ACCESS

Edited by:
Yvonne Mast,
German Collection of Microorganisms and Cell Cultures GmbH (DSMZ), Germany

Reviewed by:
Gang Liu,
Institute of Microbiology (CAS), China
Gong-Li Tang,
Shanghai Institute of Organic Chemistry (CAS), China

****Correspondence:***
Xuming Mao
xmmao@zju.edu.cn
Yongquan Li
lyq@zju.edu.cn

Specialty section:
This article was submitted to Microbial Physiology and Metabolism, a section of the journal Frontiers in Microbiology

Received: *31 October 2019*
Accepted: *26 February 2020*
Published: *24 March 2020*

Citation:
Xia H, Li X, Li Z, Zhan X, Mao X and Li Y (2020) The Application of Regulatory Cascades in Streptomyces: Yield Enhancement and Metabolite Mining. Front. Microbiol. 11:406. doi: 10.3389/fmicb.2020.00406

INTRODUCTION

Streptomyces, Gram-positive mycelial bacteria with high GC content, shows a complex morphological differentiation and belongs to actinobacteria (Hopwood, 2019). It is reported that 61% of so far discovered microorganism-derived bioactive substances are produced by actinobacteria (mainly *Streptomyce*). Most of the clinically essential drugs containing antibiotic and

other bio-active agents are derived from *Streptomyces* (Waksman et al., 2010). In the past decades, scientists have made great advances to elucidate the regulatory mechanisms related to antibiotic production in *Streptomyces*. Generally, the antibiotic production is stringently and elaborately regulated by pyramidal transcriptional regulatory cascades, including signaling pathways, global regulators, pathway-specific regulator (PSR), and feedback regulation. This interweaved networks can determine the production levels of antibiotic under specific culture condition (Chater, 2016).

With the accumulation of genome data, the number of predicted secondary biosynthetic gene clusters (SBGs) on genome is much more than that of the products has been identified. Generally, most of these gene clusters have been defined as cryptic ones because of unknown or undetectable secondary metabolites. Scientists proposed that the *Streptomyces* has been greatly underestimated for the capability to produce diversity of natural products (Baltz, 2017, 2019). Up to now, *Streptomyces* strains are still taken as the most promising candidates for novel antibiotic discovery. In the synthetic biology era, manipulation of regulatory genes has been employed to activate of some cryptic gene clusters.

The production of antibiotic in *Streptomyces* can be largely enhanced by rewiring the regulatory network. There are several reviews on the advances about the elucidation of regulatory networks and the activation of cryptic gene clusters in *Streptomyces* (Ochi, 2017; Onaka, 2017; Wei J. et al., 2018; Palazzotto et al., 2019). Antibiotics or specialized metabolites usually means same for secondary metabolites produced by *Streptomyces*. Here, the term antibiotic is used to stand for the natural products. In this review, we will focus on the production enhancement and new antibiotic discovery by manipulation of the regulatory networks in *Streptomyces*. We proposed that the systematic rewiring of regulatory networks in *Streptomyces* would play a critical role in drug discovery and production enhancement in the near future.

THE REGULATORY CASCADES OF ANTIBIOTIC PRODUCTION IN *Streptomyces*

It is commonly recognized that antibiotic production is stringently regulated by pyramidal transcriptional regulatory cascades in *Streptomyces*. Recent years, there were several reviews on the regulatory networks of *Streptomyces* (Romero-Rodriguez et al., 2018; van der Heul et al., 2018; Wei J. et al., 2018; Palazzotto et al., 2019). So here we won't go into detail of the regulatory networks involved in antibiotic production. The regulatory cascades of antibiotic production will be briefly presented from the following four levels.

The first one is the onset of antibiotic production, which is triggered by the coupled receptors of *Streptomyces* "hormones" or other signals. Among them, A-factor, the chemical structural characteristic γ-butyrolactone (GBL), is the first *Streptomyces* hormone reported as a signal triggering streptomycin production in *Streptomyces griseus* in 1967. Avenolide was identified as a new type of butenolide hormone regulating avermectin production in *Streptomyces avermitilis* (Kitani et al., 2011). The production of the methylenomycin is induced by methylenomycin furan (MMF), a furan-type autoregulator in *Streptomyces coelicolor* (Xu G. et al., 2010). It was reported that 84.1% actinomycetes probably use either GBL (64.1%) or butenolide (24%) to control the antibiotic production (Thao et al., 2017). A-factor, coupled with its receptor ArpA, controls transcription of the master positive regulator AdpA for morphological differentiation and streptomycin production in *S. griseus* (Higo et al., 2012).

The second level is the global regulators which bring pleiotropic effects on the lower level of regulators. The global regulators affect more than one metabolic pathways and may not directly affect any specific biosynthetic gene clusters (BGCs). They also respond to a variety of chemical or physiological signals, e.g., nutrient limitation, the concentration of chitin or *N*-acetylglucosamine (GlcNAc) in the medium, cell wall damage, heat shock or pH shift. Two-component systems (TCSs, consisted with a membrane-bound histidine kinase, which senses specific environmental stimuli, and a cognate regulator) play crucial roles in sensing extracellular signals. Typical TCSs mediate responses to the cellular signal, mainly through regulating the transcription of downstream genes. Moreover, TCSs, as the most abundant pleiotropic regulators, are involved in the dynamic control of the biosynthesis of secondary metabolites in *Streptomyces*. E.g., PhoP/PhoR can regulate antibiotic production and morphological differentiation (Yepes et al., 2011; Rodriguez et al., 2013). Both antibiotic production and GlcNAc uptake *via* the phosphotransferase system are directly regulated by DasR, a GntR-family allosteric regulator, with the GlcNAc as a ligand (Fillenberg et al., 2016). The major checkpoint for the onset of secondary metabolism is the accumulation of GlcNAc through the autolytic degradation of the vegetative mycelium. The antibiotic production is triggered by DasR regulon (Rigali et al., 2008). AdpA, which is ubiquitously distributed in streptomycetes as a member of the AraC/XylS family regulators, affects transcription of hundreds of genes involved in morphological differentiation and antibiotic biosynthesis (Higo et al., 2012; Guyet et al., 2014). ArpA, the receptor of A-factor, regulated the transcription of *adpA* in *S. griseus*. The transcription level of *adpA* is dynamic controlled by the interaction between ArpA and A-factor. As A-factor reached a threshold concentration, it binds to ArpA and releases the repression of *adpA* transcription (Wei J. et al., 2018). WblA and AtrA also have been extensively investigated as the global regulators involved in the biosynthesis of antibiotic. As a global repressor, WblA affects doxorubicin (DXR), tautomycetin, and daptomycin biosynthesis in their natural host strains (Noh et al., 2010; Nah et al., 2012; Kim et al., 2014). However, WblA activates natamycin biosynthesis in *Streptomyces chattanoogensis* (Yu et al., 2014).

The third level is pathway-specific regulators (PSRs), which are taken as the master switches of antibiotic production. PSRs are situated in the BGCs of secondary metabolites and directly regulate the transcription of the biosynthetic genes. So they have been called the "cluster-situated regulators (CSRs)." SARP (*Streptomyces* antibiotic regulatory proteins), LAL (large ATP-binding regulators of the LuxR family) and PAS-LuxR

family regulators usually belong to PSRs (Martin and Liras, 2012). The ActII-ORF4 and RedD of *S. coelicolor* and DnrI of *S. peucetius* are typical SARPs family activators (Song et al., 2011). The LAL family regulators, which comprise an N-terminal ATP/GTP-binding domain and a C-terminal LuxR family DNA-binding domain, usually activate the biosynthesis of antibiotic in *Streptomyces*. PimR, RapH, NysRI, AveR, and SlnR, which are typical LAL regulators, are located in type I polyketide BGCs in *Streptomyces* (Anton et al., 2004; Sekurova et al., 2004; Kuscer et al., 2007; Guo et al., 2010; Zhu et al., 2017). The whole process of avermectin biosynthesis is controlled by direct interaction between AveR and all promoters of *ave* cluster (Guo et al., 2010). The PAS-LuxR family regulator is characterized with an N-terminal PAS sensory domain and a C-terminal LuxR type DNA binding domain. PAS domain probably function as responsor to light, redox potential, oxygen, overall energy level of a cell, and small ligands (Taylor and Zhulin, 1999). For the cytosol localization, proteins containing PAS domains can sense internal signals and other environmental factors which cross the cell membrane. PimM, a PAS-LuxR family regulator, positively regulates pimaricin production in *Streptomyces natalensis* (Anton et al., 2007). The orthologs of PimM have been represented in most of the reported BGCs of antifungal polyketides like amphotericin (AmphRIV), candicidin (FscRI), nystatin (NysRIV), and filipin (PteF) gene clusters (Santos-Aberturas et al., 2011). PSRs also contain other family repressor or activator. The production of antibiotic can be positively or negatively regulated by TetR, MarR, LysR, and IclR family regulators (Molina-Henares et al., 2006; Martin and Liras, 2012; Cuthbertson and Nodwell, 2013; Zhang et al., 2015; Guo et al., 2018).

The fourth level is the feedback regulation which is brought by antibiotic and/or intermediates to coordinate antibiotic production and transport. Evidences have shown that antibiotic functions as signals to regulate the production of antibiotic besides as feedback substances for the enzymatic reactions. Antibiotic, as ligand for proper regulator, affects the final production in *Streptomyces*. The expression of antibiotic biosynthetic genes was modulated by the RedZ and undecylprodigiosin complex (Wang L. et al., 2009). The activity of AtrA, which regulates primary and secondary metabolism, is reduced by lidamycin of *Streptomyces globisporus* and actinorhodin (ACT) of *S. coelicolor* (Li et al., 2015). The biosynthesis of jadomycin is dynamically modulated by the interaction among jadomycin B, chloramphenicol, JadR1 and JadR2 in *Streptomyces venezuelae* (Wang L. et al., 2009; Xu D. et al., 2010). Daunorubicin (DNR) biosynthesis is regulated by three DNA binding regulatory proteins (DnrI, DnrN, and DnrO). The DNA binding activity of DnrO can be modulated by Rhodomycin D, a glycosylated precursor of DXR (Jiang and Hutchinson, 2006). Simocyclinone and its precursors inhibit the binding activity of SimReg1 to several promoter regions of simocyclinone biosynthesis genes and SimReg1 encoding gene (Horbal et al., 2012). As a GBL receptor-like protein, PapR5, which is the major regulator of pristinamycin biosynthesis, may sense pristinamycin or intermediate(s) of the pathway (Mast et al., 2015). SsaA can activate sansanmycin biosynthesis by binding to five different regions within the sansanmycin BGC. The sansanmycins A and H inhibit DNA-binding activity of SsaA in a concentration-dependent manner (Li et al., 2013). The rifamycin B, the end product of rifamycin biosynthesis, can relieve the repression of RifQ on the transcription of the rifamycin efflux pump (RifP) (Lei et al., 2018). Transporters may affect product maturation. The ABC transporters NysG and NysH involved in the biosynthetic export of nystatin in *Streptomyces noursei*. Deletion of either transporter gene caused ca. 35% reduction in the levels of fully formed nystatin and led to concomitant enrichment of a deoxy precursor. The authors proposed that a NysGH complex might preferentially export fully formed nystatin and that this activity would increase the efficiency of the last biosynthetic step through product removal (Sletta et al., 2005). For both class I and II lantibiotics, the function of a dedicated ABC transporter, generally termed 'LanT,' is essential for the formation of the final product (Gebhard, 2012).

Signals and regulators, dynamic fluctuating on the metabolic state of the cell and its environment, are extensively involved in regulation of secondary metabolism. The abundances of nitrogen, phosphate and carbon sources are nutrimental signal for the onset of secondary metabolism. It has been reported that GlnR and PhoR–PhoP was involved in the type of regulation depending on the carbon, nitrogen, and phosphate supply. For the similarity of binding sites, PhoP and GlnR showed competitive binding to target genes in some cases (Romero-Rodriguez et al., 2018). In *Saccharopolyspora erythraea*, the GlnR regulon is not only involved in nitrogen metabolism, but it also appears to control ABC-type transporters for uptake of carbon sources (Liao et al., 2015). In *S. avermitilis*, AveR positively regulates avermectin production and negatively affects oligomycin biosynthesis, respectively (Guo et al., 2010). AveI, an AtrA-like regulator, regulates production of avermectin, oligomycin, melanin, and morphological differentiation by directly regulating the transcription of *ave*, *olm*, *melC1C2*, *ssgRD*, *wblI* and genes in primary metabolism, including substrates transport, the metabolism of amino acids, lipids, and carbohydrates (Liu et al., 2019). Usually more than twenty secondary metabolic pathways exist in most of the *Streptomyces* (Nett et al., 2009). There is complex cross-talk regulation among different biosynthetic clusters and between the primary and secondary metabolism. With the deep understanding the regulatory mechanism of the antibiotic production, there is a consensus that the complicated and interweaved regulatory networks contribute to the dynamic antibiotic production in *Streptomyces*.

ENHANCEMENT OF ANTIBIOTIC PRODUCTION IN *Streptomyces* BY REWIRING THE REGULATORY NETWORKS

As mentioned above, the regulatory networks constitute major bottlenecks to over produce target antibiotics. The manipulation of regulatory genes can contribute to overcome these bottlenecks

to turn on the expression of gene clusters for antibiotic production. Various strategies have been taken to manipulate regulatory genes to achieve the optimal antibiotic production in both the native and/or heterologous hosts.

Enhancing Antibiotic Production by Overexpression of Positive Regulator Genes

The regulators also can be defined as positive and negative regulators according their effect on the antibiotic production. The positive regulators (activators) can promote the biosynthesis of antibiotics. But the negative ones (repressors) can repress the biosynthesis of antibiotics (Martin and Liras, 2010). Since the positive regulators activate the transcription of antibiotic BGCs, they can be manipulated to enhance the production of antibiotic in *Streptomyces*. The titer improvement can efficiently and simply be achieved by over-expression of genes encoding activators with proper promoters. As listed in **Table 1**, overexpression of genes encoding LAL family regulators, such as MilR, NemR, and AveR, has been used to increase production of milbemycin in *S. bingchenggensis* BC04, nemadectin in *S. cyaneogriseus* subsp. *non-cyanogenus* NMWT1 and avermectin in *S. avermitilis*, respectively (Guo et al., 2010; Zhang Y. et al., 2016; Li et al., 2019). Overproduction of nikkomycin has been achieved by engineering of the CSR activator gene *sanG* with different constitutive promoters (Liu et al., 2005). Overproduction of oxytetracycline (OTC) has been achieved by overexpression of the CSR activator gene *otcR* as tandem copies under the control of a constitutive SF14 promoter (Yin et al., 2015). Similar strategy has also been used to overproduce tacrolimus (FK506) in *Streptomyces tsukubaensis* NRRL18488 by overexpression of *bulZ* (Ma et al., 2018). Other examples include LysR family regulator for ascomycin production in *S. hygroscopicus* var. *ascomyceticus* (Song et al., 2017), PAS-LuxR family regulator for wuyiencin production in *Streptomyces wuyiensis* CK-15 (Liu et al., 2014), and Crp/Fnr family regulator for leinamycin production in *Streptomyces atroolivaceus* (Huang et al., 2016).

The expression level of positive regulator is not always correlated to the production of antibiotic. E.g., overexpression of *mil*R with a strong constitutive promoter led to decrease of milbemycin production in *S. bingchenggensis* (Zhang Y. et al., 2016). These showed that the threshold of the over-expressed regulator was key point to determine the production of antibiotic in *Streptomyces*.

Enhancing Antibiotic Production by Removal of Repressor Genes

The TetR and LysR family regulators are widely distributed in the genome of *Streptomyces*. Most of TetR and LysR regulators function as repressors. More details of TetR family regulators have been reviewed elsewhere (Cuthbertson and Nodwell, 2013). Deletion of TetR family repressors has been used to increase avermectin production in *S. avermitilis* (He et al., 2014), calcimycin production in *Streptomyces chartreusis* NRRL 3882 (Gou et al., 2017), and pristinamycin production in *Streptomyces pristinaespiralis* (Meng et al., 2017).

WblA, a WhiB-like protein, also widely distributes among actinomycetes (Kim et al., 2014; Huang et al., 2017). WblA affects morphological development and antibiotic biosynthesis. It generally functions as a global repressor of antibiotic biosynthesis, such as DXR biosynthesis in *S. peucetius*, tautomycetin biosynthesis in *Streptomyces* sp. CK4412, and daptomycin biosynthesis in *Streptomyces roseosporus*. Deletion of *wblA* leads to overproduction of pikromycin in *S. venezuelae* (Woo et al., 2014), daptomycin in *S. roseosporus* (Huang et al., 2017). Other examples include deletion of genes encoding GntR family regulators for platensimycin and platencin overproduction in *Streptomyces platensis* (Smanski et al., 2009).

The *nsdA*, a gene negatively affecting *Streptomyces* differentiation, had been proved a pleiotropic negative regulatory gene in *S. coelicolor* (Li et al., 2006). It plays a negative role in sporulation, morphological differentiation and antibiotic synthesis. The overproduction of ACT, calcium-dependent antibiotic (CDA), and methylenomycin was detected in a *nsdA* mutant. The *nsdA* homologous genes have been found to conservatively distribute in *Streptomyces*. The milbemycin A4 and nanchangmycin production increased in *nsdA* mutant of *S. bingchengensis* by 1.5-fold and 9-fold, respectively (Wang X. J. et al., 2009). The natamycin production can be increased 1.9-fold by deletion of *nsdA* gene in *Streptomyces lydicus* A02 (Wu et al., 2017).

γ-Butyrolactone receptors, like the A-factor receptor ArpA, repress transcription of *adpA* to affect the production of streptomycin in *S. griseus*. Deletion of the GBL receptors probably can promote antibiotic production. The validamycin production of mutants with deletion of *arpA* homologs were increased by 26% (Δ*shbR1*) and 20% (Δ*shbR3*) in *S. hygroscopicus* 5008, respectively (Tan et al., 2015). Deletion of *avaR1*, the avenolide (a novel butenolide-type autoregulator) receptor encoding gene, increased production of avermectin B1a approximately 1.75 times compared with the parent strain in a high-producing *S. avermitilis* strain (Wang et al., 2014).

Enhancing Antibiotic Production by Manipulation of Feedback and Transport

Genes encoding exporters, which are responsible for the secretion of antibiotic, often situate in their BGCs. The majority of BGC-linked antibiotic exporters belongs to various subgroups like the ATP-binding cassette (ABC) superfamily and major facilitator superfamily (MFS) of transporters. It is commonly assumed that BGC-linked exporters function in the secretion of the antibiotic made by BGC. Toxic end-products can be pumped out of the cells by exporters to realize more durable and sustainable productivity.

Importantly, even in the absence of toxicity, the ability to secrete the end-products may play key roles in affecting the expression of the BGCs. ActA (ActII-ORF2) and ActB (ActII-ORF3) are MFS and RND (root-nodulation-division) exporters, respectively, involved in ACT production in *S. coelicolor*. ActA and ActB are crucial players in the sophisticated feed-forward mechanism, by which secretion of the end-products leads to the transcriptional activation of the BGCs in the cells (Tahlan et al., 2007; Xu et al., 2012). The double *actAB* mutant could

TABLE 1 | Examples of antibiotic production enhancement in *Streptomyces* by regulatory gene manipulation.

Strategy	Antibiotics	Strains	Regulators (family)	Yield	References
Overexpression of positive genes	Milbemycin	*S. bingchenggensis*	MilR(LAL)	138%	Zhang Y. et al., 2016
	Nemadectin	*S. cyaneogriseus*	NemR(LAL)	179.9%	Li et al., 2019
	Avermectin	*S. avermitilis*	AveR(LAL)	164%	Guo et al., 2010
	Nikkomycin	*S. ansochromogenes*	SanG(SARP)	200%	Liu et al., 2005
	Oxytetracycline	*S. rimosus*	OtcR(SARP)	649%	Yin et al., 2015
	FK-506	*S. tsukubaensis*	BulZ (SARP)	∼330%	Ma et al., 2018
	Wuyiencin	*S. ahygroscopicus*	WysR(PAS-LuxR)	300%	Liu et al., 2014
	Leinamycin	*S. atroolivaceus*	LnmO(Crp/Fnr)	300%	Huang et al., 2016
	Pimaricin	*S. natalensis*	PimM(PAS-LuxR)	240%	Anton et al., 2007
	Pimaricin	*S. chattanoogensis*	ScnRII(PAS-LuxR)	400%	Du et al., 2009
	Milbemycin	*S. hygroscopicus*	MilR2 (TetR)	34.4%	Wei K. et al., 2018
	Avermectin	*S. avermitilis*	SAV4189 (MarR)	250%	Guo et al., 2018
	FK-506	*S. tsukubaensis*	FkbN (LAL)	176%	Zhang X. S. et al., 2016
	Daptomycin	*S. roseosporus*	DepR1(TetR)	141%	Yuan et al., 2016
	Daptomycin	*S. roseosporus*	DptR3(*MarR)*	131%	Zhang et al., 2015
Deletion of negative regulatory genes	Avermectin	*S. avermitilis*	SAV151(TetR)	200%	He et al., 2014
	Calcimycin	*S. chartreusis*	CalR3(TetR)	280%	Gou et al., 2017
	Pristinamycin	*S. pristinaespiralis*	PapR3(TetR)	240%	Meng et al., 2017
	Daptomycin	*S. roseosporus*	WblA	151%	Huang et al., 2017
	Pikromycin	*S. venezuelae*	WblA	350%	Woo et al., 2014
	Doxorubicin	*S. peucetius*	WblA	170%	Noh et al., 2010
	Platensimycin	*S. platensis*	PtmR1(GntR)	∼500%	Smanski et al., 2009
	Natamycin	*S. natalensis*	PhoRP(TCS)	180	Mendes et al., 2007
	Milbemycin	*S. bingchenggensis*	NsdA	150%	Wang X. J. et al., 2009
	Natamycin	*S. lydicus*	NsdA	190%	Wu et al., 2017
	Avermectin	*S. avermitilis*	AveI(AtrA)	1600%	Chen et al., 2008
	Nystatin A1	*S. ahygroscopicus*	TtmRIV(PAS-LuxR)	212%	Cui et al., 2015
	Rapamycin	*S. rapmycinicus*	RapS(TetR)	460%	Yoo et al., 2015
	Rapamycin	*S. rapmycinicus*	RapY(TetR)	370%	Yoo et al., 2015
Deletion of GBL receptors	Tylosin	*S. fradiae*	TylP	∼200%	Stratigopoulos et al., 2002
	Avermectin	*S. avermitilis*	AvaR1	∼300%	Wang et al., 2014
	Milbemycin	*S. bingchenggensis*	SbbR	125%	He et al., 2018
	Natamycin	*S. natalensis*	SngR	460%	Lee et al., 2005
	FK506	*S. tsukubaensis*	BulR1	27.8%	Salehi-Najafabadi et al., 2014
	Clavulanic acid	*S. clavuligerus*	Brp	300%	Santamarta et al., 2005
	Validamycin	*S. hygroscopicus*	ShbR1/R3	∼55%	Tan et al., 2015
Overexpression the feedback transporters	Avermectin	*S. avermitilis*	AvtAB	∼50%	Qiu et al., 2011
	Daunorubicin	*S. peucetius*	*DrrC*	510%	Malla et al., 2010
	Rifamycin	*A. mediterranei*	*RifQ*	200%	Lei et al., 2018
Ribosomal engineering	Avermectin	*S. avermitilis*	σ^{hrdB}(A56 A393)	150%	Zhuo et al., 2010
	Actinorhodin	*S. lividans*	RpsL(K88E, L90K)	290%	Okamoto-Hosoya et al., 2003b
	Actinorhodin	*S. coelicolor*	K88E, the GI92	200%	Wang G. et al., 2009
	Salinomycin	*S. albus*	RpsL(K88R), RpoB	230%	Tamehiro et al., 2003
	A21978C	*S. roseosporus*	RpsL K43N	220%	Wang et al., 2012
	Chloramphenicol	*S. coelicolor**	RpsL(K88E) RpoB(S433L)	∼1000%	Gomez-Escribano and Bibb, 2011

**Heterologous expression.*

only produce one fifth of ACT compared to WT. The activation of ACT production occurs in two waves where expression of key *act* genes, including the *actAB* operon, is initially induced by a biosynthetic intermediate. The ACT production grows into full induction only once the accumulating ACT is secreted out of the cells.

The genes encoding for the AvtAB ABC transporter are adjacent and co-expressed with the BGC for avermectin in *S. avermitilis*. In the WT strain, deletion of either *avtA* or *avtB* had no effect on avermectin production, while over-expression of *avtAB* led to the increased level of avermectin B1a with two-fold. But the production level of oligomycin A, another product from

S. avermitilis, was found unaltered. The production promotion effects of *avtAB* could be specific to avermectin in *S. avermitilis* (Qiu et al., 2011). Co-overexpression of three OTC resistance genes, including *otrA* (encoding a ribosomal protection protein), *otrB* and *otrC* (encoding two efflux proteins), led to 179% increase of OTC production in *Streptomyces rimosus* M4018 (Yin et al., 2017).

Feed-forward mechanisms may explain the regulation of BGCs for the actinobacterial ribosomally synthesized and post-translationally modified peptides (RiPPs), planosporicin and microbisporicin. The multiple ABC transporter genes in these BGCs seem to modulate their production and self-immunity (Foulston and Bibb, 2010; Sherwood et al., 2013). GouM, the MFS transporter, is responsible for the secretion of gougerotin outside of *Streptomyces graminearus* (Wei et al., 2014). The overexpression of BotT, a putative efflux pump encoded in the bottromycin BGC, increased bottromycin production about 20 times in a heterologous host (Huo et al., 2012).

Export of antibiotic is important for the producer to reduce the intracellular antibiotic concentration, which can relieve self-toxicity. In *Amycolatopsis mediterranei*, Δ*rifQ* mutant brought overexpression of RifP. The accelerated export of rifamycin may reduce the intracellular rifamycin concentration, relieve other possible feedback inhibition of rifamycin biosynthesis and finally lead to more than two-fold improvement of rifamycin B production (Lei et al., 2018). Overexpression of DrrC, which provide self-resistance to DNR and DXR, achieved 5.1-fold increase in DXR production in *S. peucetius* ATCC 27952 (Malla et al., 2010).

For there are many transporters help to transport end products or intermediates out of the cell, this can help to remove the feedback caused by the antibiotics or intermediates. Transporters enhance the efflux of the self-produced antibiotics, which can be an important strategy for self-protection from self-toxicity. Many antibiotic BGCs comprise functional exporter genes (Rees et al., 2009; Severi and Thomas, 2019). Also some exporters encoding genes for detoxification are outside of the BGCs. By systematical investigation, it has proved that more than 25 groups of genes contributed the efflux of molecules involved in natamycin biosynthesis (Shan et al., 2019).

Enhancing Antibiotic Production by Ribosome Engineering

Classical strain improvement is usually achieved by multiple rounds of random mutagenesis and repetitively screening. Although the outcome is fruitful, the weakness of this strategy is time intensive and laborious. A ribosome engineering approach has been designed to obtain antibiotic overproducing strains by corelatively screening for mutants with proper drug resistant level, e.g., streptomycin resistance mutations (Hosoya et al., 1998). It has been proven to be an effective rational strategy for strain improvement. The percentage of overproducing mutants among drug resistance mutants can be up to 2–20% in a species dependent way, which is much higher than that of random mutagenesis. S12-mutated variants, which have mutations in the *rpsL* gene with resistance to streptomycin, stabilize the open A-site conformation and prevent streptomycin from binding (Holberger and Hayes, 2009). Screening of streptomycin resistant mutations has been demonstrated a useful tool for strain improvement in many *Streptomyces* strains (Ochi, 2007). The undecylprodigiosin production in *S. lividans* was activated in RpsL mutants with K88E, L90K, and R94G substitutions (Okamoto-Hosoya et al., 2003b). The industrial strain of *S. albus*, which had RpsL (K88R) and RpoB mutation, enhanced salinomycin production by 1.5-fold (Tamehiro et al., 2003). In *S. coelicolor*, over 10-fold ACT improved in RpsL (K88E and P91S) strains than the original strain (Okamoto-Hosoya et al., 2003a). Both the K88E mutation and an insertion mutation at GI92 led to substantially higher levels of ACT in *S. coelicolor* strains (Wang G. et al., 2009). Selection of mutations in the *rpsL* gene are widely used to improve the production in a variety of industrial antibiotic-producing strains (Tamehiro et al., 2003; Beltrametti et al., 2006).

Another method of "ribosome engineering" incorporates the inactivation of the *rsmG* gene, which encodes an *S*-adenosylmethionine (SAM)-dependent 16S rRNA methyltransferase. Recombinants with deletion of *rsmG* gene resulted in overproduction of ACT in *S. coelicolor* (Nishimura et al., 2007).

Previous reports showed that ribosome engineering was an effective strategy for yield improvement in *Streptomyces*. From the reference, ribosome engineering has been employed for yield improvement in more than fifty *Streptomyces* strains (Zhu et al., 2019). As a rational and cost-effective approach, ribosome engineering could be adapted to speed up strain development for those without clear genetic background. If compared with other direct genetic manipulation approach, the ribosome engineering still be with laborious screening to overcome the phenotype uncertainty of resistant mutants.

The above data show that manipulation of regulatory cascades can be an efficient way to improve the production of antibiotic. It is obvious that the balance and synergy between primary and secondary metabolism is very important for the overproduction of antibiotic. Rewiring regulatory network combined with metabolic engineering will be a more powerful way to enhance the production of antibiotic in *Streptomyces*.

DISCOVERING NOVEL ANTIBIOTICS THROUGH ACTIVATING THE CRYPTIC GENE CLUSTERS BY UNLOCKING THEIR REGULATORY NETWORK

The genome sequencing of streptomycetes demonstrated that each genome has the genetic capacity with 20–40 distinct gene clusters for secondary metabolites. They can produce far more compounds than reported previously (Nett et al., 2009). Since many of these gene clusters are expressed at low levels under laboratory conditions, they are called cryptic gene clusters. Several strategies have been designed to activate these clusters and discover novel molecules. The feasible approaches include uses of signals probes, ribosome engineering, regulatory unlocking

and heterologous expression (Laureti et al., 2011; Ochi, 2017; Myronovskyi and Luzhetskyy, 2019). For this review is about the regulation in *Streptomyces*, the heterologous expression will not be discussed here.

Activation of Cryptic Gene Clusters by Chemical or Physical Signals

Though *Streptomyces* has the potential to produce over 20 secondary metabolites, most BGCs are cryptic or silent. As we know from the regulatory cascades, there are many signaling factors affecting the expression of secondary metabolic gene, and many culture dependent methods have been developed (Yoon and Nodwell, 2014).

The one strain many compounds (OSMACs) approach has been previously applied to explore the secondary metabolic potential of different strains with altering a single parameter in the growth conditions or eliciting a stress response (Bode et al., 2002). Heat shock and ethanol shock are two widely applied measures. *S. venezuelae* produces negligible amounts of jadomycin when it is cultured at 27°C without heat/ethanol shock. The yield of jadomycin B reach 25 μg/ml after 12 h by shifting the temperature from 27 to 42°C. Similarly, cultures with 6% ethanol enhanced yields of jadomycin to as high as 30 μg/ml at 27°C (Doull et al., 1993, 1994). Another compound that is produced in response to the heat/ethanol shock is validamycin A (VAL-A) by *Streptomyces hygroscopicus*. VAL-A rapidly accumulated at relatively higher fermentation temperatures (37°C, 40°C, and 42°C). But the production was very low at lower temperatures (28°C, 30°C, 33°C, and 35°C) (Liao et al., 2009). Several other stress responses have been explored. New metabolites can be produced by *Streptomyces parvulus* upon increasing the hydrostatic pressure during fermentation (Bode et al., 2002). *S. coelicolor* can produce ectoine and 5-hydroxyectoine under high salt conditions and temperature stress (Bursy et al., 2008). Methylenomycin production can be activated in *S. coelicolor* by either alanine growth-rate-limiting conditions and/or acidic pH shock (Hayes et al., 1997).

As we know that the autoregulators can trigger the antibiotic production in *Streptomyces*. These classes of naturally produced chemical probes like GBLs can be used to elicit the expression of cryptic SBGs. Goadsporin, a compound isolated from *Streptomyces* sp. TP-A0584, was shown to stimulate the production of prodiginine antibiotic in *S. lividans*, and promote pigment production and morphogenesis on 36 streptomycetes (Onaka et al., 2001).

In *Streptomyces*, antibiotic production, which is usually coupled with the onset of development, is triggered by the interaction between DasR and the accumulation of GlcNAc after autolytic degradation of the vegetative mycelium. So GlcNAc can be used as a signal chemical to activate pathways for secondary metabolite biosynthesis. Several *Streptomyces* species were examined for their antibiotic production on MM plates (25 mM mannitol as the sole carbon source) with or without GlcNAc (50 mM). GlcNAc had a stimulating effect on antibiotic production on *S. clavuligerus*, *S. collinus*, *S. griseus*, *S. hygroscopicus*, and *S. venezuelae* (Rigali et al., 2008).

By investigating small molecules that perturb secondary metabolism, Justin group had screen out 19 compounds from 30,569 small molecules of the Canadian Compound Collection for their ability to alter the pigmentation of *S. coelicolor*. The ARC2 series (ARC2, ARC3, ARC4, and ARC5) were structurally related to triclosan, a synthetic antibiotic (Craney et al., 2012). Particularly, ARC2 altered the secondary metabolite output in all of the tested streptomycetes (Craney et al., 2012; Ahmed et al., 2013). These probes appear to have the potential to widely use as active elicitors for mining secondary metabolite.

Since *Streptomyces* is the soil dwelling microbe, it was reported that antibiotic overproduction could be promoted by 2- to 25-fold when the rare earth, scandium (Sc), added at a low concentration (10–100 mM) to cultures of *S. coelicolor* A3(2) (ACT producer), *Streptomyces antibioticus* (actinomycin producer), and *S. griseus* (streptomycin producer). Scandium was also effective in activating the dormant ability to produce ACT in *S. lividans* (Kawai et al., 2007). The rare earth elements, scandium and/or lanthanum, can activate the expression of nine genes belonging to nine secondary metabolite–BGCs by 2.5- to 12-fold in *S. coelicolor* A3(2). Several compounds can only be detected with HPLC in the rare earth-treated cultures (Tanaka et al., 2010).

Combined-culture is a co-culture method to activate secondary metabolism in *Streptomyces* (Onaka, 2017). The biosynthesis of red pigment by *S. lividans* TK23 can be influenced by co-culture with *Tsukamurella pulmonis* TP-B0596. It was proved that the biosynthesis of cryptic natural products in *Streptomyces* species can only be induced by living mycolic acid-containing bacteria (MACB). ∼90% of *Streptomyces* species, which isolated from soil samples collected in the Hokuriku district of Japan, show changes in secondary metabolism in combined-culture with *T. pulmonis* (Onaka et al., 2011).

Binding to a specific receptor, like the A factor, is proposed as possible mechanisms of activation of secondary metabolite biosynthesis by some chemical probes. The perturbation of host metabolism can be another reason to activate cryptic clusters. The ARC2 series, similar to triclosan, repress fatty acid biosynthesis by inhibiting the enoyl reductase FabI and change the flux of precursor molecules to antibiotic biosynthesis. Quorum sensing molecules could also important factors to induce the secondary metabolite production in actinomycetes. The results from co-cultivation probably due to physical cell to cell interactions, small molecule-mediated communication or metabolite precursor supply (Abdelmohsen et al., 2015; Jones et al., 2017). Though a great many of products are discovered through activation of cryptic gene clusters by chemical or physical signals, it still lacks clearly explanation of the molecular mechanism triggering the expression of the secondary metabolic genes. But for this approach is non-genetic dependent, it can be developed to high-throughput screening model to investigate more strains easily.

Activation of the Cryptic Gene Clusters by Manipulation of the Regulatory Genes

The transcription processes of BGCs are usually modulated by specific regulatory gene clusters, including activators and

repressors, which activate or repress biosynthesis, respectively. The identification of PSRs genes offers possibility to activate the desired BGCs either by inactivation of the repressor or overexpression of the activator genes (Baral et al., 2018).

TetR family of transcription regulators, which participate in the regulatory pathways associated with the efflux of antibiotic, cell–cell signaling, antibiotic biosynthesis, biofilm formation, etc., is one of the most predominant families of transcription factors in the prokaryotic system (Bhukya and Anand, 2017). The TetR family members usually serve as repressors which possess a N-terminal DNA-binding domain and a C-terminal signal reception domain (Cuthbertson and Nodwell, 2013). The inactivation of a TetR transcriptional repressor gene *arpRII* in *Streptomyces argillaceus* promoted the activation of the cryptic gene cluster *arp*, and discovery of argimycins P, a natural product in polyketide alkaloid family (Ye et al., 2018). ScbR, another TetR-like transcriptional repressor, has been confirmed to directly control the expression of the cryptic type I polyketide BGC by binding at two different positions of *kasO* promoter in *S. coelicolor* (Takano et al., 2005; Xu D. et al., 2010; Bhukya and Anand, 2017). GdmRIII, a TetR family transcriptional regulator, was connected with the biosynthetic pathways of geldanamycin and elaiophylin in *Streptomyces autolyticus* CGMCC0516 (Jiang et al., 2017). Moreover, it has been proved that the biosynthetic pathways including jadomycin, kinamycin, and auricin, were activated after removal of TetR family repressors, JadR/JadR2 (Zhang et al., 2013), AlpW (Bunet et al., 2011), and SCO1712 (Lee et al., 2010), respectively.

LuxR superfamily is another predominant class of regulators associated with quorum sensing (Baral et al., 2018). Contrary to the TetR family, LuxR-like proteins usually act as activators during secondary metabolic regulation. LuxR proteins consist of an N-terminal DNA binding domain and a C-terminal ligand-binding domain, where ligand binding induces homodimerization and subsequent binding of protein to DNA to initiate transcription (Maddocks and Oyston, 2008). LuxR proteins, which are abundant among Actinobacteria, Proteobacteria, and Firmicutes, play significant roles in improvement of antibiotic production and activation of cryptic gene clusters after overexpression. The LuxR family members, GdmRI and GdmRII, are positive regulators required for geldanamycin biosynthesis in *S. hygroscopicus* 17997, and inactivation of them resulted in blocked production of geldanamycin (He et al., 2008). The synthesis of β-lactam antibiotic thienamycin was first observed when ThnI protein of LuxR family was induced in *Streptomyces cattleya* (Rodriguez et al., 2008). Furthermore, the LAL–proteins are large ATP-binding regulators constituting a noteworthy branch of LuxR family (De Schrijver and De Mot, 1999). The LAL–subfamily members usually contain an additional ATP binding domain at the N-terminus, which is responsible for the interaction with the inducers, maltotriose and ATP (Danot, 2001; Baral et al., 2018). Series of studies have confirmed that LAL regulators play important roles in activating the silent gene clusters. Overexpression of LAL-type regulatory factor *samR* in *Streptomyces ambofaciens* activated a 150 kb cryptic gene cluster, and promoted the discovery of a glycosylated macrolide product with anti-cancer activity (Laureti et al., 2011). Similarly, LAL-type transcriptional regulators of GdmRI and GdmRII in *S. hygroscopicus* are positive to geldanamycin biosynthesis (Martin et al., 2019). Furthermore, the LAL-like 63-amino acid protein AfsS and its homologs have been shown to relate closely with the induction of avermectin in *S. avermitilis* (Lee et al., 2000), pikromycin in *S. venezuelae* (Maharjan et al., 2009), and DXR in *S. peucetius* (Parajuli et al., 2005).

Manipulation of the regulators in cryptic gene clusters probably the most convenient way to activate the pathway. But for the uncertainty of regulatory network, the success of activation is case by case.

Activation the Cryptic Gene Clusters by Ribosome Engineering

Ribosome engineering, first proposed by Kozo Ochi, focuses on modifying ribosomal or RNA polymerases whose structural and functional changes related to the synthesis of secondary metabolites (Ochi et al., 2004). The introduction of specific mutations into the ribosome elements triggers structural changes to ribosome with affected protein synthesis, which ultimately influences secondary metabolism of the microorganism. Targeted strains are screened by mutations in antibiotic resistance acting on ribosome without special requirement of equipment or genetic background of the strains. Isoindolinomycin (Idm), an unprecedented bioactive polyketide with a novel isoindolinone-containing tetracyclic skeleton, was discovered by activation of cryptic gene through screening rifampicin-resistant (*rif*) mutants from actinobacteria strains (Thong et al., 2018). Piperidamycins production was induced in a gentamicin-resistant mutant of *Streptomyces mauvecolor*, whereas the wild strain does not produce these metabolites at any detectable level on various media (Hosaka et al., 2009; Baral et al., 2018). Ribosome engineering now is developed into an important technology for improving secondary metabolites with commercial value and stimulating new natural product production, and also contributes to increase in structural diversity of bioactive compounds. Mutations in these ribosomal genes have also been shown to activate the expression of silent or poorly expressed BGCs in *S. griseus* (Tanaka et al., 2009).

Most above strategies to activate cryptic gene clusters are by manipulating the original host. With developing of large DNA cloning, heterologous expression is extensively used to overexpress target clusters in super host strains (Yamanaka et al., 2014; Greunke et al., 2018; Choi et al., 2019). There are series of reviews on this aspect. Also some heterologous expression was solved with overexpression of regulatory genes by proper promoters in the target clusters (Fazal et al., 2019; Myronovskyi and Luzhetskyy, 2019; Nepal and Wang, 2019; Xu and Wright, 2019).

CONCLUSION AND PERSPECTIVES

Streptomyces, which has complex morphological development and cell differentiation, can adapt to diverse environments by ingenious regulation and produce variety of secondary

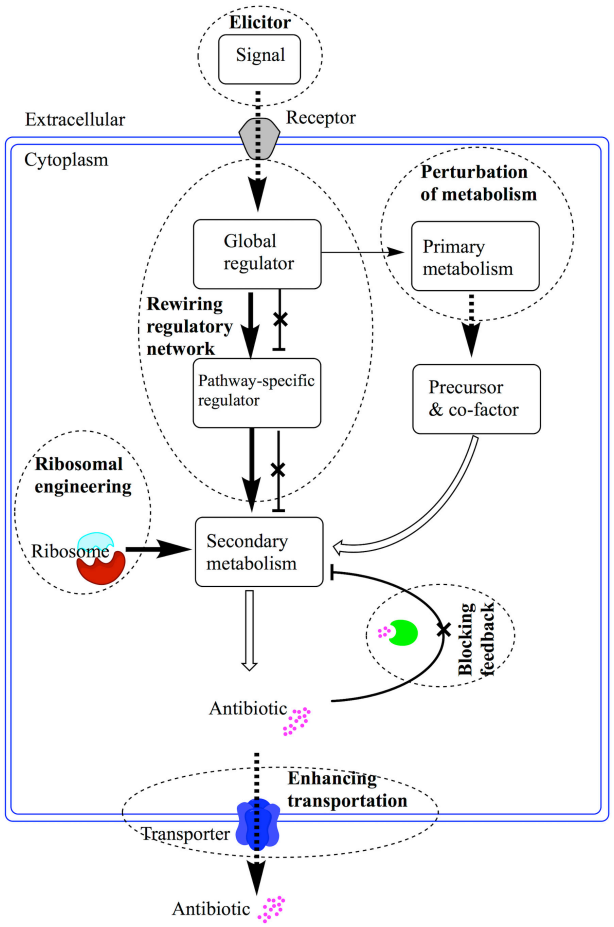

FIGURE 1 | Schematic diagram of application strategies for regulatory cascades in *Streptomyces*. The regulatory cascades are illustrated with arrow linked rectangles. The dash circles are annotated with bold text to describe the strategies employed to enhance antibiotic production or discovery of novel antibiotics. The bold arrows mean overexpression of positive regulators. The crossed perpendicular lines mean the deletion of repressors or inhibition of feedback reactions. The dash bold arrows mean enhanced supply of precursor or efflux of antibiotics.

metabolites. The regulation of antibiotic production has been extensively investigated in the past years. For the complicated interactions among primary and secondary metabolic pathways, elucidation of the regulatory network in antibiotic production still was a tough task for scientist. With further recognizing the secondary metabolism regulatory cascades, novel proposed strategies can greatly promote the production enhancement and drug discovery in *Streptomyces*. For there are several reviews on the regulation of antibiotic biosynthesis, strategy to enhance production of antibiotic in *Streptomyces* and new compounds discovery in actinobacteria by Nodwell group and van Wezel group (van Wezel et al., 2009; Yoon and Nodwell, 2014; Rigali et al., 2018; van der Heul et al., 2018). Here we drafted a review on the cascades of regulation and its application in production enhancement and compound discovery (**Figure 1**). We proposed to give an extensive review on the regulation of antibiotic production in *Streptomyces*.

The complex hierarchical regulation constitutes a major bottleneck to over produce target antibiotic. On the basis of understanding the regulation of antibiotic biosynthesis, rewiring the regulatory network is much more efficient to optimize antibiotic producers than the classical random mutagenesis methods. It has mentioned above that the enhancement of antibiotic titers can be achieved by overexpression of positive regulator, inactivation of negative regulator, tuning feedback and ribosomal engineering. Combination of different strategies to manipulate regulatory genes can achieve higher antibiotic production in both the native and/or heterologous host. It is necessary to achieve maximal level of antibiotic production by systematically rewiring the regulatory network.

With the accumulation of explosive genome sequencing data, it has been estimated that *Streptomyces* species harbor a huge unexploited potential to produce novel natural products. A new discovery approach-microbial genome mining has been well developed in the past years (Baltz, 2019). How to efficiently activate cryptic gene clusters is still challenging to scientist. Because the interweaved regulatory networks in most cases are not well studied or understood. Elucidation of the regulatory network is crucial to discover new antibiotics.

For efficient manipulation of the regulatory genes, multi-*loci* simultaneous editing technology is necessary to be invented. The recent application of CRISPR-Cas9 dependent serials genome editing system provides a new opportunity for rapid rewiring regulatory network in *Streptomyces* (Tong et al., 2019). For precisely tuning the transcription level of regulators, a panel of quantitative promoters should be defined in *Streptomyces*. This would be practical for tuning the expression of secondary metabolic pathway. Though there are many publications on promoter engineering in *Streptomyces*. Still serial quantitative promoters are necessary for predictable engineering with synthetic biology strategy in future.

AUTHOR CONTRIBUTIONS

HX, XL, ZL, and XZ prepared material for the manuscript. HX, XM, and YL wrote the manuscript. All authors read and approved the final manuscript.

FUNDING

This study was funded by the Natural Science Foundation of Zhejiang Province to HX (LY19C010002).

ACKNOWLEDGMENTS

The assistance of the colleagues of Institute of Biopharmaceuticals during preparing manuscript is gratefully acknowledged.

REFERENCES

Abdelmohsen, U. R., Grkovic, T., Balasubramanian, S., Kamel, M. S., Quinn, R. J., and Hentschel, U. (2015). Elicitation of secondary metabolism in actinomycetes. *Biotechnol. Adv.* 33, 798–811. doi: 10.1016/j.biotechadv.2015.06.003

Ahmed, S., Craney, A., Pimentel-Elardo, S. M., and Nodwell, J. R. (2013). A synthetic, species-specific activator of secondary metabolism and sporulation in *Streptomyces coelicolor*. *Chembiochem* 14, 83–91. doi: 10.1002/cbic.201200619

Anton, N., Mendes, M. V., Martin, J. F., and Aparicio, J. F. (2004). Identification of PimR as a positive regulator of pimaricin biosynthesis in *Streptomyces natalensis*. *J. Bacteriol.* 186, 2567–2575. doi: 10.1128/jb.186.9.2567-2575.2004

Anton, N., Santos-Aberturas, J., Mendes, M. V., Guerra, S. M., Martin, J. F., and Aparicio, J. F. (2007). PimM, a PAS domain positive regulator of pimaricin biosynthesis in *Streptomyces natalensis*. *Microbiology* 153, 3174–3183. doi: 10.1099/mic.0.2007/009126-0

Baltz, R. H. (2017). Gifted microbes for genome mining and natural product discovery. *J. Ind. Microbiol. Biotechnol.* 44, 573–588. doi: 10.1007/s10295-016-1815-x

Baltz, R. H. (2019). Natural product drug discovery in the genomic era: realities, conjectures, misconceptions, and opportunities. *J. Ind. Microbiol. Biotechnol.* 46, 281–299. doi: 10.1007/s10295-018-2115-4

Baral, B., Akhgari, A., and Metsa-Ketela, M. (2018). Activation of microbial secondary metabolic pathways: avenues and challenges. *Synth. Syst. Biotechnol.* 3, 163–178. doi: 10.1016/j.synbio.2018.09.001

Beltrametti, F., Rossi, R., Selva, E., and Marinelli, F. (2006). Antibiotic production improvement in the rare actinomycete *Planobispora rosea* by selection of mutants resistant to the aminoglycosides streptomycin and gentamycin and to rifamycin. *J. Ind. Microbiol. Biotechnol.* 33, 283–288. doi: 10.1007/s10295-005-0061-4

Bhukya, H., and Anand, R. (2017). TetR regulators: a structural and functional perspective. *J. Indian I Sci.* 97, 245–259. doi: 10.1007/s41745-017-0025-5

Bode, H. B., Bethe, B., Hofs, R., and Zeeck, A. (2002). Big effects from small changes: possible ways to explore nature's chemical diversity. *Chembiochem* 3, 619–627.

Bunet, R., Song, L., Mendes, M. V., Corre, C., Hotel, L., Rouhier, N., et al. (2011). Characterization and manipulation of the pathway-specific late regulator AlpW reveals *Streptomyces ambofaciens* as a new producer of kinamycins. *J. Bacteriol.* 193, 1142–1153. doi: 10.1128/jb.01269-10

Bursy, J., Kuhlmann, A. U., Pittelkow, M., Hartmann, H., Jebbar, M., Pierik, A. J., et al. (2008). Synthesis and uptake of the compatible solutes ectoine and 5-hydroxyectoine by *Streptomyces coelicolor* A3(2) in response to salt and heat stresses. *Appl. Environ. Microbiol.* 74, 7286–7296. doi: 10.1128/aem.00768-08

Chater, K. F. (2016). Recent advances in understanding *Streptomyces*. *F1000Research* 5:2795. doi: 10.12688/f1000research.9534.1

Chen, L., Lu, Y., Chen, J., Zhang, W., Shu, D., Qin, Z., et al. (2008). Characterization of a negative regulator AveI for avermectin biosynthesis in *Streptomyces avermitilis* NRRL8165. *Appl. Microbiol. Biotechnol.* 80, 277–286.

Choi, S., Nah, H. J., Choi, S., and Kim, E. S. (2019). Heterologous expression of daptomycin biosynthetic gene cluster via *Streptomyces* artificial chromosome vector system. *J. Microbiol. Biotechnol.* 29, 1931–1937. doi: 10.4014/jmb.1909.09022

Craney, A., Ozimok, C., Pimentel-Elardo, S. M., Capretta, A., and Nodwell, J. R. (2012). Chemical perturbation of secondary metabolism demonstrates important links to primary metabolism. *Chem. Biol.* 19, 1020–1027. doi: 10.1016/j.chembiol.2012.06.013

Cui, H., Ni, X., Shao, W., Su, J., Su, J., Ren, J., et al. (2015). Functional manipulations of the tetramycin positive regulatory gene *ttmRIV* to enhance the production of tetramycin A and nystatin A1 in *Streptomyces ahygroscopicus*. *J. Ind. Microbiol. Biotechnol.* 42, 1273–1282. doi: 10.1007/s10295-015-1660-3

Cuthbertson, L., and Nodwell, J. R. (2013). The TetR family of regulators. *Microbiol. Mol. Biol. Rev.* 77, 440–475. doi: 10.1128/mmbr.00018-13

Danot, O. (2001). A complex signaling module governs the activity of MalT, the prototype of an emerging transactivator family. *Proc. Natl. Acad. Sci. U.S.A.* 98, 435–440. doi: 10.1073/pnas.98.2.435

De Schrijver, A., and De Mot, R. (1999). A subfamily of MalT-related ATP-dependent regulators in the LuxR family. *Microbiology* 145, 1287–1288. doi: 10.1099/13500872-145-6-1287

Doull, J. L., Ayer, S. W., Singh, A. K., and Thibault, P. (1993). Production of a novel polyketide antibiotic, jadomycin B, by *Streptomyces venezuelae* following heat shock. *J. Antibiot.* 46, 869–871. doi: 10.7164/antibiotics.46.869

Doull, J. L., Singh, A. K., Hoare, M., and Ayer, S. W. (1994). Conditions for the production of jadomycin B by *Streptomyces venezuelae* ISP5230: effects of heat shock, ethanol treatment and phage infection. *J. Ind. Microbiol.* 13, 120–125. doi: 10.1007/bf01584109

Du, Y. L., Chen, S. F., Cheng, L. Y., Shen, X. L., Tian, Y., and Li, Y. Q. (2009). Identification of a novel *Streptomyces chattanoogensis* L10 and enhancing its natamycin production by overexpressing positive regulator ScnRII. *J. Microbiol.* 47, 506–513. doi: 10.1007/s12275-009-0014-0

Fazal, A., Thankachan, D., Harris, E., and Seipke, R. F. (2019). A chromatogram-simplified *Streptomyces albus* host for heterologous production of natural products. *Anton. Leeuw. Int.*. doi: 10.1007/s10482-019-01360-x

Fillenberg, S. B., Friess, M. D., Korner, S., Bockmann, R. A., and Muller, Y. A. (2016). Crystal structures of the global regulator DasR from *Streptomyces coelicolor*: implications for the allosteric regulation of GntR/HutC repressors. *PLoS ONE* 11:e0157691. doi: 10.1371/journal.pone.0157691

Foulston, L. C., and Bibb, M. J. (2010). Microbisporicin gene cluster reveals unusual features of lantibiotic biosynthesis in actinomycetes. *Proc. Natl. Acad. Sci. U.S.A.* 107, 13461–13466. doi: 10.1073/pnas.1008285107

Gebhard, S. (2012). ABC transporters of antimicrobial peptides in Firmicutes bacteria – Phylogeny, function and regulation. *Mol. Microbiol.* 86, 1295–1317. doi: 10.1111/mmi.12078

Gomez-Escribano, J. P., and Bibb, M. J. (2011). Engineering *Streptomyces coelicolor* for heterologous expression of secondary metabolite gene clusters. *Microb. Biotechnol.* 4, 207–215. doi: 10.1111/j.1751-7915.2010.00219.x

Gou, L., Han, T., Wang, X., Ge, J., Liu, W., Hu, F., et al. (2017). A novel TetR family transcriptional regulator, CalR3, negatively controls calcimycin biosynthesis in *Streptomyces chartreusis* NRRL 3882. *Front. Microbiol.* 8:2371. doi: 10.3389/fmicb.2017.02371

Greunke, C., Duell, E. R., D'Agostino, P. M., Glockle, A., Lamm, K., and Gulder, T. A. M. (2018). Direct pathway cloning (DiPaC) to unlock natural product biosynthetic potential. *Metab. Eng.* 47, 334–345. doi: 10.1016/j.ymben.2018.03.010

Guo, J., Zhang, X., Lu, X., Liu, W., Chen, Z., Li, J., et al. (2018). SAV4189, a MarR-family regulator in *Streptomyces avermitilis*, activates avermectin biosynthesis. *Front. Microbiol.* 9:1358. doi: 10.3389/fmicb.2018.01358

Guo, J., Zhao, J., Li, L., Chen, Z., Wen, Y., and Li, J. (2010). The pathway-specific regulator AveR from *Streptomyces avermitilis* positively regulates avermectin production while it negatively affects oligomycin biosynthesis. *Mol. Genet. Genomics* 283, 123–133. doi: 10.1007/s00438-009-0502-2

Guyet, A., Benaroudj, N., Proux, C., Gominet, M., Coppee, J. Y., and Mazodier, P. (2014). Identified members of the *Streptomyces lividans* AdpA regulon involved in differentiation and secondary metabolism. *BMC Microbiol.* 14:81. doi: 10.1186/1471-2180-14-81

Hayes, A., Hobbs, G., Smith, C. P., Oliver, S. G., and Butler, P. R. (1997). Environmental signals triggering methylenomycin production by *Streptomyces coelicolor* A3(2). *J. Bacteriol.* 179, 5511–5515. doi: 10.1128/jb.179.17.5511-5515.1997

He, F., Liu, W., Sun, D., Luo, S., Chen, Z., Wen, Y., et al. (2014). Engineering of the TetR family transcriptional regulator SAV151 and its target genes increases avermectin production in *Streptomyces avermitilis*. *Appl. Microbiol. Biotechnol.* 98, 399–409. doi: 10.1007/s00253-013-5348-1

He, H., Ye, L., Li, C., Wang, H., Guo, X., Wang, X., et al. (2018). SbbR/SbbA, an important ArpA/AfsA-like system, regulates milbemycin production in *Streptomyces bingchenggensis*. *Front. Microbiol.* 9:1064. doi: 10.3389/fmicb.2018.01064

He, W., Lei, J., Liu, Y., and Wang, Y. (2008). The LuxR family members GdmRI and GdmRII are positive regulators of geldanamycin biosynthesis in *Streptomyces hygroscopicus* 17997. *Arch. Microbiol.* 189, 501–510. doi: 10.1007/s00203-007-0346-2

Higo, A., Hara, H., Horinouchi, S., and Ohnishi, Y. (2012). Genome-wide distribution of AdpA, a global regulator for secondary metabolism and morphological differentiation in *Streptomyces*, revealed the extent and complexity of the AdpA regulatory network. *DNA Res.* 19, 259–273. doi: 10.1093/dnares/dss010

Holberger, L. E., and Hayes, C. S. (2009). Ribosomal protein S12 and aminoglycoside antibiotics modulate A-site mRNA cleavage and transfer-messenger RNA activity in *Escherichia coli*. *J. Biol. Chem.* 284, 32188–32200. doi: 10.1074/jbc.M109.062745

Hopwood, D. A. (2019). Highlights of *Streptomyces* genetics. *Heredity* 123, 23–32. doi: 10.1038/s41437-019-0196-0

Horbal, L., Rebets, Y., Rabyk, M., Makitrynskyy, R., Luzhetskyy, A., Fedorenko, V., et al. (2012). SimReg1 is a master switch for biosynthesis and export of simocyclinone D8 and its precursors. *AMB Express.* 2:1. doi: 10.1186/2191-0855-2-1

Hosaka, T., Ohnishi-Kameyama, M., Muramatsu, H., Murakami, K., Tsurumi, Y., Kodani, S., et al. (2009). Antibacterial discovery in actinomycetes strains with mutations in RNA polymerase or ribosomal protein S12. *Nat. Biotechnol.* 27, 462–464. doi: 10.1038/nbt.1538

Hosoya, Y., Okamoto, S., Muramatsu, H., and Ochi, K. (1998). Acquisition of certain streptomycin-resistant (*str*) mutations enhances antibiotic production in bacteria. *Antimicrob Agents Chemother.* 42, 2041–2047. doi: 10.1128/aac.42.8.2041

Huang, X., Ma, T., Tian, J., Shen, L., Zuo, H., Hu, C., et al. (2017). wblA, a pleiotropic regulatory gene modulating morphogenesis and daptomycin production in *Streptomyces roseosporus*. *J. Appl. Microbiol.* 123, 669–677. doi: 10.1111/jam.13512

Huang, Y., Yang, D., Pan, G., Tang, G. L., and Shen, B. (2016). Characterization of LnmO as a pathway-specific Crp/Fnr-type positive regulator for leinamycin biosynthesis in *Streptomyces atroolivaceus* and its application for titer improvement. *Appl. Microbiol. Biotechnol.* 100, 10555–10562. doi: 10.1007/s00253-016-7864-2

Huo, L., Rachid, S., Stadler, M., Wenzel, S. C., and Muller, R. (2012). Synthetic biotechnology to study and engineer ribosomal bottromycin biosynthesis. *Chem. Biol.* 19, 1278–1287. doi: 10.1016/j.chembiol.2012.08.013

Jiang, H., and Hutchinson, C. R. (2006). Feedback regulation of doxorubicin biosynthesis in *Streptomyces peucetius*. *Res. Microbiol.* 157, 666–674. doi: 10.1016/j.resmic.2006.02.004

Jiang, M., Yin, M., Wu, S., Han, X., Ji, K., Wen, M., et al. (2017). GdmRIII, a TetR family transcriptional regulator, controls geldanamycin and elaiophylin biosynthesis in *Streptomyces autolyticus* CGMCC0516. *Sci. Rep.* 7:4803. doi: 10.1038/s41598-017-05073-x

Jones, S. E., Ho, L., Rees, C. A., Hill, J. E., Nodwell, J. R., and Elliot, M. A. (2017). *Streptomyces* exploration is triggered by fungal interactions and volatile signals. *eLife* 6:e21738. doi: 10.7554/eLife.21738

Kawai, K., Wang, G., Okamoto, S., and Ochi, K. (2007). The rare earth, scandium, causes antibiotic overproduction in *Streptomyces* spp. *FEMS Microbiol. Lett.* 274, 311–315. doi: 10.1111/j.1574-6968.2007.00846.x

Kim, H. J., Kim, M. K., Jin, Y. Y., and Kim, E. S. (2014). Effect of antibiotic down-regulatory gene *wblA* ortholog on antifungal polyene production in rare actinomycetes *Pseudonocardia autotrophica*. *J. Microbiol. Biotechnol.* 24, 1226–1231. doi: 10.4014/jmb.1406.06018

Kitani, S., Miyamoto, K. T., Takamatsu, S., Herawati, E., Iguchi, H., Nishitomi, K., et al. (2011). Avenolide, a *Streptomyces* hormone controlling antibiotic production in *Streptomyces avermitilis*. *Proc. Natl. Acad. Sci. U.S.A.* 108, 16410–16415. doi: 10.1073/pnas.1113908108

Kuscer, E., Coates, N., Challis, I., Gregory, M., Wilkinson, B., Sheridan, R., et al. (2007). Roles of *rapH* and *rapG* in positive regulation of rapamycin biosynthesis in *Streptomyces hygroscopicus*. *J. Bacteriol.* 189, 4756–4763. doi: 10.1128/jb.00129-07

Laureti, L., Song, L., Huang, S., Corre, C., Leblond, P., Challis, G. L., et al. (2011). Identification of a bioactive 51-membered macrolide complex by activation of a silent polyketide synthase in *Streptomyces ambofaciens*. *Proc. Natl. Acad. Sci. U.S.A.* 108, 6258–6263. doi: 10.1073/pnas.1019077108

Lee, H. N., Huang, J., Im, J. H., Kim, S. H., Noh, J. H., Cohen, S. N., et al. (2010). Putative TetR family transcriptional regulator SCO1712 encodes an antibiotic downregulator in *Streptomyces coelicolor*. *Appl. Environ. Microbiol.* 76, 3039–3043. doi: 10.1128/aem.02426-09

Lee, J., Hwang, Y., Kim, S., Kim, E., and Choi, C. (2000). Effect of a global regulatory gene, *afsR2*, from *Streptomyces lividans* on avermectin production in *Streptomyces avermitilis*. *J. Biosci. Bioeng.* 89, 606–608. doi: 10.1016/s1389-1723(00)80065-1

Lee, K. M., Lee, C. K., Choi, S. U., Park, H. R., Kitani, S., Nihira, T., et al. (2005). Cloning and *in vivo* functional analysis by disruption of a gene encoding the gamma-butyrolactone autoregulator receptor from *Streptomyces natalensis*. *Arch. Microbiol.* 184, 249–257. doi: 10.1007/s00203-005-0047-7

Lei, C., Wang, J., Liu, Y., Liu, X., Zhao, G., and Wang, J. (2018). A feedback regulatory model for RifQ-mediated repression of rifamycin export in *Amycolatopsis mediterranei*. *Microb. Cell Fact.* 17:14.

Li, C., He, H., Wang, J., Liu, H., Wang, H., Zhu, Y., et al. (2019). Characterization of a LAL-type regulator NemR in nemadectin biosynthesis and its application for increasing nemadectin production in *Streptomyces cyaneogriseus*. *Sci. China Life Sci.* 62, 394–405. doi: 10.1007/s11427-018-9442-9

Li, Q., Wang, L., Xie, Y., Wang, S., Chen, R., and Hong, B. (2013). SsaA, a member of a novel class of transcriptional regulators, controls sansanmycin production in *Streptomyces* sp. strain SS through a feedback mechanism. *J. Bacteriol.* 195, 2232–2243. doi: 10.1128/jb.00054-13

Li, W., Ying, X., Guo, Y., Yu, Z., Zhou, X., Deng, Z., et al. (2006). Identification of a gene negatively affecting antibiotic production and morphological differentiation in *Streptomyces coelicolor* A3(2). *J. Bacteriol.* 188, 8368–8375. doi: 10.1128/jb.00933-06

Li, X., Yu, T., He, Q., McDowall, K. J., Jiang, B., Jiang, Z., et al. (2015). Binding of a biosynthetic intermediate to AtrA modulates the production of lidamycin by *Streptomyces globisporus*. *Mol. Microbiol.* 96, 1257–1271. doi: 10.1111/mmi.13004

Liao, C. H., Yao, L., Xu, Y., Liu, W. B., Zhou, Y., and Ye, B. C. (2015). Nitrogen regulator GlnR controls uptake and utilization of non-phosphotransferase-system carbon sources in actinomycetes. *Proc. Natl. Acad. Sci. U.S.A.* 112, 15630–15635. doi: 10.1073/pnas.1508465112

Liao, Y., Wei, Z. H., Bai, L., Deng, Z., and Zhong, J. J. (2009). Effect of fermentation temperature on validamycin A production by *Streptomyces hygroscopicus* 5008. *J. Biotechnol.* 142, 271–274. doi: 10.1016/j.jbiotec.2009.04.015

Liu, G., Tian, Y., Yang, H., and Tan, H. (2005). A pathway-specific transcriptional regulatory gene for nikkomycin biosynthesis in *Streptomyces ansochromogenes* that also influences colony development. *Mol. Microbiol.* 55, 1855–1866. doi: 10.1111/j.1365-2958.2005.04512.x

Liu, L., Cheng, Y., Lyu, M., Zhao, X., Wen, Y., Li, J., et al. (2019). AveI, an AtrA homolog of *Streptomyces avermitilis*, controls avermectin and oligomycin production, melanogenesis, and morphological differentiation. *Appl. Microbiol. Biotechnol.* 103, 8459–8472. doi: 10.1007/s00253-019-10062-3

Liu, Y., Ryu, H., Ge, B., Pan, G., Sun, L., Park, K., et al. (2014). Improvement of Wuyiencin biosynthesis in *Streptomyces wuyiensis* CK-15 by identification of a key regulator, WysR. *J. Microbiol. Biotechnol.* 24, 1644–1653. doi: 10.4014/jmb.1405.05017

Ma, D., Wang, C., Chen, H., and Wen, J. (2018). Manipulating the expression of SARP family regulator BulZ and its target gene product to increase tacrolimus production. *Appl. Microbiol. Biotechnol.* 102, 4887–4900. doi: 10.1007/s00253-018-8979-4

Maddocks, S. E., and Oyston, P. C. (2008). Structure and function of the LysR-type transcriptional regulator (LTTR) family proteins. *Microbiology* 154, 3609–3623. doi: 10.1099/mic.0.2008/022772-0

Maharjan, S., Oh, T. J., Lee, H. C., and Sohng, J. K. (2009). Identification and functional characterization of an *afsR* homolog regulatory gene from *Streptomyces venezuelae* ATCC 15439. *J. Microbiol. Biotechnol.* 19, 121–127.

Malla, S., Niraula, N. P., Liou, K., and Sohng, J. K. (2010). Self-resistance mechanism in *Streptomyces peucetius*: overexpression of *drrA*, *drrB* and *drrC* for doxorubicin enhancement. *Microbiol. Res.* 165, 259–267. doi: 10.1016/j.micres.2009.04.002

Martin, J.-F., and Liras, P. (2010). Engineering of regulatory cascades and networks controlling antibiotic biosynthesis in *Streptomyces*. *Curr. Opin. Microbiol.* 13, 263–273. doi: 10.1016/j.mib.2010.02.008

Martin, J. F., and Liras, P. (2012). Cascades and networks of regulatory genes that control antibiotic biosynthesis. *Subcell Biochem.* 64, 115–138. doi: 10.1007/978-94-007-5055-5_6

Martin, J. F., Ramos, A., and Liras, P. (2019). Regulation of geldanamycin biosynthesis by cluster-situated transcription factors and the master regulator PhoP. *Antibiotics* 8:E87. doi: 10.3390/antibiotics8030087

Mast, Y., Guezguez, J., Handel, F., and Schinko, E. (2015). A complex signaling cascade governs pristinamycin biosynthesis in *Streptomyces pristinaespiralis*. *Appl. Environ. Microbiol.* 81, 6621–6636. doi: 10.1128/aem.00728-15

Mendes, M. V., Tunca, S., Anton, N., Recio, E., Sola-Landa, A., Aparicio, J. F., et al. (2007). The two-component *phoR-phoP* system of *Streptomyces natalensis*: inactivation or deletion of *phoP* reduces the negative phosphate regulation of pimaricin biosynthesis. *Metab. Eng.* 9, 217–227. doi: 10.1016/j.ymben.2006.10.003

Meng, J., Feng, R., Zheng, G., Ge, M., Mast, Y., Wohlleben, W., et al. (2017). Improvement of pristinamycin I (PI) production in *Streptomyces pristinaespiralis* by metabolic engineering approaches. *Synth. Syst. Biotechnol.* 2, 130–136. doi: 10.1016/j.synbio.2017.06.001

Molina-Henares, A. J., Krell, T., Eugenia Guazzaroni, M., Segura, A., and Ramos, J. L. (2006). Members of the IclR family of bacterial transcriptional regulators function as activators and/or repressors. *FEMS Microbiol. Rev.* 30, 157–186. doi: 10.1111/j.1574-6976.2005.00008.x

Myronovskyi, M., and Luzhetskyy, A. (2019). Heterologous production of small molecules in the optimized *Streptomyces* hosts. *Nat. Prod. Rep.* 36, 1281–1294. doi: 10.1039/c9np00023b

Nah, J. H., Park, S. H., Yoon, H. M., Choi, S. S., Lee, C. H., and Kim, E. S. (2012). Identification and characterization of *wblA*-dependent *tmcT* regulation during tautomycetin biosynthesis in *Streptomyces* sp. CK4412. *Biotechnol. Adv.* 30, 202–209. doi: 10.1016/j.biotechadv.2011.05.004

Nepal, K. K., and Wang, G. (2019). Streptomycetes: surrogate hosts for the genetic manipulation of biosynthetic gene clusters and production of natural products. *Biotechnol. Adv.* 37, 1–20. doi: 10.1016/j.biotechadv.2018.10.003

Nett, M., Ikeda, H., and Moore, B. S. (2009). Genomic basis for natural product biosynthetic diversity in the actinomycetes. *Nat. Prod. Rep.* 26, 1362–1384. doi: 10.1039/b817069j

Nishimura, K., Hosaka, T., Tokuyama, S., Okamoto, S., and Ochi, K. (2007). Mutations in *rsmG*, encoding a 16S rRNA methyltransferase, result in low-level streptomycin resistance and antibiotic overproduction in *Streptomyces coelicolor* A3(2). *J. Bacteriol.* 189, 3876–3883. doi: 10.1128/jb.01776-06

Noh, J. H., Kim, S. H., Lee, H. N., Lee, S. Y., and Kim, E. S. (2010). Isolation and genetic manipulation of the antibiotic down-regulatory gene, *wblA* ortholog for doxorubicin-producing *Streptomyces* strain improvement. *Appl. Microbiol. Biotechnol.* 86, 1145–1153. doi: 10.1007/s00253-009-2391-z

Ochi, K. (2007). From microbial differentiation to ribosome engineering. *Biosci. Biotechnol. Biochem.* 71, 1373–1386. doi: 10.1271/bbb.70007

Ochi, K. (2017). Insights into microbial cryptic gene activation and strain improvement: principle, application and technical aspects. *J. Antibiot.* 70, 25–40. doi: 10.1038/ja.2016.82

Ochi, K., Okamoto, S., Tozawa, Y., Inaoka, T., Hosaka, T., Xu, J., et al. (2004). Ribosome engineering and secondary metabolite production. *Adv. Appl. Microbiol.* 56, 155–184. doi: 10.1016/s0065-2164(04)56005-7

Okamoto-Hosoya, Y., Hosaka, T., and Ochi, K. (2003a). An aberrant protein synthesis activity is linked with antibiotic overproduction in *rpsL* mutants of *Streptomyces coelicolor* A3(2). *Microbiology* 149, 3299–3309. doi: 10.1099/mic.0.26490-0

Okamoto-Hosoya, Y., Okamoto, S., and Ochi, K. (2003b). Development of antibiotic-overproducing strains by site-directed mutagenesis of the *rpsL* gene in *Streptomyces lividans*. *Appl. Environ. Microbiol.* 69, 4256–4259. doi: 10.1128/aem.69.7.4256-4259.2003

Onaka, H. (2017). Novel antibiotic screening methods to awaken silent or cryptic secondary metabolic pathways in actinomycetes. *J. Antibiot.* 70, 865–870. doi: 10.1038/ja.2017.51

Onaka, H., Mori, Y., Igarashi, Y., and Furumai, T. (2011). Mycolic acid-containing bacteria induce natural-product biosynthesis in *Streptomyces* species. *Appl. Environ. Microbiol.* 77, 400–406. doi: 10.1128/aem.01337-10

Onaka, H., Tabata, H., Igarashi, Y., Sato, Y., and Furumai, T. (2001). Goadsporin, a chemical substance which promotes secondary metabolism and morphogenesis in streptomycetes. I. Purification and characterization. *J. Antibiot.* 54, 1036–1044. doi: 10.7164/antibiotics.54.1036

Palazzotto, E., Tong, Y., Lee, S. Y., and Weber, T. (2019). Synthetic biology and metabolic engineering of actinomycetes for natural product discovery. *Biotechnol. Adv.* 37, 107366. doi: 10.1016/j.biotechadv.2019.03.005

Parajuli, N., Viet, H. T., Ishida, K., Tong, H. T., Lee, H. C., Liou, K., et al. (2005). Identification and characterization of the *afsR* homologue regulatory gene from *Streptomyces peucetius* ATCC 27952. *Res. Microbiol.* 156, 707–712. doi: 10.1016/j.resmic.2005.03.005

Qiu, J., Zhuo, Y., Zhu, D., Zhou, X., Zhang, L., Bai, L., et al. (2011). Overexpression of the ABC transporter AvtAB increases avermectin production in *Streptomyces avermitilis*. *Appl. Microbiol. Biotechnol.* 92, 337–345. doi: 10.1007/s00253-011-3439-4

Rees, D. C., Johnson, E., and Lewinson, O. (2009). ABC transporters: the power to change. *Nat. Rev. Mol. Cell Biol.* 10, 218–227. doi: 10.1038/nrm2646

Rigali, S., Anderssen, S., Naome, A., and van Wezel, G. P. (2018). Cracking the regulatory code of biosynthetic gene clusters as a strategy for natural product discovery. *Biochem. Pharmacol.* 153, 24–34. doi: 10.1016/j.bcp.2018.01.007

Rigali, S., Titgemeyer, F., Barends, S., Mulder, S., Thomae, A. W., Hopwood, D. A., et al. (2008). Feast or famine: the global regulator DasR links nutrient stress to antibiotic production by *Streptomyces*. *EMBO Rep.* 9, 670–675. doi: 10.1038/embor.2008.83

Rodriguez, H., Rico, S., Diaz, M., and Santamaria, R. I. (2013). Two-component systems in *Streptomyces*: key regulators of antibiotic complex pathways. *Microb. Cell Fact.* 12, 127. doi: 10.1186/1475-2859-12-127

Rodriguez, M., Nunez, L. E., Brana, A. F., Mendez, C., Salas, J. A., and Blanco, G. (2008). Identification of transcriptional activators for thienamycin and cephamycin C biosynthetic genes within the thienamycin gene cluster from *Streptomyces cattleya*. *Mol. Microbiol.* 69, 633–645. doi: 10.1111/j.1365-2958.2008.06312.x

Romero-Rodriguez, A., Maldonado-Carmona, N., Ruiz-Villafan, B., Koirala, N., Rocha, D., and Sanchez, S. (2018). Interplay between carbon, nitrogen and phosphate utilization in the control of secondary metabolite production in *Streptomyces*. *Antonie Van Leeuwenhoek* 111, 761–781. doi: 10.1007/s10482-018-1073-1

Salehi-Najafabadi, Z., Barreiro, C., Rodriguez-Garcia, A., Cruz, A., Lopez, G. E., and Martin, J. F. (2014). The gamma-butyrolactone receptors BulR1 and BulR2 of *Streptomyces tsukubaensis*: tacrolimus (FK506) and butyrolactone synthetases production control. *Appl. Microbiol. Biotechnol.* 98, 4919–4936. doi: 10.1007/s00253-014-5595-9

Santamarta, I., Perez-Redondo, R., Lorenzana, L. M., Martin, J. F., and Liras, P. (2005). Different proteins bind to the butyrolactone receptor protein ARE sequence located upstream of the regulatory *ccaR* gene of *Streptomyces clavuligerus*. *Mol. Microbiol.* 56, 824–835. doi: 10.1111/j.1365-2958.2005.04581.x

Santos-Aberturas, J., Payero, T. D., Vicente, C. M., Guerra, S. M., Canibano, C., Martin J. F., et al. (2011). Functional conservation of PAS-LuxR transcriptional regulators in polyene macrolide biosynthesis. *Metab. Eng.* 13, 756–767. doi: 10.1016/j.ymben.2011.09.011

Sekurova, O. N., Brautaset, T., Sletta, H., Borgos, S. E., Jakobsen, M. O., Ellingsen, T. E., et al. (2004). *In vivo* analysis of the regulatory genes in the nystatin biosynthetic gene cluster of *Streptomyces noursei* ATCC 11455 reveals their differential control over antibiotic biosynthesis. *J. Bacteriol.* 186, 1345–1354. doi: 10.1128/jb.186.5.1345-1354.2004

Severi, E., and Thomas, G. H. (2019). Antibiotic export: transporters involved in the final step of natural product production. *Microbiology* 165, 805–818. doi: 10.1099/mic.0.000794

Shan, Y., Guo, D., Gu, Q., Li, Y., Li, Y., Chen, Y., et al. (2019). Genome mining and homologous comparison strategy for digging exporters contributing self-resistance in natamycin-producing *Streptomyces* strains. *Appl. Microbiol. Biotechnol.* 104, 817–831.

Sherwood, E. J., Hesketh, A. R., and Bibb, M. J. (2013). Cloning and analysis of the planosporicin lantibiotic biosynthetic gene cluster of *Planomonospora alba*. *J. Bacteriol.* 195, 2309–2321. doi: 10.1128/jb.02291-12

Sletta, H., Borgos, S. E., Bruheim, P., Sekurova, O. N., Grasdalen, H., Aune, R., et al. (2005). Nystatin biosynthesis and transport: *nysH* and *nysG* genes encoding a putative ABC transporter system in *Streptomyces noursei* ATCC 11455 are required for efficient conversion of 10-deoxynystatin to nystatin. *Antimicrob. Agents Chemother.* 49, 4576–4583. doi: 10.1128/AAC.49.11.4576-4583.2005

Smanski, M. J., Peterson, R. M., Rajski, S. R., and Shen, B. (2009). Engineered *Streptomyces platensis* strains that overproduce antibiotics platensimycin and platencin. *Antimicrob. Agents Chemother.* 53, 1299–1304. doi: 10.1128/aac.01358-08

Song, E., Malla, S., Yang, Y. H., Lee, K., Kim, E. J., Lee, H. C., et al. (2011). Proteomic approach to enhance doxorubicin production in *panK*-integrated *Streptomyces peucetius* ATCC 27952. *J. Ind. Microbiol. Biotechnol.* 38, 1245–1253. doi: 10.1007/s10295-010-0903-6

Song, K., Wei, L., Liu, J., Wang, J., Qi, H., and Wen, J. (2017). Engineering of the LysR family transcriptional regulator FkbR1 and its target gene to improve ascomycin production. *Appl. Microbiol. Biotechnol.* 101, 4581–4592. doi: 10.1007/s00253-017-8242-4

Stratigopoulos, G., Gandecha, A. R., and Cundliffe, E. (2002). Regulation of tylosin production and morphological differentiation in *Streptomyces fradiae* by TylP, a deduced gamma-butyrolactone receptor. *Mol. Microbiol.* 45, 735–744. doi: 10.1046/j.1365-2958.2002.03044.x

Tahlan, K., Ahn, S. K., Sing, A., Bodnaruk, T. D., Willems, A. R., Davidson, A. R., et al. (2007). Initiation of actinorhodin export in *Streptomyces coelicolor*. *Mol. Microbiol.* 63, 951–961. doi: 10.1111/j.1365-2958.2006.05559.x

Takano, E., Kinoshita, H., Mersinias, V., Bucca, G., Hotchkiss, G., Nihira, T., et al. (2005). A bacterial hormone (the SCB1) directly controls the expression of a pathway-specific regulatory gene in the cryptic type I polyketide biosynthetic gene cluster of *Streptomyces coelicolor*. *Mol. Microbiol.* 56, 465–479. doi: 10.1111/j.1365-2958.2005.04543.x

Tamehiro, N., Hosaka, T., Xu, J., Hu, H., Otake, N., and Ochi, K. (2003). Innovative approach for improvement of an antibiotic-overproducing industrial strain of *Streptomyces albus*. *Appl. Environ. Microbiol.* 69, 6412–6417. doi: 10.1128/aem.69.11.6412-6417.2003

Tan, G. Y., Peng, Y., Lu, C., Bai, L., and Zhong, J. J. (2015). Engineering validamycin production by tandem deletion of gamma-butyrolactone receptor genes in *Streptomyces hygroscopicus* 5008. *Metab. Eng.* 28, 74–81. doi: 10.1016/j.ymben.2014.12.003

Tanaka, Y., Hosaka, T., and Ochi, K. (2010). Rare earth elements activate the secondary metabolite-biosynthetic gene clusters in *Streptomyces coelicolor* A3(2). *J. Antibiot. (Tokyo)* 63, 477–481. doi: 10.1038/ja.2010.53

Tanaka, Y., Komatsu, M., Okamoto, S., Tokuyama, S., Kaji, A., Ikeda, H., et al. (2009). Antibiotic overproduction by *rpsL* and *rsmG* mutants of various actinomycetes. *Appl. Environ. Microbiol.* 75, 4919–4922. doi: 10.1128/aem.00681-09

Taylor, B. L., and Zhulin, I. B. (1999). PAS domains: internal sensors of oxygen, redox potential, and light. *Microbiol. Mol. Biol. Rev.* 63, 479–506. doi: 10.1128/mmbr.63.2.479-506.1999

Thao, N. B., Kitani, S., Nitta, H., Tomioka, T., and Nihira, T. (2017). Discovering potential *Streptomyces* hormone producers by using disruptants of essential biosynthetic genes as indicator strains. *J. Antibiot.* 70, 1004–1008. doi: 10.1038/ja.2017.85

Thong, W. L., Shin-Ya, K., Nishiyama, M., and Kuzuyama, T. (2018). Discovery of an antibacterial isoindolinone-containing tetracyclic polyketide by cryptic gene asctivation and characterization of its biosynthetic gene cluster. *ACS Chem. Biol.* 13, 2615–2622. doi: 10.1021/acschembio.8b00553

Tong, Y., Weber, T., and Lee, S. Y. (2019). CRISPR/Cas-based genome engineering in natural product discovery. *Nat. Prod. Rep.* 36, 1262–1280. doi: 10.1039/c8np00089a

van der Heul, H. U., Bilyk, B. L., McDowall, K. J., Seipke, R. F., and van Wezel, G. P. (2018). Regulation of antibiotic production in actinobacteria: new perspectives from the post-genomic era. *Nat. Prod. Rep.* 35, 575–604. doi: 10.1039/c8np00012c

van Wezel, G. P., McKenzie, N. L., and Nodwell, J. R. (2009). Chapter 5. Applying the genetics of secondary metabolism in model actinomycetes to the discovery of new antibiotics. *Methods Enzymol.* 458, 117–141. doi: 10.1016/s0076-6879(09)04805-8

Waksman, S. A., Schatz, A., and Reynolds, D. M. (2010). Production of antibiotic substances by actinomycetes. *Ann. N. Y. Acad. Sci.* 1213, 112–124. doi: 10.1111/j.1749-6632.2010.05861.x

Wang, J. B., Zhang, F., Pu, J. Y., Zhao, J., Zhao, Q. F., and Tang, G. L. (2014). Characterization of AvaR1, an autoregulator receptor that negatively controls avermectins production in a high avermectin-producing strain. *Biotechnol. Lett.* 36, 813–819. doi: 10.1007/s10529-013-1416-y

Wang, L., Zhao, Y., Liu, Q., Huang, Y., Hu, C., and Liao, G. (2012). Improvement of A21978C production in *Streptomyces roseosporus* by reporter-guided *rpsL* mutation selection. *J. Appl. Microbiol.* 112, 1095–1101. doi: 10.1111/j.1365-2672.2012.05302.x

Wang, X. J., Guo, S. L., Guo, W. Q., Xi, D., and Xiang, W. S. (2009). Role of *nsdA* in negative regulation of antibiotic production and morphological differentiation in *Streptomyces bingchengensis*. *J. Antibiot.* 62, 309–313. doi: 10.1038/ja.2009.33

Wang, G., Inaoka, T., Okamoto, S., and Ochi, K. (2009). A novel insertion mutation in *Streptomyces coelicolor* ribosomal S12 protein results in paromomycin resistance and antibiotic overproduction. *Antimicrob. Agents Chemother.* 53, 1019–1026. doi: 10.1128/aac.00388-08

Wang, L., Tian, X., Wang, J., Yang, H., Fan, K., Xu, G., et al. (2009). Autoregulation of antibiotic biosynthesis by binding of the end product to an atypical response regulator. *Proc. Natl. Acad. Sci. U.S.A.* 106, 8617–8622. doi: 10.1073/pnas.0900592106

Wei, J., He, L., and Niu, G. (2018). Regulation of antibiotic biosynthesis in actinomycetes: perspectives and challenges. *Synth. Syst. Biotechnol.* 3, 229–235. doi: 10.1016/j.synbio.2018.10.005

Wei, K., Wu, Y., Li, L., Jiang, W., Hu, J., Lu, Y., et al. (2018). MilR2, a novel TetR family regulator involved in 5-oxomilbemycin A3/A4 biosynthesis in *Streptomyces hygroscopicus*. *Appl. Microbiol. Biotechnol.* 102, 8841–8853. doi: 10.1007/s00253-018-9280-2

Wei, J., Tian, Y., Niu, G., and Tan, H. (2014). GouR, a TetR family transcriptional regulator, coordinates the biosynthesis and export of gougerotin in *Streptomyces graminearus*. *Appl. Environ. Microbiol.* 80, 714–722. doi: 10.1128/aem.03003-13

Woo, M.-W., Nah, H.-J., Choi, S.-S., and Kim, E.-S. (2014). Pikromycin production stimulation through antibiotic down-regulatory gene disruption in *Streptomyces venezuelae*. *Biotechnol. Bioprocess. Eng.* 19, 973–977. doi: 10.1007/s12257-014-0407-8

Wu, H., Liu, W., Shi, L., Si, K., Liu, T., Dong, D., et al. (2017). Comparative genomic and regulatory analyses of natamycin production of *Streptomyces lydicus* A02. *Sci. Rep.* 7:9114.

Xu, D., Seghezzi, N., Esnault, C., and Virolle, M. J. (2010). Repression of antibiotic production and sporulation in *Streptomyces coelicolor* by overexpression of a TetR family transcriptional regulator. *Appl. Environ. Microbiol.* 76, 7741–7753. doi: 10.1128/aem.00819-10

Xu, G., Wang, J., Wang, L., Tian, X., Yang, H., Fan, K., et al. (2010). "Pseudo" gamma-butyrolactone receptors respond to antibiotic signals to coordinate antibiotic biosynthesis. *J. Biol. Chem.* 285, 27440–27448. doi: 10.1074/jbc.M110.143081

Xu, M., and Wright, G. D. (2019). Heterologous expression-facilitated natural products' discovery in actinomycetes. *J. Ind. Microbiol. Biotechnol.* 46, 415–431. doi: 10.1007/s10295-018-2097-2

Xu, Y., Willems, A., Au-Yeung, C., Tahlan, K., and Nodwell, J. R. (2012). A two-step mechanism for the activation of actinorhodin export and resistance in *Streptomyces coelicolor*. *MBio.* 3, e191–e112.

Yamanaka, K., Reynolds, K. A., Kersten, R. D., Ryan, K. S., Gonzalez, D. J., Nizet, V., et al. (2014). Direct cloning and refactoring of a silent lipopeptide biosynthetic gene cluster yields the antibiotic taromycin A. *Proc. Natl. Acad. Sci. U.S.A.* 111, 1957–1962. doi: 10.1073/pnas.1319584111

Ye, S., Brana, A. F., Gonzalez-Sabin, J., Moris, F., Olano, C., Salas, J. A., et al. (2018). New insights into the biosynthesis pathway of polyketide alkaloid argimycins P in *Streptomyces argillaceus*. *Front. Microbiol.* 9:252. doi: 10.3389/fmicb.2018.00252

Yepes, A., Rico, S., Rodriguez-Garcia, A., Santamaria, R. I., and Diaz, M. (2011). Novel two-component systems implied in antibiotic production in *Streptomyces coelicolor*. *PLoS ONE* 6:e19980. doi: 10.1371/journal.pone.0019980

Yin, S., Wang, W., Wang, X., Zhu, Y., Jia, X., Li, S., et al. (2015). Identification of a cluster-situated activator of oxytetracycline biosynthesis and manipulation of its expression for improved oxytetracycline production in *Streptomyces rimosus*. *Microb. Cell Fact.* 14, 46.

Yin, S., Wang, X., Shi, M., Yuan, F., Wang, H., Jia, X., et al. (2017). Improvement of oxytetracycline production mediated *via* cooperation of resistance genes in *Streptomyces rimosus*. *Sci. China Life Sci.* 60, 992–999. doi: 10.1007/s11427-017-9121-4

Yoo, Y. J., Hwang, J. Y., Shin, H. L., Cui, H., Lee, J., and Yoon, Y. J. (2015). Characterization of negative regulatory genes for the biosynthesis of rapamycin in *Streptomyces rapamycinicus* and its application for improved production. *J. Ind. Microbiol. Biotechnol.* 42, 125–135. doi: 10.1007/s10295-014-1546-9

Yoon, V., and Nodwell, J. R. (2014). Activating secondary metabolism with stress and chemicals. *J. Ind. Microbiol. Biotechnol.* 41, 415–424. doi: 10.1007/s10295-013-1387-y

Yu, P., Liu, S. P., Bu, Q. T., Zhou, Z. X., Zhu, Z. H., Huang, F. L., et al. (2014). WblAch, a pivotal activator of natamycin biosynthesis and morphological

differentiation in *Streptomyces chattanoogensis* L10, is positively regulated by AdpAch. *Appl. Environ. Microbiol.* 80, 6879–6887. doi: 10.1128/aem.01849-14

Yuan, P. H., Zhou, R. C., Chen, X., Luo, S., Wang, F., Mao, X. M., et al. (2016). DepR1, a TetR family transcriptional regulator, positively regulates daptomycin production in an Industrial producer, *Streptomyces roseosporus* SW0702. *Appl. Environ. Microbiol.* 82, 1898–1905. doi: 10.1128/aem.03002-15

Zhang, Q., Chen, Q., Zhuang, S., Chen, Z., Wen, Y., and Li, J. (2015). A MarR family transcriptional regulator, DptR3, activates daptomycin biosynthesis and morphological differentiation in *Streptomyces roseosporus*. *Appl. Environ. Microbiol.* 81, 3753–3765. doi: 10.1128/aem.00057-15

Zhang, Y., He, H., Liu, H., Wang, H., Wang, X., and Xiang, W. (2016). Characterization of a pathway-specific activator of milbemycin biosynthesis and improved milbemycin production by its overexpression in *Streptomyces bingchenggensis*. *Microb. Cell Fact.* 15:152.

Zhang, X. S., Luo, H. D., Tao, Y., Wang, Y. Y., Jiang, X. H., Jiang, H., et al. (2016). FkbN and Tcs7 are pathway-specific regulators of the FK506 biosynthetic gene cluster in *Streptomyces tsukubaensis* L19. *J. Ind. Microbiol. Biotechnol.* 43, 1693–1703. doi: 10.1007/s10295-016-1849-0

Zhang, Y., Zou, Z., Niu, G., and Tan, H. (2013). *jadR* and *jadR2* act synergistically to repress jadomycin biosynthesis. *Sci. China Life Sci.* 56, 584–590. doi: 10.1007/s11427-013-4508-y

Zhu, S., Duan, Y., and Huang, Y. (2019). The application of ribosome engineering to natural product discovery and yield improvement in *Streptomyces*. *Antibiotics* 8:E133. doi: 10.3390/antibiotics8030133

Zhu, Z., Li, H., Yu, P., Guo, Y., Luo, S., Chen, Z., et al. (2017). SlnR is a positive pathway-specific regulator for salinomycin biosynthesis in *Streptomyces albus*. *Appl. Microbiol. Biotechnol.* 101, 1547–1557. doi: 10.1007/s00253-016-7918-5

Zhuo, Y., Zhang, W., Chen, D., Gao, H., Tao, J., Liu, M., et al. (2010). Reverse biological engineering of *hrdB* to enhance the production of avermectins in an industrial strain of *Streptomyces avermitilis*. *Proc. Natl. Acad. Sci. U.S.A.* 107, 11250–11254. doi: 10.1073/pnas.1006085107

Conflict of Interest: The authors declare that the research was conducted in the absence of any commercial or financial relationships that could be construed as a potential conflict of interest.

frontiers in Microbiology

ORIGINAL RESEARCH
published: 26 March 2020
doi: 10.3389/fmicb.2020.00495

Regulation of Bottromycin Biosynthesis Involves an Internal Transcriptional Start Site and a Cluster-Situated Modulator

*Natalia M. Vior, Eva Cea-Torrescassana, Tom H. Eyles, Govind Chandra and Andrew W. Truman**

Department of Molecular Microbiology, John Innes Centre, Norwich, United Kingdom

Bottromycin is a ribosomally synthesized and post-translationally modified peptide (RiPP) produced by several streptomycetes, including the plant pathogen *Streptomyces scabies*. There is significant interest in this molecule as it possesses strong antibacterial activity against clinically relevant multidrug resistant pathogens and is structurally distinct from all other antibiotics. However, studies into its efficacy are hampered by poor yields. An understanding of how bottromycin biosynthesis is regulated could aid the development of strategies to increase titres. Here, we use 5′-tag-RNA-seq to identify the transcriptional organization of the gene cluster, which includes an internal transcriptional start site that precedes *btmD*, the gene that encodes the bottromycin precursor peptide. We show that the gene cluster does not encode a master regulator that controls pathway expression and instead encodes a regulatory gene, *btmL*, which functions as a modulator that specifically affects the expression of *btmD* but not genes up- or downstream of *btmD*. In order to identify non-cluster associated proteins involved in regulation, proteins were identified that bind to the main promoter of the pathway, which precedes *btmC*. This study provides insights into how this deceptively complex pathway is regulated in the absence of a pathway specific master regulator, and how it might coordinate with the central metabolism of the cell.

Keywords: *Streptomyces*, bottromycin, RiPP, antibiotic, regulation, transcription, RNA-seq, natural product

OPEN ACCESS

Edited by:
Yinhua Lu,
Shanghai Normal University, China

Reviewed by:
Weishan Wang,
Institute of Microbiology (CAS), China
Di Sun,
Jiangsu Normal University, China

***Correspondence:**
Andrew W. Truman
andrew.truman@jic.ac.uk

Specialty section:
This article was submitted to Antimicrobials, Resistance and Chemotherapy, a section of the journal Frontiers in Microbiology

Received: *07 August 2019*
Accepted: *06 March 2020*
Published: *26 March 2020*

Citation:
Vior NM, Cea-Torrescassana E, Eyles TH, Chandra G and Truman AW (2020) Regulation of Bottromycin Biosynthesis Involves an Internal Transcriptional Start Site and a Cluster-Situated Modulator. Front. Microbiol. 11:495. doi: 10.3389/fmicb.2020.00495

INTRODUCTION

Infectious diseases are responsible for one-fifth of deaths worldwide, and antimicrobial resistance is becoming an increasingly serious threat to global public health, which makes the development of new antibiotics a pressing need (Laxminarayan et al., 2016; Martens and Demain, 2017). The effective treatment of multidrug resistant bacteria requires the identification of compounds with either unusual chemical scaffolds or novel molecular targets, capable of overcoming multiple and widespread resistance mechanisms (Laxminarayan, 2014; Newman and Cragg, 2016; Martens and Demain, 2017). One antimicrobial compound of great interest is bottromycin, a peptide antibiotic with promising activity against multi-drug resistant Gram-positive bacterial pathogens (Shimamura et al., 2009; Tacconelli and Magrini, 2017). Bottromycin was first isolated in 1957 from cultures of *Streptomyces bottropensis* (Waisvisz et al., 1957), and then more recently as a product of

the plant pathogen *Streptomyces scabies* (Crone et al., 2012) and other *Streptomyces* species (Gomez-Escribano et al., 2012; Hou et al., 2012; Huo et al., 2012). Bottromycin is a ribosomally synthesized and post-translationally modified peptide (RiPP). In its biosynthetic pathway, a precursor peptide (BtmD) undergoes a complex and unprecedented series of modifications catalyzed by enzymes encoded in the bottromycin (*btm*) gene cluster (**Figure 1**) (Crone et al., 2012, 2016; Gomez-Escribano et al., 2012; Huo et al., 2012; Franz et al., 2017; Schwalen et al., 2017; Sikandar et al., 2019).

Bottromycin is a structurally novel compound that selectively blocks the binding of aminoacyl t-RNAs to the A-site in the 50S subunit of bacterial ribosomes, ultimately leading to protein synthesis inhibition (Otaka and Kaji, 1976, 1981, 1983). This makes bottromycin an interesting lead for development, as it attacks a molecular target that is currently unexploited in the clinic. However, bottromycin is produced in low yields, where titres in wild type producers are below 1 mg/L (Huo et al., 2012). These low production levels complicate both drug development and further biosynthetic studies of these molecules (Huo et al., 2012; Crone et al., 2016). An understanding of how bottromycin biosynthesis is regulated may enable the rational improvement of yield by modifying pathway regulation, especially as the pathway is inefficient in laboratory conditions (Crone et al., 2016; Eyles et al., 2018).

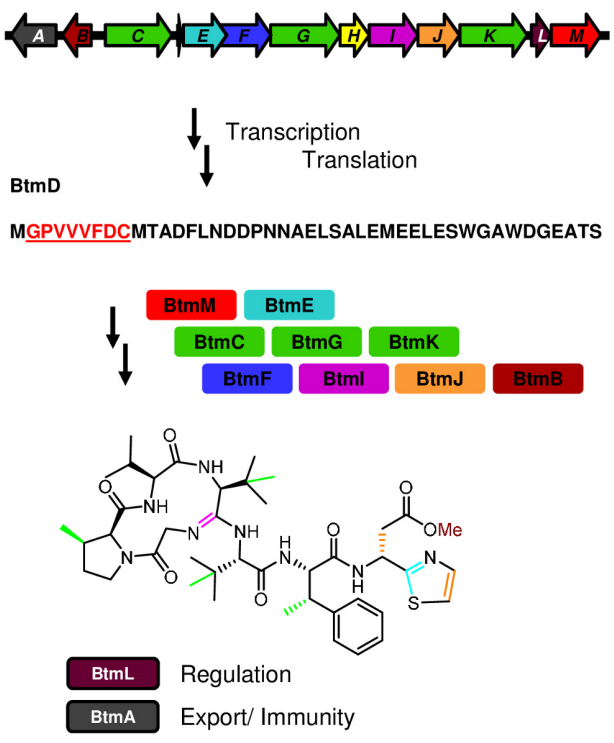

FIGURE 1 | Biosynthesis of bottromycin. The diagram shows the genetic organization of the bottromycin (*btm*) cluster and summarizes its biosynthetic pathway, from the transcription and translation of the precursor peptide gene *btmD*, to the posttranslational modifications leading to the final compound.

It is very well documented that altering the regulatory networks that control secondary metabolite biosynthesis often leads to significant yield increases, either by overexpressing positive regulators, inactivating repressors, or altering higher levels of regulation in the producer strain (Makitrynskyy et al., 2013; Vior et al., 2014; Yoo et al., 2015; Huang et al., 2016). RiPP biosynthesis, especially in the case of lantibiotics, is often regulated by classic two-component systems or orphan response regulators (Bierbaum and Sahl, 2009; Cooper et al., 2010), but this is not a mechanism common to all RiPP pathways. Systems involving sigma-anti-sigma factor pairs, SARP, LuxR, or TetR regulators have also been documented (Izawa et al., 2013; Flinspach et al., 2014; Zhang et al., 2014; Fernández-Martínez et al., 2015), and more diverse regulatory systems are likely to be found in the future, especially because many RiPP gene clusters do not encode any obvious pathway specific regulators (Bartholomae et al., 2017). The *btm* gene cluster in *S. scabies* encodes one potential regulatory protein, BtmL (**Figure 1**) (Crone et al., 2012). This protein is conserved across all characterized bottromycin gene clusters (Crone et al., 2012; Gomez-Escribano et al., 2012; Huo et al., 2012), but nothing is known about how this putative regulator controls bottromycin biosynthesis, nor whether additional regulators have critical roles in *btm* cluster regulation.

In this work, we apply transcriptomic, proteomic and metabolomic techniques in combination with qRT-PCR and reporter activity experiments in order to obtain key details on the regulation of bottromycin biosynthesis. We show that BtmL is not a master regulator of biosynthesis and instead specifically enhances expression levels of the precursor peptide gene *btmD*. This occurs in conjunction with a transcriptional start site for *btmD* that is internal to the preceding gene in the cluster. We show that this pathway is surprisingly complex and provide evidence into how it is regulated in the absence of a pathway specific master regulator.

RESULTS

BtmL Specifically Modulates the Expression of the Precursor Peptide Gene *btmD* and Is Independent of Cobalt Levels in the Medium

The *btm* gene cluster in *S. scabies* encodes a single putative regulator, BtmL, a 20.5 kDa protein that contains a *C*-terminal domain of unknown function (DUF2087 or PF09860), which has been associated with putative transcriptional regulators and is proposed to bind nucleic acids (Rigden, 2011). To date (July 2019), over 6,500 DUF2087-containing proteins have been sequenced and deposited in Genbank, of which more than 2,000 have additional DNA-binding domains. *In silico* analysis of BtmL using both Phyre2 (Crone et al., 2012; Kelley et al., 2015) and I-TASSER (Yang et al., 2015) predicted that the *N*-terminus of the protein has structural homology with SmtB-ArsR-like repressors, and therefore would feature a winged helix-turn-helix (wHTH) domain characteristic of this family of transcriptional regulators

(Busenlehner et al., 2003; Osman and Cavet, 2010; Chakravorty and Merz, 2014). However, no canonical wHTH domain was detected by sequence analysis and the protein appears to lack the conserved residues characteristically involved in ArsR-family metal binding (Osman and Cavet, 2010; Crone et al., 2012). Despite this, previous empirical evidence showed that addition of cobalt(II) to the production medium increased bottromycin yields (Crone et al., 2012), inferring that the ArsR-like structure of BtmL may control cluster expression via a metal-binding mechanism. This hypothesis was especially compelling given that several genes in the *btm* cluster encode class B radical SAM methyltransferases, which are cobalamin-dependent enzymes (Bauerle et al., 2015).

To investigate the role of BtmL in bottromycin biosynthesis, a mutant *S. scabies* strain carrying an in-frame deletion of *btmL* was generated (Crone et al., 2012) and its ability to produce bottromycin was assessed using liquid chromatography - mass spectrometry (LC-MS). Inactivation of *btmL* did not abolish bottromycin biosynthesis, but we could observe a moderate and consistent decrease in production levels to approximately 40% of wild type (WT) levels (**Figure 2A**). This result suggests that *btmL* acts as a positive modulator of bottromycin biosynthesis, but is not the master activator of the pathway. WT levels of bottromycin production were restored in Δ*btmL* upon *in trans* complementation with a copy of *btmL* under the control of the constitutive promoter *ermE**p (Bibb et al., 1985), confirming that the phenotype was due to the deletion of *btmL*. Surprisingly, when that same *btmL* expression construct was introduced in the WT strain (generating strain WT + L), there was no increase in bottromycin levels (**Figure 2A**).

To evaluate quantitatively whether *btmL* could be acting as a transcriptional regulator, qRT-PCR experiments were carried out with RNA samples from both the WT and Δ*btmL* strains (**Figure 2B**). The *btm* gene cluster is organized in two divergent groups of genes: *btmA* and *btmB* on one strand and *btmC-btmM* on the other strand (**Figure 1**). We therefore measured the expression of *btmB* from the smaller block, and *btmC*, *btmD* (the gene encoding the precursor peptide), *btmE* and *btmL* from the rest of the cluster. Expression values of these genes were normalized using the expression of *hrdB*, which encodes the principal sigma factor of RNA polymerase. A time course experiment determined that the optimal time to measure *btm* gene expression was at 72 h post-inoculation of bottromycin production medium (**Supplementary Figure S1**). At this time point, it could be observed that deletion of *btmL* has no significant effect on most of the genes tested, with one notable exception: *btmD*, the gene encoding the bottromycin precursor peptide. Transcription of *btmD* is reduced to approximately 40% of WT levels, which correlates with the reduction in bottromycin production (**Figure 2B**). Furthermore, qRT-PCR analysis of the WT + L strain revealed that transcription of *btmD* is significantly increased in this strain, confirming that BtmL is a specific and positive regulator of *btmD*. Interestingly, upstream and downstream genes (*btmB*, *btmC*, and *btmE*) are only slightly overexpressed or not overexpressed at all, suggesting the presence of an alternative operon encompassing only *btmD*.

After confirming that *btmL* is involved in bottromycin regulation, we assessed whether cobalt(II) levels influence pathway productivity, and whether this effect was mediated by *btmL*. Bottromycin production was measured in *S. scabies* WT and Δ*btmL* cultured in bottromycin production medium (BPM) supplemented with different concentrations of $CoCl_2$ (**Figure 3A**). In absolute terms, bottromycin production increased upon addition of cobalt(II), reaching a maximum at 15–25 μg/mL $CoCl_2$ after which production steadily decreased

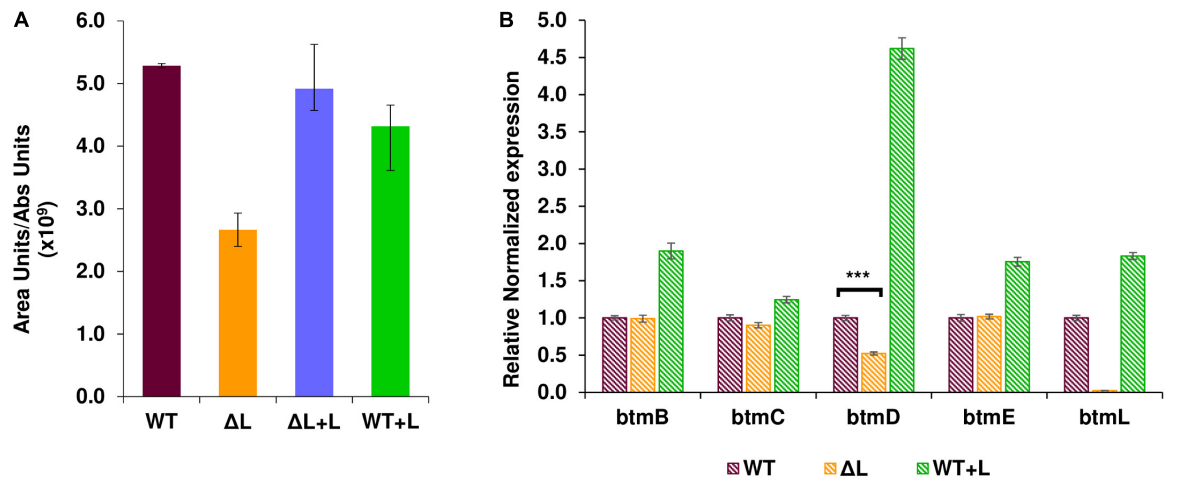

FIGURE 2 | Effect of *btmL* on bottromycin production and *btm* gene transcription. **(A)** LC-MS analysis of bottromycin production in *S. scabies* WT, Δ*btmL* (ΔL), ΔL complemented with a copy of *btmL* (ΔL + L) and the WT strain overexpressing *btmL* (WT + L). Error bars represent the standard deviation of the average production values in biological triplicates, which are normalized by culture growth. **(B)** qRT-PCR analysis of the transcription of representative *btm* genes in the WT (purple bars), Δ*btmL* (yellow bars) and WT + L (green bars) at 72 h of growth in BPM. Expression values are relative to the expression of the target gene in the WT, which was set at 1. Transcription of *hrdB* was used to normalize the expression levels across samples. Error bars represent standard error of the mean from triplicate experiments, and the asterisk represents a statistically significant difference in *btmD* expression between wt and the mutant *ΔbtmL* (*p*-value < 0.001).

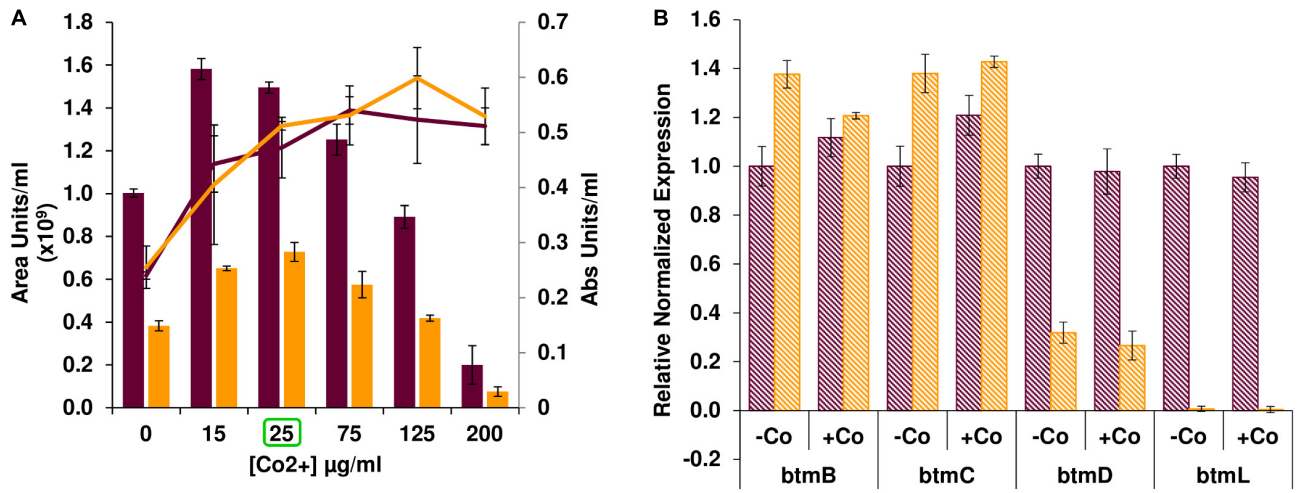

FIGURE 3 | Effect of cobalt(II) on bottromycin biosynthesis. **(A)** Bottromycin production in *S. scabies* WT (purple bars) and Δ*btmL* (yellow bars) in BPM supplemented with increasing concentrations of $CoCl_2$. Culture growth (calculated from a DNA quantification assay, see section "Materials and Methods") is overlaid and represented on the secondary axis. Error bars represent the standard deviation of biological triplicate data. The concentration of cobalt used for the qRT-PCR experiment in **(B)** appears highlighted with a green square. **(B)** qRT-PCR analysis of the expression of *btm* genes in the WT (purple bars) and Δ*btmL* mutant (yellow bars) at 72 h of growth in BPM with and without added cobalt. Expression values are relative to the expression of the target gene in the WT without added cobalt, which was set at 1. Transcription of *hrdB* was used to normalize the expression levels across samples and error bars represent standard error of the mean from triplicate experiments.

until almost disappearing at 200 µg/mL $CoCl_2$. However, the increase in production simply corresponded to a proportional increase in mycelial growth upon addition of up to 25 µg/mL of cobalt(II) in the medium (**Figure 3A**). At higher cobalt(II) concentrations mycelial growth was sustained, so the drop in production was probably due to a general inhibitory effect of excess metal in the medium, a phenomenon reported for the biosynthesis of other antibiotics (Rogers and Birnbaum, 1974; Abbas and Edwards, 1990). The growth-dependent production increase was also noticeable in Δ*btmL*, which followed a similar pattern, albeit at a reduced level of production. Moreover, a comparison of qRT-PCR data for the expression levels of several pathway genes in the presence or absence of added cobalt(II) (**Figure 3B**) showed that these are nearly identical in either condition for both the WT and Δ*btmL* strains, discarding any specific regulatory effect of this metal. This result is in accordance with the observation that *btmL* lacks the conserved metal-binding residues characteristic of ArsR-SmtB regulators (Osman and Cavet, 2010; Crone et al., 2012).

These results ruled out cobalt(II)-dependent pathway regulation by BtmL, which is instead a cobalt-independent transcriptional modulator that selectively increases *btmD* transcript levels in order to generate high levels of the precursor peptide in a feed-forward loop. Other positive loop systems have been reported in the biosynthesis of several RiPPs like microbisporicin and planosporicin, where the autoinduction mechanism relies of the detection of small quantities of precursor peptide by a sigma-antisigma complex (Sherwood and Bibb, 2013; Fernández-Martínez et al., 2015), or cinnamycin, where production is launched after onset of immunity to the compound in the producer strain (O'Rourke et al., 2017).

Overexpression of Exporter BtmA Has a Moderate Positive Effect on Bottromycin Production

The discordance between the increase in *btmD* expression and the lack of change in bottromycin production in the WT + L strain (**Figure 2A**) led us to postulate that the potential increase in available BtmD might not be effectively channeled by the pathway and exported out of the cell, leading to increased degradation of pathway intermediates and generation of shunt metabolites. Supporting this hypothesis, previous work showed that overexpression of *botT*, the major facilitator superfamily (MFS) transporter gene (Kumar et al., 2016; Quistgaard et al., 2016) in the bottromycin cluster from *Streptomyces* sp. BC16019 increased bottromycin production in a heterologous host, although it still did not reach wild type production levels (Huo et al., 2012). We therefore assessed whether overexpressing the homolog of this gene (*btmA*, 88% identity to *botT*) in the *S. scabies btm* gene cluster might increase the efficiency of the pathway and self-resistance to potentially toxic levels of the antibiotic.

Expression of a second copy of *btmA* under the control of the constitutive promoter *ermE**p provided a 25% increase in bottromycin production with respect to the WT strain (**Figure 4A**), an effect that was maintained, but not improved, when it was expressed in WT + L (generating WT + L + A). When the quantification was extended to other bottromycin related metabolites described previously (Crone et al., 2016; Eyles et al., 2018) this pattern was still observed for the total set of mature bottromycins (those including the main posttranslational modifications) (**Figure 4A**). However, in the case of the pathway

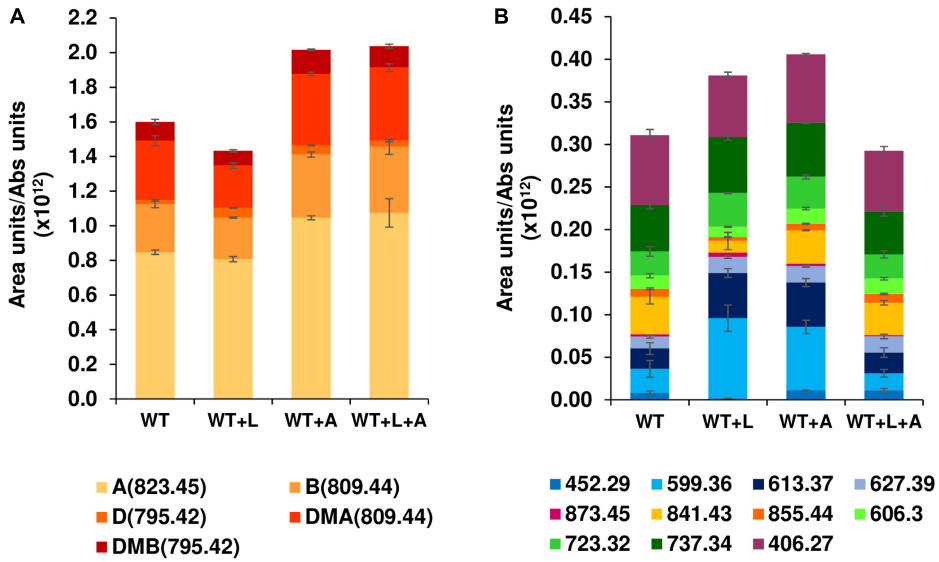

FIGURE 4 | Effect of the MFS transporter gene *btmA* on bottromycin production. Comparison of WT and WT + L strains with strains overexpressing *btmA* (WT + A and WT + L + A). **(A)** Production of mature bottromycins. **(B)** Production of intermediates and shunt products of the bottromycin pathway. Legends show all the compounds quantified in the experiment, and each compound is labeled with its observed mass as described in Crone et al. (2016) and Eyles et al. (2018). Mature bottromycins are also labeled with letters (A: bottromycin A_2, B: bottromycin B, D: bottromycin D, DMA: desmethyl bottromycin A_2 and DMB: desmethyl bottromycin B). Error bars represent the standard deviation of biological triplicate data, and production values are normalized by culture growth.

intermediates and shunt metabolites the trend was not present, with WT + L and WT + A producing more of them than the WT and the double overexpression strain WT + L + A (**Figure 4B**). This result indicates that efficiency can be increased to some extent by improving export of the molecule, but this is not the major bottleneck for bottromycin production. The main limiting factor for bottromycin production is likely to be the post-translational maturation of the precursor peptide instead, as we previously showed that the bottromycin pathway inefficiently stalls at numerous biosynthetic steps, even in the WT strain (Crone et al., 2016).

Mapping of the Transcriptional Organization of the *btm* Cluster Identifies a Secondary Transcriptional Start Site for *btmD*

Given that *btmD* appears to be situated within a larger operon, the specific increase in *btmD* transcription following *btmL* overexpression was unexpected and prompted us to investigate the transcriptional organization of the *btm* gene cluster. This cluster contains 13 genes, where 11 (*btmC-M*) are arranged in the same orientation and appear tightly clustered, with *btmE* to *btmJ* physically overlapping and *btmK* starting 8 bp after the *btmJ* stop codon. To assess the possibility of co-transcription of the remaining genes, RT-PCR experiments were performed on 72 h cultures of both WT and Δ*btmL* strains with specific primer pairs for the intergenic regions *btmA-B*, *btmC-D*, *btmD-E*, and *btmK-L* (**Figure 5A**). These showed co-transcription of all of the tested regions except *btmA-B*, indicating that genes *btmC-M* co-transcribe and can behave as a single 14.5 kb operon, whereas *btmA* and *btmB* are transcribed separately. The gene cluster was analyzed for putative terminators using WebGeSTer (Mitra et al., 2011). Consistent with the RT-PCR results, terminators were predicted spanning up to 90 bp away from the stop codon of *btmA* ($\Delta G = -19.5$), between *btmA* and *btmB* ($\Delta G = -19.43$) and 149 bp away from the stop codon of *btmM* ($\Delta G = -19.27$) (**Figure 5A**).

This evidence for *btmC-M* co-transcription did not exclude the possibility of alternative operons, and the specific increase in *btmD* transcription following *btmL* overexpression hinted toward an alternative transcription start site (TSS) for *btmD* that would explain how it is differentially regulated from its surrounding genes. In order to map the TSSs for the whole cluster we employed 5′-tag-RNA-seq (also called tagRNA-seq) (Innocenti et al., 2015) that enables the identification of TSSs in an untargeted, genome-wide fashion. This powerful technique has the advantage of differentially distinguishing primary transcripts (those generated by an RNA polymerase and therefore coming from true TSSs) from processed transcripts, which arise upon degradation or RNase mediated cleavage of the original transcripts at specific processing sites (PSs). In this particular case, with an operon spanning over 10 kb, degradation or post-transcriptional modification of the resulting transcript could also account for the difference between *btmD* expression and the remainder of the *btmC-M* operon.

5′-tag-RNA-seq reads mapped to the *S. scabies* 87-22 genome clearly showed the presence of three TSSs in the *btm* cluster: one preceding *btmB*, one before *btmC*, and an extra one preceding *btmD* and within the coding region of the upstream gene, *btmC* (**Figure 5B**). Unexpectedly, no TSS was found before *btmA*, in contrast with what was expected from the

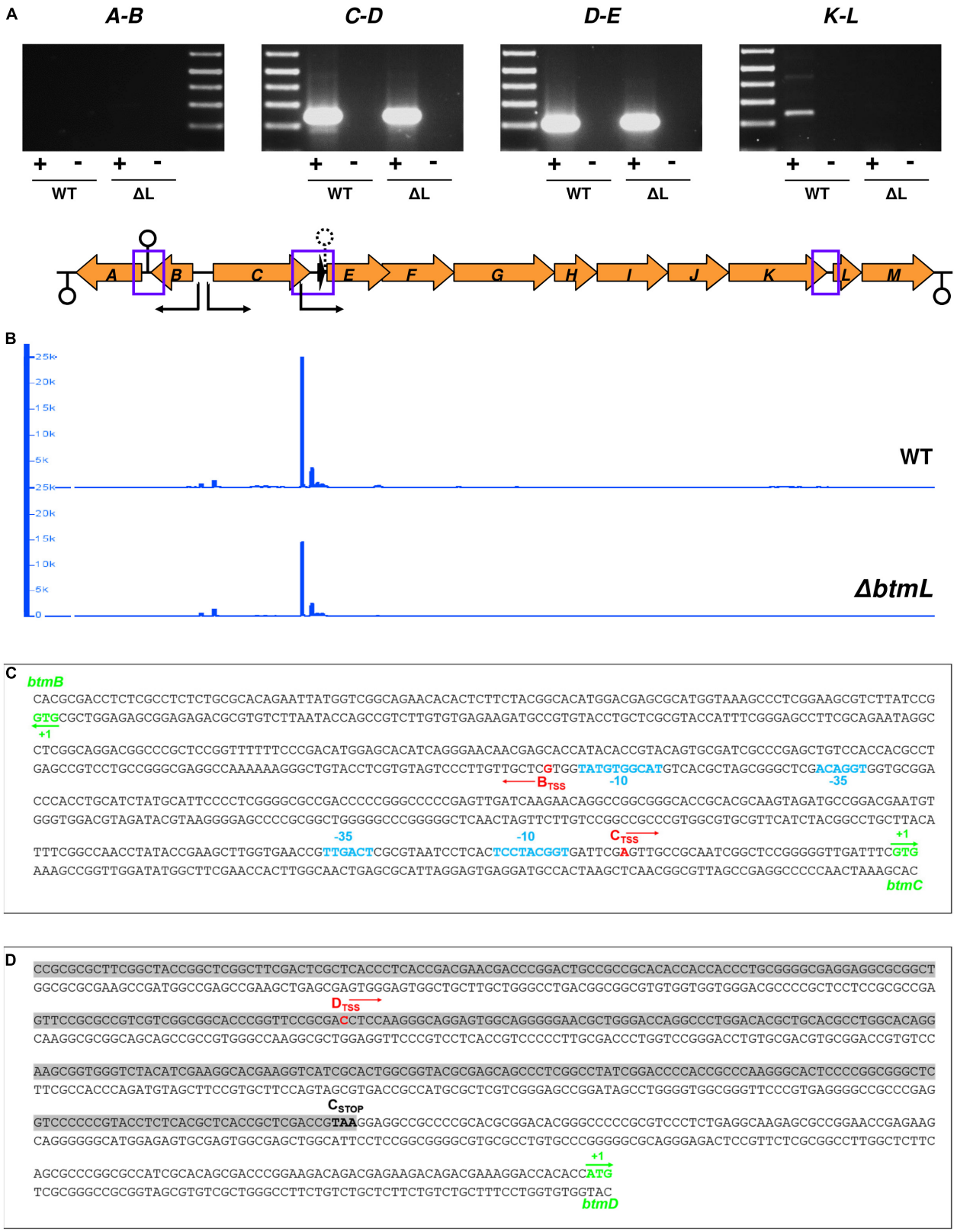

FIGURE 5 | Transcriptional organization of the *btm* gene cluster. **(A)** RT-PCR cotranscription analysis of the intergenic regions with no overlapping genes in the *btm* cluster (highlighted with blue squares in the schematic representation of the *btm* gene cluster below the gel images; loop symbols in this diagram indicate the

(Continued)

FIGURE 5 | Continued
location of predicted transcription terminators -solid line- and attenuators -dashed line- in the cluster). **(B)** Transcription start site mapping of the *btm* cluster using 5′-tag-RNA-seq. The plots (generated in IGB) show the mapping of reads with TSS tags in the *btm* cluster in the WT (top) and Δ*btmL* (bottom) strains. Sharp peaks corresponding to mapped reads precede *btmB*, *btmC,* and *btmD*, along with some non-specific transcription initiation in the *btmD* region. The vertical axis in the plots represents read counts and the horizontal axis maps to the gene cluster shown in **(A)**. The direction of transcription from the identified TSSs is represented with black arrows in the cluster. **(C)** Precise mapping of TSS and potential promoter regions in the *btmB-C* intergenic region. *btmB* and *btmC* start codons are marked in green, and the TSSs identified for *btmB* and *btmC* using both 5′tag-RNA-seq and 5′-RACE are labeled in red. −10 and −35 promoter regions for *btmC* (predicted with BPROM) and *btmB* (annotated manually) are represented in light blue. **(D)** Mapping of *btmD* TSS (red) within the coding sequence of *btmC* (shadowed in gray, with its stop codon highlighted in bold).

intergenic RT-PCR result (**Figure 5A**). To independently confirm the existence of these TSSs, we performed 5′-RACE (Rapid amplification of cDNA ends) experiments for $btmB_{TSS}$, $btmC_{TSS}$, and $btmD_{TSS}$, which yielded identical results to the 5′tag-RNA-seq (**Figures 5C,D**). $btmC_{TSS}$ is in position -32 with respect to the *btmC* start codon, and a prediction of putative σ70 promoters in the *btmB-btmC* intergenic region using BPROM (Solovyev and Salamov, 2011) identified a nearly canonical −35 sequence (TTGACT) and a poorly conserved −10 region (TCCTACGGT) that are consistent with the location of the $btmC_{TSS}$ (**Figure 5C**). It was not possible to confidently identify −10 and −35 boxes for the $btmB_{TSS}$ using BPROM or other prediction tools, so potential sequences were identified manually (**Figure 5C**). The $btmD_{TSS}$ is located 348 bp away from the start of *btmD* and 215 bp before the end of *btmC* coding sequence (**Figure 5D**), but we could not identify any suitable −10 or −35 regions for this TSS, either manually or with predictive tools. Unexpectedly, $btmD_{TSS}$ appears both in the WT and in Δ*btmL*, albeit with lower intensity in Δ*btmL* (**Figure 5B**), which indicates that although *btmL* does affect the transcription of *btmD*, it is not essential for the expression of this alternative transcript.

Interestingly, the 5′tagRNA-seq results showed that at 72 h of growth there is an extremely high level of transcription of some *btm* genes, in particular *btmD*. Transcription initiation preceding this gene seems rather promiscuous with some background noise (**Figure 5B**). Strikingly, an analysis of the full transcriptome to assess levels of gene expression as reads per kilobase per million reads (RPKM) and transcripts per million (TPM) (Wagner et al., 2012), showed that *btmD* and *btmC* are the 4th and 9th most highly transcribed genes in the genome at this time point (**Supplementary Datasheet S1**). Transcription after *btmD* drops considerably, showing that even upon overexpression of *btmL*, expression of *btmE* did not increase in a comparable way to *btmD*, in accordance with the qRT-PCR results (**Figure 2B**). The transcriptomic data also shows that all downstream genes in the operon are transcribed at lower levels than their preceding genes. This may be explained by a transcription attenuator downstream of *btmD* that likely serves to dampen transcription of downstream genes in the cluster. Accordingly, a putative terminator sequence between *btmD* and *btmE* ($\Delta G = -21.22$) is predicted by WebGeSTer (Mitra et al., 2011).

Genome-Wide Analysis of Transcriptional Start Sites in *S. scabies*

In RiPP biosynthesis, it appears to be beneficial to evolve mechanisms to selectively increase precursor peptide production in relation to catalytic proteins, given that precursor peptides are structural rather than catalytic. The mechanisms by which this happens are poorly understood, especially in pathways where the precursor peptide is apparently co-transcribed with upstream genes encoding catalytic proteins. The secondary transcriptional start site for *btmD* provides a previously unobserved mechanism by which this can occur. To assess whether this strategy was apparent in other RiPP gene clusters in *S. scabies*, we assessed their transcriptional organization using the 5′tagRNA-seq dataset. This showed that for all of the putative RiPP clusters identified in the *S. scabies* genome, the precursor peptide gene always has its own TSS (**Supplementary Figures S2, S3**). This happens even when the gene is preceded by genes predicted to encode tailoring enzymes (**Supplementary Figure S2**). Notably, in the case of SCAB_32021, which is tightly clustered with a preceding gene encoding a putative methyltransferase, its dedicated TSS overlaps with the end of this gene, in a similar scenario to *btmC* and *btmD* (**Supplementary Figure S2**). This suggests that having a dedicated TSS could be a widespread strategy for obtaining the appropriate stoichiometry of precursor peptide and tailoring enzymes in those cases where the precursor peptide gene is not at the beginning of an operon.

Reporter Assays Show Strong Transcription From the *btmC* Promoter Yet Negligible Transcription From the Putative *btmD* Promoter

To further characterize the main promoter regions in the pathway, promoter activity was measured using the β-glucuronidase reporter gene *gusA* (Myronovskyi et al., 2011). A 414 bp fragment containing the whole intergenic region *btmB-btmC*, including $btmC_{TSS}$ but not its RBS, was cloned in vector pIJ10742 (Feeney et al., 2017) to create a transcriptional fusion with *gusA*. This construct was introduced in *S. scabies* WT, Δ*btmL,* and WT + L to test whether the different genetic backgrounds would affect promoter activity. As a positive control, vector pIJ10741 carrying *gusA* under the control of the constitutive promoter *ermE**p (Feeney et al., 2017) was used, while empty pIJ10742 with no promoter was employed as a negative control. *btmC*p proved to be an exceptionally strong promoter in both in solid and in liquid culture (**Figure 6**), and at 72 h of growth its activity was comparable to *ermE**p. This result correlates with the high levels of expression of *btmC* observed in the transcriptomic analysis. The same *gusA* reporter experiment was performed with a 545 bp region that was predicted to contain the promoter preceding $btmD_{TSS}$, but no reporter activity could be detected in any of the genetic backgrounds tested (**Figure 6**).

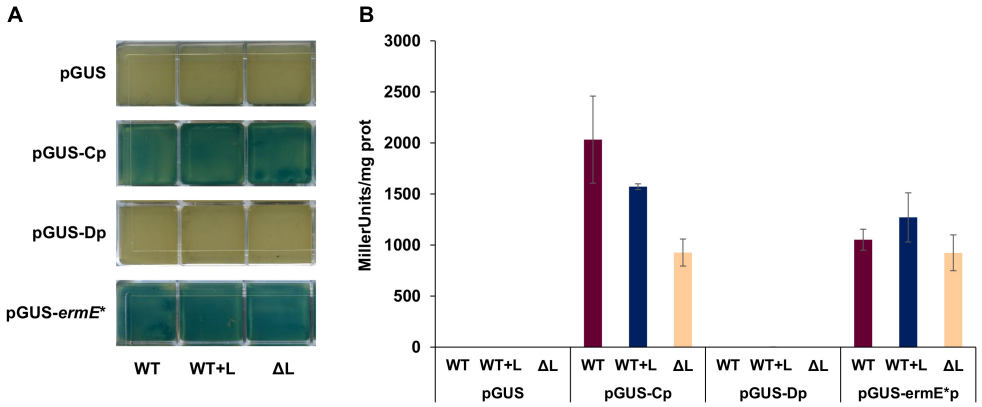

FIGURE 6 | Promoter activity using β-glucuronidase (GUS) reporter assays. The putative promoter regions for *bmtC* and *btmD* were inserted before the *gusA* gene in plasmid pIJ10740 to create transcriptional fusions. The promoterless vector was used as a negative control, and pIJ10741 (containing *gusA* under the control of *ermE**p) was used as a positive control. **(A)** Qualitative GUS assay in solid medium. Each of the squares represents one independent culture, with squares in the same row corresponding to strains containing the construct listed to their left, and the annotation at the bottom of each column indicating the genetic background. **(B)** Quantitative GUS assay in liquid medium, with reporter activity measured as Miller units/mg protein.

Therefore, further reporter constructs were made that progressively extended the region tested until it included the whole coding sequence of *btmC* (but not *btmC*p), but these provided identical negative results (**Supplementary Figures S4, S5**). This result pointed to the possibility that transcription from $btmD_{TSS}$ is not driven from its own promoter, but rather from *btmC*p, where some sort of secondary structure might help enhance transcription of this particular gene. To test this, we assessed the promoter activity of the whole region (*btmC*p, *btmC,* and the intergenic region before *btmD*) and compared its promoter activity to that of the original *btmC*p reporter. Two promoter versions were generated, one containing the WT sequence, and another one where several synonymous point mutations were introduced in the region of *btmD*TSS via yeast refactoring (**Supplementary Figure S4**) in order to disrupt possible DNA secondary structures in this region. Although these new transcriptional fusions were more active than all the other sequences lacking *btmC*p, they showed drastically reduced activity when compared to the original *btmC*p reporter, indicating that the additional DNA sequence dampened the promoter activity of *btmC*p. The mutated *btmD*TSS region did not significantly affect this phenotype (**Supplementary Figures S4, S5**).

Identification of Potential Pathway Regulators Using DNA Affinity Capture Assays

Our transcriptional analysis combined with the data from *S. scabies* Δ*btmL* and WT + L show that the master regulator(s) of the *btm* cluster are not encoded by the *btm* cluster and are therefore unlikely to be pathway-specific. Identification of such regulators could aid in improving the yield of bottromycin. Given the difficulty in predicting binding sequences for transcriptional activators in streptomycetes without extensive transcriptomic and metabolic datasets (Iqbal et al., 2012; Hwang et al., 2019), the intergenic region *btmB-C* was used as a probe in a DNA-binding protein capture experiment. This region was amplified using biotinylated primers and the resulting fragment was immobilized on streptavidin coated magnetic beads. The beads were then incubated with lysates of 72 h cultures of *S. scabies* WT grown in BPM. As a negative control, the same promoter region was incubated with lysates of cultures grown in GYM medium, where the cluster is not expressed and therefore there is no bottromycin production (**Supplementary Figure S6**). After incubation and several washes with competitor DNA to eliminate proteins binding non-specifically to the probe, the remaining proteins were eluted, washed again and analyzed using quantitative proteomics. A total of 321 proteins were identified in the 2 sets of samples, 120 of which appeared in both conditions, whereas 177 where present exclusively in the BPM samples and only 24 were specific to GYM samples. These results were filtered to identify annotated regulatory proteins or uncharacterized proteins binding to *btmC*p specifically in bottromycin production conditions. This reduced the candidates to 21 proteins (**Supplementary Table S3**), of which three were annotated as regulators, while the remainder were uncharacterized proteins.

Based on the intensity of the signal obtained or the biological relevance of the hit, we selected four promising candidates for further genetic analysis to assess their involvement in bottromycin biosynthesis: MtrA (SCAB_55281), GlnK (SCAB_61751), a putative regulatory protein (SCAB_ 85931) and an uncharacterized protein that binds specifically to *btmC*p under production conditions (SCAB_51451). MtrA forms a three-component system with the histidine kinase MtrB and LpqB, a lipoprotein that is involved in signal transduction (Hoskisson and Hutchings, 2006; Nguyen et al., 2010). This system is widely conserved in Actinobacteria, where it has been shown to regulate both development and antibiotic production in *Streptomyces venezuelae* and in *Streptomyces coelicolor* (Som et al., 2017; Zhang et al., 2017). SCAB_61751 encodes a homolog

of GlnK, a signal transduction protein with a central role in nitrogen metabolism (Thomas et al., 2000). SCAB_ 85931 is annotated as a putative regulatory protein and contains domains characteristic of RsbR-like anti-anti-sigma factors. Rsb proteins form part of the "stressosome," which responds to bacterial stress and ultimately leads to the activation of the alternative sigma factor σ^B (Lee et al., 2004). SCAB_51451 contains no conserved domains. In order to test the role of these genes in bottromycin biosynthesis, each of them was constitutively overexpressed under the control of *ermE**p in *S. scabies* WT using the integrative plasmid pIB139-RBS, a derivative of pIB139 (Wilkinson et al., 2002). The potential involvement of the MtrAB two-component system prompted us to also express *mtrB*, which encodes the cognate histidine kinase. Despite the evidence provided by DNA binding, the bottromycin titres were comparable to the WT under the conditions tested (**Supplementary Figure S7**).

DISCUSSION

An understanding of genetic regulation is required to inform rational approaches to overproduce or engineer the biosynthesis of medicinally promising specialized metabolites. In the case of bottromycin and other RiPPs, their ribosomal origin enables the rapid generation of analogs by precursor peptide mutagenesis, which can lead to the rapid generation of libraries of bioactive analogs (Yang et al., 2018). A distinct challenge for the regulation of RiPP biosynthesis is to enable the expression of a sufficiently large amount of the precursor peptide to support RiPP production, given that this is the substrate for the pathway, while producing other pathway proteins in catalytic quantities. Numerous genetic strategies have evolved that enable this differential production of the precursor peptide. Most commonly, precursor peptide genes are encoded at the beginning of RiPP operons, where they can be followed by imperfect transcriptional terminators (sometimes called "attenuators") that dampen transcript levels of the following genes (Severinov et al., 2007; Foulston and Bibb, 2010; O'Rourke et al., 2017). Alternatively, some RiPP gene clusters contain multiple precursor peptide genes (Li et al., 2010), while others feature a single precursor peptide containing multiple core peptides (Leikoski et al., 2013; Santos-Aberturas et al., 2019).

There is substantial interest in the RiPP antibiotic bottromycin due to its novel structure, unique molecular target and its activity toward multi-drug resistant pathogens, including methicillin-resistant *Staphylococcus aureus* (MRSA) and vancomycin-resistant enterococci (VRE) (Shimamura et al., 2009; Tacconelli and Magrini, 2017). Identification of the bottromycin biosynthetic gene cluster (Crone et al., 2012; Gomez-Escribano et al., 2012; Huo et al., 2012) showed that the precursor peptide gene, *btmD*, appeared to be encoded in the middle of a larger operon. In this study, we used 5′-tag-RNA-seq and 5′-RACE to reveal that the bottromycin gene cluster features an internal transcription start site that enhances transcription of *btmD* in relation to the remainder of the gene cluster (**Figure 5B**). The use of 5′-tag-RNA-seq provides confidence that this is a primary transcript and not simply the result of degradation of a longer transcript. In bottromycin production conditions, *btmD* is one of the most highly expressed genes in the genome. The presence of an internal TSS ($btmD_{TSS}$) to boost precursor peptide transcript levels has not previously been reported but our data indicate that it may be a common regulatory feature in RiPP biosynthesis. Evidence for this was provided by an analysis of other RiPP gene clusters in the *S. scabies* genome, which showed that their precursor peptides also have dedicated TSSs, in some cases overlapping with the coding sequence of the preceding genes, as with *btmD*. The occurrence of intragenic TSS is not a rare phenomenon, and recent TSS mapping work in *Streptomyces clavuligerus* has revealed the presence of 155 intragenic TSSs in its genome out of a total of 2659 identified (Hwang et al., 2019) and even higher numbers have been reported for other bacteria (Wade, 2015; Brito et al., 2017).

The gene cluster encodes one putative transcriptional regulator, BtmL (**Figure 1**), but deletion and over-expression experiments showed that this does not function as a master regulator of biosynthesis (**Figure 2**) and instead functions to increase transcript levels of *btmD*. Notably, $btmD_{TSS}$ is still present in *S. scabies* Δ*btmL* (**Figure 5B**), indicating that BtmL does not solely control this regulatory feature. Unexpectedly, a *gusA* reporter experiment did not reveal any promoter activity associated to $btmD_{TSS}$, indicating that transcription from this TSS might instead be driven from *btmC*p. This could also explain why mobility shift assays with purified BtmL using this region as probe were unsuccessful (data not shown). However, a transcriptional fusion containing the entire region from *btmC*p to the region before *btmD* provided lower GusA reporter activity than only *btmC*p. This unexpected result indicates that a complex and unusual system is functioning to regulate *btmD* gene expression, and further supports the theory that $btmD_{TSS}$ does not have its own dedicated promoter. These data highlight the need for further studies to elucidate the precise role of internal TSSs in RiPP biosynthesis.

Despite these null results, the importance of $btmD_{TSS}$ is supported by our prior work that showed that altering the region preceding *btmD* practically abolishes bottromycin production (Eyles et al., 2018), either by deletion of *btmC* or by swapping the positions of *btmC* and *btmD* in the gene cluster. Similarly, DNA affinity capture with the *btmB-C* region did not pull down BtmL (**Supplementary Table S3**). Therefore, the mechanism by which BtmL modulates *btmD* transcription remains cryptic. One possible hypothesis would be the interaction with a *cis*-regulatory region in the 5′ untranslated region (UTR) of *btmD* mRNA. Transcripts with UTRs bigger than 100–150 bp are usually considered "extended-leadered mRNAs" and are likely candidates to contain such a regulatory feature (Brito et al., 2017; Hwang et al., 2019). The *btmD* 5'UTR (347 bp) is within this category, but searches in this sequence against the Rfam database for any known RNA structures did not yield a clear result.

We sought to use our knowledge of pathway expression to increase bottromycin titre, firstly by over-expressing *btmL* either alone or along with *btmA*, which encodes a MFS transporter. While this increased *btmD* transcription (**Figure 2B**), it did not lead to higher bottromycin yields, indicating that *btmD* levels are

not the rate limiting factor for pathway expression. Similarly, in *S. scabies*, export by BtmA is not a bottleneck in this pathway. We had previously shown that the bottromycin pathway produces a significant amount of side-products in both *S. scabies* and a heterologous expression system (Crone et al., 2016; Eyles et al., 2018). Pathway refactoring in this heterologous system showed that constitutive high expression of the *btm* cluster leads to high yields of shunt metabolites and low titres of mature products, while controlled expression using a riboswitch increases overall production with higher ratios of mature bottromycins versus shunt metabolites. This is consistent with a study that refactored the bottromycin gene cluster from *Streptomyces* sp. BC16019 (Horbal et al., 2018), which also concluded that high levels of transcription did not fully correlate with increases in production. Promoter choice is a key factor for optimizing production of RiPPs, and can also depend on the timing of gene expression, such as in the heterologous production of telomestatin in *Streptomyces avermitilis* (Amagai et al., 2017).

There is surprisingly little known about the regulation of specialized metabolites that do not contain master regulators in their gene clusters. A rare example is erythromycin biosynthesis in *Saccharopolyspora erythraea*, which is regulated by BldD, a key regulator of actinomycete development, as well as two other regulatory genes which are not located within its biosynthetic cluster (Chng et al., 2008; Kirm et al., 2013; Wu et al., 2014). We sought to identify the master regulators of bottromycin biosynthesis using a DNA affinity capture experiment with the intergenic region between *btmB* and *btmC*, which contains the major promoters that control the pathway. This provided a series of promising candidate proteins, including the well-characterized regulatory proteins MtrA and GlnK. However, over-expression of these genes also did not lead to increased bottromycin production in *S. scabies*. This negative result does not disprove the involvement of these regulators, in particular in the case of MtrA and GlnK. As a member of classical two-component system the activity of the response regulator MtrA is dependent on its phosphorylation state (Kenney, 2002; Desai and Kenney, 2017). Overexpression of the gene, if it is not appropriately phosphorylated, might not be enough to reveal a phenotype. GlnK is a PII family signal transducer protein that modulates the activity of multiple biosynthetic and regulatory proteins in nitrogen metabolism (Arcondéguy et al., 2001; Gerhardt et al., 2015; Shimizu, 2016). It would make sense that nitrogen levels would exert an effect on bottromycin biosynthesis, due to the peptidic nature of bottromycin and in fact a paralog of this protein has been shown to affect secondary metabolite production in *S. coelicolor* (Waldvogel et al., 2011). These proteins also rely on post-translational modifications to properly function, which adds a layer of complication in their regulatory functions that may dampen the effect of their overexpression. Further studies will be necessary to fully characterize the role of these regulators, as well as the uncharacterized proteins identified in this work, on bottromycin production.

In summary, we have revealed that the regulation of bottromycin biosynthesis is surprisingly complex and features interplay between global regulatory proteins and a cluster-situated modulator, BtmL. Precursor peptide transcription is enhanced in relation to surrounding genes by BtmL and a cryptic internal transcriptional start site. This single-gene internal transcript makes the precursor peptide gene one of the most highly transcribed genes in the *S. scabies* genome. A wider assessment of the *S. scabies* genome shows that this strategy could represent a widespread regulatory mechanism for the expression of RiPP precursor peptide genes.

MATERIALS AND METHODS

Chemicals and Molecular Biology Reagents

Unless otherwise specified, antibiotics, media components and chemical reagents used in this work were purchased from Sigma-Aldrich (United Kingdom) with the exception of soy flour, which was purchased from Holland & Barret (United Kingdom). Enzymes and molecular biology kits were purchased from New England Biolabs and Promega Healthcare, respectively.

Bacterial Strains and Culture Conditions

The following strains were used in this work: *S. scabies* DSM 41658, both the wild-type (WT) and the mutant strain Δ*btmL* (ΔL), whose construction was described previously (Crone et al., 2012). Additionally, *Escherichia coli* K-12 strain DH5α (Invitrogen) was used for plasmid propagation and DNA manipulation, and the methylation deficient strain *E. coli* ET12567 containing pUZ8002 (Paget et al., 1999) was used for intergeneric conjugal transfer of genetic material to *S. scabies*, which was performed following standard procedures (Kieser et al., 2000). *E. coli* culture media used in this work are described in Sambrook et al. (1989). Several *Streptomyces* culture media were used: mannitol soya flour medium (SFM) (Kieser et al., 2000) was used for *Streptomyces* propagation and conjugations, and instant potato mash agar [2% Smash (Premier Foods), 2% agar] was used to grow *S. scabies* for spore harvesting. GYM medium (0.4% glucose, 0.4% yeast extract, and 1.0% malt extract, in Milli-Q water) and bottromycin production medium (BPM: 1% glucose, 1.5% soluble starch, 0.5% yeast extract, 1.0% soy flour, 0.5% NaCl, and 0.3% $CaCO_3$, in Milli-Q water) were used for bottromycin production. Production experiments were performed as follows: 30 μL of concentrated spores were used to inoculate 10 mL of GYM medium in 50 mL flasks and were incubated for 48 h at 30°C and 250 rpm. 250 μL of seed culture were used to inoculate 10 mL BPM in 50 mL Falcon tubes covered with foam bungs instead of caps. Alternatively, 1 mL of seed culture was used to inoculate 50 mL of BPM in 250 mL flasks containing a spring. When necessary, cultures were supplemented with appropriate concentrations of $CoCl_2$ (25 μg/mL unless otherwise stated). Triplicate production cultures were incubated for 5–6 days at 28°C and 230 rpm, at which point samples were collected and processed immediately, or frozen at −20°C until further processing and analysis. When antibiotic selection was necessary, culture media were supplemented with the appropriate antibiotics at the following final concentrations: kanamycin at 50 μg/mL, apramycin at 50

μg/mL, hygromycin at 50 μg/mL, chloramphenicol at 25 μg/mL, and nalidixic acid at 25 μg/mL.

Gene Expression Plasmids Construction

All the primers used for gene amplification and generation of the following constructs are listed in **Supplementary Table S1**. The gene expression vectors used in this work were pIB139-RBS-btmD (Crone et al., 2016) and pIJ10257 (Hong et al., 2005), which are both integrative plasmids containing the constitutive *ermE** promoter. pIB139-RBS-btmD is a derivative of pIB139 (Wilkinson et al., 2002) that carries the *btmD* gene preceded by a ribosome binding site (RBS) and an *Nde*I restriction site installed to facilitate cloning and improve gene expression (Crone et al., 2016). This plasmid was linearized using restriction enzymes *Nde*I and *Eco*RI, releasing *btmD* and allowing the introduction of the gene of interest, either via ligation of an *Eco*RI/*Nde*I treated PCR fragment or by Gibson assembly, following published protocols (Crone et al., 2012). The ligation method was used to introduce *btmL* and generate pIB139-RBS-*btmL*, which was used to complement the mutant Δ*btmL* and to overexpress this gene in the WT strain (WT + L). The Gibson assembly method was used to introduce *mtrA*, *mtrB*, *glnB*, SCAB_85931, and SCAB_51451, into pIB139-RBS for gene overexpression the WT strain. An empty version of pIB139-RBS was generated to use as a control in production experiments, via Gibson assembly, using the *Nde*I/*Eco*RI linearized vector and primers pIB-RBS_fw and pIB-RBS_rv, carrying the RBS sequence. pIJ10257 was used for the expression of *btmA*. This gene was amplified using primers btmA-start and btmA-end, digested with *Nde*I and *Hin*dIII and ligated into *Nde*I/*Hin*dIII digested pIJ10257. Correct construction of all expression plasmids was confirmed using colony PCR and sequencing, after which they were transferred to *E. coli* ET12567/pUZ8002 cells for conjugation into *S. scabies* (WT or Δ*btmL* as appropriate). pIB139 integrates in the ϕC31 phage integration site, and pIJ10257 integrates in the ϕBT1 site, which allowed for the simultaneous overexpression of two genes when necessary. Correct integration of the plasmids was verified by colony PCR using ermEp_chk1 in combination with the reverse amplification primer for each of the genes. As a control for the production experiments, a strain carrying the corresponding empty vector was generated in each case.

LC-MS Analysis of Bottromycin Production

Bottromycin production culture samples (1 mL) were extracted with an equal volume of methanol, mixed with shaking for a minimum of 10 min. The mixtures were then centrifuged for 4 min at 13,000 rpm to pellet cellular material and other particulate contaminants. 2 μL of the resulting supernatants were injected onto a Phenomenex Kinetex 2.6 μm XB-C18 column (50 mm × 2.1 mm, 100 Å) attached to a Shimadzu Nexera X2 UHPLC and eluted with a linear gradient of 5 to 95% acetonitrile (ACN) in water + 0.1% formic acid (FA) over 6 min, with a flow-rate of 0.6 mL/min. MS data were obtained in positive mode using a Shimadzu IT-TOF mass spectrometer coupled to the UHPLC and analyzed using LabSolutions software (Shimadzu). Bottromycin production was plotted in peak area units. To normalize production values across samples, culture growth was quantified by measuring DNA concentration with an adaptation of the Burton diphenylamine colorimetric assay (Zhao et al., 2013).

Isolation of Total RNA

Two milliliter samples of *S. scabies* liquid cultures were harvested after 72 h incubation in conditions as described above. Samples were washed with an equal volume of RNAlater (Thermo Fisher Scientific) and stored at −80°C until further processing. RNA was then extracted following previous protocols (Crone et al., 2016), resuspending the mycelium in 1 mL of RLT buffer from the RNeasy Kit (Qiagen) and homogenizing the sample in lysing matrix B tubes (MP Biomedicals) using a FastPrep instrument and a program of 3 × 30 s pulses at 6 m/s with 1 min cooling intervals on ice. The lysates were then centrifuged at 13,000 rpm and 700 μL of supernatant from each sample were then transferred to spin tubes from the RNeasy Kit to undergo purification following manufacturer instructions. Chromosomal DNA contamination was eliminated with on-column DNase I treatment (Qiagen) and a further cleanup step using TURBO DNA-free Kit (Ambion, Invitrogen). RNA concentration in the samples was quantified measuring A_{260} using a Nanodrop. In the case of the samples for 5′tag-RNAseq, further quantity and integrity measurements were performed with RNA ScreenTape (Agilent).

RT and qRT-PCR Analyses

Both RT-PCR and qRT-PCR analyses were carried out using 250 ng of total RNA as template in a two-step protocol. The first step consisted of cDNA synthesis with the QuantiTect Reverse Transcription Kit (Qiagen), as detailed in the manufacturer's instructions. For RT-PCR analyses the cDNA was then used as a template for PCR reactions using Taq polymerase and specific primers for the regions to test (**Supplementary Table S1**). The amplification conditions were as follows: initial denaturation at 95°C for 3 min followed by 33 cycles of 95°C for 30 s, 58–62°C for 30 s and 72°C for 40–60 s, with a final extension step at 72°C for 5 min. The resulting RT-PCR products were separated in 2% agarose gels and stained with ethidium bromide for visualization. For qRT-PCR analyses the aforementioned cDNA was used as template in quantitative reactions with the SensiFAST SYBR No-ROX Kit (Bioline) following the manufacturer's instructions. The reactions were run in a Bio-Rad CFX96 thermocycler and the amplification protocol was a 2-step cycling PCR program: 1 cycle at 95°C for 2 min followed by 40 cycles of 5 s at 95°C and 30 s at 60°C. An additional melting curve step was used at the end of the reaction to assess the specificity of the amplified products. The qRT-PCR results were analyzed with CFX Manager software (Bio-Rad). In both cases, negative control samples of the cDNA synthesis step with no retrotranscriptase were included, in order to control for the presence of contaminating chromosomal DNA in the RNA samples. Primers used in these analyses (**Supplementary Table S1**) were designed with a preference for

17–23 mers and $T_m \sim 65°C$ with the help of Vector NTI Advance 11.5 (Invitrogen) and Primer3 software (Untergasser et al., 2012) and validated used the online tool NetPrimer (Premier Biosoft). In the specific case of qRT-PCR primers, these were designed to amplify fragments of ∼100 bp and their efficiency was tested using serial dilutions of chromosomic DNA as template. For both RT-PCR and qRT-PCR, primers for *hrdB*, encoding a housekeeping sigma factor, were used as an internal control to assess the quality of RNA and in the latter case to normalize gene expression levels.

5′tag-RNA-Seq (tagRNA-Seq)

Library Construction and Sequencing

Total RNA samples of *S. scabies* WT and Δ*btmL* were extracted as previously described and, following quality control assays to ensure their integrity, they were submitted to Vertis Biotechnologie AG (Germany) for the construction and sequencing of tagRNA-seq libraries in a protocol adapted from the technique described in Innocenti et al. (2015). Prior to library construction, rRNA was depleted in the samples using the Ribo-Zero rRNA Removal Kit for bacteria (Epicenter). The remaining material was labeled sequentially as follows: sequence tag CTGAAGCT was ligated to transcripts presenting 5′-monophosphate groups (processed transcripts). The samples were then treated with RNA 5′ polyphosphatase (5′PP; Epicenter) to convert the 5′-triphosphate groups of primary transcripts into 5′-monophosphate ends amenable for ligation with the alternative tag sequence TAATGCGC. Once labeled, the samples were used as template for first-strand cDNA synthesis using random hexameric primers. After fragmentation and RNA clean up, Illumina TruSeq sequencing adapters were ligated in a strand specific manner to the 5′ and 3′ ends of the cDNA fragments. The cDNA was then amplified with a proof-reading enzyme to enrich the samples. At this point, it is possible to specifically PCR amplify the 5′-ends which carried the two tag sequences, but that would mean losing the information relating to the rest of the transcriptome. Therefore, a full transcriptome enrichment (for fragments that had Illumina adapters on both ends) was carried out in order to preserve the full coverage of the transcriptome in our libraries. The resulting material was purified with the Agencourt AMPure XP Kit (Beckman Coulter Genomics) and analyzed by capillary electrophoresis. The cDNA preparations were pooled in equimolar amounts and size selected (240–450 bp range) and the pooled libraries were sequenced on an Illumina NextSeq 500 system using 75 bp read lengths. RNA-seq data has been deposited in the ArrayExpress database (accession number E-MTAB-8236).

Data Analysis

Sequencing reads were first sorted according to their tags in order to generate independent fastq files for each of the datasets (see **Supplementary Table S2** for a summary of the sequencing results). Once sorted, the reads were trimmed to remove the tag sequences and aligned to *S. scabies* 87-22 genome (RefSeq NC_013929.1) using Bowtie2 (Langmead and Salzberg, 2012), which yielded SAM alignment files for each of the fastq files. Downstream processing of the SAM alignment files was performed using a series of Perl scripts supported by the Bioperl (Stajich et al., 2002) toolkit. Using the SAM alignments as input, the number of reads mapping to each nucleotide position of the *S. scabies* genome was calculated and saved in a coverage file. The coverage information was then integrated with a feature table including the coordinates of all of the gene coding sequences in the genome, in order to calculate the number of reads per gene, or gene counts. These gene counts were used to make an estimation of gene expression levels by calculating RPKM and TPM values for each gene (Wagner et al., 2012) (**Supplementary Datasheet S1**). For mapping and visualization of the transcription start sites (TSSs) in the bottromycin cluster, the SAM files containing the sequences labeled with 5′ tags were transformed into wig files suitable for visualization in the Integrated Genome Browser (IGB) software (Freese et al., 2016) plotted against the *S. scabies* genome. These files were normalized to eliminate biases due to difference in sequencing depth using the normalizeQuantiles function in the limma package (Ritchie et al., 2015) of R (R Core Team, 2014). Given the high amount of processed transcripts present in the *btmC-D* region of the bottromycin cluster, a "wig minus wig" file was generated in which processed transcript reads were subtracted from the primary transcript reads. The regions mapped in this filtered file were considered to be true TSSs.

5′-RACE Experiments

The TSSs identified in the 5′tag-RNA-seq experiment were validated using a 5′-RACE system for rapid amplification of cDNA ends (Invitrogen), using the manufacturer's instructions (version 2.0). 1 μg of total RNA from *S. scabies* WT and Δ*btmL* harvested after 72 h of growth at 28°C and 230 rpm was used to carry out cDNA synthesis with specific primers for each of the promoters tested (**Supplementary Table S1**). The cDNA was purified and treated with terminal deoxynucleotidyl transferase (TdT) to add poly(dC) tails to its 3′ends. After an initial PCR amplification of the tailed fragments with the 5′-RACE abridged anchor primer and subsequent amplifications with the universal amplification primer (both provided by the kit) and specific nested primers (**Supplementary Table S1**), defined amplification products were observed. These products were gel purified and submitted for Sanger sequencing to confirm the position of the TSSs.

gusA Transcriptional Fusions Construction and β-Glucuronidase Reporter Activity Assays

Putative promoter regions of *btmC* (*btmC*p, 414 bp) and *btmD* (*btmD*p, 545 bp) and extended promoter regions spanning different lengths of *btmC* were amplified from *S. scabies* genomic DNA or from a refactored bottromycin cluster containing 33 synonymous point mutations in the $btmD_{TTS}$ region (**Supplementary Figure S4**) with primers containing *Nde*I and *Xho*I restriction sites (**Supplementary Table S1**). These were verified by sequencing, and then ligated or

assembled into *Nde*I/*Xho*I digested pIJ10742, which contains a promoterless copy of the reporter gene *gusA* (Feeney et al., 2017). These plasmids were introduced via intergeneric conjugation into *S. scabies* (WT, Δ*btmL*, and WT + L) using *E. coli* ET12567/pUZ8002, where they integrated in the ϕBT1 phage integration site. Hygromycin resistant exconjugants were analyzed by colony PCR with primers pGUS_chk_fw and pGUS_chk_fw. β-glucuronidase assays in solid and liquid medium were carried out as described previously (Sherwood and Bibb, 2013). In the case of the liquid assays, reporter activity was represented as Miller units/mg protein. In both cases, pIJ10742 carrying no promoter was used as a negative control, and pIJ10741, carrying *gusA* under the control of *ermE**p (Feeney et al., 2017), was included as a positive control of promoter activity.

DNA Affinity Protein Capture Assay

Sample Preparation

The intergenic region *btmB-btmC* (414 bp) was PCR amplified using primers probe_BC_fw2_b and probe_BC_rv2 to generate a 5′ biotinylated probe. 40 μg of this probe were inmobilised onto 10 mg of streptavidin magnetic beads (Dynabeads® MyOne™ Streptavidin T1, Invitrogen, United Kingdom), following the manufacturer's instructions. Protein extracts from *S. scabies* wild type were obtained from 500 mL cultures in either BPM or GYM incubated for 72 h at 28°C and 250 rpm. Cell pellets were harvested by centrifugation for 15 min at 7,000 rpm, resuspended in binding buffer (20 mM TrisHCl pH7.5, 1 mM EDTA, 100 mM NaCl, 10% glycerol, and 1 mM DTT) supplemented with protease inhibitors (cOmplete™ Protease Inhibitor Cocktail, Roche, United Kingdom) and lysed by sonication with a Vibra-cell sonicator (Sonics & Materials Inc., United States) using 150 × 2 s pulses at 40% amplitude alternated by 5 s rest on ice. Binding assays were performed using a modification of the protocol reported by Bekiesch et al. (2016) using 60 mg of total protein in a 10 mL final volume of the aforementioned binding buffer supplemented with 0.1 mg/mL of salmon sperm DNA (Invitrogen, Germany). Proteins were eluted twice in 250 μL binding buffer containing 2 M NaCl and the binding assay was repeated twice for each sample, generating 1 mL of final eluate per sample. These eluates were then acidified to pH3 with trifluoroacetic acid (TFA) and applied to an C4 SPE column (OMIX C4, Agilent). The samples were washed twice with 0.1% TFA in water and three times with 0.1% FA before eluting in three fractions (200 μL 30% ACN and 0.1% FA, 200 μL 30% ACN and 200 μL 70% ACN) that were pooled and kept frozen on dry ice until analysis.

Sample Analysis

After purification and clean up, duplicate samples for each condition were analyzed by LC-MS/MS on an Orbitrap-Fusion™ mass spectrometer (Thermo Fisher, United Kingdom) equipped with an UltiMate™ 3000 RSLCnano System using an Acclaim PepMap C18 column (2 μm, 75 μm × 500 mm, Thermo). Samples were loaded and trapped using a pre-column which was then switched in-line to the analytical column for separation. Peptides were eluted with a gradient of 5–40% ACN in water/0.1% FA at a rate of 0.5% min^{-1}. The column was connected to a 10 μm SilicaTip™ nanospray emitter (New Objective, United States) for infusion into the mass spectrometer. Data dependent analysis was performed using a CID/HCD fragmentation method with the following parameters: positive ion mode, orbitrap MS resolution = 60 k, mass range (quadrupole) = 300–1500 *m/z*, AGC target $2e^5$, MS2 in ion trap, threshold $1e^4$, isolation window 1.6 Da (quadrupole), charge states 2–6, MS2 top20, AGC target $1.5e^4$, max inject time 200 ms, dynamic exclusion 1 count, 60 s exclusion, exclusion mass window ±7 ppm. MS scans were saved in profile mode while MS2 scans were saved in centroid mode. Raw files were processed with MaxQuant (version 1.5.3.30) (Tyanova et al., 2016). The peak lists were searched against a *S. scabies* protein database downloaded from Uniprot.org (25.05.2016) with 16846 entries together with the MaxQuant contaminants database (249 entries) using an in-house Mascot Server (2.4.1, Matrix Science, United Kingdom) with trypsin with 2 missed cleavages, carbamidomethylation (C) as fixed and oxidation (M), acetylation (protein N-terminus), and deamidation (N,Q) as variable modifications. Mass tolerances were 6 ppm for precursor ions and 0.6 Da for fragment ions. Mascot search results were imported into the Scaffold software (Proteome Software Inc., United States) to probabilistically validate protein identifications derived from the MS/MS sequencing results using the X!Tandem (Craig and Beavis, 2003) and ProteinProphet algorithms (Nesvizhskii et al., 2003). Validation parameters were set to 95% protein probability and 95% peptide probability.

DATA AVAILABILITY STATEMENT

The datasets generated for this study can be found in the ArrayExpress Archive of Functional Genomics Data (accession number E-MTAB-8236).

AUTHOR CONTRIBUTIONS

NV performed genetic manipulation experiments, LC-MS analyses, RNA extraction, and gene expression analyses. NV, EC-T, and TE performed promoter activity assays. GC and NV performed RNA-seq data processing and analysis. AT devised and supervised this work. NV and AT wrote the manuscript.

FUNDING

Financial support was provided by a Royal Society University Research Fellowship (AT), Biotechnology and Biological Sciences Research Council (BBSRC) MET and MfN Institute Strategic Programme grants (BB/J004596/1 and BBS/E/J/000PR9790) to the John Innes Centre (AT and NV), BBSRC grant BB/M003140/1 (AT and NV), a European Commission Erasmus+ traineeship (EC-T), and a Ph.D. studentship (BBSRC Doctoral Training Program grant BB/M011216/1) (TE). Open access publication fees are paid by a United Kingdom Research Council grant to the John Innes Centre.

ACKNOWLEDGMENTS

We thank Dr. Gerhard Saalbach (John Innes Centre Proteomics Facility) for his help with the proteomic analysis of the DNA binding protein capture samples.

SUPPLEMENTARY MATERIAL

The Supplementary Material for this article can be found online at: https://www.frontiersin.org/articles/10.3389/fmicb.2020.00495/full#supplementary-material

REFERENCES

Abbas, A. S., and Edwards, C. (1990). Effects of metals on *Streptomyces coelicolor* growth and actinorhodin production. *Appl. Environ. Microbiol.* 56, 675–680. doi: 10.1128/aem.56.3.675-680.1990

Amagai, K., Ikeda, H., Hashimoto, J., Kozone, I., Izumikawa, M., Kudo, F., et al. (2017). Identification of a gene cluster for telomestatin biosynthesis and heterologous expression using a specific promoter in a clean host. *Sci. Rep.* 7:3382. doi: 10.1038/s41598-017-03308-5

Arcondéguy, T., Jack, R., and Merrick, M. (2001). P(II) signal transduction proteins, pivotal players in microbial nitrogen control. *Microbiol. Mol. Biol. Rev.* 65, 80–105. doi: 10.1128/MMBR.65.1.80-105.2001

Bartholomae, M., Buivydas, A., Viel, J. H., Montalbán-López, M., and Kuipers, O. P. (2017). Major gene-regulatory mechanisms operating in ribosomally synthesized and post-translationally modified peptide (RiPP) biosynthesis. *Mol. Microbiol.* 106, 186–206. doi: 10.1111/mmi.13764

Bauerle, M. R., Schwalm, E. L., and Booker, S. J. (2015). Mechanistic diversity of radical S-adenosylmethionine (SAM)-dependent methylation. *J. Biol. Chem.* 290, 3995–4002. doi: 10.1074/jbc.R114.607044

Bekiesch, P., Franz-Wachtel, M., Kulik, A., Brocker, M., Forchhammer, K., Gust, B., et al. (2016). DNA affinity capturing identifies new regulators of the heterologously expressed novobiocin gene cluster in *Streptomyces coelicolor* M512. *Appl. Microbiol. Biotechnol.* 100, 4495–4509. doi: 10.1007/s00253-016-7306-1

Bibb, M. J., Janssen, G. R., and Ward, J. M. (1985). Cloning and analysis of the promoter region of the erythromycin resistance gene (ermE) of *Streptomyces erythraeus*. *Gene* 38, 215–226. doi: 10.1016/0378-1119(85)90220-3

Bierbaum, G., and Sahl, H.-G. (2009). Lantibiotics: mode of action, biosynthesis and bioengineering. *Curr. Pharm. Biotechnol.* 10, 2–18. doi: 10.2174/138920109787048616

Brito, L. F., Irla, M., Kalinowski, J., and Wendisch, V. F. (2017). Detailed transcriptome analysis of the plant growth promoting Paenibacillus riograndensis SBR5 by using RNA-seq technology. *BMC Genomics* 18:846. doi: 10.1186/s12864-017-4235-z

Busenlehner, L. S., Pennella, M. A., and Giedroc, D. P. (2003). The SmtB/ArsR family of metalloregulatory transcriptional repressors: structural insights into prokaryotic metal resistance. *FEMS Microbiol. Rev.* 27, 131–143. doi: 10.1016/S0168-6445(03)00054-8

Chakravorty, D. K., and Merz, K. M. (2014). Studying allosteric regulation in metal sensor proteins using computational methods. *Adv. Protein Chem. Struct. Biol.* 96, 181–214. doi: 10.1016/bs.apcsb.2014.06.009

Chng, C., Lum, A. M., Vroom, J. A., and Kao, C. M. (2008). A key developmental regulator controls the synthesis of the antibiotic erythromycin in Saccharopolyspora erythraea. *Proc. Natl. Acad. Sci. U.S.A.* 105, 11346–11351. doi: 10.1073/pnas.0803622105

Cooper, L. E., Li, B., and van der Donk, W. A. (2010). 5 . 08 biosynthesis and mode of action of lantibiotics. *Compr. Nat. Prod. II* 1971, 217–256. doi: 10.1016/B978-008045382-8.00116-7

Craig, R., and Beavis, R. C. (2003). A method for reducing the time required to match protein sequences with tandem mass spectra. *Rapid Commun. Mass Spectrom.* 17, 2310–2316. doi: 10.1002/rcm.1198

Crone, W. J. K., Leeper, F. J., and Truman, A. W. (2012). Identification and characterisation of the gene cluster for the anti-MRSA antibiotic bottromycin: expanding the biosynthetic diversity of ribosomal peptides. *Chem. Sci.* 3, 3516–3521. doi: 10.1039/c2sc21190d

Crone, W. J. K., Vior, N. M., Santos-Aberturas, J., Schmitz, L. G., Leeper, F. J., and Truman, A. W. (2016). Dissecting bottromycin biosynthesis using comparative untargeted metabolomics. *Angew. Chemie Int. Ed.* 55, 9639–9643. doi: 10.1002/anie.201604304

Desai, S. K., and Kenney, L. J. (2017). To P or Not to P? Non-canonical activation by two-component response regulators. *Mol. Microbiol.* 103, 203–213. doi: 10.1111/mmi.13532

Eyles, T. H., Vior, N. M., and Truman, A. W. (2018). Rapid and robust yeast-mediated pathway refactoring generates multiple new bottromycin-related metabolites. *ACS Synth. Biol.* 7, 1211–1218. doi: 10.1021/acssynbio.8b00038

Feeney, M. A., Chandra, G., Findlay, K. C., Paget, M. S. B., and Buttner, M. J. (2017). Translational control of the SigR-directed oxidative stress response in *Streptomyces* via IF3-mediated repression of a noncanonical GTC start codon. *mBio* 8, e815–e817. doi: 10.1128/mBio.00815-17

Fernández-Martínez, L. T., Gomez-Escribano, J. P., and Bibb, M. J. (2015). A relA-dependent regulatory cascade for auto-induction of microbisporicin production in *Microbispora corallina*. *Mol. Microbiol.* 97, 502–514. doi: 10.1111/mmi.13046

Flinspach, K., Kapitzke, C., Tocchetti, A., Sosio, M., and Apel, A. K. (2014). Heterologous expression of the thiopeptide antibiotic GE2270 from planobispora rosea ATCC 53733 in *Streptomyces coelicolor* requires deletion of ribosomal genes from the expression construct. *PLoS One* 9:e90499. doi: 10.1371/journal.pone.0090499

Foulston, L. C., and Bibb, M. J. (2010). Microbisporicin gene cluster reveals unusual features of lantibiotic biosynthesis in actinomycetes. *Proc. Natl. Acad. Sci. U.S.A.* 107, 13461–13466. doi: 10.1073/pnas.1008285107

Franz, L., Adam, S., Santos-Aberturas, J., Truman, A. W., and Koehnke, J. (2017). Macroamidine formation in bottromycins is catalyzed by a divergent YcaO enzyme. *J. Am. Chem. Soc.* 139, 18158–18161. doi: 10.1021/jacs.7b09898

Freese, N. H., Norris, D. C., and Loraine, A. E. (2016). Integrated genome browser: visual analytics platform for genomics. *Bioinformatics* 32, 2089–2095. doi: 10.1093/bioinformatics/btw069

Gerhardt, E. C. M., Rodrigues, T. E., Müller-Santos, M., Pedrosa, F. O., Souza, E. M., Forchhammer, K., et al. (2015). The Bacterial signal transduction protein GlnB regulates the committed step in fatty acid biosynthesis by acting as a dissociable regulatory subunit of acetyl-CoA carboxylase. *Mol. Microbiol.* 95, 1025–1035. doi: 10.1111/mmi.12912

Gomez-Escribano, J. P., Song, L., Bibb, M. J., and Challis, G. L. (2012). Posttranslational ß-methylation and macrolactamidination in the biosynthesis of the bottromycin complex of ribosomal peptide antibiotics. *Chem. Sci.* 3, 3522–3525. doi: 10.1039/C2SC21183A

Hong, H.-J., Hutchings, M. I., Hill, L. M., and Buttner, M. J. (2005). The role of the novel Fem protein VanK in vancomycin resistance in *Streptomyces coelicolor*. *J. Biol. Chem.* 280, 13055–13061. doi: 10.1074/jbc.M413801200

Horbal, L., Marques, F., Nadmid, S., Mendes, M. V., and Luzhetskyy, A. (2018). Secondary metabolites overproduction through transcriptional gene cluster refactoring. *Metab. Eng.* 49, 299–315. doi: 10.1016/J.YMBEN.2018.09.010

Hoskisson, P. A., and Hutchings, M. I. (2006). MtrAB-LpqB: a conserved three-component system in actinobacteria? *Trends Microbiol.* 14, 444–449. doi: 10.1016/j.tim.2006.08.005

Hou, Y., Tianero, M. D. B., Kwan, J. C., Wyche, T. P., Michel, C. R., Ellis, G. A., et al. (2012). Structure and biosynthesis of the antibiotic bottromycin D. *Org. Lett.* 14, 5050–5053. doi: 10.1021/ol3022758

Huang, Y., Yang, D., Pan, G., Tang, G.-L., and Shen, B. (2016). Characterization of LnmO as a pathway-specific Crp/Fnr-type positive regulator for leinamycin biosynthesis in *Streptomyces atroolivaceus* and its application for titer improvement. *Appl. Microbiol. Biotechnol.* 100, 10555–10562. doi: 10.1007/s00253-016-7864-7862

Huo, L., Rachid, S., Stadler, M., Wenzel, S. C., and Müller, R. (2012). Synthetic biotechnology to study and engineer ribosomal bottromycin biosynthesis. *Chem. Biol.* 19, 1278–1287. doi: 10.1016/j.chembiol.2012.08.013

Hwang, S., Lee, N., Jeong, Y., Lee, Y., Kim, W., Cho, S., et al. (2019). Primary transcriptome and translatome analysis determines transcriptional

and translational regulatory elements encoded in the *Streptomyces clavuligerus* genome. *Nucleic Acids Res.* 47, 6114–6129. doi: 10.1093/nar/gkz471

Innocenti, N., Golumbeanu, M., Fouquier, d'Hérouël, A., Lacoux, C., Bonnin, R. A., et al. (2015). Whole-genome mapping of 5' RNA ends in bacteria by tagged sequencing: a comprehensive view in *Enterococcus faecalis*. *RNA* 21, 1018–1030. doi: 10.1261/rna.048470.114

Iqbal, M., Mast, Y., Amin, R., Hodgson, D. A., Wohlleben, W., and Burroughs, N. J. (2012). Extracting regulator activity profiles by integration of de novo motifs and expression data: characterizing key regulators of nutrient depletion responses in *Streptomyces coelicolor*. *Nucleic Acids Res.* 40, 5227–5239. doi: 10.1093/nar/gks205

Izawa, M., Kawasaki, T., and Hayakawa, Y. (2013). Cloning and heterologous expression of the thioviridamide biosynthesis gene cluster from *Streptomyces olivoviridis*. *Appl. Environ. Microbiol.* 79, 7110–7113. doi: 10.1128/AEM.01978-13

Kelley, L. A., Mezulis, S., Yates, C. M., Wass, M. N., and Sternberg, M. J. E. (2015). The Phyre2 web portal for protein modeling, prediction and analysis. *Nat. Protoc.* 10, 845–858. doi: 10.1038/nprot.2015.053

Kenney, L. J. (2002). Structure/function relationships in OmpR and other winged-helix transcription factors. *Curr. Opin. Microbiol.* 5, 135–141. doi: 10.1016/S1369-5274(02)00310-7

Kieser, T., Bibb, M. J., Buttner, M. J., Chater, K. F., and Hopwood, D. A. (2000). *Practical Streptomyces Genetics*. Norwich: John Innes Foundation.

Kirm, B., Magdevska, V., Tome, M., Horvat, M., Karničar, K., Petek, M., et al. (2013). SACE_5599, a putative regulatory protein, is involved in morphological differentiation and erythromycin production in *Saccharopolyspora erythraea*. *Microb. Cell Fact.* 12:126. doi: 10.1186/1475-2859-12-126

Kumar, S., He, G., Kakarla, P., Shrestha, U., Ranjana, K. C., Ranaweera, I., et al. (2016). Bacterial multidrug efflux pumps of the major facilitator superfamily as targets for modulation. *Infect Disord. Drug Targets* 16, 28–43. doi: 10.2174/1871526516666160407113848 doi: 10.2174/1871526516666160407113848

Langmead, B., and Salzberg, S. L. (2012). Fast gapped-read alignment with Bowtie 2. *Nat. Methods* 9, 357–359. doi: 10.1038/nmeth.1923

Laxminarayan, R. (2014). Antibiotic effectiveness: balancing conservation against innovation. *Science* 345, 1299–1301. doi: 10.1126/science.1254163

Laxminarayan, R., Amábile-Cuevas, C. F., Cars, O., Evans, T., Heymann, D. L., Hoffman, S., et al. (2016). UN high-level meeting on antimicrobials—what do we need? *Lancet* 388, 218–220. doi: 10.1016/S0140-6736(16)31079-0

Lee, E.-J., Cho, Y.-H., Kim, H.-S., Ahn, B.-E., and Roe, J.-H. (2004). Regulation of sigmaB by an anti- and an anti-anti-sigma factor in *Streptomyces coelicolor* in response to osmotic stress. *J. Bacteriol.* 186, 8490–8498. doi: 10.1128/JB.186.24.8490-8498.2004

Leikoski, N., Liu, L., Jokela, J., Wahlsten, M., Gugger, M., Calteau, A., et al. (2013). Genome mining expands the chemical diversity of the cyanobactin family to include highly modified linear peptides. *Chem. Biol.* 20, 1033–1043. doi: 10.1016/J.CHEMBIOL.2013.06.015

Li, B., Sher, D., Kelly, L., Shi, Y., Huang, K., Knerr, P. J., et al. (2010). Catalytic promiscuity in the biosynthesis of cyclic peptide secondary metabolites in planktonic marine cyanobacteria. *Proc. Natl. Acad. Sci.* 107, 10430–10435. doi: 10.1073/PNAS.0913677107

Makitrynskyy, R., Ostash, B., Tsypik, O., Rebets, Y., Doud, E., Meredith, T., et al. (2013). Pleiotropic regulatory genes bldA, adpA and absB are implicated in production of phosphoglycolipid antibiotic moenomycin. *Open Biol.* 3:130121. doi: 10.1098/rsob.130121

Martens, E., and Demain, A. L. (2017). The antibiotic resistance crisis, with a focus on the United States. *J. Antibiot.* 70, 520–526. doi: 10.1038/ja.2017.30

Mitra, A., Kesarwani, A. K., Pal, D., and Nagaraja, V. (2011). WebGeSTer DB—a transcription terminator database. *Nucleic Acids Res.* 39, D129–D135. doi: 10.1093/nar/gkq971

Myronovskyi, M., Welle, E., Fedorenko, V., and Luzhetskyy, A. (2011). ß-Glucuronidase as a sensitive and versatile reporter in Actinomycetes. *Appl. Environ. Microbiol.* 77, 5370–5383. doi: 10.1128/AEM.00434-11

Nesvizhskii, A. I., Keller, A., Kolker, E., and Aebersold, R. (2003). A Statistical Model for Identifying Proteins by Tandem Mass Spectrometry. *Anal Chem* 75, 4646–4658. doi: 10.1021/ac0341261

Newman, D. J., and Cragg, G. M. (2016). Natural products as sources of new drugs from 1981 to 2014. *J. Nat. Prod.* 79, 629–661. doi: 10.1021/acs.jnatprod.5b01055

Nguyen, H. T., Wolff, K. A., Cartabuke, R. H., Ogwang, S., and Nguyen, L. (2010). A lipoprotein modulates activity of the MtrAB two-component system to provide intrinsic multidrug resistance, cytokinetic control and cell wall homeostasis in *Mycobacterium*. *Mol. Microbiol.* 76, 348–364. doi: 10.1111/j.1365-2958.2010.07110.x

O'Rourke, S., Widdick, D., and Bibb, M. (2017). A novel mechanism of immunity controls the onset of cinnamycin biosynthesis in *Streptomyces cinnamoneus* DSM 40646. *J. Ind. Microbiol. Biotechnol.* 44, 563–572. doi: 10.1007/s10295-016-1869-9

Osman, D., and Cavet, J. S. (2010). Bacterial metal-sensing proteins exemplified by ArsR-SmtB family repressors. *Nat. Prod. Rep.* 27, 668–680. doi: 10.1039/b906682a

Otaka, T., and Kaji, A. (1976). Mode of Action of Bottromycin A2. Release of aminoacyl- or peptidyl-tRNA from ribosomes. *J. Biol. Chem.* 251, 2299–2306.

Otaka, T., and Kaji, A. (1981). Mode of action of bottromycin A2: effect on peptide bond formation. *FEBS Lett.* 123, 173–176. doi: 10.1016/0014-5793(81)80280-3

Otaka, T., and Kaji, A. (1983). Mode of action of bottromycin A2: effect of bottromycin A2 on polysomes. *FEBS Lett.* 153, 53–59. doi: 10.1016/0014-5793(83)80118-5

Paget, M. S., Chamberlin, L., Atrih, A., Foster, S. J., and Buttner, M. J. (1999). Evidence that the extracytoplasmic function sigma factor sigmaE is required for normal cell wall structure in *Streptomyces coelicolor* A3(2). *J. Bacteriol.* 181, 204–211. doi: 10.1128/jb.181.1.204-211.1999

Quistgaard, E. M., Low, C., Guettou, F., and Nordlund, P. (2016). Understanding transport by the major facilitator superfamily (MFS): structures pave the way. *Nat. Rev. Mol. Cell Biol.* 17, 123–132. doi: 10.1038/nrm.2015.25

R Core Team (2014). *R: A Language and Environment for Statistical Computing*. Vienna: R Foundation for Statistical Computing.

Rigden, D. J. (2011). Ab initio modeling led annotation suggests nucleic acid binding function for many DUFs. *Omi. A J. Integr. Biol.* 15, 431–438. doi: 10.1089/omi.2010.0122

Ritchie, M. E., Phipson, B., Wu, D., Hu, Y., Law, C. W., Shi, W., et al. (2015). limma powers differential expression analyses for RNA-sequencing and microarray studies. *Nucleic Acids Res.* 43:e47. doi: 10.1093/nar/gkv007

Rogers, T. O., and Birnbaum, J. (1974). Biosynthesis of fosfomycin by *Streptomyces fradiae*. *Antimicrob. Agents Chemother.* 5, 121–132. doi: 10.1128/aac.5.2.121

Sambrook, J., Fritsch, E. F., and Maniatis, T. (1989). *Molecular Cloning: A Laboratory Manual*, 2nd editio Edn. New York, NY: Cold Spring Harbor Laboratory Press.

Santos-Aberturas, J., Chandra, G., Frattaruolo, L., Lacret, R., Pham, T. H., Vior, N. M., et al. (2019). Uncovering the unexplored diversity of thioamidated ribosomal peptides in Actinobacteria using the RiPPER genome mining tool. *Nucleic Acids Res.* 47, 4624–4637. doi: 10.1093/nar/gkz192

Schwalen, C. J., Hudson, G. A., Kosol, S., Mahanta, N., Challis, G. L., and Mitchell, D. A. (2017). *In vitro* biosynthetic studies of bottromycin expand the enzymatic capabilities of the YcaO superfamily. *J. Am. Chem. Soc.* 139, 18154–18157. doi: 10.1021/jacs.7b09899

Severinov, K., Semenova, E., Kazakov, A., Kazakov, T., and Gelfand, M. S. (2007). Low-molecular-weight post-translationally modified microcins. *Mol. Microbiol.* 65, 1380–1394. doi: 10.1111/j.1365-2958.2007.05874.x

Sherwood, E. J., and Bibb, M. J. (2013). The antibiotic planosporicin coordinates its own production in the actinomycete *Planomonospora alba*. *Proc. Natl. Acad. Sci. U.S.A.* 110, E2500–E2509. doi: 10.1073/pnas.1305392110

Shimamura, H., Gouda, H., Nagai, K., Hirose, T., Ichioka, M., Furuya, Y., et al. (2009). Structure determination and total synthesis of bottromycin A2: a potent antibiotic against MRSA and VRE. *Angew. Chem Int. Ed.* 48, 914–917. doi: 10.1002/anie.200804138

Shimizu, K. (2016). "Metabolic regulation and coordination of the metabolism in bacteria in response to a variety of growth conditions," in *Bioreactor Engineering Research and Industrial Applications I: Cell Factories*, eds Q. Ye, J. Bao, and J.-J. Zhong (Berlin: Springer), 1–54. doi: 10.1007/10_2015_320

Sikandar, A., Franz, L., Melse, O., Antes, I., and Koehnke, J. (2019). Thiazoline-specific amidohydrolase PurAH is the gatekeeper of bottromycin biosynthesis. *J. Am. Chem. Soc.* 141:9748. doi: 10.1021/jacs.8b12231

Solovyev, V., and Salamov, A. (2011). "Automatic annotation of microbial genomes and metagenomic sequences," in *Metagenomics & its Applications in Agriculture, Biomedicine & Environmental Studies*, ed. R. W. Li (New York, NY: Nova Science Publishers Inc), 61–78.

Som, N. F., Heine, D., Holmes, N. A., Munnoch, J. T., Chandra, G., Seipke, R. F., et al. (2017). The conserved actinobacterial two-component system MtrAB coordinates chloramphenicol production with sporulation in *Streptomyces venezuelae* NRRL B-65442. *Front. Microbiol.* 8:1145. doi: 10.3389/fmicb.2017.01145

Stajich, J. E., Block, D., Boulez, K., Brenner, S. E., Chervitz, S. A., Dagdigian, C., et al. (2002). The Bioperl toolkit: perl modules for the life sciences. *Genome Res.* 12, 1611–1618. doi: 10.1101/gr.361602

Tacconelli, E., and Magrini, N. (2017). *Global Priority List of Antibiotic-Resistant Bacteria to Guide Research, Discovery, and Development of New Antibiotics*. Geneva: World Health Organization.

Thomas, G., Coutts, G., and Merrick, M. (2000). The glnKamtB operon. A conserved gene pair in prokaryotes. *Trends Genet.* 16, 11–14. doi: 10.1016/S0168-9525(99)01887-9

Tyanova, S., Temu, T., and Cox, J. (2016). The MaxQuant computational platform for mass spectrometry-based shotgun proteomics. *Nat. Protoc.* 11, 2301–2319. doi: 10.1038/nprot.2016.136

Untergasser, A., Cutcutache, I., Koressaar, T., Ye, J., Faircloth, B. C., Remm, M., et al. (2012). Primer3–new capabilities and interfaces. *Nucleic Acids Res.* 40:e115. doi: 10.1093/nar/gks596

Vior, N. M., Olano, C., García, I., Méndez, C., and Salas, J. A. (2014). Collismycin a biosynthesis in *Streptomyces* sp. *CS*40 is regulated by iron levels through two pathway-specific regulators. *Microbiology* 160, 467–478. doi: 10.1099/mic.0.075218-0

Wade, J. T. (2015). Where to begin? Mapping transcription start sites genome-wide in *Escherichia coli*. *J. Bacteriol.* 197, 4–6. doi: 10.1128/JB.02410-14

Wagner, G. P., Kin, K., and Lynch, V. J. (2012). Measurement of mRNA abundance using RNA-seq data: RPKM measure is inconsistent among samples. *Theory Biosci.* 131, 281–285. doi: 10.1007/s12064-012-0162-3

Waisvisz, J. M., van der Hoeven, M. G., van Peppen, J., and Zwennis, W. C. M. (1957). Bottromycin. I. A new sulfur-containing antibiotic. *J. Am. Chem. Soc.* 79, 4520–4521. doi: 10.1021/ja01573a072

Waldvogel, E., Herbig, A., Battke, F., Amin, R., Nentwich, M., Nieselt, K., et al. (2011). The PII protein GlnK is a pleiotropic regulator for morphological differentiation and secondary metabolism in *Streptomyces coelicolor*. *Appl. Microbiol. Biotechnol.* 92, 1219–1236. doi: 10.1007/s00253-011-3644-1

Wilkinson, C. J., Hughes-Thomaz, Z. A., Martin, C. J., Bohm, I., Mironenko, T., Deacon, M., et al. (2002). Increasing the efficiency of heterologous promoter in actinomycetes. *J. Mol. Microbiol. Biotechnol.* 4, 417–426.

Wu, P., Pan, H., Zhang, C., Wu, H., Yuan, L., Huang, X., et al. (2014). SACE-3986, a TetR family transcriptional regulator, negatively controls erythromycin biosynthesis in *Saccharopolyspora erythraea*. *J. Ind. Microbiol. Biotechnol.* 41, 1159–1167. doi: 10.1007/s10295-014-1449-9 doi: 10.1007/s10295-014-1449-9

Yang, J., Yan, R., Roy, A., Xu, D., Poisson, J., and Zhang, Y. (2015). The I-TASSER suite: protein structure and function prediction. *Nat. Methods* 12, 7–8. doi: 10.1038/nmeth.3213

Yang, X., Lennard, K. R., He, C., Walker, M. C., Ball, A. T., Doigneaux, C., et al. (2018). A lanthipeptide library used to identify a protein–protein interaction inhibitor. *Nat. Chem. Biol.* 14, 375–380. doi: 10.1038/s41589-018-0008-5

Yoo, Y. J., Hwang, J., Shin, H., Cui, H., Lee, J., and Yoon, Y. J. (2015). Characterization of negative regulatory genes for the biosynthesis of rapamycin in *Streptomyces rapamycinicus* and its application for improved production. *J. Ind. Microbiol. Biotechnol.* 42, 125–135. doi: 10.1007/s10295-014-1546-9

Zhang, P., Wu, H., Chen, X. L., Deng, Z., Bai, L., and Pang, X. (2014). Regulation of the biosynthesis of thiopeptide antibiotic cyclothiazomycin by the transcriptional regulator SHJG8833 in *Streptomyces hygroscopicus* 5008. *Microbiology* 160, 1379–1392. doi: 10.1099/mic.0.076901-0

Zhang, P., Wu, L., Zhu, Y., Liu, M., Wang, Y., Cao, G., et al. (2017). Deletion of MtrA inhibits cellular development of *Streptomyces coelicolor* and alters expression of developmental regulatory genes. *Front. Microbiol.* 8:2013. doi: 10.3389/fmicb.2017.02013

Zhao, Y., Xiang, S., Dai, X., and Yang, K. (2013). A simplified diphenylamine colorimetric method for growth quantification. *Appl. Microbiol. Biotechnol.* 97, 5069–5077. doi: 10.1007/s00253-013-4893-y

Conflict of Interest: The authors declare that the research was conducted in the absence of any commercial or financial relationships that could be construed as a potential conflict of interest.

frontiers in Microbiology

ORIGINAL RESEARCH
published: 09 June 2020
doi: 10.3389/fmicb.2020.01089

SrrB, a Pseudo-Receptor Protein, Acts as a Negative Regulator for Lankacidin and Lankamycin Production in *Streptomyces rochei*

Yuya Misaki[1,2†], Shouji Yamamoto[2†‡], Toshihiro Suzuki[2‡], Miyuki Iwakuni[2], Hiroaki Sasaki[2], Yuzuru Takahashi[2], Kuninobu Inada[3], Haruyasu Kinashi[2] and Kenji Arakawa[1,2]*

[1] Unit of Biotechnology, Graduate School of Integrated Sciences for Life, Hiroshima University, Higashi-Hiroshima, Japan, [2] Department of Molecular Biotechnology, Graduate School of Advanced Sciences of Matter, Hiroshima University, Higashi-Hiroshima, Japan, [3] Natural Science Center for Basic Research and Development, Hiroshima University, Higashi-Hiroshima, Japan

Streptomyces rochei 7434AN4, a producer of lankacidin (LC) and lankamycin (LM), carries many regulatory genes including a biosynthesis gene for signaling molecules SRBs (*srrX*), an SRB receptor gene (*srrA*), and a SARP (*Streptomyces* antibiotic regulatory protein) family activator gene (*srrY*). Our previous study revealed that the main regulatory cascade goes from *srrX* through *srrA* to *srrY*, leading to LC production, whereas *srrY* further regulates a second SARP gene *srrZ* to synthesize LM. In this study we extensively investigated the function of *srrB*, a pseudo-receptor gene, by analyzing antibiotic production and transcription. Metabolite analysis showed that the *srrB* mutation increased both LC and LM production over four-folds. Transcription, gel shift, and DNase I footprinting experiments revealed that *srrB* and *srrY* are expressed under the SRB/SrrA regulatory system, and at the later stage, SrrB represses *srrY* expression by binding to the promoter region of *srrY*. These findings confirmed that SrrB acts as a negative regulator of the activator gene *srrY* to control LC and LM production at the later stage of fermentation in *S. rochei*.

Keywords: *Streptomyces*, regulatory cascade, pseudo-receptor, antibiotic, biosynthesis

OPEN ACCESS

Edited by:
Evi Stegmann,
University of Tübingen, Germany

Reviewed by:
Yihua Chen,
Institute of Microbiology (CAS), China
Juan F. Martin,
Universidad de León, Spain

***Correspondence:**
Kenji Arakawa
karakawa@hiroshima-u.ac.jp

† These authors have contributed equally to this work

‡Present address:
Shouji Yamamoto, Department of Bacteriology I, National Institute of Infectious Diseases, Tokyo, Japan
Toshihiro Suzuki, Department of Fermentation Science, Faculty of Applied Biosciences, Tokyo University of Agriculture, Tokyo, Japan

Specialty section:
This article was submitted to Antimicrobials, Resistance and Chemotherapy, a section of the journal Frontiers in Microbiology

Received: *17 December 2019*
Accepted: *30 April 2020*
Published: *09 June 2020*

Citation:
Misaki Y, Yamamoto S, Suzuki T, Iwakuni M, Sasaki H, Takahashi Y, Inada K, Kinashi H and Arakawa K (2020) SrrB, a Pseudo-Receptor Protein, Acts as a Negative Regulator for Lankacidin and Lankamycin Production in Streptomyces rochei. Front. Microbiol. 11:1089. doi: 10.3389/fmicb.2020.01089

INTRODUCTION

Secondary metabolites production is strictly controlled by small diffusible signaling molecules that constitute signaling-molecule/receptor regulatory systems in *Streptomyces* species (Bibb, 2005; Takano, 2006; Horinouchi and Beppu, 2007; Martín and Liras, 2019). The most-studied signaling-molecule/receptor system is A-factor/ArpA in *Streptomyces griseus* for streptomycin and grixazone production (Ohnishi et al., 1999, 2005). In the absence of A-factor, ArpA protein specifically binds to the promoter region of the target activator gene *adpA* and represses its transcription. When A-factor reaches a critical concentration, A-factor/ArpA complex dissociates from the promoter region of *adpA*, leading to the onset of *adpA* transcription. Then, the gene product of *adpA* binds to its targets (AdpA-regulons) to activate streptomycin and grixazone production and morphological differentiation (Ohnishi et al., 1999, 2005). Gene sets involved in the signaling-molecule-dependent regulatory pathways for

secondary metabolite production are listed in **Table 1** (Arakawa, 2018; Xu and Yang, 2019); e.g., streptomycin and grixazone production in *S. griseus* (Hara and Beppu, 1982; Onaka et al., 1995; Ohnishi et al., 1999, 2005), lankamycin (LM) and lankacidin (LC) (**Figure 1**) in *Streptomyces rochei* (Arakawa et al., 2007, 2012; Yamamoto et al., 2008; Suzuki et al., 2010), tylosin in *Streptomyces fradiae* (Bate et al., 1999, 2002; Stratigopoulos and Cundliffe, 2002), coelimycin P-1 in *Streptomyces coelicolor* (Takano et al., 2001, 2005; Hsiao et al., 2009; Gottelt et al., 2010; Li et al., 2015), actinorhodin and undecylprodigiosin in *Streptomyces coelicolor* (Xu et al., 2010; Wang et al., 2011), virginiamycin in *Streptomyces virginiae* (Kondo et al., 1989; Kinoshita et al., 1997; Kawauchi et al., 2000), jadomycin in *Streptomyces venezuelae* (Yang et al., 1995; Wang and Vining, 2003; Wang et al., 2009; Xu et al., 2010; Zou et al., 2014), kinamycin in *Streptomyces ambofaciens* (Aigle et al., 2005; Bunet et al., 2008, 2011), and avermectin in *Streptomyces avermitilis* (Kitani et al., 2011; Wang J. B., et al., 2014; Zhu et al., 2016).

Streptomyces rochei 7434AN4 produces two structurally unrelated polyketide antibiotics, LM and LC (**Figure 1A**) and carries three linear plasmids pSLA2-L, -M, and -S (Kinashi et al., 1994). Together with the biosynthetic genes for LM and LC, many regulatory genes including a biosynthetic gene for signaling molecules SRBs (**Figure 1B**) (*srrX*), six *tetR*-type repressor genes (*srrA*, *srrB*, *srrC*, *srrD*, *srrE*, and *srrF*), and three SARP (*Streptomyces* antibiotic regulatory protein) family activator genes (*srrY*, *srrZ*, and *srrW*) are located on giant linear plasmid pSLA2-L (210,614 bp) (Mochizuki et al., 2003). Our group revealed that SRBs/SrrA complex dissociates from the promoter region of *srrY*, leading to the activation of LC production (Yamamoto et al., 2008), whereas the gene product of *srrY* further activates a second activator gene *srrZ* to produce LM (Suzuki et al., 2010). In addition, mutation of an additional receptor gene *srrB* greatly increased the production of both LC and LM (Arakawa et al., 2007). This finding suggested that *srrB* negatively regulates LC and LM production, however, its functional role has not been clarified.

In this study, we extensively investigated the function of *srrB* by analyzing antibiotic production and transcription, the results of which indicated that SrrB acts as a negative regulator by binding to the promoter region of the activator gene *srrY* to control LC and LM production at the later stage of fermentation in *S. rochei*.

MATERIALS AND METHODS

Bacterial Strains and DNA Manipulation

S. rochei strain 51252 carrying only the linear plasmid pSLA2-L was used as the parent strain (Kinashi et al., 1994). All strains, plasmids, and oligonucleotides used in this study are listed in **Table 2**. *Streptomyces* strains were grown in YM medium (0.4% yeast extract, 1.0% malt extract, 0.4% D-glucose, pH 7.3) for antibiotic production and RNA isolation. *Escherichia coli* strains were grown in Luria-Bertani (LB) medium supplemented with ampicillin (100 μg/ml), apramycin (50 μg/ml), and/or chloramphenicol (25 μg/ml) when necessary. For protoplasts preparation, *Streptomyces* strains were grown in YEME medium (Kieser et al., 2000). Protoplasts were regenerated on R1M plates (Zhang et al., 1997). DNA manipulations for *E. coli* (Sambrook et al., 1989) and *Streptomyces* (Kieser et al., 2000) were performed according to the standard protocols. PCR amplification was done on a 2720 Thermal Cycler (Thermo Fisher Scientific, Waltham, MA, USA) with KOD-Plus- DNA polymerase (Toyobo, Osaka, Japan).

Construction of Mutant and Plasmid

Construction of *srrA* and *srrB* Double Mutant

The target plasmid pKAR3014 that carries in-frame deletion of *srrA* in *E. coli-Streptomyces* shuttle vector pRES18 (Ishikawa et al., 1996) was constructed as described previously (Arakawa et al., 2007). Targeted mutagenesis was performed as follows. Plasmid pKAR3014 was transformed into protoplasts of *S. rochei* strain KA07 (*srrB* mutant), and thiostrepton-resistant strains were obtained. Among these transformants, single-crossover strains were selected by Southern hybridization. Some single-crossover colonies were continuously grown in YEME liquid medium to facilitate a second crossover. Finally, thiostrepton sensitive strains were selected as double crossover strains, to obtain a strain TS03 (*srrAB* mutant). Gene disruption was checked by Southern hybridization analysis using DIG DNA Labeling and Detection Kit (Roche Diagnostics GmbH, Mannheim, Germany).

Construction of *srrY* and *srrB* Double Mutant

The target plasmid pKAR3055 that carries in-frame deletion of *srrY* in pRES18 was constructed as described previously (Yamamoto et al., 2008). This plasmid was transformed into protoplasts of *S. rochei* strain KA07, and an *srrB-srrY* double mutant KA64 was constructed in a similar manipulation as above mentioned.

Construction of *in vivo srrB* Expression Plasmid

The *srrB* gene was amplified using cosmid A8 (Mochizuki et al., 2003) and primers, srrB-8600f1 and srrB-8600r1. The resulting PCR product was digested with *Nde*I and *Xba*I and cloned into pIJ8600, an *E. coli-Streptomyces* shuttle vector carrying a *tipA* promoter (Sun et al., 1999), to obtain pKAR3065.

This plasmid was introduced into strain 51252, and transformants were cultured for 24 h at 28°C in YM liquid medium with 10 μg/ml apramycin. Thiostrepton (10 μg/ml as final concentration) was added at 24 h to induce *srrB* expression. After cultivation for additional 24 h, the broth filtrate was extracted twice with equal volume of ethyl acetate. The combined organic phase was dried with Na_2SO_4, and concentrated *in vacuo* to obtain crude extracts.

Construction of *srrB* Overexpression Plasmid in *E. coli*

The *srrB*-coding sequence was PCR amplified using the template cosmid A8 (Mochizuki et al., 2003) and primers, KAR7903OE and KAR7902OE. The amplified fragment was digested with *Bgl*II and *Eco*RI and cloned into pET32b(+), a $(His)_6$-tagged expression vector, to obtain pKAR3036.

TABLE 1 | Gene sets of signaling molecule(s)/receptor/pseudo-receptor for secondary metabolite production in *Streptomyces* species.

	Signaling molecule synthesis gene	Signaling molecule(s)	Receptor gene	Pseudo-receptor gene (pI of gene product)	Secondary metabolite(s)
S. griseus	*afsA*	A-factor	*arpA*		Streptomycin, grixazone
S. rochei	*srrX*	SRB1, SRB2	*srrA*	*srrB* (11.2)	Lankacidin, lankamycin
S. fradiae	ND	ND	*tylP*	*tylQ* (6.4)	Tylosin
S. coelicolor	*scbA*	SCB1-3	*scbR*	*scbR2* (5.8)	Coelimycin P-1, actinorhodin, undecylprodigiosin
S. coelicolor	*mmfL*	MMFs	*mmfR*		Methylenomycin
S. virginiae	*barX*	Virginia butanolides	*barA*	*barB* (10.2)	Virginiamycin
S. venezuelae	*jadW1*	SVB1	*jadR3*	*jadR2* (7.8)	Jadomycin
S. lavendulae	*farA*	IM-2	*farR*	*farR2* (9.7)	Showdomycin
S. ambofaciens	ND	ND	*alpZ*	*alpW* (11.6)	Kinamycins
S. avermitilis	*aco*	Avenolide	*avaR1*	*avaR2* (9.6)	Avermectins

ND, Not determined.

Isolation and Analysis of Metabolites

The 48-h cultures of *S. rochei* strains were harvested, and the supernatant was extracted twice with equal volume of ethyl acetate. The crude extracts were purified by Sephadex LH-20 chromatography (1 × 40 cm, GE Healthcare, Chicago, IL) with methanol. Then the fractions containing antibiotics were purified by silica gel chromatography with chloroform-methanol (80:1–10:1, v/v). NMR spectra were recorded on an ECA-500 spectrometer (JEOL, Tokyo, Japan) equipped with a field gradient accessory. Chloroform-*d* and methanol-d_4 were used as solvents. Chemical shifts were recorded in δ value based on the solvent signals ($\delta_C = 77.0$ in $CDCl_3$, $\delta_C = 49.0$ in CD_3OD, and $\delta_H = 3.30$ in residual CH_3OH) or an internal standard tetramethylsilane ($\delta_H = 0$). High resolution ESI-MS spectra were measured by a LTQ Orbitrap XL mass spectrometer (Thermo Fisher Scientific). The ^{1}H- and ^{13}C-NMR assignments for lankamycin (**1**), lankacidin C (**2**), lankacidin A (**3**), lankacidinol A (**4**), iso-lankacidinol (**5**), and lankacidinol (**6**) have already been reported (Suzuki et al., 2010; Arakawa et al., 2011; Yamamoto et al., 2018).

SRB Assay

Two strains KA61 (Δ*srrY*) and KA64 (Δ*srrY*Δ*srrB*) were cultured at 28°C for 30 h, and the supernatant (60 ml) was acidified to pH 3 and extracted with equal volume of ethyl acetate twice. The combined organic phase was concentrated in vacuo. Appropriately diluted culture extract (100 μl) was added to the fresh culture (5 ml) of strain KA20, an *srrX*-deficient strain, and cultured at 28°C for 36 h to restore LM and LC production.

Time-Course Analysis

S. rochei strains were grown in YM liquid medium and harvested at various time periods at 12-36 h. Cells were used for measurement of dry cell weight (dcw) and isolation of total RNA, while the culture supernatant was for measurement of antibiotic production.

Measurement of DCW

Cultures were collected at various time periods and centrifuged at 5,000 rpm for 10 min. The resulting pellet was washed twice with 10.3% sucrose, and then placed in a 60°C dry oven until the weight reaches to a constant value.

RNA Preparation and Reverse Transcription-PCR (RT-PCR)

S. rochei strains were cultured at 28°C in YM liquid medium for various time periods. Total RNAs was extracted from cells with a TRI reagent (Invitrogen, Carlsbad, CA) according to the manufacturer's instructions. Trace amounts of DNA were removed with RNase-free DNase I (Takara, Kyoto, Japan). The concentration of purified RNA was determined by UV absorbance at 260 nm using Ultrospec 3300 pro spectrometer (GE Healthcare). The cDNAs were synthesized using Transcriptor Reverse Transcriptase (Roche Diagnostics). Each reaction mixture contained 1 μg of total RNA and 0.08 A_{260} units random primer. Each mixture was sequentially treated at 85°C for 5 min, at 25°C for 10 min, and 55°C for 45 min for the cDNA synthesis. The 16S rRNA was used as an internal standard (Lane, 1991;Turner et al., 1999).

5′ Rapid Amplification of cDNA Ends (5′ RACE)

Transcriptional start site (TSS) of *srrB* was determined using 5′RACE System, Version 2.0 (Invitrogen, Carlsbad, CA, USA). Total RNA was prepared from a 24-h culture sample of parent strain. One microgram of total RNA was converted to the cDNA using specific primer srrB-GSP1, and the resultant was treated with ribonuclease and purified through spin column to afford cDNA. A homopolymeric tail was then added to the 3'-end of cDNA using terminal deoxynucleotidyl transferase and dCTP. PCR was performed with poly C tailed cDNA as a template using abridged anchor primer and

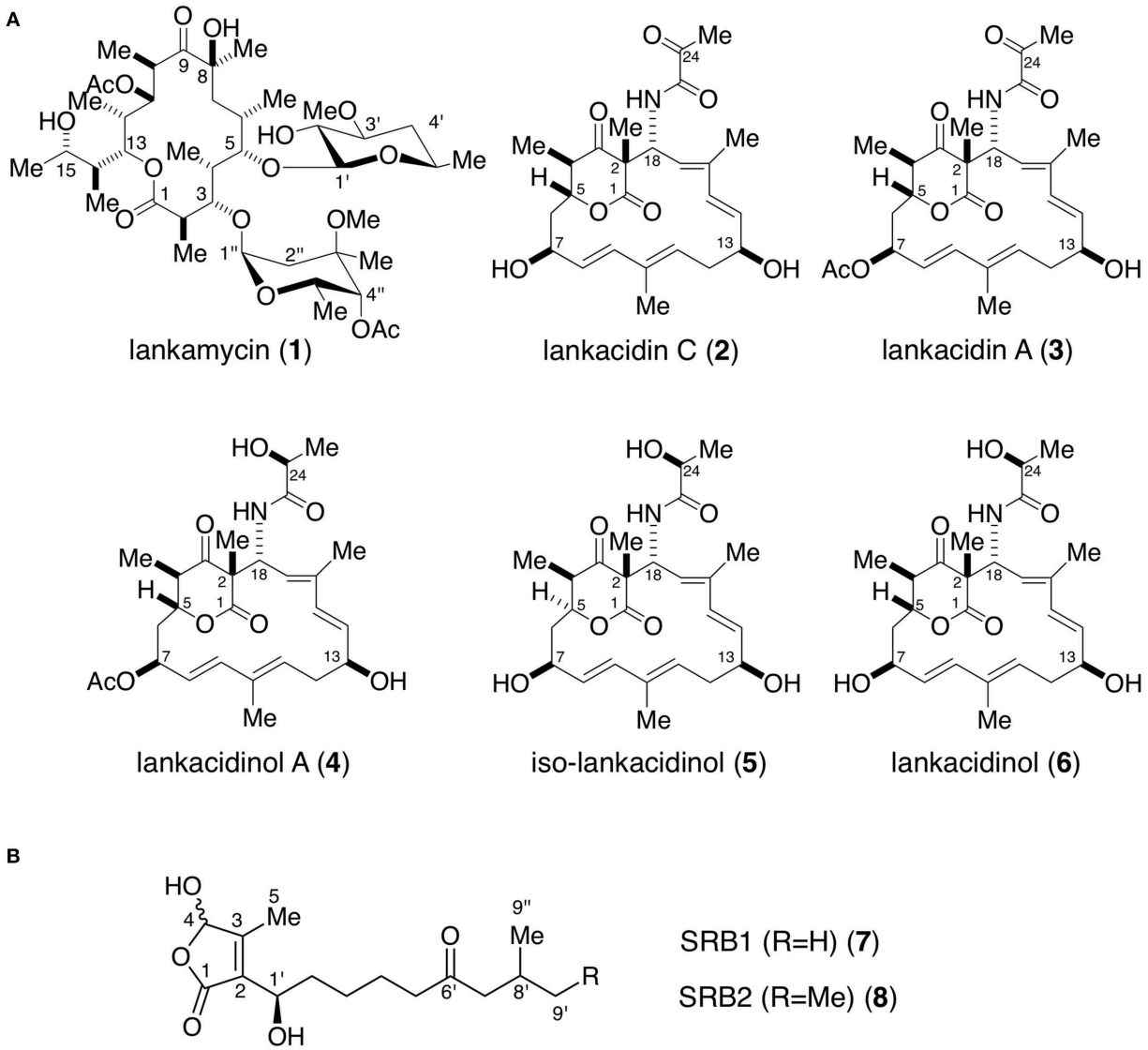

FIGURE 1 | Chemical structures of antibiotics **(A)** and signaling molecules **(B)** produced in *Streptomyces rochei*. **(A)** Antibiotics lankamycin (**1**), lankacidin C (**2**), lankacidin A (**3**), lankacidinol A (**4**), iso-lankacidinol (**5**), and lankacidinol (**6**). **(B)** Signaling molecules SRB1 (**7**) and SRB2 (**8**). Me, methyl; Ac, acetyl.

inner specific primer RT79-R2. TSS was determined from nucleotide sequence of amplified PCR product using ABI PRISM 310 Genetic Analyzer (Life Technologies, Carlsbad, CA, USA).

Overexpression and Purification of SrrB Protein

E. coli BL21(DE3)pLysS was used as hosts for plasmid pKAR3036. Cells were grown in LB liquid medium supplemented with 100 μg/ml ampicillin and 25 μg/ml chloramphenicol at 37°C to OD_{600} = 0.6 and then were induced with 1 mM isopropyl β-thiogalactopyranoside (IPTG). Cultivation was continued for 12 h at 16°C, and then cells were harvested and disrupted by SONIFER 250 ultrasonic homogenizer (Branson Ultrasonics Corporation, Danbury, CT, USA). The $(His)_6$-fusion protein was purified by Ni^{2+}-nitrotriacetic acid agarose (Qiagen GmbH, Hilden, Germany) according to the manufacture's protocol. After dialysis with PBS buffer (137 mM NaCl, 8.1mM $Na_2HPO_4{\cdot}12H_2O$, 2.68 mM KCl, 1.47 mM KH_2PO_4), the $(His)_6$-tagged SrrB protein was treated with enterokinase (Novagen, Madison, WI, USA), and the $(His)_6$-tag peptide upstream of the N-terminal SrrB was removed by Enterokinase Cleavage Capture Kit (Novagen) according to the manufacture's protocol. The protein was analyzed by SDS-PAGE with 15% polyacrylamide gel. The protein concentration was determined according to the methods of Bradford using Bio-Rad protein assay (Bio-Rad, Hercules, CA, USA) with bovine serum albumin as a standard.

TABLE 2 | Bacterial strains, plasmids, and oligonucleotides used in this study.

Strains/plasmids/oligonucleotides	Description	Source/References
BACTERIAL STRAINS		
Streptomyces rochei 7434AN4	Wild type (pSLA2-L, M, S)	Kinashi et al., 1994
Streptomyces rochei 51252	Ultraviolet irradiation of 7434AN4 (pSLA2-L)	Kinashi et al., 1994
Streptomyces rochei KA07	*in frame* deletion of *srrB* in 51252 (Δ*srrB*)	Arakawa et al., 2007
Streptomyces rochei KA12	*in frame* deletion of *srrA* in 51252 (Δ*srrA*)	Arakawa et al., 2007
Streptomyces rochei TS03	*in frame* deletion of *srrA* in KA07 (Δ*srrAB*)	This study
Streptomyces rochei KA61	*in frame* deletion of *srrY* in 51252 (Δ*srrY*)	Yamamoto et al., 2008
Streptomyces rochei KA64	*in frame* deletion of *srrY* in KA07 (Δ*srrBY*)	This study
Streptomyces rochei KA20	*kan*::*srrX* in KA07 (Δ*srrXB*)	Arakawa et al., 2012
Escherichia coli XL1-Blue	*recA1 endA1 gyrA96 thi-1 hsdR17 supE44 relA1 lac* F' *proAB lacIqZ*Δ[*M15* Tn10 (Tet^r)]	Stratagene
Escherichia coli BL21(DE3)pLysS	F' *ompT hsdS$_B$* (r_B^- m_B^-) *gal dcm* (DE3) pLysS(Cam^r)	Novagen
PLASMIDS		
Cosmid A8	38.9-kb pSLA2-L DNA (nt 106,868-145,771) cloned into SuperCos-1 at *Bam*HI site	Mochizuki et al., 2003
pKAR3004	4.3 kb *Pst*I-*Eco*47III fragment containing *srrB* in pUC19	(Arakawa et al., 2007)
pKAR3014	3.0 kb *Nco*I-*Sac*I fragment deleted 207-bp *Bsp*EI fragment from *srrA*	Arakawa et al., 2007
pKAR3055	1.5 kb EcoRI-PstI fragment deleted 267-bp *Pvu*II fragment from *srrY*	(Yamamoto et al., 2008)
pKAR3036	1.0 kb *Bgl*II-*Eco*RI fragment containing *srrB* in pET32b(+)	This study
pKAR4002	9.2 kb *Pst*I fragment containing *srrY* in pUC19	(Yamamoto et al., 2008)
pUC19	Cloning vector; *amp*	Takara
pET32b(+)	T7 expression vector for histidine-tagging, *amp*	Novagen
pIJ8600	Integrative *E. coli-Streptomyces* shuttle vector, inducible *tipA* promoter, *apr*, *tsr*	Sun et al., 1999
pKAR3065	0.68 kb *Nde*I-*Xba*I PCR fragment containing srrB in pIJ8600	This study
***OLIGONUCLEOTIDES* (5′-3′)**		
KAR7903OE	CGCAGATCTACATATGGCCATGCAGGAACGT	This study
KAR7902OE	CTAGAATTCGTACAGCTCGGCCACCATGGC	This study
SRRBf3	ACCCGCACGGCCCGTACATC	This study
SRRBr3	GTACCCCTCTTCCGCGAACA	This study
SRRYf2	GGCGTCGTCTGCCTGCTGCC	Yamamoto et al., 2008
SRRYr2	ATATCCGCCGGGGGCGGTGG	Yamamoto et al., 2008
SRRYf4	CTCCCCTTGTCGTCGTCGAG	This study
SRRYr4	GCGCCCGCGGCGTCACCGAGA	Yamamoto et al., 2008
RT75-F	CAGGTTCTCGTGCGTGCGGTA	This study
RT75-R	GTGCGACGTACAAGCGGGACC	This study
KA82010E	CTAGGATCCGCATATGGCACAGCAGGAAC	This study
SRRAr2B	GGGGGATCCCACCAGCACCGAGGGCACCGC	This study
SRRBf1E	GGGGAATTCGAGCGGTGGAGGACCAGGCCG	This study
SRRBr4	AGGAGCAGTTCCCAGAACGC	This study
16S-357F	CCTACGGGAGGCAGCAG	Turner et al., 1999
16S-907R	CCCCGTCAATTCCTTTGAGTT	Lane 1991
KA-RT079S1	GCGAGACACCGGGAGCCAACTG	This study
KA-RT079AS1	TCGCGGAAGAGGGGTACGTGCC	This study
srrB-8600f1	GAACATATGGCCATGCAGGAA	This study
srrB-8600r1	TGAAGATCTCACTGTCGGGCTG	This study
srrB-GSP1	GCTGCGAACCCAGCTCGAAAC	This study
RT79-R2	CGCCTTCTTGTTCTCGAAGTG	This study
srrB-GSP3	TCCCCGCCGGTGACCGCTCCGTCC	This study

Preparation of DNA Probes and Gel Shift Assay

The *srrB* probes for gel shift assay were prepared as follows. For preparation of probe B1, a 564-bp DNA fragment containing the upstream region of *srrB* was amplified using pKAR3004 as a template and primers SRRBf3 and SRRBr3 (positions −81 to +483 from TSS of *srrB*; nt 140,677-141,240 of pSLA2-L). For preparation of probe B2, a 386-bp DNA fragment containing the internal region of *srrB* was amplified using pKAR3004 as a template and primers SRRBf1E and SRRBr4 (positions +574 to +959 from TSS of *srrB*; nt 140,201-140,586 of pSLA2-L).

Probe B1 was then 3′ -end labeled with [γ-^{32}P]ATP (GE Healthcare) and T4 polynucleotide kinase (Toyobo). The reaction mixture contained the binding buffer (20 mM Tris-HCl [pH 8.0], 100 mM NaCl, 1 mM dithiothreitol, 0.1 mg of bovine serum albumin and 5% glycerol), 0.5 nM labeled DNA and 2 μM SrrA protein. SrrA protein was prepared as reported previously (Yamamoto et al., 2008). When necessary, synthetic SRB1 [(1–′*R*)-isomer; **Figure 1B**] (Arakawa et al., 2012) was added to the reaction mixture. For competition experiment, unlabeled probes B1 and B2 were used at a final concentration of 200 nM. The reaction mixture was incubated at 26°C for 30 min, and subjected to electrophoresis at room temperature on a native 4.5% polyacrylamide gel in 0.5 × TBE buffer (46 mM Tris base, 46 mM boric acid, 1 mM EDTA). The ^{32}P-labeled DNAs were detected by autoradiography.

Preparation of *srrY* probes for gel shift assay was described previously (Yamamoto et al., 2008). To analyze the effect of SRB on the binding of SrrA and SrrB, various concentration of synthetic SRB1 [(1′*R*)-isomer; **Figure 1B**] (Arakawa et al., 2012) was added to the reaction mixture. In order to evaluate the effect of endogenous metabolites in *S. rochei* and other antibiotics on the binding of SrrB, the following compounds (1 mM) were separately added to the reaction mixture; LC, LM, chlorotetracycline, kanamycin, and ampicillin.

DNase I Footprinting

The method used for DNase I footprinting analysis for the upstream region of *srrY* was described previously (Yamamoto et al., 2008). For the upstream region of *srrB*, the primer SRRBf3 was 5′-end labeled using [γ-^{32}P]ATP (GE Healthcare) and T4 polynucleotide kinase (Toyobo), and then PCR reaction was performed with unlabeled primer SRRBr3 and pKAR3004 as a template to afford a 564-bp product containing the upstream region of *srrB* (positions −81 to +483 from TSS of *srrB*; nt 140,677-141,240 of pSLA2-L). Binding reaction mixture (50 μl) contained 10 nM labeled DNA, 20 mM Tris-HCl (pH8.0), 1 mM $MgCl_2$, 100 mM NaCl, 1 mM dithiothreitol, 0.1 mg/ml BSA, 5% glycerol, and various concentrations of SrrA. The binding reaction mixture was incubated for 30 min at 25°C, and then a mixture was treated with DNase I (Roche Diagnostics) solution [1 ng in 50 μl of 5 mM $MgCl_2$ and 5 mM $CaCl_2$] for 2 minutes at room temperature. The reaction was terminated by 100 μl of phenol-chloroform. The aqueous fraction containing DNAs was precipitated by ethanol and separated on a 5% polyacrylamide gel containing 6 M urea. The labeled DNAs were detected by autoradiography. Sequencing ladders were generated by Maxam-Gilbert sequencing of the labeled DNA used for binding reaction.

Comparative Sequence Analysis

Alignment of Amino acid sequences of the pseudo-receptors including SrrB was performed by BioEdit version 7.2.5 software (https://bioedit.software.informer.com/) (Hall, 1999) (**Figure S1A**). Phylogenetic tree was constructed by the neighbor-joining algorithm of MEGA X version 10.1.5 software (Kumar et al., 2018) (**Figure S1B**).

RESULTS

SrrB Acts as a Negative Regulator for Lankacidin and Lankamycin Production

The gene product of *srrB* belongs to the TetR-type transcriptional regulator family proteins, which contains a helix-turn-helix DNA binding motif at the N-terminal region (**Figure S1**). We previously reported overproduction of LM and LC in the *srrB* mutant KA07 based on TLC bioautography (Arakawa et al., 2007). In this study, we performed comparative metabolite analysis of the *srrB* mutant and its parent strain 51252. As shown in **Figures 2A,B**, the *srrB* mutant KA07 accumulated larger amount of compounds **1**-**6** compared with the parent strain 51252. Namely, KA07 produced 6-folds of lankamycin (**1**) (**Figure 2A**) and 9.9, 25, 4.2, and 5.7-folds of lankacidin C (**2**), lankacidinol A (**4**), iso-lankacidinol (**5**), and lankacidinol (**6**), respectively (**Figure 2B**). To investigate the effect of SrrA on antibiotic production, we further analyzed two mutants, an *srrA* mutant KA12 and an *srrA-srrB* double mutant TS03 (**Figure S2**). KA12 produced about 40% of metabolites when compared with the parent, while TS03 overproduced metabolites **1**-**6** at the same level with the *srrB* mutant KA07 (**Figures 2A,B**). These results confirmed the following two aspects; *srrA* mutation causes a slight decrease of the metabolic titer, whereas SrrB acts as a negative regulator for lankacidin and lankamycin production in *S. rochei*.

To determine the role of *srrB* in the regulation of lankacidin and lankamycin production, we further performed time-course analysis of metabolite profile, growth curve, and transcription in the parent and three mutants (KA07, KA12, and TS03) at various time periods. As shown in **Figure 2C**, all strains grew in a similar proportion, indicating that overproduction in KA07 and TS03 was due to *srrB* mutation but not to cell growth difference. The time-course of antibiotic production was analyzed by the titer of **2**, a major product among lankacidin derivatives (**2**-**6**; **Figure 1A**). As shown in **Figure 2D**, **2** was detected after 18 h, and its titer at 48-h growth in the *srrB* deficient strains, KA07 and TS03, were 9.0- and 7.2-times of 51252, respectively, which agrees with the overproduction profiles in KA07 and TS03 in **Figures 2A,B**. To confirm the negative regulatory property of SrrB *in vivo*, overexpression of SrrB in *S. rochei* was carried out. The intact *srrB* gene was introduced into plasmid pIJ8600, an *E. coli-Streptomyces* shuttle plasmid with a thiostrepton-inducible *tipA* promoter, to give pKAR3065. We tested antibiotic production in the *S. rochei* 51252 recombinants containing either the empty vector pIJ8600 or the *srrB* overexpression plasmid (pKAR3065). Compared with the control recombinant *S. rochei*

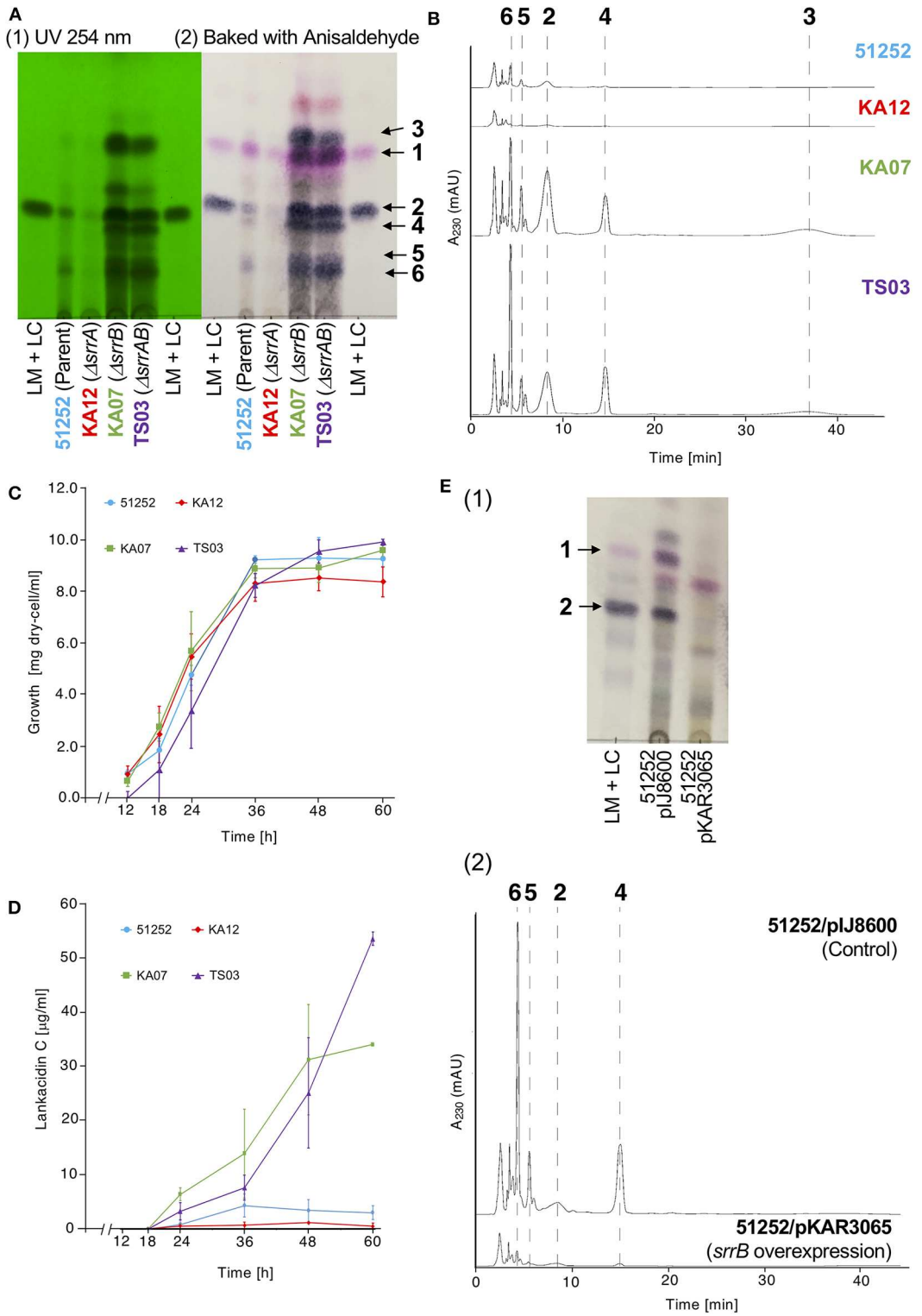

FIGURE 2 | Metabolite profiles and cell growth of four *S. rochei* strains; 51252 (parent), KA12 (Δ*srrA*), KA07 (Δ*srrB*), and TS03 (Δ*srrA-srrB*). **(A)** TLC analysis of the crude extract of *S. rochei* strains. All strains were grown at 28°C for 48 h. The left panel represents the TLC plate under ultraviolet irradiation (254 nm). The right panel represents the TLC plate after baking with anisaldehyde-H_2SO_4. TLC plates were developed with chloroform-methanol = 15:1 (v/v). **(B)** HPLC analysis of metabolites produced by *S. rochei* strains. The crude extracts were applied on a COSMOSIL Cholester column (4.6 × 250 mm, Nacalai Tesque) and eluted with a mixture of acetonitrile-10 mM sodium phosphate buffer (pH 8.2) (3:7, v/v) at a flow rate of 1.0 ml/min. **(C)** Time-course growth of *S. rochei* strains. Symbols represent

(Continued)

FIGURE 2 | each dry cell weight (DCW; g/l); strain 51252, blue circles and line; strain KA12, red diamonds and line; strain KA07, green squares and line; TS03, purple triangles and line. Results are representative of at least three independent experiments. **(D)** Time-course production of **2** in *S. rochei* strains. Symbols represent each production yield of **2** (μg/ml); strain 51252, blue circles and line; strain KA12, red diamonds and line; strain KA07, green squares and line; TS03, purple triangles and line. Results are representative of at least three independent experiments. **(E)** Effect of *srrB* overexpression on antibiotic production. Thiostrepton (10 μg/ml) was added to the 24-h culture of *S. rochei* 51252 recombinants harboring either pIJ8600 (control) or pKAR3065 (intact *srrB*), and then the cultures were further incubated at 28°C for 24 h. (1) TLC analysis of crude extracts. Crude extracts were separated by TLC [eluent; chloroform-methanol = 15:1 (v/v)] and detected by baking with anisaldehyde-H_2SO_4. Lane 1, LM and LC standard; lane 2, recombinant harboring pIJ8600 (control); lane 3, recombinant harboring pKAR3065 (intact *srrB*). (2) HPLC analysis of crude extracts. The crude extracts were applied on a COSMOSIL Cholester column (4.6 x 250 mm, Nacalai Tesque) and eluted with a mixture of acetonitrile-10 mM sodium phosphate buffer (pH 8.2) (3:7, v/v) at a flow rate of 1.0 ml/min.

51252/pIJ8600, the *S. rochei* 51252/pKAR3065 recombinant significantly reduced antibiotic production (**Figure 2E**). These results clearly indicated that SrrB acts as a negative regulator for antibiotic production in *S. rochei*.

In our preliminary experiment, gel shift assay indicated that SrrA and SrrB could bind to the upstream region of *srrX*, a gene responsible for SRB biosynthesis. This finding suggested that the signaling molecule receptor/pseudo-repressor repress the transcription of *srrX*. Two strains were used to evaluate the comparative yield of SRB; an *srrY* single mutant KA61 and an *srrY-srrB* double mutant KA64 (**Figure S3**), both of which are unable to produce LC or LM due to a mutation on the major activator *srrY*. The yields of SRBs were evaluated by a help of bioassay using an *srrX*-deficient mutant as described previously (Arakawa et al., 2012). One-eighth of the crude extract of KA64 contained an equivalent amount of SRBs to that of KA61 (**Figure S4**), suggesting that *srrB* negatively controls the titer of SRBs.

srrB and *srrY* Are Expressed Under the SRB/SrrA Regulatory System, and SrrB Then Represses *srrY* Expression at the Later Stage

To analyze the role of *srrB* in the SRB/SrrA regulatory system in *S. rochei*, we performed comparative transcriptional analysis of the selected regulatory genes in the parent and three mutants (*srrA*, *srrB*, and *srrA-srrB*). Transcription of *srrY* in the parent appeared around 18 h and diminished after 32 h (**Figure 3A**), while that in the *srrB* mutant KA07 continued until the later stage (**Figure 3C**). On the other hand, *srrB* transcription in the parent appeared around 16 h and prolonged until the late stage of fermentation (**Figure 3A**). In the *srrA* mutant KA12, transcription of both *srrY* and *srrB* appeared at 12 h or earlier (**Figure 3B**), whereas *srrY* transcription in the *srrA-srrB* mutant TS03 was detected through all time periods (12–36 h) (**Figure 3D**). These findings together with our previous result (Yamamoto et al., 2008) showed that SRB/*srrA* regulatory system controls transcription of both *srrY* and *srrB*, and SrrB represses *srrY* transcription at the later stage.

SrrA Binds to the Promoter Region of *srrB*

A transcriptional start point (TSS) of *srrB* was determined be 401-bp upstream of its translational start codon by 5′-RACE (**Figure 4** and **Figure S5**). To determine whether SrrA binds to the upstream promoter region of *srrB* (*srrBp*), gel shift assay was performed using ^{32}P-labeled probe B1 (nt 140,677-141,240 of pSLA2-L) that contained the upstream region of *srrB* (**Figure 5A**). SrrA protein was overexpressed in *E. coli* as described previously (Yamamoto et al., 2008). A band shift of probe B1 was observed in the presence of SrrA protein in a concentration-dependent manner (**Figure 5B**). Competition experiments using unlabeled probes B1 and B2 (nt 140,201-140,585 of pSLA2-L) (**Figure 5C**) were performed to determine the specific binding of SrrA to the region of probe B1. A band shift disappeared in the large excess of unlabeled probe B1, whereas probe B2 gave no effect on band shift (**Figure 5C**). Addition of SRB led to dissociation of SrrA from probe B1 (**Figure 5C**), indicating that the *srrB* transcription is controlled by SRB/SrrA regulatory system.

DNase I footprinting experiment was performed to identify the SrrA binding sequence in the upstream of *srrB*. Positions −36 to −11 of the non-template strand was protected by SrrA (**Figure 5D**). The protected region overlapped with a possible *srrB* promoter containing a palindromic sequence (asterisks in **Figure 4B**), whose sequence well-matched with the SrrA-binding sequence of *srrY* (Yamamoto et al., 2008). Taking account of transcriptional analysis above mentioned, SrrA binds to the upstream regions of both *srrB* and *srrY* to repress their transcription at the early growth phase (∼16 h).

SrrB Represses *srrY* Transcription at the Later Stage of Fermentation by Binding to the Promoter Region of *srrY*

To analyze whether SrrB binds to the promoter region of *srrY* (*srrYp*), gel shift assay was performed using probe Y1 (positions −452 to +100 from TSS of *srrY*) (**Figure 6A**) containing the promoter region of *srrY*, which was constructed previously (Yamamoto et al., 2008). SrrB protein was overexpressed in the *E. coli* BL21(DE3)pLysS/pKAR3036 recombinant with IPTG induction and purified by Ni-NTA agarose (**Figure S6**). The addition of SrrB protein gave a shifted band of probe Y1 in a concentration-dependent manner (**Figure 6B**). Competitive experiments (**Figure 6C**) revealed that SrrB specifically binds to probe Y1, not to probe Y2 (positions +101 to +333 from TSS of *srrY*). The pseudoreceptors hitherto studied are insensitive to endogenous signaling molecules and interact with endogenous antibiotics (Martín and Liras, 2019; Xu and Yang, 2019) (details are described in Discussion Section). We tested the effects of various signaling-molecule/antibiotics on the binding of SrrB to *srrYp* through gel shift analysis by using endogenous signaling molecule SRB, endogenous antibiotics (LC and LM),

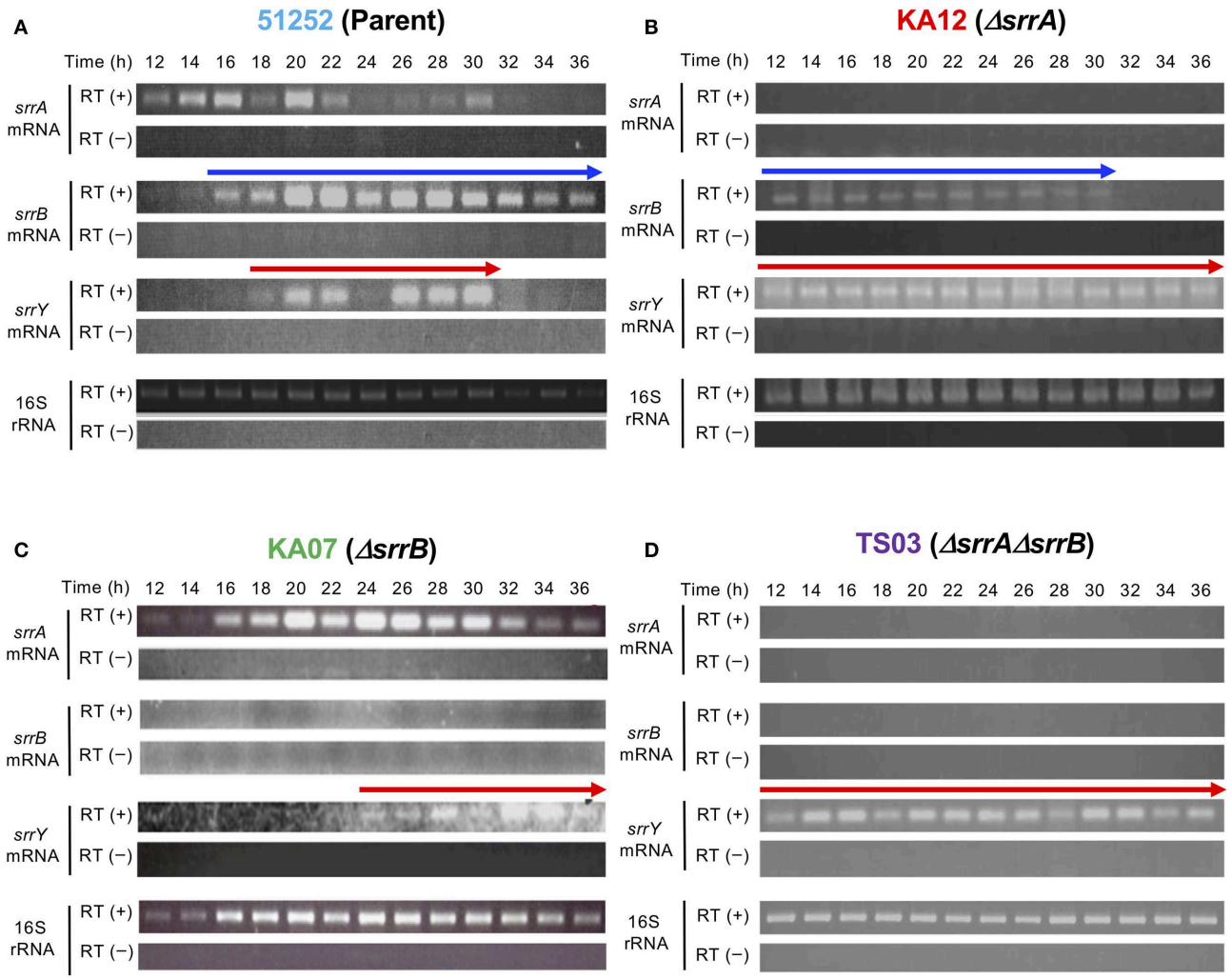

FIGURE 3 | Time-course RT-PCR analysis of strains 51252 **(A)**, KA12 **(B)**, KA07 **(C)**, and TS03 **(D)**. Three upper panels represent *srrA* mRNA, *srrB* mRNA, and *srrY* mRNA. The lowest panels represents 16S rRNA gene as a control. RT (+) indicates the treatment of total RNA with Transcriptor Reverse Transcriptase, while RT (–) dues no treatment of transcriptase. Red arrow indicates transcription of *srrY*, while blue arrow does transcription of *srrB*.

and other exogenous antibiotics (**Figures 6D,E**). Dissociation of SrrB from *srrYp* could be caused by SRB, however, a higher concentration of 1 mM was required (500-fold excess against SrrB protein). The sensitivity of SrrB against SRB was 50-fold lower compared with the signaling molecule receptor SrrA (**Figure 6D**). Dissociation of SrrB from *srrYp* was not caused by endogenous antibiotics LC and LM in *S. rochei* and neither by exogenous antibiotics (chlorotetracycline, kanamycin, ampicillin) at even 1 mM concentration (500-fold excess against SrrB protein) (**Figure 6E**).

We further performed DNase I footprinting experiment to identify the SrrB binding sequence in the upstream of *srrY*. As shown in **Figure 6F**, positions −61 to −4 of non-template strand were protected by SrrB. Although SrrB covers larger upstream region (58 bp) than SrrA does (28 bp; blue letters in **Figure 6F**), both SrrA and SrrB could bind to the promoter region of *srrY* (**Figure 4B**).

DISCUSSION

In this study, we revealed that *srrB* acts as a negative regulator by binding to the promoter region of the target gene *srrY* to repress LC and LM production in *S. rochei*. Expression of *srrB* is controlled by SRB/SrrA regulatory system.

TetR-type receptors have a conserved DNA-binding helix-turn-helix motif in the N-terminus and a ligand-binding pocket in the C-terminus (Yu et al., 2010). Particularly, the signaling molecule receptors and the pseudo-receptors constitute one of a major class of TetR-type regulators (**Figure S1**). The signaling molecule receptors have a helix-turn-helix DNA-binding motif in the N-terminus and a ligand-binding Trp residue in the C-terminus. It is noteworthy that the signaling molecule synthase and its cognate receptor gene pairs usually locate adjacently on the genome (Biarnes-Carrera et al., 2015), which allows us to predict signaling molecule/receptor systems

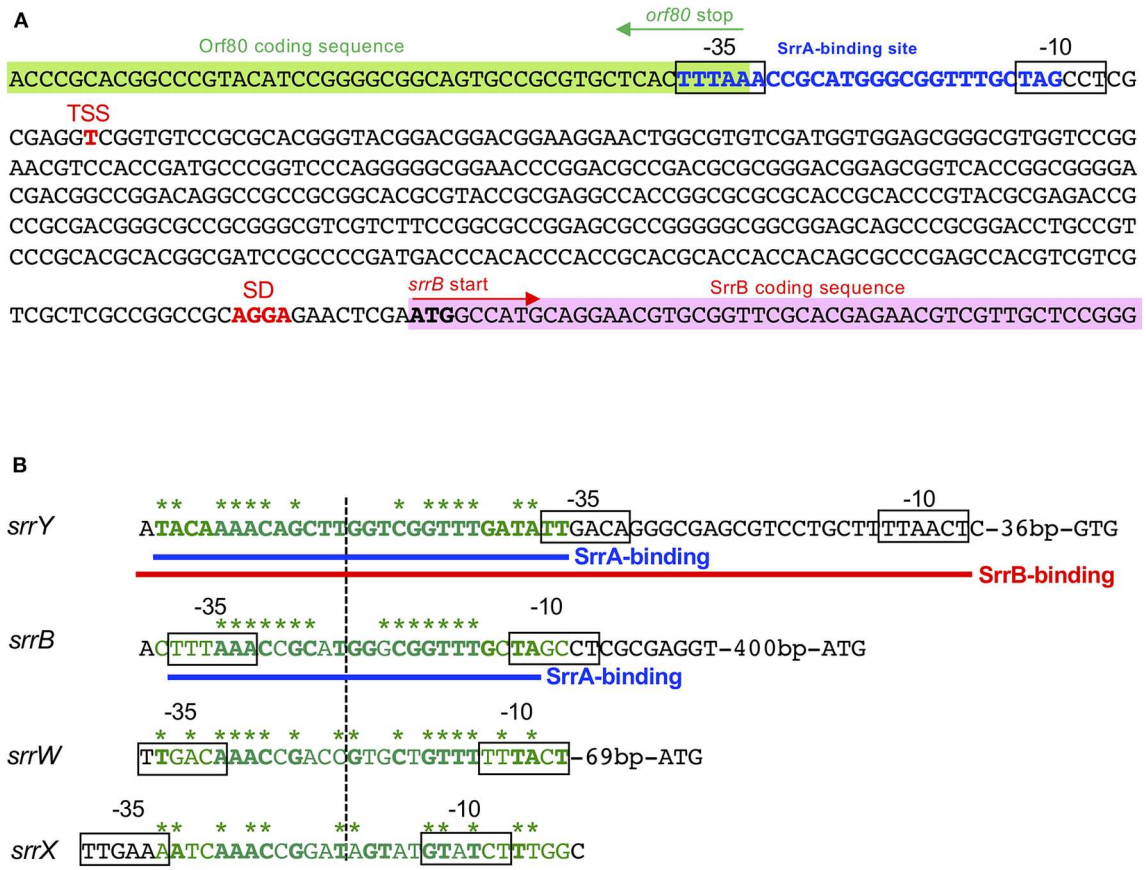

FIGURE 4 | SrrA/SrrB binding sequences. **(A)** Characterization of the upstream region of *srrB*. Putative *srrB* promoter regions (−35 and −10) are boxed. Shine-Dalgarno (SD) sequence and transcriptional start site (TSS) are shown as red boldface letters. SrrA-binding sequence is shown as blue boldface letters. Pink and green highlights indicate SrrB and Orf80 coding sequences, respectively. **(B)** Comparison of the binding sequences for SrrA and SrrB. The confirmed SrrA- and SrrB-binding sequences are shown as blue and red underlines, respectively. Possible SrrA-binding sites at upstream of *srrW* and *srrX* are deduced from sequence data. For comparison of consensus sequence, SrrA-binding sites at the upstream of *srrY* (SrrA-*srrY*) are shown as green. Bases identical with SrrA-*srrY* are shown in boldface letters. Complementary bases are indicated as asterisks. The center of palindromes is shown as a vertical dashed line.

in *Streptomyces* species (Niu et al., 2016). On the other hand, the pseudo-receptors also have a conserved DNA-binding motif like the signaling molecule receptors (**Figure S1A**), however, their location has no relationship with the signaling molecule synthase genes. Many of them act as negative regulators for antibiotic production; for example, TylQ for tylosin production in *Streptomyces fradiae* (Stratigopoulos and Cundliffe, 2002), BarB for virginiamycin in *Streptomyces virginiae* (Matsuno et al., 2004), ScbR2 for coelimycin P-1 in *Streptomyces coelicolor* (Gottelt et al., 2010), AlpW for orange pigment kinamycin in *Streptomyces ambofaciens* (Bunet et al., 2008), and AvaR2 for avermectin in *Streptomyces avermitilis* (Zhu et al., 2016) (**Table 1**).

In general, the pseudo-receptors are insensitive to endogenous signaling molecules. BarB has no binding affinity to virginia butanolides in *S. virginiae* (Matsuno et al., 2004). Surprisingly, ScbR2 from *S. coelicolor* does not bind to the signaling molecules SCB1-3 but binds to two endogenous antibiotics, actinorhodin and undecylprodigiosin (Xu et al., 2010), and exogenous antibiotic jadomycin (Wang W., 2014). In *S. venezuelae*, JadR2 binds to endogenous jadomycin and chloramphenicol as ligands, (Xu et al., 2010). Thus, ScbR2 and JadR2 bind to multiple antibiotics, and coordinate their biosynthesis (Xu et al., 2010; Zou et al., 2014). In *S. avermitilis*; AvaR2 binds to the endogenous signaling molecule avenolide, but not to oligomycin and avermectin (Zhu et al., 2016). Its mutational analysis revealed that AvaR2 plays a negative regulatory role in avermectin production and cell growth (Zhu et al., 2016). In *S. rochei*, SrrB-*srrYp* complex was disrupted by endogenous signaling molecule SRB at 1 mM concentration, although its minimum dissociation concentration for SrrB was 50-fold higher than that for SrrA, the SRB receptor. SrrB showed no binding activity to endogenous polyketide antibiotics LM or LC in *S. rochei* and neither to exogenous antibiotics including aromatic polyketide chlorotetracycline, aminoglycoside antibiotic kanamycin, and β-lactam antibiotic ampicillin even at 1 mM concentration (500-fold excess against SrrB). Thus, functions of the pseudo-receptors are variable in *Streptomyces* species.

The possible regulatory pathway in *S. rochei* is shown in **Figure 7**. At the early growth phase, SrrA represses transcription

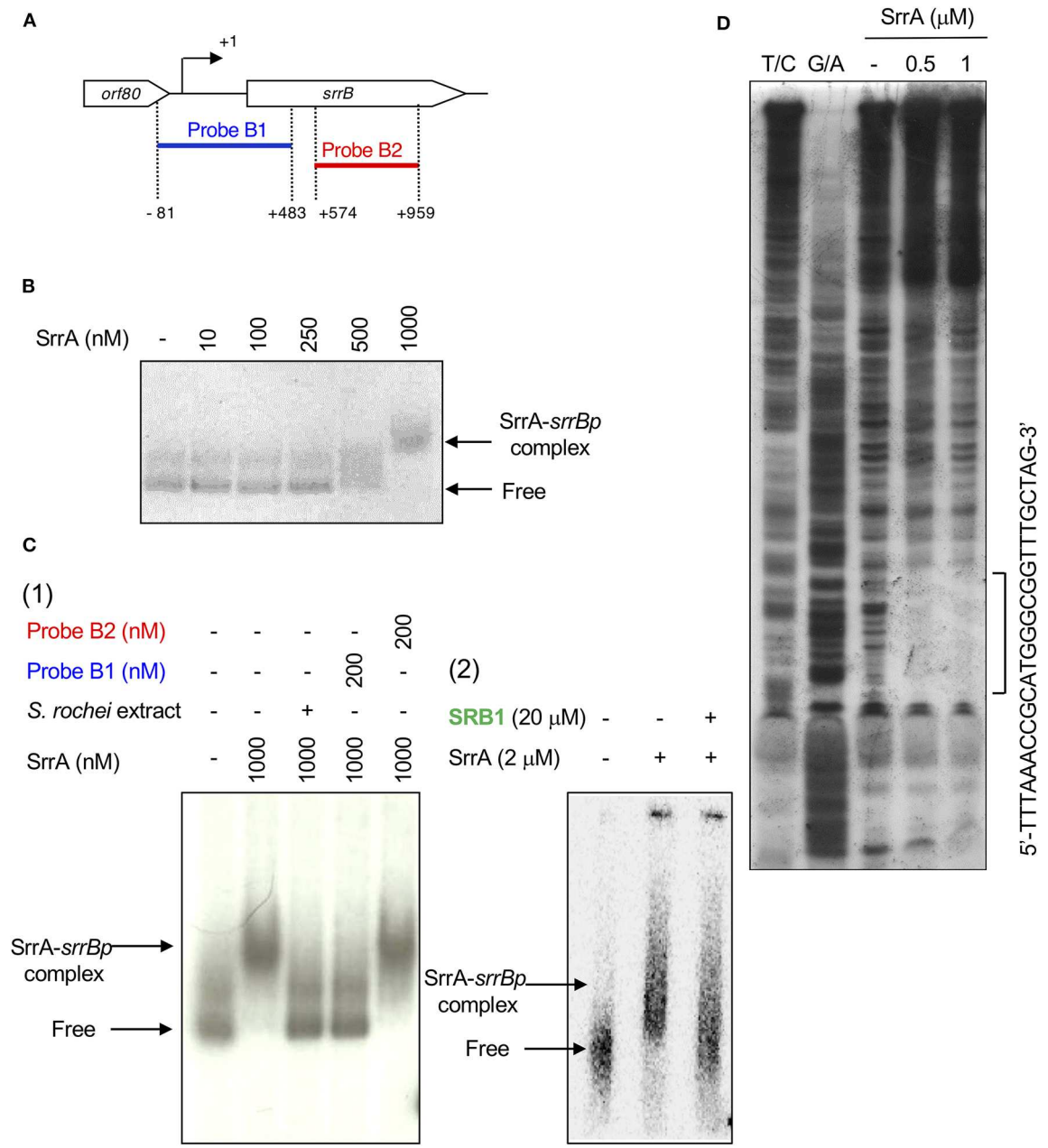

FIGURE 5 | Gel shift assay and DNase I footprinting analysis of SrrA-binding in the upstream region of *srrB*. **(A)** Location of the two probes B1 and B2. The TSS of *srrB* is numbered +1. **(B)** The concentration-dependent binding of SrrA to the upstream promoter region of *srrB* (*srrBp*). The ^{32}P-labeled probe B1 (1 nM) was mixed with various concentration of SrrA (0–1,000 nM). **(C)** (1) Competition experiments to investigate specific binding of SrrA to the upstream region of *srrB*. Each reaction mixture contained 0.5 nM ^{32}P-labeled probe B1 (lane 1) and 1,000 nM SrrA (lane 2). Then, *S. rochei* culture extract (lane 3), 200 nM unlabeled probe B1 (lane 4) or unlabeled probe B2 (lane 5) was added. (2) Effect of endogenous SRB to investigate specific binding of SrrA to the upstream region of *srrB*. Each reaction mixture contained 0.5 nM ^{32}P-labeled probe B1 (lane 1) and 2,000 nM SrrA (lane 2). Then, 20 μM synthetic SRB1 [(1′*R*)-isomer; **Figure 1B**] (Arakawa et al., 2012) (lane 3) was added. **(D)** DNase I footprinting analysis of SrrA-binding site on the upstream of *srrB*. Probe B1 was end labeled on the non-template strand. Each reaction mixture contained 2 nM labeled DNA and SrrA (0.5 and 1 μM). Sequencing ladders were generated by Maxam-Gilbert sequencing of the labeled probe B1. Capital letters at right side indicate SrrA-binding sequences.

of both *srrY* and *srrB* (panel A). When SRB reaches a critical concentration, SrrA-SRB complex dissociates from both promoter regions to induce expression of *srrY* and *srrB* (panel B). Then SrrB represses *srrY* transcription at the later stage fermentation (panel C), suggesting a transient expression of *srrY* by two receptor proteins SrrA and SrrB in *S. rochei*. A similar regulatory pathway was proposed for kinamycin production in *S. ambofaciens* (Bunet et al., 2008) although

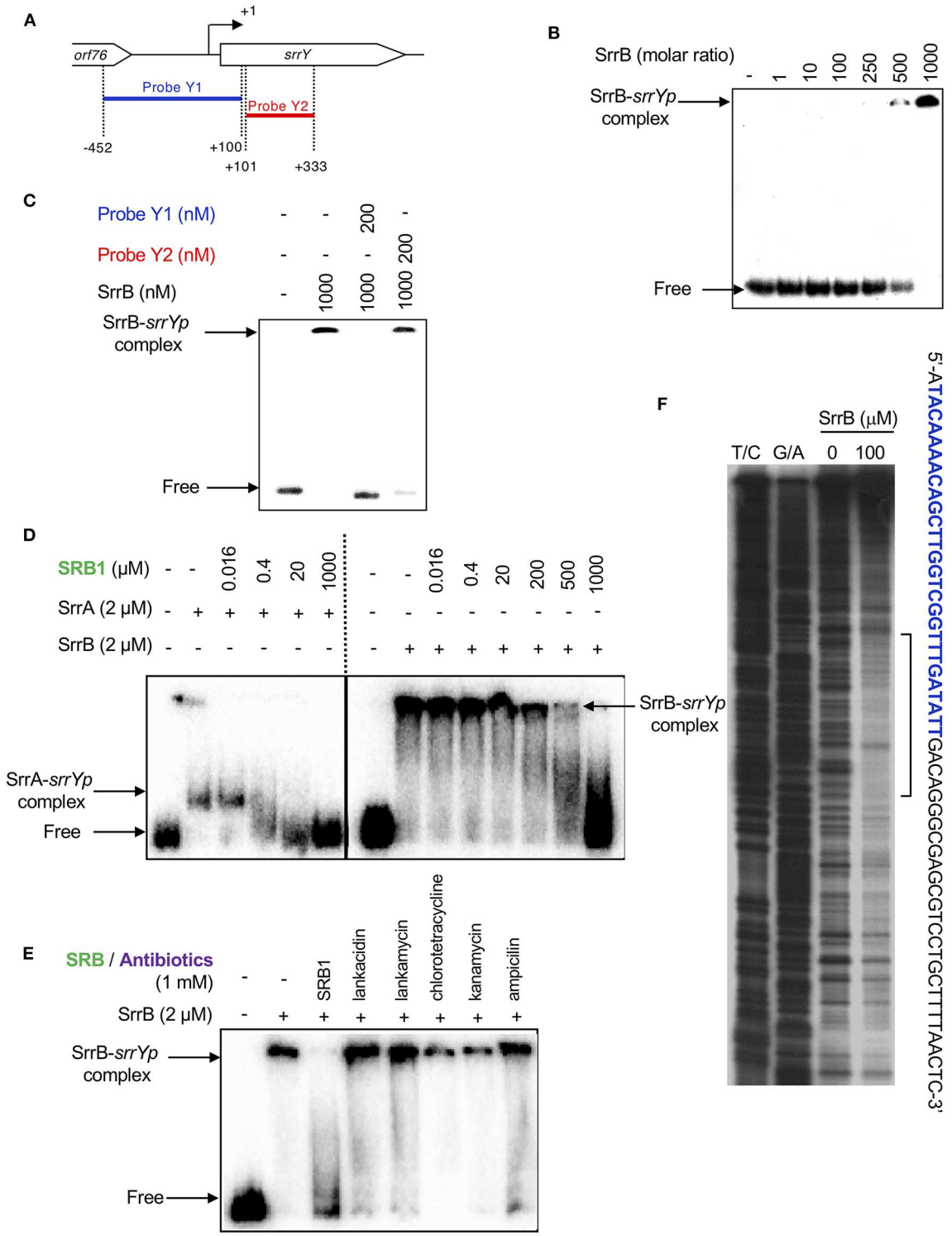

FIGURE 6 | Gel shift assay and DNase I footprinting analysis of SrrB-binding in the upstream region of *srrY*. **(A)** Location of the two probes, probe Y1 and Y2. The description of probe preparation was described previously (Yamamoto et al., 2008). **(B)** The concentration-dependent binding of SrrB to the upstream promoter region of *srrY* (*srrYp*). Labeled probe Y1 (1 nM) was mixed with various concentration of SrrB (0–1,000 nM). **(C)** Competition experiments to investigate specific binding of SrrB to the upstream region of *srrY*. Each reaction mixture contained 1 nM ^{32}P-labeled probe Y1 and 1,000 nM SrrB. Then, 200 nM unlabeled probe Y1 (lane 3) or unlabeled probe Y2 (lane 4) was added. **(D)** Effect of SRB1 on the binding of SrrA (Right panel) and SrrB (left panel). Each reaction mixture contained 0.5 nM probe Y1 and 2,000 nM recombinant protein. To the reaction mixture, various concentration of synthetic SRB1 [(1′*R*)-isomer; **Figure 1B**) (Arakawa et al., 2012) was added.

(Continued)

FIGURE 6 | (E) Effect of endogenous metabolites in *S. rochei* and other antibiotics on the binding of SrrB. To the same reaction mixture described for panel D, various compounds including SRB1, LC, LM, chlorotetracycline, kanamycin, and ampicillin (each 1 mM) were separately added. **(F)** DNase I footprint analysis of SrrB-binding site on the upstream of *srrY*. Probe Y1 was end labeled on the non-template strand. Each reaction mixture contained 2 nM labeled DNA and SrrB (100 nM). Sequencing ladders were generated by Maxam-Gilbert sequencing of the labeled probe Y1. Capital letters at right side indicate SrrB-binding sequences, among which blue letters indicate SrrA-binding sequences.

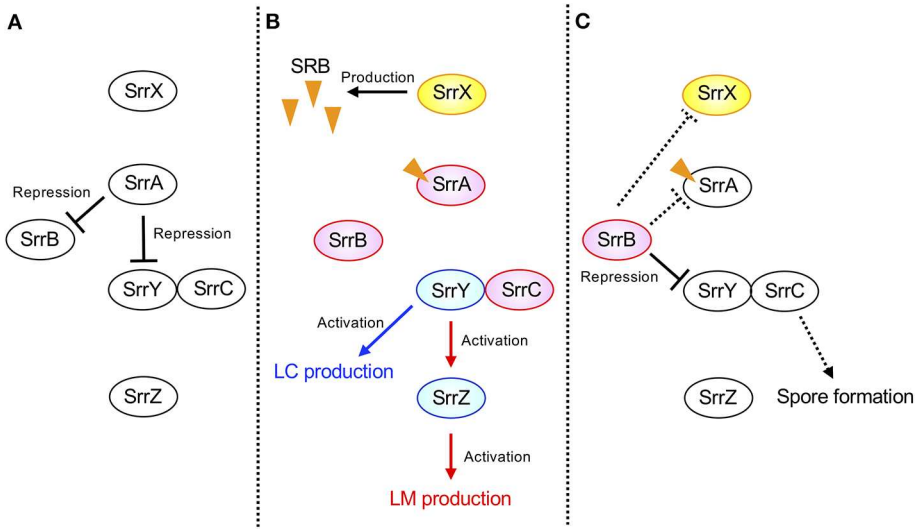

FIGURE 7 | Model of transient *srrY* expression for LM and LC production in *S. rochei.* **(A)** SrrA represses both *srrY* and *srrB* expression in the early stage of growth. **(B)** Dissociation of SrrA from the promoter region of both *srrY* and *srrB* by SRB in middle stage of growth. **(C)** Repression of *srrY* by SrrB in the late stage of growth. Solid lines indicate the confirmed regulatory pathway hitherto. Additional dashed lines were suggested by unpublished results. Orange triangles indicate the signaling molecules SRBs.

its ligand has not yet been identified. In the early stage of growth, the signaling molecule receptor AlpZ represses both transcription of *alpV* (an SARP-type activator gene) and *alpW* (a pseudo-receptor gene). When an unidentified ligand interacts with AlpZ, this protein dissociates from the promoter regions in both *alpV* and *alpW*, leading to kinamycin production. At the later stage of fermentation, AlpW represses *alpV* transcription again to cease kinamycin production. Another interesting features in the *S. rochei* regulatory pathway is the presence of *srrY-srrC* cistron (**Figure 7**). The *srrC* mutant showed no sporulation, suggesting that *srrC* acts as a positive regulator for morphological differentiation (Arakawa et al., 2007). As shown in **Figure 7**, *srrB* negatively regulates the transcription of both *srrY* and *srrC*, which leads to transient controls for antibiotic production and morphological differentiation, respectively.

The *srrB* mutation increased the titers of antibiotics as well as SRBs. This result well agreed with our preliminary gel shift assay that both SrrA and SrrB bind to the upstream region of SRB biosynthesis gene *srrX* (data not shown). Large excess of SRBs has no effect on antibiotic overexpression in *S. rochei* (Arakawa et al., 2012), hence, exact mechanism of the *srrX* repression by SrrB at the later stage remains to be clarified.

Manipulation of regulatory genes often causes activation of "silent" secondary metabolites (Olano et al., 2008; Zerikly and Challis, 2009; Rutledge and Challis, 2015; Arakawa, 2018). In *S. ambofaciens*, a mutant of the pseudo-receptor gene *alpW* accumulated kinamycin (Bunet et al., 2011). A mutant of the repressor gene *ksbC* accumulated β-carboline compound kitasetaline in *Kitasatospora setae* (Aroonsri et al., 2012). To our surprise, azoxyalkene compound KA57-A accumulated in a triple knockout mutant of *S. rochei* that have mutations on two biosynthetic gene clusters for LC, LM, and *srrB* (Kunitake et al., 2015). The genome sequence of the *S. rochei* chromosome has been determined to be 8.36 Mb in size, and at least 35 secondary metabolites gene clusters are coded on the chromosome (Nindita et al., 2019). Comprehensive mutational analysis on various regulatory genes may lead to activate silent secondary metabolite gene clusters in *S. rochei*, which is in progress in our laboratory. In conclusion, we have extensively characterized the role of the pseudo-receptor SrrB for antibiotic production in *S. rochei*. Further understanding and manipulation of the regulatory system in *Streptomyces* will lead to a natural product discovery with notable biological activities.

DATA AVAILABILITY STATEMENT

The datasets generated for this study are available on request to the corresponding author.

AUTHOR CONTRIBUTIONS

YM, SY, TS, HK, and KA designed the experiments. YM, SY, TS, MI, HS, YT, KI, and KA performed the experiments. YM, SY, TS, MI, HS, and KA analyzed the data. YM, SY, TS, HK, and KA wrote the manuscript with input from all of the authors. All authors approved the final version of the manuscript.

FUNDING

This work was supported by Grants-in-Aid for Scientific Research on Innovative Areas (23108515, 25108718, 17H05446, and 19H04659 to KA) from Ministry of Education, Culture, Sports, Science and Technology of Japan (MEXT), Grants-in-Aid for Scientific Research (B) (16H04917 to KA) from the Japan Society for the Promotion of Science (JSPS), and JSPS A3 Foresight Program.

ACKNOWLEDGMENTS

We would like to thank Dr. D. Kajiya and Mrs. T. Amimoto (N-BARD, Hiroshima University) for measurement of the high resolution mass spectra.

SUPPLEMENTARY MATERIAL

The Supplementary Material for this article can be found online at: https://www.frontiersin.org/articles/10.3389/fmicb.2020.01089/full#supplementary-material

REFERENCES

Aigle, B., Pang, X., Decaris, B., and Leblond, P. (2005). Involvement of AlpV, a new member of the Streptomyces antibiotic regulatory protein family, in regulation of the duplicated type II polyketide synthase alp gene cluster in Streptomyces ambofaciens. *J. Bacteriol.* 187, 2491–2500. doi: 10.1128/JB.187.7.2491-2500.2005

Arakawa, K. (2018). Manipulation of metabolic pathways controlled by signaling molecules, inducers of antibiotic production, for genome mining in Streptomyces spp. *Antonie. Leeuwen.* 111, 743–751. doi: 10.1007/s10482-018-1052-6

Arakawa, K., Cao, Z., Suzuki, N., and Kinashi, H. (2011). Isolation, structural elucidation, and biosynthesis of 15-norlankamycin derivatives produced by a type-II thioesterase disruptant of Streptomyces rochei. *Tetrahedron* 67, 5199–5205doi: 10.1016/j.tet.2011.05.047

Arakawa, K., Mochizuki, S., Yamada, K., Noma, T., and Kinashi, H. (2007). γ-Butyrolactone autoregulator-receptor system involved in lankacidin and lankamycin production and morphological differentiation in Streptomyces rochei. *Microbiology* 153, 1817–1827. doi: 10.1099/mic.0.2006/002170-0

Arakawa, K., Tsuda, N., Taniguchi, A., and Kinashi, H. (2012). The butenolide signaling molecules SRB1 and SRB2 induce lankacidin and lankamycin production in Streptomyces rochei. *ChemBioChem* 13, 1447–1457. doi: 10.1002/cbic.201200149

Aroonsri, A., Kitani, S., Hashimoto, J., Kosone, I., Izumikawa, M., Komatsu, M., et al. (2012). Pleiotropic control of secondary metabolism and morphological development by KsbC, a butyrolactone autoregulator receptor homologue in Kitasatospora setae. *Appl. Environ. Microbiol.* 78, 8015–8024. doi: 10.1128/AEM.02355-12

Bate, N., Butler, A. R., Gandecha, A. R., and Cundliffe, E. (1999). Multiple regulatory genes in the tylosin biosynthetic cluster of Streptomyces fradiae. *Chem. Biol.* 6, 617–624. doi: 10.1016/S1074-5521(99)80113-6

Bate, N., Stratigopoulos, G., and Cundliffe, E. (2002). Differential roles of two SARP-encoding regulatory genes during tylosin biosynthesis. *Mol. Microbiol.* 43, 449–458. doi: 10.1046/j.1365-2958.2002.02756.x

Biarnes-Carrera, M., Breitling, R., and Takano, E. (2015). Butyrolactone signaling circuits for synthetic biology. *Curr. Opin. Chem. Biol.* 28, 91–98. doi: 10.1016/j.cbpa.2015.06.024

Bibb, M. J. (2005). Regulation of secondary metabolism in streptomycetes. *Curr. Opin. Microbiol.* 8, 208–215. doi: 10.1016/j.mib.2005.02.016

Bunet, R., Mendes, M. V., Rouhier, N., Pang, X., Hotel, L., Leblond, P., et al. (2008). Regulation of the synthesis of the angucyclinone antibiotic alpomycin in Streptomyces ambofaciens by the autoregulator receptor AlpZ and its specific ligand. *J. Bacteriol.* 190, 3293–3305. doi: 10.1128/JB.01989-07

Bunet, R., Song, L., Mendes, M. V., Corre, C., Hotel, L., Rouhier, N., et al. (2011). Characterization and manipulation of the pathway-specific late regulator AlpW reveals Streptomyces ambofaciens as a new producer of kinamycins. *J. Bacteriol.* 193, 1142–1153. doi: 10.1128/JB.01269-10

Gottelt, M., Kol, S., Gomez-Escribano, J. P., Bibb, M., and Takano, E. (2010). Deletion of a regulatory gene within the cpk gene cluster reveals novel antibacterial activity in Streptomyces coelicolor A3(2). *Microbiology* 156, 2343–2353. doi: 10.1099/mic.0.038281-0

Hall, T. A. (1999). BioEdit: a user-friendly biological sequence alignment editor and analysis program for Windows 95/98/NT. Nucl. Acids. Symp. *Ser.* 41, 95–98.

Hara, O., and Beppu, T. (1982). Mutants blocked in streptomycin production in streptomyces griseus - The role of A-factor. *J. Antibiot.* 35, 349–358. doi: 10.7164/antibiotics.35.349

Horinouchi, S., and Beppu, T. (2007). Hormonal control by A-factor of morphological development and secondary metabolism in streptomyces. *Proc. Jpn. Acad. Ser. B Phys. Biol. Sci.* 83, 277–295. doi: 10.2183/pjab.83.277

Hsiao, N. H., Nakayama, S., Merlo, M. E., de Vries, M., Bunet, R., Kitani, S., et al. (2009). Analysis of two additional signaling molecules in streptomyces coelicolor and the development of a butyrolactone-specific reporter system. *Chem. Biol.* 16, 951–960. doi: 10.1016/j.chembiol.2009.08.010

Ishikawa, J., Niino, Y., and, Hotta, K. (1996). Construction of pRES18 and pRES19, streptomyces-escherichia coli shuttle vectors carrying multiple cloning sites. *FEMS Microbiol. Lett.* 145, 113–116. doi: 10.1016/0378-1097(96)00397-7

Kawauchi, R., Akashi, T., Kamitani, Y., Sy, A., Wangchaisoonthorn, U., Nihira, T., et al. (2000). Identification of an AfsA homologue (BarX) from streptomyces virginiae as a pleiotropic regulator controlling autoregulator biosynthesis, virginiamycin biosynthesis and virginiamycin M1 resistance. *Mol. Microbiol.* 36, 302–313. doi: 10.1046/j.1365-2958.2000.01819.x

Kieser, T., Bibb, M. J., Buttner, M. J., Chater, K. F., and Hopwood, D. A. (2000). *Practical Streptomyces Genetic: A Laboratory Manual*. Norwich: John Innes Foundation.

Kinashi, H., Mori, E., Hatani, A., and Nimi, O. (1994). Isolation and characterization of large linear plasmids from lankacidin-producing Streptomyces species. *J. Antibiot.* 47, 1447–1455. doi: 10.7164/antibiotics.47.1447

Kinoshita, H., Ipposhi, H., Okamoto, S., Nakano, H., Nihira, T., and Yamada, Y. (1997). Butyrolactone autoregulator receptor protein (BarA) as a transcriptional regulator in Streptomyces virginiae. *J. Bacteriol.* 179, 6986–6993. doi: 10.1128/JB.179.22.6986-6993.1997

Kitani, S., Miyamoto, K. T., Takamatsu, S., Herawati, E., Iguchi, H., Nishitomi, K., et al. (2011). Avenolide, a Streptomyces hormone controlling antibiotic production in streptomyces avermitilis. *Proc.*

Natl. Acad. Sci. U.S.A. 108, 16410–16415. doi: 10.1073/pnas.1113908108

Kondo, K., Higuchi, Y., Sakuda, S., Nihira, T., and Yamada, Y. (1989). New virginiae butanolides from *Streptomyces virginiae*. *J. Antibiot.* 42, 1873–1876. doi: 10.7164/antibiotics.42.1873

Kumar, S., Stecher, G., Li, M., Knyaz, C., and Tamura, K. (2018). MEGA X: molecular evolutionary genetics analysis across computing platforms. *Mol. Biol. Evol.* 35, 1547–1549. doi: 10.1093/molbev/msy096

Kunitake, H., Hiramatsu, T., Kinashi, H., and Arakawa, K. (2015). Isolation and biosynthesis of an azoxyalkene compound produced by a multiple gene disruptant of streptomyces rochei. *ChemBioChem* 16, 2237–2243. doi: 10.1002/cbic.201500393

Lane, D. J. (1991). "16S/23S rRNA sequencing," in *Nucleic Acid Techniques in Bacterial Systematics*, eds E. Stackebrandt and M. Goodfellow (New York, NY: John Wiley and Sons), 115–175.

Li, X., Wang, J., Li, S., Ji, J., Wang, W., and Yang, K. (2015). ScbR- and ScbR2-mediated signal transduction networks coordinate complex physiological responses in Streptomyces coelicolor. *Sci. Rep.* 5:14831. doi: 10.1038/srep14831

Martín, J. F., and Liras, P. (2019). Harnessing microbiota interactions to produce bioactive metabolites: communication signals and receptor proteins. *Curr, Opin. Pharmacol.* 48, 8–16. doi: 10.1016/j.coph.2019.02.014

Matsuno, K., Yamada, Y., Lee, C. K., and Nihira, T. (2004). Identification by gene deletion analysis of barB as a negative regulator controlling an early process of virginiamycin biosynthesis in Streptomyces virginiae. *Arch. Microbiol.* 181, 52–59. doi: 10.1007/s00203-003-0625-5

Mochizuki, S., Hiratsu, K., Suwa, M., Ishii, T., Sugino, F., Yamada, K., et al. (2003). The large linear plasmid pSLA2-L of Streptomyces rochei has an unusually condensed gene organization for secondary metabolism. *Mol. Microbiol.* 48, 1501–1510. doi: 10.1046/j.1365-2958.2003.03523.x

Nindita, Y., Cao, Z., Fauzi, A. A., Teshima, A., Misaki, Y., Muslimin, R., et al. (2019). The genome sequence of Streptomyces rochei 7434AN4, which carries a linear chromosome and three characteristic linear plasmids. *Sci. Rep.* 9:10973. doi: 10.1038/s41598-019-47406-y

Niu, G., Chater, K. F., Tian, Y., Zhang, J., and Tan, H. (2016). Specialized metabolites regulating antibiotic biosynthesis in streptomyces spp. *FEMS Microbiol. Rev.* 40, 554–573. doi: 10.1093/femsre/fuw012

Ohnishi, Y., Kameyama, S., Onaka, H., and Horinouchi, S. (1999). The A-factor regulatory cascade leading to streptomycin production in streptomyces griseus: identification of a target gene of the A-factor receptor. *Mol. Microbiol.* 34, 102–111. doi: 10.1046/j.1365-2958.1999.01579.x

Ohnishi, Y., Yamazaki, H., Kato, J. Y., Tomono, A., and Horinouchi, S. (2005). AdpA, a central transcriptional regulator in the A-factor regulatory cascade that leads to morphological development and secondary metabolism in Streptomyces griseus. *Biosci. Biotechnol. Biochem.* 69, 431–439. doi: 10.1271/bbb.69.431

Olano, C., Lomb,ó, F., Méndez, C., and Salas, J. A. (2008). Improving production of bioactive secondary metabolites in actinomycetes by metabolic engineering. *Metab. Eng.* 10, 281–292. doi: 10.1016/j.ymben.2008.07.001

Onaka, H., Ando, N., Nihira, T., Yamada, Y., Beppu, T., and Horinouchi, S. (1995). Cloning and characterization of the A-factor receptor gene from Streptomyces griseus. *J. Bacteriol.* 177, 6083–6092. doi: 10.1128/JB.177.21.6083-6092.1995

Rutledge, P. J., and Challis, G. L. (2015). Discovery of microbial natural products by activation of silent biosynthetic gene clusters. *Nat. Rev. Microbiol.* 13, 509–523. doi: 10.1038/nrmicro3496

Sambrook, J., Fritsch, E. F., and Maniatis, T. (1989). *Molecular Cloning: A Laboratory Manual*. Cold Spring Harbor, NY: Cold Spring Harbor Laboratory Press.

Stratigopoulos, G., and Cundliffe, E. (2002). Expression analysis of the tylosin-biosynthetic gene cluster: pivotal regulatory role of the tylQ product. *Chem. Biol.* 9, 71–78. doi: 10.1016/S1074-5521(01)00095-3

Sun, J., Kelemen, G. H., Fernandez-Abalos, J. M., and Bibb, M. J. (1999). Green fluorescent protein as a reporter for spatial and temporal gene expression in Streptomyces coelicolor A3(2). *Microbiology* 145, 2221–2227. doi: 10.1099/00221287-145-9-2221

Suzuki, T., Mochizuki, S., Yamamoto, S., Arakawa, K., and Kinashi, H. (2010). Regulation of lankamycin biosynthesis in streptomyces rochei by two SARP genes, srrY and srrZ. *Biosci. Biotechnol. Biochem.* 74, 819–827. doi: 10.1271/bbb.90927

Takano, E. (2006). γ-Butyrolactones: Streptomyces signaling molecules regulating antibiotic production and differentiation. *Curr. Opin. Microbiol.* 9, 287–294. doi: 10.1016/j.mib.2006.04.003

Takano, E., Chakaraburtty, R., Nihira, T., Yamada, Y., and Bibb, M. J. (2001). A complex role for the γ-butyrolactone SCB1 in regulating antibiotic production in streptomyces coelicolor A3(2). *Mol. Microbiol.* 41, 1015–1028. doi: 10.1046/j.1365-2958.2001.02562.x

Takano, E., Kinoshita, H., Mersinias, V., Bucca, G., Hotchkiss, G., Nihira, T., et al. (2005). A bacterial hormone (the SCB1) directly controls the expression of a pathway-specific regulatory gene in the cryptic type I polyketide biosynthetic gene cluster of Streptomyces coelicolor. *Mol. Microbiol.* 56, 465–479. doi: 10.1111/j.1365-2958.2005.04543.x

Turner, S., Pryer, K. M., Miao, V. P., and Palmer, J. D. (1999). Investigating deep phylogenetic relationships among cyanobacteria and plastids by small subunit rRNA sequence analysis. *J. Eukaryot. Microbiol.* 46, 327–338. doi: 10.1111/j.1550-7408.1999.tb04612.x

Wang, J., Wang, W., Wang, L., Zhang, G., Fan, K., Tan, H., et al. (2011). A novel role of 'pseudo' γ-butyrolactone receptors in controlling γ-butyrolactone biosynthesis in streptomyces. *Mol. Microbiol.* 82, 236–250. doi: 10.1111/j.1365-2958.2011.07811.x

Wang, J. B., Zhang, F., Pu, J. Y., Zhao, J., Zhao, Q. F., and Tang, G. L. (2014). Characterization of AvaR1, an autoregulator receptor that negatively controls avermectins production in a high avermectin-producing strain. *Biotechnol. Lett.* 36, 813–819. doi: 10.1007/s10529-013-1416-y

Wang, L., Tian, X., Wang, J., Yang, H., Fan, K., Xu, G., et al. (2009). Autoregulation of antibiotic biosynthesis by binding of the end product to an atypical response regulator. *Proc. Natl. Acad. Sci. U.S.A.* 106, 8617–8622. doi: 10.1073/pnas.0900592106

Wang, L., and Vining, L. C. (2003). Control of growth, secondary metabolism and sporulation in Streptomyces venezuelae ISP5230 by jadW1, a member of the afsA family of γ-butyrolactone regulatory genes. *Microbiology* 149, 1991–2004. doi: 10.1099/mic.0.26209-0

Wang, W., Ji, J., Li, X., Wang, J., Li, S., Pan, G., et al. (2014). Angucyclines as signals modulate the behaviors of Streptomyces coelicolor. *Proc. Natl. Acad. Sci. U.S.A.* 111, 5688-5693. doi: 10.1073/pnas.1324253111

Xu, G., Wang, J., Wang, L., Tian, X., Yang, H., Fan, K., et al. (2010). "Pseudo" γ-butyrolactone receptors respond to antibiotic signals to coordinate antibiotic biosynthesis. *J. Biol. Chem.* 285, 27440–27448. doi: 10.1074/jbc.M110.143081

Xu, G., and Yang, S. (2019). Regulatory and evolutionary roles of pseudo γ-butyrolactone receptors in antibiotic biosynthesis and resistance. *Appl. Microbiol. Biotechnol.* 103, 9373–9378. doi: 10.1007/s00253-019-10219-0

Yamamoto, S., He, Y., Arakawa, K., and Kinashi, H. (2008). γ-Butyrolactone-dependent expression of the SARP gene srrY plays a central role in the regulatory cascade leading to lankacidin and lankamycin production in Streptomyces rochei. *J. Bacteriol.* 190, 1308–1316. doi: 10.1128/JB.01383-07

Yamauchi, Y., Nindita, Y., Hara, K., Umeshiro, A., Yabuuchi, Y., Suzuki, T., et al. (2018). Quinoprotein dehydrogenase functions at the final oxidation step of lankacidin biosynthesis in Streptomyces rochei 7434AN4. *J. Biosci. Bioeng.* 126, 145–152. doi: 10.1016/j.jbiosc.2018.03.006

Yang, K., Han, L., and Vining, L. C. (1995). Regulation of jadomycin B production in Streptomyces venezuelae ISP5230: involvement of a repressor gene, jadR2. *J. Bacteriol.* 177, 6111–6117. doi: 10.1128/JB.177.21.6111-6117.1995

Yu, Z., Reichheld, S. E., Savchenko, A., Parkinson, J., and Davidson, A. R. (2010). A comprehensive analysis of structural and sequence conservation in the TetR family transcriptional regulators. *J. Mol. Biol.* 400, 847–864. doi: 10.1016/j.jmb.2010.05.062

Zerikly, M., and Challis, G. L. (2009). Strategies for the discovery of new natural products by genome mining. *ChemBioChem* 10, 625–633. doi: 10.1002/cbic.200800389

Zhang, H., Shinkawa, H., Ishikawa, J., Kinashi, H., and Nimi, O. (1997). Improvement of transformation system in Streptomyces using a modified regeneration medium. *J. Ferment. Bioeng.* 83, 217–221. doi: 10.1016/S0922-338X(97)80982-8

Zhu, J., Sun, D., Liu, W., Chen, Z., Li, J., and Wen, Y. (2016). AvaR2, a pseudo γ-butyrolactone receptor homologue from Streptomyces avermitilis, is a pleiotropic repressor of avermectin and avenolide biosynthesis and cell growth. *Mol. Microbiol.* 102, 562–578. doi: 10.1111/mmi.13479

Zou, Z., Du, D., Zhang, Y., Zhang, J., Niu, G., and Tan, H. (2014). A γ-butyrolactone-sensing activator/repressor, JadR3, controls a regulatory mini-network for jadomycin biosynthesis. *Mol. Microbiol.* 94, 490–505. doi: 10.1111/mmi.12752

Conflict of Interest: The authors declare that the research was conducted in the absence of any commercial or financial relationships that could be construed as a potential conflict of interest.

frontiers in Microbiology

ORIGINAL RESEARCH
published: 02 July 2020
doi: 10.3389/fmicb.2020.01255

Molecular Dynamics to Elucidate the DNA-Binding Activity of AlpZ, a Member of the Gamma-Butyrolactone Receptor Family in *Streptomyces ambofaciens*

Cláudia M. Vicente[1†], Jean-Michel Girardet[2], Laurence Hôtel[1] and Bertrand Aigle[1*]*

[1] Université de Lorraine, INRAE, DynAMic, Nancy, France, [2] Université de Lorraine, INRAE, IAM, Nancy, France

OPEN ACCESS

Edited by:
Yvonne Mast, German Collection of Microorganisms and Cell Cultures GmbH (DSMZ), Germany

Reviewed by:
Shigeru Kitani, Osaka University, Japan
Wenqing Chen, Wuhan University, China

***Correspondence:**
Cláudia M. Vicente
claudia.vicente@insa-toulouse.fr
Bertrand Aigle
bertrand.aigle@univ-lorraine.fr

†Present address:
Cláudia M. Vicente, TBI, CNRS, INRAE, INSA, Université de Toulouse, Toulouse, France

Specialty section:
This article was submitted to Antimicrobials, Resistance and Chemotherapy, a section of the journal Frontiers in Microbiology

Received: *08 December 2019*
Accepted: *18 May 2020*
Published: *02 July 2020*

Citation:
Vicente CM, Girardet J-M, Hôtel L and Aigle B (2020) Molecular Dynamics to Elucidate the DNA-Binding Activity of AlpZ, a Member of the Gamma-Butyrolactone Receptor Family in Streptomyces ambofaciens. Front. Microbiol. 11:1255. doi: 10.3389/fmicb.2020.01255

Signaling molecule receptors play a central role in quorum sensing and in the coordination onset of specialized metabolite biosynthesis in *Streptomyces* due to their dual function in signal detection and gene expression control through DNA-binding in the promoter region of their target genes. In *Streptomyces ambofaciens* the *alp* biosynthetic gene cluster includes the signaling molecule receptor AlpZ that negatively regulates through a complex regulatory cascade the expression of key genes involved in the kinamycin antibiotic production until its cognate ligand, a yet unidentified signaling molecule, prompts its release from target promoters. Here we use an original molecular dynamics method to evaluate the DNA-binding properties of AlpZ to its target DNA sequence and the impact the signaling molecule has on the interaction. It is the first time this approach is used to characterize a regulator from the γ-butyrolactone receptor family. The observed K_D in the nanomolar range indicates that AlpZ-DNA constitute a particularly stable complex. The signaling molecule ably disturbs this binding while kinamycin has no effect on the activity of AlpZ. Regulator size was determined and found to be considerably large regarding protein sequence, indicating that AlpZ regulates gene expression by binding the DNA as a homodimer, and structural modeling comparison with closely related γ-butyrolactone receptors supports this conclusion.

Keywords: molecular dynamics, DNA-binding, signaling molecule receptor, quorum sensing, kinamycin

INTRODUCTION

Bacterial quorum sensing is a well-established phenomenon by which bacteria produce and sense chemical signals to communicate with neighboring cells. These diffusible signaling molecules are able to trigger a plethora of activities such as genetic exchange, antibiotic production, motility, virulence, biofilm formation, among others. The signaling molecule accumulates extracellularly during cell growth and when the concentration reaches a certain threshold it is detected by a receptor that elicits a downstream signal transduction cascade, triggering a specific gene expression program. An array of signaling molecules are used for cellular communication. For example, the acylhomoserine lactones (AHL) are the representatives and most studied chemical signals in Gram-negative bacteria, while Firmicutes mainly use peptides as signaling molecules

(Waters and Bassler, 2005). *Streptomyces*, ubiquitous filamentous Gram-positive bacteria characterized for their complex life cycle, linear chromosome and their ability to produce a wide variety of specialized metabolites including antibiotics, herbicides, immunosuppresssants and anticancer agents, display a different profile of signaling molecules.

The vast majority of signaling molecules produced by Streptomycetes and identified to date are classified into three major groups, γ-butyrolactones (GBL) (Yamada et al., 1987; Ohnishi et al., 1999; Takano et al., 2000; Takano, 2006), 2-alkyl-4-hydroxymethylfuran-3-carboxylic acids (AHFCA) (Corre et al., 2008) and γ-butenolides (Kitani et al., 2011; Arakawa et al., 2012). Two other less studied signaling molecules with quite different structures exist, the PI factor and the N-methylphenylalanyl-dehydrobutyrine diketopiperazine (Recio et al., 2004; Matselyukh et al., 2015). These molecules are widespread in the genus, often controlling both specialized metabolism and morphological differentiation (McCormick and Flärdh, 2012). Many of these molecules are active at nanomolar concentrations.

Gamma-butyrolactones constitute the largest and most studied group of signaling molecules in *Streptomyces*, and the first bacterial signaling molecule to be discovered was the A-factor of *Streptomyces griseus* (Khokhlov et al., 1967), a γ-butyrolactone type signaling molecule that governs a vast regulon of genes involved in both the morphological differentiation and specialized metabolism (Horinouchi et al., 2001; Horinouchi, 2002). Specialized metabolite biosynthetic pathway expression is a much regulated process (Liu et al., 2013). The onset of production is tightly controlled by a regulatory network comprised of different transcriptional regulators incorporating various environmental and physiological signals (Bibb, 2005; van Wezel and McDowall, 2011; Martín and Liras, 2012). Cluster-situated regulators (CSRs) play an important role, directly controlling gene transcription within the specialized metabolite biosynthetic gene cluster [although some CSRs have been described to cross regulate other biosynthetic gene clusters (Vicente et al., 2015; McLean et al., 2019)], while pleiotropic regulators modulate the biosynthesis of several specialized metabolites and often morphological development as well. Some of these transcriptional regulators are central to the quorum sensing phenomenon, acting as receptors of the diffusible signaling molecules, and usually belong to the large and widely distributed TetR family of transcriptional regulators (Ramos et al., 2005). A typical TetR-family GABR (γ-butyrolactone receptor) is comprised of two functional domains, a N-terminal helix-turn-helix DNA-binding domain that can interact with specific DNA target sequences in promoter regions, and a C-terminal signaling molecule-binding domain that interacts with cognate ligands (Cuthbertson and Nodwell, 2013). The promoter-bound signaling molecule receptor prevents transcription, and binding of the cognate signaling molecule leads to its release from the DNA allowing gene expression (Willey and Gaskell, 2011; Sidda and Corre, 2012).

The type II polyketide synthase (PKS) *alp* biosynthetic gene cluster of *Streptomyces ambofaciens* is responsible for the production of the antibiotic kinamycin and its regulatory network has been previously elucidated (Pang et al., 2004; Aigle et al., 2005; Bunet et al., 2008, 2011). Several forms of kinamycin have been identified (Bunet et al., 2011) and for the purpose of this work will be referred to as kinamycin. The cluster is duplicated (two identical copies) due to its location in the terminal inverted repeat (TIR) sequences at both ends of the chromosome and was initially identified as comprising 27 genes including three genes that compose the minimal PKS (*alpA*, *alpB*, and *alpC*) and five regulatory genes. Recent reports indicate that the cluster size could be extended to include a 24 gene region containing 6 genes responsible for the synthesis of the diazo functional group (Wang et al., 2015). Of the regulator genes, *alpT*, *alpU*, and *alpV* are members of the SARP (*Streptomyces* antibiotic regulatory proteins) family (Wietzorrek and Bibb, 1997), and *alpW* and *alpZ* belong to pseudo-GABR and GABR family, respectively (Matsuno et al., 2004; Nishida et al., 2007). Pseudo-GABRs are paralogs of GABR but are unable to interact with the cognate GBL. In the regulatory cascade (**Supplementary Figure S1**), the positive regulator AlpV activates kinamycin biosynthesis promoting the expression of the minimal PKS-encoding genes. During the initial growth phase, the negative regulator AlpZ specifically binds and prevents expression of the operon *alpXW* and of *alpV* as well as its own, hindering antibiotic biosynthesis particularly through the repression of *alpV*. The binding sites of AlpZ, as well as those of AlpW, have been characterized (Bunet et al., 2008, 2011) and show high homology to previously defined ARE (autoregulatory elements) motifs (Folcher et al., 2001). Following synthesis and build-up of the yet unknown *S. ambofaciens* signaling molecule, it binds to the regulator AlpZ releasing it from the target promoters and allowing gene expression that leads to kinamycin production (Bunet et al., 2008). At this stage late negative regulator AlpW accumulates and blocks *alpV* expression thus switching off kinamycin biosynthesis, at which point the signaling molecule concentration also decreases and based on transcription analysis data it is hypothesized that the negative control exerted by AlpZ on the expression of both *alpV* and *alpXW* resumes (Bunet et al., 2008, 2011). Although it remains unidentified, the signaling molecule responsible for the quorum sensing regulation of kinamycin production in *S. ambofaciens* has been characterized to some extent. Initial studies predict that it is not a γ-butyrolactone type signaling molecule, based on its physical properties such as its resistance to alkaline conditions and also to high temperatures (Bunet et al., 2008), but rather perhaps a AHFCA-like molecule. Furthermore, an *afsA*-like gene responsible for its biosynthesis was identified close to the *alp* cluster (unpublished data). AfsA-like enzymes have been shown to be key in both γ-butyrolactones and AHFCA synthesis (Hsiao et al., 2007; Kato et al., 2007; Corre et al., 2008).

As in the case of kinamycin biosynthesis, these signaling molecules and their receptors constitute one of the most extended regulatory systems to elicit the biosynthesis of specialized metabolites and/or morphological differentiation in a coordinated fashion in *Streptomyces* (Polkade et al., 2016). Several signaling molecules have been identified so far with more expected to exist (Thao et al., 2017). For this reason, signaling molecule receptors are central to modulate specialized metabolite biosynthesis and can be used as a strategy for cryptic gene

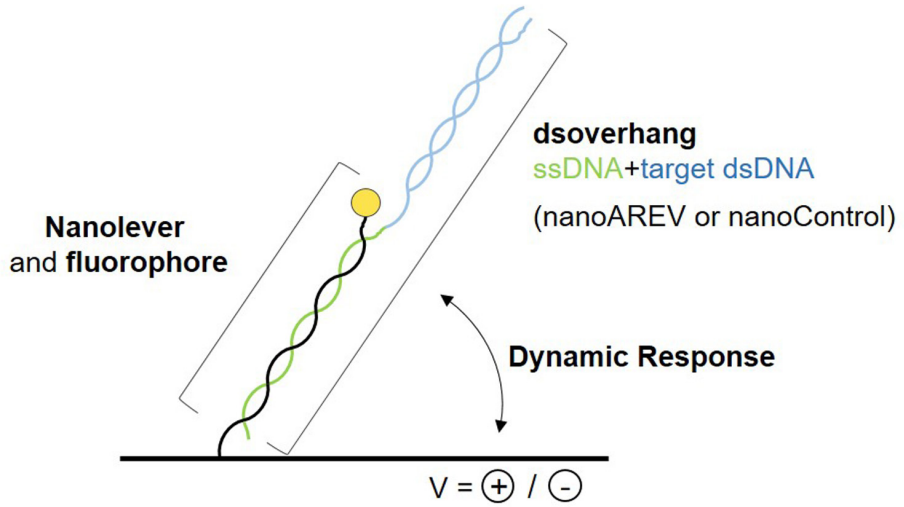

FIGURE 1 | Schematic representation of the molecular dynamics system. The dsoverhangs, the nanoAREV and nanoControl, include a dsDNA region containing either the protein's model target DNA or an unspecific DNA region, respectively (blue), and a ssDNA sequence (green) that is complementary to the tethered nanolever (black), which has a fluorophore linked at its end (yellow circle). Alternating the electric potentials applied to the gold microchip surface will either attract or repel the negatively charged dsDNA. The distance to the surface affects the intensity of the fluorescent light emitted by the dye due to the quenching effect of the gold surface, allowing the accurate measurement of the oscillating orientation change of the DNA in dynamic response.

cluster activation (Aigle and Corre, 2012; Sidda and Corre, 2012), shaping regulatory systems and to develop expression control tools (Bowyer et al., 2017; Biarnes-Carrera et al., 2018).

In this study, we address the role of AlpZ, a negative regulator and receptor of an unknown signaling molecule in *S. ambofaciens* that controls kinamycin biosynthesis, using a novel biophysical-based approach that allows a detailed depiction of the regulator's DNA-binding activity and how it is affected by the signaling molecule.

RESULTS

Regulator AlpZ Has High Affinity to Its Target Sequence

A recently developed technology was used to perform molecular dynamics studies and characterize the putative signaling molecule receptor AlpZ, the switchSENSE®. It is based on the electric properties of negatively charged double stranded DNA sequences, that when grafted to a gold microelectrode and subjected to alternating electric potentials are either attracted or repelled from the surface. Real-time tracking of the fluorescence emission from the fluorescent dye attached to the dsDNA nanolevers that depends on its proximity to the gold surface, allows to assess variations in the switching movement. To determine the affinity of AlpZ to its target sequences through molecular dynamics, specific DNA sequences were designed, the dsoverhangs. These contain both the target dsDNA sequence and a ssDNA region complementary to the biochip attached nanolevers (**Figure 1**). The AREV sequence located in the promoter region of the *alpV* gene (i.e., AREV) was used as a model of the known recognized sequences in the gene cluster (Bunet et al., 2008) and to create the dsoverhang nanoAREV. Functionalization of the dsoverhangs on the biochip was verified before each assay through increased fluorescence signal detection.

First, different concentrations of protein from 1.6 to 55.6 μM were used to assess the DNA-binding activity of AlpZ to the nanoAREV. Results show a strong affinity and remarkable stable binding of AlpZ to its target sequence. Indeed, in these conditions binding rate constant k_{ON} values reached 1.46 to 4.43 × 10^4 $M^{-1}.s^{-1}$ (**Table 1**), respectively. Notably, with increasingly higher protein concentrations the k_{ON} remains unchanged suggesting a saturation phenomenon occurs easily (**Figure 2A** left panel, **Table 1**). Furthermore, in these conditions no dissociation was observed even after a long period of time in dissociation favoring conditions (**Figure 2A** right panel). To better analyze the binding properties of AlpZ to the nanoAREV, assays were then performed using a lower concentration of protein (50 nM). It was observed that in these conditions protein binding occurs more slowly, with a k_{ON} of 1.38 × 10^5 $M^{-1}.s^{-1}$ (**Figure 2B** left panel, **Table 1**). Additionally, a slow dissociation is finally observed, although an even longer period of time is necessary to reach a steady state. This dissociation is however, enough to determine the binding rate constant k_{OFF}, which is of 1.05 × 10^{-4} s^{-1}.

TABLE 1 | Kinetic parameters of AlpZ with target DNA sequence.

Concentration (M)	k_{ON} ($M^{-1}.s^{-1}$)	k_{OFF} (s^{-1})	K_D (nM)
55.6 × 10^{-6}	4.43 ± 0.16 × 10^4	N/A	N/A
5.0 × 10^{-6}	4.68 ± 0.16 × 10^4	N/A	N/A
1.7 × 10^{-6}	1.46 ± 0.05 × 10^4	N/A	N/A
50.0 × 10^{-9}	1.38 ± 0.06 × 10^5	1.05 ± 0.08 × 10^{-4}	37.1 ± 3.3

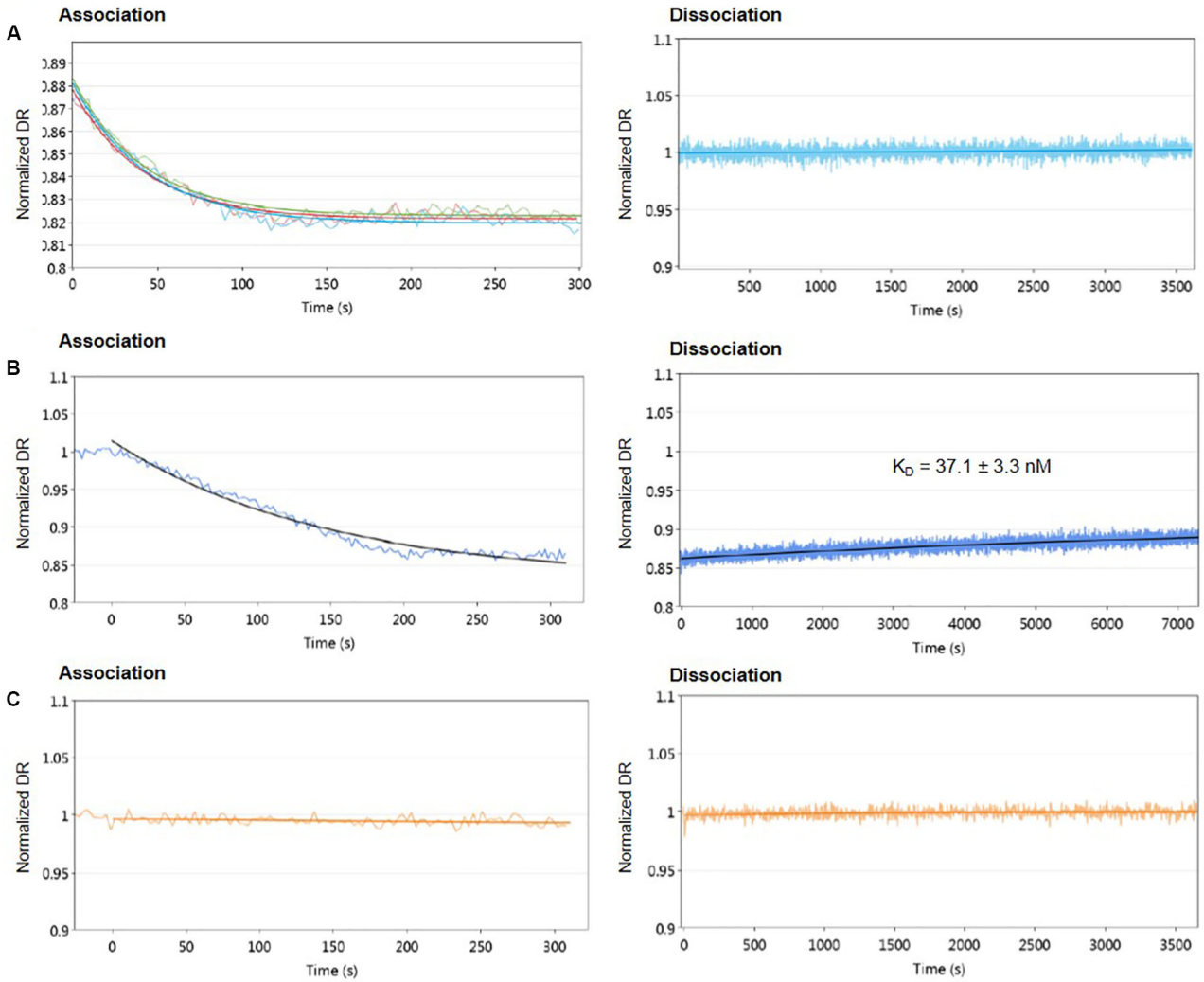

FIGURE 2 | Real-time measurements of molecular dynamics of AlpZ using molecular dynamics. Both association and dissociation analysis were performed. Different AlpZ protein concentrations were used with the nanoAREV dsoverhang. Colored lines in green, light blue and red represent the protein concentrations 55.6 μM, 5 μM, and 1.6 μM, respectively **(A)**. Assays were also carried out with 50 nM of AlpZ and nanoAREV dsoverhang **(B)**, and with 50 nM AlpZ and nanoControl dsoverhang **(C)**. Dissociation constant (K_D) shows the mean and standard deviation of three independent assays. Signal expressed as normalized dynamic response (DR).

The dissociation constant K_D of AlpZ to its target model sequence was found to be 37.1 nM (**Figure 2B** right panel, **Table 1**). These results indicate that the AlpZ-DNA complex is substantially stable.

To ensure AlpZ specificity in binding DNA during the assays, an unspecific dsoverhang was designed, the nanoControl. Instead of the AREV sequence it contains the AREU sequence originally located in the promoter region of *alpU* from the kinamycin gene cluster. It has been previously demonstrated that this sequence, which contains a weakly conserved ARE motif, is neither recognized nor bound by the regulator (Bunet et al., 2008). Molecular dynamic analysis using the established conditions and the nanoControl indicate that AlpZ does not bind to the dsoverhang. There is no observed association and consequently no dissociation (**Figure 2C**), confirming that AlpZ recognizes and specifically binds its target DNA sequences.

Sizing and Protein Structure Modeling Suggest AlpZ Functions as a Homodimer

The used molecular dynamics approach enables the measurement of protein friction, ultimately allowing protein size determination through hydrodynamic diameter (D_H) measurements. As the experimental set-up uses dsoverhangs, the movements of the biochip's nanolevers with the dsoverhangs used for the analysis have increased friction and lower dynamic response (DR) compared to those of the nanolevers alone. It is therefore necessary to first determine the relative size of the dsoverhang (different from the actual D_H as the dsoverhangs

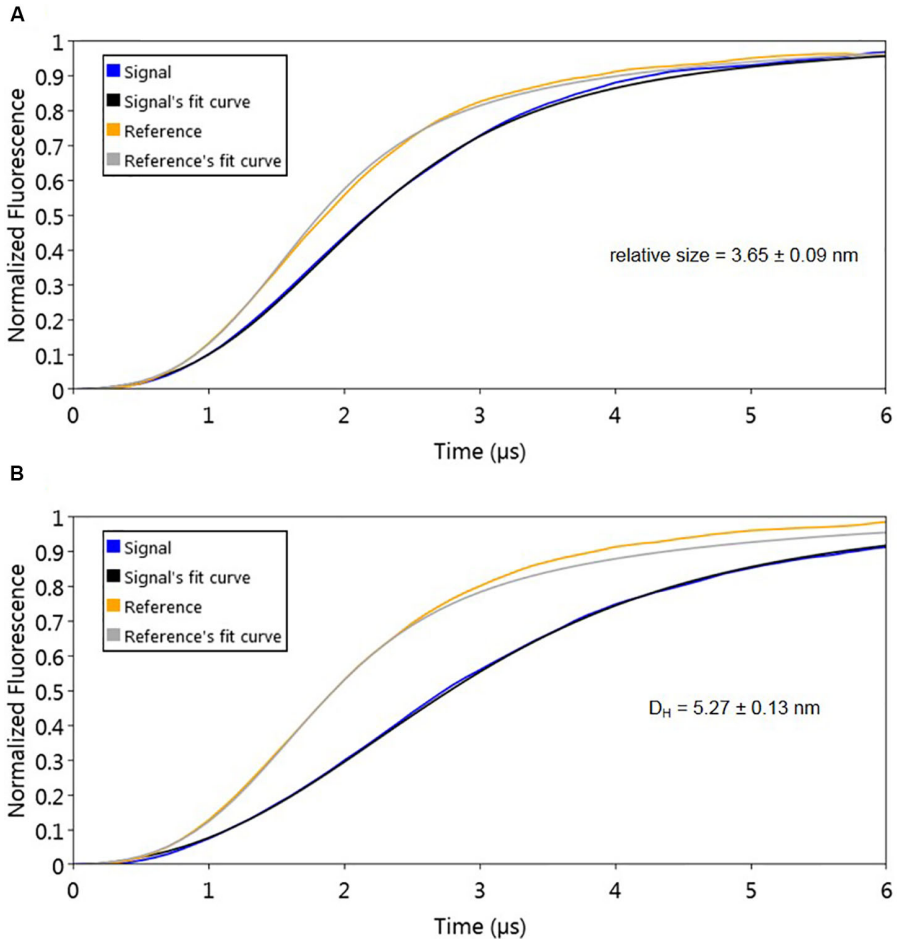

FIGURE 3 | Protein size analysis. Hydrodynamic diameter (D_H) was determined by comparing size of the nanoAREV dsoverhang **(A)** with that of dsoverhang nanoAREV + AlpZ complex **(B)**. Results show the mean and standard deviation using at least 3 independent assays. Signal expressed in normalized fluorescence.

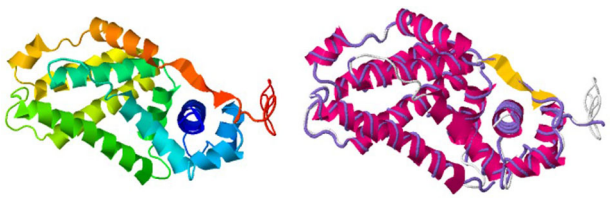

FIGURE 4 | AlpZ structure prediction. Predicted model of AlpZ **(left)** and alignment with TylP, a TetR regulator of tylosin biosynthesis in *S. fradiae* (**right**, structure analog in purple).

do not have a globular shape that is assumed in the model for size calculation). By comparing the switching dynamics of the dsoverhang to those of the reference nanolevers, the nanoAREV was shown to have 3.65 nm in relative size (**Figure 3A**), identical to the size of the nanoControl, as expected since the dsovehangs have the same length (data not shown).

Interestingly, we determined that AlpZ has a D_H of 5.27 nm (**Figure 3B**). AlpZ is a relatively small protein with 237 aa and a theoretical MW of 25.7 kDa, however, this result suggests its size is considerable. The only other related γ-butyrolactone receptor with structural data available is CprB from *Streptomyces coelicolor* A3(2) (Natsume et al., 2004). AlpZ and CprB belong to the GABR and pseudo-GABR family, respectively and show significant similarity (almost 30% identity and CprB has 26.4 kDa, and moreover similar predicted structures). Although it has been demonstrated that CprB binds DNA as a dimer of dimers (Bhukya et al., 2014), further biophysical modeling analysis using the switchANALYSIS software and the structural data of the apo-form of CprB (Natsume et al., 2004) predicted its D_H to be 5.21 nm, a very similar size to that of AlpZ. This result indicates that the form of AlpZ that binds the nanoAREV could be a homodimer. Furthermore, using a threading/fold recognition method (Zhang, 2009; Yang and Zhang, 2015) to modelize AlpZ it was possible to predict its single molecule structure. The best model has a relatively good C-score of −0.60 and is structurally very close to the homodimer structure of the TetR family regulator TylP from *Streptomyces fradiae* (Ray et al., 2017), showing a TM-score of 0.87 and coverage of 0.822

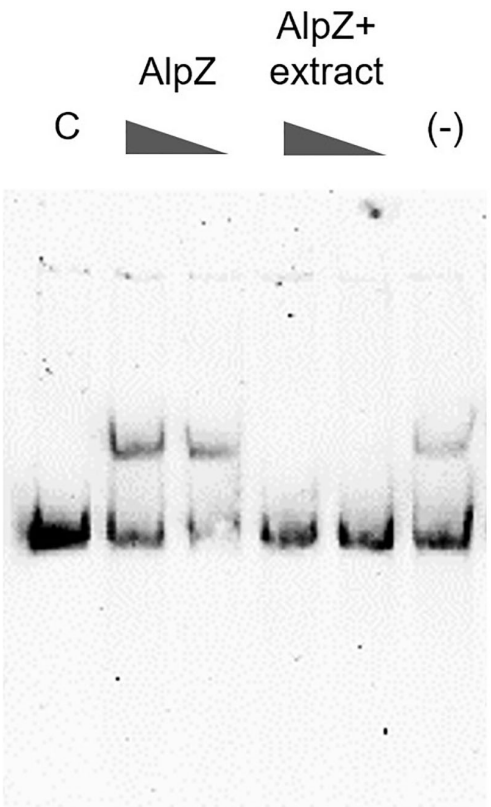

FIGURE 5 | Analysis of the presence of signaling molecule in mutant strain extracts. Electrophoretic mobility shift assays (EMSA) were used to assess AlpZ protein DNA-binding activity to a probe comprising the AREV sequence, with conditions of decreasing protein concentration (160 and 80 nM, respectively) and decreasing amounts of a *S. ambofaciens* ΔΔ*alpW* ΔΔ*alpID* strain supernatant extract containing the signaling molecule (25 μg/ml and 2.5 μg/ml, respectively) using 80 nM of protein. The loss of shifted bands indicates the presence of signaling molecule. Lane *C* contains the control without protein and lane *(-)* methanol 50%.

(**Figure 4**). This result further strengths the hypothesis that AlpZ is active as a homodimer.

Signaling Molecule Drastically Disrupts AlpZ-DNA Complex

It has been previously reported that a yet unidentified *S. ambofaciens* signaling molecule is able to affect the DNA binding by AlpZ, effectively modulating the regulation of kinamycin biosynthesis (Bunet et al., 2008). To obtain signaling molecule containing extracts, the *S. ambofaciens* ΔΔ*alpW* ΔΔ*alpID* mutant strain was used as it lacks the late regulator *alpW* leading a constitutive production of signaling molecule (unpublished data). This strain is also deficient in kinamycin production [loci *alpIABCD* deleted, in which the *alpABC* locus encodes the minimal PKS (Pang et al., 2004)], allowing therefore analysis without the putative interference of the biosynthetic pathway products (i.e., kinamycins or its intermediates). Extracts obtained from the culture supernatant were routinely checked for the presence of signaling molecule using electrophoretic mobility shift assays (EMSA), as seen in **Figure 5**.

To evaluate the effect of signaling molecule on AlpZ and its binding to the nanoAREV, an assay was designed to accurately detect protein release from the dsoverhang. The correct binding of AlpZ to the dsoverhang is first verified, and then an extract containing signaling molecule is added and molecular dynamics analysis are performed. Size analysis confirmed that the signaling molecule drastically alters the DNA binding function of AlpZ. The protein that was steadily bound to the dsoverhang (**Figure 6A**) shows a size of 5.7 nm, and is released when signaling molecule is present, changing the detected size to that of the dsoverhang and reference with 3.5 nm (**Figure 6B**). Additionally, kinetics analysis also demonstrates that the impact of the signaling molecule can be significant. Concentrated extracts of 0.5 mg/ml induce an almost immediate release, showing a considerably high k_{OFF} of 1.95×10^{-1} s^{-1} (**Figure 7A**), whereas more diluted samples lead to a fast but steady dissociation event with no protein molecule remaining bound to the dsoverhangs after just 5 minutes (**Figures 7B,C**). The observed effect is manifestly concentration dependent, and even small modifications of concentration affect the k_{OFF} values. Extract samples from the ΔΔ*alpW* ΔΔ*alpID* strain at 25 and 50 μg/ml display k_{OFF} values of 1.04×10^{-2} and 1.79×10^{-2} s^{-1}, respectively. Other solutions were previously proven to have no effect on the DNA-binding activity of AlpZ, including the used culture medium and purified molecules of the three subclasses of γ-butyrolactones, the A-factor, SCB1 and IM-2 (Bunet et al., 2008), confirming the observed phenomenon is specifically related to the unknown *S. ambofaciens* signaling molecule.

The interactions involving the three players AlpZ, target DNA and signaling molecule are clearly visible with a conformational analysis. The assay was designed and performed to analyze AlpZ binding to the nanoAREV dsoverhang and subsequently adding PE40 buffer (control) and signaling molecule containing extract to observe its effects on the association, followed by a conformational analysis (**Figure 8**). As in every performed assay, six electrodes are used, the first two of which are the controls without neither ligand nor analytes, and the following four electrodes are used for the assay itself (**Figure 8a**). As expected, the functionalization of the dsoverhangs (the first step of the assay), already has a negative impact on the dynamic response (**Figure 8b**). When AlpZ is introduced the dynamic response further decreases, as the protein tightly binds to the dsoverhangs (**Figure 8c**). The complex protein-DNA is very stable and not altered by solutions like the buffer PE40 (**Figure 8d**). However, when in the presence of signaling molecule containing extracts the dynamic response increases to the original levels upon release of the dsoverhangs by AlpZ (**Figure 8e**). During the entire assay, the control electrodes remain unchanged, confirming that no unspecific protein binding occurs to the nanolevers.

Kinamycin Does Not Impact AlpZ DNA-Binding Activity

Some regulator-receptors have been demonstrated to bind the product of their biosynthetic gene clusters in *Streptomyces*, such

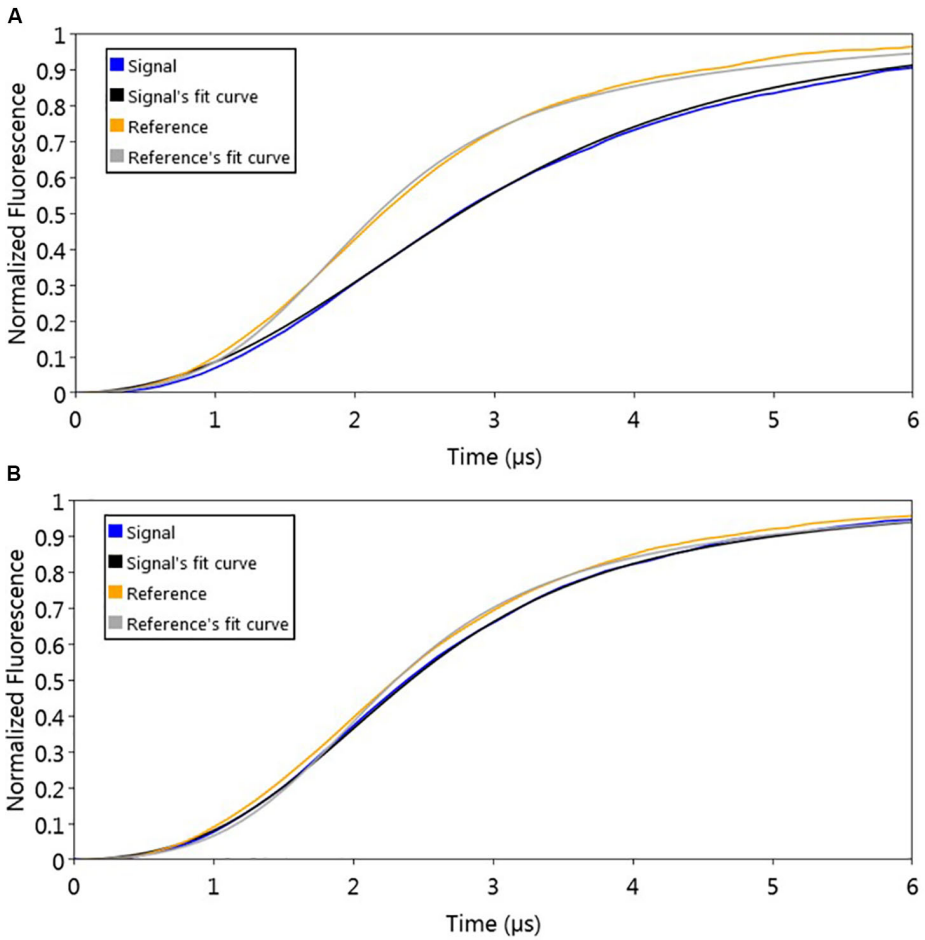

FIGURE 6 | Sizing analysis used to determine signaling molecule effect on AlpZ DNA-binding activity. **(A)** Analysis following preparation step with AlpZ binding to nanoAREV and **(B)** after adding signaling-molecule containing extract (0,5 mg/ml). Signal expressed in normalized fluorescence.

as JadR2 (Xu et al., 2010).To analyze if kinamycin could also act as a ligand of AlpZ, we performed molecular dynamic assays in the presence of purified kinamycin D and the results were analyzed (**Figure 9**). No dissociation of AlpZ was observed when kinamycin was used, confirming the regulator does not respond to kinamycin as a signal to modulate transcriptional control. Although the *S. ambofaciens* signaling molecule remains elusive, these results support the initially proposed classification of AlpZ as a true GABR.

DISCUSSION

The TetR regulator AlpZ plays a key role in the regulatory network of kinamycin biosynthesis in *S. ambofaciens* ATCC 23877, coupling it to the production of a yet unknown signaling molecule. As a negative transcriptional regulator, it exerts its control by binding specific promoter located sequences and hence blocking gene expression. An in-depth molecular characterization of this regulator is crucial to understand how it responses to target promoters and triggering signals.

The present study indicates that AlpZ has a strong affinity for its target DNA sequences and forms very stable complexes upon binding, as seen by a K_D in the nanomolar range. This result is also in good agreement with the EMSA experiments performed. Signaling molecule receptors such as GABRs have long been known for their affinity to DNA targets (Miyake et al., 1989; Onaka et al., 1995), though recent characterization of the binding activity of CprB to its target DNA shows a considerably higher K_D in the micromolar range (Biswas et al., 2015). The stable AlpZ-DNA complex explains how the regulator achieves a steady control on gene expression and on subsequence kinamycin biosynthesis. Protein size was determined through molecular dynamics, an approach validated in previous studies by comparing it with other more recurrent methods (Blocquel et al., 2017). The determined size of DNA-bound AlpZ is hence consistent and nonetheless unexpectedly large, suggesting that the regulator could be in a homodimer form. A model of AlpZ structure obtained through a threading/fold recognition prediction method shows high similarities with that of TylP, also a homodimer (Ray et al., 2017), strengthening the hypothesis that AlpZ binds its target DNA as an homodimer.

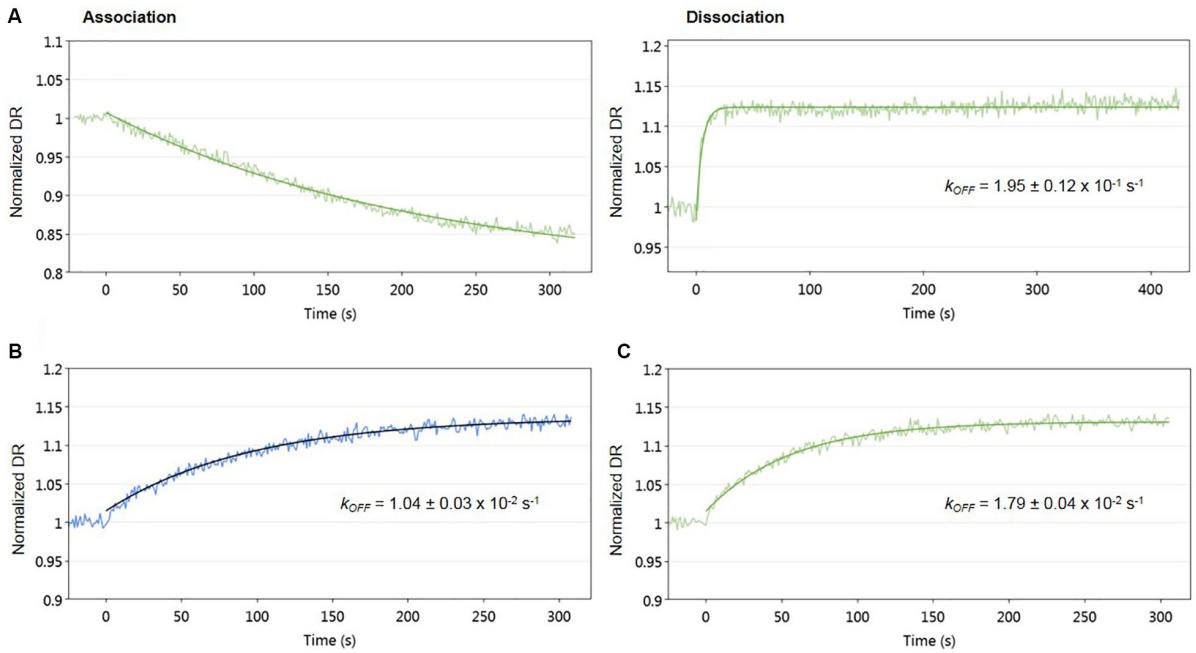

FIGURE 7 | Impact of signaling molecule on AlpZ binding activity. Kinetic analysis of AlpZ binding to the nanoAREV and its release in presence of concentrated signaling molecule containing extract **(A)** and protein dissociation with 25 μg/ml **(B)** and 50 μg/ml **(C)** of signaling molecule containing extract. Signal expressed as normalized dynamic response (DR).

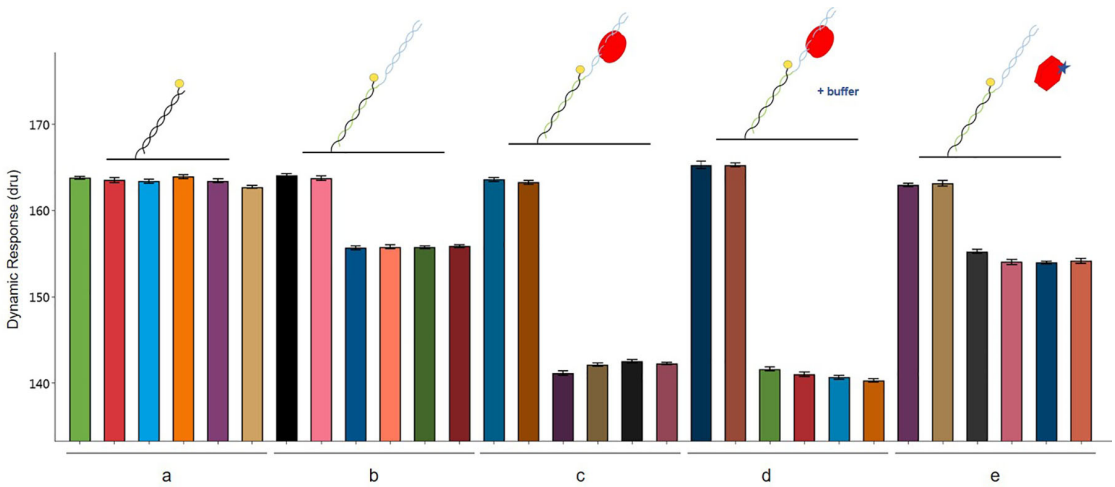

FIGURE 8 | Conformation analysis of AlpZ binding activity. Comparing changes in dynamic response of nanolevers alone **(a)**, after annealing of the dsoverhangs **(b)**, following binding of 50 nM of AlpZ **(c)**, in presence of PE40 buffer **(d)**, and signaling molecule-containing extract **(e)**. Above the graph are representations of the assay conditions and kinetics on the nanolevers, nanoAREV dsoverhang, with AlpZ (red circles), in the presence of buffer (+buffer) and signaling molecule (star). Vertical bars show dynamic response in the 6 electrodes present in the biochip. In each case the first two electrodes are the controls with nanolevers to verify the absence of unspecific binding to this region, and the next four electrodes were subjected to the different conditions. Assay was performed with 50 nM of AlpZ and a concentrated signaling molecule containing extract (0.5 mg/ml). Signal expressed in dynamic response units (dru). Error bars represent the standard deviation.

Only one trigger has been identified to actively interfere with the AlpZ-DNA complex, the yet unidentified *S. ambofaciens* signaling molecule. When present, the signaling molecule prompts a rapid AlpZ dissociation and the slightest amount variation is detected and impacts the dissociation rate. Consistent data were found both with molecular dynamics and sizing assays, substantiating this conclusion.

It is unclear if the DNA release is a result of an interference mechanism (e.g., competition for the same binding site), or rather the induction of structural conformational changes on the regulator hindering its DNA-binding capability. Based on

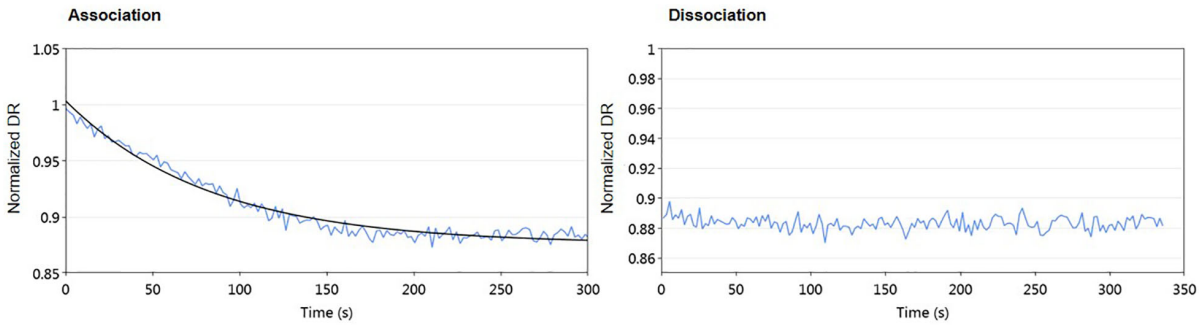

FIGURE 9 | Kinamycin has no effect on DNA-binding activity of AlpZ. A solution of pure kinamycin D at 50 μg/ml was used. Association analysis from AlpZ binding to nanoAREV in preparation for the assay **(left panel)**, and dissociation analysis after adding kinamycin D **(right panel)**.

previous studies, the latter hypothesis seems more probable, as TetR regulators appear to shift between mutually exclusive conformational states, either binding DNA or their cognate ligand of choice (Ramos et al., 2005; Bhukya et al., 2014), unlike the LuxR receptor regulator in proteobacteria whose structure has been resolved in complex with both the target DNA and the cognate pheromone (Zhang et al., 2002). Some bacterial compounds have been described to function as both antibiotics and signaling molecules (Beyersmann et al., 2017), however, that does not seem to be the case of kinamycin in regard to AlpZ. The DNA-binding activity of AlpZ is not impacted by kinamycin, indicating the regulator is not able to bind the antibiotic in contrast with other regulators that have been described to bind intermediates or products of their gene cluster, such as TylP (Ray et al., 2017), MphR(A) regulator of erythromycin biosynthesis (Zheng et al., 2009), SimR in *Streptomyces antibioticus* (Le et al., 2009) and the regulator of tetracyclin production TetR (Hinrichs et al., 1994). However, we hypothesize that one of the other regulators present in the *alp* cluster, AlpW, could perhaps be able to bind kinamycin or one of its biosynthetic pathway intermediates, as it has been described to be the case for other pseudo-GABRs, such as JadR2 and jadomycin (Xu et al., 2010).

The interactions between AlpZ-DNA complex and signaling molecule constitute a remarkably sensible system for gene regulation and induction of kinamycin biosynthesis, where even small concentration changes are sensed and impact protein-DNA complex stability. The promoter region of the *afsA*-like gene identified in the proximity of the *alp* cluster has been shown to contain an ARE motif (unpublished). It would be interesting to explore the role of AlpZ in the expression regulation of the *afsA*-like gene. One could envision that the AlpZ-ARE*afs*A-like complex would activate gene expression for a positive feed-back loop of induction of production of signaling molecule. Even though the nature of this signaling molecule continues to elude us, this work clearly demonstrates that the response of AlpZ to the extract of *S. ambofaciens* is in no way linked to kinamycin and broadens the knowledge on AlpZ regulatory role, possibly paving the way for similar autoregulator receptors. Efforts are underway for the purification and identification of the *S. ambofaciens* signaling molecule. The discovery of new signaling molecules in *Streptomyces* is impaired by the fact that these compounds are typically produced in very small amounts. Moreover, purification scale can be highly variable, avenolide in *S. avermitilis* required 2000 L of fermentation broth whereas *S. coelicolor* furans were identified using only 40 squared Petri dishes (Corre et al., 2008; Kitani et al., 2011). Approaches being used include the traditional large-scale fermentation method and specific capture using GABRs (Yang et al., 2005; Zou et al., 2014).

Although several studies exist on autoregulator receptors, there is still a long way to go to identify the cognate ligands of all TetR regulators identified to date (Cuthbertson and Nodwell, 2013). The present work constitutes the first described study of a signaling molecule receptor using an innovative molecular dynamics approach and provides a further step on the way to identifying the signaling molecule in *S. ambofaciens*. Furthermore, understanding how these regulators control gene expression and respond to the trigger of signaling molecules will ultimately contribute to the development of new approaches for specialized metabolite discovery and production improvement, as well as advancing other application tools.

MATERIALS AND METHODS

Strains, Media, and Growth Conditions

Strains used in this study are listed in **Table 2**. *Streptomyces* strains were grown in R2 medium (Kieser et al., 2000) and *Bacillus subtilis* was grown in LB. Kinamycin production was

TABLE 2 | Bacterial strains and cosmids/plasmids used in this work.

Strain	Description	References
S. ambofaciens ATCC 23877	Wild type	Pinnert-Sindico, 1954
S. ambofaciens Δ*alpW*	*alpW* loci replaced by a scar	Bunet et al., 2011
S. ambofaciens Δ*alpW* Δ*alpID*	*alpW* and *alpIABCD* loci replaced by a scar	This work
F6Δ*alpID*:scar	genomic library cosmid F6 with locus *alpID* replaced by a scar	Pang et al., 2004
Escherichia coli ET12567	strain used for interspecific conjugation	MacNeil, 1988
pUZ8002	for in *trans* mobilization of *oriT* containing cosmid	Paget et al., 1999

assessed on R2 medium as described previously (Pang et al., 2004; Aigle et al., 2005).

Construction of the Mutant Strain ΔΔ*alpW*ΔΔ*alpID*

To obtain a strain of *S. ambofaciens* producing the signaling molecule controlling the biosynthesis of kinamycin but unable to synthetize the antibiotic itself, we first made an in-frame deletion in the Δ*alpW* mutant strain (Bunet et al., 2011) of the locus *alpID* on both chromosomal arms. This locus includes the *alpA*, *alpB* and *alpC* genes encoding the minimal PKS and was replaced by a scar. The strategy was based on the REDIRECT system (Gust et al., 2003) and was carried out as described previously (Pang et al., 2004; Bunet et al., 2008). Only the start and stop codons of *alpI* and *alpD*, respectively remained after deletion and gene replacement was confirmed by Southern blot and PCR analysis using the CK1 and CK2 primer pair (**Supplementary Table S1**, data not shown).

Extraction of AlpZ Signaling Molecule

To study the effect of *S. ambofaciens* signaling molecule on AlpZ DNA-binding crude extracts were prepared as follows. The mutant strain ΔΔ*alpW*ΔΔ*alpID* was grown in 50 ml R2 medium in 250 ml flasks and incubated at 30°C until late exponential-stationary transition phase. Supernatant was collected and extracted twice with 1 volume of ethyl acetate, dried in a rotavapor, and dissolved in 100 μl methanol-H_2O 1:1 and stored at −20°C.

DNA-Protein Binding Assays

DNA binding assays were performed by EMSA as described previously (Bunet et al., 2008). Briefly, AREV DNA probe was obtained by PCR using the primers listed in **Supplementary Table S1** and directly labeled with digoxigenin using the DIG Oligonucleotide 3'-End Labeling kit, 2nd Generation (Roche Applied Science). Binding assays were performed with AlpZ protein, purified as described previously (Bunet et al., 2008). Labeled probes (0.4 ng) were incubated at 30°C for 10 min with AlpZ protein (80–160 nM) in binding buffer (20 mM HEPES pH7.6, 1 mM EDTA, 10 mM $(NH_4)_2SO_4$, 1 mM DTT, 0.2% Tween 20, 30 mM KCl) containing 50 μg/ml poly(dI-C) in a 20 μl final volume. When necessary, *S. ambofaciens* ΔΔ*alpW*ΔΔ*alpID* extracts (1 μl) were added after the incubation period and incubated for further 10 min to verify the presence of signaling molecule. Binding reactions were analyzed with 5% native PAGE and run in 0.5X TBE buffer. DNA was then transferred onto a positively charged nylon membrane (Amersham Hybon-N^+) by electroblotting, then fixed by UV crosslinking, detected with anti-digoxigenin antibodies, and developed by chemiluminescence with the CDP-StarTM reagent (Roche Applied Science).

Binding Kinetics and Hydrodynamic Diameter Measurements

A switchSENSE® DRX instrument and MPC-48-2-R1-S biochips (Dynamic Biosensors GmbH, Martinsried, Germany) were used to characterize the binding kinetics and protein size changes (Knezevic et al., 2012; Langer et al., 2013).

Specific dsDNA sequences coupled with ssDNA overhang regions complementary to the ssDNA sequences tethered to the biochip (nanolevers) called dsoverhangs, were designed. To prepare the dsoverhangs 2 μM of the two comprising ssDNA sequences (listed in **Supplementary Table S1**) were annealed by heating at 95°C for 10 min and slowly cooled to room temperature in PE40 buffer pH 7.4 (10 mM Na_2HPO_4/NaH_2PO_4, 40 mM NaCl, 0.05% Tween20, 50 μM EDTA, 50 μM EGTA). For the analysis of protein affinity to the dsoverhang, 150 μl of AlpZ at a range of concentrations were injected with a flow rate of 30 μl/min, and dissociation was measured with running buffer at a flow rate of 30 μl/min over 120 min to 4 h. Assays to assess the effect of signaling molecule on the binding of AlpZ to DNA started with a preparation step with dsoverhang (the ligand, either nanoAREV or nanoControl) and 150 μl of AlpZ (the analyte) at 50nM with a flow rate of 30 μl/min without dissociation, followed by a sandwich type of capture injecting 140 μl of signaling molecule containing extract (second analyte) at different concentrations (dilutions performed in PE40) with a flow rate of 20 μl/min. All assays used dsoverhangs at 500 nM and were performed at 30°C, combining both association/dissociation and size measurements and used PE40 as running buffer. A regeneration solution (alkaline solution pH 13) was used to remove the ligand after each assay.

Binding rates constants (k_{ON} and k_{OFF}) and dissociation constants (K_D) were determined using real-time measurements of the switching dynamics. Protein size was estimated by comparing the switching dynamics of bound protein with those of bare DNA and with the lollipop biophysical model (Langer et al., 2013). Analysis was performed with the switchANALYSIS software from Dynamic Biosensors and using at least three independent assays.

Protein Structure Modeling

Structure prediction was performed using a threading/fold recognition method and the server I-TASSER (Zhang, 2009; Yang and Zhang, 2015). After predicting secondary and solvent accessibility, structure templates with the highest significance in threading alignments are identified with LOMETS (Wu and Zhang, 2007). Structure models are predicted and ranked based on the C-score, a confidence score to estimate the quality of models predicted by I-TASSER. It is calculated based on the significance of threading template alignments and the convergence parameters of the structure assembly simulations, and values vary in a range of [−5, 2] where models with high confidence show higher C-score values (Zhang, 2008; Yang et al., 2015).

Kinamycin D Purification

A solution of kinamycin D was purified by semipreparative HPLC on an Agilent 1100 instrument equipped with an Agilent Zorbax Eclipse RP-C18 column (21 × 100 mm, 5 μm) monitoring the absorbance at 420 nm as described previously (Bunet et al., 2011).

DATA AVAILABILITY STATEMENT

All datasets generated for this study are included in the article/**Supplementary Material**.

AUTHOR CONTRIBUTIONS

CV and LH performed the experiments. CV, J-MG, and BA analyzed the data. CV and BA conceived the experiments and wrote the manuscript. BA supervised the project and obtained the funding. All authors have read and approved the final manuscript.

FUNDING

This work was funded by the French National Research Agency through Project ANR MiGenIs (ANR-13-BSV6-0009) and the French National Institute for Agricultural Research (INRA) and Laboratory Excellence ARBRE (ANR-11-LABX-0002-01). CV was also supported by the AgreenSkillsPlus Program (FP7-609398.0000) and the Région Grand Est.

ACKNOWLEDGMENTS

Real-time biomolecular interactions were investigated with the switchSENSE® technology available on the ASIA platform (Université de Lorraine-INRAE, https://a2f.univ-lorraine.fr/asia/).

SUPPLEMENTARY MATERIAL

The Supplementary Material for this article can be found online at: https://www.frontiersin.org/articles/10.3389/fmicb.2020.01255/full#supplementary-material

REFERENCES

Aigle, B., and Corre, C. (2012). Waking up *Streptomyces* secondary metabolism by constitutive expression of activators or genetic disruption of repressors. *Methods Enzymol.* 517, 343–366. doi: 10.1016/B978-0-12-404634-4.00017-6

Aigle, B., Pang, X., Decaris, B., and Leblond, P. (2005). Involvement of AlpV, a new member of the *Streptomyces* antibiotic regulatory protein family, in regulation of the duplicated type II polyketide synthase alp gene cluster in *Streptomyces ambofaciens*. *J. Bacteriol.* 187, 2491–2500. doi: 10.1128/JB.187.7.2491-2500.2005

Arakawa, K., Tsuda, N., Taniguchi, A., and Kinashi, H. (2012). The butenolide signaling molecules SRB1 and SRB2 induce lankacidin and lankamycin production in *Streptomyces rochei*. *Chembiochem* 13, 1447–1457. doi: 10.1002/cbic.201200149

Beyersmann, P. G., Tomasch, J., Son, K., Stocker, R., Göker, M., Wagner-Döbler, I., et al. (2017). Dual function of tropodithietic acid as antibiotic and signaling molecule in global gene regulation of the probiotic bacterium *Phaeobacter inhibens*. *Sci. Rep.* 7:730. doi: 10.1038/s41598-017-00784-7

Bhukya, H., Bhujbalrao, R., Bitra, A., and Anand, R. (2014). Structural and functional basis of transcriptional regulation by TetR family protein CprB from S. coelicolor A3(2). *Nucleic Acids Res.* 42, 10122–10133. doi: 10.1093/nar/gku587

Biarnes-Carrera, M., Lee, C.-K., Nihira, T., Breitling, R., and Takano, E. (2018). Orthogonal regulatory circuits for *Escherichia coli* based on the γ-butyrolactone system of *Streptomyces coelicolor*. *ACS Synth. Biol.* 7, 1043–1055. doi: 10.1021/acssynbio.7b00425

Bibb, M. J. (2005). Regulation of secondary metabolism in *Streptomycetes*. *Curr. Opin. Microbiol.* 8, 208–215. doi: 10.1016/j.mib.2005.02.016

Biswas, A., Narayan, S., Kallianpur, M. V., Krishnamoorthy, G., and Anand, R. (2015). Mode of DNA binding with γ-butyrolactone receptor protein CprB from *Streptomyces coelicolor* revealed by site-specific fluorescence dynamics. *Biochim. Biophys. Acta* 1850, 2283–2292. doi: 10.1016/j.bbagen.2015.08.008

Blocquel, D., Li, S., Wei, N., Daub, H., Sajish, M., Erfurth, M.-L., et al. (2017). Alternative stable conformation capable of protein misinteraction links tRNA synthetase to peripheral neuropathy. *Nucleic Acids Res.* 45, 8091–8104. doi: 10.1093/nar/gkx455

Bowyer, J. E., Lc de Los Santos, E., Styles, K. M., Fullwood, A., Corre, C., and Bates, D. G. (2017). Modeling the architecture of the regulatory system controlling methylenomycin production in *Streptomyces coelicolor*. *J. Biol. Eng.* 11:30. doi: 10.1186/s13036-017-0071-6

Bunet, R., Mendes, M. V., Rouhier, N., Pang, X., Hotel, L., Leblond, P., et al. (2008). Regulation of the synthesis of the angucyclinone antibiotic alpomycin in *Streptomyces ambofaciens* by the autoregulator receptor AlpZ and its specific ligand. *J. Bacteriol.* 190, 3293–3305. doi: 10.1128/JB.01989-07

Bunet, R., Song, L., Mendes, M. V., Corre, C., Hotel, L., Rouhier, N., et al. (2011). Characterization and manipulation of the pathway-specific late regulator AlpW reveals *Streptomyces ambofaciens* as a new producer of Kinamycins. *J. Bacteriol.* 193, 1142–1153. doi: 10.1128/JB.01269-10

Corre, C., Song, L., O'Rourke, S., Chater, K. F., and Challis, G. L. (2008). 2-Alkyl-4-hydroxymethylfuran-3-carboxylic acids, antibiotic production inducers discovered by *Streptomyces coelicolor* genome mining. *Proc. Natl. Acad. Sci. U.S.A.* 105, 17510–17515. doi: 10.1073/pnas.0805530105

Cuthbertson, L., and Nodwell, J. R. (2013). The TetR family of regulators. *Microbiol. Mol. Biol. Rev.* 77, 440–475. doi: 10.1128/MMBR.00018-13

Folcher, M., Gaillard, H., Nguyen, L. T., Nguyen, K. T., Lacroix, P., Bamas-Jacques, N., et al. (2001). Pleiotropic functions of a *Streptomyces* pristinaespiralis autoregulator receptor in development, antibiotic biosynthesis, and expression of a superoxide dismutase. *J. Biol. Chem.* 276, 44297–44306. doi: 10.1074/jbc.M101109200

Gust, B., Challis, G. L., Fowler, K., Kieser, T., and Chater, K. F. (2003). PCR-targeted *Streptomyces* gene replacement identifies a protein domain needed for biosynthesis of the sesquiterpene soil odor geosmin. *Proc. Natl. Acad. Sci. U.S.A.* 100, 1541–1546. doi: 10.1073/pnas.0337542100

Hinrichs, W., Kisker, C., Düvel, M., Müller, A., Tovar, K., Hillen, W., et al. (1994). Structure of the Tet repressor-tetracycline complex and regulation of antibiotic resistance. *Science* 264, 418–420. doi: 10.1126/science.8153629

Horinouchi, S. (2002). A microbial hormone, a-factor, as a master switch for morphological differentiation and secondary metabolism in *Streptomyces griseus*. *Front. Biosci.* 7:d2045–d2057. doi: 10.2741/horinouc

Horinouchi, S., Ohnishi, Y., and Kang, D. K. (2001). The a-factor regulatory cascade and cAMP in the regulation of physiological and morphological development in *Streptomyces griseus*. *J. Ind. Microbiol. Biotechnol.* 27, 177–182. doi: 10.1038/sj.jim.7000068

Hsiao, N.-H., Söding, J., Linke, D., Lange, C., Hertweck, C., Wohlleben, W., et al. (2007). ScbA from *Streptomyces coelicolor* A3(2) has homology to fatty acid synthases and is able to synthesize gamma-butyrolactones. *Microbiology* 153, 1394–1404. doi: 10.1099/mic.0.2006/004432-0

Kato, J., Funa, N., Watanabe, H., Ohnishi, Y., and Horinouchi, S. (2007). Biosynthesis of gamma-butyrolactone autoregulators that switch on secondary metabolism and morphological development in *Streptomyces*. *Proc. Natl. Acad. Sci. U.S.A.* 104, 2378–2383. doi: 10.1073/pnas.0607472104

Khokhlov, A. S., Tovarova, I. I., Borisova, L. N., Pliner, S. A., Shevchenko, L. N., Kornitskaia, E. I., et al. (1967). [The A-factor, responsible for streptomycin biosynthesis by mutant strains of *Actinomyces streptomycini*]. *Dokl. Akad. Nauk SSSR* 177, 232–235.

Kieser, T., Bibb, M., Buttner, M., Chater, K., and Hopwood, D. A. (2000). *Practical Streptomyces Genetics*. London: The John Innes Foundation.

Kitani, S., Miyamoto, K. T., Takamatsu, S., Herawati, E., Iguchi, H., Nishitomi, K., et al. (2011). Avenolide, a *Streptomyces* hormone controlling antibiotic production in *Streptomyces avermitilis*. *Proc. Natl. Acad. Sci. U.S.A.* 108, 16410–16415. doi: 10.1073/pnas.1113908108

Knezevic, J., Langer, A., Hampel, P. A., Kaiser, W., Strasser, R., and Rant, U. (2012). Quantitation of affinity, avidity, and binding kinetics of protein analytes with a dynamically switchable biosurface. *J. Am. Chem. Soc.* 134, 15225–15228. doi: 10.1021/ja3061276

Langer, A., Hampel, P. A., Kaiser, W., Knezevic, J., Welte, T., Villa, V., et al. (2013). Protein analysis by time-resolved measurements with an electro-switchable DNA chip. *Nat. Commun.* 4:2099. doi: 10.1038/ncomms3099

Le, T. B. K., Fiedler, H.-P., den Hengst, C. D., Ahn, S. K., Maxwell, A., and Buttner, M. J. (2009). Coupling of the biosynthesis and export of the DNA gyrase inhibitor simocyclinone in *Streptomyces antibioticus*. *Mol. Microbiol.* 72, 1462–1474. doi: 10.1111/j.1365-2958.2009.06735.x

Liu, G., Chater, K. F., Chandra, G., Niu, G., and Tan, H. (2013). Molecular regulation of antibiotic biosynthesis in *Streptomyces*. *Microbiol. Mol. Biol. Rev.* 77, 112–143. doi: 10.1128/MMBR.00054-12

MacNeil, D. J. (1988). Characterization of a unique methyl-specific restriction system in *Streptomyces avermitilis*. *J. Bacteriol.* 170, 5607–5612. doi: 10.1128/jb.170.12.5607-5612.1988

Martín, J. F., and Liras, P. (2012). Cascades and networks of regulatory genes that control antibiotic biosynthesis. *Subcell. Biochem.* 64, 115–138. doi: 10.1007/978-94-007-5055-5_6

Matselyukh, B., Mohammadipanah, F., Laatsch, H., Rohr, J., Efremenkova, O., and Khilya, V. (2015). N-methylphenylalanyl-dehydrobutyrine diketopiperazine, an a-factor mimic that restores antibiotic biosynthesis and morphogenesis in *Streptomyces globisporus* 1912-B2 and *Streptomyces griseus* 1439. *J. Antibiot.* 68, 9–14. doi: 10.1038/ja.2014.86

Matsuno, K., Yamada, Y., Lee, C.-K., and Nihira, T. (2004). Identification by gene deletion analysis of barB as a negative regulator controlling an early process of virginiamycin biosynthesis in *Streptomyces virginiae*. *Arch. Microbiol.* 181, 52–59. doi: 10.1007/s00203-003-0625-5

McCormick, J. R., and Flärdh, K. (2012). Signals and regulators that govern *Streptomyces* development. *FEMS Microbiol. Rev.* 36, 206–231. doi: 10.1111/j.1574-6976.2011.00317.x

McLean, T. C., Wilkinson, B., Hutchings, M. I., and Devine, R. (2019). Dissolution of the disparate: co-ordinate regulation in antibiotic biosynthesis. *Antibiotics* 8:83. doi: 10.3390/antibiotics8020083

Miyake, K., Horinouchi, S., Yoshida, M., Chiba, N., Mori, K., Nogawa, N., et al. (1989). Detection and properties of a-factor-binding protein from *Streptomyces griseus*. *J. Bacteriol.* 171, 4298–4302. doi: 10.1128/jb.171.8.4298-4302.1989

Natsume, R., Ohnishi, Y., Senda, T., and Horinouchi, S. (2004). Crystal structure of a γ-butyrolactone autoregulator receptor protein in *Streptomyces coelicolor* A3(2). *J. Mol. Biol.* 336, 409–419. doi: 10.1016/j.jmb.2003.12.040

Nishida, H., Ohnishi, Y., Beppu, T., and Horinouchi, S. (2007). Evolution of gamma-butyrolactone synthases and receptors in *Streptomyces*. *Environ. Microbiol.* 9, 1986–1994. doi: 10.1111/j.1462-2920.2007.01314.x

Ohnishi, Y., Kameyama, S., Onaka, H., and Horinouchi, S. (1999). The A-factor regulatory cascade leading to streptomycin biosynthesis in *Streptomyces griseus*: identification of a target gene of the A-factor receptor. *Mol. Microbiol.* 34, 102–111. doi: 10.1046/j.1365-2958.1999.01579.x

Onaka, H., Ando, N., Nihira, T., Yamada, Y., Beppu, T., and Horinouchi, S. (1995). Cloning and characterization of the A-factor receptor gene from *Streptomyces griseus*. *J. Bacteriol.* 177, 6083–6092. doi: 10.1128/jb.177.21.6083-6092.1995

Paget, M. S., Chamberlin, L., Atrih, A., Foster, S. J., and Buttner, M. J. (1999). Evidence that the extracytoplasmic function sigma factor sigmaE is required for normal cell wall structure in *Streptomyces coelicolor* A3(2). *J. Bacteriol.* 181, 204–211. doi: 10.1128/jb.181.1.204-211.1999

Pang, X., Aigle, B., Girardet, J.-M., Mangenot, S., Pernodet, J.-L., Decaris, B., et al. (2004). Functional angucycline-like antibiotic gene cluster in the terminal inverted repeats of the *Streptomyces ambofaciens* linear chromosome. *Antimicrob. Agents Chemother.* 48, 575–588. doi: 10.1128/aac.48.2.575-588.2004

Pinnert-Sindico, S. (1954). Une nouvelle espèce de *Streptomyces* productrice d'antibiotiques: *Streptomyces ambofaciens* n. sp., caracteres culturaux. *Ann. Inst. Pasteur* 87, 702–707.

Polkade, A. V., Mantri, S. S., Patwekar, U. J., and Jangid, K. (2016). Quorum sensing: an under-explored phenomenon in the phylum actinobacteria. *Front. Microbiol.* 7:131. doi: 10.3389/fmicb.2016.00131

Ramos, J. L., Martínez-Bueno, M., Molina-Henares, A. J., Terán, W., Watanabe, K., Zhang, X., et al. (2005). The TetR family of transcriptional repressors. *Microbiol. Mol. Biol. Rev.* 69, 326–356. doi: 10.1128/MMBR.69.2.326-356.2005

Ray, S., Maitra, A., Biswas, A., Panjikar, S., Mondal, J., and Anand, R. (2017). Functional insights into the mode of DNA and ligand binding of the TetR family regulator TylP from *Streptomyces fradiae*. *J. Biol. Chem.* 292, 15301–15311. doi: 10.1074/jbc.M117.788000

Recio, E., Colinas, A., Rumbero, A., Aparicio, J. F., and Martín, J. F. (2004). PI factor, a novel type quorum-sensing inducer elicits pimaricin production in *Streptomyces natalensis*. *J. Biol. Chem.* 279, 41586–41593. doi: 10.1074/jbc.M402340200

Sidda, J. D., and Corre, C. (2012). Gamma-butyrolactone and furan signaling systems in *Streptomyces*. *Methods Enzymol.* 517, 71–87. doi: 10.1016/B978-0-12-404634-4.00004-8

Takano, E. (2006). Gamma-butyrolactones: *Streptomyces* signalling molecules regulating antibiotic production and differentiation. *Curr. Opin. Microbiol.* 9, 287–294. doi: 10.1016/j.mib.2006.04.003

Takano, E., Nihira, T., Hara, Y., Jones, J. J., Gershater, C. J., Yamada, Y., et al. (2000). Purification and structural determination of SCB1, a gamma-butyrolactone that elicits antibiotic production in *Streptomyces coelicolor* A3(2). *J. Biol. Chem.* 275, 11010–11016. doi: 10.1074/jbc.275.15.11010

Thao, N. B., Kitani, S., Nitta, H., Tomioka, T., and Nihira, T. (2017). Discovering potential *Streptomyces* hormone producers by using disruptants of essential biosynthetic genes as indicator strains. *J. Antibiot.* 70, 1004–1008. doi: 10.1038/ja.2017.85

van Wezel, G. P., and McDowall, K. J. (2011). The regulation of the secondary metabolism of *Streptomyces*: new links and experimental advances. *Nat. Prod. Rep.* 28, 1311–1333. doi: 10.1039/c1np00003a

Vicente, C. M., Payero, T. D., Santos-Aberturas, J., Barreales, E. G., de Pedro, A., and Aparicio, J. F. (2015). Pathway-specific regulation revisited: cross-regulation of multiple disparate gene clusters by PAS-LuxR transcriptional regulators. *Appl. Microbiol. Biotechnol.* 99, 5123–5135. doi: 10.1007/s00253-015-6472-x

Wang, B., Guo, F., Ren, J., Ai, G., Aigle, B., Fan, K., et al. (2015). Identification of Alp1U and Lom6 as epoxy hydrolases and implications for kinamycin and lomaiviticin biosynthesis. *Nat. Commun.* 6:7674. doi: 10.1038/ncomms8674

Waters, C. M., and Bassler, B. L. (2005). Quorum sensing: cell-to-cell communication in bacteria. *Annu. Rev. Cell Dev. Biol.* 21, 319–346. doi: 10.1146/annurev.cellbio.21.012704.131001

Wietzorrek, A., and Bibb, M. (1997). A novel family of proteins that regulates antibiotic production in *Streptomycetes* appears to contain an OmpR-like DNA-binding fold. *Mol. Microbiol.* 25, 1181–1184. doi: 10.1046/j.1365-2958.1997.5421903.x

Willey, J. M., and Gaskell, A. A. (2011). Morphogenetic signaling molecules of the *Streptomycetes*. *Chem. Rev.* 111, 174–187. doi: 10.1021/cr1000404

Wu, S., and Zhang, Y. (2007). LOMETS: a local meta-threading-server for protein structure prediction. *Nucleic Acids Res.* 35, 3375–3382. doi: 10.1093/nar/gkm251

Xu, G., Wang, J., Wang, L., Tian, X., Yang, H., Fan, K., et al. (2010). "Pseudo" gamma-butyrolactone receptors respond to antibiotic signals to coordinate antibiotic biosynthesis. *J. Biol. Chem.* 285, 27440–27448. doi: 10.1074/jbc.M110.143081

Yamada, Y., Sugamura, K., Kondo, K., Yanagimoto, M., and Okada, H. (1987). The structure of inducing factors for virginiamycin production in *Streptomyces virginiae*. *J. Antibiot.* 40, 496–504. doi: 10.7164/antibiotics.40.496

Yang, J., Yan, R., Roy, A., Xu, D., Poisson, J., and Zhang, Y. (2015). The I-TASSER suite: protein structure and function prediction. *Nat. Methods* 12, 7–8. doi: 10.1038/nmeth.3213

Yang, J., and Zhang, Y. (2015). I-TASSER server: new development for protein structure and function predictions. *Nucleic Acids Res.* 43, W174–W181. doi: 10.1093/nar/gkv342

Yang, Y.-H., Joo, H.-S., Lee, K., Liou, K.-K., Lee, H.-C., Sohng, J.-K., et al. (2005). Novel method for detection of butanolides in *Streptomyces coelicolor* culture broth, using a His-tagged receptor (ScbR) and mass spectrometry. *Appl. Environ. Microbiol.* 71, 5050–5055. doi: 10.1128/AEM.71.9.5050-5055.2005

Zhang, R., Pappas, K. M., Pappas, T., Brace, J. L., Miller, P. C., Oulmassov, T., et al. (2002). Structure of a bacterial quorum-sensing transcription factor complexed with pheromone and DNA. *Nature* 417, 971–974. doi: 10.1038/nature00833

Zhang, Y. (2008). I-TASSER server for protein 3D structure prediction. *BMC Bioinformatics* 9:40. doi: 10.1186/1471-2105-9-40

Zhang, Y. (2009). I-TASSER: fully automated protein structure prediction in CASP8. *Proteins* 77(Suppl. 9), 100–113. doi: 10.1002/prot.22588

Zheng, J., Sagar, V., Smolinsky, A., Bourke, C., LaRonde-LeBlanc, N., and Cropp, T. A. (2009). Structure and function of the macrolide biosensor protein, MphR(A), with and without erythromycin. *J. Mol. Biol.* 387, 1250–1260. doi: 10.1016/j.jmb.2009.02.058

Zou, Z., Du, D., Zhang, Y., Zhang, J., Niu, G., and Tan, H. (2014). A γ-butyrolactone-sensing activator/repressor, JadR3, controls a regulatory mini-network for jadomycin biosynthesis. *Mol. Microbiol.* 94, 490–505. doi: 10.1111/mmi.12752

Conflict of Interest: The authors declare that the research was conducted in the absence of any commercial or financial relationships that could be construed as a potential conflict of interest.

Advantages of publishing in Frontiers

OPEN ACCESS
Articles are free to read for greatest visibility and readership

FAST PUBLICATION
Around 90 days from submission to decision

HIGH QUALITY PEER-REVIEW
Rigorous, collaborative, and constructive peer-review

TRANSPARENT PEER-REVIEW
Editors and reviewers acknowledged by name on published articles

Frontiers
Avenue du Tribunal-Fédéral 34
1005 Lausanne | Switzerland

Visit us: www.frontiersin.org
Contact us: info@frontiersin.org | +41 21 510 17 00

REPRODUCIBILITY OF RESEARCH
Support open data and methods to enhance research reproducibility

DIGITAL PUBLISHING
Articles designed for optimal readership across devices

FOLLOW US
@frontiersin

IMPACT METRICS
Advanced article metrics track visibility across digital media

EXTENSIVE PROMOTION
Marketing and promotion of impactful research

LOOP RESEARCH NETWORK
Our network increases your article's readership